# 海外出張報告書

# 第33回OECD/NEA炉物理委員会



1990年12月

# 技術資料コード 開示区分 レポートNo. ハタカロ タ のー の/ 3 この資料は 図書室保存資料です 閲覧には技術資料閲覧票が必要です 動力炉・核燃料開発事業団大洗工学センター技術管理室

動力炉・核燃料開発事業団 大 洗 工 学 セン ター

複製又はこの資料の入手については、下記にお問い合わせください。 〒311-13 茨城県東茨城郡大洗町成田町4002 動力炉・核燃料開発事業団 大洗工学センター システム開発推進部・技術管理室

Enquires about copyright and reproduction should be addressed to: Technology Management Section O-arai Engineering Center, Power Reactor and Nuclear Fuel Development Corporation 4002 Narita-cho, O-arai-machi, Higashi-Ibaraki, Ibaraki-ken, 311-13, Japan

動力炉·核燃料開発事業団 (Power Reactor and Nuclear Fuel Development Corporation)

## 海 外 出 張 報 告 書 第33回 OECD/NEA炉物理委員会

若林 利男\*

### 要旨

第33回NEACRP(参加国17ヶ国)に日本の委員として参加し、日本の技術論文の内、PNC発表分5件を紹介するとともに討議を行った。また、NEACRPの将来展望についての討議に参加した。

技術論文発表数54件の内、日本は15件を占め、内容的にも優れたものが多く、NEACRPへの日本の技術的な寄与は非常に大きいと思われる。

また、今回の会合は、NEAがおかれている厳しい状況(経費削減等)の中、NEACRPとしての位置付けの明確化、長期計画の策定が要求された会合でもあった。NEACRPの活動は炉物理分野に限られているが、この分野は原子力の他の分野(安全性、廃棄物等)への基礎的な技術データベースの提供と炉物理面での革新的アイディアの創出という役割を持っている。このため、NDACRP活動の重要性は益々高まってくると思われる。

現在、炉物理のすべての分野にわたって1つの国が実施することは、予算、人的な面で難しくなってきており、その点NEACRPのような国際協力の場で情報交換と共同作業(ベンチマークも含む)を行うことは、資源の有効利用の点からも必要である。

NEACRPのリーダーシップを取っているのは米国、フランス、ドイツ及び日本であり、特に日本への期待は高まっていると思われる。

<sup>\*</sup> 技術開発部プラント工学室

# 目 次

| 1. | 出强   | 概要           | *************************************** | 1  |
|----|------|--------------|-----------------------------------------|----|
| ]  | . 1  | 目            | 的                                       | 1  |
|    | . 2  | 期            | 間                                       | 1  |
|    | . 3  | 出 張          | 者                                       | 1  |
|    | . 4  | 場所・          | 出席者等                                    | 1  |
| 2. | 報告   | 内容           |                                         | 2  |
| 6  | 2. 1 | Agenda       | a                                       | 2  |
| 2  | 2. 2 | 会議の          | )概要                                     | 2  |
|    | 2. 2 | .1 框         | Í松NEA 局長の挨拶                             | 2  |
|    | 2. 2 | . 2 技        | な術セッション                                 | 3  |
|    | 2. 2 | . 3 追        | 『営セッションでの討議                             | 18 |
|    | 2. 2 | . 4 <i>ひ</i> | (回の予定                                   | 18 |
| 3  | 2. 3 | 所            | 感                                       | 18 |
| 3. | 添作   | <b></b> 資料   |                                         | 23 |
| (  | 1) 角 | ₹33回N        | EACRP会合出席者リスト                           | 23 |
| (  | 2) A | genda        |                                         | 25 |
| 1  | Q) 🚉 | ☆女佳          |                                         | 29 |

### 1. 出 張 概 要

### 1.1 目 的

OECD • NEA 主催炉物理委員会 (NEACRP)\*の第33回年次会合に参加して情報・意見交換を行い、併せて動力炉開発における炉物理分野の研究開発課題について討議する。

### 1.2 期 間

1990年10月14日(日)~1990年10月21日(日)

### 1.3 出張者

若林 利男 (動燃大洗, 技開部プラント工学部担当役)

### 1.4 場所、出席者等

会議は1990年10月15日から19日の間、パリのOECD本部において開催された。出席者は各国委員16名(日本からは原研金子氏と若林が出席)のほか、NEA本部(事務局)より7名、さらにオブザーバーとしてIAEA3名が加わり、合計26名の会議となった。議長はスイス代表のP. Wydlerが務めた。添付資料1に出席者リストを示す。

<sup>\*</sup> NEACRPはOECD・NEAの下部委員会であり、原子力研究開発の炉物理分野におけるNBA加盟国の協力を図ることを目的としている。すなわち、各国の情報や意見を交換し、新たな技術的課題の解決のために各国が協力し、また協力に必要な事柄を各国の研究開発の政策に反映してもらうことである。

### 2. 報告內容

### 2. 1 Agenda

添付資料 2 に第33回NEACRP会合のAgendaを示す。

### 2.2 会議の概要

本会合は委員会運営セッションと技術セッションに別けて討議した。以下それぞれのセッションの概要について示す。

### 2.2.1 植松NEA局長の挨拶

会合の初めにOECD・NEA 植松局長がNEA のおかれている状況, NEACRPに期待する事項等の 挨拶があった。以下に要点を示す。

- 原子力工業はしばらく新しい発注がなく厳しい状態におかれている。しかし、原子力エネルギーに対して長い目で見ると、地球環境の変化や最近の世界的な石油供給のもろさを考えると少しは良い方に向かっていると思われる。
- NEA は現在長期計画を検討し採用しようとしている。そのためにいくつかの「シンクタンク」を設置した。
- それら「シンクタンク」の1つでは、高速炉に対して議論を行っている。その中には長 半減期核種の消滅に関する検討も含まれており、高速炉をアクチナイド消滅装置の1つと して提案できる可能性もある。
- NEACRPは原子力開発における新型炉及び革新的技術を取り入れた炉の研究に取り組んできている。その内以下のものが注目される。
  - (イ) 安全性向上を考慮した中小型炉の設計研究
- (ロ) 高速炉の将来の研究開発
- (ハ) アクチナイドの取扱も含む燃料サイクル改善の研究
- (二) プラント寿命延長の研究
- 原子力発電所建設が沈滞しているOECD加盟国のいくつかでは新型炉開発への態度が不確 定なところもある。しかし、中小型炉は単純であることや安全性に対するPAの問題解決等 により将来のオプションとして魅力的なものであると考えているところもある。
- NEACRPが加盟国に炉物理に関して多くの情報を提供していることは開発計画を作る上で 重要である。
- NEAには多くの委員会があるが,その内科学的な委員会であるNEACRP,NEANDC(Nuclear

Energy Agency Nuclear Data Committee), CSNI (Committee on the Safety of Nuclear Installations)の間で、仕事の連携にギャップがあるように見える。重複した仕事がないように適切に役割分担をする必要がある。

● NEAはソ連を含めた東ヨーロッパとの関係を深めるために、今年の12月6日、7日に特別にセミナーを開催する予定である。NEAでは安全性、廃棄物処理等それら国々が注目している事項について協力の可能性を模索する予定である。

### 2.2.2 技術セッション

Technical Session ではそれぞれのトピックスに関して各国が提出した論文の紹介と討議が行われた。また、NEACRPが関与しているベンチマーク問題及びデータベースの状況、国際協力プログラムや各国炉物理活動の状況等の紹介と討議が行われた。

### (1) トピックスの概要

表1にトピックスの項目と発表論文数を示す。各セッションの論文の概要を以下に示す。なお、PNCに関連する論文は少し詳しく示した。また、これら論文を添付資料に示す。

1) 軽水炉によるPuリサイクルの当面の課題(セッション1.1)

論文A-1047~A1049(ベルギー)は、VIP計画について述べたものである。この計画はLWR におけるMOX燃料の利用に関する炉物理・炉工学上の問題の解決について研究炉(VENUS)等の施設を使って実験的根拠を得ようとするものであり、日本の LWRメーカーも参加することになっている。

論文A-1055(CEA)は、フランスのPWRでのプルトニウム装荷の2年間の経験についてまとめてある。

論文A-1116 (ドイツ) は、西独でのPuリサイクル研究活動のまとめである。

論文A-1066(日本)は、燃料の対減速材比を0.3程度に低くした新型の BWRの提案であり、Pu残存率約1.0を達成し得るとしている。

論文A-1067 (日本PNC)は、ATR原型炉におけるMOX燃料の利用についての経験について述べ、DUPLEXペレットの燃料体が燃焼度の向上に有効とした。この論文についてはPuサーマルとATRの位置付け、Gd入り燃料の臨界実験計画等について質問があった。

討論において、Puリサイクルの経済的優位制は明確にされなかった。また、議論が廃棄物処理に及ぶことも考えるべきだとされた。

2) 中性子(炉物理)計算コードを検証する方法に対する要求(セッション1.2) 論文A-1056と1084(フランス)は、中性子物理関係のコードの評価と記録について、 コード管理及び標準版の保護の観点から論じている。

論文A-1085は、EPRIのLWR安全審査用炉物理解析コードの解析手法をまとめている。 論文A-1091(USA)は、MHTGRに重要な安全上のパラメータの不確かさとその評価の要求 についてまとめている。新しい手法による実験の解析が必要としている。

論文A-1096(カナダ)は、CANDUダーリントン発電所における停止系のソフトの許可に あたって遭遇した困難について述べている。この困難さは、ソフトに基礎をおいた系を 採用することの潜在的な利点を無視してしまった。そして、ソフトに依存した安全系の 許可を得ようとするときの問題点を浮き彫りにした。

討論では、NEACRPのベンチマーク試験が、炉物理計算コードの評価に役立っているという認識が得られた。

- 3) 高速炉に係わる炉物理特性(セッション1.3) 全部で6件の論文が提出され、その内日本から1件報告した。
  - ① NEACRP-A-1057

"Comparative Study of the Neutronic Performances of a Large LMFBR Using Oxide Fuel or Metallic Fuel." J. C. Garnier et al., CEA

- ◆ 本論文は、大型FBRに金属燃料を使用した場合の核特性に関する予備検討結果を 示している。
  - Burn-up Reactivity の大幅な低減は図れるものの,正のボイド反応度はMOXに比べ約2倍大きくなり、ドップラー反応度は約1/2になる。
- ② NEACRP-A-1058

"Sodium Voiding Reactivity Effect Reduction in Fast Breeder Reactors,"

J. Tommusi et al., CEA

- 本論文は、Naボイド係数低減のためのパラメータサーベイ結果について述べている。
- パラメータとしては、炉心構成(体積比、富化度、燃料タイプ(窒化物、金属、酸化物)等)、形状(H/D、体積)、炉心概念(均質、軸/径非均質、モジュール等)を選定した。
- Naボイド係数低減の有効な炉心概念としては、H型炉心(内側/外側高さ: 50/160cm,約4.3\$(ref.5.9\$)),軸方向ブランケット無し(1\$減少),径方向 非均質炉心(約2.7\$)がある。
- (3) NEACRP-1059

"Modular Island Cores." C. De Pascale et al., CEA

- 本論文は、Naボイド反応度低減のためのモジュラー炉心の検討結果について述べている。
- 150MWeのモジュラー炉心を7モジュラー炉心(1050MWe) にして、Naボイド反応度を1.3\$まで低減している。(基準は5\$~8\$)
- 問題点としては、Pu富化度が高くなる、燃焼反応度が大きくなる、各モジュラー

の出力制御が困難等があげられる。

### 4 NEACRP-A-1086

"A Measurement-Based Method for Predicting Margins and Uncertainties for Unprotected Accidents in the Integral Fast Reactor." R. Vilim, ANL

● IFRでのPassiveな炉停止機能を実証するために、EBR-Ⅱの動特性試験データを用いて、安全保護系不作動時の炉心応答を予測する手法を開発している。

### (5) NEACRP-A-1111

"Sensitivities to Nuclear Constants and Related Calculational Errors in Safety Characteristics of Fast Reacotrs with Different Coolants,"G.G.Kuliko et al.. USSR

- 本論文はkerr, Naボイド係数, ドップラー係数等に対する核データの感度係数を 求め, 核データの不確かさに起因する核特性精度を評価している。
- 重核の生成・吸収断面積の不確かさに起因する誤差が大きい。
- (6) NEACRP-A-1068

"Study on Enhanced Safety Core Characteristics of Nitride Fuel FBR,"
Y. Ohkubo et al., PNC

- 本論文は窒化物燃料炉心でのNaボイド反応度低減について検討したものである。
- 炉心が偏平になることによる炉心安定性について検討すべきであるとのコメントがあった。
- 4) 炉物理研究が重要な位置を占める新計画(セッション1.4) 論文A-1052(スイス)は、CW核破砕中性子源SINQの冷中性子源の設計について述べ ている。

論文A-1087(USA)では、ANLが計画している核融合材料試験用の高中性子束施設計画が紹介された。これは、FMITよりずっと費用を削減したものである。

5) 核データの不確かさに重点を置いた中性子遮蔽(セッション1.5)

論文A-1053(スイス)は、ITERの増殖ブランケットの核特性についてのBeの核データの誤差の影響を検討した。トリチウム増殖比及び超伝導コイルの損傷について、それぞれ7%及び27%の差異が出るとしている。

論文A-1060(フランス)は、NETのブランケット及び遮蔽パラメータの感度解析をまとめており、鉄の断面積の不確かさから超伝導コイルにおいて±25%の高速中性子及びDPAの差異を生ずるとし、核加熱についても同様とした。

論文A-1069(日本)は、単純形状でのBe及びPbの中性子増倍性能評価のための積分 実験を紹介している。

|論文A-1070(日本) は、DT炉のトロイダル線状源のシミュレーション実験について

述べている。

論文A-1071 (日本)は、Be円柱での積分実験から、JENDL-3の核データの妥当性を推論した。

論文A-1101(CEC) は、ANIT計画について紹介している。ここでは、中性子照射後の放射化物のインベントリーのほか、熱の発生、摂取のリスク、線量、ガンマ線スペクトルが計算される。

論文A-1113(ソ連)は,クルチャトフ研究所とモスクワの工学・物理研究所が共同で,OTR 計画の枠組みの中で進めているブランケット実験について記述しいてる。  $^{238}$ Uを中性子増倍材として,水を減速材としてい用い, $^6$ Li に中性子を吸収させる構成の体系を対象としている。中性子発生量は $5 \times 10^{10}$ n/sである。

このセッションでの議論では、核データ上の問題は、かなり解決されたのではないかという意見があった。

- 6) 高速炉の燃焼に起因する反応度の不確かさの評価(セッション2.1) 全部で3件の論文が提出され、その内日本から2件報告した。
  - ① NEACRP-A-1089

"Pin Power and Depletion of EBR-II", W. S. Yang et al., ANL

- 本論文は、FBR燃料の出力、燃焼度、原子数密度の燃料ピン単位の値を求める手法の開発と精度検証について書かれたものである。
- 本手法は、またIFRの燃料サイクル実証、EBR-Ⅱ実験解析、新しいFBR設計にも 適用できるようにすることも目的としている。
- REBUS-3/DIF3D Argonneコードシステムを用い、Hexagonal-Z体系で実行された ノード拡散燃焼計算から求めた出力密度、燃焼度、原子数密度、各群のFlux及び フルエンスについて、ノード内での分布を求めるコード(RCT)を開発した。
- RCTコードによる原子数密度の空間分布は、各群のFluxと同じように高次多項 式展開を基に求める。(Fluxに対し6次、原子数密度に対して4次)
- ベンチマークテストは、2次元では450及び950MWtのLMRで、3次元では450MWt
   のLMRとEBR-Ⅱ炉心で実施した。

ポイントワイズ出力密度計算の最大誤差はドライバーで  $2 \sim 3\%$ , ブランケットで  $3 \sim 6\%$ であった。また,燃焼計算のベンチマークテストは, 3 サイクルについて 450MW to LMRで行った。

出力密度の最大誤差はBOCにおいて、ドライバーで1.5%、ブランケットで4%であった。

● EBR-Ⅱの燃焼計算をREBUSU/RCTコードシステムで実施した。 RCTコードは特定のS/As解析に対して用いられた。

- S/A X419, X420, X421の燃焼解析を REBUS/RCTコードで実施した。実測値と解析 値は良く一致した。G/E値は0.94~1.09の間で求まった。
- ② NEACRP-A-1072

"Prediction Accuracies of Safety Related Core Design Parameters for FBR." K. Shirakata et al.. PNC

- 本論文は大型炉の目標核計算精度と現状の精度を比較したものである。
- 測定誤差に対する質問があった。
- ③ NEACRP-A-1115

"Analysis of JOYO Burnup Characteristics," A. Hara et al., PNC

- 常陽での燃焼解析精度評価に関する論文であった。
- 今後の計画について質問があった。
- 7) 改良型ガス炉及び軽水炉の炉物理特性

日本からの論文A-1073は、HTTR炉心での中性子のチャンネルストリーミングについてVHTRC炉心でのパルス中性子実験から、Benoistの非等方拡散係数の使用が必要であることを結論とした。

同じく日本からの論文A-1074は、VHTRC及びSHEでの反応度温度係数の実験をHTTR設計コードで解析し、実験との比較からHTTRの炉心設計が十分な精度で実施されていることを示した。

ソ連の論文A-1050は、PWR とHCLWR の格子についてのベンチマークに対するSPEKTR コードの計算結果について発表したが、核データを含めて精密化が指摘された。

同じくソ連からの論文A-1109は、オブニンスクで実施しているウラン炉心でのHCLWR の実験計画について述べている。この実験では、温度が20℃から 240℃まで変化できる。

IAEAのNuernberg会議のまとめがあり、NEACRPへのコメントとして、

- 転換比についての不一致の減少
- 集合体単位及び全炉心でのBenchmarkの必要性
- 熱水力と結合した動特性解析手法開発

があげられる。

- 8) 原子炉及び加速器によるTRU消滅に関する炉物理・炉工学(セッション2.3) 全部で7件の論文が提出され、その内2件日本から報告した。
  - ① NEACRP-A-1090

"Hazard Quantification for LWR Spent Fuel," R. N. Hill, ANL

- 本論文は、LWR使用済燃料中の各種同位体の危険性を評価したものである。
- 危険性の解析は被曝によるガン発生線量(CD)に着目した。

- 同位体放射能は、典型的なLWRの燃料100万 t 当りとし0RIGENコードで1000万年まで計算した。
- 規格化は、燃料100万 t を作るに必要な天然 U によるCDで行った。
- FPは燃料取出直後は危険性の主な寄与を示すが、500年で1.0以下になる。
- TRUの危険性は長く続く。1.0になるまで100万年近くかかる。
- 最初の500年は<sup>241</sup>Am(半減期432年)が主で、10000年までは<sup>238</sup>Puと<sup>248</sup>Puが、それ以後は<sup>237</sup>Np(半減期200万年)が主な寄与となり100万年以上続く。

### ② NEACRP-A-1062

"Radiotoxicity of Wastes Impact of Plutonium Recycling", M. Darrouzed et al., CEA

- 本論文では、PWRでのPuリサイクル (Puサーマル) が放射性廃棄物の長期的な 放射能毒性低減に効果的かどうかを検討したものである。
- Puは放射線学的にはインパクトは大きい。放射能毒性の評価は、ICRP30ガイドラインで採用されている年間公衆摂取制限法を利用した。
- 100MWe級 PWRを対象とし、U0₂燃料(3.7%<sup>238</sup>U, 45GWd/t)とMOX燃料(7.6%Pu, 45GWd/t)で比較した。
- U0₂燃料においては、100万年後にはPuの寄与はなくなり<sup>238</sup>Uと同じ放射能毒性となる。
- MOX 燃料においては、新燃料より照射済燃料の方が、長期的な放射能毒性では 小さくなる。これは、Puリサイクルとした方が、Puをリサイクルしないで貯蔵す る場合より放射能毒性は小さいことになる。
- フランスにおけるPuリサイクル有無が長期的な放射能毒性に与える影響を調べた結果、Puリサイクルを行った方が廃棄物の放射能毒性低減に役立つことが分かった。

### ③ NEACRP-A-1054

"Reduction of the Long-Term Toxicity of Neptunium by Nuclear Spallation", H. U. Wenger, et al., Switzerland

- 本論文では、<sup>237</sup>Np の放射能毒性の低減のための高エネルギー粒子による反応 (スポレーション及び核分裂)の可能性について研究したものである。
- <sup>237</sup>Np を低減する加速器システムの可能性が確認された。
- <sup>237</sup>Np ターゲットに1GeVの陽子を入射させることにより、優れた消滅特性が得られることが明らかになった。
- このシステムでは(Fission/スポレーション反応)の比率が大きいことが必要である。また、このシステムでは<sup>235</sup>U, <sup>236</sup>Uのような不必要な長半減期核種も生

成する。

- このシステムで生成される長半減期の核種はスポレーション反応によるものが 主である。
- しかし、スポレーション反応による放射能毒性は、<sup>237</sup>Npと<sup>237</sup>Npの崩壊物質によるものより40~500倍小さい。
- 理論解析の精度は、高エネルギーにおける核分裂モデルに依存する。精度向上 のために、実験が必要である。
- 本システムは高エネルギー反応だけの利用ではエネルギーバランスはとれない。しかし、15MeV 以下の多数の中性子を多重ターゲットアセンブリにあて、核反応による熱を利用すればエネルギーバランスが確保される可能性もある。

### (4) NEACRP-A-1112(1)

示す。

"On Actinides Transmutation Possibility in Fast Reactor with Various Coolants", D. F. Tzurickov, et al., USSR

- 本論文ではアクチナイド専焼FBRの特性の研究に関するものである。
- BN-350クラスのFBRに対し、冷却材としてNa、鉛、水-蒸気混合を用いた場合の特性(消滅率、β・11、崩壊熱等)を解析している。
- TRUとしては、VVER-1000の使用済燃料(燃焼度: 40,000MWd/t,冷却3年)のNp, Am, Cmを対象とした。
- 計算結果をTable 1に示す。
  表の中でAACは消滅率(全fission に対して)、qvは崩壊熱、Lは冷却材密度係数[(dKerr/Kerr)/(dρ/ρ)], enr. は燃料中のTRU核種(Pu, Np, Am, Cm)の平均濃縮度を
- 消滅率の点からはNp, Am, Cmだけで燃料を作った場合の方が、Puも含めた場合より良い。しかし、Np, Am, Cmだけの場合は、 $\beta$  。 $\epsilon$  、 $\epsilon$  、 $\epsilon$  、 $\epsilon$  、 $\epsilon$  が小さく、崩壊熱も大きくなる。
- この対策としては、β<sub>\*ff</sub>を大きくする物質(例えば<sup>233</sup>U, <sup>235</sup>U, <sup>240</sup>Pu, <sup>241</sup>Pu,
   <sup>242</sup>Pu等)を入れることも考えられる。
- Cmについては崩壊熱を低減するために、燃料には添加しない方が良い。 又はある程度、崩壊するまで貯蔵しておくのが望ましい。

| Coolant          | WWER                | enr.  | α 9    | AAC   | Beff   | 1                  | qv    | L      | vari |
|------------------|---------------------|-------|--------|-------|--------|--------------------|-------|--------|------|
| COUTAIN          | fuel                | %     |        | %     | %      | 10 <sup>-7</sup> s | kw/kg |        | ant  |
|                  | pu<br>present       | 17. 7 | 0. 267 | 1. 7  | 0.345  | 3. 41              | 22. 7 | -0.004 | 1    |
| sodium           | Pu<br>extract<br>ed | 77.8  | 0. 154 | 72. 0 | 0.110  | 0. 49              | 118.5 | -0.052 | 2    |
| melted           | pu<br>present       | 17. 3 | 0. 253 | 1. 7  | 0, 334 | 3. 34              | 22. 7 | +0.004 | 3    |
| lead             | Pu<br>extract<br>ed | 78. 8 | 0. 150 | 71.6  | 0. 115 | 0.52               | 118.5 | -0.057 | 4    |
| Steam-           | pu<br>present       | 18. 7 | 0. 427 | 1. 6  | 0. 354 | 4. 94              | 22. 7 | +0.003 | 5    |
| water<br>mixture | Pu<br>extract<br>ed | 92. 5 | 0. 222 | 75. 4 | 0. 089 | 0.39               | 118.5 | -0.121 | 6    |

Table 1 Parameters of BN-350-type core with various coolants

### ⑤ NEACRP-A-1112 (2)

"Investigations for Designs Justification of Actinides", Bednyakov et al.. USSR

- ◆ 本論文では、LMFBRにおいてTRUを消滅する場合の核データの精度について評価したものである。
- BN-800タイプ原子炉に対してTRU添加量をパラメータ(25%, 50%, 75%, 100%) にしてK。rr計算における核データの不確かさについて解析した。その結果、以下の事が明らかになった。
  - TRU添加量が増えると不確かさは増大する。MOXでTRU を添加しない場合に比べて、TRUを100%添加した燃料では不確かさは2倍以上になる。
  - K<sub>• f</sub> 計算における不確かさは、臨界実験装置や動力炉での積分実験を基に評価及び補正すれば著しく低減できる可能性がある。
  - K<sub>e</sub>rr計算における不確かさは、50%以上TRUを添加した場合においては、<sup>237</sup>Np、 <sup>241</sup>Am, <sup>243</sup>Am, <sup>238</sup>Pu の核分裂及び非弾性散乱断面積の不確かさによるところが 大きい。
  - TRUを75%以上添加した場合のKerr 計算における不確かさは、主に237Np と

<sup>241</sup>Amの非弾性散乱断面積の不確かさに依存する。

- TRU添加FBR概念検討には以下の核データの評価、補正が必要である。
  - <sup>237</sup>Np, <sup>241</sup>Am, <sup>243</sup>Am, <sup>238</sup>PuのFP収率
  - これらの核種の遅発中性子データ
  - ドップラー自己遮蔽効果のデータ
- TRUの予備的な反応度実験解析より以下の事が分かった。
  - 反応度実験の解析において、adjoint fluxの共鳴と空間分布の無視が大きな 誤差を及ぼす。
  - FCAとBFS臨界実験装置の<sup>240</sup>Pu 反応度の実験結果に相違が見られる。
- 6 NEACRP-A-1075

"Study of TRU Transmutation Plant with Proton Accelerator," T. Nishida et al., JAERI

NEACRP-A-1076

"TRU Transmutation in an LMFBR,"M. Ishikawa et al., PNC この分野の各国の関心は非常に高いが、ドイツのクスター氏が指摘したように現実的な消滅処理についてもっと研究すべきであると思われる。

9) 軽水炉及び重水炉の3次元効果を考慮した安定性

論文A-1077(日本)は、BWR の領域振動についてのTOSDYN-2による解析を実施し、 Out of Phase振動の起るシナリオを確定した。もともと出力密度の高いチャンネルが 熱水力的に不安定に成りやすいが、中性子的結合により、Out of Phase振動が励起される。

論文A-1078 (日本)は、BWRの 3 次元・核熱結合解析から、Out of Phase振動は炉心外での流れの抵抗が大きい場合炉心流量の総量が変化せず、チャンネル流量の再配分が起こることになるので特定の領域に熱発生についての外乱を加えると核的結合の助けを得て発生する。これを抑制する効果は中性子の流れによる実効的なボイド係数の低減によるとした。また、炉心全体の同位相振動は、炉心外での流れの抵抗が小さい場合に起るという見通しを得た。

論文A-1107(スウェーデン)は、1989年に経験した出力振動に関係したRinghals 1 での炉雑音実験について、Decay-Ratioの監視が可能とした。

論文A-1098 (カナダ) は、CANDU の軸方向振動について述べ、LOCA時に一様にボイドが発生することが重要としている。 3 次元動特性に炉物理に寄与すべきという意見があった。

10) 燃料の非破壊計量に関する物理的方法

論文A-1063 (フランス) は、燃料集合体の発送前に燃焼度、冷却時間、実効増倍率

を測定する手法の開発に関するものである。

一方, 論文A-1079(日本)は,返還廃棄物の中の微量のアクチノイドの非破壊測定に関してのパッシブ及びアクティブの手法で,数nCi/gの感度に達したことを報告している。

### (2) ベンチマークとデータベース

NEACRPが現在組織しているベンチマーク問題としては以下のものがある。

- ① 遮蔽ベンチマークとデータベース
- ② 臨界安全
- ③ 輸送容器の遮蔽
- ④ 炉雜音解析
- ⑤ 高転換軽水炉
- ⑥ トリチウム生成率測定
- ⑦ 3次元輸送計算ベンチマーク
- ⑧ 遅発中性子データの検証
- ⑨ 大型高速炉のC/E値の径方向依存性 以下にベンチマークの現状を今後の計画について示す。

### ① 遮蔽ベンチマーク

1988年のボンマスでの遮蔽国際会議に於てなされたデータベース構築の提案が進展している。

論文A-1093では、今後の進め方についてまとめている。問題は、今後誰がこのプロジェクトを進めていくかであり、ORNLのIngersoll が候補になっている。個別の問題に入ると、共鳴自己遮蔽効果の評価は課題としては解決済みのようにみえる。次にブタペストでの別の提案では、最適なバイアススキームの決定と非専門家の利用が問題とされている。遮蔽ベンチマークのリーダーが要請されている。

### ② 臨界安全

燃焼による核分裂性物質の減少及びFPの増大を臨界安全評価に組入れる努力が、燃料の濃縮度の増大とともに課題となっている。3次元、軸方向に燃焼度の異なる場合の計算が重要であり、体系の構成の複雑さと自己遮蔽効果をうまく取扱えるようにする必要があるとした。次回に計画をWorking Groupがまとめてくることとなった。

### ③ 輸送容器の遮蔽

論文A-1107は、TN-12実験ベンチマークについての会合について報告している。実験・計算の不一致が大きいが、測定器の特性も不確定である。

1991年、春に会合をもち、不一致を縮めようとしている。中性子ドジメータの応答関数が問題であり、実験的な対応が必要とする日本の提案が受入れられている。

### ④ 炉雑音解析

1989年のベンチマーク試験は、SMORN-V のフォローアップで、ARモデル化及び異常検 出の改良を求めるものであった。15グループのうち 8 グループが回答を出し、1990年の 6 月に会合をもって議論をした。IRIで回答を解析中であり、SMORV-VIで報告の予定であ る。

### ⑤ 高転換軽水炉

Bernnatがまとめた第2フェーズのBenchmarkは、NEACRP-L-321で公表される。実験データの提供があれば、第3フェーズも可能であると考えられるが、かなり困難な見通しである。今一番欲しいのは、温度係数に関するものであるという意見もあった。Benchmarkは一年間休んで、実験上もしくは計算上新事実が現れたら再開することとなった。

### ⑥ トリチウム生成率測定

論文A-1080(日本)は,トリチウム生成率測定国際比較について,現状報告を行った。 8 機関が参加しているが,第1回の照射については5%という目標をはかるに超える差異があった。原因探求のため,ANLからの供給された標準トリチウム水の分析を各機関に依頼したが,不一致は約3%にとどまり,不一致の主たる原因は,サンプルからトリチウムを抽出してトリチウム水を作る過程にあることがはっきりした。この過程についての改善を行った後,第2回の照射をする提案を行い,了承された。照射は,1991年4~5月の予定である。

### ⑦ 3次元輸送ベンチマーク

論文A-1081 (日本) は、 $K_{eff}$ を中心とする 3 次元ベンチマークの中間報告を行った。 3 ケのXYZ形状と 1 ケのhexagonal-Z形状の問題に対して、19機関からの参加があった。 小型のLWRについては、-致は良い。( $\Delta K_{eff}\sim 0.5\%$ )。

小型のFBRについては、制御棒効果の不一致がSnとモンテカルロ間にあり、大型のFBRになると、さらにこの不一致は拡大される。1990年10月22日と23日に専門家会議をもつ。

### ⑧ 遅発中性子データ

論文A-1041は,遅発中性子データの現状についてまとめたものであり,論文A-1064は,MASURCAでの実験ベンチマーク準備について述べ,イタリア(ENEA),日本(JAERI)及びソ連(Obninsk)その他の参加が予定されている。実験は,1992年年頭からの予定である。

### ⑨ FBRの炉物理量のC/E値の径方向依存

Benchmarkの案が、CEA, ANLから発表された。問題が1990年12月に各国へ配布され、検討された後、次回のNEACRPで成案を得ることになった。日本も参加の意志を表示した。また、JENDL-3 の使用が有効であることも付加えておいた。

### ⑩ 集合体内部での燃料ピン出力分布

EdfのWestから提案説明があった。議論の結果, Benchmark のリーダーはKWUのWagner と相談することとした。粗案は, 各参加予定者に配布されたコメントを受け, Westのもとに集められて, 次回正式提案する。日本からの参加の意志表示を行った。

また、新たに次のベンチマークが提案され、各国が賛成したため詳細データが次回提出されることとなった。

- ⑩ 集合体内ピン出力分布(フランスEdfより提案)
- ① 3次元動特性解析(イタリアより提案)

3次元動特性解析は過渡事象を対象とし当面は軽水炉で行い、次のステップでFBR へ対象を広げていくこととなった。

### (3) 各国の炉物理研究活動

オーストラリア、ベルギー、カナダ、デンマーク、フィンランド、フランス、ドイツ、イタリア、日本、オランダ、スウェーデン、スイス、イギリス、アメリカ、IAEAオブザーバー (ソ連)、CECの炉物理活動及び国家プログラムの状況について各国委員より説明があった。

ヨーロッパ全体として原子力開発に関する状況は予算上もPA上も厳しく、特に新型炉開発に関しては厳しい状況にあることが認識された。

以下に主要な国の活動状況を示す。

### ① 米 国

米国において炉開発の最高の優先度がおかれているのは、軽水炉産業の再活性化であり、そのため、新しいLWRの建設についての技術、許可取得及び制度上の負担の軽減に努力している。開発努力は、単純化、制度の高度化及び受動的安全性の採用である。中型炉(600MWe)の設計が進行している。また、モジュラー型HTGRとALMRの開発が続けられていて、前者は熱電併給炉で、後者はウラン資源の節約、燃料サイクルコストの低減が特長である。炉物理は、これらの開発を支援するのが主眼とされている。

炉心設計研究では、高速炉のボイド係数の低減化であるが、燃焼に伴う反応度swing がトレードオフとして問題である。また、金属燃料についての消滅処理も検討された。また、窒化物燃料が良い安全特性を与えることも推察されている。

臨界実験では、ZPPRでIFRの支援実験が実施された。MCNPの計算については、delayed  $\gamma$  線を取り入れたことと、FFTFでのRIの生産の効率向上に利用された。

手法の開発については、新しいノード法とSn法による輸送計算手法がコード化された。実際的な不規則問題への適用も可能のように見える。3次元のノード法による動特性解析コードが開発中である。また、3次元の熱水力コードも手がつけられた。

遮蔽については、日米協力によるLMRの軸方向遮蔽設計に対する実験及び解析が実施

されている。また、モジュラーHTGRについての制御棒孔からの中性子ストリーミングが 重要視され、実験が計画されている。SP-100の地上工学試験施設の計算が始まってい る。

ANS計画では、炉心の最適化が継続された。核データについては、ENDF/B-IVの中でも中性子、光子及び熱中性子散乱則の部分が公表された。

### ② スイス

1990年の9月に国民投票があり、全核エネルギーを段階的に廃止する提案は僅かの差で否決されたが、新しい計画をここ10年凍結する提案は採決された。現在全発電量の40%を賄っている5基の原子力発電所の運転に直接影響はないものの政府予算は非核部門に流れる傾向が強まっている。PSI研究所の核工学部門の主たる努力は既存炉の安全な運転に役立つことと、高レベル廃棄物の処分への寄与である。小型の地域暖房用原子炉の開発の如き炉開発は正当化しにくい状況にある。

炉物理の部門では、PROTEUS での低濃縮ウランを用いたペブル型高温ガス炉の研究に 集中する計画である。1985年から実施してきた HCLWRの第2期実験は、1990年末に終了 する。

ペブル炉の実験は、中小型炉の設計と安全審査に係わる不確定さを減少させようというもので、特に水侵入反応度効果、制御棒価値及び反応度と出力分布へのボロンとハフニウムの効果が中心になる。この実験はIAEAのCRP"Validation of Safety-Related Reactor Physics Calculations for Low Enriched HTGRs"として採択され、ソ連、スイス、ドイツ、日本、中国、USAが参加する。臨界実験は、1991年の夏から開始される。

以上のほか、LWRの過渡解析、SINQの増力計画、TRUの消滅の基礎研究として、核破砕 生成物の計算と実験がある。

### ③ スウェーデン

全ての原子力発電所の停止を2010年までに行うとした国民投票が見直されそうである。この2年間で公衆の意見は原子力発電を認める方向に動きつつある。ことしの9月に社会党の大会は、同党によって構成されている政府に対してエネルギー政策の変更を他党と交渉することを要請した。1995年及び1996年に2基の炉を停止するという提案は、議会はCO2の放出を1988年レベルに押えるという一年前に定めた事由を実行する上で実際上難しくなっている。

炉物理研究の面では、プルトニウムの生産とリサイクル、それから KRITZ実験データ の公開がある。

### ④ ドイツ

670MWe BWR型のWurgassen が停止された。これは、弁の閉じるのが遅いことによる。

THTR-300とSNR-300の状況は不変であり、停止している。

カールスルーエ研究所については、<sup>241</sup>Puの断面積評価、ウランとMOX燃料のderay heat 計算コード開発、Puリサイクルに関する研究、核融合炉ブランケット実験解析のための ANTRA 2(2次元輸送) コードの開発及び核廃棄物の長期リスクの低減等の活動がある。

SIEMENS/KWUについては、BWRシミュレータ用の核・水力計算コードの開発、安全因子の評価がある。

IKEについては、BWR・自立対流炉の安定性の解析がある。

### ⑤ フランス

1989年末の国民議会でこれまでの原子力エネルギー政策が再承認された。エネルギー源外国依存からの独立と環境汚染との斗いが重要という認識がある。また、MELOX プラント(120ton/年のMOX燃料生産)建設が決定された。現在、90万kWと130万kWのPWRがそれぞれ34及び14基稼働している。さらに、130万kW3基が1990年中に運転に入り、5基が建設中である。140万kWのCivauxの発注も1992年には実施されよう。一方、高速炉は、LWRに比較して運転実績が不満足である。PHENIXはアルゴンの泡の炉心通過と考えられるスクラムが1990年の9月にあり、炉は停止されている。SUPER-PHENIXは、炉のアルゴンへの空気の混入により1990年6月に停止されている。再処理に関しては、UP3プラント(800トンU/年)が始動している。

CEA の組織変更があった。開発研究部門は原子炉工学,ウラン濃縮,再処理及び技術拡散に分れた。また、基礎研究部門は生物科学,物質科学に分離された。安全研究部門は現在議論中である。

炉物理研究については、昨年の継続であり、特に新しい問題の提起はない。運転中の 炉の改善と燃焼度の増加が目標になっている。EFRとREP2000に努力が注がれた。

データと手法の開発については、SUPER-PHENIXの起動実験に基づいた設計上の不確か さの評価、ECCO及びERANOSの開発が進んでいる。

遮蔽研究については、ヨーロッパ共通の JANUS計画が進行している。鉄・Na系の解析が終了した。

核融合の炉物理については、NETの感度解析がある。

### ⑥ ソ 連

炉物理研究は、現用炉及び新型炉の概念研究に主眼がある。新型炉としては、VVER (PWR)モジュールHTGR, VTRS(溶解塩炉), LMR, 蒸気冷却高速共鳴中性子スペクトル(SWPR)及びTRU消滅炉がある。

炉物理研究の主たる方向としてあげているのは,

- (1) 炉の安全特性のシミュレーションに対する最近の要請に答えるためのコード開発 と検証
- (2) 受動的な安全特性を保証するための新型炉の安全性に係わる炉物理
- (3) 次世代発電炉の設計研究
- (4) 苛酷事故に対する既存炉の耐性の改善

### としている。

高速炉物理に関しては、理論的な領域については、Naボイド効果の低減、TRU 消滅への高速炉の利用、新型燃料高速炉、小型炉心、核データ BNABファイル、Thの利用、BN-350、BN-600の炉心解析がある。また、転換比が1でボイド反応度が0になる大型FBRの検討もしている。

実験研究の領域については、BR-10 でのRIの生産、BR-1臨界実験装置での炉物理計測機器試験、BFS-1臨界実験装置でのHCLWR炉心実験、BFS-2での径方向非均質実験、KOBRA 臨界実験装置での核データ実験及びKBR-18炉心でのTh実験がある。

これから始めようとする新型炉の炉物理研究に二つがある。いずれもHTGRの球状燃料を用いるものであるが、一つは超臨界軽水を、もう一つは溶融塩を冷却材として用いることになっている。

### (4) NEACRPに関係する他機関の活動

NEANDC, NEA Data Bank, CSNI(原子炉装置の安全性に関する委員会), NDC(原子力開発委員会), IAEAの活動について説明があった。

NEANDC及びNEA Data Bank とは核データ精度への要求,必要な核種の評価等でNEACRPは密接な関係にある。NEA の経費削減からNEANDCとNEACRPの統合が事務局長より諮問されている。これについては運営セッションで論議された。

CSNIの活動の中に過渡・事故解析用コードの開発と評価があるが、NEACRPと重複するところであり今後調整が必要であるとの指摘があった。(特に3次元動特性解析コードの開発)

NDCとはNDCが推進しているOMEGA計画と密接な関係があり、今後仕事の分担について討議していくこととなった。

### 2.2.3 運営セッションでの討議

本セッションでは今回は特にNEACRPの位置付けと長期計画が討議された。これは NEAの経費削減からくる各委員会の統合要求に基づいている。討議の結果,以下の内容のステートメントがNEA事務局長に出されることとなった。

- NEACRPは科学的かつ技術的委員会である。
- NEACRPは参加各国の炉物理プログラムの連携,ノウハウのプール,情報の交換によって成り立っている。
- NEACRPの活動は、炉心核特性解析、炉心設計、コード及び手法の開発、遮蔽や臨界安全解析、燃料サイクル解析、核融合のブランケットや遮蔽解析、原子炉制御やサーベイランス、安全性の炉物理的評価、革新的原子力システムの炉物理的評価、研究及び実験炉、中性子及び炉物理研究に対して重要な新しい装置(原子炉又は原子炉以外)等が含まれる。
- 本委員会活動で最近注目しているものとしては、革新的原子炉概念の炉物理評価、原子炉状態のオンラインモニタリング、3次元動特性解析のためのコード開発等がある。 炉物理分野において、本委員会はその専門性とスコープにおいて特出している。
- NEACRP参加各国は、炉物理分野で最近の開発及び優先順位等のすべての状況を把握する機構をそなえたNEACRPを支持している。
- 加えて、NEACRPは参加各国の限られた成果を集め、最も効率良く利用できるようにする協力プログラムをプロモートしている。
- NEACRPとCSNIの活動の間には、両委員会が適切に協力できる広範囲の関連する分野がある。
- NEA事務局は同じ様な分野の仕事の種分けすることに協力すべきである。多くの場合、 炉物理は、安全解析や基準決定の基礎となる物理的な情報を与えている。
- NEACRPとNEANDCの統合については役割と仕事の内容が異なるため統合することには反対する。

### 2.2.4 次回の予定

次回第34回NEACRP会合は1991年10月7日から11日の間,スイスのPSIで行われることとなった。表2に次回のトピックスを示す。

### 2.3 所 感

今回の会合は、NEAがおかれている厳しい状況(経費削減等)の中、NEACRPとしての位置付けの明確化、長期計画策定が要求された会合であった。NEACRPの活動は炉物理分野に限られ

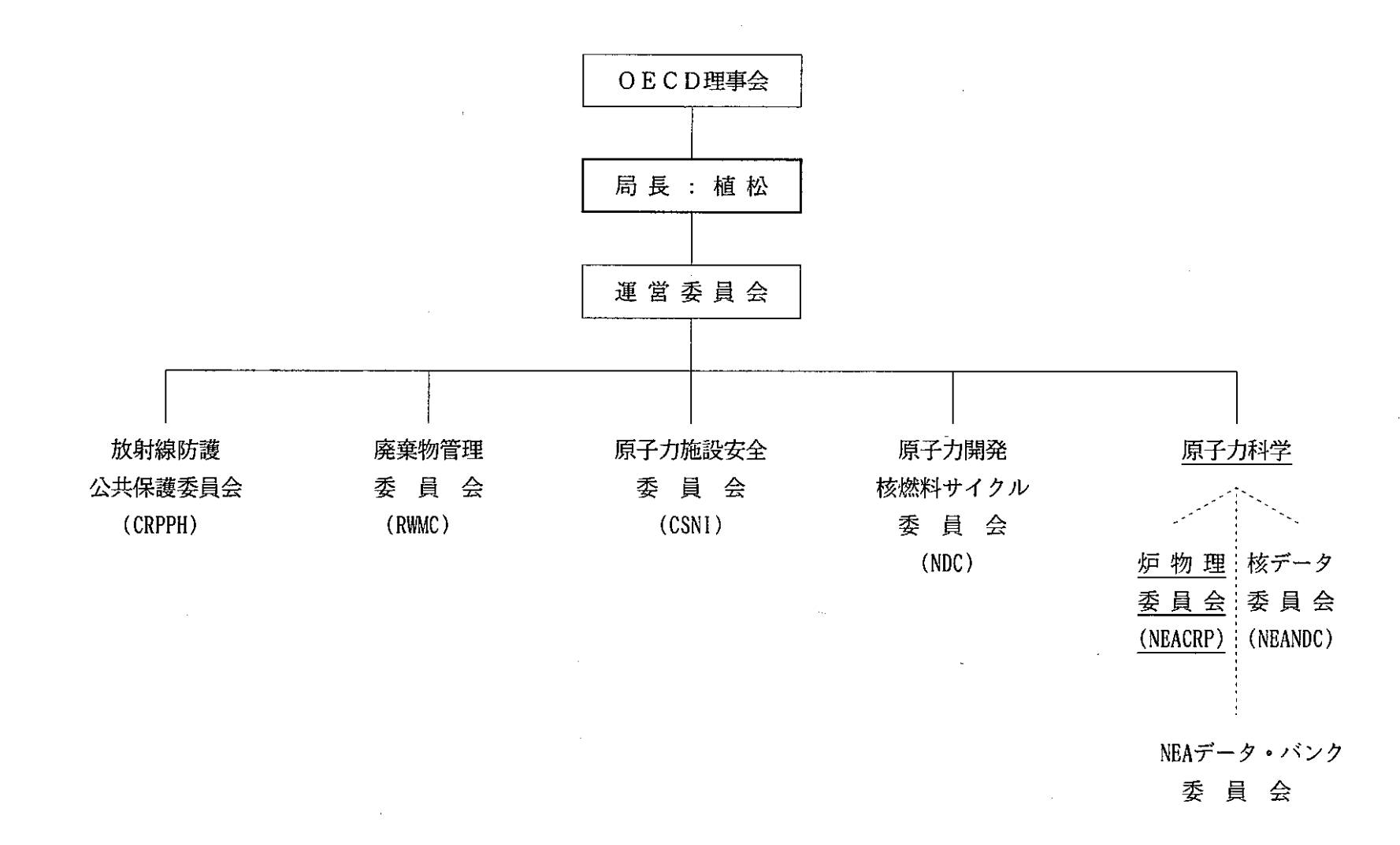
ているが、この分野は原子力の他の分野(安全性、廃棄物等)への基礎的、基盤的な技術データベースの提供と炉物理面での革新的アイディアの創出という役割を持っている。このため、NEACRPの活動の重要性は益々高まってくると思われる。現在、炉物理のすべての分野にわたって1国が実施することは予算、人的な面出難しくなってきており、その点でNEACRPのような国際協力の場で情報交換と共同作業(ベンチマークも含む)を行うことは資源の有効利用の点からも必要である。NEACRPのリーダーシップを取っているのは米国、フランス、ドイツ及び日本であり、特に日本への期待は高まっている。今回の会議の場で、たびたび日本の意見、賛否を求められることがあり、これからの日本のリーダーシップの発揮が重要になると思われる。

表 1 第33回NEACRP会合のトピックスと発表論文件数

| セッション | トピックス                   | 論文数 | 日本の論文数    |
|-------|-------------------------|-----|-----------|
|       |                         |     | (PNCの論文数) |
| 1. 1  | 軽水炉によるPuリサイクルの当面の課題     | 7   | 2(1)      |
| 1. 2  | 中性子(炉物理)計算コードを検証する方法に対  | 7   |           |
|       | する要求                    |     |           |
| 1. 3  | 高速炉の安全性に係わる炉物理特性        | 6   | 1(1)      |
| 1. 4  | 中性子工学及び炉物理研究に関する新装置     | 2   |           |
| 1. 5  | 核融合ブランケット-核データの不確かさに重点  | 9   | 3         |
|       | を置いた中性子遮蔽               |     |           |
| 2. 1  | 高速炉の燃焼に起因する反応度の不確かさの評価  | 3   | 2 (2)     |
| 2. 2  | 改良型ガス炉及び軽水炉の炉物理特性       | 6   | 2         |
| 2. 3  | 原子炉及び加速器によるTRU 消滅に関する炉物 | 7   | 2(1)      |
|       | 理•炉工学                   |     |           |
| 2. 4  | 軽水炉及び重水炉の3次元効果を考慮した安    | 5   | 2         |
| 2. 5  | 定性燃料の非破壊計量に関する炉物理手法     | 2   | . 1       |
|       |                         |     |           |
|       |                         | 54  | 15(5)     |

### 表 2 第34回NEACRP会合のトピックスの予定

|         | トピックス                                                                 | ,    |
|---------|-----------------------------------------------------------------------|------|
| 1.      | . 放射線輸送コードの利用に関する新しい計算機構成のインパクト(ベクトル及はパラレル計算機,新型ワークステーション,トランスピューター等) | なび,又 |
| 2.      | . 中性子ラジオグラフィーの新しい応用                                                   |      |
| 3.      | . 軽水炉におけるPuリサイクル                                                      |      |
| 4.      | . 中性子(炉物理)計算コードを検証する方法に対する要求                                          |      |
| 5.      | . 高速及び他の新型炉の炉物理課題(反応度フィードバック特性,設計における<br>と経済性のトレードオフ)                 | 安全性  |
| 6.      | . 原子力分野における原子炉以外の新装置                                                  |      |
| 7.      | . 核融合ブランケットの遮蔽性能                                                      |      |
| 8.<br>- | . TRU消滅炉及び加速器性能の物理的及び安全性上の課題(NEACRPとして研究の存<br>ついてステートメントをまとめる予定)      | Eり方に |
| 9.      | . 3次元オンライン監視の物理的問題                                                    |      |
|         | 新 し い ベ ン チ マ ー ク                                                     |      |
| 1.      | . 軽水炉炉心の3次元動特性解析                                                      |      |
| 2.      | 集合体内の燃料ピン単位出力分布解析                                                     |      |



22

図1 OECD·NEA委員会組織図

# 3. 添付資料

### (1) 第33回NEACRP会合出席者リスト

Belgium Dr. Pierre D'HONDT

Dr. Heinz KUESTERS Germany

Centre d'Etude de

Inst. fuer Neutronenphysik

l'Energie Nucleaire

und Reaktortechnik

Dept. de Phys. des Reactors

Kernforschungsz. Karlsruhe

France

M. Michel DARROUZET

U.S.A Dr. Leo LESAGE

C. E. N. Cadarache

Applied Phys. Div.

Argonne National Laboratory

Dr. Eric FORT

C. E. N. Cadarache

Italy

Dr. Renato MARTINELLI

ENEA, CIRENE-PASI

Dr. Massimo SALVATORES

C. E. N. Cadarache

Dr. Herbert W. RIEF

Department A

Mr. Jean-Pierre WEST

Info. Analysis & Handling Div.

Dept. Physique des Reacteurs

Joint Research Centre

EDF/DER

Ispra Establishment

U.K.

Dr. M. J. HALSALL

U. S. S. R. Dr. Igor P. MATVEENKO

AEA Technology

FEI

Winfrith Technology Centre

Prof. Igor S. SLESAREV

Dr. Gerald INGRAM

Nuclear Reactor Department

AEA Technology

I. V. Kurchatov Institute

Winfrith Technology Centre

Canada

Dr. F. N. McDONNELL

Sweden

Mr. Klas JIRLOW

Studsvik Energiteknik

Atomic Energy of Canada Ltd.

Chalk River Nuclear Labs.

### PNC TN9600 90-013

Japan

Dr. Yoshihiko KANEKO

Dept. of Reactor Engineering

JAERI

Switzerland

Dr. Peter WYDLER

Paul Scherrer Institute

Dr. Toshio WAKABAYASHI

Technology Development Div.

PNC

I. A. E. A. Mr. Martin CRIJINS

Advanced Nuclear Power

Technology Section

Austria

### OECD/NEA Secretariat

Dr. Kunihiko UEMATSU, Director General

Mr. Jonny ROSEN, Deputy Director

Dr. Donald Mc PHERSON, Safety Division

Dr. Geoffrey STEVENS, Nuclear Development Division

Dr. Nigel TUBBS, OECD/NEA Data Bank

Dr. Cleas NORDBORG, OECD/NEA Data Bank

Dr. Enrico SARTORI, OECD/NEACRP Secretariat

# 添付資料(2) Agenda

Proposed Agenda for the 33rd NEACRP Meeting (Id Numbers of papers discussed at each topic are listed) (Papers in brackets have been distributed in advance of the meeting)

### 15. October (Monday)

10:30 am Introductory Remarks by the Director General, Dr. K. Wematsu

### PART A : EXECUTIVE SESSION

10:45 am

- 1.a Participants in the Meeting
- 1.b Committee Membership
- 2. Adoption of the Final Summary Record of the 32nd Heeting.
- 3. Adoption of the Agenda of the Heeting.
- 4. Completion of Actions Arising from Previous Meetings.

11.30 am

PART B: TECHNICAL SESSIONS

(Time assigned for Technical Papers: 10' + 2' for discussion)

- 1. New Topics
  - 1.1 Current Issues of Plutonium Recycling in LWRs 1047, 1048, 1049, 1055, 1066, 1067
  - 1.2 Review of Requirements for the Methods of Validating Neutronics Codes (i.e. Quality Assurance for Neutronics Codes) 1056, 1084, 1085, 1091, 1094, 1095, 1096
  - 1.3 Physics Related Safety Aspects of Fast Reactors. (Reactivity Feedback Properties, Design tradeoffs and Safety Implications) 1050, 1051, 1057, 1058, 1059, 1068, 1086, 1111
  - 1.4 New Facilities of Importance for Neutronics and Reactor Physics Research (Intense Neutron Sources, MAPLE, etc.) 1052, 1087, 1097
  - 1.5 Fusion Blanket Shield Neutronics with Emphasis on the Effects of Data Uncertainties (Including Effects of Double Differential Data) 1053, 1060, 1069, 1070, 1071, 1088, 1092, 1101, 1113
- Topics Carried over from Previous Meetings
  - 2.1 Evaluation of the Uncertainty in FBR Burn-up Reactivity Swing 1072, 1089
  - 2.2 The Reactor Physics of Advanced Gas-Cooled and Water Reactors. 1061, 1073, 1074, 1109
  - 2.3 Engineering and Physics Aspects of Transuranium Burning by Reactors and Accelerators. 1054, 1062, 1075, 1076, 1090, 1112
  - 2.4 Local Stability in LWRs and HWRs with Emphasis on 3D Effects. 1077, 1078, 1098, 1099, 1102
  - 2.5 Physics Methods in Fuel Accountability. 1063, 1079

### 17. October (Wednesday)

9:00 am

- 3. Benchmarks and Data Bases
  - 3.1 Radiation Shielding Benchmark Data Base. (1044), 1093
  - 3.2 Criticality of Fuel Undergoing Dissolution. (including irradiated fuel - burnup) 1114
  - 3.3 Shielding of Transport Casks. 1107
  - 3.4 Noise Analysis. 1046
  - 3.5 HCLWR Benchmarks. 1108, 1110
  - 3.6 Heasurement of Tritium Production Rates. 1080
  - 3.7 Three-Dimensional Transport Benchmark. 1081
  - 3.8 Validation of Delayed Neutron Data. 1041
  - 3.9 Radial C/E Trends in Large FBRs.
  - 3.10 Pin Power Distribution within Assemblies. 1065
- 4. International and National Programmes
  - 4.1 Activities of Other International Bodies of Interest to NEACRP.
    - NEANDC Topics of Interest to NEACRP
      - Progress Report from Evaluated Data File Projects
      - International Cooperation on Evaluated Data Files
    - NEA Data Bank,
    - NEA Committee on Safety of Nuclear Installations
    - NEA Nuclear Development Committee
    - IAEA
  - 4.2 Review of Recent Activities and National Programmes (Reports from: Australia, Belgium, Canada, Denmark, Finland, France, F.R. Germany, Italy, Japan, Netherlands, Spain, Sweden, Switzerland, United Kingdom, United States, IAEA Observers)
- 18. October (Thursday)

9:15 am

PART A : EXECUTIVE SESSION (Cont.)

- Trends for future work of NEACRP, (follow-up of the discussion held at the 32nd meeting)
- 19. October (Friday)

9:00 am

PART B : TECHNICAL SESSION (Cont.)

5. Keetings

------

- 5.1 Highlights of Recent Meetings of Interest to NEACRP.
- 5.2 Future Meetings of Interest to the NEACRP.

PART A : EXECUTIVE SESSION (Cont.)

- 6. Distribution and Discussion of Summaries by Session Rapporteurs Selection of Topics for Next Meeting
- 7. Arrangements for the 34th Meeting of the Committee.
- 8. Other Business.
- 9. Election of Committee Officers

# Proposed Agenda for the 33rd NEACRP Meeting (DETAILS)

### 15. October (Monday)

10:30 am Introductory Remarks by the Director General, Dr. K. Uenatsu

### PART A : EXECUTIVE SESSION

10:45 am

- 1.a Participants in the Meeting
- 1.b Committee Membership
- Adoption of the Final Summary Record of the 32nd Heeting. (NEACRP-A-964)
- Adoption of the Agenda of the Meeting.
- Completion of Actions Arising from Previous Meetings. (page 53 and 54 of MEACRP-1-964)

11.30 am PART B: TECHNICAL SESSIONS

(Time assigned for Technical Papers: 10' + 2' for discussion)

### 1. REW TOPICS

1.1 Current Issues of Plutonium Recycling in LWRs

### REACRP-A-1047

Yenus International Programme (VIP),

A Muclear Data Package for LWR Pu recycle

P. D'Hondt

### NEACRP-A-1048

Yenus International Programme (VIP),

A Buclear Data Package for BWR Pu recycle

P. D'Hondt

### NEACRP-1-1049

Yenus International Programme (VIP),

A Nuclear Data Package for PWR Pu recycle

P. D'Hondt

### NEACRP-A-1055

Plutonium Reload Experience and Perspective in French PWR Plants September 1990

M. Rome, M. Salvatores, J. Mondot, M. Le Bars

### ○ NEACRP-A-1066

Plutonium Generation Boiling Water Reactor Concept September 1990

Japan

### NEACRP-A-1067

Utilization of MOX Fuel Assembly Containing Gd203 in ATR September 1990
Japan

### NEACRP-A-1116

Investigations on Pu-Recycling and High Burnup for LARs in the Federal Republic of Germany

1.2 Review of Requirements for the Methods of Validating
-----Neutronics Codes (i.e. Quality Assurance for Neutronics Codes)

NEACRP-A-1056
Quality Assurance Provisions for EANOS
September 1990
J.M. Rieunier

NEACRP-A-1084
Quality Assurance for Neutronics Codes at ANL
September 1990
USA

WEACRP-A-1085
Requirements for Validating (LVR) Neutronics Codes
September 1990
USA

\*\*BELCRP-1-1091

A Review of Reactor Physics Uncertainties and Validation
Requirements for the Modular High-Temperature Gas-Cooled Reactor
May 1990

A.M. Baxter, R.K. Lane, E. Hettergott, W. Lefler

WEACRP-A-1094 Verification of the Shutdown System Software at the Darlington Nuclear Generating Station September 1990 G.W. Archivoff et al.

WEACRP-A-1095
The Canadian Process for Regulatory Approval of
Safety Critical Software in Suclear Power Reactors
September 1990
G.J.K. Asmis et al.

WEACRP-A-1096
Licencing Safety Critical Software
September 1990
G.H. Archivoff

1.3 Physics Related Safety Aspects of Fast Reactors.

(Reactivity Feedback Properties, Design tradeoffs and Safety Implications)

SEACR?-A-1050

Requirements to Calculational Methods of New Generation Reactors

I.S. Slesarev

YEACRP-A-1051
Experimental Investigations of Reactivity Effects for FBRs I.P. Katveenko

### NEACRP-A-1057

Comparative Studies of the Reutronic Performances of a Large LMFBR Using Oxide Fuel or Metallic Fuel.

September 1990

J.C. Garnier, A. Zaetta

### NEACRP-A-1058

Sodium-Voiding Reactivity Effect Reduction in Fast Breeder Reactors September 1990

J. Thomas, A. Zaetta

### NEACRP-A-1059

Modular Island Cores September 1990 C. De Pascale, I. Zaetta

### MEACRP-A-1068

Study of Enhanced Safety Core Characteristics of Mitride Fuel Core September 1990 Japan

### NEACRP-A-1086

Measurement Based Method for Predicting Margins—and Uncertainties for Unprotected Accident s in the IFR USA

### MEACRP-A-1111

Sensitivity of Nuclear Constants and Related Calculational Errors in Safety Characteristics of Fast Reactors September 1990 USSR

# 1.4 New Facilities of Importance for Neutronics and Reactor Physics Research (Intense Neutron Sources, MAPLE, etc.)

### YEACRP-1-1052

The Cold Neutron Moderator for the Continuous Spallation Neutron Source  ${\tt SINQ}$ 

F. Atchison, G. Bauer, W. Fischer, K. Skala, H. Spitzer

### NEACRP-1-1087

High Neutron Flux Fusion Materials Test Facility USA

### YEACRP-A-1097

The idvanced MAPLE Concept September 1990 R.F. Lilstone et al. 1.5 Fusion Blanket - Shield Neutronics with Emphasis on the Effects of Data Uncertainties (Including Effects of Double \_\_\_\_\_\_ Differential Data)

### NEACRP-A-1053

On the Effect of ENDF/B-VI Beryllium Data on the Neutronics of ITER Blankets S. Pelloni, M.J. Embrechts, E.T Cheng

### NEACRP-A-1060

Sensitivities Analysis of the T.F. Coil Shielding Parameters in the NET Design to the Nuclear Data Uncertainties September 1990 A. Santamarina, H. Smith

O WEACRP-A-1069

Integral Experiments to Improve Tritium Breeding Ratio September 1990 Japan

D WEACRP-1-1070

Phase-IIIA Experiment of the JAERI/USDOE Collaborative Program on Fusion Neutronics September 1990 Japan

NEACRP-A-1071

Benchmark Test of Be Nuclear Data in JENDL-3 Trough Analyses of Time of Flight and Integral Experiments on Be Assemblies at FMS September 1990 Japan

### MEACRP-1-1088

Note on Effects of Data Uncertainties on Shield Meutronics September 1990 USA

### WEACRP-A-1092

Reaction Rate Distributions and Related Data in the FNS Phase II Experiments July 1990 R.T. Santoro, R.G. Alsmiller, J.M. Barnes (ORNL)

### MEACRP-A-1101

ANITA - Analysis of Neutron Induced Transmutation and Activation April 1990 C. Ponti, S. Stramaccia, (JRC Ispra)

### NEACRP-A-1113

Fusion Blanket Benchmark Experiments September 1990 USSP.

۵

## 2. TOPICS CARRIED OVER FROM PREVIOUS MEETINGS

### 2:1 Evaluation of the Uncertainty in FBR Burn-up Reactivity Swing

NEACRP-A-1072

Prediction Accuracies of Safety Related Core Design Parameters for FBR September 1990 Japan

NEACRP-A-1089

Pin Power and Depletion in EBR-II

September 1990

USA

2.2 The Reactor Physics of Advanced Gas-Cooled and Water Reactors.

WEACRP-1-1061
Reactor Physics Studies at CEA on Advanced Water Reactors
September 1990
A. Leridon et al.

O MELCRP-1-1073

Heasurement of Void Reactivity Worth of HTTR Mockup
Control Rod Hole in VHTRC-1 Core
September 1990
Japan

O MEACRP-A-1074
Analysis of Temperature Effect of Reactivity for VHTRC and SHE with Muclear Design Code System for High Temperature Engineering Test Reactor (HTTR)
September 1990
Japan

NEACRP-A-1109
Calculation of Neutron Physical Parameters of the Advanced LWR
Fuel Lattices
September 1990
USSR

2./
NEACRP-A-1115
Analysis of JOYO Burnup Characteristics
Japan

2.3 Engineering and Physics Aspects of Transuranium Burning by
-----Reactors and Accelerators.

### NEACRP-A-1054

Reduction of the Long -term Toxicity of Meptunium by Muclear Spallation H.U. Wenger, P. Wydler, S. Atchison

### NEACRP-A-1062

Radiotoxicity of Wastes Impact of Plutonium Recycling September 1990 M. Darrouzet, G. Flamenbaum, J.P. Grouiller

### O NEACRP-A-1075

Study of TRU Transmutation Plant with Proton Accelerator September 1990 Japan

### MEACRP-1-1076

TRU Transmutation in LMFBR(II) September 1990 Japan

### MEACRP-4-1090

Eazard Quantification for LWR Spent Fuel September 1990 USA

### **WEACRP-A-1112**

On the Actinide Transmutation Possibility in Fast Reactors September 1990 USSR

- 2.4 Local Stability in LWRs and HWRs with Emphasis on 3D Effects.
- O WELCRP-A-1077
  A Study of Regional Oscillation with TOSDYN-2
  September 1990
  Japan
- O WEACRP-A-1078

  Examination of Nuclear Thermal Hydraulic Oscillation Modes in BWR Core.

September 1990 Japan

### NEACRP-A-1098

Neutronic Decoupling and Coolant Void Reactivity in CANDU September 1990 V.K. Mohindra, A.R. Dastur

### REACRP-A-1099

SMOKIN - A Code for Time-dependent Tree-Dimensional Neutronics Calculations in CANDU-PHW Reactors Based on Nodal Kinetics Theory - Application to Loss of Coolant Accidents September 1990 M. Gold, J.C. Luxat

### NEACRP-A-1102

BWR Stability Investigation in Ringhals 1 Studsvik (1990) Bengt-Goeran Bergdahl, Ritsuo Oguma

2.5 Physics Methods in Fuel Accountability.

### NEACRP-A-1063

Active and Passive non Destructive Measurements for Muclear Monitoring of Spent Assemblies
. September 1990
G. Bignan, L. Martin Deidier

### O WEACRP-1-1079

Development of Mon-Destructive Measuring Techniques for Trace Amount of Fissile and Fertile Materials in Drum-Sized Waste. September 1990 Japan

## 17. October (Wednesday)

9:00 am

## 3. BENCHMARKS AND DATA BASES

3.1 Radiation Shielding Benchmark Data Base.

NEACRP-A-1044 (already distributed)

The Establishment of a Shielding Experimental Benchmark at the OECD/NEA Data Bank

June 1990

A.K. McCRACKEN

NEACRP-A-1093

Considerations for a Shielding Experimental Benchmark Data Base
October 1990
W.W. Engle and D.T. Ingersoll (ORKL)

3.2 Criticality of Fuel Undergoing Dissolution.

(including irradiated fuel - burnup)

MEACRP-A-1114
Activity Report of the Criticality Working Group
October 1990
G.E. Whitesides, E. Sartori

3.3 Shielding of Transport Casks.

HEACRP-A-1107

Status Report on the Shielding of Transport Casks Benchmark
October 1990

A. Avery

3.4 Noise Analysis.

NEACRP-1-1046
Status of the 1989 Noise Analysis Benchmark Test
September 1990.
Eduard Hoogenboom

### 3.5 ECLVR Benchmarks.

### NEACRP-A-1108

Status Report of the WEICRP HCLWR Benchmark Working Group October 1990

W. Bernnat, E. Sartori

#### NEACRP-A-1110

Set of Interrelated Benchmarks Test for Investigation of LWR with Resonance Neutron Spectrum September 1990 USSR

3.6 Keasurement of Tritium Production Rates.

### O MEACRP-A-1080

International Comparison on Measuring Techniques of Tritium Production Rate for Fusion Neutronics Experiments.

September 1990

Japan

- 3.7 Three-Dimensional Transport Benchmark.
- O MELCRP-1-1081
  Summary Report of 3-D Meutron Benchmark Problems
  September 1990
  Japan

3.8 Validation of Delayed Neutron Data.

### NEACRP-1-1064

NEICRP Beta-effective Benchmark Measurements at MISURCI. Proposal of the Experimental Programme. September 1990 M. Martini, J.C. Gauthier, G. Granget, R. Soule

MEACRP-1-1041

Status of Delayed Neutron Data, 1990
October 1990
J. Blachot, M.C. Brady, A. Filip, R.W. Mills, D.R. Weaver
Draft - circulated to NEACRP members
To be published as NEICRP-L-323, NEANDC-2990

3.9 Radial C/E Trends in Large FBRs.

3.7

NEACRP-A-1117
Benchmark 3-D Neutron Transport Calculations
USSR

NEACRP-A-1118
3-D Neutron Transport Benchmark Problems
USSR

3.10 Pin Power Distribution within Assemblies.

### NEACRP-A-1065

Benchmark Calculation of Power Distribution Within an Assembly Using Standard or Hodal Diffusion Schemes September 1990

J.C. Lefebvre, J. Mondot, J.P. West et al.

- 4. INTERNATIONAL AND NATIONAL PROGRAMMES
  - 4.1 Activities of Other International Bodies of Interest to MEACRP.
    - REANDC Topics of Interest to NEACRP

NEACRP-A-1100

Twenty-eigth WELNDC Meeting: Report on Matters of Interest to WELCRP October 1990 E. Fort

### NEACRP-A-1104

Summary Record of the Twenty-eigth WEARDC Meeting Harvell, 26-30 March 1990, (Technical Minutes) Herbert Yonach, IRK

- Progress Report from Evaluated Data File Projects

WEACRP-A-1043 (already distributed)
Summary Record of the Twelfth Meeting of the Scientific Coordination
Group (SCG) of the Joint Evaluated File Project
OECD, 1st June 1990
WEA Data Bank Secretariat

- International Cooperation on Evaluated Data Files

NEACRP-A-1042 (already distributed)

Summary record of the Second meeting of the

Working Group on International Evaluation Cooperation

Marseille, 30th April - 1st May 1990

NEA Data Bank Secretariat

- NEW Data Bank,

NEACRP-A-1106

Activity Report of the OECD/NEA Data Bank for the NEACRP Meeting October 1990 NEA Data Bank Secretariat - WEA Committee on Safety of Muclear Installations

### NEACRP-A-1082

Viewgraphs on the Activities of the Committee on the Safety of Nuclear Installations (CSNI) September 1990 CSNI Secretariat

- WEA Nuclear Development Committee

### NEACRP-1-1083

Summary of Activities of the Nuclear Development Committee (NDC) September 1990 HDC Secretariat

- IYEY

NEACRP-A-1105

Overview of the IAEA Reactor Physics Activities 1989/1990 October 1990 M. Crijns, IAEA

4.2 Review of Recent Activities and Mational Programmes

### NEACRP-L-322

(Reports from: Australia, Belgium, Canada, Denmark, Finland, France, F.R. Germany, Italy, Japan, Metherlands, Spain, Sweden, Switzerland, United Kingdom, United States, IAEA Observers)

18. October (Thursday)

9:15 am PART A : EXECUTIVE SESSION (Cont.)

 TRENDS FOR FUTURE WORK OF MELCRP, (follow-up of the discussion held at the 32nd meeting) 19. October (Friday)

9:00 am

PART B : TECHNICAL SESSION (Cont.)

5. Meetings

-----

5.1 Highlights of Recent Heetings of Interest to NEACRP.

NEACRP-A-1103

PHYSOR'90: Conference Summary

May 1990

J. Rowlands

5.2 Future Meetings of Interest to the NEACRP.

PART A : EXECUTIVE SESSION (Cont.)

- 6. Distribution and Discussion of Summaries by Session Rapporteurs Selection of Topics for Next Meeting
- 7. Arrangements for the 34th Meeting of the Committee.
- 8. Other Business.
- 9. Election of Committee Officers

添付資料(3) 各セッションの論文集の抜粋

NEACRP-A-1047

VENUS International Programme (VIP)

A Nuclear Data Package for LWR Pu Recycle

Charlier A., Basselier J. BELGONUCLEAIRE, Brussels

Leenders L. SCK/CEN, MOL, Belgium

VENUS International Programme (VIP)
A Nuclear Data Package for LWR Pu Recycle

A. Charlier\*, J. Basselier\*, L. Leenders\*\*

\*BELGONUCLEAIRE, 1050 Brussels, Belgium
\*\*CEN/SCK, 2400 Mol, Belgium

### ABSTRACT

Large-scale MOX irradiation campaigns are now considered in various industrial countries. Consequently, there is a need to develop, to improve and to validate nuclear computer codes.

The objective of the VIP programme is to constitute a complete set of experimental measurements performed with UO2 and MOX fuel rods in order to provide an extensive nuclear data base for the development and the validation of nuclear calculation methods for MOX fuels used in LWRs. A VIP programme will be devoted to Pu recycle in PWRs and another one in BWRs. The VIP programme is starting now.

### INTRODUCTION

Since about 25 years, BELGONUCLEAIRE has been collaborating with the Belgian National Nuclear Centre (CEN/SCK) and has been proceeding with R and D work to understand and predict the behaviour of the fuel in light water reactors. In particular, the VENUS zero-power facility located at the CEN/SCK at Mol has been used to support this kind of investigation.

The operating data obtained from the power reactors, the continuing increase of the fuel performance, the new fuel characteristics, the decision recently taken by major Utilities in various countries to recycle in their power plants the plutonium obtained from reprocessing and the necessity to demonstrate to the Licensing Authority that the differences in the neutronic, safety and thermal-hydraulic features are properly taken into account show that there are still subjects of concern which require new experimental investigation for code validation. This is specially the case of MOX fuel in which the fuel composition markedly differs from the ones generally experimented up to now.

Moreover, an insufficient validation might induce a dramatic increase of the uncertainty factor with a possible reduction of the reactor power and it appears that most of the organizations concerned with MOX fuel development do not dispose of enough experimental data for their own neutronic calculation tool improvement and calibration.

Therefore, based on the experience accumulated during these 25-year collaboration, CEN/SCK together with BELGONUCLEAIRE have decided to implement a new experimental programme in the VENUS facility.

This new VENUS International Programme called VIP includes a complete set of experimental measurements performed with existing  $\rm UO_2$  and MOX fuel rods in order to provide an extensive nuclear data base for the development, the improvement and the validation of nuclear calculation methods for MOX fuels used in LWRs.

A programme is devoted to Pu recycle in PWRs and another one in BWRs. The VIP Programme is starting now in 1990.

### OBJECTIVES AND MAJOR FEATURES OF THE VIP LWR PROGRAMME

The MOX fuel fabrication and large-scale MOX irradiation campaigns are now considered in various industrial countries. Consequently there is a need to develop or to improve the design and in-core management codes and to benchmark and validate them against experimental data.

The objective of the VIP programme is to constitute a nuclear data base on MOX and  $\rm UO_2$  fuels very similar to current LWR fuels in order to cover a wide range of the problems arising in the neutronic field of the Pu recycle in LWR. This experimental programme emphasizes the following major features :

- (1) Use of rods containing U and Pu with isotopic compositions similar to those of MOX fuel used in current LWR MOX fabrication campaigns.
- (2) Basic measurements and reactivity effects related to modern LWR lattices as close as possible of their conditions in core management studies by the simulation of current LWR assemblies in mock-up configurations.
- (3) Experimental support to items such as the instrumentation response, the equivalent factors determination and the various significant reactivity effects.

The selection of investigated experiments directly based on mock-up configurations will cover the major topics of interest for any participant in the calibration of his own methods. Furthermore, some options specific to particular reactivity effects are proposed in addition to the programme and could be included in the programme itself upon request.

### MAIN CHARACTERISTICS OF THE FUEL RODS

The main characteristics of fuel rods that are incorporated in this new programme are given in Table I.

TABLE I

VENUS Programme Fuel

Rod outer diameter : 0.95 cm

Lattice pitch : square 1.26 cm Rod cladding : Zircaloy-4

Fuel types available:

| TYPE    | U <sup>235</sup><br>Enrich-<br>ment | Pu <sup>tot</sup> U + Pu <sup>tot</sup> | Isotopic<br>Composition<br>Plutonium<br>238/239/240/241/242 | Rods<br>Avail-<br>able |
|---------|-------------------------------------|-----------------------------------------|-------------------------------------------------------------|------------------------|
| 3/0     | 3.3 %                               | 0                                       |                                                             | 1200                   |
| 0.3/5.4 | 0.3 %                               | 5.4 %                                   | 1/63/24/8/4                                                 | 80                     |
| 0.2/5.8 | 0.2 %                               | 5.8 %                                   | 1/58/25/10/6                                                | 80                     |
| 0.3/9.7 | 0.3 %                               | 9.7 %                                   | 1/61/24/9/5                                                 | 550                    |
| 0.3/10  | 0.3 %                               | 10.2 %                                  | 1/58/25/10/6                                                | 100                    |
| 0.4/14  | 0.4 %                               | 14.4 %                                  | 1/62/23/9/5                                                 | 300                    |

### PWR PROGRAMME DESCRIPTION

The programme is devoted to sophisticated configurations that are as close as possible to the actual and future PWR MOX assemblies. The purpose is to demonstrate that the calculation methods applied to the analysis of these experiments are able to achieve a good accuracy for mock-up assemblies simulating real parts of PWR core configurations with various significant reactivity effects.

The programme is divided into different phases. The Phase l is devoted to rodwise power distribution in MOX fuel assemblies and to detector response in  $\rm UO_2$  and  $\rm MOX$  assemblies.

### Phase 1

The first mock-up configuration (Figure 1) consists of a central MOX assembly of 17 x 17 RCC type surrounded by four UO2 assemblies and by a UO2 feeding zone, if necessary. The central MOX assembly consists of 3 different Pu content rods distributed inside the assembly in a similar way than for MOX assemblies loaded in modern PWRs. The UO2 fuel assemblies will be made of 3.3 w/o U-235 enriched fuel rods (type 3/0).

The second mock-up configuration is similar to the first one but in this case several MOX rods will be replaced by  $\rm UO_2-Gi_2O_3$  rods. These Gd rods are containing 7 w/o  $\rm Gd_2O_3$  and their U-235 enrichment is 3.5 w/o.

The following measurements will be carried out :

- critical mass,
- axial buckling for the various types of fuel rods,
- the rodwise power distribution in the central MOX assembly and in an adjacent UO2 assembly,
- the response of a U-235 fission detector located in the centre of the MOX assembly and the response of the same detector located in the centre of the UO<sub>2</sub> assembly. The detector response is particularly affected by the neutron spectrum and the flux level.

### Phase 2

The Phase 2 should be specially devoted to the reactivity measurements in the MOX fuel assembly. Various measurements are suggested at the present stage of the programme.

Reference MOX Mock-Up for Reactivity Measurements. This MOX mock-up configuration is introduced in the programme as a reference configuration for some significant reactivity effects. This reference mock-up configuration must be critical at a reduced water level in order to compensate by a water level variation for the reactivity loss due to some predetermined perturbations in the core.

Control Rod Effects. One effect of the Pu recycle in PWRs is the reduction of control rod worth when inserted into MOX assemblies and consequently a reduction of the shutdown margin. This measurement will provide the reactivity effect of Ag-In-Cd in MOX assemblies by measuring the critical level and  $\Delta\rho/\Delta h$  reactivity curve as obtained by inserting a progressive number of Ag-In-Cd rods in the central MOX assembly.

This option also proposes to investigate this point by measuring the benefit of introducing enriched B4C control rods instead of Ag-In-Cd.

Boric Acid Worth Measurements. The boron worth will be measured by adding boric acid to the moderator by taking as a reference, the reference MOX mock-up.

Moderation Ratio Effect in the MOX Assembly. The moderation reduction affects differently UO $_2$  and MOX lattices. This effect measured by the new critical level and the  $\Delta\rho/\Delta h$  will be created by the insertion of aluminium microrods between the fuel rods of the MOX assembly.

Two moderation ratios will be considered. This effect will also be combined with inserted control rods.

Reactivity of  ${\tt UO}_2$  Central Fuel Assembly. The reactivity difference between the  ${\tt UO}_2$  and MOX central assembly will be measured by replacing the MOX rods by  ${\tt UO}_2$  rods and by adjusting the water level to be critical.

Options. If requested by the participants, additional measurements could be carried out in the configurations defined in the present VIP programme. These optional measurements are:

- Measurement of the power tilt inside a MOX fuel rod located at the  $UO_2/MOX$  interface.
- Beta effective measurement.
- Other MOX assembly mock-up with other repartitions of Pu enrichments in the MOX assembly.
- Other Pu vector in the mock-up.
- Am-241 effect by measuring the critical mass after more than one year.

### BWR PROGRAMME DESCRIPTION

This programme is also divided into different phases. Some options, as in PWR programme, could be included in the programme at the participants' request.

### Phase 1

The Phase 1, now underway, is devoted to three configurations simulating as close as possible advanced BWR bundles. For each of these three mock-ups where the water density reduction is reached by Al microrods insertion between fuel rods, the following measurements will be carried out:

- critical mass,
- axial buckling measurement, -
- rodwise power distribution in the bundles of interest and along main axis.

The reactivity effect of moderation density variation will also be measured for the Pu-island bundle. The three configurations are as follows.

UO2 BWR Bundle Mock-Up. This configuration, illustrated in Figure 2, consists of simulating 4 BWR 8 x 8 UO2 bundles surrounded by a UO2 rod feeding zone. A 2 x 2 water hole is located in the centre of each bundle. Two bundles diagonally opposite, contains 8 UO2-Gd2O3 rods (7 w/o Gd2O3 and 3.5 w/o U-235 enriched).

I-MOX Mock-Up (8 x 8). This configuration consists of simulating 2 BWR 8 x 8 UO $_2$ -MOX island-type bundles and 2 UO $_2$  bundles surrounded by a feeding zone of UO $_2$  rods. Each of the MOX bundle will consist of :

- 8 central medium-enriched MOX fuel rods,
- 12 low-enriched MOX fuel rods,
- 10 UO2-Gd203 rods,
- 30  $\mathbb{C}_{02}$  fuel rods located at the periphery of the bundle.

This basic I-MOX configuration is illustrated in Figure 2.

A-MOX Mock-Up. This configuration consists of simulating 2 BWR 8 x 8 all-MOX type bundles surrounded by a feeding zone of  $\rm UO_2$  rods. Each of the MOX bundle will consist of :

- 4 central high-enriched MOX fuel rods,
- 12 medium-enriched MOX fuel rods,
- 14 UO<sub>2</sub>-Gd<sub>2</sub>O<sub>3</sub> rods,
- 30 low-enriched MOX fuel rods at the periphery.

### Phase 2

This Phase 2 will be devoted to reactivity measurements for MOX bundles. Various measurements are suggested at the present stage of the programme.

Reference MOX Mock-Up for Reactivity Measurements. This mock-up configuration is used as a reference configuration for some significant reactivity effects. This reference mock-up configuration must be critical at a reduced power level in order to compensate by a water level variation for the reactivity loss due to some predetermined perturbations in the core.

 $B_4C$  Control Rod or Blade Effects. One effect of the Pu recycle in BWRs is the reduction of control rod worth when inserted close to MOX bundles and consequently a reduction of the shutdown margin. This measurement will provide the reactivity effect of  $B_4C$  close to MOX bundles by measuring the critical level and  $\Delta\rho$  /  $\Delta h$  after the insertion of  $B_4C$  rods or blades in the water gaps between central bundles.

Moderation Ratio Effect. This effect measured by the new critical level and the  $\Delta\rho$  /  $\Delta h$  will be created by the insertion of aluminium microrods between the fuel rods. Two moderation ratios will be considered.

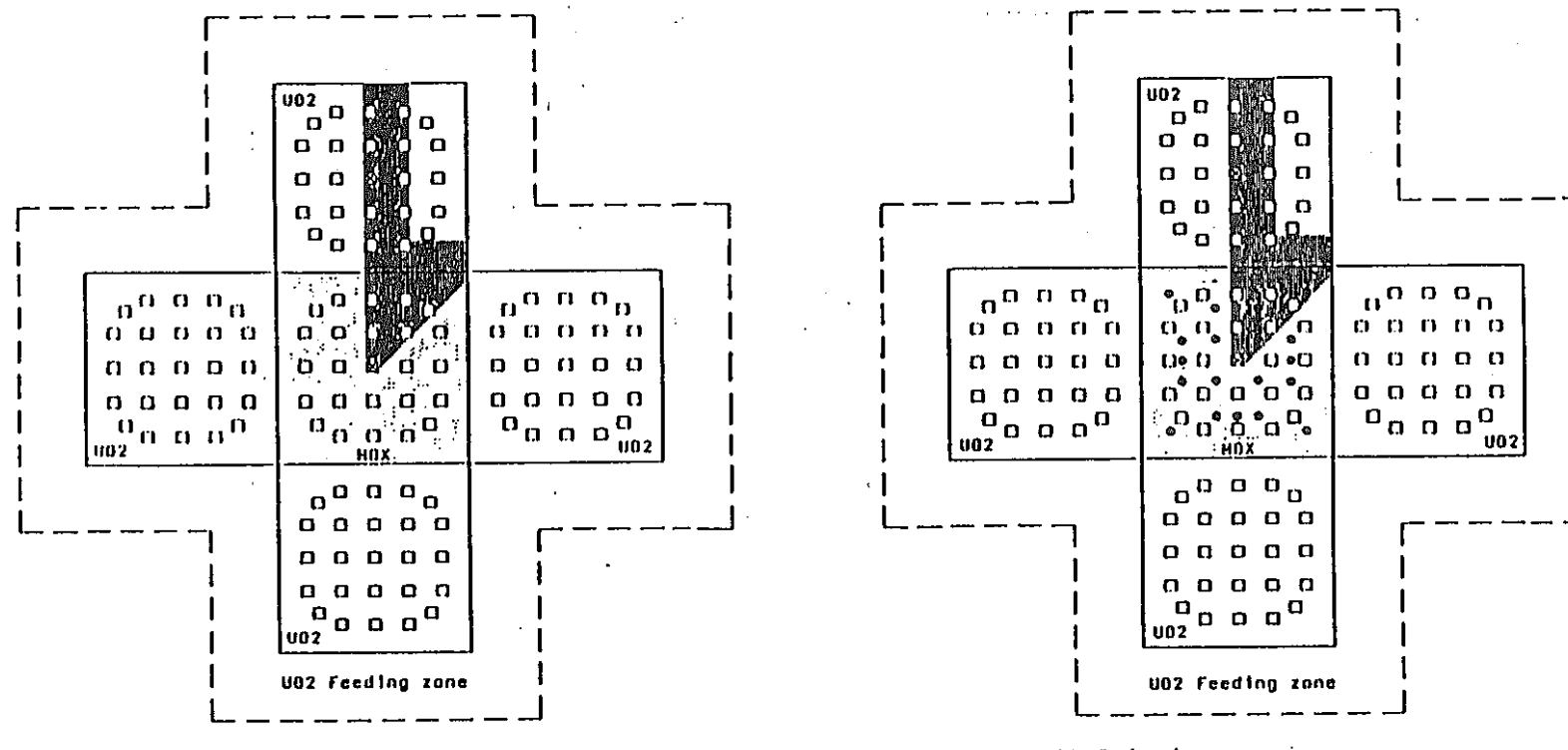
Reactivity of  ${\tt UO}_2$  and  ${\tt MOX}$  Central Bundles. The reactivity difference between the  ${\tt UO}_2$  and  ${\tt MOX}$  central bundles will be measured by replacing the  ${\tt MOX}$  bundles by  ${\tt UO}_2$  bundle and by adjusting the water level to be critical.

Options. If requested by the participants, additional measurements could be carried out in the configuration defined in the present VIP programme. These optional measurements are:

- Beta effective measurement.
- Other MOX assembly mock-up with other repartitions of Pu enrichments in the MOX assembly.
- Other Pu vector in the mock-up.
- Am-241 effect by measuring the critical mass after more than one year.



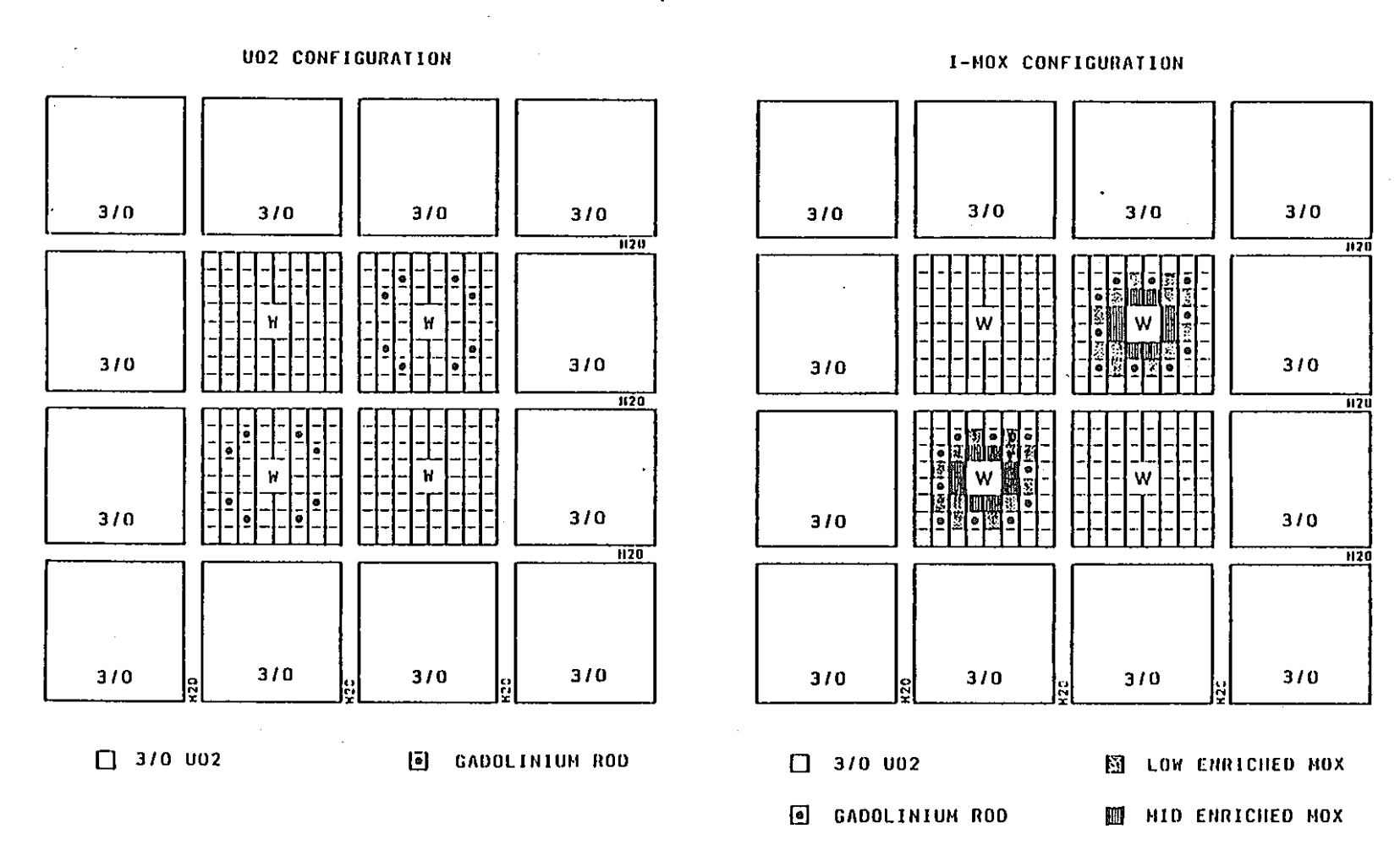




- U235 Detector
- □ Water hole
- 🏻 Heasurement area
- **HEASUREMENTS: Critical mass**
- ----- Rodwise power distribution
  - Axial buckling
  - U235 detector response

- ₩ U235 Detector
- 🗆 Water hole
- Gd203 U02 Rod
- M Measurement area
- MEASUREMENTS : Critical mass
  - - Axial buckling
    - U235 detector response

## VENUS BWR MOX PROGRAMME (PHASE 1)



NEACRP-A-1048

## VENUS International Programme (VIP) A Nuclear Data Package for BWR Pu Recycle

- Phase 1 -

## TECHNICAL PROPOSAL

Basselier J., Charlier A. BELGONUCLEAIRE, Brussels

D'hondt P., Leenders L., Minsart G. SCK/CEN, MOL, Belgium

### - TABLE OF CONTENTS -

|    |                                                        | Pages |
|----|--------------------------------------------------------|-------|
| l. | INTRODUCTION                                           | 2     |
| 2. | OBJECTIVES AND MAJOR FEATURES OF THE VIP BWR PROGRAMME | 3     |
| 3. | THE VENUS ZERO-POWER FACILITY                          | 4     |
| 4. | MAIN CHARACTERISTICS OF THE FUEL RODS                  | 5     |
| 5. | PROGRAMME DESCRIPTION                                  | 7     |
| 6. | PLANNING                                               | 10    |

0 0 0 0 0

### 1. INTRODUCTION

Since about 25 years, BELGONUCLEAIRE has been collaborating with the Belgian National Nuclear Centre (CEN/SCK) and has been proceeding with R and D work to understand and predict the behaviour of the fuel in light water reactors. In particular, the VENUS zero-power facility located at the CEN/SCK at Mol has been used to support this kind of investigation. As an example, this VENUS facility was used to develop the Belgian pluto-nium recycling programme in LWRs. The experimental data obtained in the frame of this programme include: basic characteristics ( $k_{\rm eff}$ , critical bucklings, power distribution), perturbation measurements (reactivity effects, flux measurements, ...) or mock-up experiments where parts of LWR cores are simulated, for the measurements of major characteristics such as critical masses, power distribution, control rod worth, etc.

The operating data obtained from the power reactors, the continuing increase of the fuel performance, the new fuel characteristics, the decision recently taken by major Utilities in various countries to recycle in their power plants the plutonium obtained from reprocessing and the necessity to demonstrate to the Licensing Authority that the differences in the neutronic, safety and thermal-hydraulic features are properly taken into account show that there are still subjects of concern which require new expermimental investigation for code validation. This is specially the case of MOX fuel in which the fuel composition markedly differs from the ones generally experimented up to now.

Moreover, an insufficient validation might induce a dramatic increase of the uncertainty factor with a possible reduction of the reactor power and it appears that most of the organizations concerned with MOX fuel development do not dispose of enough experimental data for their own neutronic calculation tool improvement and calibration.

Therefore, based on the experience accumulated during these 25-year collaboration, CEN/SCK together with BELGONUCLEAIRE have decided to implement a new experimental programme in the VENUS facility.

This new VENUS International Programme called VIP will include a complete set of experimental measurements performed with existing UO<sub>2</sub> and MOX fuel rods in order to provide an extensive nuclear data base for the development, the improvement and the validation of nuclear calculation methods for MOX fuels used in BWRs. A more complete description of the VIP programme for BWR application was provided in the technical document VIP-3 89/01.

However, in a first stage, only a part of the work scope will be carried out, to cope with the available budget and with the most urgent topics of this experimental programme. This Phase I of the VIP Programme is described in this report. It mainly includes the facility preparation, fuel rod deliveries and three mock-up experiments. It is to be expected that it will be followed by Phase 2, incorporating several reactivity effects measurements.

### 2. OBJECTIVES AND MAJOR FEATURES OF THE VIP BWR PROGRAMME

The MOX fuel fabrication and large-scale MOX irradiation campaigns are now considered in various industrial countries. Consequently there is a need to develop or to improve the design and in-core management codes and to benchmark and validate them against experimental data.

The objective of the VIP programme is to constitute a nuclear data base on MOX and  ${\rm UO}_2$  fuels in order to cover a wide range of the problems arising in the neutronic field of the Pu recycle in BWR. This experimental programme emphasizes the following major features :

- (1) Use of rods containing U and Pu with isotopic compositions representative of those of MOX fuel used in current BWR MOX fabrication campaigns.
- (2) Power measurements and reactivity effects related to modern BWR lattices as close as possible of their conditions in core management studies by the simulation of current BWR bundles in mock-up configurations.
- (3) Experimental support to items such as the instrumentation response, the equivalent factors determination and the various significant reactivity effects.

Phase 1 of the programme, described in item 5 hereafter, is relative to one BWR UO $_2$  mock-up followed by two BWR-MOX mock-ups simulating 8 x 8 BWR bundles in order to validate the rodwise power distribution and the detector response.

Each of these configurations will include some Gadolinium rods and the water density reduction will be simulated by the introduction of aluminium microrods within the fuel lattice.

A An additional reduction of water density will be simulated in the I-MOX mock-up by the introduction of additional aluminium rods surrounding the fuel rods and adjusted between the existing Al microrods.

### 3. THE VENUS ZERO-POWER FACILITY

A general description of the VENUS facility that was originally constructed to support the design of the spectral shift VULCAIN reactor was given in VIP-8 89/01.

In 1966-1967, the VENUS facility was specially adapted to the requirements of the plutonium physics programme. Its main characteristics are now:

- 1.26 cm square pitch grids, with individually inserted fuel rods,
  - between the holes for fuel rods, smaller holes are made in the grids, allowing the introduction of aluminium microrods in the lattice when the water density reduction corresponding to the nominal power reactor operation average coolant temperature has to be simulated,
  - there are a few demountable parts in the grids, enabling the easy introduction into the core of certain measurement or detection devices or fuel loading,
  - due to the adoption of a fast moderator dump system, allowing an emergency drain of the water from the active part of the core in less than one second, no control rod guide tubes perturb the lattices,
  - fine reactivity regulation can be done by water level variation (the level indication precision is 0.01 cm) or by regulating rods if the local perturbation they create does not affect the measured characteristics.

Straightly connected to the utilization and the operation of the critical facility, are a gamma-scanning and a gamma-spectrometry installation and a plutonium laboratory. The gamma-scanning installation is used to count the gamma-activity of fission products in the selected experimental fuel rods, in order to determine fission density distributions. This installation is fully automatic. The detector is a 2" x 2" NaI(T1) crystal.

## - 5 - (Revision A)

### 4. MAIN CHARACTERISTICS OF THE FUEL RODS

The main characteristics of fuel rods that will be incorporated in the programme are provided in Tables 1 and 2 hereafter.

- TABLE 1 MOX Fuel Isotopic Composition (w/o)

|               | Low<br>Enrichment | Medium<br>Enrichment | High<br>Enrichment |
|---------------|-------------------|----------------------|--------------------|
| U-235/U tot   | 0.20 - 0.60       | 0.3                  | 0.4                |
| Pu-238/Pu tot | 1.2 - 1.6         | 1.4 - 1.6            | 1.2                |
| Pu-239/Pu tot | 58 - 63           | 58 - 60              | 61.6               |
| Pu-240/Pu tot | 24                | 24                   | 23.4               |
| Pu-241/Pu tot | 7.9 <b>-</b> 10   | 9 - 10               | 9.3                |
| Pu-242/Pu tot | 4.2 - 5.5         | 7.7 - 5.5            | 4.4                |
| Am-241/Pu tot | 0.1 - 0.5         | 0.14 - 0.33          | 0.25               |

NB1: These values are approximate values, they will be confirmed after the selection and the characterization work to be performed on the rods for the VIP programme.

NB2: The reference date is February 1, 1985.

 $\frac{\text{NB3}}{\text{The low enrichment is about}}: \text{ The low enrichment is about} \qquad \begin{array}{c} 5.5 \text{ w/o } \text{Pu}_{\text{tot}} / \text{U} + \text{Pu}_{\text{tot}}. \\ 9.7 \text{ w/o } \text{Pu}_{\text{tot}} / \text{U} + \text{Pu}_{\text{tot}}. \\ \text{The high enrichment is about} \qquad \begin{array}{c} 14.4 \text{ w/o } \text{Pu}_{\text{tot}} / \text{U} + \text{Pu}_{\text{tot}}. \end{array}$ 

A Uranium content in the MOX fuel is in the range of 0.2 to 0.6 w/o U=235/U\_{COT}.

- 6 -(Revision A)

- TABLE 2 VIP Rods Preliminary Specifications

|                                                                                              | MOX Rods  | UO <sub>2</sub> Rods | Gd Rods | B <sub>4</sub> C Rods | Microrods |
|----------------------------------------------------------------------------------------------|-----------|----------------------|---------|-----------------------|-----------|
| Active length (cm)                                                                           | 100       | 50                   | 100     | 50                    |           |
| Cladding material                                                                            | Zry-4     | Zry-4                | Zry-4   | SS                    | Al        |
| Cladding O.D. (mm)                                                                           | 9.63      | 9.50                 | 9.50    | 9.78                  | 5.5 ,.    |
| Cladding I.D. (mm)                                                                           | 3.42      | 3.36                 | - 8.24  | 9.02                  |           |
| Pellet Ø (mm)                                                                                | 8.23      | 8.19                 | 8.04    |                       |           |
| Available rod No.                                                                            | 300 - 400 | > 7000               | ≈ 70    | ≈ 50                  | > 1000    |
| Density (% TD)                                                                               | 95        |                      | 95      | 60                    |           |
| Density (g/cm)                                                                               |           | 5.4                  |         |                       |           |
| U-235/U (W/o)                                                                                | 0.3       | 3.3                  | 3.5     |                       |           |
| Gd <sub>2</sub> 0 <sub>3</sub> /(UO <sub>2</sub> + Gd <sub>2</sub> O <sub>3</sub> )<br>(w/o) |           |                      | 7       |                       |           |

NB: For information only. These characteristics will be updated during the characterization work to be performed on the selected rods for the VIP programme.

A

## - 7 - (Revision A)

### 5. PROGRAMME DESCRIPTION (Phase 1)

The proposed Phase I of the VIP (BWR) Programme will be divided into four different tasks as follows:

### TASK 1: Fuel and Components Procurements and Licensing

The task which will include all items belonging to the preparation of the facility and of the procurement of the fuel rods is presently divided into several subtasks, such as:

- Task l.l: Licensing application, safety requirements, preparation of the facility and orientation calculations.
- Task 1.2 : Fuel rods procurement.
- Task 1.3: Fuel rods selection and characterization.
- Task 1.4: Fuel rods transportations.
- Task 1.5: Storage and facility hardware adaptation.
- A Task 1.6: Fabrication and procurement of Al rods for additional density reduction.
  - Task 1.7: Final disposal of the fuel rods after the experimental campaign.

### TASK 2 : Mock-up Programme

This experimental part of the programme will be devoted to three sophisticated configurations that are as close as possible to the BWR MOX bundles. The purpose is to demonstrate that the calculation methods applied to the analysis of these experiments are able to achieve a good accuracy for mock-up assemblies simulating real parts of BWR core configurations.

For each of these three configurations, the following major parameters will be measured:

- critical mass,
- axial buckling measurement,
- rodwise power distribution in one half of a bundle and in some adjacent rods to this bundle.

Task 2 of the programme is divided into five different subtasks :

### Task 2.1 : Orientation

Safety aspects and preparation of the facility for the mock-up programme.

## - 8 - (Revision A)

### Task 2.2 : UO2 BWR Mock-up (8 x 8)

- A This task consists in one VENUS symmetrical configuration simulating 2 BWR  $8\times8$  UO $_2$  bundles surrounded by a feeding zone of UO $_2$  rods. Each of the
- A bundle will content 8 UO<sub>2</sub>-Gd<sub>2</sub>O<sub>3</sub> rods, as illustrated in Figure 1. A density of 0.73 will be simulated by the introduction of Al microrods.

### Task 2.3 : A-MOX Mock-up

This task consists in one VENUS symmetrical configuration simulating 2 BWR 8 x 8 all-MOX type bundles surrounded by a feeding zone of  $\rm UO_2$  rods. Each of the bundle will consist of :

- 4 central high-enriched MOX fuel rods,
- 12 medium-enriched MOX fuel rods,
- 14 UO<sub>2</sub>-Gd<sub>2</sub>O<sub>3</sub> rods,
- 30 low-enriched MOX fuel rods at the periphery.
- A A density of 0.73 will be simulated by the introduction of Al microrods.

  A water density effect will be performed at the end of the measurement by extraction of the Aluminium microbars.
- A This basic A-MOX configuration is illustrated in Figure 2.

### Task 2.4 : I-MOX Mock-up (8 x 8)

- A This task consists in one VENUS symmetrical configuration simulating 2 BWR 8 x 8 UO2-MOX island-type bundles surrounded by a feeding zone of UO2 rods. Each of the bundle will consist of :
  - 8 central medium-enriched MOX fuel rods,
  - 12 low-enriched MOX fuel rods,
  - 10 UO2-Gd2O3 rods,
  - 30 UO2 fuel rods located at the periphery of the bundle.
- A A density of 0.5 will be simulated by the introduction of Al existing microrods and additional Al tubes.
- A This basic I-MOX configuration is illustrated in Figure 3.

### Task 2.5 : Theoretical Support

This task includes the design, the orientation calculation, supply of theoretical data for measurement treatment, the follow-up, the review and checking and all the theoretical support to the experimental programme of Task 2.

- 9 - (Revision A)

### TASK 3: Project Management

This task will include the co-ordination and administration of the programme with the transfer of the fuel rods as well as the preparation and follow-up of the new experiments.

As far as reporting is concerned, topical reports will be issued in the frame of each technical task. The Project Management will issue semestral progress reports and a final report summarizing the work performed and giving the main conclusions of the programme.

For Phase 1, two Programme Committee Meetings are scheduled to discuss the progress of the work and to decide on further actions or modifications of the programme. Moreover, additional technical meetings may be held upon participants' request to handle urgent matters. A visit of the VENUS experimental facility will be organized in conjunction with one of the progress meetings.

Task 3 has been divided into three parts:

Task 3.1 : Pre-programme implementation.

Task 3.2 : Administration and programme management.

Task 3.3 : Co-ordination and Follow-up.

### TASK 4 : PIE Data

This task will include some post-irradiation experiments and results on a two MOX BWR rods (PG34 and PG56) irradiated to high burnup in DODEWAARD.

- A This task is divided into several subtasks:
  - Task 4.1 : Rod post-irradiation examination.
  - Task 4.2 : Fuel pellet post-irradiation examination.
  - Task 4.3: PIE additional services (marking, sectioning, sample storage, waste disposal).
  - Task 4.4 : Transportation.
  - Task 4.5 : Reporting.
  - Task 4.6 : Co-ordination and follow-up of Task 4.

## - 10 - (Revision A)

A The PIE test matrix is provided hereafter:

|                         | Rod PG34 | Rod PG56 |
|-------------------------|----------|----------|
| Gross gamma-scanning    | 1 (*)    | 1        |
| Cs-137 gamma-scanning   | 1 (*)    | 1        |
| Puncture + gas analysis | 1 (*)    | 1        |
| Alpha aucoradiography   | 2        | 1        |
| EPMA                    | 3        | . 3      |
| Peller burnup           | 5        | 4        |
| Pellet radial burnup    | 2        | 1        |
| SIMS                    | 2        | 1        |

(\*) These measurements on rod PG34 are released in the frame of the DOMO programme.

### 6. PLANNING

Beginning of Phase 1: November 1, 1989.

A UO2 and A-MOX mock-up : From March to October 1990.

A I-MOX mock-up : From April to August 1991.

A PIE on two rods : From August 1990 to March 1991.

The general planning is pointed out in Figure 4.

0 0 0 0 0

### VENUS BWR MOX PROGRAMME

(PHASE 1)

### UO2 CONFIGURATION

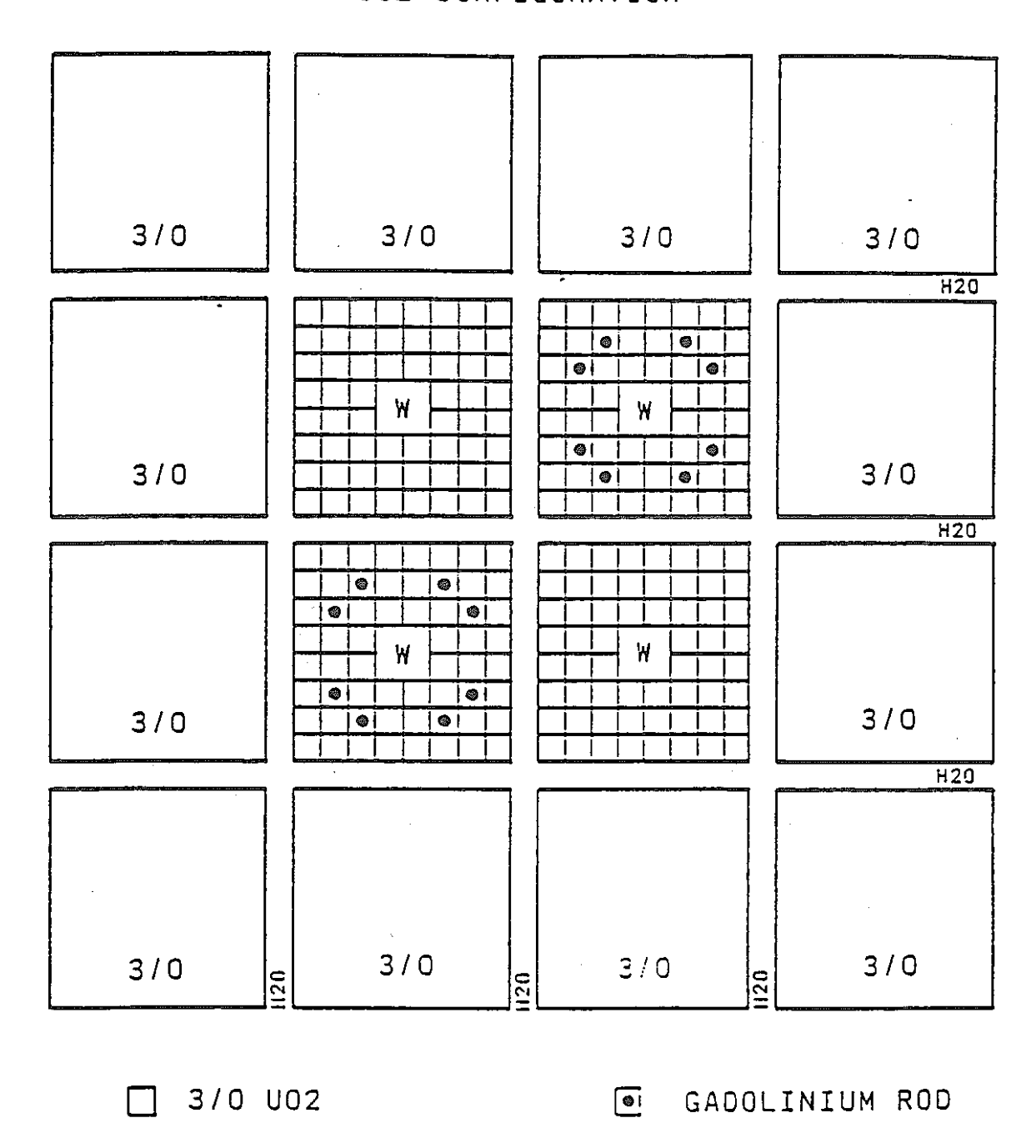


FIGURE 1.

# VENUS BWR MOX PROGRAMME (PHASE 1)

A-MOX CONFIGURATION (Preliminary)

| 3/0 | 3/0           | 3/0   | 3/0        |
|-----|---------------|-------|------------|
| 3/0 |               |       | 3/0<br>H20 |
| 3/0 |               |       | 3/0        |
| 3/0 | 1120<br>O \ E | 3 / O | H20        |

- GADOLINIUM ROD -
- MID ENRICHED MOX
- LOW ENRICHED MOX
- HIGH ENRIHCED MOX

# VENUS BWR MOX PROGRAMME (PHASE 1)

### I-MOX CONFIGURATION

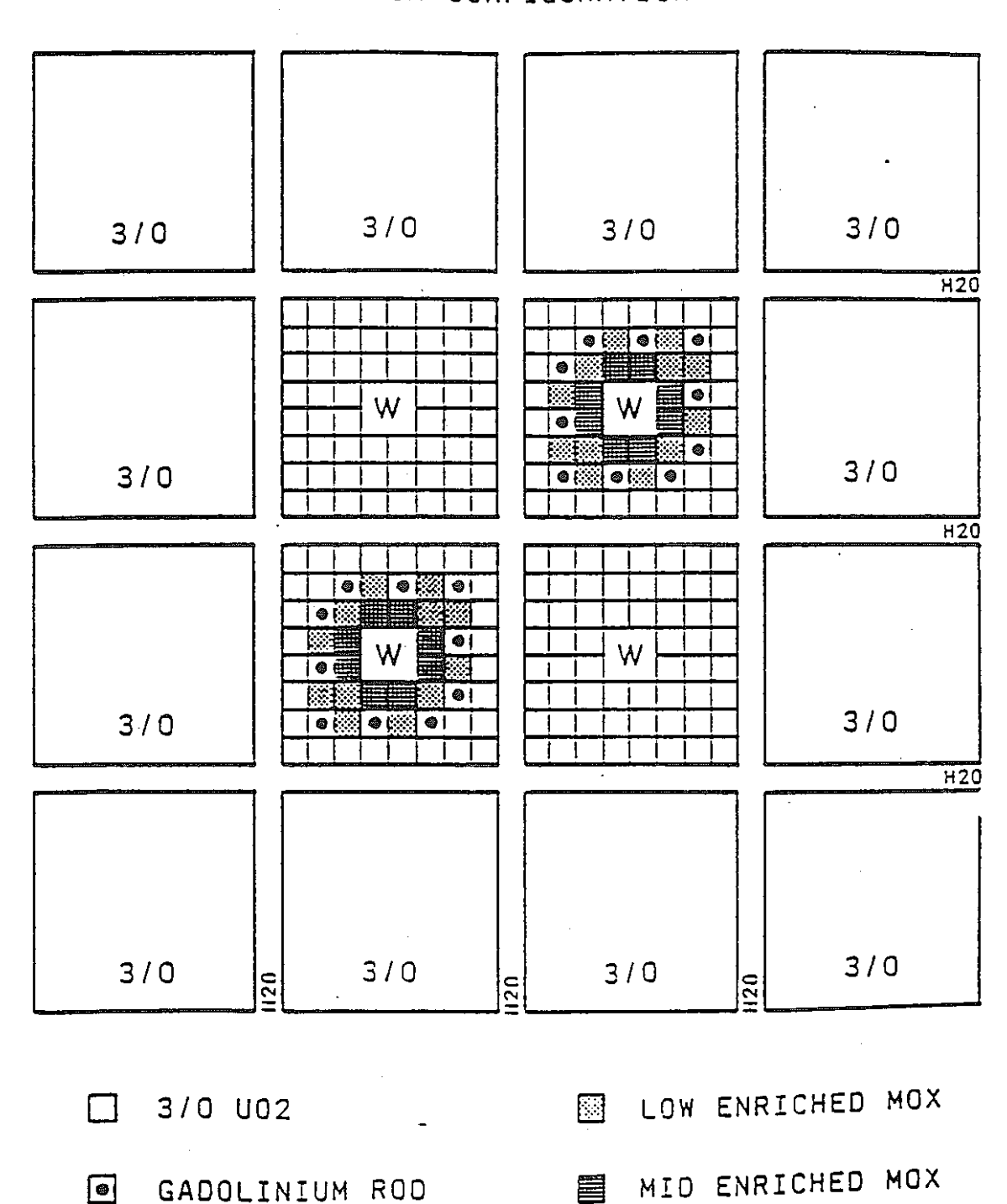


FIGURE 4: VIP-BWR Phase 1 - General Planning (Revision A)

| TASKS                                                                                                                                                                                                                                                                                                                                            |  | 1989 1990 |     |      |     |     |     |   |   |   |   | 1991 |   |       |     |     |    |   |   |    |   |   |
|--------------------------------------------------------------------------------------------------------------------------------------------------------------------------------------------------------------------------------------------------------------------------------------------------------------------------------------------------|--|-----------|-----|------|-----|-----|-----|---|---|---|---|------|---|-------|-----|-----|----|---|---|----|---|---|
|                                                                                                                                                                                                                                                                                                                                                  |  | D         | J.J | F    | М   | Α   | М   | J | J | A | s | 0    | N | D     | Į.j | F   | Н  | A | M | .j | ı | A |
| <ul> <li>1.1 Licensing, safety, preparation.</li> <li>1.2 MOX fuel rods procurement.</li> <li>1.3 Fuel rods selection and characterization.</li> <li>1.4 Fuel rods transportation.</li> <li>1.5 Storage and facility hardware adaptation.</li> <li>1.6 Al rods procurement.</li> <li>1.7 Final disposal of rods (not yet applicable).</li> </ul> |  |           |     |      |     |     |     |   |   |   |   |      |   |       |     |     |    |   |   |    |   |   |
| <ul> <li>2.1 Orientation work.</li> <li>2.2 1002 mock-up until reporting.</li> <li>2.3 A-MOX mock-up until reporting.</li> <li>2.4 1-MOX mock-up until reporting.</li> <li>2.5 Theoretical support until final reporting.</li> </ul>                                                                                                             |  |           | BM  | c De | )·2 | A - | NOX |   |   |   |   |      | 4 | ( PWI | P   | l-i | ). |   |   |    |   |   |
| 3.1 Pre-programme implementation.  3.2 Administration and programme management.  3.3 Co-ordination and follow-up.                                                                                                                                                                                                                                |  |           |     |      |     |     |     |   |   |   |   |      |   |       |     |     |    |   |   |    |   |   |
| 4.1 to 4.6 PIE + reporting (*)                                                                                                                                                                                                                                                                                                                   |  |           |     |      |     |     |     |   | - |   |   |      |   |       |     |     |    |   |   |    |   |   |

(\*) Final reporting of SIMS results will be fixed later on.

NEACRP-A-1049

1.1

## VENUS International Programme (VIP) A Nuclear Data Package for PWR Pu Recycle

- Phase 1 -

### TECHNICAL PROPOSAL

Basselier J., Charlier A. BELGONUCLEAIRE, Brussels

D'hondt P., Leenders L., Minsart G. SCK/CEN, MOL, Belgium

### - TABLE OF CONTENTS -

|    |                                                        | Pages |
|----|--------------------------------------------------------|-------|
| 1. | INTRODUCTION                                           | 2     |
| 2. | OBJECTIVES AND MAJOR FEATURES OF THE VIP PWR PROGRAMME | 3     |
| 3. | THE VENUS ZERO-POWER FACILITY                          | 4     |
| 4. | MAIN CHARACTERISTICS OF THE FUEL RODS                  | , 5   |
| 5. | PROGRAMME DESCRIPTION                                  | 7     |
| 6. | PLANNING                                               | 9     |

00000

### 1. INTRODUCTION

Since about 25 years, BELGONUCLEAIRE has been collaborating with the Belgian National Nuclear Centre (CEN/SCK) and has been proceeding with R and D work to understand and predict the behaviour of the fuel in light water reactors. In particular, the VENUS zero-power facility located at the CEN/SCK at Mol has been used to support this kind of investigation. As an example, this VENUS facility was used to develop the Belgian pluto-nium recycling programme in LWRs. The experimental data obtained in the frame of this programme include: basic characteristics (keff, critical bucklings, power distribution), perturbation measurements (reactivity effects, flux measurements, ...) or mock-up experiments where parts of LWR cores are simulated, for the measurements of major characteristics such as critical masses, power distribution, control rod worth, etc.

The operating data obtained from the power reactors, the continuing increase of the fuel performance, the new fuel characteristics, the decision recently taken by major Utilities in various countries to recycle in their power plants the plutonium obtained from reprocessing and the necessity to demonstrate to the Licensing Authority that the differences in the neutronic, safety and thermal-hydraulic features are properly taken into account show that there are still subjects of concern which require new expermimental investigation for code validation. This is specially the case of MOX fuel in which the fuel composition markedly differs from the ones generally experimented up to now.

Moreover, an insufficient validation might induce a dramatic increase of the uncertainty factor with a possible reduction of the reactor power and it appears that most of the organizations concerned with MOX fuel development do not dispose of enough experimental data for their own neutronic calculation tool improvement and calibration.

Therefore, based on the experience accumulated during these 25-year collaboration, CEN/SCK together with BELGONUCLEAIRE have decided to implement a new experimental programme in the VENUS facility.

This new VENUS International Programme called VIP will include a complete set of experimental measurements performed with existing UO<sub>2</sub>, UO<sub>2</sub>-Gd<sub>2</sub>O<sub>3</sub> and MOX fuel rods in order to provide an extensive nuclear data base for the development, the improvement and the validation of nuclear calculation methods for MOX fuels used in PWRs. A more complete description of the VIP programme for PWR application was provided in the technical document VIP-P 89/O1.

However, in a first stage, only a part of the work scope will be carried out, to cope with the available budget and with the most urgent topics of this experimental programme. This Phase I of the VIP Programme is described in this report. It mainly includes the facility preparation, fuel rod deliveries and two mock-up experiments. It is to be expected that it will be followed by Phase 2, incorporating several reactivity effects measurements.

#### 2. OBJECTIVES AND MAJOR FEATURES OF THE VIP PWR PROGRAMME

The MOX fuel fabrication and large-scale MOX irradiation campaigns are now considered in various industrial countries. Consequently there is a need to develop or to improve the design and in-core management codes and to benchmark and validate them against experimental data.

The objective of the VIP programme is to constitute a nuclear data base on MOX and  $\rm UO_2$  fuels in order to cover a wide range of the problems arising in the neutronic field of the Pu recycle in PWR. This experimental programme emphasizes the following major features:

- Use of rods containing U and Pu with isotopic compositions representative of those of MOX fuel used in current PWR MOX fabrication campaigns.
- (2) Power measurements and reactivity effects related to modern PWR lattices as close as possible of their conditions in core management studies by the simulation of current PWR assemblies in mock-up configurations.
- (3) Experimental support to items such as the instrumentation response, the equivalent factors determination and the various significant reactivity effects.

Phase 1 of the programme, described in item 5 hereafter, is relative to one PWR MOX mock-up followed by one PWR MOX mock-up with gadolinium rods simulating PWR assemblies in order to validate the rodwise power distribution and the detector response.

The second configuration will include some Gadolinium rods and the water density reduction could be simulated by the introduction of aluminium microrods within the fuel lattice.

#### 3. THE VENUS ZERO-POWER FACILITY

A general description of the VENUS facility that was originally constructed to support the design of the spectral shift VULCAIN reactor was given in VIP-P 89/01.

In 1966-1967, the VENUS facility was specially adapted to the requirements of the plutonium physics programme. Its main characteristics are now:

- 1.26 cm square pitch grids, with individually inserted fuel rods,
- between the holes for fuel rods, smaller holes are made in the grids, allowing the introduction of aluminium microrods in the lattice when the water density reduction corresponding to the nominal power reactor operation average coolant temperature has to be simulated.
- there are a few demountable parts in the grids, enabling the easy introduction into the core of certain measurement or detection devices or fuel loading,
- due to the adoption of a fast moderator dump system, allowing an emergency drain of the water from the active part of the core in less than one second, no control rod guide tubes perturb the lattices,
- fine reactivity regulation can be done by water level variation (the level indication precision is 0.01 cm) or by regulating rods if the local perturbation they create does not affect the measured characteristics.

Straightly connected to the utilization and the operation of the critical facility, are a gamma-scanning and a gamma-spectrometry installation and a plutonium laboratory. The gamma-scanning installation is used to count the gamma-activity of fission products in the selected experimental fuel rods, in order to determine fission density distributions. This installation is fully automatic. The detector is a 2" x 2" NaI(T1) crystal.

#### 4. MAIN CHARACTERISTICS OF THE FUEL RODS

The main characteristics of fuel rods that will be incorporated in the programme are provided in Tables 1 and 2 hereafter.

- TABLE 1 MOX Fuel Isotopic Composition (w/o)

|               | Low<br>Enrichment | Medium<br>Enrichment | High<br>Enrichment |
|---------------|-------------------|----------------------|--------------------|
| U-235/U tot   | 0.20 - 0.60       | 0.3                  | 0.4                |
| Pu-238/Pu tot | 1.2 - 1.6         | 1.4 - 1.6            | 1.2                |
| Pu-239/Pu tot | 58 - 63           | 58 - 60              | 61.6               |
| Pu-240/Pu tot | ≈ 24              | ≈ 24                 | 23.4               |
| Pu-241/Pu tot | 7.9 - 10          | 9 - 10               | 9.3                |
| Pu-242/Pu tot | 4.2 - 5.5         | 7.7 - 5.5            | 4.4                |
| Am-241/Pu tot | 0.1 - 0.5         | 0.14 - 0.33          | 0.25               |

NB1 : These values are approximate values, they will be confirmed after the selection and the characterization work to be performed on the rods for the VIP programme.

NB2: The reference date is February 1, 1985.

 $\frac{\text{NB3}}{\text{The low enrichment is about}}: \text{ The low enrichment is about} \qquad \begin{array}{c} 5.5 \text{ w/o } \text{Pu}_{\text{tot}} / \text{U} + \text{Pu}_{\text{tot}}. \\ 9.7 \text{ w/o } \text{Pu}_{\text{tot}} / \text{U} + \text{Pu}_{\text{tot}}. \\ \\ \text{The high enrichment is about} \qquad 14.4 \text{ w/o } \text{Pu}_{\text{tot}} / \text{U} + \text{Pu}_{\text{tot}}. \\ \end{array}$ 

Uranium content in the MOX fuel is in the range of 0.2 to 0.4 w/o U-235/U tot.

- TABLE 2 VIP Rods Preliminary Specifications

|                                                                                              | MOX Rods  | UO <sub>2</sub> Rods | Gd Rods | B <sub>4</sub> C Rods | Microrods |
|----------------------------------------------------------------------------------------------|-----------|----------------------|---------|-----------------------|-----------|
| Active length (cm)                                                                           | 100       | 50                   | 100     | 50                    |           |
| Cladding material                                                                            | Zry-4     | Zry-4                | Zry-4   | SS                    | A1        |
| Cladding O.D. (mm)                                                                           | 9.63      | 9.50                 | 9.50    | 9.78                  | 5.5       |
| Cladding I.D. (mm)                                                                           | 8.42      | 8.36                 | 8.24    | 9.02                  |           |
| Pellet Ø (mm)                                                                                | 8.23      | 8.19                 | 8.04    |                       |           |
| Available rod No.                                                                            | 300 - 400 | > 1000               | ≈ 70    | ≈ 50                  | > 1000    |
| Density (% TD)                                                                               | 95        |                      | 95      | 60                    |           |
| Density (g/cm)                                                                               |           | 5.4                  |         |                       |           |
| U-235/UO <sub>2</sub> (w/o)                                                                  | 0.3       | 3.3                  | 3.5     |                       |           |
| Gd <sub>2</sub> 0 <sub>3</sub> /(U0 <sub>2</sub> + Gd <sub>2</sub> 0 <sub>3</sub> )<br>(w/o) |           |                      | . 7     |                       |           |

 $\frac{NB}{}$ : For information only. These characteristics will be updated during the characterization work to be performed on the selected rods for the VIP programme.

#### 5. PROGRAMME DESCRIPTION (Phase 1)

The proposed Phase 1 of the VIP (PWR) Programme will be divided into three different tasks as follows:

#### TASK 1: Fuel and Components Procurements and Licensing

This task which will include all items belonging to the preparation of the facility and of the procurement of the fuel rods is presently divided into several subtasks, such as:

- Task 1.1: Licensing application, safety requirements, preparation of the facility and orientation calculations.
- Task 1.2: Fuel rods procurement.
- Task 1.3: Fuel rods selection and characterization.
- Task 1.4: Fuel rods transportations.
- Task 1.5: Storage and facility hardware adaptation.
- Task 1.6: Final disposal of the fuel rods after the experimental campaign.

#### TASK 2 : Mock-up Programme

This experimental part of the programme will be devoted to two sophisticated configurations that are as close as possible to the PWR MOX assemblies. The purpose is to demonstrate that the calculation methods applied to the analysis of these experiments are able to achieve a good accuracy for mock-up assemblies simulating real parts of PWR core configurations.

For each of these two configurations, the following major parameters will be measured:

- critical mass,
- axial buckling measurement,
- rodwise power distribution in one eighth of a MOX assembly and in a large part of one half of one adjacent UO2 assembly,
- U-235 detector response located in the centre of the MOX assembly and in the centre of one  ${\rm UO}_2$  assembly.
- Task 2 of the programme is divided into four different subtasks:

#### Task 2.1 : Orientation

Safety aspects and preparation of the facility for the mock-up programme.

#### Task 2.2 : MOX Mock-up

This task consists in one VENUS symmetrical configuration simulating one central all-MOX assembly surrounded by four  ${\tt UO_2}$  assemblies and by a possible  ${\tt UO_2}$  feeding zone.

This basic all-MOX configuration is illustrated in Figure 1.

#### Task 2.3 : MOX-Gd Mock-up

This task consists in one VENUS symmetrical configuration simulating one PWR MOX assembly with gadolinium rods surrounded by four  ${\rm UO}_2$  assemblies and by a possible  ${\rm UO}_2$  feeding zone.

This basic MOX-Gd configuration is illustrated in Figure 2, the number and the position of Gd rods is not yet definitively fixed.

#### Task 2.4: Theoretical Support

This task includes the design, the orientation calculation, supply of theoretical data for measurement treatment, the follow-up, the review and checking and all the theoretical support to the experimental programme of Task 2.

#### TASK 3: Project Management

This task will include the co-ordination and administration of the programme with the transfer of the fuel rods as well as the preparation and follow-up of the new experiments.

As far as reporting is concerned, topical reports will be issued in the frame of each technical task. The Project Management will issue semestral progress reports and a final report summarizing the work performed and giving the main conclusions of the programme.

For Phase 1, two Programme Committee Meetings are scheduled to discuss the progress of the work and to decide on further actions or modifications of the programme. Moreover, additional technical meetings may be held upon participants' request to handle urgent matters. A visit of the VENUS experimental facility will be organized in conjunction with one of the progress meetings.

Task 3 has been divided into three parts:

Task 3.1: Pre-programme implementation.

Task 3.2: Administration and programme management.

Task 3.3: Co-ordination and Follow-up.

#### 6. PLANNING (\*)

Beginning of Phase 1: September 15, 1990.

MOX mock-up : October 1990 - March 1991.

MOX-Gd mock-up : January 1991 - April 1991.

Final report : End of April 1991.

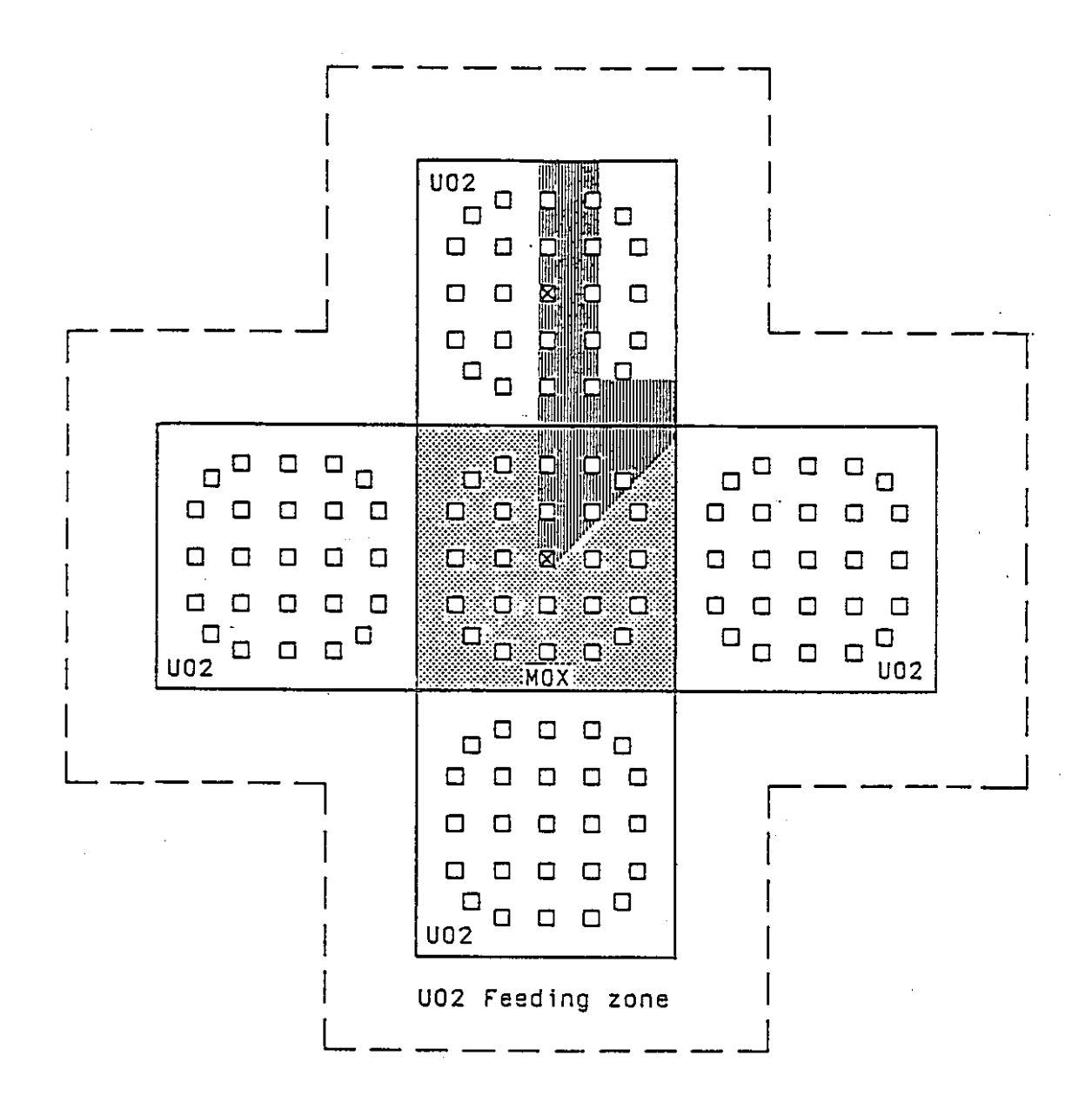
The general planning is pointed in Figure 3.

(\*) The tentative planning defined for this VIP PWR Phase 1 is based on the agreement with the VIP-BWR Phase 1 partners to interrupt for several months the VIP-BWR programme. It therefore assumes a complete unloading of one BWR configuration to perform both PWR mock-ups and a complete unloading of the second PWR configuration to start again with the next BWR configuration.

0 0 0 0 0

#### VIP - PWR (Phase 1)

#### MOX MOCK-UP



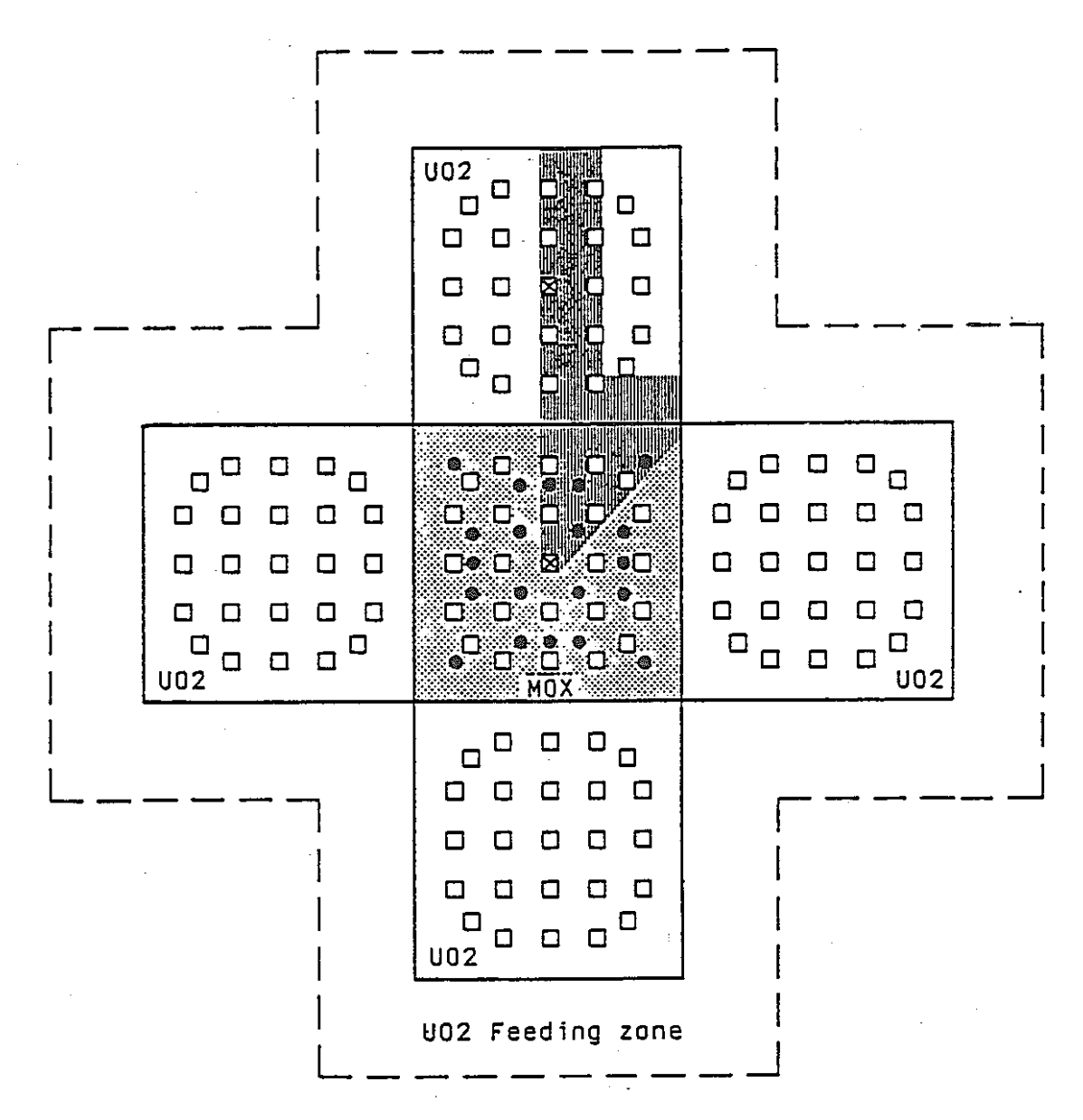
- ☑ U235 Detector
- ☐ Water hole
- 🎹 Measurement area

MEASUREMENTS :

- Critical mass
- Rodwise power distribution
- Axial buckling
- U235 detector response

#### VIP - PWR (Phase 1)

MOX Gd MOCK-UP (Preliminary)



- ☑ U235 Detector
- □ Water hole
- Gd203 U02 Rod
- Measurement area

**MEASUREMENTS**:

- Critical mass

----- - Rodwise power distribution

- Axial buckling

- U235 detector response

FIGURE 3: VIP-PWR Phase 1 - General Planning

| 1989 |                 |          | 1990 |          |   |          |          |          |              |              |   | 1991 |          |   |                     |   |              |
|------|-----------------|----------|------|----------|---|----------|----------|----------|--------------|--------------|---|------|----------|---|---------------------|---|--------------|
| N    | D               | J        | F    | М        | A | М        | J        | J        | Λ            | s            | 0 | N    | D        | J | F                   | М | A            |
|      |                 |          |      | -        |   |          |          | <b> </b> |              | <del> </del> |   |      |          |   | ,                   |   |              |
|      |                 | 1        |      |          |   |          |          |          | <del> </del> | -            |   |      | <u> </u> |   |                     |   | <del> </del> |
|      |                 |          |      |          | - |          |          |          |              |              |   |      |          |   |                     |   |              |
|      |                 |          |      |          |   |          |          |          |              |              |   |      |          |   |                     |   |              |
| -    |                 |          |      |          |   |          |          |          |              |              |   |      |          |   |                     |   |              |
|      |                 |          |      |          |   |          |          |          |              |              |   |      | į        |   |                     |   |              |
|      |                 |          |      |          |   |          |          |          |              | <del> </del> |   |      |          |   |                     |   |              |
|      |                 |          |      | :        |   |          |          |          |              |              |   |      |          |   |                     |   |              |
|      |                 |          | . :  |          |   |          |          |          |              |              |   |      |          |   |                     |   | ┦—           |
|      |                 |          | <br> | <br>     |   |          |          |          |              |              |   |      |          |   |                     |   | <u> </u>     |
|      | - بالمحدودة الم |          |      |          |   |          |          |          |              |              |   | -    |          |   |                     |   | <u> </u>     |
|      | -               | <b> </b> |      |          |   |          |          |          |              |              |   |      |          |   |                     |   |              |
|      |                 |          |      |          |   |          |          |          |              |              |   |      |          |   |                     |   |              |
|      |                 |          |      |          |   |          | <u> </u> |          |              |              |   |      |          |   | · <del>······</del> |   | _            |
|      | <b> </b>        | <b> </b> |      | <u> </u> |   | <u> </u> | <u> </u> | <u> </u> | <u> </u>     |              |   |      |          |   |                     |   | <del></del>  |

NEACRP-A-1055 Topic 1.1

# 93rd NEACRP MEETING PARIS OCTOBER 15-19, 1990

## PLUTONIUM RELOAD EXPERIENCE AND PERSPECTIVE IN FRENCH PWR PLANTS

by

M. ROME\*, M. SALVATORES\*\*, J. MONDOT\*\*, M. LE BARS\*

- \* EDF
- \*\* CEA

October 1990

#### INFORMATION ABSTRACT

Spent fuel reprocessing has been chosen in France since the beginning of the French nuclear program.

Plutonium recycling in French PWR plants was decided in june 1985.

A generic safety report for plutonium recycling, established by FRAGEMA for EDF 900 MW PWR, at the end of 1986, demonstrated the feasability of MOX recycling with 30 % maximum ratio of MOX assemblies in each reload for one third of the core annual cycling.

A first reload of 52 assemblies including 16 MOX assemblies was introduced in ST LAURENT B1 in november 1987. At the beginning of 1990, seven MOX reloads of the same type were introduced in 4 reactors. This program should affect up to the 16 EDF 900 MW PWR for which the authorization of plutonium recycling was attributed.

This paper describes a two-year experience of plutonium reload operation in 900 MW PWR now acquired in France.

## PLUTONIUM RELOAD EXPERIENCE AND PERSPECTIVE IN FRENCH PWR PLANTS

#### 1 - INTRODUCTION

A significant amount of plutonium from PWR spent fuel reprocessing is available in France. Due to the FBR (fast breeder reactor) program delay, this amount is sufficient to allow for the plutonium recycle in a large part of french PWR plants.

Following the french policy of spent fuel reprocessing, the plutonium recycle presents two main interests:

- reduction of natural uranium needs for PWR plants,
- temporary solution for the plutonium storage during the intermediate period before the FBR program economic interest is demonstrated.

Plutonium recycling in French PWR plants was decided in june 1985.

A generic safety report for plutonium recycling was established by FRAGEMA for EDF 900 MW PWR at the end of 1986. It demonstrates the feasability of MOX recycling with 30 % maximum ratio of MOX assemblies in each reload for one third of the core annual cycling.

In october 1987, EDF received the Safety Authority agreement to load MOX in 900 PWR.

A first reload of 52 assemblies including 16 MOX assemblies was introduced in ST LAURENT B1 in november 1987 (cf. Table 1).

A second MOX reload of the same type (except for the plutonium concentration) was introduced in 1988 in this reactor so long as a first Pu reload was introduced in ST LAURENT B2, the same year.

Three MOX reloads were introduced in 1989: one in ST LAURENT B2 and two in GRAVELINES 3 and 4. A third MOX reload was introduced in ST LAURENT B1 at the beginning of 1990.

One may thereby notice that this reactor will reach the equilibrium MOX core in 1990.

This program should affect up to the 16 EDF 900 MW PWR for which the Authorization of Plutonium recycling was attributed.

A two-year experience of Plutonium reload operation in 900 MW PWR is now acquired in France.

#### This paper describes:

- neutronic calculations organization and methods,
- critical experiments performed by CEA,
- available neutronic calculations and measurements of PWR MOX cycles obtained by EDF,
- available radiation measurements during MOX cycles in french PWR plants,
- MOX fuel behaviour,
- economic aspect and EDF program.

#### II - NEUTRONIC CALCULATIONS ORGANIZATION AND METHODS (Ref 1)

Within the French nuclear organization for licensing with respect to Safety Authority, the fuel reloads are calculated by two independant computer codes systems using EDF and FRAMATOME neutronic codes.

This allows cross checking and verification insuring guarantee of safety.

The justification of the reload studies with respect to Safety Authority falls within the responsibility of EDF.

The shift of neutronic spectrum to higher energies with MOX assemblies lead to the following changes:

- plutonium neutronic absorption in thermal range higher than uranium's one,
- higher critical boron concentration,
- lower boron efficiency,
- more negative moderator temperature coefficient,
- lower antireactivity of RCC.

To accommodate the first characteristic, a zoned MOX assembly is used with three concentric zones of increasing plutonium concentration from the periphery to the center of the assembly to avoid power peaks in the boundary with the neighbouring uranium assemblies (Cf. Fig 1).

To compensate lower boron efficiency, boron concentration of RWST (refueling water storage tank) is increased from 2000 ppm to 2400 ppm and boron concentration of boric acid make-up tanks is increased from 7000 to 7500 ppm.

Lower RCC antireactivity with plutonium recycle was anticipated by 8 Pu non equipped RCC in upper head core vessel internals of 16 900 MW PWR.

Two RCC dispositions are taken for plutonium recycle (Cf. Fig 2):

- reoptimization of RCC positions: SA bank (4 RCC) set in core periphery Pu RCC positions leading to 200 pcm hot shut-down margin increase,
- increase of RCC number (53 to 57): 4 new RCC's are set in core center Pu RCC positions giving 300 pcm hot shut-down margin increase.

MOX reloads are calculated by EDF using the same cross-section set and codes as for UO<sub>2</sub> reloads:

- CEA 1979 cross-section set (from ENDF/B 3 and 4, UKAEA 1973 and CEA sources),
- APOLLO 1 for cell calculations (Ref 2),
- LIBELLULE 3 for axial calculations (Ref. 3),
- JANUS 3 for xy calculations (Ref. 4),
- COCCINELLE for 3D calculations (Ref. 5).

However, it was necessary to use a different mesh distribution in the assembly for MOX reload JANUS xy calculations ( $8 \times 8$  in MOX reload instead of  $4 \times 4$  in UO<sub>2</sub> reload) to represent more accurately the zoning of the MOX assemblies (with three zones of different plutonium enrichments as shown on fig. 1).

The ability of predicting the power distribution and the fission chamber activity in U-PuO2 lattice, with EDF and FRAMATOME codes and methods, was investigated through EDF and FRAMATOME participations in critical experiments made by CEA in the reactors of MINERVE and EOLE in CADARACHE.

#### III - CRITICAL EXPERIMENTS PERFORMED BY CEA

#### 3.1 - MINERVE AND ERASME L

EDF and CEA decided in 1987, prior to the first loading of MOX in ST LAURENT B1, to validate experimentally the calculational tools to be used for determining power distributions throughout flux maps measured in PWR partially loaded with recycled plutonium assemblies.

For this purpose a special measurement program was carried out in the MINERVE experimental reactor which operates at cold temperature (20° C) and atmospheric pressure. Pin by pin power distributions were determined in a small core with a central zone of 4 % Pu MOX pins (11 x 11) surrounded by 3 % enriched UO<sub>2</sub> pins.

The power distribution was measured using a classical gamma scanning technique, across the interface between UO<sub>2</sub> and MOX zones. In parallel, measurements were performed with U235 fission chambers similar to those used for in-core instrumentation in PWR reactors. These chambers were placed in the center of the MOX zone and in the symetric position with respect to the interface in the UO<sub>2</sub> zone.

These measurements allowed us to validate our calculational schemes concerning the relative values of the power/activity ratio in MOX and UO<sub>2</sub> assemblies.

At the same time, in the EOLE experimental reactor which operates at cold temperature (20° C) and atmospheric pressure, the ERASME/L configuration was available.

ERASME was an extensive program devoted to studies on the HCLWR (High Conversion LWR) concept (Ref. 6).

The last stage of this program, referred to as L (standing for large with respect to the moderating ratio), was also aimed at validating the calculational schemes for Pu recycling in PWR's.

The core was loaded with about 1600 MOX pins (11 % Pu) with a moderating ratio of 2.1 and an active length of 80 cm.

Data concerning such parameters as:

- multiplication factors,
- spectrum index,
- worth of several absorbers, etc,

were obtained from this experiment.

At the end of the program, a power/activity measurement similar to the one performed in MINERVE was repeated in the ERASME/L core to determine the trend of variation of uncertainties with respect to the plutonium enrichment.

The power distributions obtained with EDF codes and methods, in the MOX zone and in the transition zone UO<sub>2</sub>-MOX, are as good as UO<sub>2</sub> ones as shown on figures 3 and 4. Thus, the same fine power uncertainty of 3 % already applied to UO<sub>2</sub> assemblies, is applied to MOX assemblies in EDF calculations.

For the movable fission chamber activity in MOX lattice, a temporary bias has to be applied to detector cross sections in EDF calculations to counterbalance the rough modelisation of the transport-diffusion equivalence in the instrumentation cell. An improvement of this modelisation is in progress.

As this problem is not completely solved, a 2 % uncertainty factor increase is applied to MOX assemblies power peak obtained from core flux map, in agreement with Safety Authority.

In parallel, since 1987, physicists from CEA, FRAMATOME and EDF have collaborated in a study of the possibility of reducing the remaining uncertainties in a mixed UO<sub>2</sub>-MOX loaded PWR core. The object of this exercice was to ensure the same core performance as a classical UO<sub>2</sub> core, with of course, the same safety criteria.

PNC TN9600 90-013

This group concluded that available experimental programs were not representative enough to lead to a real reduction of the uncertainties, mainly for the calculation of power peaks.

Thus, a new experimental program named EPICURE was decided in 1988.

#### 3.2 - THE EPICURE PROGRAM

The EPICURE program in the EOLE experimental reactor started in july 1989. Its main characteristic is to represent as close as possible the physical and neutronic conditions encountered in a mixed loaded PWR core (Ref. 7).

The fuel pins, especially constructed for this experiment, are exactly the same as those for a power reactor, except, of course, the length (80 cm) and the internal pressure (atm).

The composition of the fuel pins is as follow:

1500 UO<sub>2</sub> pins (3.7 % 235U)

( 200 with 4.3 % Pu 2000 MOX pins ( 1600 with 7.0 % Pu ( 200 with 8.7 % Pu

The three Pu enrichments will allow us to study the real neutronic environment of a three zones MOX assembly, designed to minimise the power peak near the MOX-UO<sub>2</sub> interface. UO<sub>2</sub> and MOX enrichments were chosen to be representative also of future core management (ie 1/4 loading and high burn-up).

The fuel pins are over-cladded to match, in the experiment, the moderating ratio of a PWR core at operating conditions (water density effect).

A number of configurations like the one presented on the fig. 5, will be devoted to pin by pin power measurements with fission chamber measurements in the center of assemblies. "Checkerboard" configurations will also be studied.

In addition, fundamental parameters such as:

- multiplication factors,
- effective fraction of delayed neutrons,
- temperature coefficients (spectrum and water density effects),
- worths of several absorbers (single or in a cluster),
- local void effect, bowing effect on power distributions will be investigated successively in clean UO<sub>2</sub> and MOX cores.

The EPICURE program, planned to last up to three years, will give us a solid experimental basis to assess present uncertainties and will allow us to reduce uncertainties through improvements in both:

- basic nuclear data,
- algorithms, models and calculational schemes.

## IV - AVAILABLE NEUTRONIC CALCULATIONS AND MEASUREMENTS OF FRENCH PWR MOX CYCLES (1/3 CORE RELOAD) (Ref. 1)

The 30 % MOX reloads which are considered consist of:

- 36 enriched uranium assemblies (UO<sub>2</sub>),
- 16 mixed oxide assemblies (MOX),

according to the third of the core annual fuel management.

The average plutonium concentration of the MOX assemblies in the tail uranium (0.225 %) matrix was chosen to obtain the same natural cycle length as an entire UO<sub>2</sub> reload (3.25 % U235) and varies according to the plutonium origin (isotopic composition) cf. tables 1 and 2.

The MOX fuel assembly structure is the FRAGEMA AFA 17  $\times$  17. The average UO<sub>2</sub> and MOX fuel discharge burn.up is 33 Gwd/t.

The available results concern the first two MOX cycles in ST LAURENT B1 and first MOX cycle in ST LAURENT B2 and GRAVELINES 3.

#### 4.1 - MOX CYCLES START-UP TESTS AT ZERO POWER

These tests include usual start-up tests and specific first MOX cycles tests.

Three types of tests were performed:

- critical boron concentrations all rods out, R bank inserted and grey banks inserted,
- isothermal coefficients during the same conditions,
- control rod worths of R bank (using dilution measurement method) and other RCC banks (using RCC banks exchange measurement method).

RCC banks and MOX assemblies positions are given figure 6.

Deviations between EDF calculations and measurements are given in table 3.

All the deviations meet design criteria:

- ΔCB calculation-measurement < 50 ppm</li>
- Δα iso calculation-measurement < 5.4 pcm/°C</li>

with an exception concerning G1 bank worth at GRAVELINES 3 which exceeds slightly 10 %.

Table 3 shows that SD1 bank which is inserted in MOX assemblies is as well calculated as banks inserted in UO<sub>2</sub> assemblies.

#### 4.2 - MOX CYCLES FLUX MAPS AT FULL POWER

According to the standard out-in strategy, the reload constituted by the new fuel assemblies is loaded in the periphery of the core. However new MOX assemblies are not loaded immediately near the baffle in order to minimize their contribution to the vessel fluence (fig. 6).

In the loading pattern, three of the new MOX assemblies have movable detectors (fission chambers). During the second MOX cycle, irradiated MOX assemblies are located in the center of the core and four of them have movable detectors.

A 3 % increase is applied to the cross sections of MOX assemblies movable detectors in EDF calculations, based on MINERVE experimental reactor results (cf. 3.1).

Deviations between EDF calculations and measurements of integrated activities, after azimutal tilt correction, are given in fig. 7 for each percentage of deviation in instrumented MOX assemblies.

The average deviation is around 0 (- 0.75 %) and the range of deviation (- 5 %, 3 %) is similar to that of UO<sub>2</sub> cores.

Power peak factors, obtained from the first core flux maps at full power, are given in table 4 for the four MOX cycles already run or in progress and compared to design or safety criteria.

Following data are indicated:

- power peaking factor (FQ) taking into account 8.6 % uncertainty factor (including 1 % increase of the technological factor for MOX assemblies), compared to 2.35 (LOCA limit),

- hot channel factor (F $\Delta$ H) taking into account 4% uncertainty factor, compared to 1.55,
- radial power peaking factors (Fxy(z)) in upper part (40 %) and lower part (60 %) of the core compared to design criteria.

Power peak values met all the criteria with reduced margins at GRAVELINES 3 (1st MOX cycle) and more particularly at ST LAURENT B1 (2nd MOX cycle) due to the 2% uncertainty factor increase applied to MOX assemblies power peak obtained from core flux map, since october 1988, and the relatively high azimutal tilt (2.4%) which is less than tilt value taken into account in accidents analysis (3%) but nethertheless increases the power peaking factors.

#### 4.3 - <u>CRITICAL BORON CONCENTRATIONS VERSUS CORE CYCLE</u> IRRADIATION AT FULL POWER

Critical boron concentration versus core cycle irradiation at full power is given in fig. 8 for ST LAURENT B1 (1st MOX cycle).

Calculation-measurement agreement is excellent for ST LAURENT B1 (1st MOX cycle) and is in the range +/- 40 ppm for the three other MOX cycles, which is not different from standard UO<sub>2</sub> cycles.

## V - AVAILABLE RADIATION MEASUREMENTS DURING MOX CYCLES IN FRENCH PWR

Plutonium recycle doesn't induce any new risk of radiation in PWR plants as plutonium is already generated in standard UO<sub>2</sub> assemblies during their irradiation, the risk is only different because plutonium concentration in MOX assemblies is always higher than UO<sub>2</sub> one.

There are two causes of irradiation increase due to the plutonium recycle:

- neutron and gamma irradiation increase due essentially to Americium 241 (low energy 60 Kev gamma emitter) during the site reception of new MOX assemblies; visual examinations are performed behind protective glass to mitigate this risk,
- alpha emitter risk increase during maintenance operations in case of fissile contamination due to MOX fuel rod rupture. Released MOX alpha activity in reactor primary coolant will be ten times higher than standard UO<sub>2</sub> one at 30 GWd/t, (cf. fig. 9) but primary coolant activity surveillance is sufficient to mitigate the risk without any change of technical specifications on this measurement.

The EDF/SEPTEN prediction of the total integrated dose for a MOX reload reception (950 mrem including 450 mrem due to the neutrons) was not reached during the first MOX reload reception at ST LAURENT B1 (550 mrem including 450 rem due to the neutrons) because americium 241 concentration obtained from plutonium 241 in MOX fuel was low due to the short time delay between plutonium production (spent fuel reprocessing) and new MOX assemblies delivery at ST LAURENT B1 in the case of this first MOX reload.

Detailed neutron dose measurements during the first MOX reload reception at ST LAURENT B1 are given fig. 10. The integrated dose of the first delivery of 8 assemblies was higher than the second one due to encountered difficulties in opening the MOX containers and higher number of participating people during the first delivery.

Presently, plutonium recycle is performed in the french PWR plants without any MOX assembly defect and no particular risk of alpha emitter due to plutonium recycle has been encountered.

This "hybrid cycle" is performed with four-batch fuel management for  $UO_2$  assemblies and three-batch fuel management for MOX assemblies, the reload will consist of 28  $UO_2$  assemblies for 4 cycles and 16 MOX assemblies for 3 cycles.

EDF and FRAMATOME will establish a generic safety report for this "hybrid cycle" at the end of 1991 and expect to obtain Safety Authority agreement to operate 900 MW PWR in this way starting in 1992.

The 900 MW PWR plants reserved for MOX recycling will then be converted from one third core annual fuel management to this hybrid cycle as soon as the documents and justifications are completed.

Plants presently planned for MOX recycling in France and dates of first MOX reload are given below:

| ST LAURENT B1 | 1987 |
|---------------|------|
| ST LAURENT B2 | 1988 |
| GRAVELINES 3  | 1989 |
| GRAVELINES 4  | 1989 |
| DAMPIERRE 1   | 1990 |
| DAMPIERRE 2   | 1991 |
| TRICASTIN 2   | 1992 |
| TRICASTIN 1   | 1992 |

The 8 other EDF 900 MW PWR for which the authorization of Plutonium recycling has been attributed, will have their first MOX reload as soon as the new MOX assemblies fabrication facility called MELOX, under construction in MARCOULE (FRANCE), is available (around 1995).

#### VI - MOX FUEL BEHAVIOUR

Several MOX fuel rods of different fabrications irradiated to 27 GWd/t in CHOOZ A (FRANCE) and 72 GWd/t in BR3 (BELGIUM) between 1970 and 1980, were examinated on site and in Research Centers in early 1980 s.

Post-irradiation analysis (neutronography, fission gaz release and clad profilometry measurements,...) were performed in CEA (SACLAY-FRANCE) and CEN-SCK(MOL-BELGIUM).

A new version of the thermo-mechanical fuel rod behaviour calculational code used by EDF, called CYRANO 2 C, was established and qualified through these experiments.

EDF participates also in different programs in experimental reactors to improve its knowledge in MOX fuel behaviour:

- PRIMO: the main objective of this BELGONUCLEAIRE program is to determine the mechanical, thermal and neutronic properties of MOX fuel rods with power histories representative of those of large PWR's following irradiation to various burn-up levels, up to a maximum of 55 GWd/t. Emphasis is placed on the behaviour under ramp conditions at MOL and at CEA-SACLAY,
- PROMOX: CEA and FRAMATOME program concerning MOX fuel rod behaviour (fission gaz release, pellet temperature versus power) in SILOE (FRANCE), (Ref. 8).

Through these experiments, EDF intends to determine MOX fuel rod PCI (pellet clad interaction) limit and to check that MOX fuel assemblies in the 900 MW PWR satisfy this limit during load follow considering that UO<sub>2</sub> assemblies power decreases whereas MOX assemblies have almost a constant power during the successive cycles due to the higher conversion factor in these assemblies.

#### VII - ECONOMIC ASPECT AND EDF PROGRAM

Considering the economic aspect of plutonium recycle, 30 % MOX recycle in three-batch fuel management, presently authorized in 900 MW PWR in France, gives a reduction of 30 % in the amount of natural uranium and separative work and a cycle cost 5 % lower than UO<sub>2</sub> three-batch fuel management (assuming a worthless plutonium, reprocessing always needed). This MOX cycle cost is still 5 % higher than the UO<sub>2</sub> "four-batch fuel management" one currently used in these reactors.

Feasibility study of "four-batch fuel management" with 30 % MOX recycling, undertaken in 1989, led to an average plutonium concentration of 6.5 %, energetically equivalent to  $UO_2$  (3.7 %), and an average MOX assemblies discharge burn-up of 46 GWd/t higher than  $UO_2$  assemblies one.

As MOX behaviour is not well known at this burn-up, in load-follow operation, EDF and FRAMATOME have investigated another plutonium recycle fuel management called "hybrid cycle" with a reduced MOX assemblies discharge burn-up which should lead to the same cycle cost as UO<sub>2</sub> "four-batch fuel management".

This "hybrid cycle" will be performed with "four-batch fuel management" for UO<sub>2</sub> assemblies and "three-batch fuel management" for MOX assemblies (the reload will be made of 28 UO<sub>2</sub> assemblies for 4 cycles and 16 MOX assemblies for 3 cycles Fig. 11).

The following table summarizes the average fuel burn-up of these MOX fuel managements.

| Type of fuel     | Equilibrium average | Equilibrium  |
|------------------|---------------------|--------------|
| management       | burn-up             | cycle length |
| Three-batch      | U:32 GWd/tM         | 290 EFPD     |
| (presently used) | MOX: 36 GWd/tM      |              |
| Hybrid           | U: 38.5 GWd/tM      | 270 EFPD     |
| (investigated)   | MOX: 34 GWd/tM      |              |

#### VIII - CONCLUSIONS

Plutonium recycling is performed in french 900 MW PWR plants with minor changes (57 instead of 53 RCCS, increase of boron tanks concentrations).

Available neutronic calculations and measurements concerning MOX cycles do not show any significant deviation (as compared to standard cycling, with uranium fuel) and all safety criteria are respected.

Moreover EDF and FRAMATOME will continue to implement and to qualify their codes and methods in U-PuO2 lattice in participating to critical experiments like EPICURE performed by CEA in CADARACHE.

Radiation measurements confirm the low expected increase of integrated dose due to the plutonium recycle in PWR plants.

Considering the economic aspects of plutonium recycle, 30 % MOX recycle in three-batch fuel management presently authorized in 900 MW PWR in France has a cycle cost 5 % higher than that of the UO<sub>2</sub> "four-batch fuel management" one currently used in these reactors.

As MOX four-batch fuel management can't be presently justified considering the limited experience of MOX fuel behaviour to high burn-up and PCI limit in load follow operation, EDF and FRAMATOME are investigating another plutonium recycle fuel management called "hybrid cycle" which should lead to the same cycle cost as UO<sub>2</sub> "four-batch fuel management".

## PLUTONIUM RECYCLE MOX RELOADS

| PLANT<br>CYCLE | ANTICIPATION (A)/ STRECH-OUT (P) | DATE OF<br>CRITICALITY | NUMBER OF MOX ASSEMBLIES PLUTONIUM CONCENTRATION |
|----------------|----------------------------------|------------------------|--------------------------------------------------|
|                | CYCLE IN EFPD                    |                        |                                                  |
| SLB 105        | P8                               | 11/87                  | 16 MOX1 / 4.5 %                                  |
| SLB 206        | P16                              | 08/88                  | 14 MOX2 / 5.1 %                                  |
|                |                                  |                        | 2 MOX1 / 4.5 %                                   |
| SLB 106        | P36                              | 12/88                  | 12 MOX3 / 5.1 %                                  |
| 322 700        | 130                              | 12,00                  | 4 MOX2 / 5.1 %                                   |
| GR 308         | P59                              | 04/89                  | 12 MOX4 / 4.5 %                                  |
| J. Sicolo      | 137                              | 04/62                  | 4 MOX3 / 5.1 %                                   |
| GR 408         | P51                              | 11/89                  | 12 MOX5 / 4.8 %                                  |
| GR 400         | 151                              | 11/09                  | 4 MOX4 / 4.5 %                                   |
| SLB 207        | P47                              | 11/00                  | 12 MOYE 14 9 01                                  |
| SLB 207        | P41                              | 11/89                  | 12 MOX6 / 4.8 %<br>4 MOX5 / 4.8 %                |
|                |                                  | _                      |                                                  |
| SLB 107        | P38                              | 02/90                  | 12 MOX 7 / 4.8 %                                 |
|                |                                  |                        | 4 MOX6 / 4.8 %                                   |
| GR 309         | P60                              | 04/90                  | 12 MOX8 / 4.9 %                                  |
|                |                                  |                        | 4 MOX7 / 4.8 %                                   |

#### TABLE 1

MOXi: MOX assemblies which are made with the Pu concentration number i

SLBioj: reload number j of SLB unit i

## PLUTONIUM RECYCLE MOX RELOAD ISOTOPES COMPOSITIONS (%)

| RELOADS           | 2,0271 | 10770  | 2.0272 | 3.607/4 | 24075  | MONG   |
|-------------------|--------|--------|--------|---------|--------|--------|
| ISOTOPES          | MOX1   | MOX2   | MOX3   | MOX4    | MOX5   | MOX6   |
| Pu 238            | 0.856  | 1.242  | 1.079  | 0.752   | 0.985  | 0.981  |
|                   |        |        |        |         |        |        |
| Pu 239            | 66.465 | 61.382 | 61.752 | 66.508  | 64.632 | 64.65  |
| Pu 240            | 20.770 | 23.155 | 23,446 | 22.178  | 22.905 | 22.942 |
| 1 4 240           | 20.770 | 25.155 | 23.440 | 22.170  | 22.703 | 22.772 |
| Pu 241            | 7.680  | 8.629  | 8.611  | 6.895   | 7.164  | 7.093  |
|                   |        |        | _      |         |        |        |
| Pu 242            | 2.954  | 4.333  | 4.032  | 2.690   | 3.316  | 3.348  |
| Am 241            | 1.276  | 1.259  | 1.080  | 0.977   | 0.998  | 0.983  |
| 1 2 - 1           | 1.270  | 1.20   | 1.000  | 0.577   | 0.220  | 0.703  |
| U 235             | 0.229  | 0.240  | 0.236  | 0.231   | 0.233  | 0.233  |
| AVERAGE PLUTONIUM |        |        |        |         |        |        |
| CONCENTRATION     | ·      |        |        |         |        |        |
| (Am + Pu)         | 4.546  | 5.116  | 5.006  | 4.554   | 4.786  | 4.761  |

TABLE 2

#### PLUTONIUM RECYCLE

### START-UP TESTS AT ZERO POWER

## DEVIATIONS BETWEEN CALCULATIONS AND MEASUREMENTS (EDF CALCULATIONS)

|               | PLANT-<br>CYCLE | SLB105   | SLB206<br>T TRANSIT | GR308           | SLB106<br>2ND<br>TRANSITION | AVERAGE  |
|---------------|-----------------|----------|---------------------|-----------------|-----------------------------|----------|
| PARAMETER-    | •               |          |                     |                 |                             |          |
| CONFIGURATION |                 | <u> </u> |                     |                 |                             | <u> </u> |
| ΔСВ           | ARØ             | - 27     | 0                   | -5              | + 32                        | 0        |
| IN            | R IN            | - 20     | + 1                 | - 11            | + 21                        | - 2      |
| PPM           | GG IN           | - 14     | - 14                | - 6             | + 24                        | - 2      |
| ΔαΙSΟ         | ARØ             | + 0.7    | - 0.8               | + 0.2           | - 0.4                       | - 0.1    |
| IN            | R IN            | - 0.3    | - 0.9               | + 0.1           | - 1.0                       | - 0.5    |
| PCM/°C        | GG IN           | + 1.5    | - 0.6               | - 0.5           | - 3.3                       | - 0.7    |
| Δρ            | R               | + 2.8    | - 2.5               | + 3.4           | + 2.3                       | + 1.5    |
| RCC           | G1              | - 5.2    | + 2.5               | <u>+ 11.2</u> · | + 1.3                       | + 2.4    |
| IN            | G2              | + 0.1    | + 3.2               | + 2.1           | + 1.5                       | + 1.7    |
| %             | N1              | + 4.2    | - 0.6               | + 2.9           | + 4.7                       | + 2.8    |
|               | N2              | + 7.7    | + 0.6               | + 4.3           | + 3.4                       | + 5.3    |
|               | SB              | + 5.1    | + 4.1               | + 5.9           | + 0.8                       | + 4.0    |
|               | SC              | - 4.3    | - 1.1               | + 4.2           | + 3.8                       | + 0.6    |
|               | SA+SD2          | + 1.9    | - 0.7               | + 1.3           | + 7.0                       | + 2.4    |
| SD1(SA        | +SD2IN)         | - 6.4    | + 4.5               | + 7.7           | + 3.1                       | + 5.4    |
| N2-1(SA       | +SD2IN)         | + 7.9    | + 4.9               | + 6.8           | + 3.1                       | + 5.7    |
|               | GG IN           | + 4.1    | - 6.4               | + 4.1           | - 0.2                       | - 0.1    |

TABLE 3

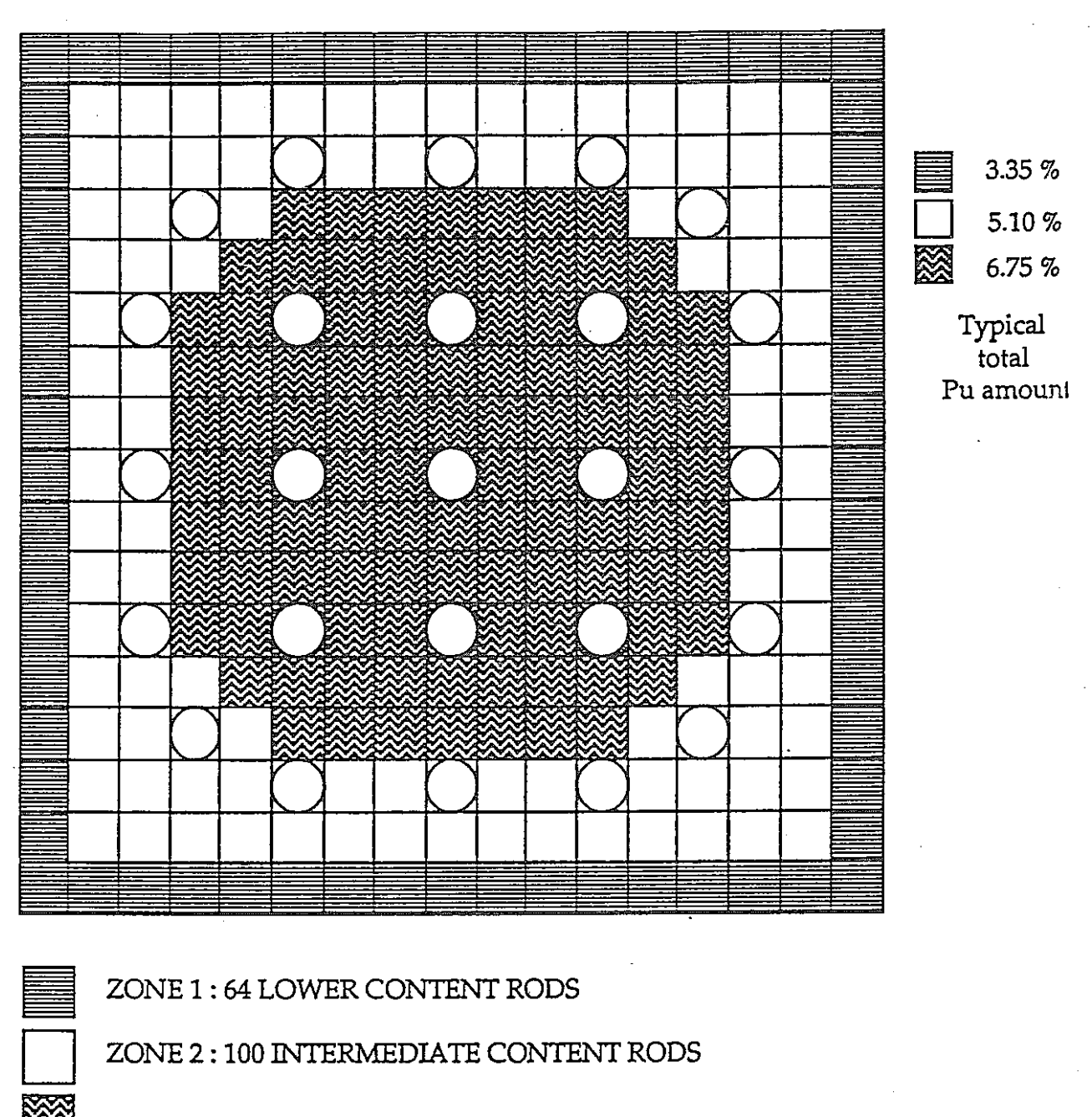
PNC TN9600 90-013 22

# PLUTONIUM RECYCLE FLUX MAPS AT FULL POWER-BOL POWER PEAK FACTORS

| PLANT-<br>CYCLE                   |        |        |       |               |          |
|-----------------------------------|--------|--------|-------|---------------|----------|
| PARAMETER                         | SLB105 | SLB206 | GR308 | SLB106        | CRITERIA |
| PARAIVIETER                       |        |        | 1     | <br>          |          |
| FQ (x 1.086)                      | 1.88   | 1.80   | 1.91* | 2.01*         | 2.35     |
| FΔH (x 1.04)                      | 1.49   | 1.46   | 1.47* | 1.53*         | 1.55     |
| MAX FXY(Z) UPPER PART OF THE CORE | 1.46   | 1.45   | 1.44* | 1.48*         | 1.56     |
| MAX FXY(Z) LOWER PART             |        |        |       |               |          |
| OF THE CORE                       | 1.44   | 1.43   | 1.46* | 1.54*         | 1.60     |
| AZIMUTAL TILT (%)                 |        |        | PNC   | TN9600 90-013 |          |
| (MAX PR - 1)                      | + 2.1  | + 1.2  | + 2.3 | + 2.4         |          |
|                                   | ·      |        |       | , i           |          |
| AXIAL-OFFSET (%)                  | - 1.7  | - 1.4  | - 4.5 | - 4.5         |          |

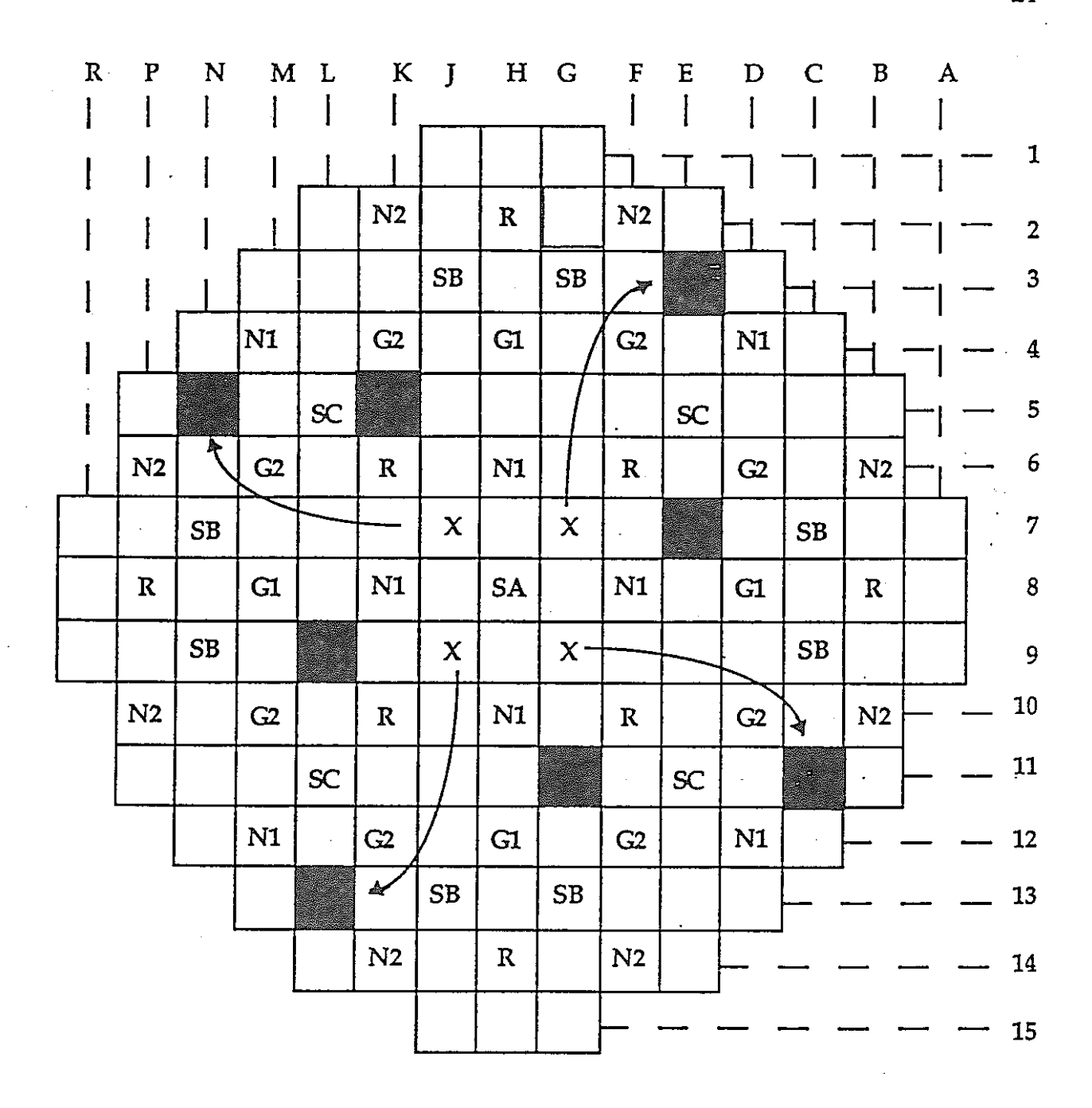
<sup>\*</sup> WITH 2 % UNCERTAINTY FACTOR INCREASE APPLIED TO MOX ASSEMBLIES PEAK

TABLE 4



ZONE 3: 100 HIGHER CONTENT RODS
GUIDES THIMBLES AND INSTRUMENTATION TUBE

FIGURE 1: MOX ASSEMBLY ZONING





Pu RCC reserved positions

FIGURE 2: RCC POSITIONS FOR Pu RECYCLE
57 RCC's

MINERVE: MELODIE B CORE

DEVIATIONS BETWEEN POWER CALCULATIONS AND MEASUREMENTS

(EDF CALCULATIONS) IN %

|            |      |     | -2.2 |      | -    |      |      |      |              |       |     |
|------------|------|-----|------|------|------|------|------|------|--------------|-------|-----|
|            |      |     |      | -1.7 |      |      |      |      |              | ·<br> |     |
|            |      |     |      |      | -2   |      |      |      |              |       |     |
|            |      |     |      |      | -0.4 | -0.3 |      |      |              |       | ·   |
|            |      |     |      | 2.6  | 3.1  | 0.4  | 0.8  |      |              |       |     |
|            |      |     | 3.8  |      |      | 1.9  |      | -0.5 |              |       |     |
|            |      | 0.8 |      |      |      | -0.3 |      |      | <b>-1.</b> 3 |       |     |
| -2.4       | -1.1 | 1   | 2.2  | 1.5  | 0.9  | 19   | -0.2 | 0.7  | -1.9         | 2.3   | 2.2 |
| <b>X</b> D | -1   | 0.1 | 2.6  | 1.7  | 0    | 2.8  | 2.4  | 1.9  | -0.6         | -0.5  | MD  |

| $\sigma = 1.8$       | transant.               |    |
|----------------------|-------------------------|----|
| 0 - 1.0              | MOX (4 % PU)            | )  |
| MD: Movable detector | UO <sub>2</sub> (3 % U2 | 35 |

FIGURE 3

MINERVE: MELODIE A CORE

DEVIATIONS BETWEEN POWER CALCULATIONS AND MEASUREMENTS

(EDF CALCULATIONS) IN %

|      |      |      | -1.2 |      |      | ·    |     |     |     |      |    |      |
|------|------|------|------|------|------|------|-----|-----|-----|------|----|------|
|      |      |      |      | -0.4 |      |      |     |     |     |      |    |      |
|      |      |      |      |      | -0.9 |      |     |     |     |      |    |      |
|      |      |      |      |      | -0.6 | -0.6 |     |     |     |      |    |      |
|      |      |      |      | 2    |      |      | 1.7 |     |     |      |    |      |
|      |      | ·    | 3.5  |      |      |      |     | 0.8 |     |      |    |      |
|      |      | 0.6  |      |      |      |      |     |     | 0.4 |      |    |      |
| -2.8 | -0.2 |      |      |      |      |      | •   |     |     | -0.7 |    | -0.8 |
| MD   | 0.4  | -0.1 | 1.5  | 0.8  | -0.4 | 0.6  | 0.7 | 1.8 | 1.1 | -0.7 | MD | -2.5 |

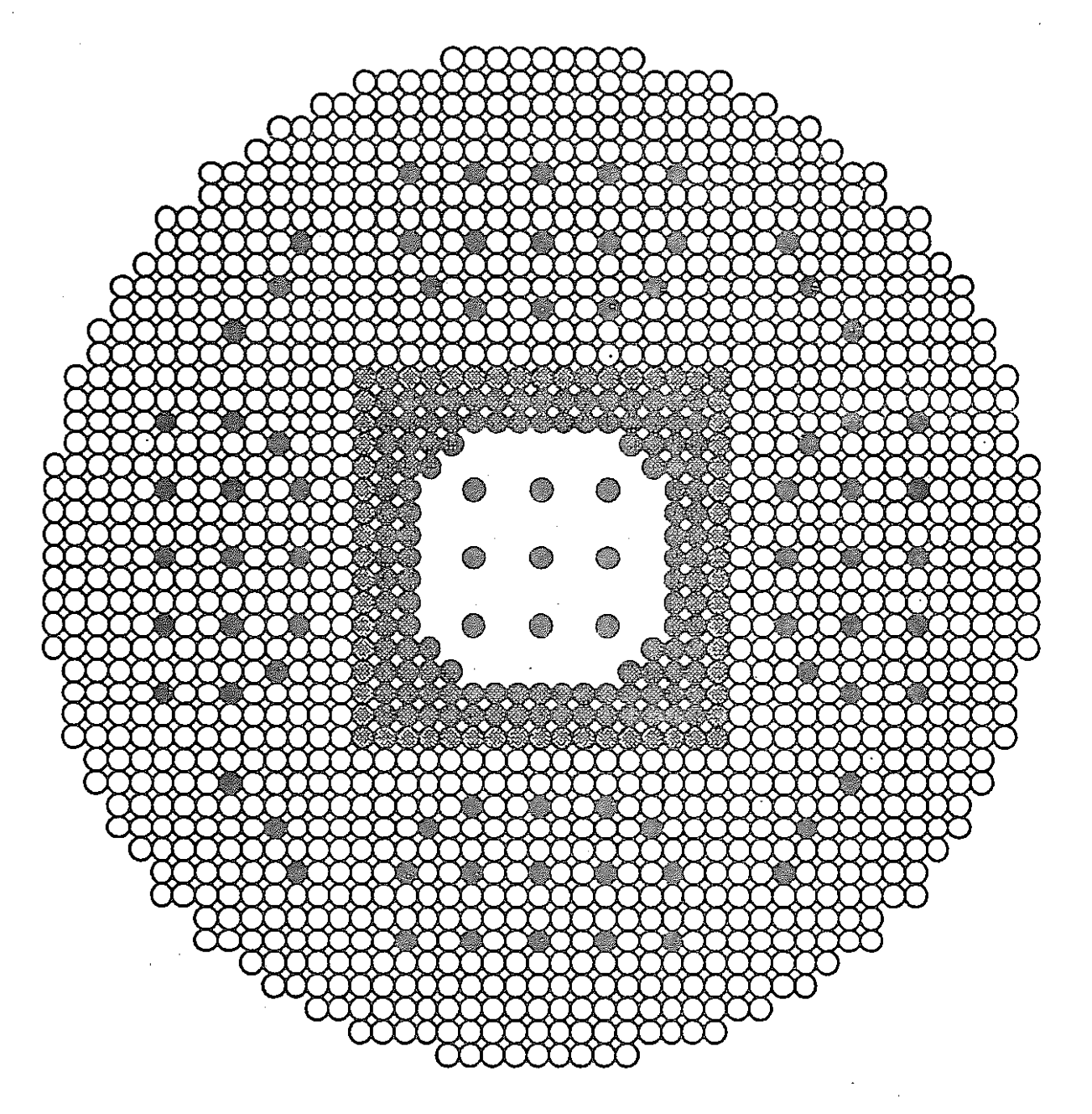
| $\sigma = 1.3$ |  | UO <sub>2</sub> | (3 % U235) |
|----------------|--|-----------------|------------|
|                |  |                 |            |

MD: Movable detector

FIGURE 4

PNC TN9600 90-013 27

# EPICURE: 3 ZONES MOX ASSEMBLY IN UO2 CORE

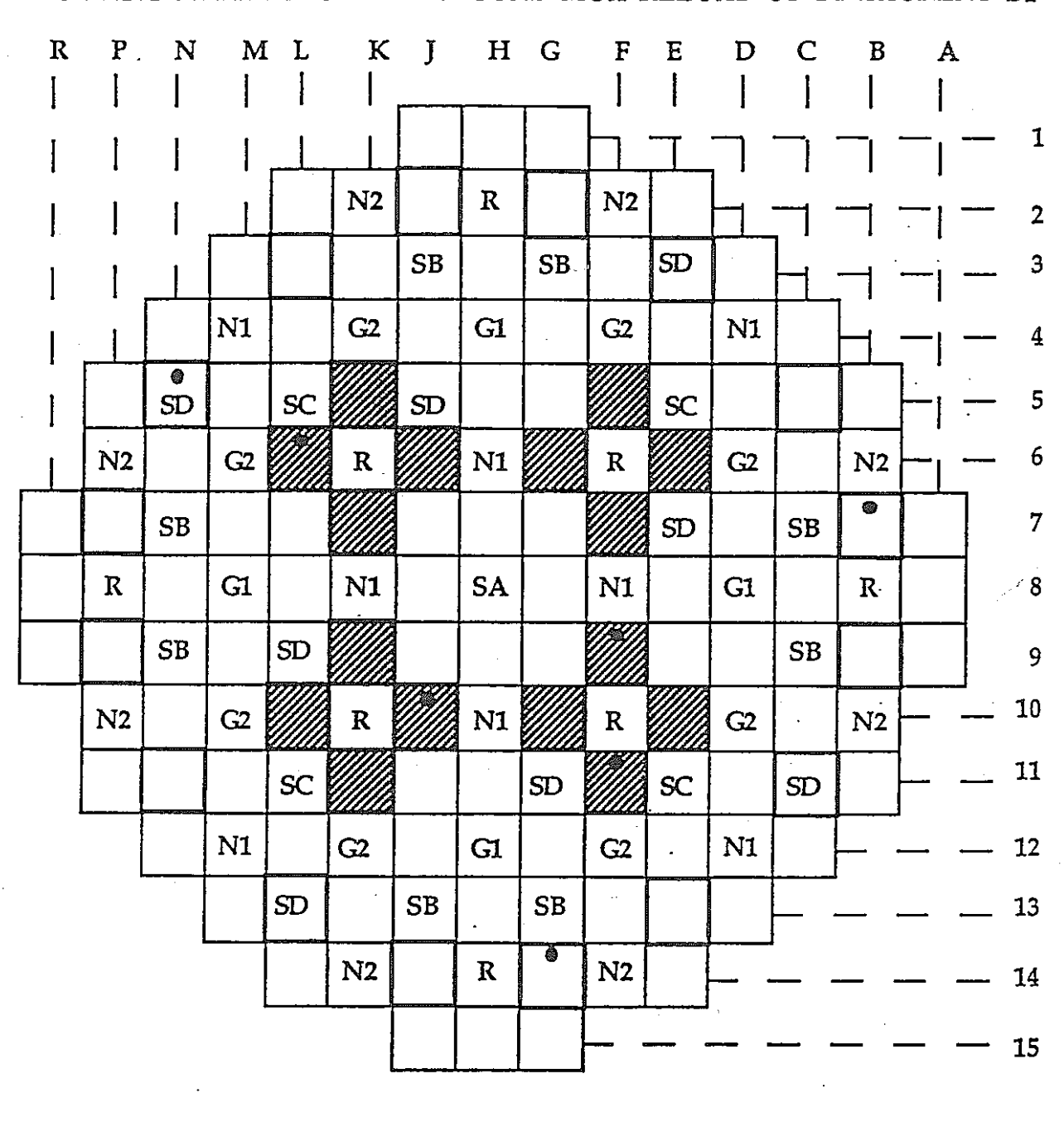


UO2 PuO2 4.3 % Pu

- **UO2** Pu02 7.0 % Pu
- UO2 Pu02 8.7 % Pu
- O UO2 3.7 % Pu
- water hole

total number of fuel pins : 1264 UO2, 264 MOX

# PLUTONIUM RECYCLING IN 900MWe PWR UNITS LOADING PATTERN OF THE SECOND MOX RELOAD OF ST-LAURENT B1

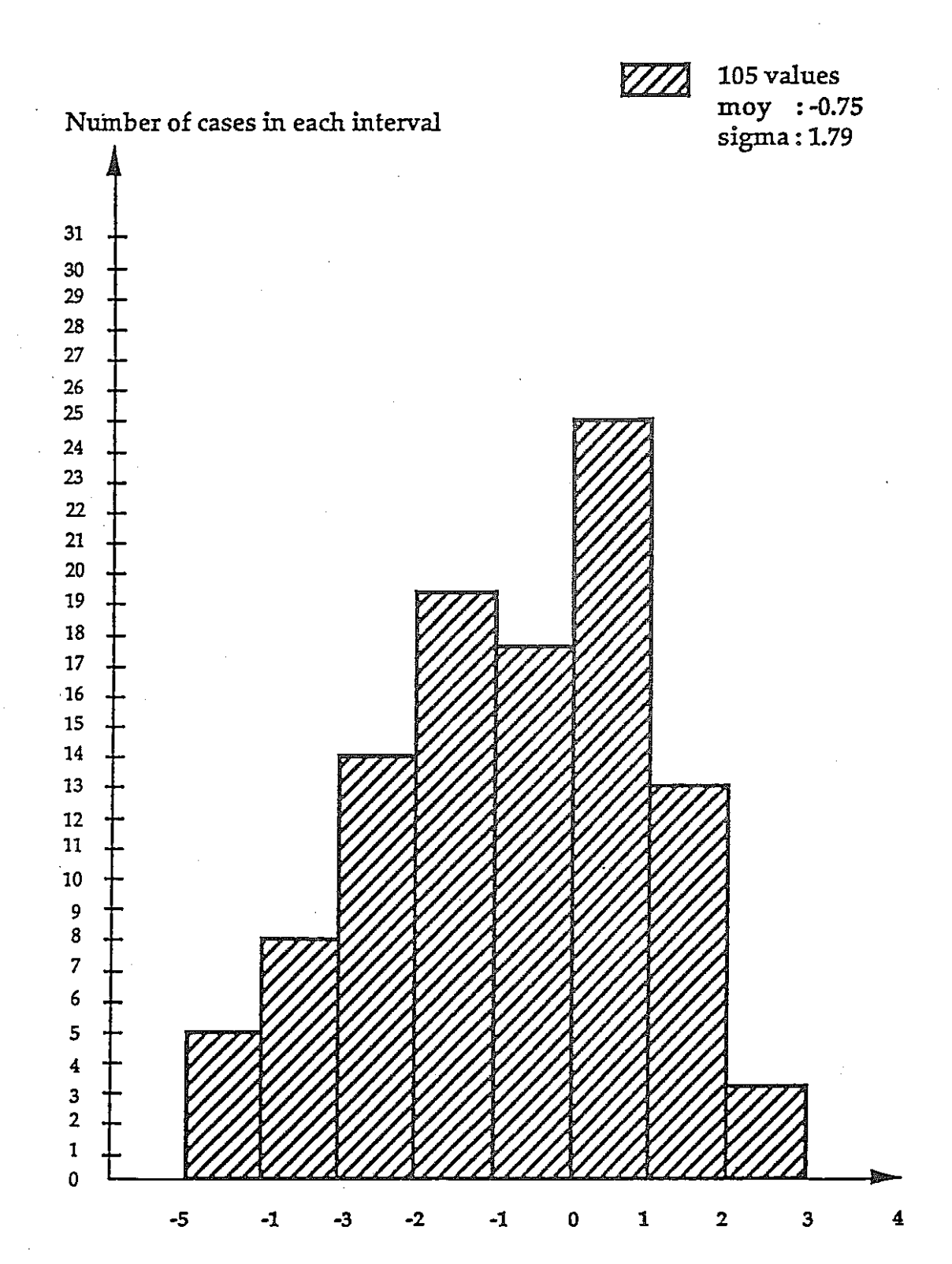


NEW MOX

INSTRUMENTED POSITION

IRRADIATED MOX (SLB106)

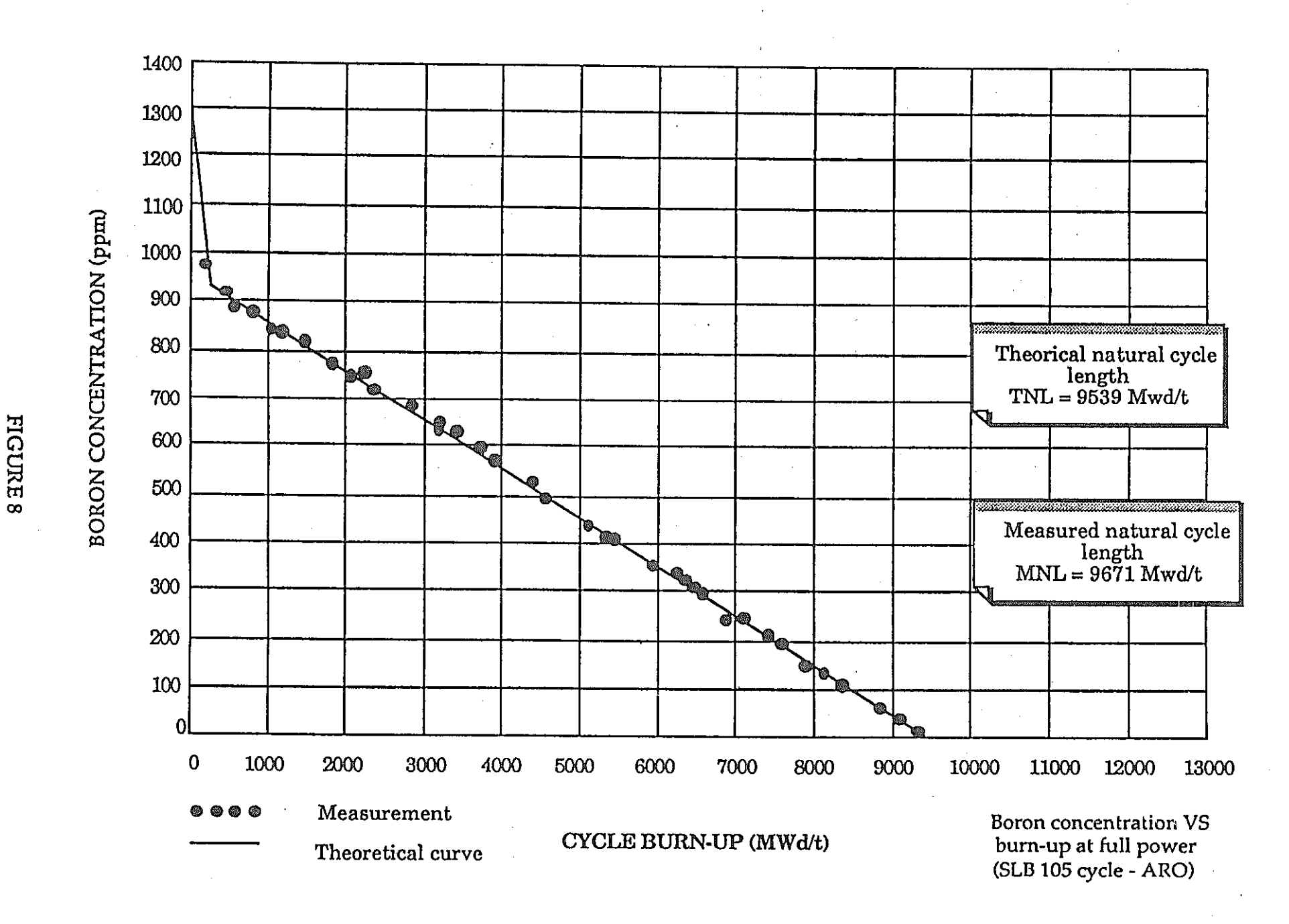
FIGURE 6



HISTOGRAM OF DEVIATIONS BETWEEN EDF CALCULATIONS AND MEASUREMENTS OF INTEGRATED ACTIVITIES AFTER-AZIMUTAL TILT CORRECTION IN %

SL105, SL206, GR308, SL106 CYCLES

FIGURE 7



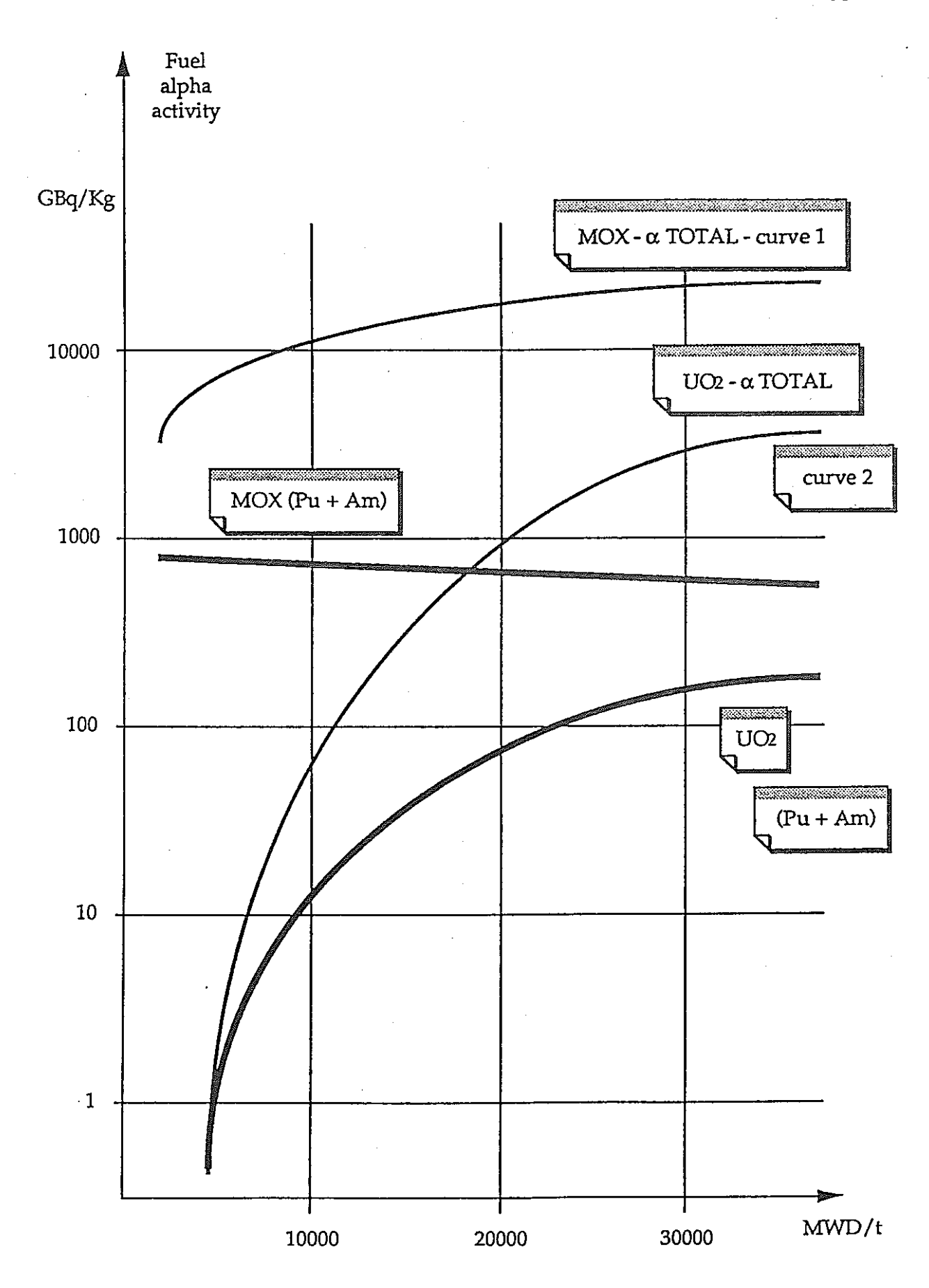
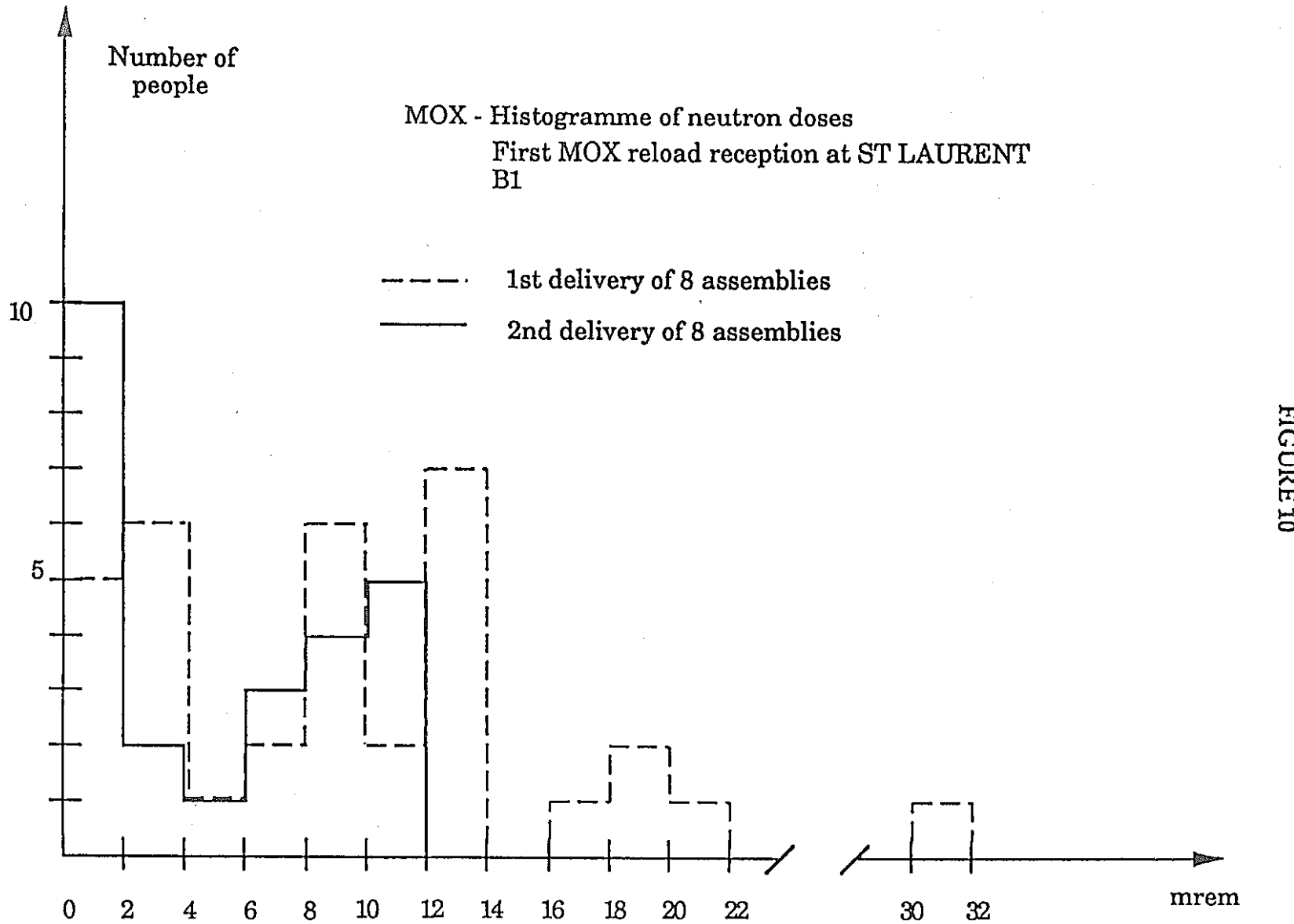


FIGURE 9: FUEL ALPHA-ACTIVITY VERSUS BURN-UP



# PLUTONIUM RECYCLING IN 900 MW PWR UNITS LOADING PATTERN OF THE HYBRID CYCLE (EQUILIBRIUM CYCLE)

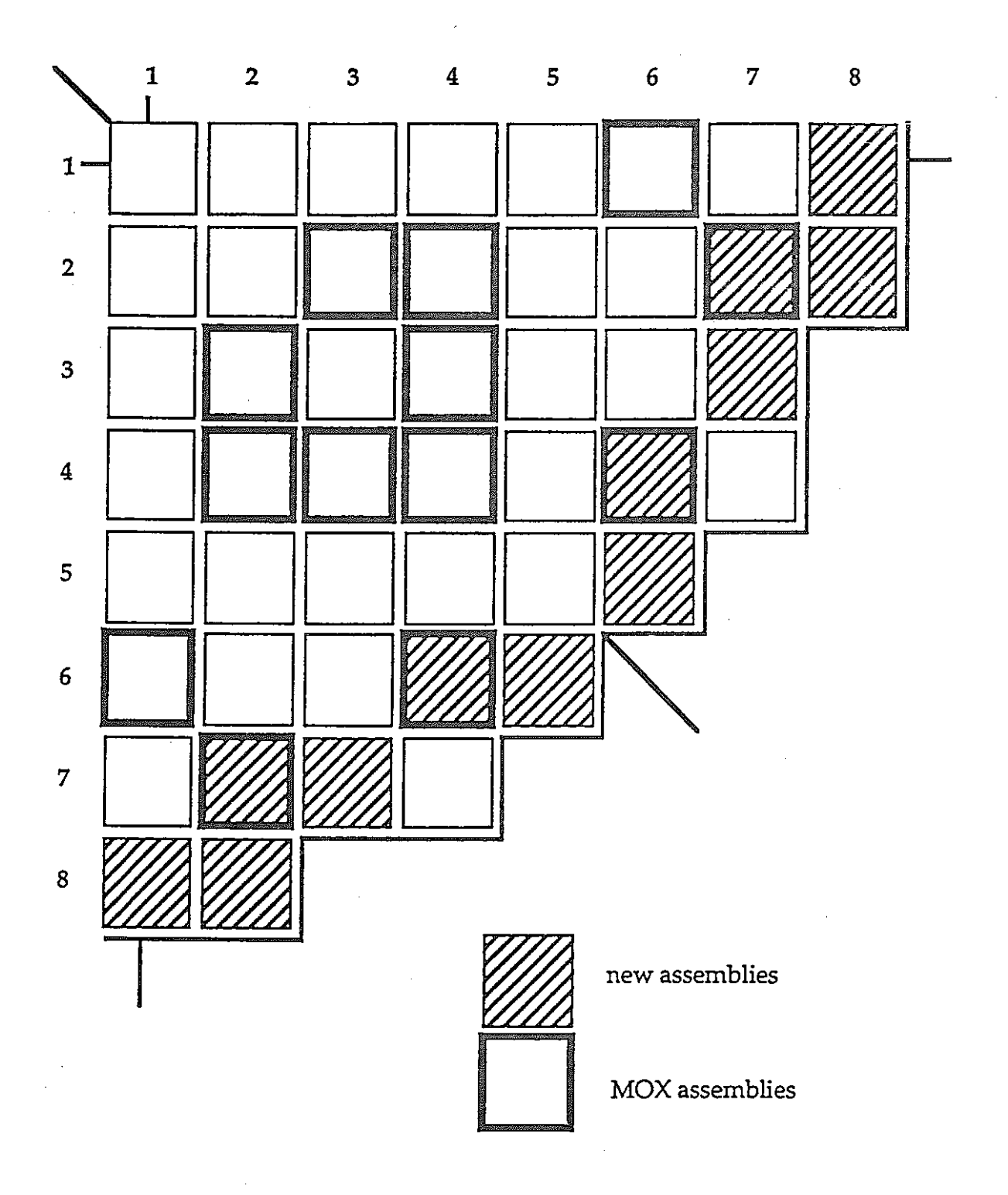


FIGURE 11

# REFERENCES

- 1 M. ROME M. FRANCILLON M. LE BARS "Plutonium Recycling Experience in French PWR plants, neutronic results" IAEA - Technical Committee Meeting - CADARACHE - November 1989
- 2 P. REUSS"APOLLO 1 Presentation Report"CEA SACLAY (France) SERMA/DIR/85-726/6 1985
- 3 J. FIORONI
  LIBELLULE 3 Presentation Report
  EDF/SEPTEN VILLEURBANNE (France) SE/T/PN 85.58 A 1986
- 4 A. VASSALLO
   JANUS 3 Presentation Report
   EDF/SEPTEN VILLEURBANNE (France) SE/T/PN 85-49 A 1986
- 5 A. VASSALLO
  COCCINELLE Presentation Report
  EDF/SEPTEN VILLEURBANNE (France) SE/T/PN 86-25 A 1986
- 6- JP. CHAUVIN G. PALMIOTTI

  ERASME: an experimental programme to validate the fundamental neutronic parameters in HCLWR spectrum

  Experiment and sensitivity analysis

  International conference on the physics of reactor: operation, design and computation "PHYSOR"

  April 23-27 1990 Maseille France Vol III, p. 1-58

7 - J. MONDOT - JC. GAUTHIER - P. CHAUCHEPRAT - JP. CHAUVIN - A. VALLEE

EPICURE: an experimental programme devoted to the validation of the calculation schemes for plutonium recycling in PWR's

International conference on the physics of reactor: operation design and computation "PHYSOR"

April 23-27 1990 - Marseille - France Vol VI p. 53

8 - A. CHOTARD - Y. MUSANTE - P. GUEDENEY - M. TROTABAS - B. GAUTIER - X. THIBAULT

PROMOX - The French RD program on MOX fuel-IAEA Technical Committee Meeting - CADARACHE - November 1989

Utilization of MOX Fuel Assembly Containing Gd<sub>2</sub>O<sub>3</sub> in ATR

Norio Kawata and Toshio Wakabayashi
Plant Engineering Office,
O-arai Engineering Center,
Power Reactor and Nuclear Fuel
Development Corp.

#### Abstract

A heavy-water moderated boiling-light-water cooled pressure tube type reactor ATR has been smoothly operated by utilizing plutonium in its core in the form of MOX fuel assemblies.

Like in light-water reactors (LWRs), Gadolinium (Gd) in fuel is useful in heavy-water reactors (HWRs) for reducing excess reactivity and power mismatching between fresh and old fuels.

In the pressure tube type heavy-water reactors where the amount of neutron absorption is small, and neutrons are moderated in the heavy water region far from the fuel region. Gd can be used in a variety of ways differing from those in LWR.

In ATR fuel assembly is composed of 28 or 36 fuel rods, which are arranged in cylindrical three layers.

In the demonstration plant of ATR under planning, several fuel rods, where fuel pellets containing 1 to 2 % Gd<sub>2</sub>O<sub>3</sub> homogeneously, are positioned in the intermediate layer and this led to the improvement of peaking due to reduction in fuel-channel power mismatching. Such fuel assembly (homogeneous Gd fuel) has been subjected to a series of irradiation tests in Fugen, the prototype reactor of ATR and results as expected in the design stage have been obtained for both fuel integrity and reactivity-controlling effect.

Moreover, many R & D projects aiming at burnup extension and high power of fuel assemblies were undertaken. O-arai Engineering Center, PNC has developed duplex-region fuel pellets, in which the outer-region and inner-region of a pellet are made of MOX and Gd<sub>2</sub>O<sub>3</sub> respectively. For adequate control of the reactivity by Gd as well as for controlling period by utilizing the shielding effect of the outer-region of pellet. The fuel assembly (Duplex pellet fuel), where the fuel rods consisting of the duplex region pellets occupy all positions allocated for the outer fuel rods of a fuel assembly, show more improved local peaking than those of the homogeneous Gd fuel. As hollow MOX pellets and inner pellets of Gd<sub>2</sub>O<sub>3</sub> is made independently in the case of Duplex pellet fuel, fissile and poison materials are not mixed in the pellet making line differing from the case of homogeneous Gd fuel. The clean-up possess for removing Gd becomes unnecessary, and degradation of fissile materials due to the inclusion

of Gd doesn't occur in the fabrication line.

## 1. Introduction

The heavy-water moderated boiling-light-water cooled pressure tube type reactor ATR has been smoothly operated by utilizing plutonium in its core in the form of MOX fuel assemblies (See Fig. 1).

In the field of fuel development, the technologies for burnup extension and higher power of fuel assemblies have been developed, aiming at reduction in fuel cycle costs and at compact cores. Gd has been adopted to reduce power mismatching between fresh and old fuel assemblies associated with burnup extension.

In ATR, since neutrons are well moderated and less absorbed in the wide heavy water (moderator) region, the dilute Gd concentrations in the fuel pellets can sufficiently reduce the excess reactivity of the fuel. In addition, as well moderated neutrons are supplied from heavy water region to fuel region, many types of burnup-extended fuel can be fabricated by arranging the positions of Gd-containing fuel rods in a fuel assembly and by employing the method of adding Gd to the fuel pellets.

This report describes the analysis of changes in the characteristics of the fuel assemblies due to the addition of Gd as the utilization of Gd-containing

fuel rods in ATR, and the irradiation results. It also introduces new types of Gd-containing fuel currently designed and studied for high-burnup fuel assemblies.

# 2. Objectives of Gd Utilization in ATR

Generally, the enrichment of fuel (in MOX fuel assembly Pu-fissile content) increases as its burnup is extended.

In ATR, as reactivity compensation due to fuel burnup is carried out by adjusting the <sup>10</sup>B concentration of heavy water (moderator), the reduction of excess reactivity, which is a main objective of Gd utilization in BWR, is not so important.

The ATR core area including the heavy water region is large. In order to make the core compact, the power per unit channel of a pressure tube is required to be as large as possible. The followings are important in aspect of core design.

- ① reduction of the radial peaking factor in the core by improvement of power mismatching between fresh and old fuel.
- 2 reduction of the local power peaking factor in fuel assembly.
- Features in Reactor Physics of ATR regarding Gd Utilization
   The prototype reactor of ATR in Fugen, the fuel assemblies are loaded into

224 pressure tubes surrounded by the heavy-water charged in calandria tank, and cooled by boiling light-water for heat removal (See Fig. 2).

As shown in Fig. 3, the shape of the fuel assembly is cylindrical three-layer type, and each assembly generally consists of 28 fuel rods. Further, the special fuel assemblies for the irradiation tests of pressure tube materials and the standard fuel assemblies (36 fuel rods per assembly) of the demonstration plant of ATR for the check of integrity of fuel assembly, have been loaded.

Figure 4 shows the fuel lattice structures of ATR and BWR. In ATR, the heavy water region independent from the fuel region is extremely wide, and its lattice structure is quite different from that of BWR, whereas in BWR the state of each fuel rod is nearly the same, thus, a single fuel rod can be approximately regarded as an unit cell for evaluation. On the other hand, since almost all of the neutrons are moderated in the heavy water region in ATR, thermal neutrons are supplied from the outside of the fuel assemblies; accordingly, the conditions for the outer, intermediate and inner fuel rods are relatively different.

Figure 5 gives the neutron spectra of the ATR fuel assemblies located in each region.

From Fig. 5, it is clearly understood that the neutron fluxes in the heavy water region and outer fuel rods are the same in the low energy area but low in the inner fuel rods; such facts would lead to the flow of thermal neutrons from the heavy water region to the inside of the fuel assemblies. Arranging the Gd-containing fuel rods adequately in a fuel assembly permits the reduction value of reactivity and reduction period to keep on a suitable degree.

# 4. Utilization of Gd-containing MOX Fuel Assemblies in the ATR

In order to attain burnup extension and high power, the Pu-fissile content and the number of fuel rods per assembly have been increased and the radial and axial Pu-fissile content distributions in the assembly have been adjusted. In addition, the Gd-containing fuel assemblies have been employed for burnup extension.

Tables 1 and 2 show the progress in the development of the MOX fuelassemblies and the schedule of their development respectively.

4.1 MOX Fuel Assemblies (Homogeneous Gd Fuels) Containing Homogeneous UO<sub>2</sub>-Gd<sub>2</sub>O<sub>3</sub>
Fuel Rods:

Like in LWR,  $Gd_2O_3$  is homogeneously mixed with  $UO_2$  powder, and sintered into pellets. The  $UO_2$ - $Gd_2O_3$  fuel rods fabricated then by using these pellets are assembled as part of a MOX fuel assembly.

#### 4.1.1 Characteristics of Homogeneous Gd Fuel

The reduction effect of reactivity varies greatly with the positions of the Gd-containing fuel rods (See Fig. 6).

# ① Gd-containing Fuel Rods as Outer Ones

As already explained, since thermal neutrons are supplied from the heavy water region, neutron importance of the outer fuel rods is very large. Gd in outer fuel rods shows the extremely great reactivity reduction effect. Moreover, because of the rapid decrease in Gd isotopes which absorb neutrons, the reactivity reduction effect of Gd disappears and the characteristics of the fuel return to that of the base fuel which has no Gd in short term.

#### ② Gd-containing Fuel Rods as Inner Ones

Since the supply of neutrons from the heavy water side to the inner fuel rods are shielded by the outer and intermediate fuel rods, the neutron importance of inner fuel rod is smallest. Therefore, if a few Gd-containing fuel rods are used as part of the inner fuel rods, then the reactivity-reduction effect of Gd is low, and Gd remains till end of cycle without diminishing, leading to lower discharged burnup.

#### 3 Gd-containing Fuel Rods as Intermediate Ones

Although the reactivity reduction effect of Gd is lower than that of the outer fuel rods, Gd disappears slowly and the reactivity reduction effect lasts

in a some degree.

The Gd content of pellets should be determined in such way that all of Gd disappear in the end of a cycle not to decrease the discharged burnup of fuel. The degree of reactivity reduction, moreover, is controlled by the number of the Gd-containing fuel rods located in the intermediate fuel layer.

# 4.1.2 Design of Homogeneous Gd Fuel

Figure 7 shows an example of the Gd-containing fuel assembly to be employed for the demonstration plant of ATR, and Fig. 8 gives the burnup history of the fuel. As these figures indicate, the optimum reactivity reduction has been performed by adjusting the number of the Gd-containing fuel rods located in the intermediate fuel layer and the Gd content. Figure 9 shows the radial power distribution at the beginning of cycle in the equilibrium core when the Gd-containing fuel is used and when it is not used. The power of the fresh fuel is high, but the adoption of the Gd-containing fuel tends to lower such tendency.

As explained above, in the heavy water reactor, the presence of a few low content Gd-containing fuel rods enables to reduce power mismatching between fresh and old fuel.

#### 4.1.3 Results of Irradiation of Homogeneous Gd Fuel Assemblies

The characteristics of the Gd-containing fuel in the ATR have been verified

by measurement namely, prior to their adoption in the demonstration plant of the ATR, the fuel with the same specifications was tested in Duterium Critical Assembly (DCA) to measure their nuclear characteristics (local power peaking factor, reactivity etc.) in the initial stage without irradiation. And this was followed by loading them into Fugen, in order to check the characteristic during irradiation.

The experiments in DCA indicated that even if several Gd-containing fuel rods which are very low power, located in the intermediate fuel rods, the main characteristics such as the local peaking factor could be predicted with the same accuracy as that of standard fuel.

The location of the Gd-containing fuel assemblies loaded in Fugen is shown in Fig 10. To measure the irradiation characteristics of the Gd-containing fuel assemblies in terms of time, 4 Gd-containing fuel assemblies have been loaded around the fixed in-core monitor LPM (local power monitor).

The loading pattern of the fuel assemblies in Fugen, is 90° rotating symmetry in principle and the fresh fuel assemblies in the positions of 90° rotating symmetry generally show the same burnup trend. Figure 11 shows the predicted value of power history in four fresh fuel assemblies (including one Gd-containing fuel assembly) in the position of 90° rotating symmetry together with the measured values by LPMs. In standard fresh fuel assemblies generally, neutron multiplication factor (k-eff.) decreases and channel power thereby reduces with burnup, but in the Gd-containing fresh fuel assemblies, the

reduction of neutron multiplication factor with burnup is canceled by the disappearance of Gd and the channel power increases relatively. As Fig. 11 indicates, the predicted values are in good agreement with the measured ones in both Gd-containing and standard fresh fuel assemblies. It was verified, therefore, that the burnup characteristics of the Gd-containing fuel assemblies could be analysed with high accuracy by using the design code.

4.2 MOX Fuel Assemblies (Duplex Pellet Fuels) Utilizing Duplex Pellets with Gd<sub>2</sub>O<sub>3</sub> Inner Pellets

In the aspects of reduction of reactivity, the addition of Gd to outer fuel rod homogeneously is most effective, but keeping reactivity reduction effect during burnup becomes difficult. Accordingly, in the homogeneous Gd fuel, Gd was added to the several intermediate fuel rods to make use of the self-shielding effect of a fuel assembly as a whole. Although this method can reduce the power of the fuel assembly, it has the demerit of increasing the local power peaking factor within the fuel assembly because of the low power of the several intermediate fuel rods containing Gd. In the duplex pellet fuel, the all outer fuel rods consist of the duplex pellets, and the reactivity during burnup is reduced by making use of the self-shielding effect of the pellets themselves. Since all of the outer rods are made of the duplex pellets, their power can be made uniform, and so the local peaking factor within a fuel assembly does not increase. In addition, to fabricate these pellets, for example, hollow pellets are firstly fabricated, followed by the insertion of

inner region pellet made of natural Gd<sub>2</sub>O<sub>3</sub> diluted with ZrO. Unlike the fabrication of the homogeneous Gd<sub>2</sub>O<sub>3</sub>-UO<sub>2</sub> pellets, in which the poison is mixed with fissile materials, the fuel fabrication line is not contaminated with the Gd poison. Therefore, the clean-up process for removing Gd becomes unnecessary, and degradation of fissile materials due to inclusion of Gd doesn't occur in the fabrication line.

One of the unique features of the ATR, in which thermal neutron flux takes place from the heavy-water region to the fuel assemblies, is that the power of fuel assembly is depressed by the duplex pellets in outer fuel rods. Consequently the radial power peaking of the core and local power peaking of the fuel assembly become smaller in size. The effect of this kind may be smaller in BWR in which the light-water moderator is distributed almost uniformly in the reactor core.

Figure 12 shows the cross section of the fuel assembly in which all the outer fuel rods are composed of the duplex pellets.

The nuclear characteristics of the duplex pellet fuel depend on the shape of the fuel assembly, Gd content (Gd/ (Zr+Gd)), diameter of Gd inner pellet, Pu-fissile content of MOX etc. The reference fuel assembly investigated for high burnup in this study is of multi-cluster type which consists of 54 fuel rods.

Figure 13 shows the Gd content dependency of the burnup history of keff. It indicates that the degree of reducing the reactivity in the initial stage of burnup is slightly dependent on the Gd content because of saturation effect of absorption by Gd, but that the reactivity-reducing period increases with the increasing Gd content.

The effects of the diameter of the Gd inner pellet on the characteristics of burnup reactivity are given in Fig. 14, which indicates that degree of reducing the initial reactivity can be adjusted by the diameter of the Gd inner pellet.

The fuel specifications set up this study are 48,000 MWd/t fuel average burnup and 12,000 MWd/t burnup increment per cycle, where 1.0 mm diameter of the Gd inner pellet and 70 to 100% Gd content are adequate as shown in Fig. 15 to minimize the reactivity change when Gd isotopes, which depress the power and absorb neutrons during this period would disappear.

If the increase in the degree of the reduction reactivity and the reactivity-reducing period is required due to higher burnup, this can be met by increasing both the diameter of the Gd inner pellet and Gd content.

As to the local power peaking in the fuel assembly, little difference from the base fuel with no Gd has been found and this is to be attributed to the uniform loading of the duplex pellets taking place in the all outer fuel rods. In the conventional homogeneous Gd fuel, on the other hand, increase in local power peaking is unavoidable because the power of several Gd-containing fuel rods becomes locally low in intermediate fuel layer (See Fig. 16).

Since the increase in local power peaking reduces the critical heat power due to the increase in linear heat generation rate from the viewpoint of heat removal, the duplex pellet fuel showing the uniform power distribution is more advantageous than the homogeneous Gd fuel.

#### 5. Conclusions

The development of the Gd-containing MOX fuel has yielded some progress to meet the requirement for burnup extension and high performance in ATR.

As the fuel utilizing the features of the pressure tube type heavy water reactor, the fuel assembly, in which part of its MOX intermediate fuel rods are replaced with the fuel rods using UO<sub>2</sub>-Gd<sub>2</sub>O<sub>3</sub> pellets, has been developed. Although such homogeneous Gd fuels have the demerit of increasing the local power peaking factor within fuel assembly, there can reduce total peaking factor by improvement of power mismatching between fresh and old fuel and carry out extention of burnup. Those fuel assemblies were subjected to critical experiments and irradiation tests and their performance has been verified, in Fugen.

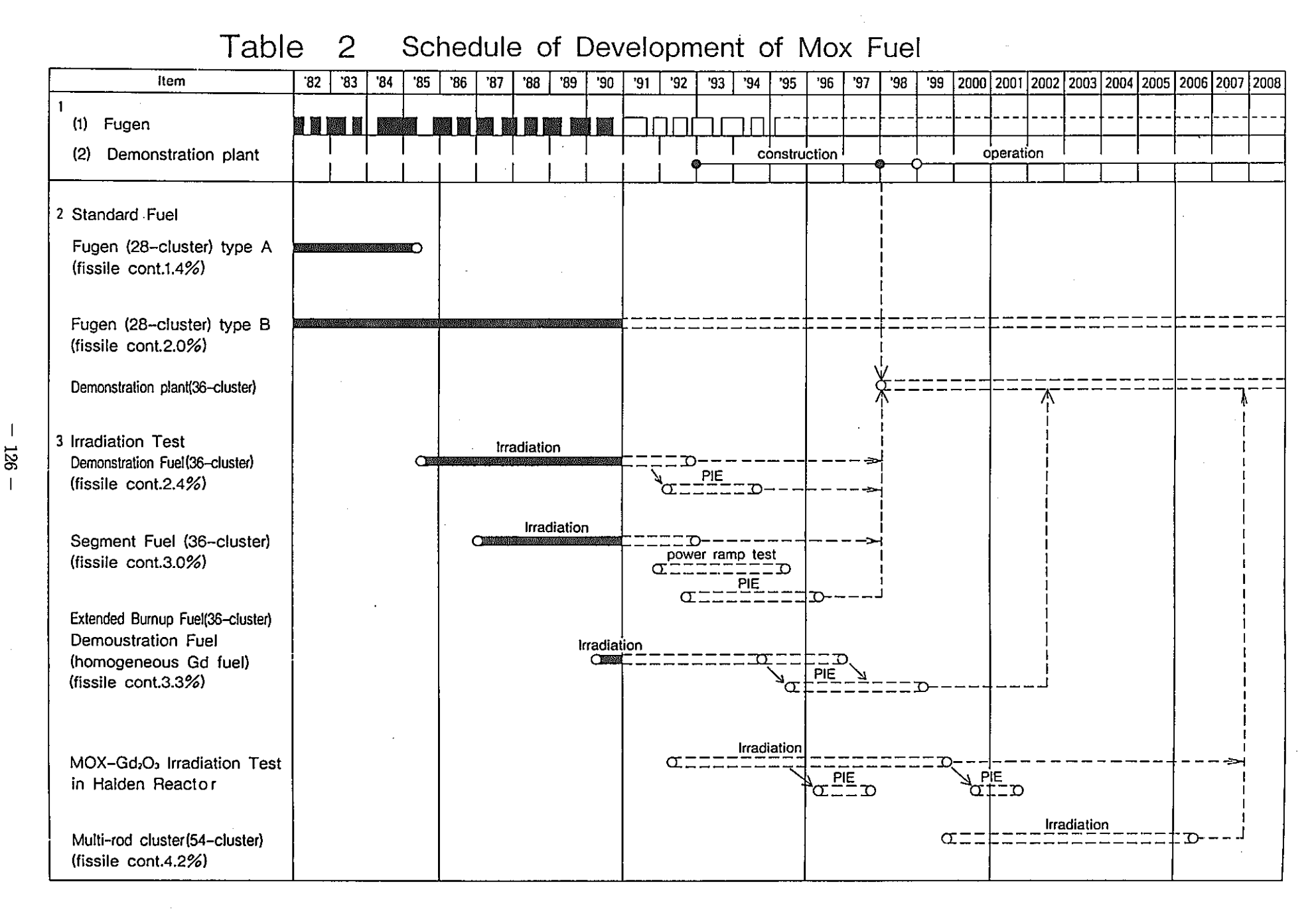
It has also been found that the duplex-pellet (inner pellet made of  $Gd_2O_3$ ) fuel rods replacing all the outer fuel rods could reduce the reactivity to a suitable degree without increasing local power peaking. Duplex pellet fuel can be applied for higher burnup fuel. Moreover, it is possible to avoid degradation of fissile materials due to the inclusion of Gd in fuel fabrication line.

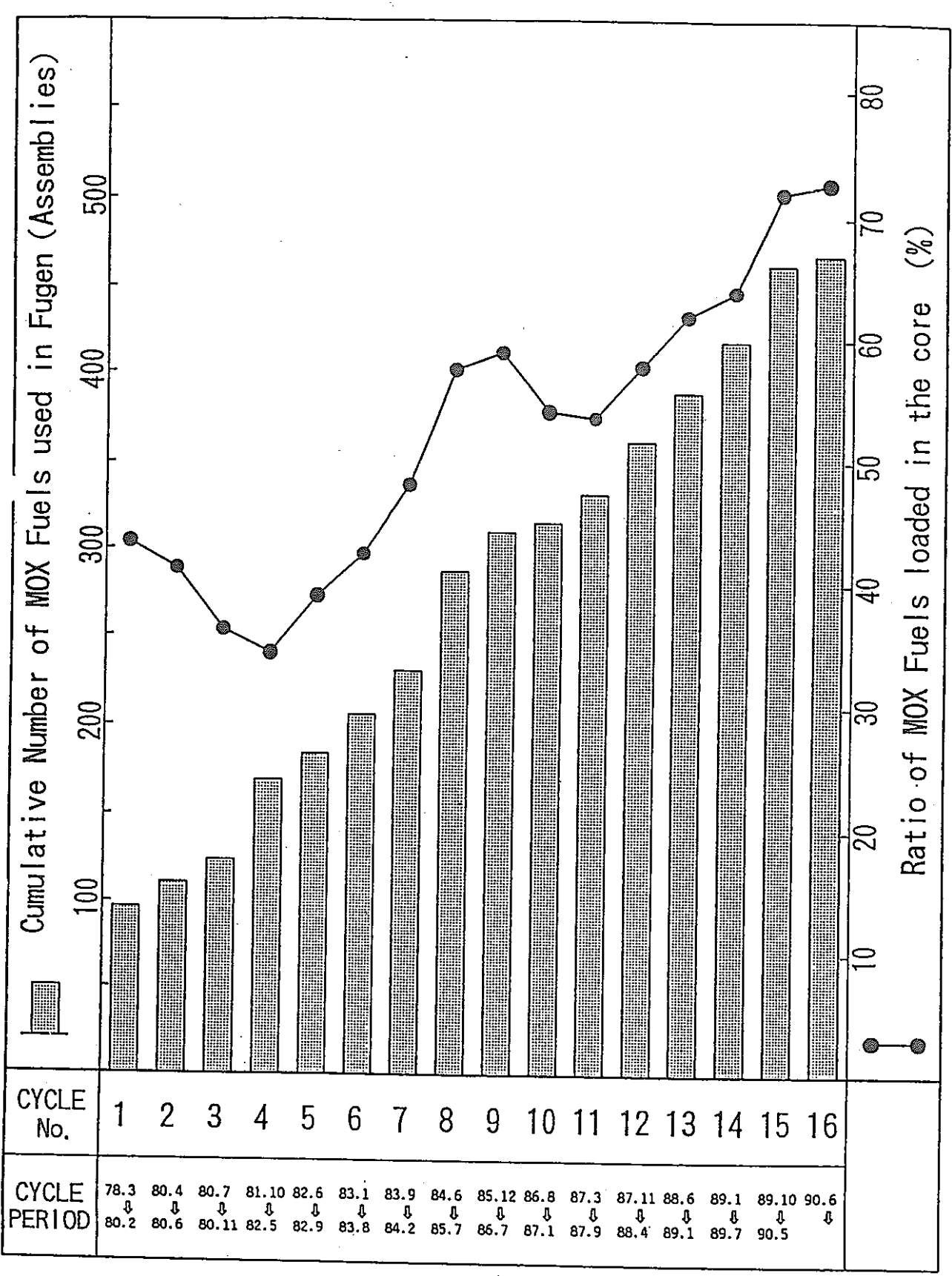
## 6. reference

- (1) S.SAWAI, "Development of a FUGEN type HWR in Japan", J.British Nucl. Energy Soc., 20, 5, 367 (1981).
- (2) Y.MIYAWAKI, S.OHTERU, Y.ASANO, "Reactor physics test of FUGEN", (Proc. 25th ANS Winter Meeting, San Francisco, 1979), Trans. Am. Nucl. Soc., 33, 760(1979).
- (3) HAGA T. KATO H., et al, "Core-Management Analysis of the Fugen Heavy Water-Moderated Plutonium-Uranium Mixed-Oxide Reactor", Nuclear Science Engineering 87, 361-380 (1984).
- (4) HAGA T. KATO H., "Physics and Control of Pu-Fueled Heavy Water Reactor Fugen", CNA Meeting, Toronto, Canada, (1973).
- (5) J.R.ASKEW, et al, "A General Description of the Lattice Code WIMS", Journal of British Nuclear Society, 5, 564 (1966).
- (6) DESHIMARU T., "Core Management of Fugen", First Annual Meeting, between Ontario Hydro and PNC. Toronto, Canada, (1988).
- (7) SHIRATORI.Y "Core Management of Fugen" Second Animal Meeting between Ontario Hydro and PNC. Tsuruga, Japan. (1989)
- (8) T.WAKABAYASHI, Y.HACHIYA, "Thermal-Neutron Behavior in Cluster-Type Plutonium Fuel Lattices", Nucl. Sci. Eng., 63, 292 (1977).
- (9) N.FUKUMURA, "Measurement of Local Power Factors in Heavy-Water Moderated Plutonium", J.Nucl. Sci. Technol. 18, 285 (1981).
- (10) T.WAKABAYASHI et al., "Characteristic of Plutonium Utilizazation in ATR", NEACRP-A744 (1985).
- (11) R.P.HARRIS. "Use of Gd in PWR extended burnup fuel cycles" Final report. CEND-397. (1982)
- (12) E.Vanden Benden. G.LeBastard. H.Bairiot. "Excellent Performance of MOX Fuel" Proceedings of an International Symposium, Good Performance in Nuclear Projects. Tokyo (1983)

Table 1 Development of Gd-containing fuel in ATR

| Fuel Type                                     | Number of fuel rods<br>per assembly | Mean fissile content<br>(235U+236Pu +241Pu)(%) | Gd-adding mode                                                                                    | Note                                                                                                                                                 |  |
|-----------------------------------------------|-------------------------------------|------------------------------------------------|---------------------------------------------------------------------------------------------------|------------------------------------------------------------------------------------------------------------------------------------------------------|--|
| Standard Fuel                                 | 28                                  | 2. 0                                           |                                                                                                   | Standard fuel of Prototype<br>reactor of ATR, "Fugen"                                                                                                |  |
| Demonstration Fuel                            | 36                                  | 2. 4                                           |                                                                                                   | Under irradiation tests in Pugen                                                                                                                     |  |
| Extended Burnup Fuel<br>(homogeneous Gd fuel) | 36                                  | 3. 3                                           | 3 to 4 intermediate fuel rods<br>consisting of pellets containing<br>0.7 to 1.4% Gd homogeneously | <ul> <li>Utilized as the replacement<br/>fuel assemblies for the demon-<br/>stration plant of ATR</li> <li>Under irradiation test in Puen</li> </ul> |  |
| Multi-cluster fuel                            | 54                                  | 4. 2                                           | G intermediate fuel rods<br>consisting of pellets containing<br>about 3% Gd homogeneously         | Design studies; In the R & D stage                                                                                                                   |  |
| Multi-cluster fuel<br>(Duplex pellet fuel)    | 54                                  | 4. 2                                           | All the outer fuel rods (24 rods)<br>consisting of the duplex pellet<br>with Gd inner pellet      | Design studies; In the R & D<br>stage                                                                                                                |  |





(Including Demonstration Fuel Assemblies)

Fig 1 MOX FUEL UTILIZATION IN FUGEN

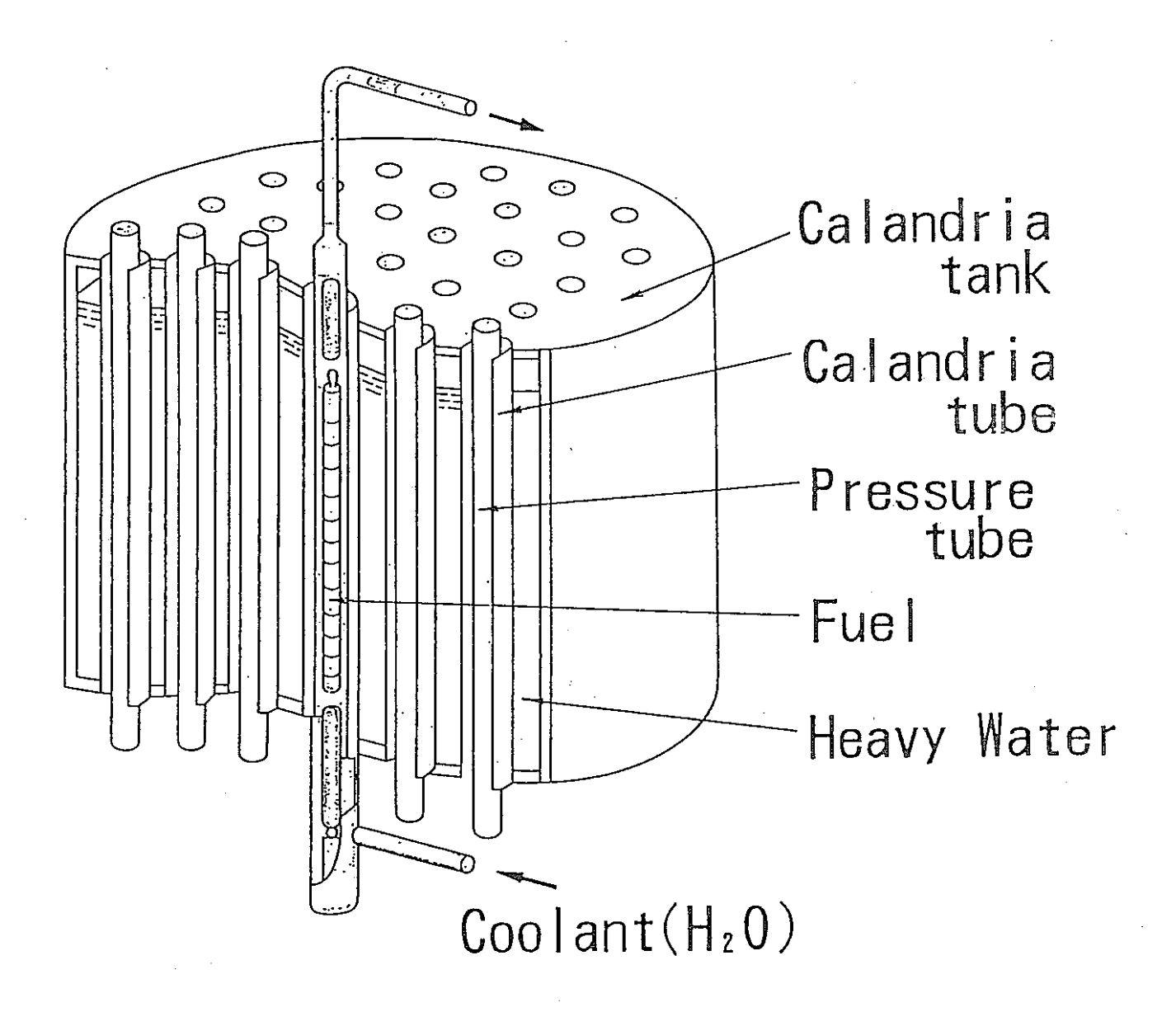


Fig 2 Reactor cross section

Fig. 3 Schematic view of Fugen fuel assembly

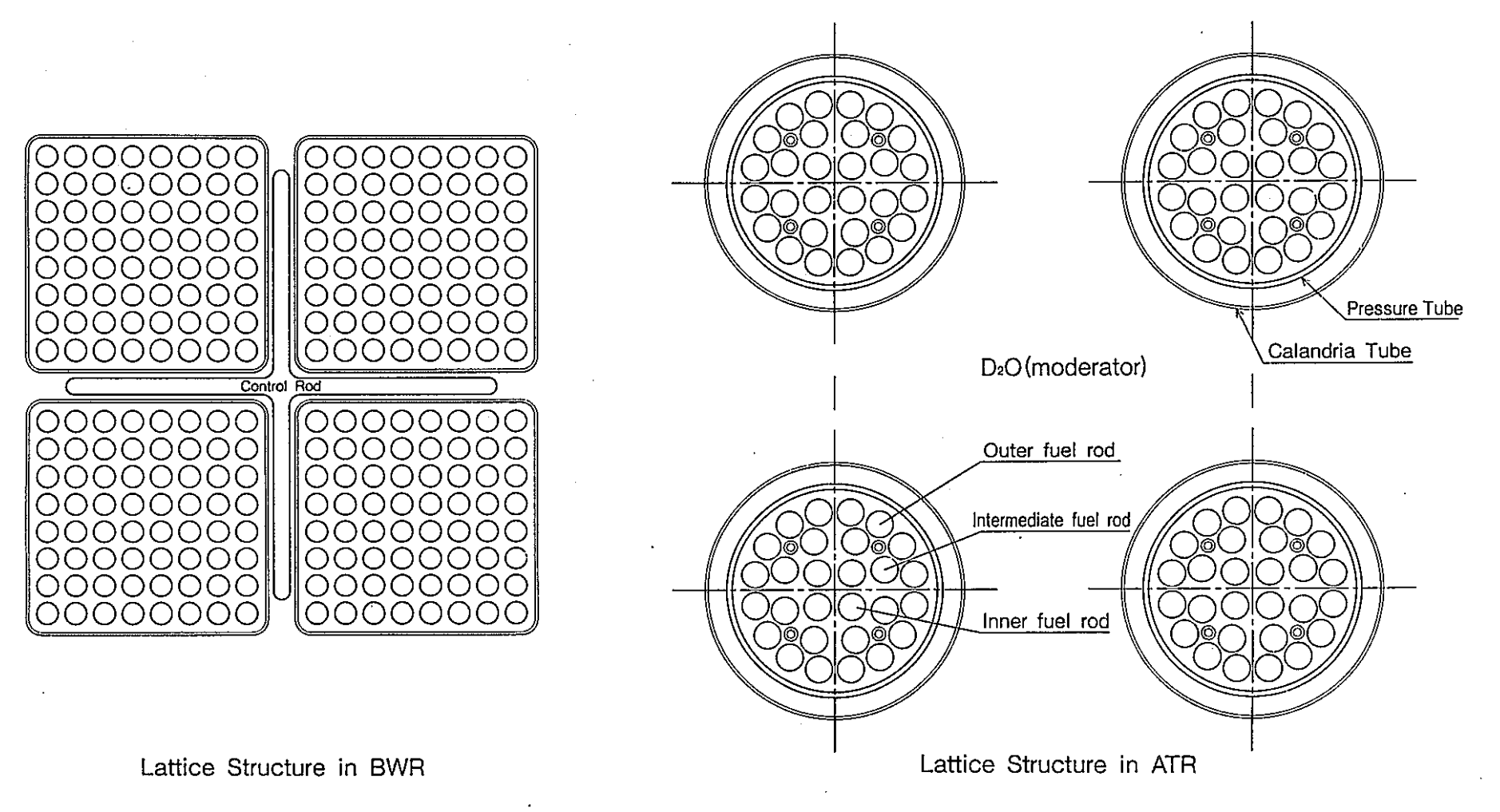


Fig 4 Fuel Lattice Structure



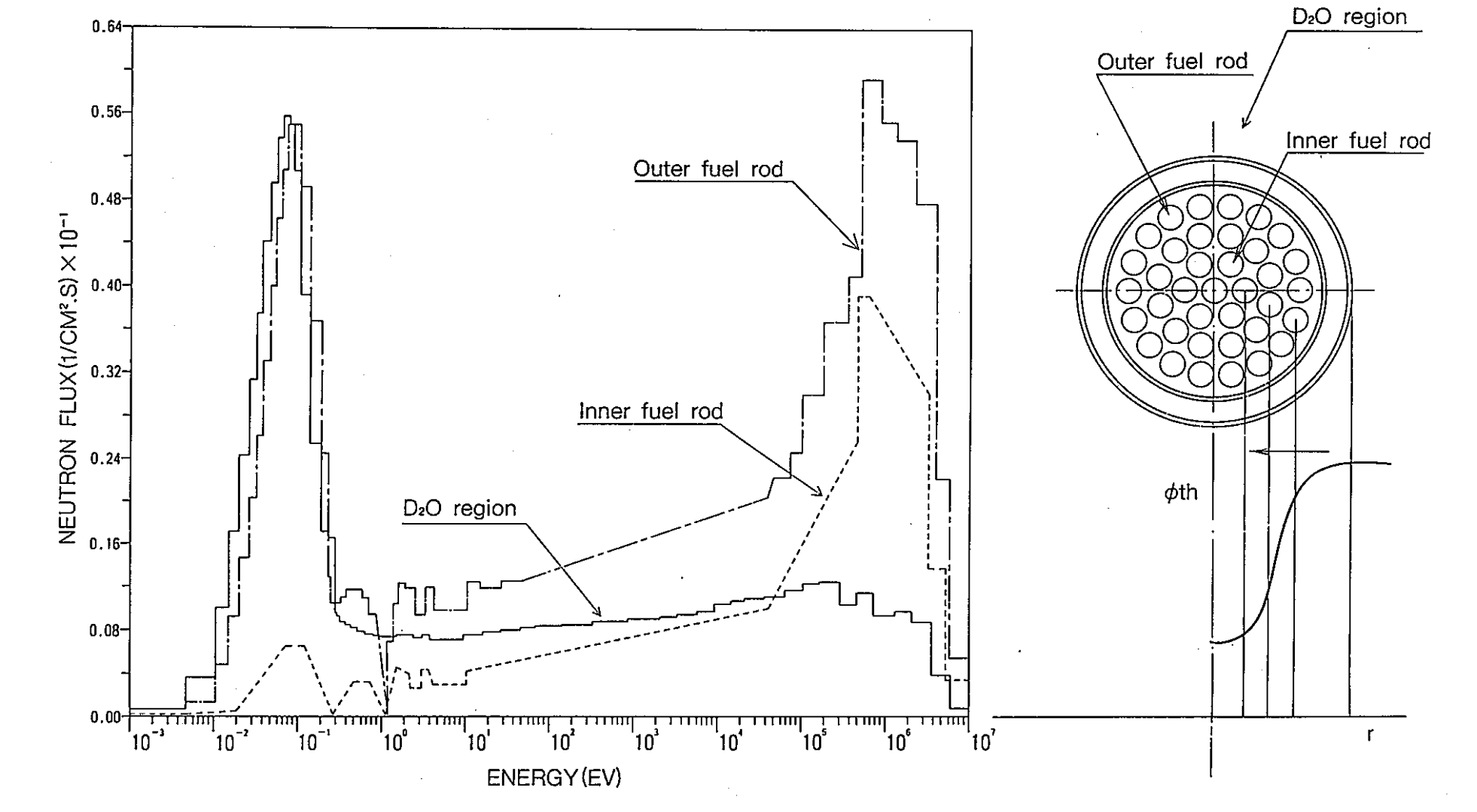


Fig 5 Neutron spectra in each region of ATR core

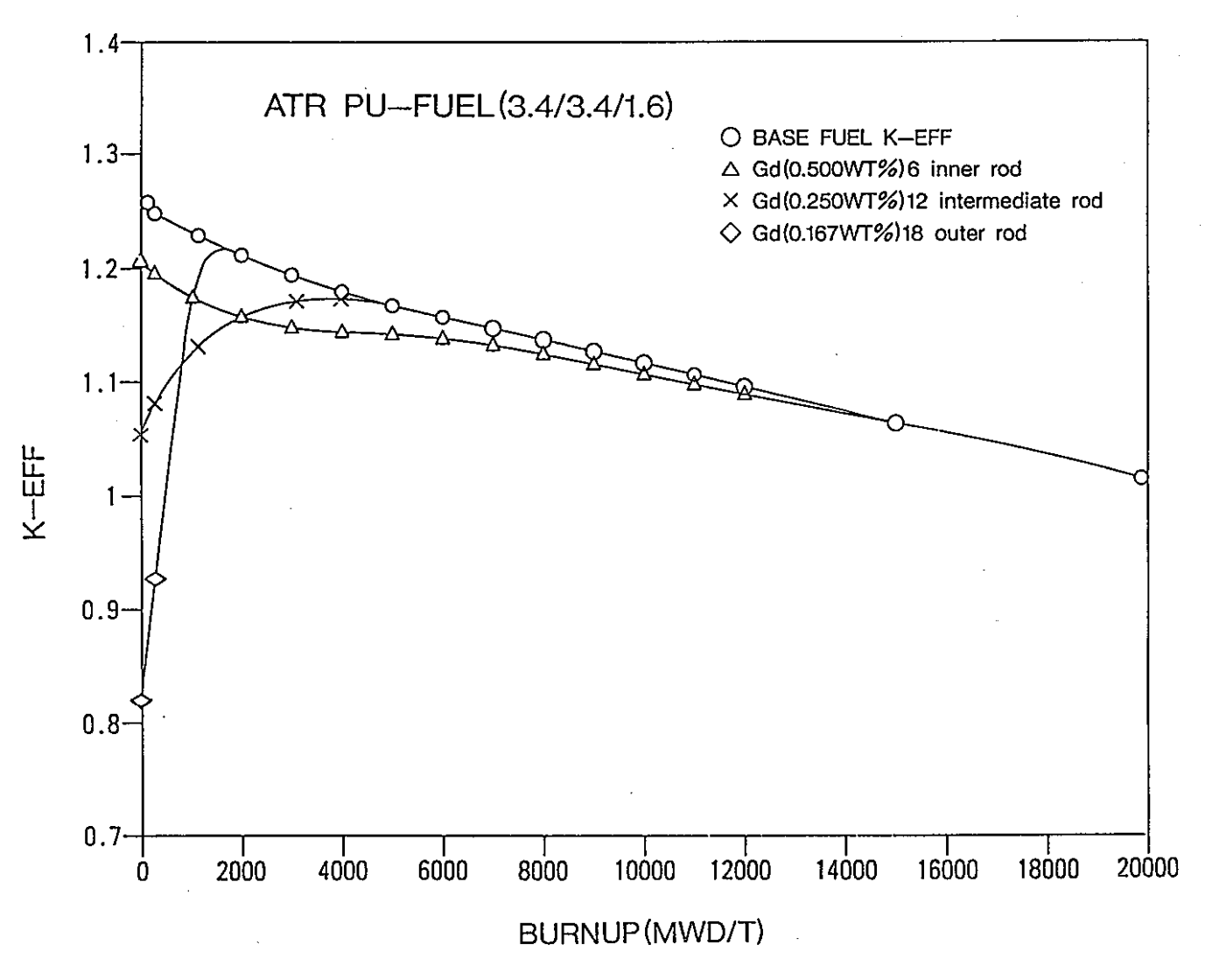


Fig 6 Characteristics of Keff vs. Burnup with the Position of the Gd-contauring Fuel rods

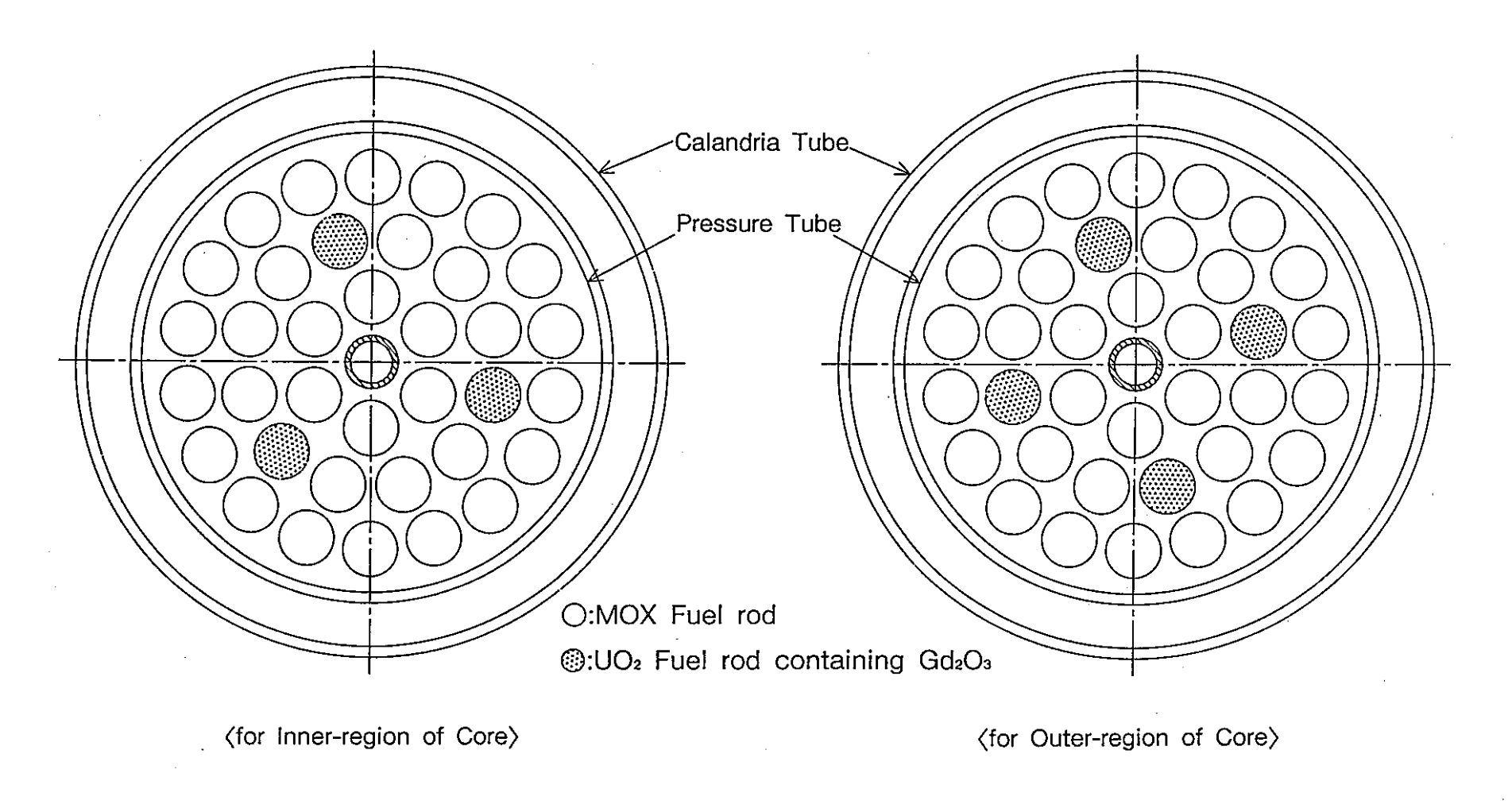


Fig 7 Cross Section of Fuel Assemblies of Demonstration Plant (Homogeneous Gd fuel)

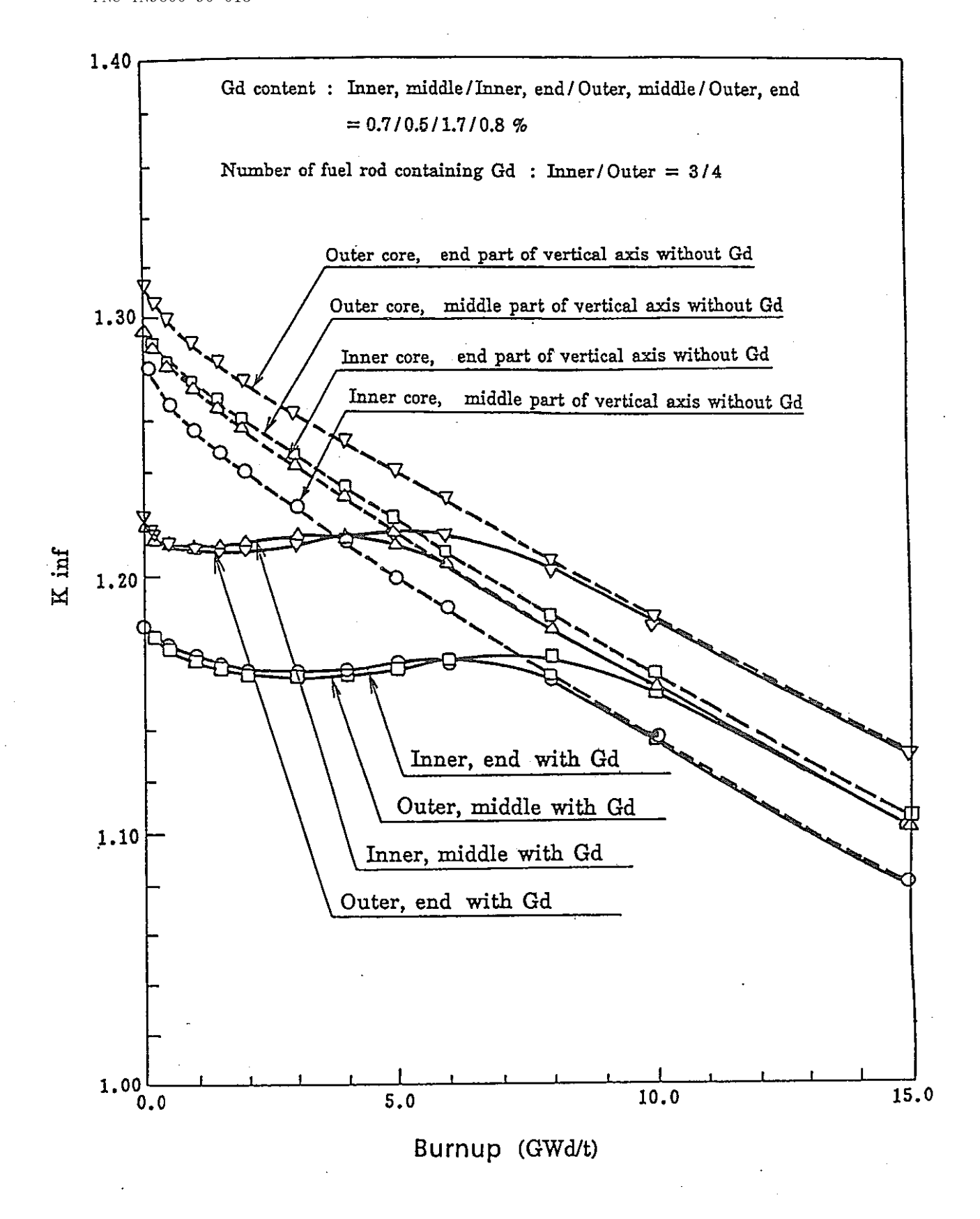


Fig 8. Characteristics of Kinf vs. Burnup of Fuel Assemblies of Demonstration Plant (homogeneous Gd fuel)



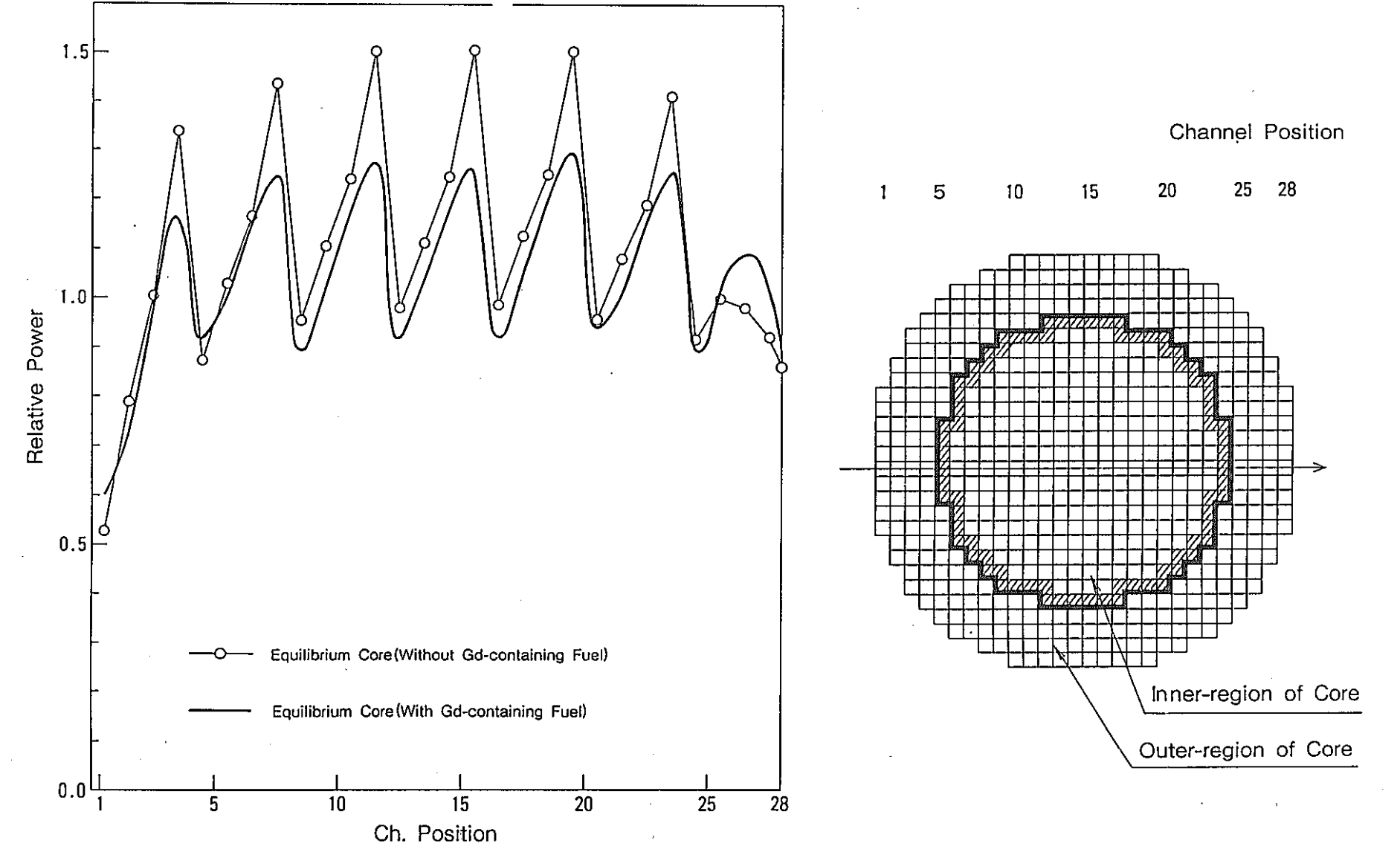
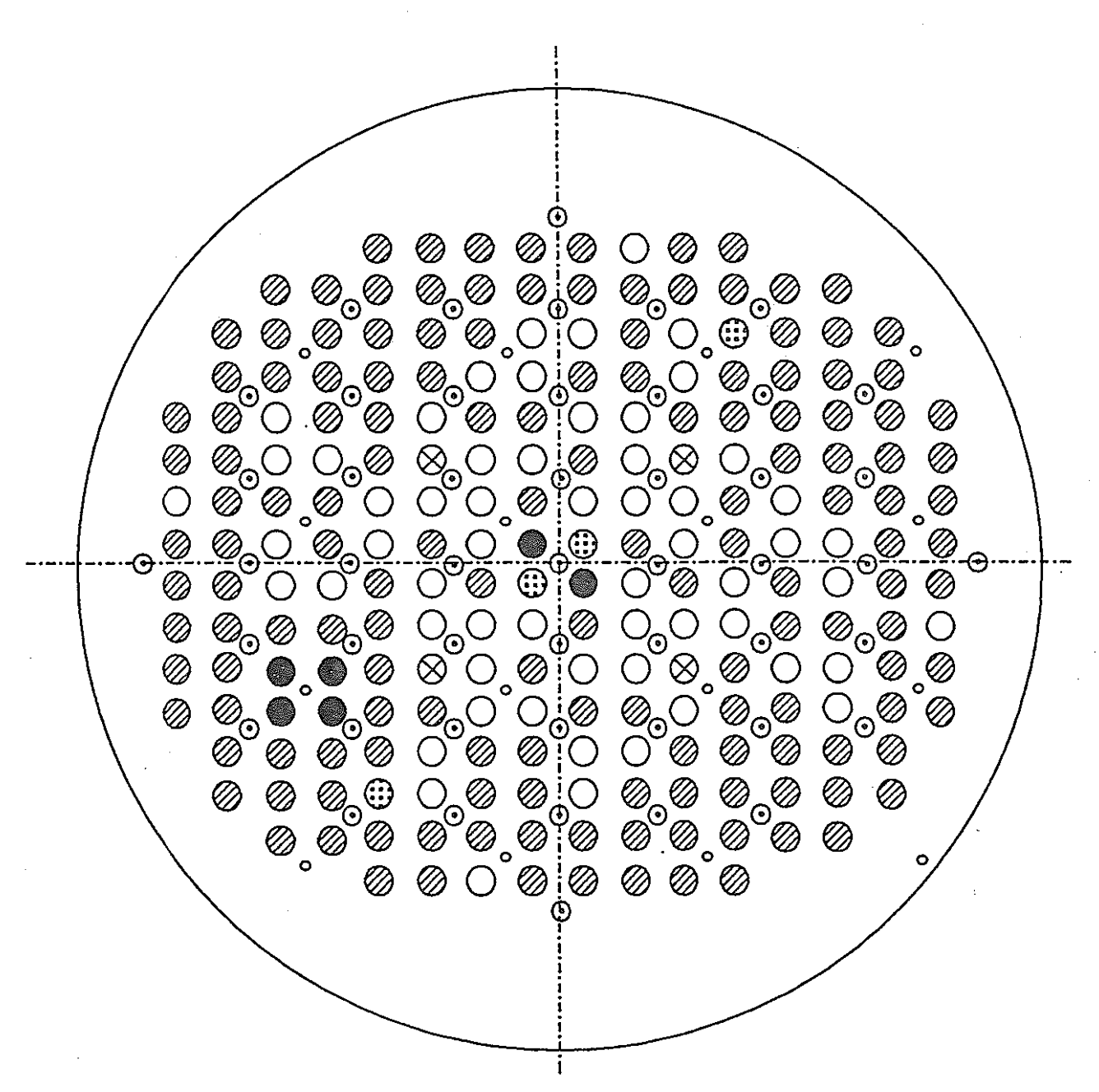


Fig 9 Radial Power Distribution at BOC in the Equibrium Core



| Note       | Equipment                   | No. | Note | Equipment                                                     | No.  |
|------------|-----------------------------|-----|------|---------------------------------------------------------------|------|
| 0          | Uranium dioxide fuel (UO2)  | 59  |      | High-Burnup fuel (containing Gd <sub>2</sub> O <sub>3</sub> ) | 6    |
| 0          | Mixed oxide fuel (PuO2+UO2) | 151 | 0    | Control rod                                                   | 49   |
| $\otimes$  | Special fuel                |     | 4    | Local power monitor                                           | 16×4 |
| <b>(1)</b> | Demonstration fuel          | 4   |      | Channel of Power Caribration Monitor                          | 16   |

Fig.10 Core configuration (16th cycle) of the Fugen

RECION.3 129-751 HOX-0

REGION-4 (15-79) HOX-0

Fig 11 Channel power history of Homogeneous Gd-fuel and Standard fuels in Fugen.

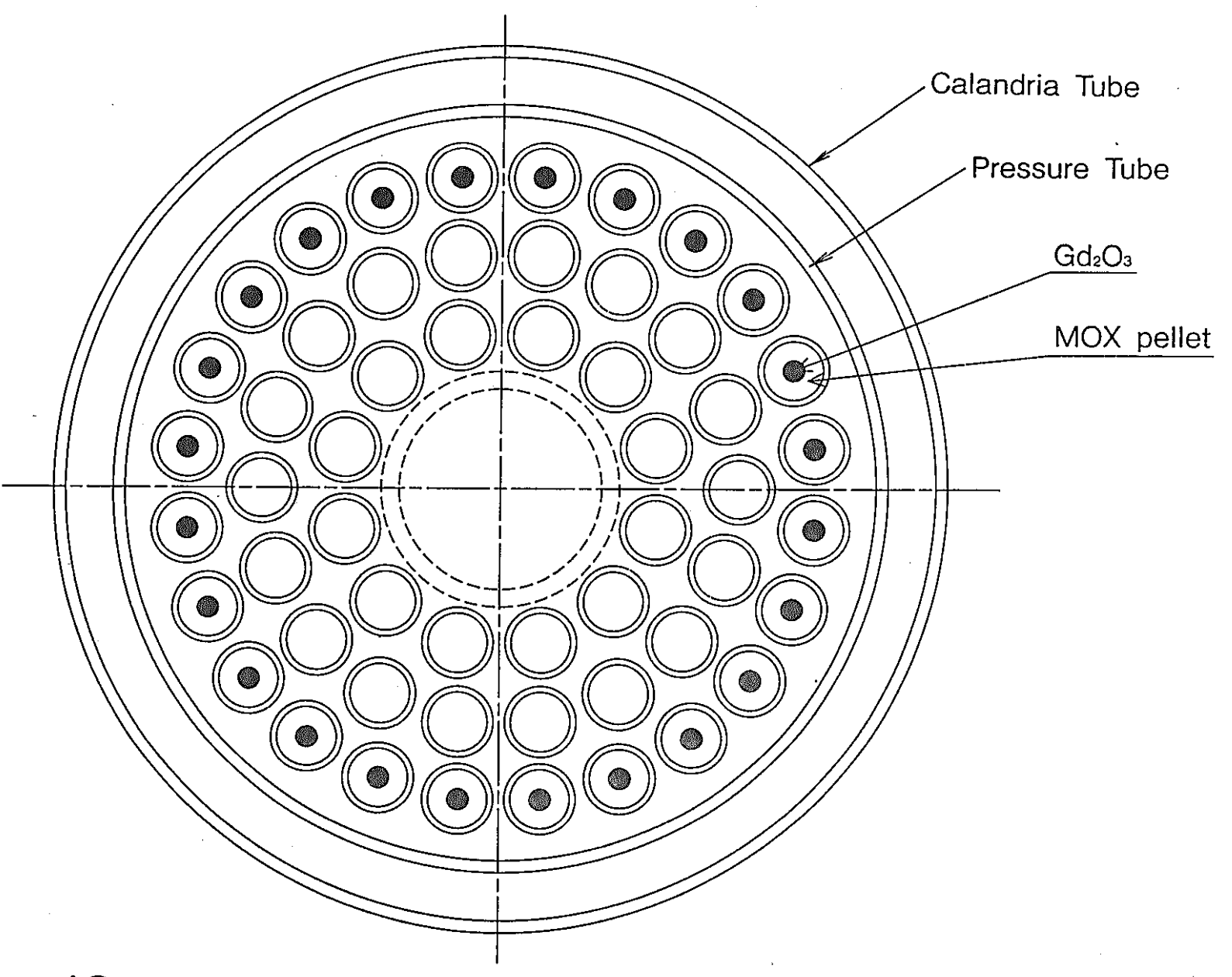


Fig 12 Cross Section of Duplex Pellet Fuel

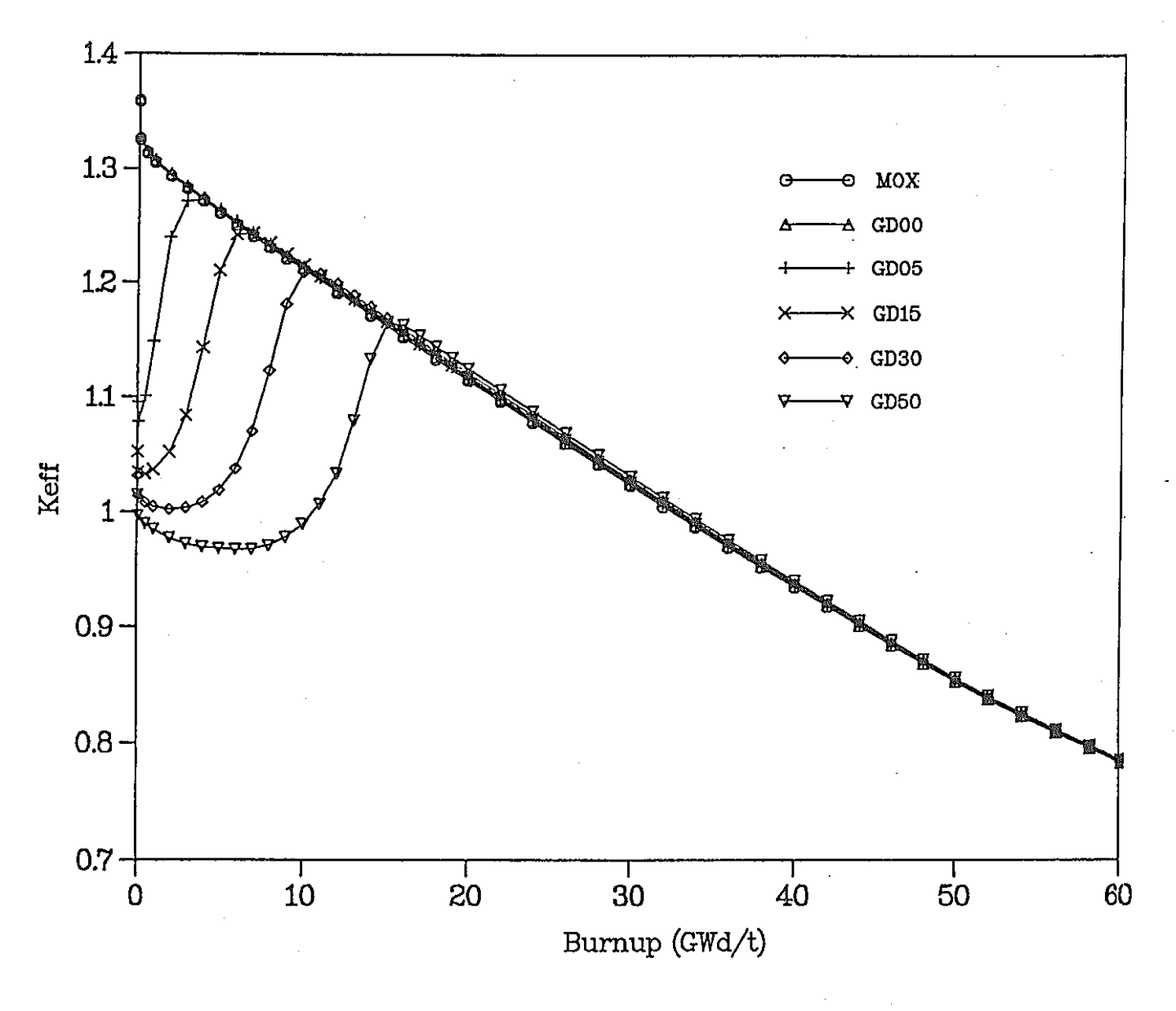


Fig 13. Characteristics of Keff vs. Burnup dependent on Gd content of Duplex pellet fuel (Dia. of  $Gd_2O_3 = 3.0 mm_{\phi}$ )

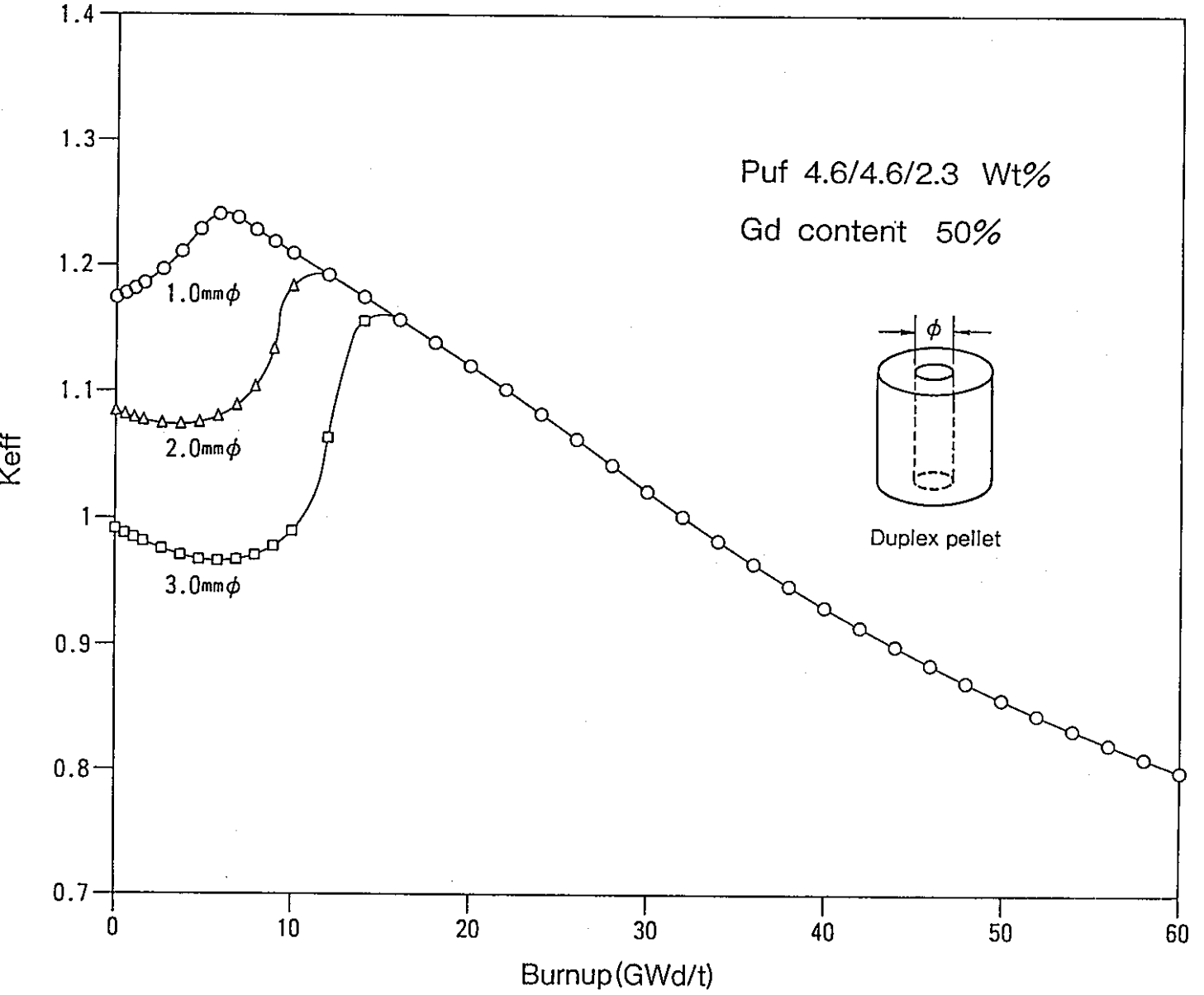


Fig 14 Characteristics of Keff vs. Barnup with the Diameter of Gd<sub>2</sub>O<sub>3</sub> in Duplex pellet

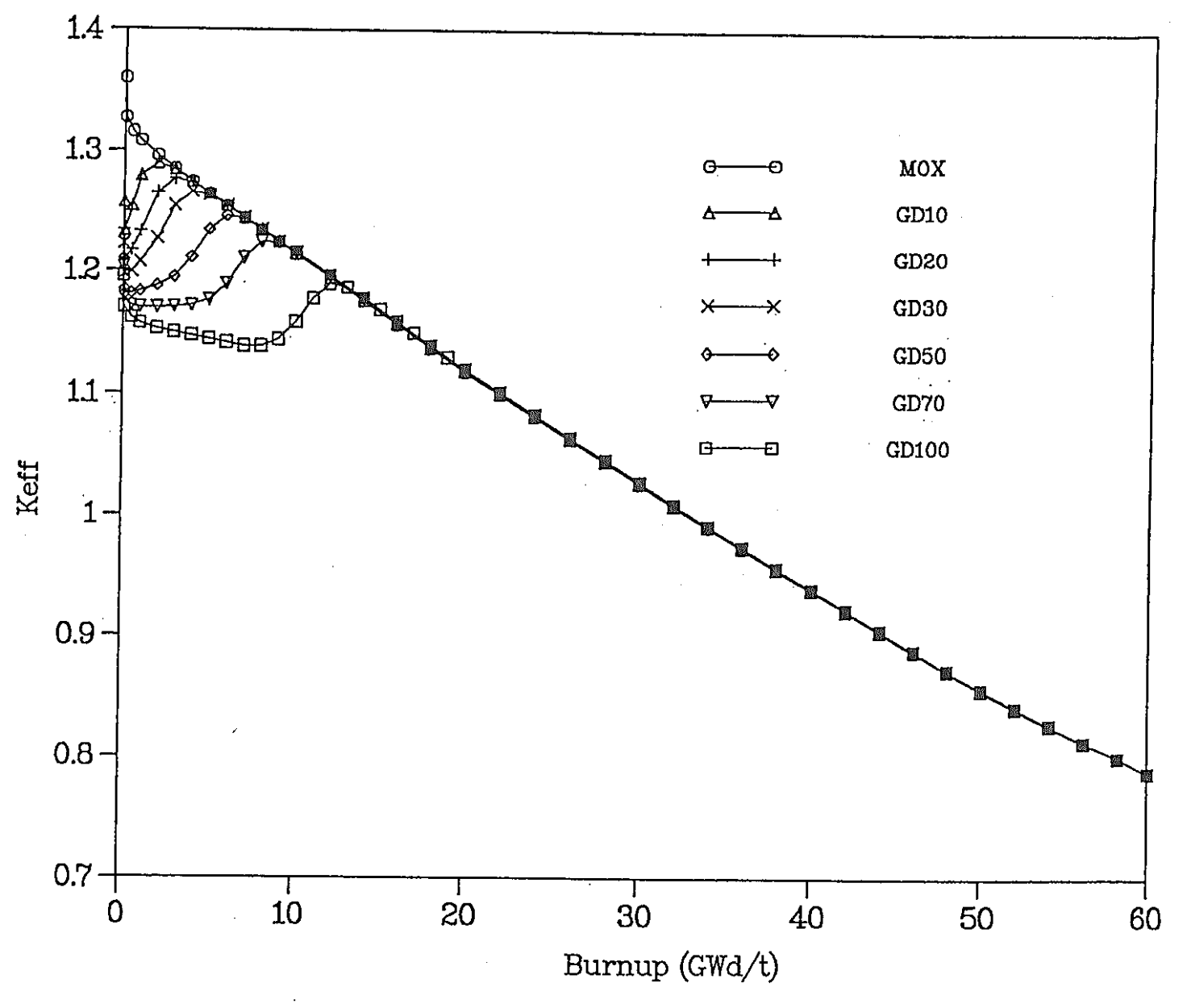


Fig 15. Characteristics of Keff vs. Burnup dependent on Gd content of Duplex pellet fuel (Dia. of  $Gd_2O_3=1.0$ mm $\phi$ )

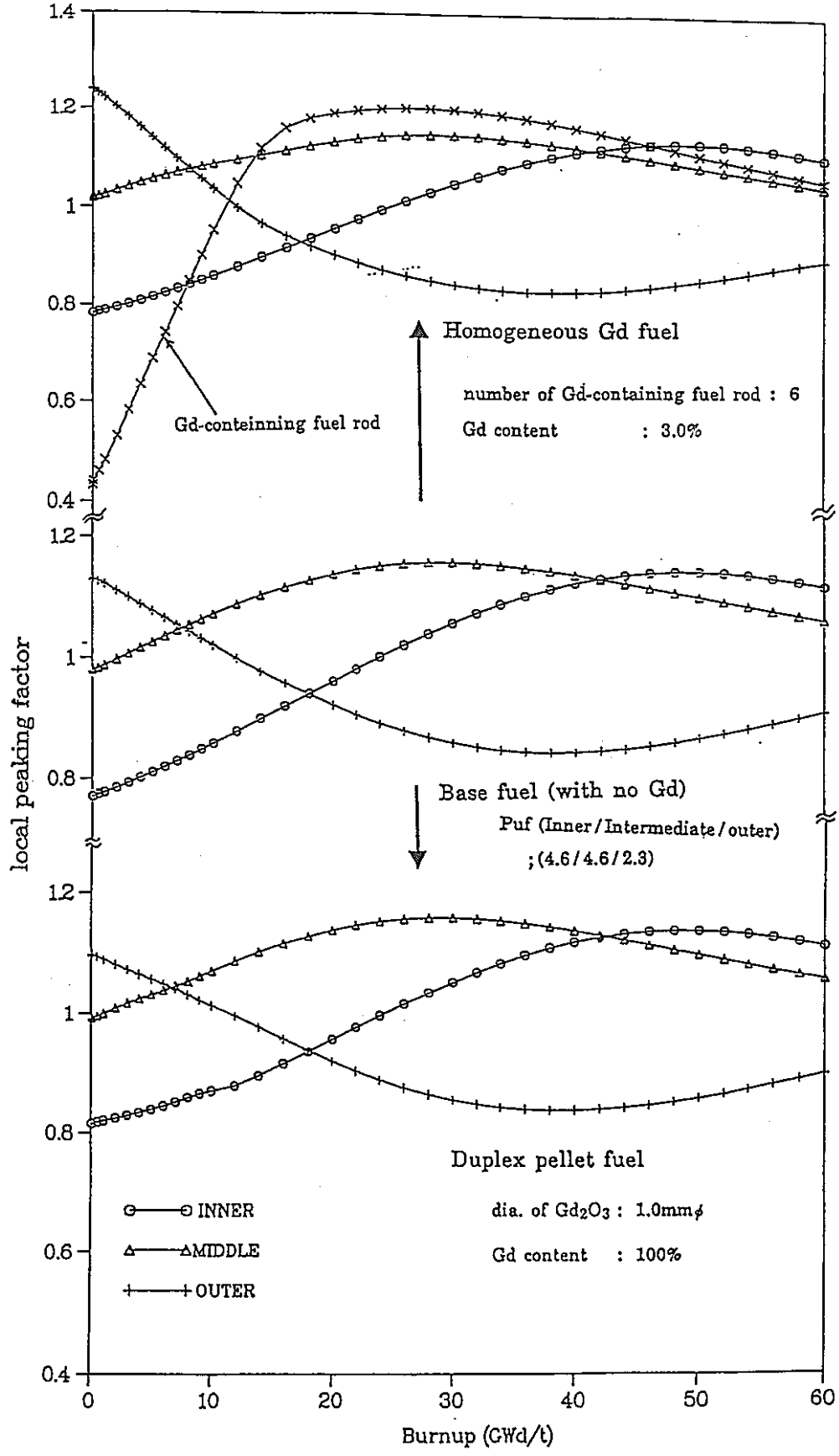


Fig 16. Burnup History of Local Peaking Factor of Base fuel, Homogeneous Gd fuel, and Duplex pellet fuel.

#### PLUTONIUM GENERATION BOILING WATER REACTOR CONCEPT

Renzou Takeda, Motoo Aoyama, Yoshiniko Ishii, Osamu Yokomizo, Kazuya Ishii, Noriyuki Sadaoka and Sadao Uchikawa

Energy Research Laboratory, Hitachi, Ltd. 1168 Moriyama-cho, Hitachi-shi, Ibaraki-ken 316, Japan

#### ABSTRACT

A design concept for a plutonium generation BWR (PGBR) is proposed, in which the effective moderator-to-fuel volume ratio less than 0.3 is realized in the design concept of the BWR with a closely packed hexagonal lattice and a higher core exit quality of coolant to achieve 1.0 of plutonium generation ratio. Three kinds of PGBR core designs are evaluated from the view points of nuclear, thermal hydraulic, mechanical, and safety performance. Evaluations show that the proposed designs are feasible, and that the PGBR concept has a potential of realizing a new recycle system in which plutonium and other actinide are confined to only nuclear reactors and reprocessing plants.

#### INTRODUCTION

In studies on high conversion light water reactors, it is recognized that a higher-conversion-ratio close to 1.0 is required to achieve an greater improvement on natural uranium utilization by a factor of 5-10 compared with current LWRs<sup>1-4</sup>. The authors has proposed a concept of plutonium generation boiling water reactor (PGBR)<sup>5-6</sup> having 1.0 of plutonium generation ratio, which means that the amount of fissile plutonium obtained from reprocessing of discharged fuel is almost the same as that of new loaded fuel, thereby enabling to continue to operate commercial reactors at rated power in plutonium recycling by compensating only natural uranium.

This paper deals with conceptual design studies on three kinds of PGBR cores.

MAIN FEATURES OF PLUTONIUM GENERATION BWR

On the basis of neutron balance, a CR can be written by

$$CR = \alpha \times (1 + \beta) - (1 + \gamma), \tag{1}$$

where,

$$\alpha = \left(\frac{v\Sigma_{f}}{\Sigma_{a}}\right)^{25+49+41} \qquad \beta = \left(\frac{(v-1)\Sigma_{f}^{28+40+42}}{v\Sigma_{f}^{25+49+41}}\right) \qquad \gamma = \frac{\Sigma_{a}^{M}}{\Sigma_{a}^{25+49+41}}$$

The a-factor represents the ratio of the number of neutrons produced by fission to that of neutrons absorbed in fissile materials. The (1+ $\beta$ )-factor corresponds to the additional contribution by fast fission of fertile materials, and  $\Sigma_a{}^M$  represents the parasitic neutron capture rate of fission products, transplutonium elements, structure materials, and so

Figure 1 shows the relation between the effective moderatorto-fuel volume ratio and the factors included in expression The effective moderator-(1). to-fuel volume ratio is defined as a moderator-to-fuel volume ratio taking into account the moderator voidage effect such as boiling. The a and B-factors increase the effective as volume ratio moderator-to-fuel decreases, in particular, this tendency of the  $\beta$ -factor is remarkable in the range of the low effective moderator-to-fuel volume ratio. This is caused by the increase in v value. The 7factor including  $\Sigma_a{}^M$  has a value of about 0.3, and decreases with the effective moderator-to-fuel volume ratio. To realize the CR close to 1.0, the utilization of of fertile fission materials is essential, and the first term in expression must be more than 2.3. means that the moderator-to-fuel volume ratio must be less than 0.3.

Under the practical constraint of a rod-to-rod clearance of more than 1mm, such a low effective moderator-to-fuel volume ratio can be realized in boiling water reactor (BWR) due to void generation in fuel bundles.

Figure 2 shows the relation between the effective moderator-to-fuel volume ratio and the required Pu-fissile enrichment and CR, which is evaluated under a typical operating condition of a cycle exposure of 9GWd/t and a discharge exposure of 45GWd/t. In case of less than 0.3 of effective moderator-to-fuel volume ratio, the required plutonium enrichment fed to natural uranium is reduced less

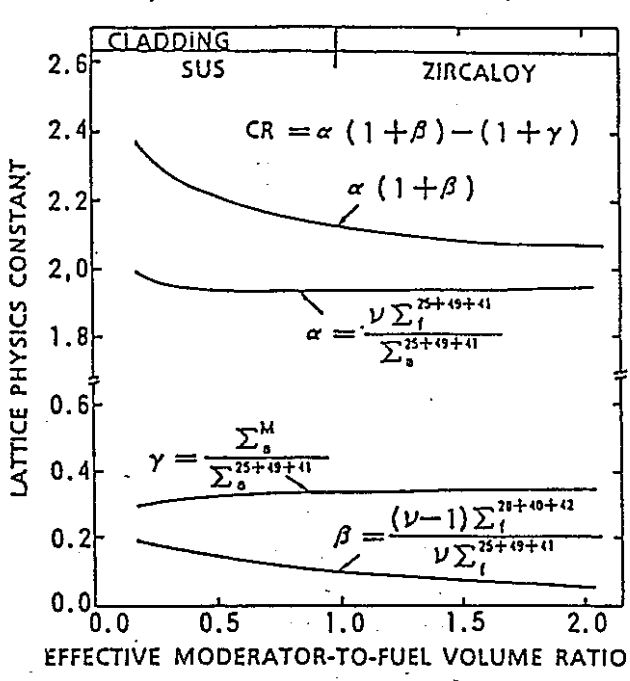


Fig. 1. Relation between the effective moderator-to-fuel volume ratio and the lattice physics constants

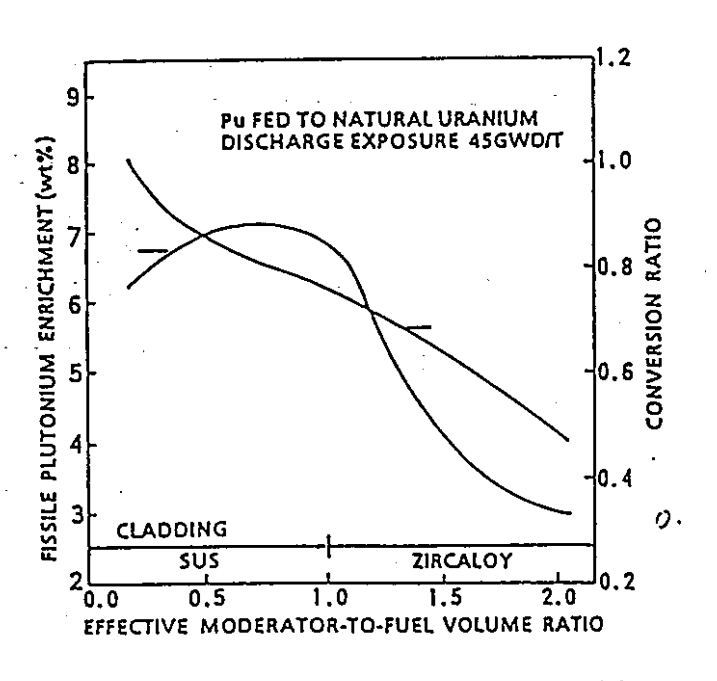


Fig.2. Relation between the effective moderator-to-fuel volume ratio and fissile Pu enrichment and conversion ratio

than 6.5 percent due to increase in  $\beta$ -values as well as  $\alpha$ -values of fissile plutonium isotopes following decrease in parasitic absorption rates of fission products and structure materials. This causes the void coefficient on PGBR to be improved to the same levels as those of a number of heavy-moderator commercial nuclear reactors in operation, which has a possibility to make void coefficient zero by adapting the flattened core. It must be emphasized in characteristics of PGBR in safety that excess reactivity during operation cycle is about one tenth and doppler coefficient is more than 50% larger in comparison with those of the current BWR because of little change in the number densities of fissile plutonium and the large portion of neutron absorptions in resonance energy region.

# CONCEPTUAL DESIGN OF PLUTONIUM GENERATION BWR

To confirm the feasibility of the plutonium generation BWR, three kind of designs have been investigated. Basic design parameters are summarized in TABLE I.

PGBR-I is a 600 MWe prototype reactor having the same power density as those of current BWRs, and some results of core performances were presented in Ref. 6.

TABLE 1
Specifications of Plutonium Generation BWR

| Parameter.                             |               | PGBR-I | PGBR-II | PGBR-III |
|----------------------------------------|---------------|--------|---------|----------|
| Electric power                         | (MW)          | 600    | 900     | 900      |
| Dome pressure                          | (MPa)         | 7.2    | 7.2     | 7.2      |
| Coolant flow rate                      | $(10^{4}t/h)$ | 1.04   | 2.25    | 2.19     |
| Core active length                     | (m)           | 2.00   | 2.00    | 1.35     |
| Core outer diameter                    | (m)           | 4.9    | 4.7     | 5.3      |
| Number of fuel bundle                  |               | 601    | 601     | 781      |
| Number of fuel rods per                | bundle        | 151    | 151     | 151      |
| Fuel rod outer diameter                | (mm)          | 12.3   | 11.8    | -11.8    |
| Fuel rod-to-rod clearar                | ice (mm)      | 1,5    | 1.3     | 1.3      |
| Moderator-to-fuel volum                | ne ratio      | 0.53   | 0.50    | 0.50     |
| Specific power                         | (kw/kg)       | 10.7   | 17.5    | 20.0     |
| Average power density                  | (kw/l)        | 51.4   | 85.1    | 97.0     |
| Average linear heat<br>generation rate | (kw/m)        | 9.9    | 14.9    | 17.0     |
| Core outlet quality                    | (%)           | 40     | 27      | 28       |
| Core average void fract                | ion (%)       | 56     | 51      | 51       |

PGBR-II is a 900 MWe commercial reactor of which fissile plutonium inventory per unit power is minimized in order to start up a 900 MWe commercial PGBR by using fissile plutonium obtained from reprocessing of discharged fuels corresponding to 80GWe-Year electric power production of the current BWR.

PGBR-M was designed to make void coefficient zero by shortening the height of the core from 2.0m of PGBR-I and II to 1.35m in considering that people are sensitive for void coefficients of which signs have no intrinsic problem as far as its absolute values are small.

In these designs, the effective moderator-to-fuel volume ratio of less than 0.3 can be realized by the closely packed hexagonal lattice with the rod-to-rod clearance of  $1.3\sim1.5$ mm and the core averaged void fraction more than 50%.

#### Fuel Bundle Design

The PGBR fuel bundle consists of 151 fuel rods, 18 control rod guide thimbles, 5 (or 4) spacers, a hexagonal channel box and upper and lower tie plates. Stainless-steel (SUS) is chosen for fuel cladding and channel materials instead of Zircaloy in the current BWRs. Stainless steel is considerably stronger than Zircaloy, so thinner stainless steel is sufficient to suppress the deformation of fuel cladding and channel box during operation.

Main specifications of fuel bundle design are summarized in TABLE II. These specifications enable the fuel bundle to keep within the design limit both mechanically and thermal-hydraulicaly. The key design concepts include the ring cell type spacer, thin channel box and narrow channel-box gap.—In the ring cell type spacer one cell is overlapped with neighboring cells each other because of narrow fuel rods gap. Inconel is adopted as spacer material. The thin channel box and narrow channel box gap are accomplished by reducing the pressure difference between channel box inside and outside by maintaining the constant flow in a channel box gap.

TABLE II
Specifications of Fuel Bundles in PGBR

| Parameter                 |       | PGBR-I | PGBR-II      | PGBR-Ш |
|---------------------------|-------|--------|--------------|--------|
| Bundle geometry           |       | He     | xagonal Latt | ice    |
| Bundle pitch              | (cm)  | 18.34  | 17.46        | 17.46  |
| Number of fuel rods       |       | 151    | 151          | 151    |
| Number of control rods    |       | 18     | 18           | 18     |
| Channel water gap         | (mm)  | 0.8    | 0.8          | 0.8    |
| Channel box thickness     | (mm)  | 0.95   | 0.95         | 0.95   |
| Fuel rod outer diameter   | (mm)  | 12.3   | 11.8         | 11.8   |
| Fuel rod-to-rod clearance | (mm)  | 1.5    | 1.3          | 1.3    |
| Cladding and channel mate | rials |        | Stainless-st | eel    |
| Pellet diameter           | (mm)  | 11.3   | 10.8         | 10.8   |
| Space type / material     |       | Ring   | cell type/I  | nconel |

#### Design of Reactor Internals

The control rod assembly consists of cluster type rods and has one rod drive for three fuel bundles. Figure 3 shows a cross section of fuel bundle and control rod assembly. Each control rod is equipped with a follower in its upper region. The control rods are inserted to the fuel bundles from the lower part of the core.

An upper core plate connected with the upper shroud is set on the top of all fuel bundles. This configuration prevents the fuel bundles from rising by the hydraulic lift force caused by upward coolant flow.

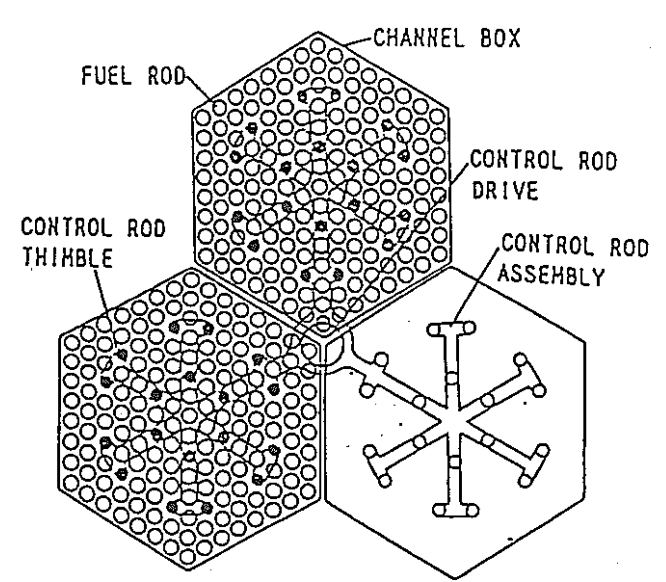


Fig.3. Cross section of fuel bundle and control rod assembly

The steam driers and separators of PGBR are designed as the same as that of the current BWR.

#### PERFORMANCE EVALUATION

#### Calculation methods

One of the remarkable features of the plutonium generation BWR is that the effective moderator-to-fuel volume ratio is smaller than in current BWRs, so that the calculation method for microscopic epithermal cross sections and the nuclear data library for resonance energy range have an important role in nuclear characteristic evaluation. In particular,—evaluations of burnup characteristics for the resonance-dominated neutron spectrum have some uncertainty. For precise numerical evaluation of fuel bundle designs, the VMONT7, in which a vectorized Monte Carlo neutron transport method is coupled with the burnup calculation, has been developed. The applicability of the VMONT code to tight lattice configurations was confirmed using the PROTEUS experimental data<sup>8</sup>.

For thermal hydraulic analysis, the critical power correlation for the tight lattice configuration gains increasingly in importance. So, the modified CISE critical power correlation9, which is based on the critical quality-boiling length correlation developed by CISE10, has been developed and verified using data from the experiment for the critical power of the closely packed lattice bundles. The proposed correlation can reproduce the experimental data within a standard deviation error of 919.

The transient behavior of a BWR involves a complex interplay between the inherent system thermal-hydraulics and neutronics and the active components. The transient behaviors in the reactor vessel were evaluated by a lumped-region model for in-reactor component thermal hydraulics coupled with a point reactor neutron kinetics model, followed by one-dimensional single channel analysis to estimate flow transient in a fuel bundle. More precise analyses by a three dimensional nodal kinetic code<sup>11</sup> are now in preparation. The modified CISE critical power correlation was used for thermal margin calculations.

#### Core performance

Performances of the proposed three designs of the plutonium generation BWR are summarized in TABLE III. In the study, the average exposure of discharged fuel bundles and the operational cycle were assumed to be 45GWd/t and 12 months respectively.

Figure 4 shows comparison of the core averaged axial void distributions of PGBR-II that of current BWRs. The steam void is generated at a lower part of core than the current BWR designs due to the PGBR design concept of a higher outlet coolant quality. As a result, the core averaged void fraction is 51% for the PGBR-II and the effective moderator-tofuel volume ratio less than 0.3 realized. The required enrichments of fissile plutonium fed to natural uranium for discharged exposure of 45GWd/t are 6.5% for PGBR-I and II, 7.0% for PGBR-II. Evaluation confirms that the proposed designs have the plutonium generation ratios of ~1.0, which means that consumption of fissile plutonium is equal to generation of fissile plutonium.

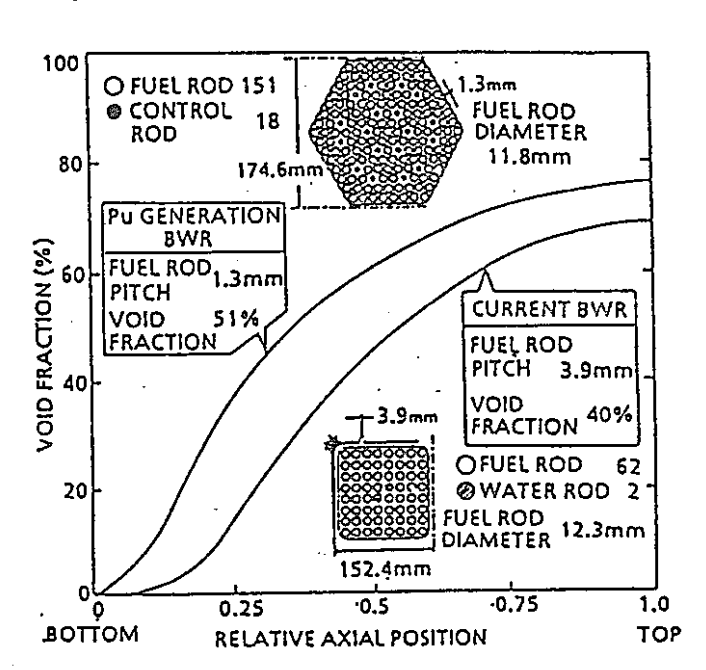


Fig.4. Comparison of fuel bundle configurations and axial distributions of void fraction

|      |             |    | ABLE III  |            |     |
|------|-------------|----|-----------|------------|-----|
| Core | Performance | of | Plutonium | Generation | BWR |
|      |             |    |           | •          |     |

| Parameter                         | PGBR- I | PGBR-II | PGBR-II |
|-----------------------------------|---------|---------|---------|
| Discharge exposure (GWd/t)        | 45      | 45      | 45      |
| Operational cycle length (months) | 12      | 12      | 12      |
| Pu-fissile enrichment* (W/o)      | 6.5     | 6.5     | 7.0     |
| Plutonium fissile inventory (t)   | 10.9    | 10.0    | 9.4     |
| Plutnium generation ratio**       | 1.02    | 1.02    | 1.0     |
| Maximum linear heat rate (kW/m)   | 18      | 27      | 30      |
| Minimum critical power ratio      | >1.3    | >1.3    | >1.3    |

<sup>\*</sup> The fissile plutonium is fed to the natural uranium.

Pu-fissile amount in discharged fuel

<sup>\*\*</sup> Plutonium Generation Ratio

Pu-fissile amount in new fuel

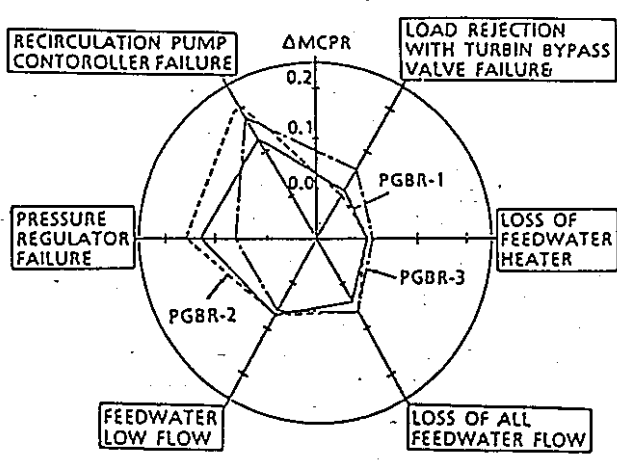
Thermal margin was evaluated using the modified CISE critical power correlation and the proposed designs are confirmed capable of having minimum critical power ratio (MCPR) of more than 1.3.

#### Transient and Safety Analysis

The proposed designs of the plutonium generation BWR have negative reactivity power coefficients. The typical transients were analysed and the  $\Delta \text{MCPR}$ , that is, decrease in thermal margin during transients was evaluated. On the evaluation, the characteristics of the active components in PGBR were assumed to have those of the ABWR's  $^{12}$ . For example, internal pumps are utilized as recirculation pumps instead of

jet pumps in the current BWRs.

Figure 5 shows the results of transient analyses. The maximal  $\Delta MCPR$  of the PGBR-I is 0.13, which is nearly the same as the current BWRs'. The PGBR-II has an increasing power density compared with the PGBR-I. Though the maximal  $\Delta$ MCPR of the PGBR-II is 0.21, which is larger than the currents BWR's, boiling transient will not occur. and the fuel integrity can be maintained because of the MCPR more than 1.3 in the rated power normal operation. margin of the PGBR-III is



Thermal - Fig.5. Thermal margin during typical transients

improved compared with the PGBR-II by improving a void reactivity coefficients and decreasing the bundle power.

In all cases, the maximum heat flux and the maximum vessel pressure during transients were confirmed to be maintained below the limiting values of the current BWRs.

From the safety aspects, a HCPS line break accident, which seems to be the most severe loss-of-coolant accident for the PGBRs, was also analysed. Analyses showed that the peak cladding temperature in LOCA is

550°C for the PGBR-II, which is less than the limiting value (1200°C) of the current BWRs.

#### ACTINIDE TRANSMUTATION

The design concept of the plutonium generation BWR seems to play an important role from a view point of storage of long-life actinide elements. In the second phase of PGBR development divided into two phase other actinide elements as well as plutonium are recycled together taking one step forward from only plutonium recycling in the first phases. Figure 6 shows that accumulation of neptunium-237 of which half life is about

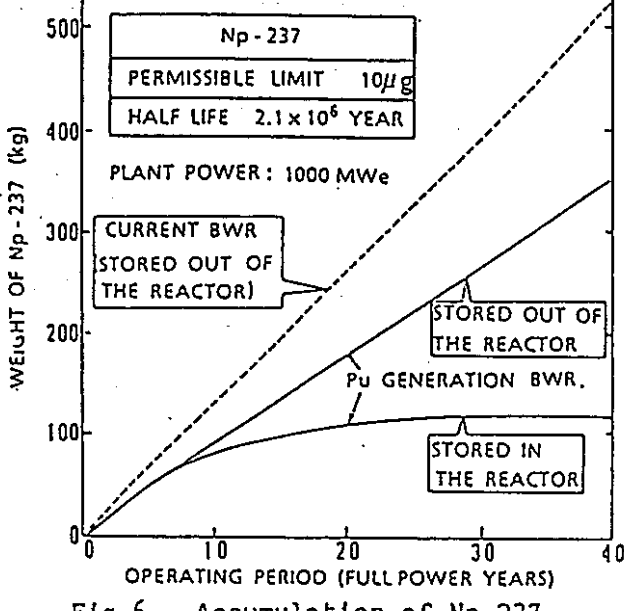


Fig.6. Accumulation of Np-237

 $2\times10^6$  year becomes equilibrium at the amount of 120kg per 1GWe PGBR core. This result means that equilibrium state of neptunium between production rates and consumption rates is kept in PGBR under the condition that 120kg of neptunium-237 generated in current BWRs is fed to the plutonium-enriched natural uranium fuel bundles in the initial core of 1GWe PGBR, and a new recycle system can be realized with light water reactor technology, in which plutonium and other actinides are confined to only nuclear reactors and reprocessing plants.

#### CONCLUSION

The design concept of a plutonium generation BWR was proposed, which has a potential for achieving a plutonium generation ratio close to 1.0 and better natural uranium utilization by a factor of 5~10 compared with current LWRs. To achieve a higher conversion ratio, the effective moderator-to-fuel volume ratio of less than 0.3 was realized in the BWR by using a closely packed hexagonal lattice with the rod-to-rod clearance of 1.3~1.5mm and a higher core average void fraction of more than 50%. Numerical evaluation for three kinds of designs for BWRs with electric power of 600MW and 900MW showed that the proposed designs are feasible from nuclear, thermal-hydraulic and safety aspects, and that the concept has another potential of realizing a new recycle system in which plutonium and other actinide are confined to only nuclear reactors and reprocessing plants.

#### REFERENCES

- 1. M. C. EDLUND, "High Conversion Ratio Plutonium Recycle in Pressurized Water Reactors," Ann. Nucl. Energy, 2, 801 (1975)
- 2. W. OLDEKOP et al., "General Features of Advanced Pressurized Water Reactors with Improved Fuel Utilization," Nucl. Technol., <u>59</u>, 212 (1982)
- 3. V. G. RODRIGUES, "Untersuchungen zum Hochkonvertierenden Siedewasserreaktor," PhD Thesis, Hannover University, (1983)
- 4. R. TAKEDA and M. AOYAMA, "Natural Uranium Utilization and the Role of HCR in the New Generation LWR," Preprint 1986 Fall Meeting At. Energy Soc. Japan, F-8 (1986)
- 5. R.TAKEDA et al., "Study on Plutonium Generation BWR Core," Preprint 1987 Fall Meeting At. Energy Soc. Japan, D-4 (1987) (in Japanese)
- 6. R. TAKEDA et al., "A Conceptual Core Design of Plutonium Generation Boiling Water Reactor", Proc. of the 1988 International Reactor Physics Conf. Vol. M., 119 (1988)
- 7. H. MARUYAMA et al., "A Monte Carlo Method with Pseudo Scattering for Neutron Transport Analysis," in Proceedings of International Topical Meeting on Advances in Reactor Physics, Mathematics and Computation, Paris (Apr. 1987)

- 8. Y. MORIMOTO et al., "Development of Vectorized Monte Carlo Nuclear Analysis Program VMONT(3) -Analysis of Tight Lattice Cell-," Preprint 1987 Fall Meeting At. Energy Soc. Japan, D-60 (1987) (in Japanese)
- 9. T. MATSUMOTO et al., "Development of Critical Power Correlation for :Tight Lattice Fuel Assembly," Preprint 1987 Annu. Meeting At. Energy Soc. Japan, E-40 (1987) (in Japanese)
- 10. 'S. BERTOLETTI et al., "Heat Transfer Crisis with Steam-Water Mixtures," Energia Nucleare, 12, 121 (1965)
- 11. Y. Bessho et al., "Development Program Based on Nodal Expansion Method," submitted to ANS 1990 Annual Meeting, (1990)
- 12. S. A. Hucik et al., "Outline of the Advanced Boiling Water Reactor (ABWR)," Proc. of Second International Topical Meeting on Nuclear Power Plant Thermal Hydraulics and Operations, 4-10, (1986)

NEA-CLF-A-1116 NEA-A Session B11

# Investigations on Pu-Recycling and High Burnup for LWRs in the Federal Republic of Germany

#### **Contributions**

- F.U. Schlemmer, G.J. Schlosser (SIEMENS):
   Development of Thermal Plutonium Recycling (1986)
- W.D. Krebs, G.J. Schlosser (SIEMENS):
   Status of Fuel Assembly Design and Core Management with MOX Fuel in the FRG for SIEMENS/KWU Type LWRs (1989)
- W.D. Krebs, G.J. Schlosser (SIEMENS):
   Status of Design and Operational Experience with Enriched Reprocessed
   Uranium (ERU) Fuel in the FRG for SIEMENS/KWU Type LWRs (1989)
- F.U. Schlemmer, H.P. Fuchs, R. Manzel (SIEMENS):
   Status of Irradiation Experience with Recycled Fuel Materials in the FRG for SIEMENS/KWU Type Fuel Assemblies (1989)
- 5. H.W. Wiese (KfK):
  Investigation of High-Burnup LWR Uranium, MOX and Recycled Uranium
  Fuel on the Basis of JEF-1 Data Validated at KfK (contribution to PHYSOR,
  Marseille 1990)



FUEL CYCLES

# DEVELOPMENT OF THERMAL PLUTONIUM RECYCLING

HORST ROEPENACK Alkem GmbH, Rodenbacher Chaussee 6 6450 Hanau 11, Federal Republic of Germany

FRITZ U. SCHLEMMER and GERHARD J. SCHLOSSER Kraftwerk Union AG, Postfach 3220, Hammerbacherstrasse, Erlangen Federal Republic of Germany

Received April 9, 1986
Accepted for Publication November 21, 1986

Thermal plutonium recycling has been demonstrated by Kraftwerk Union AG/Alkem on a large scale since 1972 in power plants at Obrigheim and Gundremmingen, Federal Republic of Germany (FRG). An improved mixed-oxide (MOX) fuel fabrication technology has been available since 1981. Such improved MOX fuel is currently being used at Obrigheim, Neckarwestheim, Unterweser, Grafenrheinfeld, FRG, and Beznau 2, Switzerland. The MOX fuel assemblies currently inserted exhibit an operating performance that is comparable to that of uranium fuel assemblies. Postirradiation investigations on MOX fuel show high mechanical stability, low shrinkage and swelling, and good behavior during power transients. On the basis of this experience, large-scale use of MOX fuel is technically feasible.

#### INTRODUCTION

Reprocessing of spent fuel from light water reactors (LWRs) on an industrial basis is becoming a reality. This recent development can be expected to continue, and increasing amounts of plutonium will become available in the near future.

The situation for the Federal Republic of Germany (FRG) is explained in Fig. 1. It shows the annual plutonium amounts resulting from the reprocessing of German LWR fuel according to present planning. The first 10 years essentially concern reprocessing contracts with COGEMA (France) and British Nuclear Fuels plc. Increasing amounts of plutonium are also expected from the German reprocessing plant currently under construction at Wackersdorf.

This plutonium could, of course, be used best in the fast breeder reactor (FBR) fuel cycle. As shown in Fig. 1, the plutonium amounts available in the near future will be much higher than the requirements of the German FBR program. On the other hand, longterm storage of plutonium is expensive and undesirable because the buildup of gamma active decay products negatively affects processing of such plutonium at a later date. As a result, there are strong incentives to use the plutonium that is not required for the German FBR program as soon as it becomes available for thermal recycling in LWRs (Refs. 1, 2, and 3).

#### DEVELOPMENT OF THE MANUFACTURING TECHNOLOGY

The development of the manufacturing technology at Kraftwerk Union AG (KWU)/Alkem began in 1965 when the first LWR mixed-oxide (MOX) fuel rods were manufactured for the boiling water reactor (BWR) Versuchsatomkraftwerk Kahl (VAK), FRG. Since then, increasing amounts of LWR MOX fuel rods have been manufactured (see Table I).

The basic technology for LWR MOX fuel fabrication is to a large extent the same as that for LWR uranium fuel. Therefore, Alkem could take over a considerable part of the fabrication processes and equipment technology that are already in use at RBU on an industrial scale. RBU, having the same shareholders and situated on the same site as Alkem, is responsible for KWU's fabrication of uranium fuel for LWRs. Some differences in fabrication technology exist in pellet fabrication; however, for this fabrication process a considerable amount of expertise could be adopted from uranium production and then adapted to MOX fabrication.

On a larger scale, MOX fuel rods were manufactured in the early 1970s for the 345-MW(electric) pressurized water reactor (PWR) at Obrigheim and the 250-MW(electric) BWR at Gundremmingen. During this campaign, where plutonium was recycled in amounts generated by these reactors, it was demonstrated that the technology at that time was able to produce fuel of a quality comparable to the established

NUCLEAR TECHNOLOGY VOL. 77 MAY 1987

175

Roepenack et al. THERMAL PLUTONIUM RECYCLING

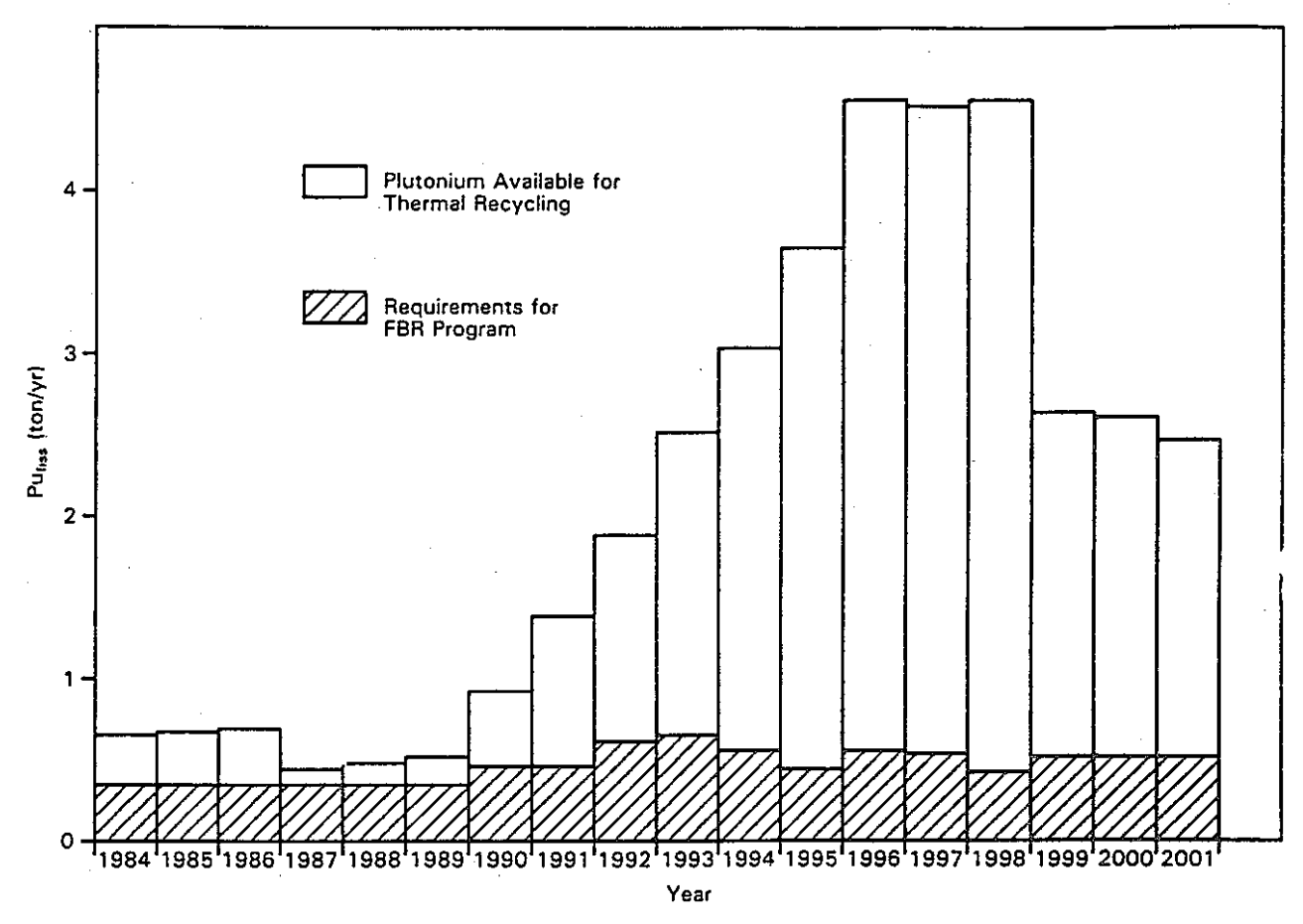


Fig. 1. Plutonium from the reprocessing of German LWR fuel and FBR requirements.

TABLE I
KWU/Alkem Operating Experience with MOX Fuel Assemblies (Status December 1986)

|                        | Power Plant<br>(Type)                             | Insertion of MOX Fuel Assemblies | Type<br>of Fuel<br>Assembly  | All-MOX<br>Fuel<br>Assemblies | MOX<br>Island Fuel<br>Assemblies | Number<br>of MOX<br>Fuel Rods             | Maximum<br>Local Burnur<br>[MWd/kg<br>(Heavy Metal)] |
|------------------------|---------------------------------------------------|----------------------------------|------------------------------|-------------------------------|----------------------------------|-------------------------------------------|------------------------------------------------------|
| VAK,<br>KWL,<br>KRB-A, | Kahl (BWR)<br>Lingen (BWR)<br>Gundremmingen (BWR) | After 1966<br>1970<br>After 1974 | 6 × f<br>6 × 6<br>6 × 6      | 7<br><br>64                   | 88<br>I (Pu/Th)                  | 1101<br>15<br>2240                        | 21<br>26<br>20                                       |
| MZFR,                  | Karlsruhe (PHWR)                                  | 1972                             | 37 rods                      | 8                             |                                  | 296                                       | 14                                                   |
| KWO,                   | Obrigheim (PWR)                                   | After 1972                       | 14 × 14 – 16 <sup>2</sup>    | 33<br>13                      |                                  | 5940<br>2282 (OCOM)<br>58 (AUPuC)         | 41<br>44<br>44                                       |
| GKN,<br>KKU,           | Neckarwestheim (PWR)<br>Unterweser (PWR)          | After 1982<br>After 1984         | 15 × 15 - 20<br>16 × 16 - 20 | 20<br>12                      |                                  | 4100 (OCOM)<br>1883 (OCOM)<br>949 (AUPuC) | 46<br>33<br>33                                       |
| BZN-2,<br>KKG/BAG,     | Beznau-2 (PWR)<br>Grafenrheinfeld (PWR)           | After 1984<br>After 1985         | 14 × 14 – 17<br>16 × 16 – 20 | 16<br>16                      |                                  | 2864 (OCOM)<br>3264 (OCOM)<br>512 (AUPuC) | 31<br>27<br>27                                       |
| Total                  |                                                   |                                  |                              | 189                           | 89 .                             | 25 504                                    |                                                      |

<sup>&</sup>lt;sup>a</sup>For example, rod array 14 by 14 minus 16 control rod positions.

LWR technology for uranium fuel.<sup>4,5</sup> Later results from reprocessing of such fuel showed a residual insolubility of the plutonium contained in nitric acid. Therefore, some modifications had to be made to the manufacturing process.

To meet the new solubility specification, two modified manufacturing processes were developed. These new processes, which result in a MOX fuel with reprocessing properties that are as good as those of uranium fuel, have been used since the new plutonium recycling campaign started in 1981 and are currently used for five PWRs.

As the main process for the long-term future, Alkem developed the AUPuC co-conversion process. 6.7 This process, which was developed from the AUC process, as used on an industrial scale for many years at RBU, produces a MOX powder from a mixture of plutonium nitrate and uranyl nitrate. Soluble MOX powder can be obtained with mixtures containing up to 40% plutonium. In its physical properties, the powder resulting from this process is very similar to the UO<sub>2</sub> powder as produced by RBU's AUC process and has very good flowability properties. The rather coarse grains lead to the high specific surface and good sintering behavior by nature of their porous structure.

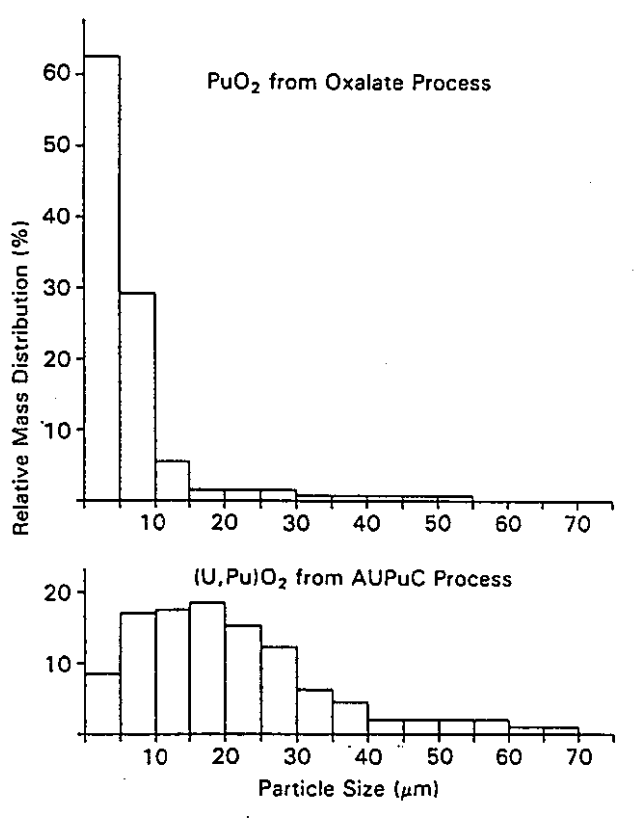


Fig. 2. Particle size distribution.

The coarse grains result in less dust formation, which is very important in minimizing radiation doses. Powders with considerable dust formation give rise in a short time to a dust layer on the equipment and on the inner walls of the glovebox, and thus to a high dose rate for the operating personnel.

The grain size distribution is shown in Fig. 2. It is compared in this diagram to plutonium oxide as obtained by the oxalate process, which was used at Alkem before the development of the AUPuC process. In contrast to the PuO<sub>2</sub> from the oxalate conversion process, 90% of the MOX powder grains from co-conversion are so coarse that they are unable to penetrate the lung. For health considerations, especially under hypothetical accident conditions, this is very important.

The process can be used for both LWR and FBR fuels. In the case of FBR fuel, the MOX powder is converted with a plutonium content as specified for the fuel and can be directly pressed into pellets. In the case of LWR fuel that requires a lower plutonium content, it is more economical, to use the mastermix concept, as shown in Fig. 3. The plutonium content for the co-conversion is adjusted to ~40%, and the resulting MOX powder is blended in an additional step with free-flowing UO<sub>2</sub> powder to the specified low plutonium content. Since the MOX powder is physically similar to the free-flowing UO<sub>2</sub> powder ex AUC, there are no difficulties in mixing both components.

The advantages of this process are as follows:

- There are only a few process steps, particularly in the powder phase, resulting in lower radiation doses to working personnel.
- 2. In all steps of the process, plutonium is present only in a highly diluted form, leading also to a lower radiation dose.
- 3. The MOX powder is fully soluble, thus facilitating scrap recovery in all stages of the process.
- 4. There is a low percentage of powder fraction fine enough to enter human lungs.
- 5. It is possible to extract the americium built up during longer plutonium storage time.
- 6. Properties are favorable for further treatment of the MOX powder.
- The experience from RBU's AUC process can also be used to a very high extent in this process.
- The process is suitable for FBR as well as for LWR fuel.

A prerequisite for the AUPuC process, however, is the availability of plutonium in the nitrate form. This prerequisite will be satisfied in the future by the

#### Roepenack et al. THERMAL PLUTONIUM RECYCLING

Wackersdorf reprocessing plant, which will deliver plutonium in the form of nitrate solution or in a mixture of plutonium and uranium nitrate solution. For Alkem's MOX fabrication as currently performed, this prerequisite, however, is only met to a small degree, because only ~20% of Alkem's plutonium supply comes in the nitrate form from the German Wiederaufarbeitungsanlage Karlsruhe (WAK) reprocessing plant. Over 80% of the plutonium supply currently comes from COGEMA's La Hague reprocessing plant in the form of PuO<sub>2</sub> powder.

Therefore, Alkem developed a second process the Optimized Co-Milling (OCOM) process - which is used in the case of plutonium supply in the oxide form. By optimization, the co-milling of UO2 and PuO2 powders was developed to such an extent that this process could also manufacture fully soluble MOX fuel. For economic reasons in the OCOM process, a mastermix concept is used (Fig. 3). This means that a mixture containing ~30% plutonium is made from UO2 and PuO<sub>2</sub> powder, and this mixture is then milled using the OCOM milling process. The MOX powder that results after the milling process is no longer free flowing. By mixing this masterblend with the eight- to tenfold amount of free-flowing UO2 powder to obtain the required plutonium content for LWR MOX fuel, a feed material is obtained with a flowability sufficient for direct pelletizing. The remaining process steps are the same as for the AUPuC process.

An area requiring special attention for the OCOM process is the homogeneity of the plutonium distribution. In contrast to the AUPuC process, two materials of very different physical properties have to be mixed together. One part is the master blend of PuO<sub>2</sub> and UO<sub>2</sub>, which after milling consists of a powder with very fine nonflowable grains with a high tendency to self-agglomeration, and the second part is the free-flowing UO<sub>2</sub> powder from the AUC process with its rather coarse grains. The mixing of the components and the preventing of segregation during further processing therefore require special attention and expertise.

As can be seen from Fig. 3, Alkem's two new processes as used for the manufacturing of LWR fuel differ only in the first part of the process. Also, most of the manufacturing equipment is identical for both processes. The properties of the MOX fuel manufactured by these new processes are very similar. As an example, Fig. 4 shows typical alpha autoradiographs of the cross section of two LWR pellets manufactured by the new processes.

Both new processes were sufficiently developed by 1980 to produce the first fuel rods for reactor tests. After 1981 LWR MOX fuel rods were exclusively manufactured using the AUPuC and the OCOM process. Since then increasing amounts of MOX fuel rods have been manufactured and inserted into various LWR power plants (see Table I).

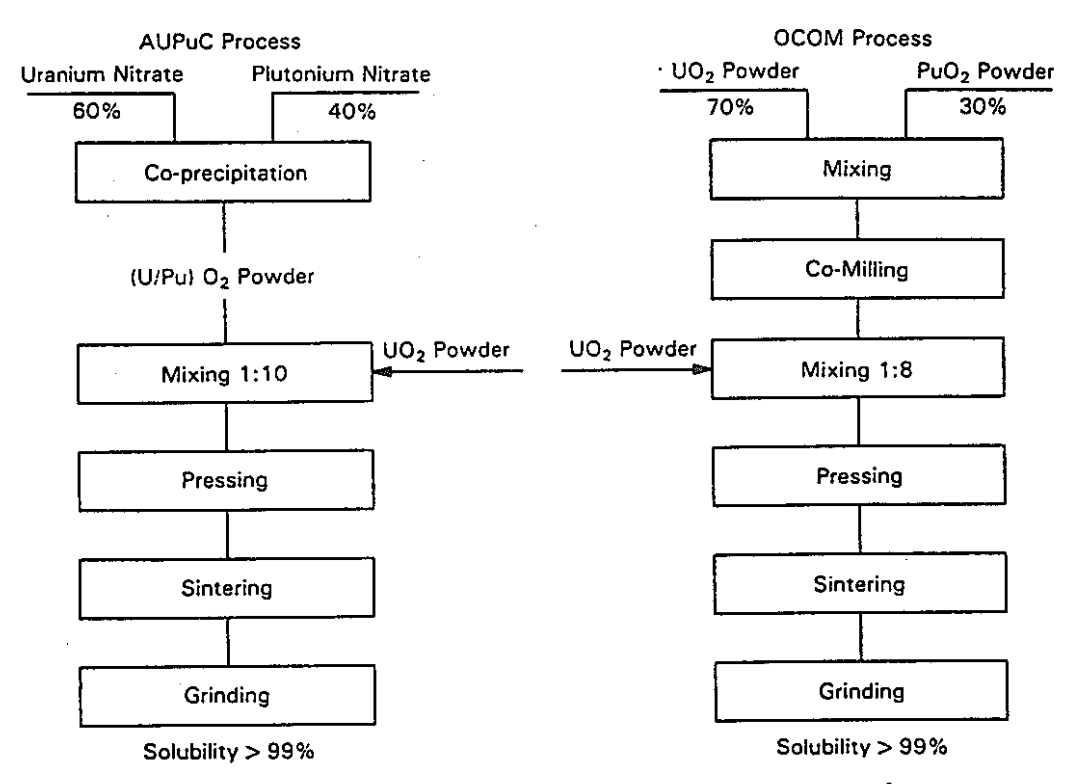


Fig. 3. Schematic description of Alkem processes for pellet manufacture.

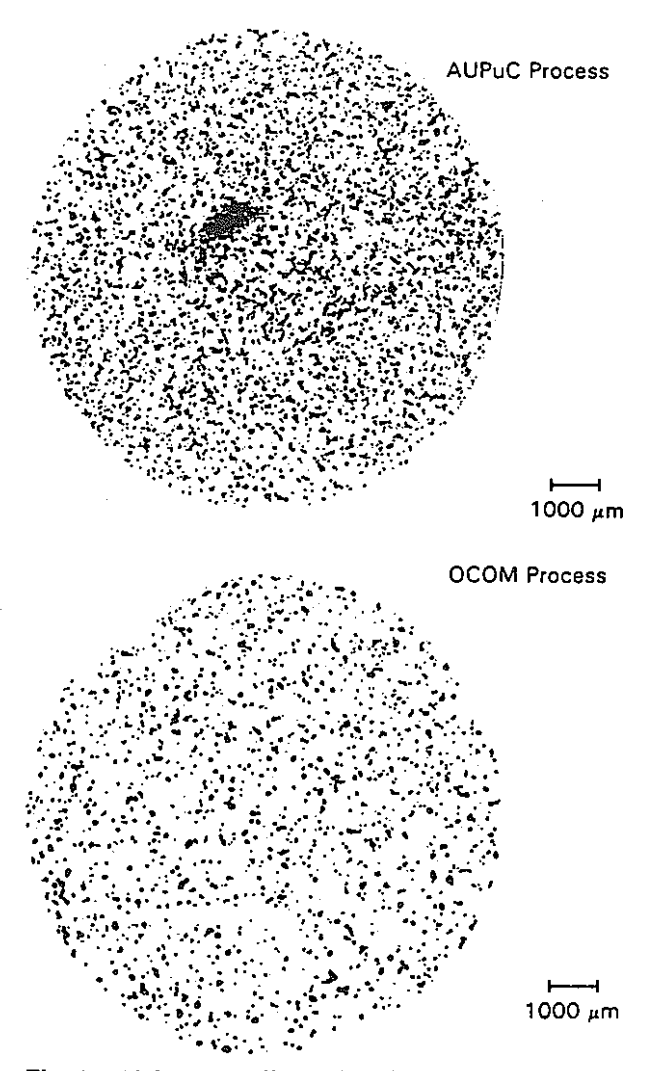


Fig. 4. Alpha autoradiography of MOX pellets (LWR).

#### **DESIGN OF MOX FUEL ASSEMBLIES**

To meet the compatibility requirements of MOX fuel assemblies with the other fuel assemblies in the core, MOX fuel rods and assemblies follow the same thermohydraulic, thermal, and mechanical design limits as uranium fuel. The mechanical design of the MOX fuel assemblies, except for the fissile material, is identical to the mechanical design of uranium fuel assemblies. In particular, the same geometry and structural materials are used. Where the neutron physics design is concerned, MOX fuel assemblies should provide a mean reactivity equivalent to that of uranium fuel assemblies and should achieve an equivalent discharge burnup. 2.3.5.9-11

Fuel elements based on a MOX island concept should be preferred for BWRs but the concept of the all-plutonium design can also be applied under special conditions. It was found that the use of an allplutonium design is always advantageous in PWRs.

#### Roepenack et al. THERMAL PLUTONIUM RECYCLING

Flattening of the power distribution is achieved by employing graded plutonium concentrations. A lower plutonium content is applied in those MOX fuel pins that are adjacent to fuel regions enriched by <sup>235</sup>U or to water gaps.

The German utilities initially decided to concentrate plutonium recycling on PWRs. However, at Alkem and KWU considerable experience in design, fabrication, and irradiation also exists for MOX fuel assemblies in BWRs. The anticipated quantities of plutonium will force recycling in BWRs to be used in the near future.

The power distribution within the PWR MOX fuel assembly that is surrounded by uranium fuel assemblies needs to be flattened by the appropriate choice of at least two plutonium enrichments and their distribution.

The design calculations use a macrocell model consisting of a pattern of one MOX fuel assembly surrounded by three uranium fuel assemblies. The results of an optimization with the MEDIUM-/FASER program system are the enrichment and power density distribution. A MOX fuel assembly with an average Pufiss content of 2.83 wt % in Unat is depicted in Fig. 5. This figure shows the design of a MOX fuel assembly, type  $16 \times 16 - 20$ , which is currently in use at the power stations at Unterweser (KKU) and Grafenrheinfeld (KKG/BAG). With only two different plutonium enrichments, a sufficiently flat power density distribution is achieved. The enrichment structure of these MOX fuel assemblies is identical to the MOX fuel assemblies of Obrigheim (KWO) and Beznau-2 (BZN-2) (types  $14 \times 14 - 17$  and  $14 \times 14 - 16$ , respectively), and of Neckarwestheim (GKN) (type 15 x 15 - 20) nuclear power stations.

Improved designs for type  $16 \times 16 - 20$  MOX fuel assemblies, which are currently in the licensing procedure for the greater part of the 1300-MW(electric) PWRs in the FRG, meet the following intentions:

- 1. Higher plutonium content to make the MOX fuel assemblies equivalent to uranium fuel assemblies of higher <sup>235</sup>U enrichment. This may be done by MOX rods of 2.1 and 3.5 wt% Pu<sub>fiss</sub> at an average Pu<sub>fiss</sub> content of 3.07 wt% in natural uranium.
- 2. MOX fuel assemblies with improvements, e.g., to be inserted at low leakage cores related to a better flattened power and burnup distribution. This new design uses MOX rods of 1.9, 2.3, and 3.3 wt% Pufiss (at an average content of 2.91 wt% Pufiss) in natural uranium and four water-flooded rods.

A comparison of these designs is given in Table II, which shows the results of shuffling studies for 1300-MW(electric) PWRs containing 48 MOX fuel assemblies in a core of 193 fuel assemblies. It is also intended to increase the number of MOX fuel assemblies in the cores by greater reloads and/or increased time of

Roepenack et al. THERMAL PLUTONIUM RECYCLING

| 0.92 | 0.93 | 0.95       | 0.99 | 0.98 | 0.99       | 1.05 | 0.95   | 0.84 | 0.93 | 0.98 | Enrichment                                                |
|------|------|------------|------|------|------------|------|--------|------|------|------|-----------------------------------------------------------|
|      | 0.94 | 0.98       | 0    | 1,02 | 1.03       | 1.07 | 0.96   | 0.85 | 0.94 | 1.00 | 3.2% Pu <sub>liss</sub> Mass Fraction in U <sub>nat</sub> |
|      |      | J.98       | 1.00 | 1.02 | 0          | 1.10 | 0.97   | 0.85 | 0.95 | 0    | 2.0% Pu <sub>liss</sub> Mass Fraction in U <sub>nat</sub> |
|      | 0    |            | 0.98 | 0.99 | 1.05       | 1.09 | 0.97   | 0.85 | 0.94 | 1.00 | 3.1% <sup>235</sup> U Mass Fraction                       |
|      |      |            |      | 1.01 | 1.06       | 1.11 | 0.98   | 0.86 | 0.95 | 1.00 | 3.1% Wass Fraction                                        |
|      |      | $\bigcirc$ |      |      | 0          | 0.94 | 1.01   | 0.87 | 0.96 | 0    | RCC Position                                              |
|      |      |            |      |      |            | 0.97 | 1.04   | 0.88 | 0.95 | 1.00 |                                                           |
|      |      |            |      |      |            |      | 1.10   | 0.90 | 0.95 | 0.99 |                                                           |
|      |      |            |      |      |            |      |        | 0.94 | 0.97 | 1.00 |                                                           |
|      |      |            |      |      |            |      | I<br>I |      | 1.00 | 1.02 |                                                           |
|      |      | $\bigcirc$ |      |      | $\bigcirc$ |      |        |      |      | 0    |                                                           |

Fig. 5. Enrichment and relative power density distribution for the PWR, MOX fuel assembly type  $16 \times 16 - 20$ .

TABLE II

Data of Out-In-In Fuel Cycles with Different MOX Fuel Assembly Designs in a Large PWR

| •                                                                                                                                                                      |         |         |         |
|------------------------------------------------------------------------------------------------------------------------------------------------------------------------|---------|---------|---------|
| Reload:  MOX fuel assembly number/Pu <sub>fiss</sub> content (wt%)  Uranium fuel assembly number/ <sup>235</sup> U enrichment (wt%)                                    | 16/2.83 | 16/3.07 | 16/2.91 |
|                                                                                                                                                                        | 48/3.4  | 48/3.4  | 48/3.4  |
| Data of equilibrium cycles Initial boron concentration (ppm) Cycle length (day) Average burnup of unloaded batch (MWd/kg)                                              | 1241    | 1252    | 1247    |
|                                                                                                                                                                        | 326     | 331     | 329     |
|                                                                                                                                                                        | 35.4    | 35.9    | 35.5    |
| Fissile content of MOX fuel assemblies  Fresh fuel  235U (kg per fuel assembly)  Pu <sub>fiss</sub> (kg per fuel assembly)  Plutonium (kg per fuel assembly)           | 3.7     | 3.6     | 3.6     |
|                                                                                                                                                                        | 15.2    | 16.5    | 15.4    |
|                                                                                                                                                                        | 21.0    | 22.7    | 21.2    |
| Burnt fuel Burnup (MWd/kg)  235U (kg per fuel assembly) Pu <sub>fiss</sub> (kg per fuel assembly) Plutonium (kg per fuel assembly)                                     | 37.1    | 37.5    | 37.4    |
|                                                                                                                                                                        | 1.4     | 1.6     | 1.5     |
|                                                                                                                                                                        | 7.7     | 8.6     | 7.7     |
|                                                                                                                                                                        | 13.9    | 15.2    | 14.0    |
| Reactivity data  Net control rod worth, end of cycle (%)  Moderator temperature coefficient, end of cycle (pcm/°C)  Reciprocal boron worth, beginning of cycle (ppm/%) | 7.6     | 7.5     | 7.5     |
|                                                                                                                                                                        | -60.6   | 61.8    | -59.5   |
|                                                                                                                                                                        | -136    | 137     | -135    |

insertion of them. Both were found possible by detailed fuel shuffling studies.

With regard to BWRs, it was intended to design a MOX fuel assembly that concentrated a maximum amount of plutonium in a minimum of reload fuel assemblies. This aims at a reduction in the economic penalty of island-type MOX fuel assemblies caused by

the assembling procedure, the transportation under safeguards measures, and the interim storage needs preceding reprocessing.

In any case, reactivity coefficients, kinetic data, hot channel factors, and the worth of the shutdown systems must meet the design criteria and fulfill requirements for safe reactor operation.

#### RECYCLING PROGRAM

KWU/Alkem began their thermal plutonium recycling program with the insertion of a test assembly into the BWR at Kahl in 1966. In the following years, further MOX fuel test assemblies were irradiated in the power plants at Kahl (VAK), KWL (Lingen, BWR) and MZFR [Karlsruhe, pressurized heavy water reactor (PHWR)]. The irradiation of MOX fuel assemblies was continued on a large scale at KWO (Obrigheim, PWR) since 1972 and at KRB-A (Gundremmingen, BWR) since 1974 (Ref. 5).

Plutonium recycling in PWRs has been performed with the improved MOX fuel (OCOM and AUPuC) in KWO since 1981, in GKN (Neckarwestheim) since 1982, in KKU (Unterweser) and Beznau-2 since 1984, and in KKG/BAG (Grafenrheinfeld) since 1985 (Refs. 1 and 3).

As shown in Table I, 25 504 MOX fuel rods (= 278 fuel assemblies) currently have been irradiated to a maximum local burnup of 46 MWd/kg (M), to a maximum average burnup per fuel assembly of 37 MWd/kg (M). These include 14 393 fuel rods with MOX OCOM fuel and 1519 with MOX AUPuC fuel.

#### Irradiation Experience with MOX Fuel

The MOX fuel assemblies exhibited an operating performance that is equal to that of the uranium fuel assemblies supplied by KWU. There are no reasons why an extension of the burnup to higher values is not possible. Continuous pool inspections during refueling and at the end of the irradiation using wet sipping and visual inspections with a television camera have confirmed the excellent behavior of the MOX fuel assemblies.

To obtain more detailed data, 23 KWO fuel rods—13 with former standard MOX fuel, 6 with AUPuC fuel, and 4 with OCOM fuel, with burnups from 6 to 37 MWd/kg (M)—have been investigated in the KWU hot cells at Karlstein. The examinations showed no significant differences in the materials performance of MOX fuel as compared to UO<sub>2</sub> fuel. Both behaved identically with regard to changes in outer diameter (cladding creep down), as shown in Fig. 6, and in increase of length (irradiation growth), as shown in Fig. 7.

Related to the average burnup, the integral volume changes of the MOX fuel due to densification and later due to swelling are smaller compared to that of UO<sub>2</sub> fuel. This has been determined from gamma scans of MOX fuel pellet columns (length changes) and additional density measurements on MOX pellets with burnups from 5.5 to 40.5 MWd/kg (M).

A difference has been observed in the fission gas release of the MOX and UO<sub>2</sub> fuel rods. The fractional fission gas release in the former standard MOX fuel was found to be higher compared to the UO<sub>2</sub> fuel

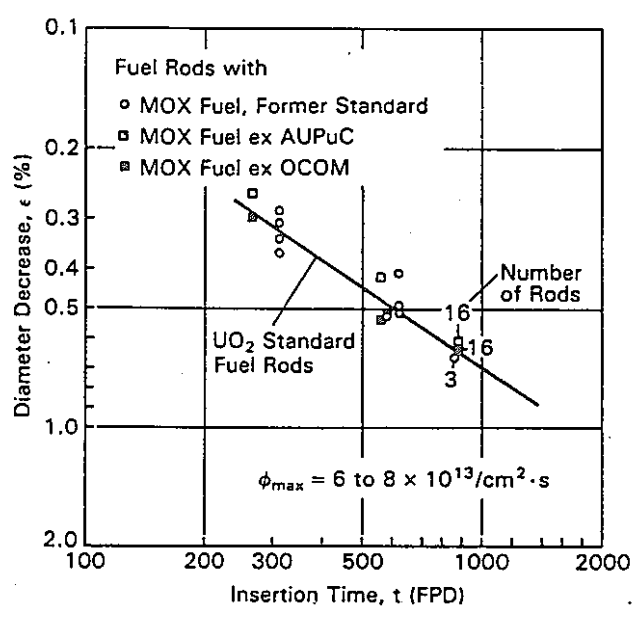


Fig. 6. Maximum diameter decrease of KWO MOX fuel rods as a function of insertion time.

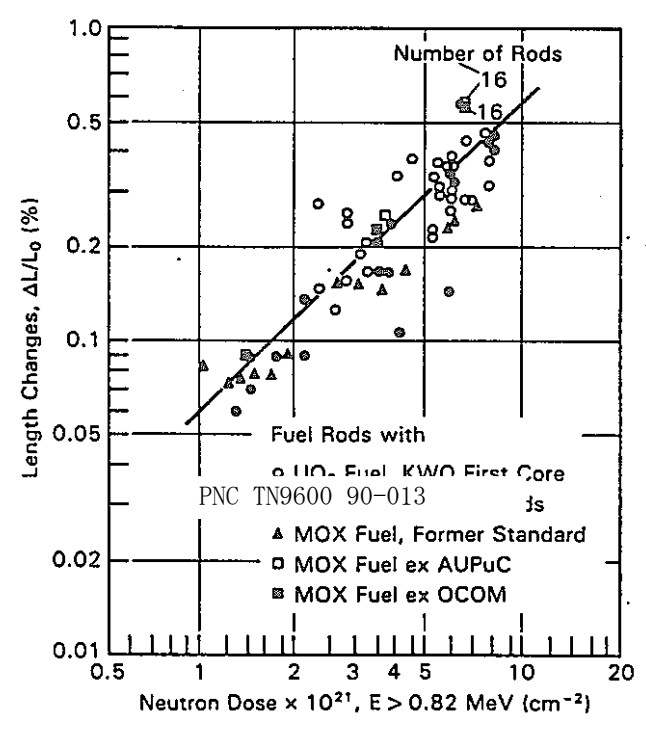


Fig. 7. Length increase of KWO UO<sub>2</sub> and MOX fuel rods as a function of neutron dose.

rods, particularly up to burnups of  $\sim$ 25 MWd/kg (M) (two-cycle rods). This is mainly attributed to the lower initial bulk density of the former standard MOX fuel (9.9 compared to 10.35 g/cm<sup>3</sup> of the UO<sub>2</sub> fuel), the

#### Roepenack et al. THERMAL PLUTONIUM RECYCLING

high open porosity ( $\sim 80\%$ ), the higher fission density associated with the discrete PuO<sub>2</sub> particles [local burnups in the PuO<sub>2</sub> particles of  $\sim 300$  MWd/kg (M)], and hence the microscopically inhomogeneous fissioning. Moreover, some MOX fuel rods were irradiated at higher heat generation rates (260 to 300 W/cm) than the UO<sub>2</sub> fuel rods (200 to 250 W/cm).

With increasing burnup and decreasing heat generation rate, the fractional fission gas release decreased toward the values known from UO<sub>2</sub>. It is assumed that this is the result of a continuous homogenization of plutonium in the surrounding matrix, a reduction in open porosity, and an increased contribution in

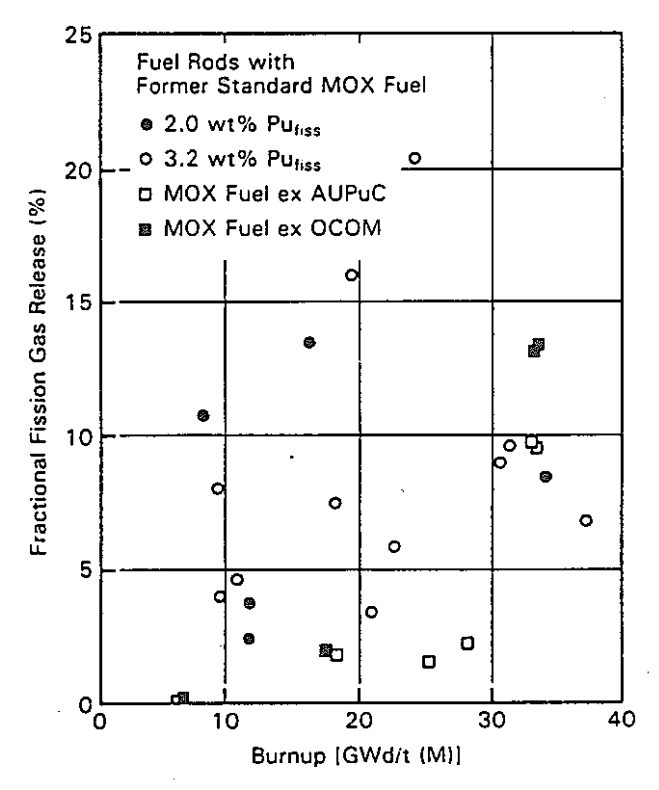


Fig. 8. Fractional fission gas release of MOX fuel rods irradiated in KWO.

power generation from plutonium generated in the UO<sub>2</sub> matrix. However, no macroscopic redistribution of plutonium was observed.

Because of its more homogeneous structure, higher density (~10.4 g/cm³), and lower open porosity (<40%), the improved MOX fuel (AUPuC, OCOM) shows a smaller fractional fission gas release at lower heat generation rates (<260 W/cm) than the former standard MOX fuel. After irradiation up to a burnup of ~33 MWd/kg (M) at heat generation rates of ~290 W/cm during the second and third cycle, however, the fission gas release is comparable to that of the former standard MOX fuel. Figure 8 contains the measured fractional fission gas release of KWO MOX fuel rods with former standard, AUPuC, and OCOM fuel as a function of burnup.

As described, the performance of MOX fuel rods at stationary operation (constant power) has been very satisfactory. Fuel rods in power reactors are subject a power variations during their lifetime, however, whic means power increases after a prolonged period at part-load and from control rod movements combined with xenon-effects.

To simulate such typical power changes, several ramping experiments have been performed with short fuel rods made from former standard MOX fuel and AUPuC-MOX fuel at KWO and HFR Petten (for design data of test rods, see Table III) (Ref. 12).

The following ramp experiments revealed the superior ramping behavior of these MOX fuel rods:

- 1. In KWO, 14 test rods with former standard MOX fuel, preirradiated at KWO to a burnup range of 9.0 to 21.8 MWd/kg (M), were ramp tested starting at 160 to 360 W/cm and leading to 270 to 420 W/cm. Thereafter, two of these ramp-tested rods were ramp tested a second time after a further preirradiation period at 165 to 230 W/cm and a burnup of 17 to 27 MWd/kg (M) to 260 W/cm.
- 2. In the High Flux Reactor (HFR), Petten, T Netherlands, 10 test rods with former standard MOA fuel, preirradiated at KWO to a burnup range of 9.3 to 32.1 MWd/kg (M), were ramp tested between 290 and 480 to 560 W/cm.

TABLE III

Ramp Experiments with MOX Fuel Rods at KWO and HFR Petten, Design Data of the Ramped Test Rods

| Pu <sub>fiss</sub> in natural uranium (wt%)                                                         | 3.2                                                     | Fuel length (mm) Fuel rod length (mm)          | 310           |
|-----------------------------------------------------------------------------------------------------|---------------------------------------------------------|------------------------------------------------|---------------|
| Pellet diameter (mm)                                                                                | 9.08                                                    |                                                | 385           |
| Mox fuel density Former standard (g/cm³) AUPuC (g/cm³) Zircaloy-4 cladding Cladding dimensions (mm) | 9.9 to 10.2<br>10.35<br>Stress relieved<br>10.75 × 9.28 | Diametric gap (mm)<br>Helium prepressure (bar) | 0.200<br>22.5 |

3. In the HFR Petten, three test rods with AUPuC-MOX fuel, preirradiated to ~35 MWd/kg (M), were ramped from 250 W/cm to 420 to 490 W/cm.

The power ramp rates in all 30 tests were in the 70 to 120 W/(cm·min) range. No defective MOX test rod has been found.

Figure 9 shows the ramp terminal linear heat generating rate as a function of burnup of the 30 ramptested rods in comparison to the power thresholds that have been elaborated for the UO<sub>2</sub> fuel rods. It can be seen that these power thresholds for UO<sub>2</sub> fuel rods were clearly exceeded by the MOX fuel rods.

Postirradiation examinations of these 30 MOX test rods after ramps at a higher burnup still reveal no diameter increase. The dimensional behavior is nearly equal to that of UO<sub>2</sub> fuel rods with a corresponding power history. The measured fission gas release of the ramped MOX fuel rods also tends to higher values in comparison with ramped UO<sub>2</sub> fuel rods.

#### **Experimental Verification Related to Neutron Physics**

The success of the neutron physics design of MOX fuel assemblies is demonstrated by the behavior during the recycle program as predicted and as verified by in-core measurements both at startup and during the cycle. This experience has been complemented by some special experiments that cannot be conducted in power reactors. Further verification of the neutron physics design stems from postirradiation examinations using gamma scans and isotopic composition and burnup measurements. 5.9,11

Some examples of this experience are as follows:

- 1. Burnup behavior. The cycle length is the most interesting quantity for fuel shuffling planning and economy. During KWO plutonium recycling after 1972, it has been shown that the predicted results with changing amounts of MOX fuel assemblies were as good as for pure uranium cores. The cycles show that fresh MOX fuel assemblies have the tendency to shorten the cycle by ~1 to 2 days related to different designs and plutonium composition per MOX fuel assembly. By appropriate design this effect can be overcome during the second and particularly the third irradiation period.
- 2. Power density distribution. Control of the power density distribution is done by aeroball activation measurements. No differences are to be seen between the interpretation of the activation in, near, and far from MOX fuel assemblies.
- 3. Control rod worth. MOX fuel assemblies can be loaded at any core position. It has been shown by means of experiments at KWO and at the KRITZ facility that the control rod worth is reduced significantly by fresh MOX fuel assemblies and at high coolant temperature. This is shown in Fig. 10. As the stuck rod worth is reduced by the presence of MOX fuel assemblies in the core in most cases, no restrictions for their loading scheme result.
- 4. Burnup and isotopic composition measurements. Isotopic analyses have been carried out on several MOX fuel samples with an initial Pu<sub>fiss</sub> content of 2 and 3.2%, covering a range of burnup up to 40 MWd/kg (M). The comparison of predicted and measured isotopic compositions can be considered

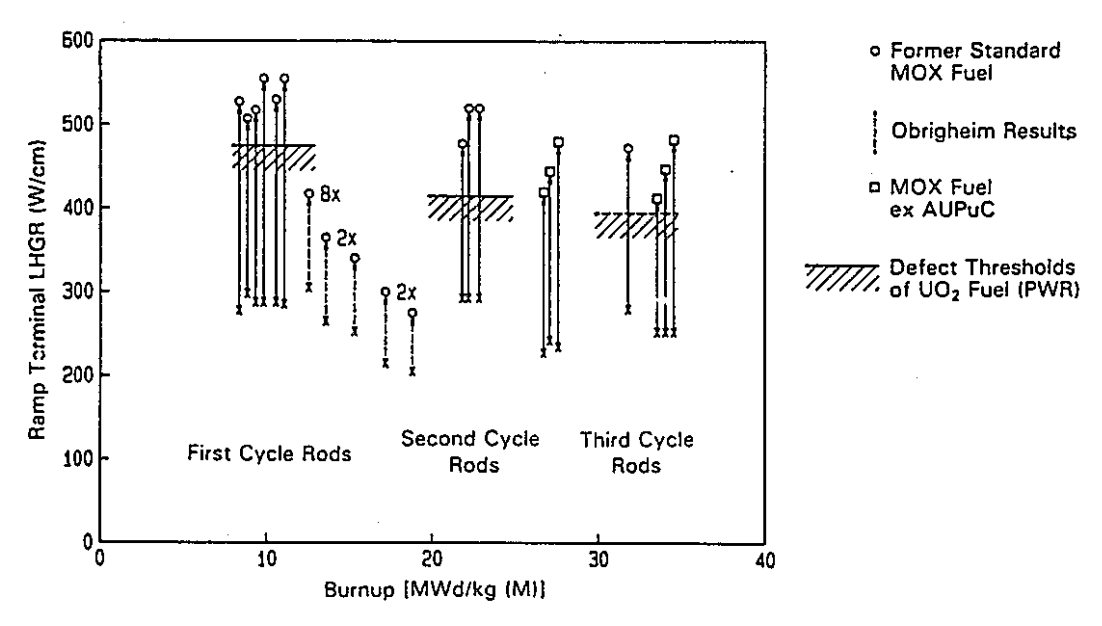


Fig. 9. Ramping experiments with MOX fuel rods in KWO and in HFR Petten (all rods are nondefective).

#### Roepenack et al. THERMAL PLUTONIUM RECYCLING

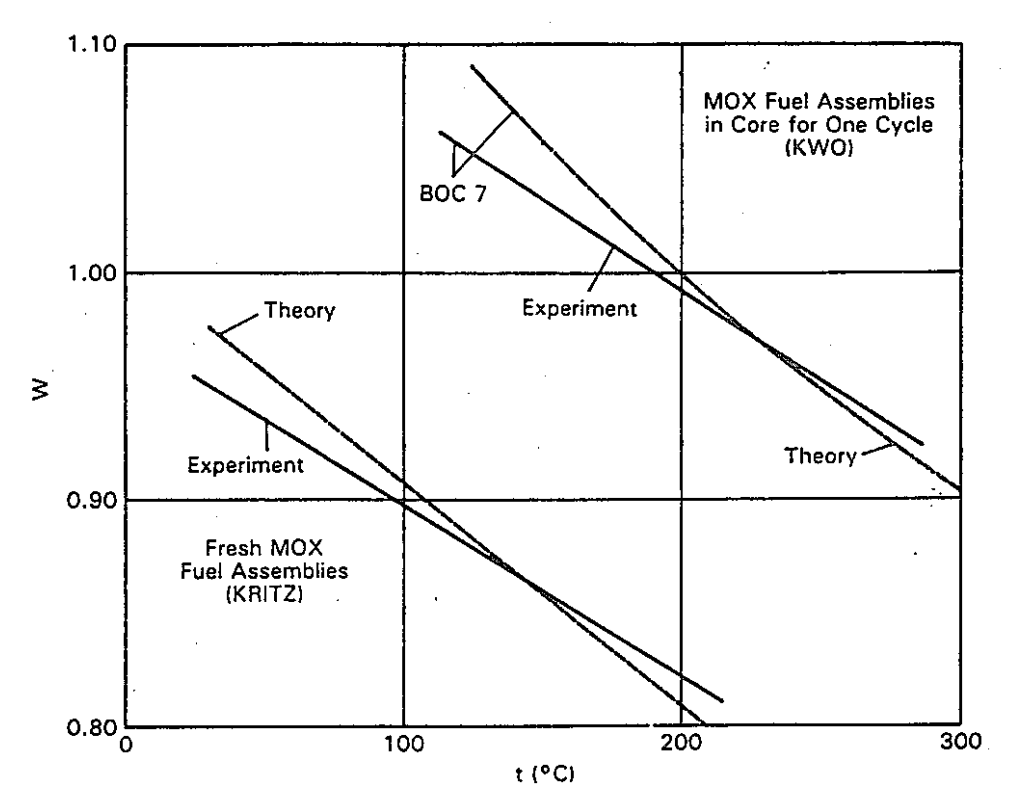


Fig. 10. Ratio W of the reactivity worth of control rods in MOX fuel assemblies to that in uranium fuel assemblies versus moderator temperature.

highly satisfactory for all plutonium isotopes. Higher actinides such as americium and curium isotopes, which are of special interest related to waste disposal, are also determined well by the calculations.

#### **FUTURE DEVELOPMENT**

Following the development for uranium fuel, higher burnups and therefore higher plutonium contents will also become necessary for MOX fuel. In accordance with expected  $^{235}$ U enrichments of 4% in the uranium fuel, corresponding MOX rod  $Pu_{fiss}$  contents up to 4.1% in the natural uranium matrix are expected. Such MOX fuel assemblies (e.g.,  $18 \times 18 - 24$ ) may contain rods with only two different plutonium percentages and four additional water rods.  $^{13}$  For low leakage loadings, MOX fuel assembly designs with burnable poisons may become necessary, especially for BWRs.

To close the fuel cycle, one must consider plutonium recycling as well as the recycling of reprocessed uranium<sup>2,3</sup> (RU). Recycling of this RU for the greater part should be performed by separate reenrichment to enriched reprocessed uranium (ERU) and fabrication of ERU fuel assemblies. As shown in Fig. 11, separate reprocessing of ERU fuel assemblies opens the possi-

bility to use the whole second generation RU (RU2) as carrier material for MOX fuel assemblies. This recycling strategy

- 1. reduces possible radiological hazards due to <sup>232</sup>U and <sup>234</sup>U decay products
- 2. reduces the amount of <sup>236</sup>U in the fuel cycle
- 3. utilizes the whole potential of natural resource

The future MOX recycling program in the Fk includes the continuation of the postirradiation examinations on fuel rods currently under irradiation. For AUPuC and OCOM fuel rods, such examinations will be performed both at the pool sites of the different PWRs and at the hot cells.

In addition, further ramp experiments are planned in the HFR Petten using short test rods with AUPuC and OCOM fuel after preirradiation for two, three, and four cycles in KWO.

Further development of the MOX fabrication both for FBR and for LWR purposes will depend mainly on the experience that can be gained from the fabrication quantities of MOX fuel in the next few years and on the introduction of this experience into the future development of processes and equipment. With such development, we expect that the costs of MOX fuel fabrication can be lowered considerably. Therefore, it

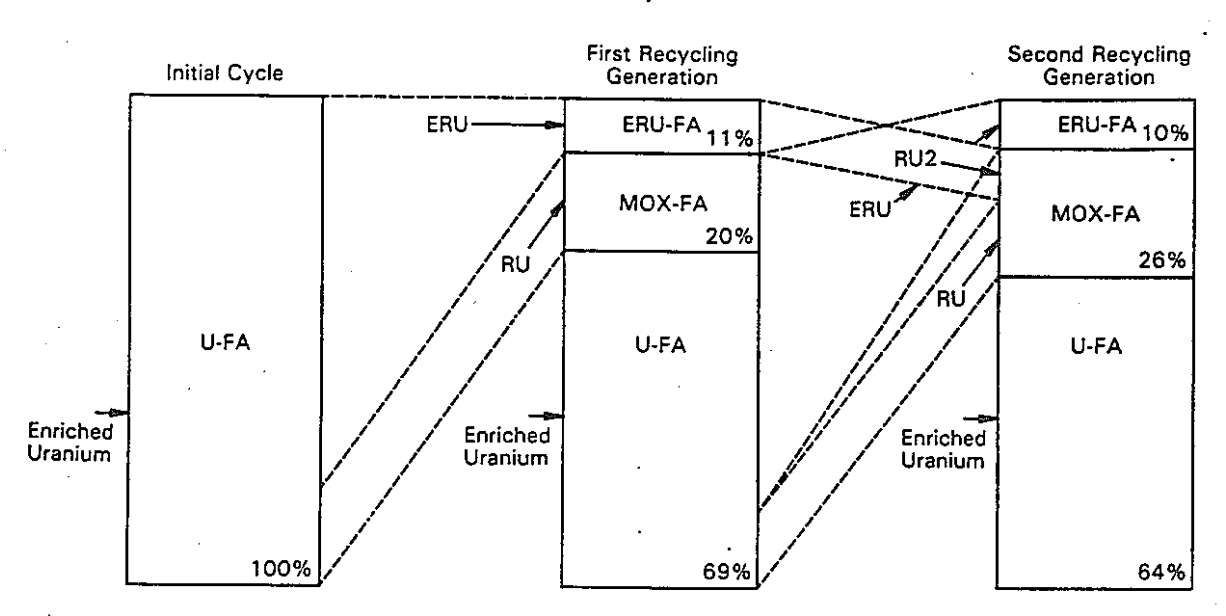


Fig. 11. Plutonium recycling strategy with use of RU as ERU in ERU fuel assemblies and as RU and RU2 in MOX fuel assemblies.

seems reasonable that the closed fuel cycle, including reprocessing and refabrication, can also become economically competitive to the so-called once-through fuel cycle.

#### CONCLUSION

Thermal recycling of uranium and plutonium is a technically and economically convenient technique for utilizing the fissile materials gained by reprocessing. This is demonstrated by the existing large-scale recycling experience in the FRG. This conclusion remains valid if further improvements in uranium fuel assembly and core design were also to be applied to the closed fuel cycle.

#### REFERENCES

- 1. H. ROEPENACK, F. SCHLEMMER, and G. SCHLOSSER, "KWU/ALKEM Experience in Thermal Pu-Recycling," Proc. Specialists' Mtg. Improved Utilization of Water Reactor Fuel with Special Emphasis on Extended Burnups and Plutonium Recycling, Mol, Belgium, May 1984, IWGFPT/20, p. 208, International Atomic Energy Agency, Vienna (1984).
- 2. O. BEER, G. SCHLOSSER, and F. SPIELVOGEL, "Experience with Thermal Recycling of Plutonium and Uranium," *Trans. Am. Nucl. Soc.*, 49, Suppl. 1, 224 (1985).
- 3. O. BEER and G. J. SCHLOSSER, "Advanced Uranium Utilization in LWR by Recycling of Uranium and

Plutonium," Proc. Technical Committee and Workshop on Advanced Light and Heavy Water Reactor Technology, Vienna, Austria, November 1984, IAEA-TECDOC-344, p. 91, International Atomic Energy Agency, Vienna (1985).

- 4. H. J. SCHENK, K. L. HUPPERT, and W. STOLL, "Experience with the Use of Recycle Plutonium in Mixed-Oxide Fuel in Light Water Reactors in the Federal Republic of Germany," *Nucl. Technol.*, 43, 174 (1979).
- 5. G. SCHLOSSER and R. MANZEL, "Recycling of Plutonium in Light Water Reactors, Part 1, Demonstration Programs," Siemens Forsch. Entwicklungsber., 8, 108 (1979).
- 6. V. SCHNEIDER, F. HERRMANN, and W. G. DRUCKENBRODT, "The AUPuC-Process: A Coprecipitation Process with Good Product Homogeneity to the Full Scale of Plutonium Concentration," *Trans. Am. Nucl. Soc.*, 31, 176 (1979).
- 7. H. ROEPENACK, V. SCHNEIDER, and W. G. DRUCKENBRODT, "Experience with the AUPuC-Co-Conversion Process for Mixed Oxide Fuel Fabrication," Am. Ceram. Soc. Bull., 63, 1051 (1984).
- 8. K. GRUBER, G. LATZEL, and H. ROEPENACK, "Fabrication and Quality Control of Mixed Oxide LWR Fuel with Regard to Homogeneity of Fissile Content," Proc. Seminar Practical Experience in the Application of Quality Control in Water Reactor Fuel Fabrication, KfK-Bericht 3777, IAEA-SR-102/23, p. 353, International Atomic Energy Agency, Vienna (July 1984).
- 9. G. SCHLOSSER, P. UYTTENDAELE, P. KAAS, and P. STROHBACH, "Plutoniui.) Recycling in LWRs:

#### Roepenack et al. THERMAL PLUTONIUM RECYCI ING

- KWU Experience and Commercial Designs," Trans. Am. Nucl. Soc., 31, 281 (1979).
- 10. G. SCHLOSSER and P. UYTTENDAELE, "Recycling of Plutonium in Light Water Reactors, Part 2, Prospective Commercial Recycling," Siemens Forsch. Entwicklungsber., 8, 153 (1979).
- 11. G. SCHLOSSER, F. SCHLEMMER, F. WUNDER-LICH, and H. UNGER, Stand und Weiterführung des Plutoniumeinsatzes in Leichtwasserreaktoren, p. 73, Deutsches Atomforum, Bonn, Jahrestagung Kerntechnik,
- Düsseldorf, Fachsitzung Brennelemente und Brennelementwerkstoffe (1981).
- 12. R. MANZEL, F. SCHLEMMER, F. SONTHEIMER, and W. VOGL, "Leistungsrampenversuche mit plutonium-haltigen Brennstäben," German Federal Ministry for Research and Technology Forschungsbericht K82-001, Kernforschung (Aug. 1982).
- 13. W. BÖHM, "Stand und Entwicklungstendenzen der BE-Einsatzplanung in Leichtwasserreaktoren," atw, 28, 126 (1983).

# STATUS OF FUEL ASSEMBLY DESIGN AND CORE MANAGEMENT EXPERIENCE WITH MOX FUEL IN THE FRG FOR SIEMENS / KWU TYPE LWRs

by
W. D. KREBS\*), G. J. SCHLOSSER\*)
SIEMENS AG KWU Group
Nuclear Fuel Cycle Division
Erlangen,
Federal Republic of Germany

# IAEA

Technical Committee Meeting on Recycling of Plutonium and Uranium in Water Reactor Fuels Cadarache, France 13 - 16 November 1989

\*) Siemens AG
KWU B3
Hammerbacherstr. 12 + 14
Postfach 32 20
D-8520 Erlangen
FRG

#### **ABSTRACT**

The Federal Republic of Germany has adopted the strategy of a closed fuel cycle using reprocessing and recycling. The central issue today in this context is plutonium recycling in operating PWRs and most recently in BWRs as well. Optimized designs of MOX fuel assemblies for PWRs presently use up to 3 types of MOX fuel rods having different plutonium contents with natural or tails uranium as carrier material but without burnable absorbers. The MOX fuel assembly designs for BWRs submitted for licensing use 4 to 5 rods with different plutonium contents and Gd<sub>2</sub>0<sub>3</sub>-U0<sub>2</sub> burnable absorber rods. Both the PWR and the BWR designs attain good equivalence and compatibility with uranium fuel assemblies. High flexibility exists in the number of MOX fuel assemblies loaded in LWR cores. Siemens/KWU experience with MOX fuel assemblies is based on the insertion of 242 MOX fuel assemblies in 8 PWR and 168 in BWR and PHWR so far. Primary operating results include information on cycle length, power distribution, reactivity coefficients and control rod worth of cores containing MOX fuel assemblies. Normal levels of reliability and safety can be maintained in reactor operation even with increased MOX fuel fractions, higher fissile contents and at high burnup.

#### 1. INTRODUCTION

The Atomic Energy Act of the Federal Republic of Germany calls for the fuel cycle to be closed by reprocessing and for the products of reprocessing to be recycled [1, 2]. Plutonium recycling in existing LWRs is a central issue in this context [3, 4]. In addition to the research supported by the BMFT\*) (Federal Ministry for Research and Technology) the German electric power utilities have formed a plutonium pool [5] intended to provide early benefit to all owners. Experience with design and operation has been accumulated quickly due to the possibility of concentrating use of the available stocks of plutonium on reactors for which recycling licenses had already been granted and is an advantage in substantiating applications for further licenses. The aim of the utilities' agreement was to establish cost-effective plutonium recycling by the earliest possible date. This drive was based primarily on the standardization potential of the existing PWR; now licenses have been awarded or are pending for the use of mixed oxide fuel in nearly all PWR. Licensing procedures are currently in progress for BWR as well, so that all utilities, including those which have no PWR, will be able to use plutonium. The aim of mixed oxide fuel assembly design is to place the greatest possible amount of plutonium in the smallest possible number of fuel assemblies and to achieve approximately the same burnup as is obtained in a uranium fuel assembly so that there are no negative effects on cycle length, loading scheme and power distribution.

<sup>\*</sup> This work was supported by the Federal Ministry for Research and Technology (BMFT) under project nos. KWA 7703 6 and 7704 7.

On the basis of the licensing requirements the present paper describes MOX fuel assembly designs for PWR and BWR and the relevant core management. This is followed by a discussion of the present status of recycling and finally a description of important experience.

#### 2. NUCLEAR DESIGN-

# 2.1 FUEL ASSEMBLY DESIGN FOR LARGE PWR

Prerequisite for plutonium recycling is the granting of a license for the use of MOX fuel assemblies in the reactor. Therefore the technical feasibility is examined on the basis of realistic and enveloping designs. For this purpose, studies are carried out in various areas of analysis for different categories of requirements [6], as is shown schematically in Fig. 1. On this basis, the technically and legally validated limits of MOX fuel use are defined in the licensing procedure. Within these limits, licensing for individual cycles is then simply a matter of proving that existing analyses cover the case to hand or of extending their coverage by additional analyses.

Plutonium recycling in MOX fuel assemblies of the type shown in Fig. 2 is being carried out in five of the seven 1300 MWe PWRs designed by Siemens/KWU containing 193 type 16x16-20 fuel assemblies. Three rod types are used, one containing 1.9 w/o Pufiss in the corner rods, one with a content of 2.3 w/o Pufiss preferentially for the fuel assembly periphery and one with 3.3 w/o used in the MOX fuel assembly interior. To date the carrier material has been natural uranium. Water-filled cladding tubes are placed in four positions to increase power output in the fuel assembly interior by improved moderation. The design of these MOX fuel assemblies is such that, in conjuction with the currently normal reload batches and reload strategies with or without U-Gd fuel assemblies, they achieve burnups comparable to uranium fuel assemblies with enrichments of 3.4 w/o U235 and do not noticeably alter the length of the cycle. This design approach produces early in life slightly lower average linear heat generation rates than are obtained with uranium fuel assemblies. A fuel assembly as shown in Fig.3 is included as a further example of a MOX fuel assembly in the current licensing procedures. Tails-uranium is used in this fuel assembly as carrier material as is Pu from high burn-up uranium fuel assemblies with correspondingly higher Pufiss contents of 2.2, 3.0 and 4.6 w/o. An equilibrium core based on full lowleakage loading with altogether 81 MOX fuel assemblies (42 % of the core) of this design is illustrated in Fig. 4. This equilibrium core has a reload batch

consisting of 24 MOX fuel assemblies and 32 uranium fuel assemblies of which the majority are gadolinium-poisoned.

Important cycle characteristics for various equilibrium cores with MOX fuel assemblies are listed in Table I. The first three columns refer to the above-mentioned type 16x16-20 fuel assemblies. This is followed by examples of equilibrium cycles for 1300 MWe reactors of the CONVOY type with type 18x18-24 fuel assemblies. Two cases are considered, namely 50% MOX loading and, as an extreme, a long cycle in a reactor fully loaded with MOX fuel assemblies (Pu burner). The decisive factor here is that it has been possible to provide verifications for these cycles as required in Fig. 1. Finally, the assessment of the core characteristics is considered in Table I with reference to the differences from comparable, pure uranium equilibrium cycles. With MOX fuel assemblies present in the core, the more negative temperature coefficient of the coolant and the smaller boron worth are especially apparent. As regards the net control assembly worth for the stuck rod configuration at the end of cycle in the hot standby condition, data depend more on the loading scheme than on the fraction of MOX fuel assemblies in the core.

#### 2.2 FUEL ASSEMBLY AND CORE DESIGN FOR LARGE BWRs

In BWRs, too, preference is given to concentrating MOX fuel rods in as few reload fuel assemblies as possible for reasons of fabrication, number of shipments and backend considerations. Only the necessity to have Gd-poisoned fuel rods leads to the provision of U-Gd rods in the MOX fuel assembly rather than developing special U-Pu-Gd fuel. Fig. 5 is a design example of a type 9x9-9Q MOX fuel assembly containing four MOX fuel rod types having different Pufiss contents and tailsuranium carrier material. The 12 U-Gd fuel rods are arranged in the vicinity of the water channel which replaces the nine central fuel rod positions and which is an important contribution to power flattening and better moderation for the MOX fuel. The central water channel also has a favorable effect on the void coefficient and hot-to-cold swing. Table II illustrates the important characteristics of an equilibrium core with 31% MOX fuel assemblies for a 1300 MWe BWR. However, loadings with 38% and 54% MOX fuel assemblies have been investigated for consideration in other licensing procedures. In this context, we await positive assessments from TUEV and the corresponding licenses.

# 3. LICENSING STATUS

The present status of licensing for German pressurized water reactors is collated in Table III. The Swiss reactor BZN-2 is also included, since plutonium recycling started out very similar to KWO (Obrigheim). Although it was possible to treat the reactors KKU (Unterweser) to KBR (Brokdorf) in the same way with regard to fuel assembly design and core management in the course of time due to the decentralized licensing procedure in the FRG different licensing practices evolved with regard to acceptable reload batches, MOX fuel assembly fractions in the core, and in particular with regard to the maximum permissible content of Pufiss and permissible carrier materials. Such differences are even found in the licenses of the identical CONVOY reactors KKI-2 (Isar), GKN-2 (Neckarwestheim) and KKE (Emsland). The documents being prepared at present for Biblis A and B incorporate an attempt to anticipate future necessary changes in the design of MOX fuel assemblies as regards carrier materials and plutonium vector and content so as to prepare the way for evolution in plutonium recycling. This involves not just verifying compliance with neutron physics design requirements but also generating legally unambiguous formulations. Table IV shows the corresponding licensing information for BWRs. It is hoped that the preparations in progress for licensing of boiling water reactors will lead to the first application of MOX in large BWRs as scheduled for 1990.

# 4. RECYCLING STATUS AND NEUTRON PHYSICS EXPERIENCE

Now that the boiling water reactors VAK (Kahl) and KRB-A (Gundremmingen A), and also the MZFR heavy water reactor, which were the first users of mixed oxide fuel in the seventies, have been taken out of service, KWO is now the only reactor at which mixed oxide fuel has been in uninterrupted use since 1972. The maximum number of MOX fuel assemblies used in a reload batch in each PWR and the number of MOX fuel assemblies used to date are listed in Table V. The maximum fraction of MOX fuel assemblies in a core load so far is 23% at BZN-2. In this case, a large fraction of 4-cycle MOX fuel assemblies is present in the core, as is illustrated by the loading in Fig. 6, and a partial low-leakage scheme without burnable poisons is in operation.

Neutron physics experience is based on start-up measurements, inservice cycle monitoring and individual measurements required under licensing commitments. The reliability of the design methods is confirmed by measurements of cycle length, reactivity coefficients such as for coolant temperature and boron

concentration and power density distribution. This also applies to control assembly worth measurements which were substantiated in 1989 by measurements on fresh MOX fuel assemblies inserted at rodded positions.

Very different compositions or vectors of plutonium have been used, starting with plutonium from Magnox reactors and progressing to plutonium from high-burnup fuel comprising up to 2.2% Pu238 and only 54.5% Pu239. Pathfinder rods of second recycling generation plutonium contained only 43.8% Pu239 and 14.2% Pu241 but 34.3% Pu240.

The fabrication experience [7] and the results of fuel examinations [8] are presented separately at this conference.

A survey of the chronological development of MOX fuel use in PWRs is collated in Fig. 7. In particular since new methods of manufacturing MOX fuel became available in 1981, numbers of MOX fuel assemblies inserted per year and of course the total in service have strongly increased; of the total of approx. 53,000 fuel rods which have been incorporated in reload batches, just under 30,000 of them are now operating in reactor cores.

#### PROSPECTS

In addition to the above-mentioned current licensing procedures, developments are paralleling uranium fuel in the design of and obtaining operating licenses for correspondingly higher enriched MOX fuel assemblies for higher burn-up. Major factors in this respect are plutonium with a smaller proportion of thermally fissile isotopes and the use of other carrier materials. As long as the licensed MOX fractions in cores has not been exhausted, no additional licensing will be needed for the time being. It is, however, to be pointed out that the MOX fraction which can be considered safe from the neutron physics standpoint has not yet been exhausted, by the limits licensed up to now.

# 6. REFERENCES

- [1] SCHLOSSER, G. J., WINNIK, S., "Thermal recycling of plutonium and uranium in the Federal Republic of Germany. Strategy and current status", Back end of the nuclear fuel cycle: strategies and options (Proc. International Symposium Vienna, 1987) IAEA-SM-294/33, Vienna (1987) 541-549.
- [2] BEER, O., SCHLOSSSER, G. J., "Advanced uranium utilization in LWR by recycling of uranium and plutonium", Advanced light and heavy water reactors for improved fuel utilization (Proc. of a technical committee and workshop Vienna, 1984) IAEA-TECDOC-344, Vienna (1985) 91-103.
- [3] ROEPENACK, H., SCHLEMMER, F. U., SCHLOSSER, G. J., Development of thermal plutonium recycling, NUCLEAR TECHNOLOGY 77 (1987) 175 186.
- [4] ROEPENACK, H., SCHLEMMER, F., SCHLOSSER, G., "KWU/ALKEM experience in thermal Pu-recycling", Proc. Specialists' Mtg. Improved Utilization of Water Reactor Fuel with Special Emphasis on Extended Burnups and Plutonium Recycling, Mol, Belgium 1984, IWGFPT/20 208-227, IAEA, Vienna (1984).
- [5] DIBBERT, H.J., HUBER, J., WINNIK, S. L., Technische und wirtschaftliche Aspekte der Plutoniumrückführung, atomwirtschaft 33 (1988) 452 454.
- [6] KREBS, W.-D., HOLZER, R., WUNDERLICH, F., Auslegung und Einsatzplanung für fortschrittliche Nachlade-Brennelemente, atomwirtschaft 33 (1988) 442 448.
- [7] SCHNEIDER, V. W., GÜLDNER, R., BRÄHLER, G., "MOX-Fuel Fabrication in the Federal Republic of Germany", Technical Committee Meeting on Recycling of Plutonium and Uranium in Water Reactor Fuels, Cadarache, France, Nov. 1989.
- [8] SCHLEMMER, F. U., FUCHS, H.-P., MANZEL, R., "Status of irradiation experience with recycled fuel materials in the FRG for SIEMENS/KWU type fuel assemblies", Technical Committee Meeting on Recycling of Plutonium and Uranium in Water Reactor Fuels, Cadarache, France, Nov. 1989.

SIEMENS Table I

| MOX-FA Loading                     | no./%   | 48/25       | 81/42       | 81/42       | 97/50           | 193/100  |               |
|------------------------------------|---------|-------------|-------------|-------------|-----------------|----------|---------------|
| Loading Scheme                     |         | out-in-in   | LL with Gd  | LL with Gd  | part LL         | part LL  | Effect        |
| Reload MOX-FA/U-FA                 | no./no. | 16/48       | 24/32       | 24/32       | 24/24           | 64/0     | Compared      |
| MOX-FA Type                        |         | 16+16-20-4  | 16+16-20-4  | 16+16-20-4  | 18-18-24-4      | 18*18-24 | to            |
| Pu <sub>fiss</sub> -Contents       | w/o     | 1.9/2.3/3.3 | 1.9/2.3/3.3 | 2.2/3.0/4.6 | 2.0/2.6/3.9/5.0 | 4.1      | U-Cores       |
| U <sub>235</sub> -Contents         | w/o     | 0.7         | 0.7         | 0.25        | 0.7             | 0.7      | ·             |
| U-FA, U <sub>235</sub> -Enrichment | w/o     | 3.4         | 3.5         | 3.5         | 4.0             | -        |               |
| Cycle Length                       | d       | 329         | 310         | 318         | 323             | 454      | same          |
| MOX-FA Burnup                      |         |             |             |             |                 |          | U-FABatch:    |
| MOX-Batch                          | ·MWd/kg | 37.4        | 35.3        | 37.3        | 48.2            | 49.8     | Burnups       |
| max. MOX-FA                        | MWd/kg  | 39.0        | 41.9        | 43.7        | 54.6            | 57.6     | about same    |
| Initial Boron                      | ppm B   | 1247        | 1088.       | 1085        | 1256            | 1996     | less          |
| Concentration                      |         |             |             |             |                 |          |               |
| Reciprocal Boron                   | مد%/mqq | - 135       | - 147       | - 158       | - 178           | - 298    | higher        |
| Worth, BOC                         |         |             |             |             |                 |          | (about - 120) |
| Mod. Temerature                    | pcm/K   | - 59.5      | - 69.1      | - 61.4      | - 77.4          | - 78.5   | higher (about |
| Coeff., EOC                        |         |             |             |             | 1               | -        | - 55 to - 65) |
| Net Control Rod                    | مد%     | 5.5         | 6.6         | 4.7         | 5.4             | 5.3      | less to same  |
| WORTH, EOC, HZP                    |         |             |             |             | 1               |          |               |

Data of Equilibrium Fuel Cycles in Large PWRs with Different MOX Fuel (009)

Assembly Designs used in the Licensing Process

# SIEMENS

Table II

| MOX-FA Loading                |           | no./%       | 264/31 | 0/0  |
|-------------------------------|-----------|-------------|--------|------|
| Loading Scheme                |           |             | LL     | LL   |
| Reload: MOX-FA                |           | no.         | 40     | 0    |
| average Pu <sub>fiss</sub> -C | ontent    | w/o         | 3.26   | •    |
| average U235-C                |           | w/o         | 0.80   | -    |
| U-FA                          |           | no.         | 96     | 136  |
| average U235-E                | nrichment | <b>∨</b> /o | 3.4    | 3.4  |
| Cycle Length, including Coa   | st Down   | d           | 296    | 298  |
| MOX-FA Burnup                 |           | *           |        |      |
| MOX-Batch                     |           | MWd/kg      | 45.2   | -    |
| max. MOX-FA                   |           | MWd/kg      | 47.3   | -    |
| Hot Excess Reactivity, BOC    |           | % Ap        | . 1.3  | 1.1  |
| Cold Shutdown Margin, 80      | C         | ود %        | 1.4    | 1.3  |
| MCPR: U-BE                    |           | _           | 1.35   | 1.38 |
| MOX-BE                        |           |             | 1.50   | -    |
| Max. Linear Heat Rate: U      | -BE       | W/cm        | 412    | 437  |
| <b>f</b> ∨                    | IOX-BE    | W/cm        | 399    | •    |

# **SIEMENS**

Table III

|             | MOX Fuel Rods |                    | MOX-FA quantities  |                |              |  |
|-------------|---------------|--------------------|--------------------|----------------|--------------|--|
| Power Plant | per FA        | Status of licenses | no. per<br>reload. | no. in<br>core | %<br>in core |  |
| KWO         | 180           | in use             | 8                  | 28             | 26           |  |
| BZN-2       | 179           | in use             | 8                  | 32             | 26           |  |
| GKN-1       | 205           | in use             | 8                  | 16             | 9            |  |
| KKU         | 232/236       | in use             | 16                 | 48             | 25           |  |
| KKGf        | 232/236       | in use             | 16                 | 64             | - 33         |  |
| KWG         | 232/236       | in use             | 16                 | 64             | 33           |  |
| KKP-2       | 232/236       | in use             | 24                 | 72*            | 37*          |  |
| KBR         | 232/236       | in use             | 16                 | 64             | 33           |  |
| KKI-2       | 296           | granted            | 24                 | 96             | 50           |  |
| GKN-2       | 296           | granted            | 24                 | 72*            | 37*          |  |
| KKE         | 296           | granted            | 16                 | 48             | 25           |  |
| KWB-A       | 232/236       | in preparation     | 24                 | 81             | 42           |  |
| KWB-B       | 232/236       | in preparation     | 24                 | 81             | 42           |  |
| KMK         | 264           | in preparation     | 20                 | 80             | 39           |  |

\* interim limit

# Status of MOX Licenses for PWR

KWU 83 10/89

# SIEMENS

Table IV

| •           | 11071                   |                    | MOX-FA quantities  |                |              |  |  |
|-------------|-------------------------|--------------------|--------------------|----------------|--------------|--|--|
| Power Plant | MOX Fuel<br>Rods per FA | Status of licenses | no. per<br>reload. | no. in<br>core | %<br>in core |  |  |
| KRB-B       | 68                      | applied for        | 60                 | 300            | 38           |  |  |
| KRB-C       | 68                      | applied for        | 60                 | 300            | 38           |  |  |
| KKB         | 58                      | applied for        | 32                 | 136            | 25           |  |  |
| KKK         | 60                      | in preparation     | 40                 | 264            | 31           |  |  |
| KKI-1       | 60                      | in preparation     | 64                 | 320            | 54           |  |  |

|             | Reached Recycle Quantities      |                       |                               |  |  |  |  |
|-------------|---------------------------------|-----------------------|-------------------------------|--|--|--|--|
| Power Plant | max no.<br>MOX-FA<br>per reload | no.<br>MOX-FA<br>used | max.<br>percentage<br>in core |  |  |  |  |
| KWO         | 8                               | 62                    | 22                            |  |  |  |  |
| BZN-2       | 8                               | 36                    | 23                            |  |  |  |  |
| GKN-1       | 8                               | 32                    | 10                            |  |  |  |  |
| KKU         | 12                              | 44                    | 17                            |  |  |  |  |
| KKGf        | 16                              | 32                    | 17                            |  |  |  |  |
| KWG         | 16                              | 20                    | 10                            |  |  |  |  |
| KKP-2       | 8                               | 12                    | 6                             |  |  |  |  |
| KBR         | 4                               | 4                     | 2                             |  |  |  |  |

MOX insertion in PWR by SIEMENS KWU Group

KWU 93 10:89

# SIEMENS

Figure 1

| Categories of<br>Requirements | Normal Operati                        | ion Ac                                | cidents                                                     |
|-------------------------------|---------------------------------------|---------------------------------------|-------------------------------------------------------------|
| Areas of Analysis             | Reactor Core                          | Spent Fuel Pool and<br>New Fuel Store | Transients, LOCA,<br>External Events                        |
| Neutron Physics               | MOX-FA-Design<br>Core Characteristics | Sub-Criticality<br>Decay Heat         | Boron Worth<br>Reactivity Coefficients<br>Control Rod Worth |
| Thermal Hydraulics            | unchanged                             |                                       |                                                             |
| System Dynamics               | Control Rod Worth                     |                                       | as above                                                    |
| Fuel Rod Design               | Fission Gas Pressure<br>Corrosion     |                                       | Fuel Rod Failure Limit                                      |
| FA Structure Design           | unchanged                             |                                       | unchanged                                                   |
| LOCA Analysis                 |                                       | _                                     | evaluated                                                   |
| Radiological Aspects          | Activity Inventory                    | Activity Inventory<br>Release Rates   | Activity Releases                                           |

| A                                                                                                                                                                                                                                                                                                                                                                                                                                                                                                                                                                                                                                                                                                                                                                                                                                                                                                                                                                                                                                                                                                                                                                                                                                                                                                                                                                                                                                                                                                                                                                                                                                                                                                                                                                                                                                                                                                                                                                                                                                                                                                                                                                                                                                                                                                                                                                                                                                                                                                                                                                                                                                                                                                                                                                                                                                                                                                                                        | IEM  | ENS  | <u></u> |      |        |      |             |              |      |      |          |     | Figure 2                                       |
|------------------------------------------------------------------------------------------------------------------------------------------------------------------------------------------------------------------------------------------------------------------------------------------------------------------------------------------------------------------------------------------------------------------------------------------------------------------------------------------------------------------------------------------------------------------------------------------------------------------------------------------------------------------------------------------------------------------------------------------------------------------------------------------------------------------------------------------------------------------------------------------------------------------------------------------------------------------------------------------------------------------------------------------------------------------------------------------------------------------------------------------------------------------------------------------------------------------------------------------------------------------------------------------------------------------------------------------------------------------------------------------------------------------------------------------------------------------------------------------------------------------------------------------------------------------------------------------------------------------------------------------------------------------------------------------------------------------------------------------------------------------------------------------------------------------------------------------------------------------------------------------------------------------------------------------------------------------------------------------------------------------------------------------------------------------------------------------------------------------------------------------------------------------------------------------------------------------------------------------------------------------------------------------------------------------------------------------------------------------------------------------------------------------------------------------------------------------------------------------------------------------------------------------------------------------------------------------------------------------------------------------------------------------------------------------------------------------------------------------------------------------------------------------------------------------------------------------------------------------------------------------------------------------------------------------|------|------|---------|------|--------|------|-------------|--------------|------|------|----------|-----|------------------------------------------------|
| Mass Fraction in U <sub>max</sub>   Mass Fraction in | 0.83 | 1.∞̂ | 0.99    | 1.∞  | 0.93   | 0.91 | 0.98        | 0.97         | 0.82 | 0.90 | 0.96     |     |                                                |
| 1.03   1.02   1.02   1.06   1.00   0.83   0.96   RCC                                                                                                                                                                                                                                                                                                                                                                                                                                                                                                                                                                                                                                                                                                                                                                                                                                                                                                                                                                                                                                                                                                                                                                                                                                                                                                                                                                                                                                                                                                                                                                                                                                                                                                                                                                                                                                                                                                                                                                                                                                                                                                                                                                                                                                                                                                                                                                                                                                                                                                                                                                                                                                                                                                                                                                                                                                                                                     | Δ    | W    | 0.90    | RCC  | 1.02   | 1.∞  | 1.œੰ        | 0.9 <u>ě</u> | 0.83 | 0.93 | 1.01     |     | 1.9% Pu <sub>fis</sub>                         |
| Mass Fraction in U_mail                                                                                                                                                                                                                                                                                                                                                                                                                                                                                                                                                                                                                                                                                                                                                                                                                                                                                                                                                                                                                                                                                                                                                                                                                                                                                                                                                                                                                                                                                                                                                                                                                                                                                                                                                                                                                                                                                                                                                                                                                                                                                                                                                                                                                                                                                                                                                                                                                                                                                                                                                                                                                                                                                                                                                                                                                                                                                                                  | Δ    | ×    | 1.αŜ    | 1.∞  | 1.02   | RCC  | 0.89        | 1.00         | 0.83 | 0.96 | RCC      |     |                                                |
| 0.95   1.03   1.06   1.04   0.94   1.02                                                                                                                                                                                                                                                                                                                                                                                                                                                                                                                                                                                                                                                                                                                                                                                                                                                                                                                                                                                                                                                                                                                                                                                                                                                                                                                                                                                                                                                                                                                                                                                                                                                                                                                                                                                                                                                                                                                                                                                                                                                                                                                                                                                                                                                                                                                                                                                                                                                                                                                                                                                                                                                                                                                                                                                                                                                                                                  | Δ    | RCC  | Δ       | 0.92 | 0.94   | 1.02 | 1.05        | 1.00         | 0.84 | 0.94 | 1.02     |     | 2.3% $Pu_{fiss}$<br>Mass Fraction in $U_{nat}$ |
| RCC                                                                                                                                                                                                                                                                                                                                                                                                                                                                                                                                                                                                                                                                                                                                                                                                                                                                                                                                                                                                                                                                                                                                                                                                                                                                                                                                                                                                                                                                                                                                                                                                                                                                                                                                                                                                                                                                                                                                                                                                                                                                                                                                                                                                                                                                                                                                                                                                                                                                                                                                                                                                                                                                                                                                                                                                                                                                                                                                      | Δ    | Δ    | Δ       | Δ    | 0.95   | 1.03 | 1.06        | 1.01         | 0.84 | 0.94 | 1.02     | Δ   | 3.3% Pu <sub>fiss</sub>                        |
| 0.97   1.08   0.97   0.96   0.99   0.96   0.99   0.96   0.99   0.96   0.98   1.00   0.96   0.98   1.00   0.96   0.98   1.00   0.96   0.98   0.96   0.96   0.96   0.96   0.96   0.96   0.96   0.96   0.96   0.96   0.96   0.96   0.96   0.96   0.96   0.96   0.96   0.96   0.96   0.96   0.96   0.96   0.96   0.96   0.96   0.96   0.96   0.96   0.96   0.96   0.96   0.96   0.96   0.96   0.96   0.96   0.96   0.96   0.96   0.96   0.96   0.96   0.96   0.96   0.96   0.96   0.96   0.96   0.96   0.96   0.96   0.96   0.96   0.96   0.96   0.96   0.96   0.96   0.96   0.96   0.96   0.96   0.96   0.96   0.96   0.96   0.96   0.96   0.96   0.96   0.96   0.96   0.96   0.96   0.96   0.96   0.96   0.96   0.96   0.96   0.96   0.96   0.96   0.96   0.96   0.96   0.96   0.96   0.96   0.96   0.96   0.96   0.96   0.96   0.96   0.96   0.96   0.96   0.96   0.96   0.96   0.96   0.96   0.96   0.96   0.96   0.96   0.96   0.96   0.96   0.96   0.96   0.96   0.96   0.96   0.96   0.96   0.96   0.96   0.96   0.96   0.96   0.96   0.96   0.96   0.96   0.96   0.96   0.96   0.96   0.96   0.96   0.96   0.96   0.96   0.96   0.96   0.96   0.96   0.96   0.96   0.96   0.96   0.96   0.96   0.96   0.96   0.96   0.96   0.96   0.96   0.96   0.96   0.96   0.96   0.96   0.96   0.96   0.96   0.96   0.96   0.96   0.96   0.96   0.96   0.96   0.96   0.96   0.96   0.96   0.96   0.96   0.96   0.96   0.96   0.96   0.96   0.96   0.96   0.96   0.96   0.96   0.96   0.96   0.96   0.96   0.96   0.96   0.96   0.96   0.96   0.96   0.96   0.96   0.96   0.96   0.96   0.96   0.96   0.96   0.96   0.96   0.96   0.96   0.96   0.96   0.96   0.96   0.96   0.96   0.96   0.96   0.96   0.96   0.96   0.96   0.96   0.96   0.96   0.96   0.96   0.96   0.96   0.96   0.96   0.96   0.96   0.96   0.96   0.96   0.96   0.96   0.96   0.96   0.96   0.96   0.96   0.96   0.96   0.96   0.96   0.96   0.96   0.96   0.96   0.96   0.96   0.96   0.96   0.96   0.96   0.96   0.96   0.96   0.96   0.96   0.96   0.96   0.96   0.96   0.96   0.96   0.96   0.96   0.96   0.96   0.96   0.96   0.96   0.96   0.96   0.96                                                                                                                                                                                                                                                                                                                                                                                                                                                                                                                                                                                                                                                                                                                                                                                                                | Δ    | Δ    | RCC     | . Δ  | Δ      | RCC  | 0.94        | 1.04         | 0.85 | 0.97 | RCC      |     | Mass Fraction in Unat                          |
| 1.08 0.91 0.96 0.99                                                                                                                                                                                                                                                                                                                                                                                                                                                                                                                                                                                                                                                                                                                                                                                                                                                                                                                                                                                                                                                                                                                                                                                                                                                                                                                                                                                                                                                                                                                                                                                                                                                                                                                                                                                                                                                                                                                                                                                                                                                                                                                                                                                                                                                                                                                                                                                                                                                                                                                                                                                                                                                                                                                                                                                                                                                                                                                      | Δ    | Δ    | ×       | Δ    | Δ      | ×    | 0.97        | 1.œ̈́        | 0.87 | 0.95 | 1.01     |     | 3.4% U <sup>235</sup>                          |
|                                                                                                                                                                                                                                                                                                                                                                                                                                                                                                                                                                                                                                                                                                                                                                                                                                                                                                                                                                                                                                                                                                                                                                                                                                                                                                                                                                                                                                                                                                                                                                                                                                                                                                                                                                                                                                                                                                                                                                                                                                                                                                                                                                                                                                                                                                                                                                                                                                                                                                                                                                                                                                                                                                                                                                                                                                                                                                                                          | ×    | ×    | ×       | ×    | ×      | ×    | ×           | 1.08         | 0.91 | 0.96 | 0.99     | 1A/ | Walas Dad                                      |
| PWR, MOX Fuel Assembly Type 16x16-20-4 Enrichment and Relative Power Density Distribution  EMENS  Figure 3  D.89 0.96 0.93 0.96 0.90 0.89 0.96 0.96 0.79 0.89 0.98  W 1.03 RCC 0.98 0.97 1.00 0.96 0.80 0.91 1.00  A 0.97 0.96 0.98 RCC 1.06 0.97 0.80 0.94 RCC  RCC 0.89 0.92 0.99 1.03 0.98 0.81 0.93 1.01  A 0.93 1.02 1.07 1.00 0.82 0.93 1.01  A 0.93 1.02 1.07 1.00 0.82 0.93 1.01  A 0.93 1.02 1.07 1.00 0.82 0.93 1.01  A 0.93 1.02 0.95 0.86 0.95 1.01  A 0.98 0.98 0.95 0.86 0.95 1.01  X X X X X X X X X X X X X X X X X X X                                                                                                                                                                                                                                                                                                                                                                                                                                                                                                                                                                                                                                                                                                                                                                                                                                                                                                                                                                                                                                                                                                                                                                                                                                                                                                                                                                                                                                                                                                                                                                                                                                                                                                                                                                                                                                                                                                                                                                                                                                                                                                                                                                                                                                                                                                                                                                                                  |      |      |         |      |        | ,    |             |              | 0.96 | 0.98 | 1.00     |     | water koa                                      |
| PWR, MOX Fuel Assembly Type 16x16-20-4 Enrichment and Relative Power Density Distribution    EMENS   Figure 3                                                                                                                                                                                                                                                                                                                                                                                                                                                                                                                                                                                                                                                                                                                                                                                                                                                                                                                                                                                                                                                                                                                                                                                                                                                                                                                                                                                                                                                                                                                                                                                                                                                                                                                                                                                                                                                                                                                                                                                                                                                                                                                                                                                                                                                                                                                                                                                                                                                                                                                                                                                                                                                                                                                                                                                                                            |      |      |         |      |        |      |             |              |      | 1.00 | 1.04     | RCC | RCC Position                                   |
| EMENS  Figure 3  D.890.960.960.960.960.960.960.960.960.960.9                                                                                                                                                                                                                                                                                                                                                                                                                                                                                                                                                                                                                                                                                                                                                                                                                                                                                                                                                                                                                                                                                                                                                                                                                                                                                                                                                                                                                                                                                                                                                                                                                                                                                                                                                                                                                                                                                                                                                                                                                                                                                                                                                                                                                                                                                                                                                                                                                                                                                                                                                                                                                                                                                                                                                                                                                                                                             |      |      | RCC     |      |        | RCC  |             |              |      |      | RCC      |     |                                                |
| △       W       1.03 RCC 0.98 0.97 1.00 0.96 0.80 0.91 1.00       □       2.2% Pu <sub>fiss</sub> Mass Fraction in U <sub>tai</sub> △       ○       0.97 0.96 0.98 RCC 1.06 0.97 0.80 0.94 RCC       □       3.0% Pu <sub>fiss</sub> Mass Fraction in U <sub>tai</sub> △       ○       0.89 0.92 0.99 1.03 0.98 0.81 0.93 1.01       □       4.6% Fu <sub>fiss</sub> Mass Fraction in U <sub>tai</sub> △       ○       ○       ○       ○       ○       ○       ○       ○       ○       ○       ○       ○       ○       ○       ○       ○       ○       ○       ○       ○       ○       ○       ○       ○       ○       ○       ○       ○       ○       ○       ○       ○       ○       ○       ○       ○       ○       ○       ○       ○       ○       ○       ○       ○       ○       ○       ○       ○       ○       ○       ○       ○       ○       ○       ○       ○       ○       ○       ○       ○       ○       ○       ○       ○       ○       ○       ○       ○       ○       ○       ○       ○       ○       ○       ○       ○       ○       ○       ○       ○       ○       ○       ○       ○       ○       ○                                                                                                                                                                                                                                                                                                                                                                                                                                                                                                                                                                                                                                                                                                                                                                                                                                                                                                                                                                                                                                                                                                                                                                                                                                                                                                                                                                                                                                                                                                                                                                                                                                                                                                                                                                                                                 | EM   | ENS  | i       |      |        |      |             |              | ,    |      |          |     | Figure 3                                       |
| △       W       1.03 RCC 0.98 0.97 1.00 0.96 0.80 0.91 1.00       □       2.2% Pu <sub>fiss</sub> Mass Fraction in U <sub>tai</sub> △       △       ○       0.97 0.96 0.98 RCC 1.06 0.97 0.80 0.94 RCC       □       3.0% Pu <sub>fiss</sub> Mass Fraction in U <sub>tai</sub> △       ○       ○       ○       ○       ○       ○       ○       ○       ○       ○       ○       ○       ○       ○       ○       ○       ○       ○       ○       ○       ○       ○       ○       ○       ○       ○       ○       ○       ○       ○       ○       ○       ○       ○       ○       ○       ○       ○       ○       ○       ○       ○       ○       ○       ○       ○       ○       ○       ○       ○       ○       ○       ○       ○       ○       ○       ○       ○       ○       ○       ○       ○       ○       ○       ○       ○       ○       ○       ○       ○       ○       ○       ○       ○       ○       ○       ○       ○       ○       ○       ○       ○       ○       ○       ○       ○       ○       ○       ○       ○       ○       ○       ○       ○       ○       ○<                                                                                                                                                                                                                                                                                                                                                                                                                                                                                                                                                                                                                                                                                                                                                                                                                                                                                                                                                                                                                                                                                                                                                                                                                                                                                                                                                                                                                                                                                                                                                                                                                                                                                                                                                                                                                                                        | ΔΙ   | ΔΪ   |         | Δ    |        |      |             |              |      |      |          | -   |                                                |
| W   1.03   RCC   0.98   0.97   1.00   0.96   0.80   0.91   1.00                                                                                                                                                                                                                                                                                                                                                                                                                                                                                                                                                                                                                                                                                                                                                                                                                                                                                                                                                                                                                                                                                                                                                                                                                                                                                                                                                                                                                                                                                                                                                                                                                                                                                                                                                                                                                                                                                                                                                                                                                                                                                                                                                                                                                                                                                                                                                                                                                                                                                                                                                                                                                                                                                                                                                                                                                                                                          |      | 0.95 | 0.93    | 0.95 | 0.90   | 0.89 | 0.96        | 0.96         | 0.79 | 0.89 | 0.96     |     |                                                |
| 0.97   0.96   0.98   RCC   1.06   0.97   0.80   0.94   RCC                                                                                                                                                                                                                                                                                                                                                                                                                                                                                                                                                                                                                                                                                                                                                                                                                                                                                                                                                                                                                                                                                                                                                                                                                                                                                                                                                                                                                                                                                                                                                                                                                                                                                                                                                                                                                                                                                                                                                                                                                                                                                                                                                                                                                                                                                                                                                                                                                                                                                                                                                                                                                                                                                                                                                                                                                                                                               |      |      |         |      |        |      | <del></del> |              |      |      | igsquare | 2   | 2.2% Pu <sub>fiss</sub> Mass Fraction in U     |
| RCC   0.89   0.92   0.99   1.03   0.98   0.81   0.93   1.01                                                                                                                                                                                                                                                                                                                                                                                                                                                                                                                                                                                                                                                                                                                                                                                                                                                                                                                                                                                                                                                                                                                                                                                                                                                                                                                                                                                                                                                                                                                                                                                                                                                                                                                                                                                                                                                                                                                                                                                                                                                                                                                                                                                                                                                                                                                                                                                                                                                                                                                                                                                                                                                                                                                                                                                                                                                                              | .    |      | - 1     |      |        |      |             | <u>!</u>     | Į.   |      | 1 1      |     |                                                |
| 0.93 1.02 1.07 1.00 0.82 0.93 1.01  A RCC A RCC 0.93 1.05 0.84 0.96 RCC  A A A A A A A A A A A A A A A A A A                                                                                                                                                                                                                                                                                                                                                                                                                                                                                                                                                                                                                                                                                                                                                                                                                                                                                                                                                                                                                                                                                                                                                                                                                                                                                                                                                                                                                                                                                                                                                                                                                                                                                                                                                                                                                                                                                                                                                                                                                                                                                                                                                                                                                                                                                                                                                                                                                                                                                                                                                                                                                                                                                                                                                                                                                             |      | RCC  |         |      |        |      | Ь.          | <del></del>  |      |      |          |     | Mass Fraction in Utali                         |
| A A A A X 0.98 0.95 0.86 0.95 1.01  X X X X X X X X X X X X X X X X X X X                                                                                                                                                                                                                                                                                                                                                                                                                                                                                                                                                                                                                                                                                                                                                                                                                                                                                                                                                                                                                                                                                                                                                                                                                                                                                                                                                                                                                                                                                                                                                                                                                                                                                                                                                                                                                                                                                                                                                                                                                                                                                                                                                                                                                                                                                                                                                                                                                                                                                                                                                                                                                                                                                                                                                                                                                                                                |      |      |         |      | 0.9ဒိ  | 1.02 | 1.07        | 1.∞          | 0.82 | 0.93 | 1.01     | Δ   | 4.6% Fu <sub>fiss</sub>                        |
| 0.98 0.95 0.86 0.95 1.01 3.5% U <sup>235</sup> X X X X X X 1.06 0.91 0.96 0.99  0.96 0.98 1.01  1.01 1.05 RCC RCC Position                                                                                                                                                                                                                                                                                                                                                                                                                                                                                                                                                                                                                                                                                                                                                                                                                                                                                                                                                                                                                                                                                                                                                                                                                                                                                                                                                                                                                                                                                                                                                                                                                                                                                                                                                                                                                                                                                                                                                                                                                                                                                                                                                                                                                                                                                                                                                                                                                                                                                                                                                                                                                                                                                                                                                                                                               |      |      |         |      |        |      | 0.9Ĝ        | 1.0ŝ         | 0.84 | 0.96 | RCC      |     |                                                |
| 1.06 0.91 0.96 0.99 W Water Rod 0.96 0.98 1.01 1.01 1.05 RCC RCC Position                                                                                                                                                                                                                                                                                                                                                                                                                                                                                                                                                                                                                                                                                                                                                                                                                                                                                                                                                                                                                                                                                                                                                                                                                                                                                                                                                                                                                                                                                                                                                                                                                                                                                                                                                                                                                                                                                                                                                                                                                                                                                                                                                                                                                                                                                                                                                                                                                                                                                                                                                                                                                                                                                                                                                                                                                                                                |      |      |         |      |        |      |             | 0.95         | 0.86 | 0.95 | 1.01     |     | 3.5% U <sup>235</sup>                          |
| 0.96 0.98 1.01<br>1.01 1.05 RCC RCC Position                                                                                                                                                                                                                                                                                                                                                                                                                                                                                                                                                                                                                                                                                                                                                                                                                                                                                                                                                                                                                                                                                                                                                                                                                                                                                                                                                                                                                                                                                                                                                                                                                                                                                                                                                                                                                                                                                                                                                                                                                                                                                                                                                                                                                                                                                                                                                                                                                                                                                                                                                                                                                                                                                                                                                                                                                                                                                             |      |      |         |      |        | Ŷ    |             | 1.06         | 0.91 | 0.96 | 0.99     | . W | Water Rod                                      |
|                                                                                                                                                                                                                                                                                                                                                                                                                                                                                                                                                                                                                                                                                                                                                                                                                                                                                                                                                                                                                                                                                                                                                                                                                                                                                                                                                                                                                                                                                                                                                                                                                                                                                                                                                                                                                                                                                                                                                                                                                                                                                                                                                                                                                                                                                                                                                                                                                                                                                                                                                                                                                                                                                                                                                                                                                                                                                                                                          |      |      |         |      |        |      |             |              | 0.96 |      |          |     | ···• •                                         |
| RCC   RCC     RCC                                                                                                                                                                                                                                                                                                                                                                                                                                                                                                                                                                                                                                                                                                                                                                                                                                                                                                                                                                                                                                                                                                                                                                                                                                                                                                                                                                                                                                                                                                                                                                                                                                                                                                                                                                                                                                                                                                                                                                                                                                                                                                                                                                                                                                                                                                                                                                                                                                                                                                                                                                                                                                                                                                                                                                                                                                                                                                                        |      |      |         |      |        |      |             |              |      | 1.01 | 1.05     | RCC | RCC Position                                   |
|                                                                                                                                                                                                                                                                                                                                                                                                                                                                                                                                                                                                                                                                                                                                                                                                                                                                                                                                                                                                                                                                                                                                                                                                                                                                                                                                                                                                                                                                                                                                                                                                                                                                                                                                                                                                                                                                                                                                                                                                                                                                                                                                                                                                                                                                                                                                                                                                                                                                                                                                                                                                                                                                                                                                                                                                                                                                                                                                          |      |      | RCC     |      | ļ.<br> | RCC  |             |              |      |      | RCC      |     |                                                |

PWR, MOX Fuel Assembly Type 16x16—20—4 Enrichment and Relative Power Density Distribution

| -  | _ |   | _ |   | _ |
|----|---|---|---|---|---|
| SI | Е | M | F | N | 5 |

Figure 4

|     | 1                                                        | 2           | 3           | 4           | 5           | 6           | 7           | 8           |  |  |  |
|-----|----------------------------------------------------------|-------------|-------------|-------------|-------------|-------------|-------------|-------------|--|--|--|
| 1   | Pu4<br>1.09                                              | Pu2<br>1.25 | Pu3<br>1.21 | Pu3<br>1.16 | Pu2<br>1.20 | U 3<br>0.94 | Pu1<br>1.13 | Pu3<br>0.45 |  |  |  |
| 2   |                                                          | Pu3<br>1.19 | Pu2<br>1.32 | Pu1<br>1.44 | U 3<br>0.99 | U 2<br>1.19 | U 1<br>1.07 | U 4<br>0.32 |  |  |  |
| 3   |                                                          |             | ປ 2<br>1.28 | U 3<br>1.12 | U 1<br>1.40 | U 3<br>0.96 | Pu1<br>1.14 | Pu3<br>0.43 |  |  |  |
| 4   |                                                          |             |             | U 2<br>1.30 | U 2<br>1.24 | U 2<br>1.22 | U 1<br>1.12 | U 4<br>0.27 |  |  |  |
| 5   |                                                          |             |             | U 3<br>1.02 | U 1<br>1.18 | Pu2<br>0.73 |             |             |  |  |  |
| 6 _ |                                                          |             |             |             | •           | Pu1<br>0.94 | Pu4<br>0.34 |             |  |  |  |
|     | Pu4 Type of FA, Insertion Period 1.09 Rel. Power Density |             |             |             |             |             |             |             |  |  |  |

Equilibrium Low Leakage Loading Cycle for a large PWR with 81 MOX Fuel Assemblies

## SIEMENS

Figure 5

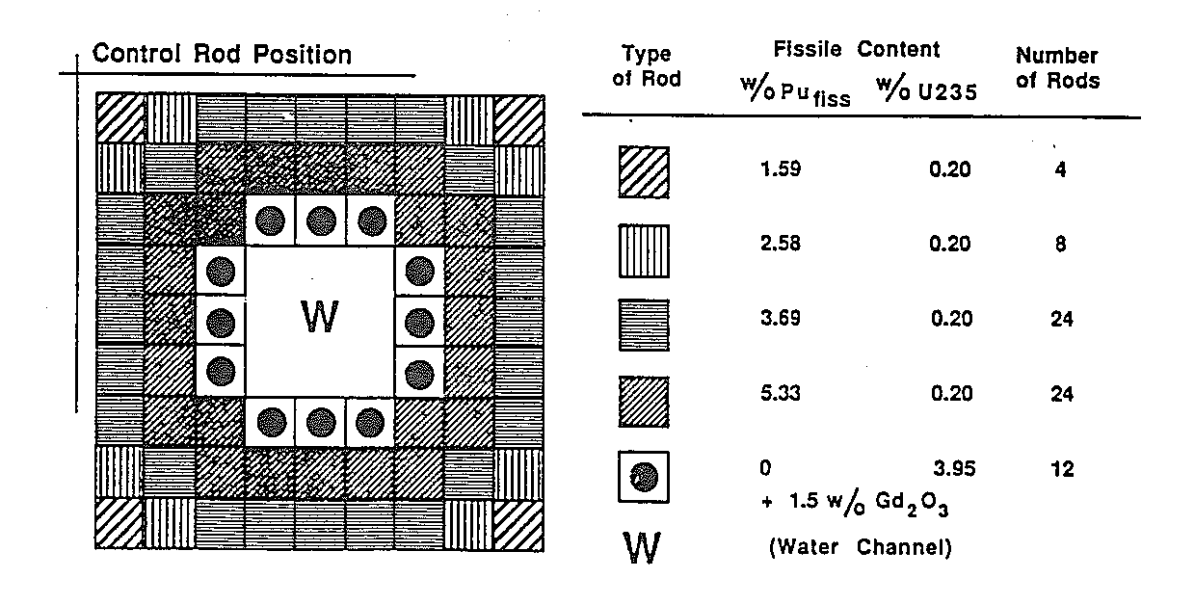
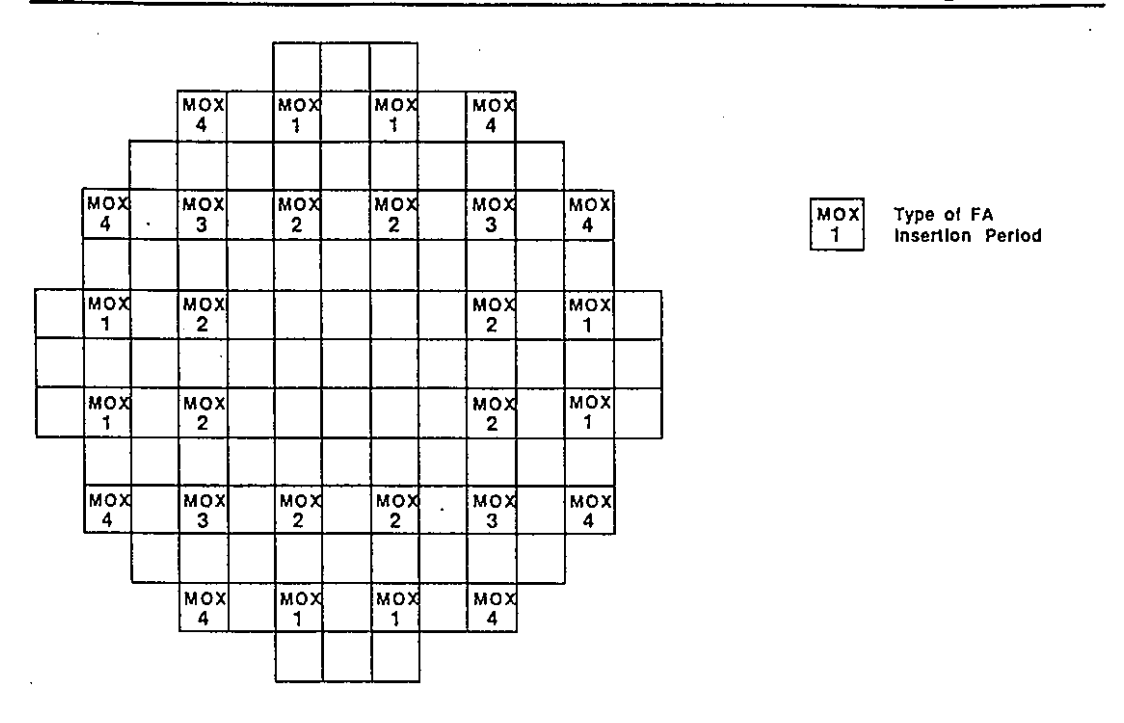
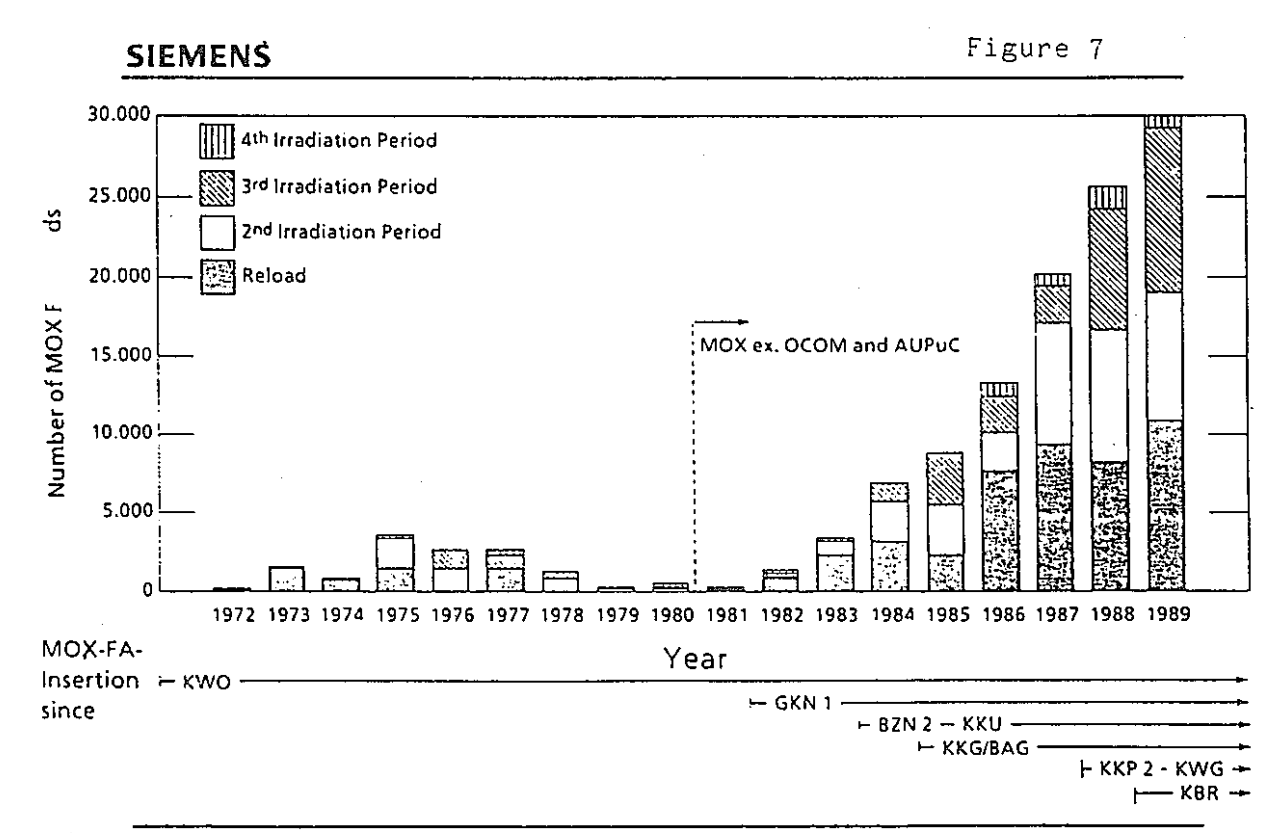


Figure 6



Actual MOX Loading Pattern at BEZNAU-2 Cycle 17 (1988-89), 28 MOX Fuel Assemblies



MOX Fuel Loading in PWRs by SIEMENS/KWU

XWU 83

# STATUS OF DESIGN AND OPERATIONAL EXPERIENCE WITH ENRICHED REPROCESSED URANIUM (ERU) FUEL IN THE FRG FOR SIEMENS/KWU TYPE LWRs

by
W. D. KREBS\*), G. J. SCHLOSSER\*)
SIEMENS AG KWU Group
Nuclear Fuel Cycle Division
Erlangen,
Federal Republic of Germany

## IAEA

Technical Committee Meeting on Recycling of Plutonium and Uranium in Water Reactor Fuels Cadarache, France 13 - 16 November 1989

\*) Siemens AG KWU B3 Hammerbacherstr. 12 + 14 Postfach 32 20 D-8520 Erlangen FRG

#### **ABSTRACT**

The technical feasibility of recycling of enriched reprocessed uranium (ERU) has been clearly proven by design investigations and by the insertion of 9 lead test assemblies. Since only a small portion of reprocessed uranium (RU) can be used as carrier material for the plutonium in mixed oxide (MOX) fuel assemblies if this is desired at all, the greater share of RU is to be processed into enriched reprocessed uranium (ERU) fuel assemblies. Design studies for ERU fuel assemblies show the equivalence to U fuel assemblies. No significant deviations in the neutron physics characteristics of cores containing rather high quantities of ERU fuel assemblies have been found. For testing U recycling, reprocessed uranium was reenriched to a somewhat higher U235 content to compensate the parasitic neutron absorption of U236. No adverse effects have been found during reactor insertion of such ERU fuel assemblies. The recycle potential of reprocessed uranium is reduced significantly with increasing burnups. Highly selective enrichment technologies (e. g. LA-SER enrichment) can reduce the burden of increasing quantities of U236. ERU recycling can be performed as early and as long the utilities see the need and the economic attractiveness.

#### 1. INTRODUCTION

The Atomic Law of the FRG demands the utilization of the fissile material contained in spent fuel assemblies unless, according to the state of the art, it is not safely possible or not reasonably economical. The reason for closing the nuclear fuel cycle by reprocessing spent fuel assemblies is manifold:

- better utilization of the natural uranium resources
- minimization of nuclear fuel imports
- long term option of fast breeder reactors
- reduction of long half-life activities in ultimate waste disposal.

The main goal of a closed fuel cycle via reprocessing [1-3] is to recover the plutonium (Pu). These Pu supplies would, of course, be best utilized in the fast breeder reactor (FBR). However for the foreseeable future, the expected Pu supply far exceeds the Pu demand of the European FBR programs. Therefore Pu recycling in thermal power reactors by mixed oxide (MOX) fuel assemblies (FA) has been performed to a growing extend in the FRG. The status of MOX-FA design, fabrication, core management and irradiation experience in the FRG is covered by three separate papers at this meeting.

This work was supported by the "Federal Ministry for Research and Technology (BMFT)" under contract nos. AtT 7645, KWA 7703 6 and 7704 7

In addition to Pu increasing amounts of reprocessed uranium (RU) are projected to be generated (Fig. 1). In principle this RU can be used to a smaller portion as carrier material for the Pu in MOX-FA and/or be processed into enriched RU fuel assemblies (ERU-FA).

By design studies and irradiation of lead test assemblies it has been demonstrated that recycling of ERU is safely possible. The second provision of the Atomic Law, whether it is reasonably economical, seems to be fulfilled for U reprocessed up to now and in the near future i. e. from fuel with low and intermediate burnup. A higher burnup significantly reduces the recycle potential of the recovered uranium due to a more and more limited U235 content and the degradation by the presence of larger amounts of the parasitic neutron absorber U236.

A technical oriented criterion on the value of RU is given in Fig. 2. The scheme depicts the combinations of initial U235 enrichment and reached final burnup of U-FA which yield RU being equivalent to natural uranium and uranium of 0.5 and 0.3 w/o U235, respectively. The possible improvements related to future highly selective enrichment processes are included, too. It can be seen that up to burnups far beyond todays experience there is a decreasing but still significant potential for better utilization of the natural uranium resources. The utilities therefore have to decide whether they prefer an early but restricted use of the RU or store it and wait for a more selective enrichment process like the atomic vapor laser isotopic separation and thus better usage of the RU.

A reprocessing of spent ERU fuel is technically and economically not recommendable due to the even worse degradation by U236 and the large increase in the Pu 238 content. Thus for spent ERU-FA final storage in geological repositories is considered rather than reprocessing them, while for spent MOX-FA multiple reprocessing is feasible [1].

In the following these statements will be explained in more detail.

#### 2. DESIGN STUDIES

The goal in designing ERU fuel assemblies, which exhibit full in-core compatibility with standard U fuel assemblies and any number of which may be inserted into the core, is to achieve burnup levels equivalent to those for standard fuel assemblies without a negative impact on cycle length. Burnable poison in the form of standard U/Gd fuel rods is inserted into ERU fuel assemblies as it is into U fuel assemblies.

The negative reactivity provided by the relatively large amounts of U236 plus U234 present in ERU fuel, which act as neutron absorber, have to be compensated for by increased U235 enrichment by an amount up to about 1/3 of the U236 content in order to achieve an equivalent reactivity (see Figure 3). Curves for the infinite multiplication factor  $k_{\infty}$  as a function of burnup for U fuel assemblies with 3.5 w/o U235 and equivalent ERU fuel assemblies with 3.8 w/o U235 and 1 w/o U236 are nearly identical up to the target burnup [3-4] of about 42 MWd/kg.

Actual fuel assembly design consists of performing rod-by-rod calculations for a so-called macrocell. An ERU macrocell consists of an ERU fuel assembly and three U fuel assemblies. Figure 4 shows for both the relative linear heat generation rate (LHGR) for individual rods at beginning of cycle. As designed for there is almost no difference in average LHGR for the two fuel assembly types (ERU-A is  $\sim 2$  % higher). The fuel rods with the highest thermal loadings, which are located adjacent to the control rod guide tubes, also exhibit a power increase of  $\sim 2$  % relative to the average rod power. There is a difference in LHGR between the peripheral ERU fuel rods and the adjacent U fuel rods of up to  $\sim 5$  %. This difference can be attributed to the fact that the increased absorption in ERU fuel leads to a hardening of the neutron spectrum compared to that for U fuel.

An in-core study was conducted to investigate the effect of ERU fuel assemblies with 3.8 W/o U235 and 1 W/o U236 on a reactor core at burnup equilibrium.

Two alternative ERU reload strategies were employed for a reload study comprising reloads of 64 fuel assemblies for a 1300 MWe PWR with 193 FA in total:

- 24 ERU fuel assemblies per each reload
- 64 ERU fuel assemblies inserted as one complete reload batch.

The data for the equilibrium cycle of the first reload strategy is compiled in Fig. 5. The reactivity coefficients and control rod worths for the equilibrium cycle are shown in comparison to a pure fresh U reload strategy. The second reload strategy investigated involved inserting a single reload batch consisting solely of ERU fuel assemblies; this batch was then investigated for three subsequent cycles, with the next two reloads consisting of fresh U-FA. In conclusion, it can be said that the two reload variants for ERU fuel assemblies can be viewed as extreme alternatives for all possible realistic reloads. There were no significant safety-related differences between the two variants. Both alternatives investigated would accommodate far more RU in the form of ERU fuel assemblies than could

be obtained from reprocessing fuel discharged from the reactor concerned. From these results it can be expected that also complete ERU-reactor-cores will show no significant difference.

#### EXPERIENCE WITH ERU FUEL ASSEMBLIES IN THE FRG

Uranium fuel assemblies containing enriched reprocessed uranium obtained through the reprocessing of burned U fuel assemblies have been inserted in the following plants in the FRG [1]:

 108 ERU fuel rods with a U235 content of 3.5 w/o and 72 U fuel rods with 3.2 w/o U235 were employed in 1 FA which was inserted into the core of KWO from 1983 to 1986 [3, 5].

The ERU fuel rods had the following composition:

 $U232/U234/U235/U236/U238 = 0.3 \times 10^{-6}/0.07/3.50/0.85/95.58 \text{ w/o}$ 

In 1986, 4 complete ERU fuel assemblies with a total of 820 fuel rods having an U235 content of 3.76 W/o were inserted in GKN-1.

The fuel had the following composition:

 $U232/U234/U235/U236/U238 = 0.5 \times 10^{-6}/0.07/3.76/1.03/95.14 \text{ w/o}$ 

- In 1987, 4 additional ERU fuel assemblies were inserted in GKN 1. They had the following composition:

 $U232/U234/U235/U236/U238 = 0.55 \times 10^{-6} / 0.06/3.72/0.81/95.41 \text{ w/o}$ 

The ERU test fuel assembly for KWO (see Figure 6) has the same structure as the standard fuel assemblies inserted in KWO and contains, as described above, fuel rods of varying enrichment. The test fuel assembly was inserted in 1983 and, after 3 operating cycles, was discharged from the core with a FA-average burnup of 33 MWd/kg HM in 1986. During each shut down for reload, one ERU and one U fuel rod were removed from the FA through a cruciform opening provided for this purpose in the top nozzle and were subjected to post-irradiation examination. The irradiation history of the assembly is given in Fig. 7. Two ERU fuel rods were inserted in another FA for a 4th cycle and reached a maximum burnup of 42 MWd/kg.

The operating behavior of the ERU test fuel assembly over 3 cycles and of the two fuel rods inserted for a 4<sup>th</sup> cycle was good.

On the basis of the post-irradiation examinations performed [7], it is concluded that there is no significant difference in the operating behavior of ERU and U fuel assemblies.

These results have been confirmed by the experience with the 8 ERU lead test assemblies irradiated at GKN-1 during the period since 1986.

#### 4. RADIOLOGICAL ASPECTS OF ERU FUEL - DECAY HEAT

The decay of U232 and U234 lead to an increase in the activity of RU and ERU during processing. Calculations were performed to obtain a quantitative determination of the activity inventory of the ERU fuel prior to insertion in KWO. This fuel had the following composition:

 $U232/U234/U235/U236/U238 = 0.3 \times 10^{-6}/0.07/3.50/0.85/95.58 \text{ w/o}$ 

The calculations were performed using the KORIGEN [5] computer program developed at the Karlsruhe Nuclear Research Center. The data obtained were compared with the activity inventory for standard fuel assemblies with an initial enrichment of 3.1 weight per cent. The activity of the ERU fuel in question was found higher than that of the enriched uranium fuel by a factor of 2.6. Whereas the effect of the U234 decay chain plays a predominate role in photon yield, the total photon energy emitted is increasingly affected by the U232 decay chain, which builds up over a period of years and to which the two hard γ-emitters, Bi 212 and TI208 make a significant contribution.

This increase in activity is characteristic of fresh fuel and is a determining factor in establishing requirements for the production and handling of new ERU fuel assemblies. It is apparent from Figure 8, which shows the major  $\gamma$ -energy levels, that radiation exposure from U232/Th228 decay products can be significantly reduced if work proceeds quickly following cleaning during reprocessing and conversion.

The activity inventory in the core depends mainly on fission products which reach equilibrium fairly quickly during reactor operation. The level of fission products present depends in turn on the power density in the core. The concentration of fission products with long half-lives increases proportional to burnup. A calculation of the overall activity inventory for U and ERU fuel assemblies in the core at reactor shutdown at the end of an operating cycle shows that the activity of the ERU fuel assemblies is almost identical (0.4 % lower) than that of the U fuel assemblies.

The levels of activity and decay heat as a function of decay time drop more slowly for ERU than for U fuel. The resulting activity in a storage pool filled with ERU fuel assemblies is about 7 % higher compared to U fuel assemblies.

The slightly higher decay heat exhibited by the ERU fuel is a result of the significantly higher decay heat of the actinides present. However, the decay heat of the actinides is generally one order of magnitude smaller than that of the fission products and thus has only a minor effect on the overall decay heat to be discharged from the storage pool.

#### 5. CONCLUSIONS

The TÜV, the authorized experts in FRG, have already certified that the use of ERU fuel assemblies a in PWR in no way degrades plant behavior under normal operation as well as accident conditions.

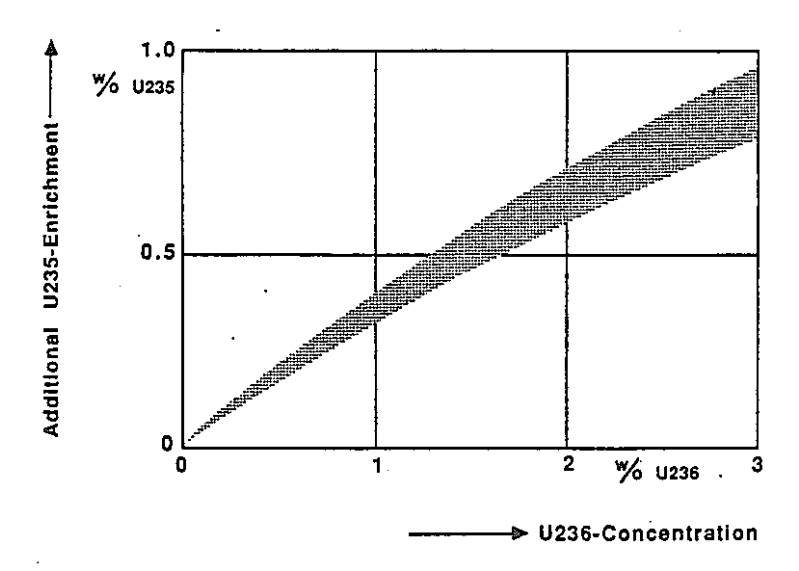
On the basis of the above mentioned designs and the experience gained with ERU-FA at KWO and GKN-1 some licenses on ERU fuel assembly insertion have been granted. They follow the concept of "equivalence" to licensed U fuel assemblies in relation to enrichment, burnup and criticality safety. The licenses for ERU fuel assembly insertion at KKP-2 and the KONVOI plants KKI-2 and GKN-2 can be seen as examples for licenses for other reactors.

Furthermore, it can be concluded from the experience with the use of ERU lead test fuel assemblies that no major technical difficulties with a future use of ERU fuel at a PWR are to be expected. These results can be transferred to BWR ERU fuel assemblies without restrictions.

The recycle potential of reprocessed uranium is reduced significantly with increasing burnup. Highly selective enrichment technologies (e. g. LASER enrichment) can reduce the burden of increasing quantities of U236. Recycling of RU can therefore be performed as early and as long the utilities see the need and the economic attractiveness.

#### 6. REFERENCES

- [1] SCHLOSSER, G. J., WINNIK, S., "Thermal recycling of plutonium and uranium in the Federal Republic of Germany. Strategy and current status", Back end of the nuclear fuel cycle; strategies and options (Proc. International Symposium Vienna, 1987) IAEA-SM-294/33, Vienna (1987) 541-549.
- [2] ROEPENACK, H., SCHLEMMER, F. U., SCHLOSSER, G. J., Development of thermal plutonium recycling, NUCLEAR TECHNOLOGY 77 (1987) 175 186.
- [3] SCHLOSSER, G. J., PORSCH, D., SCHLEMMER, F., "Uranrückführung: Strategieüberlegungen, nukleare Auslegung, Aktivitätsfragen und Einsatz eines WAU-Test-BE bei KWO", Tagungsbericht Jahrestagung Kerntechnik JK' 84, Frankfurt (1984) 297 - 300.
- [4] UYTTENDAELE, P., PORSCH, D., SCHLOSSER, G. J., "Untersuchungen zur Verwendung von wiederaufgearbeitetem Uran", Tagungsbericht Jahrestagung Kerntechnik JK' 80, Berlin (1980) 409 412.
- [5] GOLL, W., PORSCH, D., SCHLEMMER, F., "Betriebsverhalten von Brennstäben mit wiederangereichertem Uran (WAU-1)", Jahrestagung Kerntechnik JK' 87, Karlsruhe (1987) 421 - 424.
- [6] FISCHER, U., WIESE, H. W., "Verbesserte konsistente Berechnung des nuklearen Inventars abgebrannter DWR-Brennstoffe auf der Basis von Zell-Abbrand-Verfahren mit KORIGEN", KFK 3014, Kernforschungszentrum Karlsruhe (1983).
- [7] SCHLEMMER, F. U., FUCHS, H.-P., MANZEL, R., "Status of irradiation experience with recycled fuel materials in the FRG for SIEMENS/KWU type fuel assemblies", Technical Committee Meeting on Recycling of Plutonium and Uranium in Water Reactor Fuels, Cadarache, France, Nov. 1989.



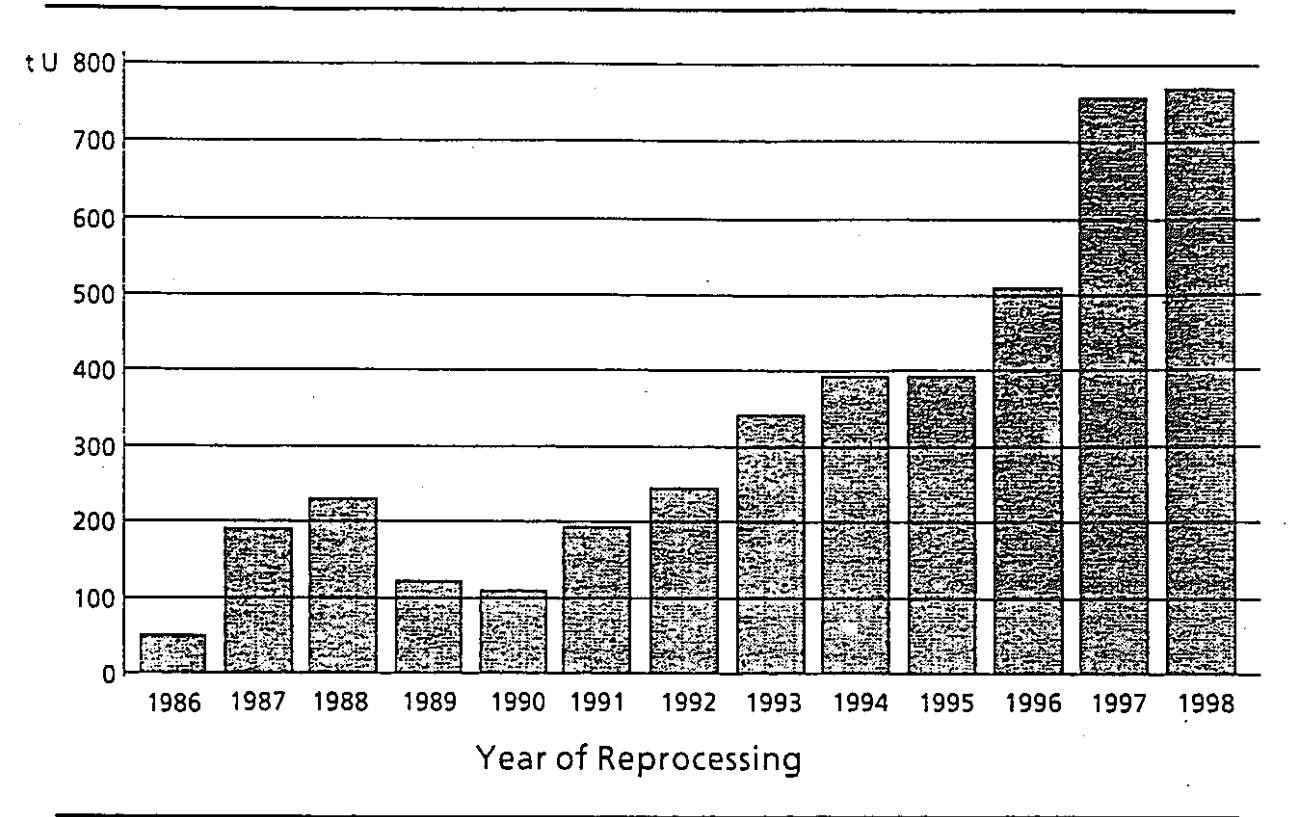
Compensation of U236 and U234 by Additional U235- Enrichment

# SIEMENS Figure 4

| 0.96 | 0.97 | 1.∞  | 1.ੴ          | 1.01 | o.sŝ | 0.89 | 1.01 | 0.95 | 0.96 | 0.98 |       |                       |  |
|------|------|------|--------------|------|------|------|------|------|------|------|-------|-----------------------|--|
| Δ    | 0.98 | 1.02 | RCC          | 1.05 | 1.ੴ  | 1.01 | 1.01 | 0.96 | 0.98 | 1.01 |       |                       |  |
| Δ    | Δ    | 1.02 | 1.04<br>1.04 | 1.05 | RCC  | 1.03 | 1.02 | 0.96 | 1.00 | RCC  |       |                       |  |
| Δ    | RCC  | Δ    | 1.01         | 1.02 | 1.04 | 1.02 | 1.02 | 0.96 | 0.98 | 1.01 |       |                       |  |
| ^    | Δ    | ۵    | Δ            | 1.02 | 1.04 | 1.02 | 1.02 | 0.96 | 0.98 | 1.01 | Δ     | 3.8% U <sup>235</sup> |  |
|      | Δ    | RCC  | Δ            | Δ    | RCC  | 1.04 | 1.02 | 0.97 | 1.00 | RCC  |       | 1.0% U <sup>235</sup> |  |
|      | Δ    | Δ    | Δ            | Δ    | Δ    | 1.02 | 1.03 | 0.97 | 0.98 | 1.00 |       | 3.5% U <sup>235</sup> |  |
| Δ    | Δ    | Δ    | Δ            | Δ    | ۵    | 4    | 1.04 | 0.98 | 0.98 | 0.98 | - RCC | RCC Position          |  |
|      |      |      |              |      |      |      |      | 0.99 | 0.98 | 0.99 |       | RCC FOSITION          |  |
|      |      |      |              |      |      |      |      |      | 0.99 | 1.01 |       |                       |  |
|      |      | RCC  |              |      | RCC  |      |      |      |      | RCC  |       |                       |  |

PWR, ERU Fuel Assembly Type 16x16—20 Enrichment and Relative Power Density Distribution

Figure 1

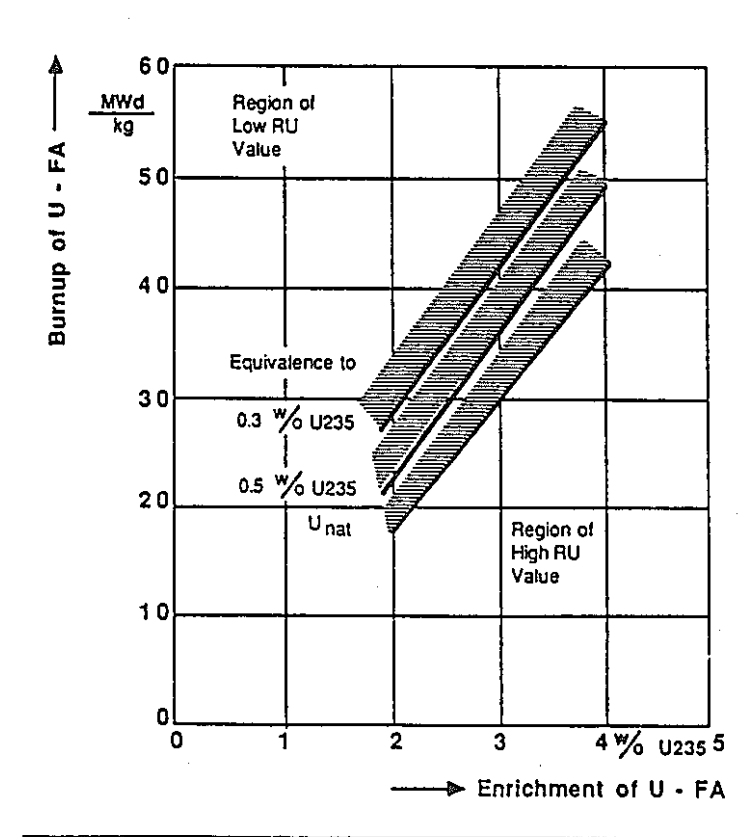


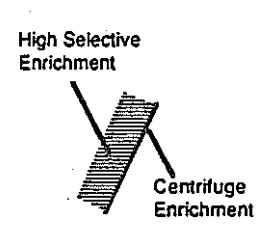
Quantities of Reprocessed Uranium from German LWR Fuel

KWU 53 10-89

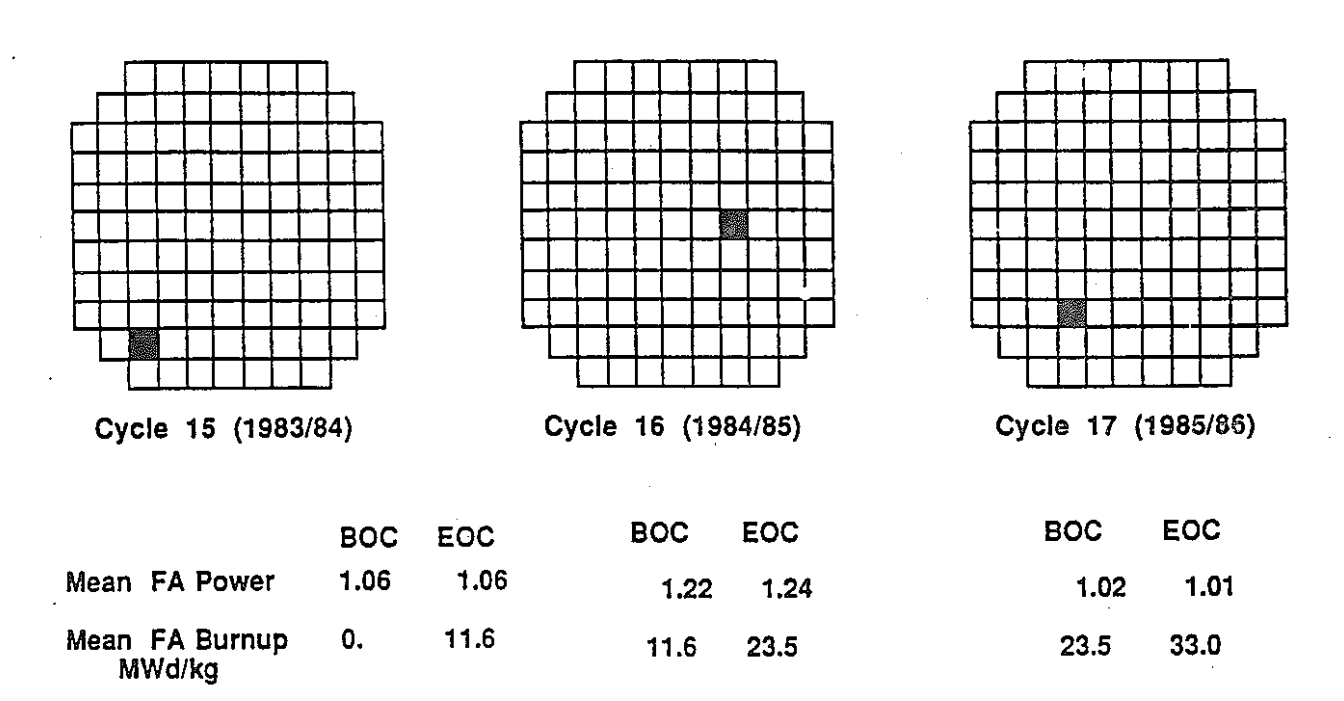
# SIEMENS

Figure 2





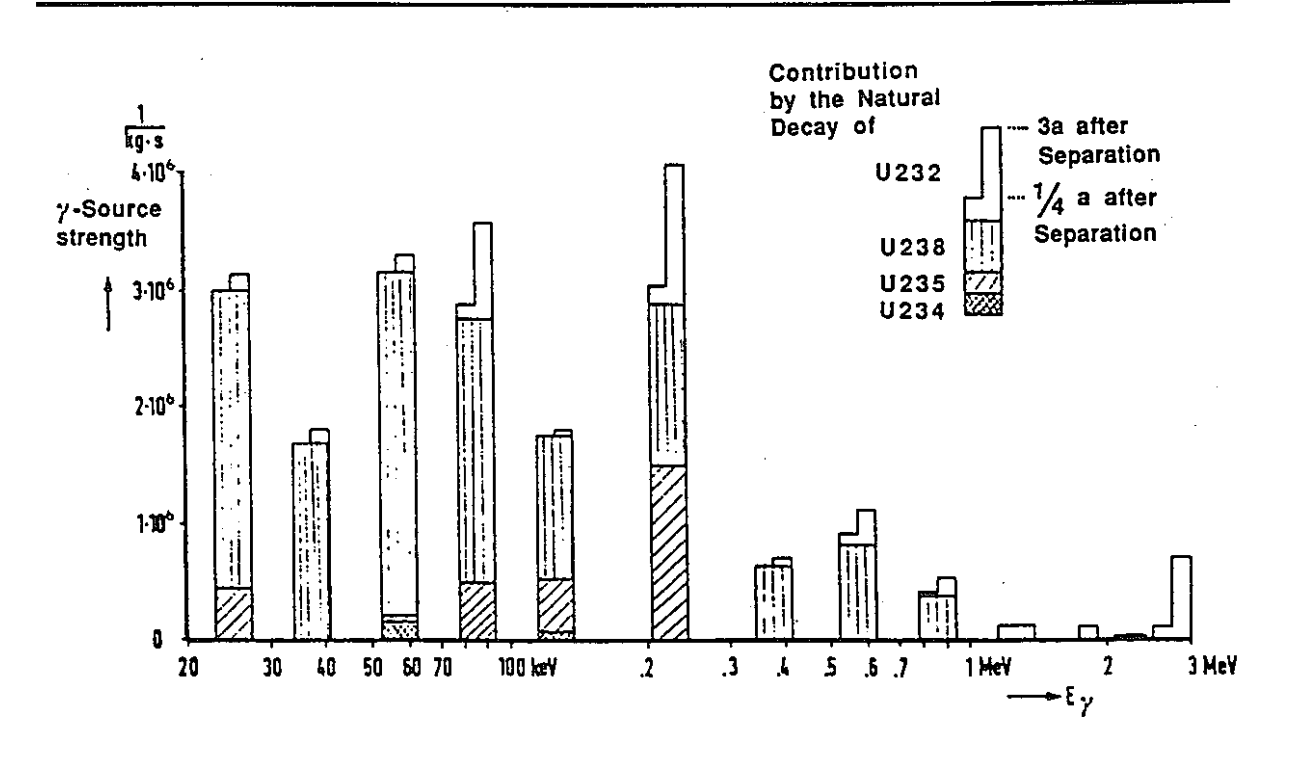
Equivalence of Reprocessed Uranium



Irradiation History of ERU Fuel Assembly inserted in KWO

#### SIEMENS

Figure 8



| ERU-FA L                    | oading                  | No/%        | 72/37     | . 0/0      |
|-----------------------------|-------------------------|-------------|-----------|------------|
| Loading :                   | Scheme                  |             | out-in-in | out-in-in. |
| Reload:                     | ERU-FA                  | No '        | 24        | -          |
|                             | ERU-FA, U235-Enrichment | <b>w</b> /o | 3.8       | -          |
|                             | ERU-FA, U236-Content    | <b>w</b> /o | 1.0       | -          |
|                             | U-FA                    | No          | 40        | 64         |
| ,                           | U-FA, U235-Enrichment   | w/o         | 3.5       | 3.5        |
| Cycle Len                   | ngth,                   | d           | 342       | 342        |
| Mean Bu                     | rnup                    | · MWd/kg    | 37.4      | 37.5       |
| Initial Bo                  | ron Concentration       | ppm B       | 1304      | 1287       |
| Reciprocal Boron Worth, BOC |                         | ppm/% Δρ    | 127       | 123        |
| Mod. Ter                    | mperature Coeff., EOC   | pcm/K       | - 59.5    | - 57.7     |
| Net Cont                    | rol Rod Worth, EOC, HZP | % Δρ        | 4.9       | 4.9        |

Data of Equilibrium Fuel Cycles in Large PWR with and without Uranium Recyling

KWU/63 10/89

# SIEMENS

Figure 6

|     |      |      |      |      |      | ليحم |      |      |
|-----|------|------|------|------|------|------|------|------|
| 0.9 | į    |      |      |      |      |      |      |      |
|     | 1.02 | 1.08 | 1.08 | RCC  | 0.99 | 0.96 | 0.96 | 1.01 |
| Δ   | Δ    | RCC  | 1.10 | 1.09 | 0.97 | 1.03 | 0.98 | 0.99 |
| Δ   | ۵    | Δ    | 1.00 | 1.09 | 0.97 | 0.96 | 0.98 | 0.99 |
| Δ   | RCC  | Δ    | Δ    | RCC  | 0.99 | 1.ထိ | 0.96 | 1.01 |
| Δ   |      |      |      |      | 1.04 | 0.96 | 0.96 | 0.98 |
| Δ   |      | Δ    |      | Δ    |      | 0.96 | 0.97 | 0.97 |
|     |      |      |      |      |      |      | 0.97 | 0.97 |
|     |      |      |      |      |      |      |      | 0.98 |

| Δ | 3.5%  | $U^{235}$ |
|---|-------|-----------|
| ŀ | በ ጸ5% | 11236     |

|  | 3.2% | U <sup>235</sup> |
|--|------|------------------|
|  |      |                  |

KWO, ERU Fuel Assembly Type 14x14—16 Enrichment and Relative Power Density Distribution

# STATUS OF IRRADIATION EXPERIENCE WITH RECYCLED FUEL MATERIALS IN THE FRG FOR SIEMENS / KWU TYPE FUEL ASSEMBLIES

by
F. U. SCHLEMMER\*), H.-P. FUCHS\*) and R. MANZEL \*)
SIEMENS AG KWU Group
Nuclear Fuel Cycle Division
Erlangen,
Federal Republic of Germany

\*) Siemens AG KWU B4 Hammerbacherstr. 12 + 14 Postfach 32 20 D-8520 Erlangen

#### Abstract

Up to now SIEMENS/KWU's operational experience with recycled fuel materials is based on the irradiation of 410 MOX (mixed oxide) and 9 ERU (enriched reprocessed uranium) fuel assemblies in 8 PWRs, 3 BWRs and 1 PHWR. That corresponds to about 53 800 MOX and 1 750 ERU fuel rods. 209 MOX fuel assemblies (about 44 350 fuel rods) have been fabricated with MOX fuel of the new OCOM and AUPuC processes. The maximum assembly burnups achieved are 42 GWd/t(HM) (MOX) and 33 GWd/tU (ERU), respectively. The irradiation behaviour of the MOX and ERU fuel has been followed and investigated in detail by special operational surveillance programmes in the different spent fuel pools on many standard MOX and ERU fuel assemblies and additional irradiation programmes with pathfinder MOX fuel rods in special carrier fuel assemblies and with special MOX test rods in test rigs in the NPP Obrigheim as well as in the HFR Petten (power ramping experiments) followed by hot cell examinations. Postirradiation examinations of MOX fuel at burnups of up to 47 GWd/t(HM) showed no significant differences in the materials performance under stationary and transient power conditions as compared to UO, standard fuel. The irradiation behaviour of ERU fuel was almost identical to UO standard fuel, too. Altogether, the irradiation experience with MOX and ERU fuel is very encouraging and their large-scale use in LWRs is technically feasible.

#### 1. INTRODUCTION

Up to 1980 SIEMENS/KWU used as standard mixed oxide (MOX) fuel a mechanically blended fuel type. The irradiation experience on fuel assemblies with this MOX fuel, gained on 201 fuel assemblies (= 9463 fuel rods) in 3 BWR, 1 PHWR and 1 PWR (see Table I), was excellent /1-2/. However, this MOX fuel did not satisfy the necessary reprocessing requirements such as complete solubility of plutonium in pure nitric acid (> 99 %). This led to the development of new MOX powder preparation processes named AUPuC and OCOM which yield pellets of better plutonium solubility in pure nitric acid already in the as-fabricated condition /3/.

Since 1981 SIEMENS/KWU has inserted MOX/AUPuC/CCOM fuel assemblies on a large scale in 8 PWRs. 209 fuel assemblies (= 44352 fuel rods) have been irradiated up to 4 cycles. A maximum fuel assembly burnup of 42 GWd/t(HM) has been achieved (see Table I) /3-5/.

In 1983 the recycling of fuel with enriched reprocessed uranium (ERU) was started in two PWRs. Meanwhile 9 ERU fuel assemblies (= 1748 fuel rods) have been irradiated for 3 cycles corresponding to a maximum fuel assembly burnup of 33 GWd/tU /6-8/.

During the last years many surveillance and investigation programmes on the new MOX and the ERU fuel have been performed to supplement the previous irradiation experience gained on fuel rods with the former standard MOX fuel.

In the following it will be exclusively reported about the performance and the results of the programmes on MOX/AUPuC/OCOM and ERU fuel.\*)

<sup>\*)</sup> This work was supported by the "Bundesminister für Forschung und Technologie" under Contract Nos ATT 7685/8, 7688/0 and 7692/3 and partly by the "Deutsche Gesellschaft für Wiederaufarbeitung von Kernbrennstoffen mbH", Hannover.

#### OPERATIONAL SURVEILLANCE AND POOL-SITE INSPECTIONS

To determine the irradiation benaviour of fuel assemblies and special test rods a large number of operational data, e.g., power history, neutron flux distribution measured with the aeroball system and the stationary incore detectors, primary coolant temperatures, pressure, chemistry etc. have been collected and evaluated. Based on these data for each fuel assembly or test rod investigated, e.g. the history of linear heat generation rate, burnup and fast neutron flux have been calculated.

First information on fuel rod integrity of the fuel assemblies in the reactor core was gained by measurements of the fission product activity in the primary coolant (e.g., I131, I133, Xe133, Xe135, Kr85m, Cs134, Cs137 etc.). In case of an increased coolant activity wet sipping tests on every fuel assembly have been performed immediately after reactor shutdown during refueling.

Additional information about the irradiation behaviour was obtained by continuous pool-site inspections on the fuel assemblies during refueling or at the end of irradiation.

Table II shows the number of fuel assemblies with MOX/AUPuC/OCOM and ERU fuel, respectively, irradiated up to 4 cycles with burnups up to 42 GWd/t(HM), and inspected in the spent fuel pools.

The visual inspections have been performed using a radiation-resistant underwater television camera. The length variations of the fuel assemblies (guide tubes) were measured with a special device built on the principle of the calliper rule and calibrated against standards. The axial clearance of the fuel rods to the assembly end fittings was determined using measuring rulers attached to the TV camera. The oxide layer thickness on fuel rods in the outer positions of fuel assemblies was measured by means of an eddy current probe.

Table III contains a summary of measurements on individual MOX and ERU fuel rods in the spent fuel pools as well as in the hot cells.

For the measurements the fuel rods were withdrawn from the fuel assemblies and passed through a multiple fuel rod measuring device. This vice allows simultaneous measurements of diameter, oxide layer thickness well as eddy current defect testing and visual inspection. Length meangements were performed with a vernier calliper device.

Additional hot cell work has been done on a selected number of precharacterized fuel rods with burnups ranging from 6 to 42 GWd/t(M) (see Table III). The most important items which have been examined in the hot cells were fission gas release, dimensional and microstructural behaviour of the fuel pellets and the cladding (densification, swelling, changes in pore and grain size, corrosion, hydrogen pick-up) and mechanical behaviour of the cladding e.g. creep down and growth.

#### POWER RAMPING EXPERIMENTS

Fuel rods in power reactors are subject to power ramps during their lifetime, e.g., power increases after a prolonged period at part-load and by control rod movements combined with xenon-effects /9/.

To simulate such typical power changes several ramping experiments have been performed with short fuel rods containing MOX/AUPuC and MOX/OCOM fuel, respectively, in the High Flux Reactor (HFR), Petten, The Netherlands. The short rodlets were pre-irradiated in segmented fuel rods at the NPP Obrigheim (KWO) up to 4 cycles.

Table IV shows the main design data of the ramped test rods. In addition to the 10 ramp tests with former standard MOX fuel /1, 2/, 7 MOX/AUPuC fuel rodlets with burnups of 26 to 43 GWd/t(HM) and 2 MOX/OCCM fuel rodlets with a burnup of about 24 GWd/t(HM) have been ramp tested. The ramp terminal power was up to 490 W/cm starting from 250 and 300 W/cm, respectively (see Figure 1).

The power ramp rate in all the tests was about 100 W/(cm min). No defects of MOX test rods have occurred.

Figure 1 shows the ramp terminal linear heat generating rate (LHGR) as a function of burnup for the 9 ramptested rods in comparison to the defect thresholds that have been established for UO<sub>2</sub> fuel rods. It can be seen that the defect thresholds for UO<sub>2</sub> fuel rods could clearly be exceeded with the MOX fuel rods without defects.

#### 4. MAIN RESULTS OF POOL-INSPECTIONS AND HOT CELL EXAMINATIONS

The overall behaviour of MOX/AUPuC/CCOM and ERU fuel assemblies was comparable to that of uranium fuel assemblies supplied by SIEMENS/KWU.

Fuel rod failures, (4 MOX FAs and 1 ERU FA), could definitely be attributed to fretting by debris and were not specific to MOX and ERU fuel. Surveillance of the primary coolant activity gave no indication for a different fission product release characteristic of MOX and ERU fuel assemblies compared to uranium fuel assemblies. A comparison of the relevant physical properties governing the fission product release did not show any significant differences between MOX and uranium fuel, hence supporting an almost identical defect behaviour for MOX and uranium fuel.

The dimensional behaviour, length and diameter changes, is fully comparable to that of UO, fuel rods. Figure 2 describes the length increase of MOX/AUPuC/OCOM and ERO fuel rods, as a function of fast neutron fluence. Up to a fast fluence of about  $5\times10^{-2}$  cm $^{-2}$  (E > 0.82 MeV) the length increase follows a linear relationship with fast fluence, as deduced from empty tube measurements. At higher fast fluences an increasing scatter in the data and a deviation from linear behaviour is observed. Both, the deviation from the linear relationship and the increased scatter could be attributed to pellet/clad interaction. Compared to uranium fuel rods whose growth with 95 % confidence is also shown in Figure 2 the MOX and ERU fuel rods reveal an identical growth behaviour.

This is also true for the maximum diameter decrease of MOX/AUPuC/OCOM and ERU fuel rods as shown in Figure 3. The diameter of MOX and ERU fuel rods like that of uranium fuel rods of similar rod power decreases steadily with time and does not indicate any support by the swelling fuel up to burnups of  $42~\mathrm{GWd/t(HM)}$ .

As expected, oxide layer thickness measurements on MOX and ERU fuel rods gave values identical to uranium fuel rods for comparable power history.

The densification and swelling behaviour of the MOX/AUPuC, MOX/OCOM and ERU fuel have been examined in dependence on the fuel burnup. The results are presented in Figure 4 in comparison to the densification and swelling data band for UC standard fuel (dotted lines). Apart from the ERU fuel, whose density data fit well into the UC data band, the density data of the MOX/AUPuC and MOX/OCOM fuel altogether are positioned at the lower boundary of the UC data band; that means the dimensional changes of the MOX fuel up to fuel burnups of about 40 GWd/t(HM) seem to be somewhat smaller.

Figure 5 shows the stationary fractional fission gas release of MOX/AUPuC/OCOM and ERU fuel in dependence on fuel rod burnup. The fractional fission gas release of MOX/AUPuC/OCOM and ERU fuel at high burnup ranges from 2 % to 17 %. This wide range in fractional fission gas release is attributed to the also wide range of power histories and consequently fuel temperatures of the fuel rods examined. Cycle average LHGRs of about 250 W/cm in the second and third operational cycle generally lead to high fission gas releases (about 17 %) while LHGRs lower than 210 W/cm, as for instance in the case of the ERU fuel rods, caused fission gas releases of about 2 %. Altogether fractional fission gas release of MOX/AUPuC/OCOM fuel was found to be somewhat higher at comparable power history in relation to UO<sub>2</sub> fuel.

The measured transient fission gas release of MOX/AUPuC fuel rodlets pre-irradiated to burnups of about 26 to 43 GWd/t(HM) and ramped to terminal power levels of 420 to 490 W/cm ranges from 23 to 46 % and is comparable to ramped UO $_2$  fuel rods.

#### SOLUBILITY TESTS ON IRRADIATED MOX/AUPuc/OCOM FUEL

To determine the solubility behaviour of plutonium from irradiated MOX fuel rods fuel samples were examined from one, two, three and four cycle rods with MOX/AUPuC and MOX/OCOM fuel, respectively. The content of fissile plutonium was about 3.2 %, the burnup of the samples in the range of 3 to 46 GWd/t(HM). The solubility tests on these samples were performed in pure nitric acid. They altogether yielded high plutonium solubilities (> 99.8 %) thus comparable to UO $_2$  fuel /10/.

#### 6. IRRADIATION TESTS WITH PLUTONIUM OF 2ND GENERATION

In 1980 SIEMENS/KWU started an irradiation programme with segmented MOX fuel rods containing plutonium of the second generation. This material was gained in the reprocessing plant MILLI at the WAK in Karlsruhe from first-generation material, which was irradiated for 3 cycles in the NPP Obrigheim.

14 MOX fuel segments, fabricated at ALKEM by using the AUPuC process, were irradiated in different KWO MOX fuel assemblies for 2, 3 and ycles.

The fuel rodlets achieved burnups from 26 to 47  $\,\mathrm{GWd/t(HM)}$ . They did not reveal any fuel rod defects. The overall operating performance was comparable to that of MOX fuel rods with first-generation plutonium, although fission gas release was considerably higher.

A comparison of neutron physics results with the performed isotopic analyses confirmed that the fuel rod power histories and thus the reactivity pattern can be predicted with a high degree of accuracy. The nuclides relevant to neutron physics are described with sufficient accuracy.

#### 7. CONCLUSIONS

The operating behaviour of the recycled fuel materials MOX/AUPuC, MOX/OCOM and ERU fuel was investigated in detail by systematic inspections on many fuel assemblies and individual fuel rods in the spent fuel pools and by hot cell examinations on selected, precharacterized fuel rods. Supplementary power ramping experiments in the HFR Petten yielded additional information about the operating behaviour under transient power conditions.

The results of the postirradiation examinations up to local burnups of 47~GWd/t(HM) can be summarized as follows

- no fuel rod defects specificly caused by recycled fuel material,
- no significant differences in dimension and corrosion behaviour of MOX/AUPuC/OCOM fuel but somewhat higher fission gas release at comparable power history in relation to UO fuel,
- excellent load following behaviour of the MOX/AUPuC/OCOM fuel,
- very good solubility behaviour of plutonium in pure nitric acid which is important for the reprocessing procedure of irradiated fuel
- almost identical irradiation behaviour of ERU fuel to UO standard fuel.

  MOX recycling with plutonium of the second generation has been successfully tested by irradiation of test fuel rods in KWO up to a burnup of 47 GWd/t(HM).

#### 8. REFERENCES

- . / 1/ MANZEL, R., SCHLEMMER, F., SONTHEIMER, F., VOGL, W., "Leistungsrampenversuche mit plutoniumhaltigen Brennstäben", German Federal Ministry for Research and Technology, Forschungsbericht K82-001, Kernforschung (Aug. 1982)
  - / 2/ ROEPENACK, H., SCHLEMMER, F., SCHLOSSER, G., "KWU/ALKEM Experience in Thermal Pu-Recycling", Proc. Specialists' Mtg. Improved Utilization of Water Reactor Fuel with Special Emphasis on Extended Burnups and Plutonium Recycling, Mol, Belgium, May 1984, IWGFPT/20, 208, IAEA, Vienna (1984)
  - / 3/ ROEPENACK, H., SCHLEMMER, F., SCHLOSSER, G., "Development of Thermal Plutonium Recycling", J. of Nucl. Techn., Vol. 77, No. 2, (May 1987), 175-186
  - / 4/ SCHNEIDER, V., GUELDNER, R., BRAEHLER, G., "MOX-Fuel Fabrication in the Federal Republic of Germany", this Meeting
  - / 5/ KREBS, W.D., SCHLOSSER, G.J., "Status of Fuel Assembly Design and Core Management Experience with MOX Fuel in the FRG for SIEMENS/KWU Type LWRs", this Meeting
  - / 6/ SCHLOSSER, G., PORSCH, D., SCHLEMMER, F., "Uranrückführung: Strategieüberlegungen, Nukleare Auslegung, Aktivitätsfragen und Einsatz eines WAU-Test-BE bei KWO", Jahrestagung Kerntechnik 1984, 297 -300
  - / 7/ GOLL, W., PORSCH, D., SCHLEMMER, F., "Betriebsverhalten von Brennstäben mit wiederangereichertem Uran (WAU-1)", Jahrestagung Kerntechnik 1987, 421-424
  - / 8/ KREBS, W.D., SCHLOSSER, G.J., "Status of Design and Operational Experience with Enriched Reprocessed Uranium (ERU) Fuel in the FRG for SIEMENS/KWU Type LWRs", this Meeting
  - / 9/ FISCHER, G., GOLL, W., RUYTER, I., MARKGRAF, J., "Verhalten von DWR-U/Pu-Mischoxid-Brennstäben bei Leistungstransienten", Jahrestagung Kerntechnik 1989, 421-424
  - /10/ WUERTZ, R., "Löslichkeit bestrahlter MOX-Brennelemente bei der Wiederaufarbeitung", Atomwirtschaft, April 1987, 190-192

|          | Ruclear Power + Innt<br>(Type) | First<br>Insertion/<br>Year | PA-Type<br>•:Rol Array• |     | MOX<br>Island<br>6.4 | Number of<br>Fuel Rocs | Fuel Type           | Haximum<br>FA-burnud<br>70k3/t<br>Decayy Metali/ |
|----------|--------------------------------|-----------------------------|-------------------------|-----|----------------------|------------------------|---------------------|--------------------------------------------------|
| VAK,     | Kahi (EWR)                     | 1950                        | - <del></del>           | ,   |                      | 972                    | former Std. MOX     |                                                  |
| .Wi      | Lingen (bañ)                   | 1970                        | 6×5-0                   | -   | 1                    | 15                     | Pu/In, form.Stc.MGX | 2                                                |
| KRB-A.   | Gundremmingen (BWR)            | 1574                        | 6x0-0                   | 54, |                      | 2240                   | Former Std. MOX     | Fi:                                              |
| 1/FR,    | Karlsrune (PHWR)               | 1372                        | 37-0                    | ŝ   |                      | 296                    | Former Std. MOX     | 14                                               |
| KWO.     | Obrigheim (P#8)                | 1972                        | 14x14-16                | 33  |                      | 5940                   | Former Std. MOX     | 35                                               |
| KWO.     | Obrigheim (PWR)                | 1981                        | 14x14-16                | 29  |                      | 5220                   | GCOM                | 35                                               |
|          |                                | 1983                        | 14x14-16                | 1   |                      | 106                    | _RU                 | 33                                               |
| ĿKN-1,   | Neckarwestheim (PRR)           | 1982                        | 15x15-20                | 32  |                      | 6560                   | OCOM                | 42                                               |
|          |                                | 1986                        | 15x15-20                | â   |                      | 1640                   | ERU                 | 31                                               |
| KKU.     | Unicrweser (PWR)               | 1984                        | 16x16-20                | 20  |                      | 4720                   | OCOM/AUPUC          | 37                                               |
|          | ů.                             | 1987                        | 16×16-24                | 24  |                      | 55 <del>6</del> 8      | OCOM/AUPUC          | 25                                               |
| B/N-2.   | Beznau-2 (PWR)                 | 1984                        | 14x14-17                | 36  |                      | 6444                   | OCOM/AUPuC          | * 36                                             |
| KKG/BAG. | Grafenrheinfeld (PWR)          | 1985                        | 16×16-20                | 16  |                      | 3776                   | OCOM/AUPUC          | 34                                               |
|          |                                | 1987                        | 16:16-24                | 16  |                      | 3712                   | OE047AdPuC          | 29                                               |
| (KP-2,   | Philippsburg (PWR)             | 1988                        | 16=16-24                | 12  |                      | 2784                   | OCOM/AUPuC          | 16                                               |
|          | Gronnde (PWR)                  | 1988                        | 16×16-24                | 20  |                      | . 4640                 | OCOR/AUPuC          | ŽtI                                              |
| KBH.     | Brokdorf (PWR)                 | 1989                        | 16×16-24                | ц   |                      | 928                    | GCOM/AUPuC          | 1                                                |
|          | Total MOX:                     |                             | ··                      | 321 | 89                   | 53815                  |                     | 42                                               |
|          | Total ERU:                     |                             |                         | 9   |                      | 1748                   | •                   | 33                                               |

Table I: SIEMENS'/KWU's Operating Experience with MOX and ERU Fuel Assemblies (Status 10/89)

| Fuel  | Irradiation     | Range of<br>FA Burnup<br>(GWd/t(HM)) | FA<br>Failures | FA Inspections in the Spent Fuel Pools |                                                     |                         |                                                                 |  |  |  |
|-------|-----------------|--------------------------------------|----------------|----------------------------------------|-----------------------------------------------------|-------------------------|-----------------------------------------------------------------|--|--|--|
| Type  | Cycles<br>of FA |                                      |                | Visual TV<br>Inspection                | Axial Clearance of Periph- eral FRs to End Fittings | Guide<br>Tube<br>Length | Oxide Mea-<br>surements<br>on Periph-<br>eral FRs<br>(8 per FA) |  |  |  |
| x     | 1               | 7 - 14                               | 2*             | 30                                     | 1                                                   | 2                       | -                                                               |  |  |  |
|       | 2               | 15 - 29                              | 1 *            | 28                                     | 5                                                   | 6                       | . 8                                                             |  |  |  |
|       | 3               | 22 - 37                              | 1 *            | 23                                     | 4 .                                                 | 5                       | 7                                                               |  |  |  |
|       | 4               | 42                                   | 0              | 4                                      | 4                                                   | 7                       | 4                                                               |  |  |  |
| Total |                 | 7 - 42                               | 4              | 85                                     | 14                                                  | 13                      | 19                                                              |  |  |  |
| ERU   | 1               | 9 - 12                               | 1 #            | 3                                      | -                                                   | -                       | -                                                               |  |  |  |
|       | 2               | 18 - 24                              | 0              | 2                                      | -                                                   | -                       | -                                                               |  |  |  |
|       | 3               | 30 - 33                              | 0              | 2                                      | -                                                   | -                       | -                                                               |  |  |  |
| Total |                 | 9 - 33                               | 1              | 7                                      | -                                                   | -                       | -                                                               |  |  |  |

<sup>\*</sup> FA-failures caused by debris: 1 fuel rod per FA; FAs were repaired and achieved their final burnup after 3 cycles;

Table II: SIEMENS'/KWU's Pool-Inspections on Fuel Assemblies with MOX-OCOM/AUPuC and ERU Fuel (Status Oct. 89)

| Nuclear<br>Power Plant/<br>Fuel Ass.    | Fuel Rod<br>Type           | Average Fuel<br>Rod Burnup         | Measured Fuel<br>Rods in the<br>Spent Fuel Pool*<br>MOX/ MOX/ ERU |              |                   | Measurement<br>aľter<br>Cycles | Hot Cell<br>Examinations |             |             |
|-----------------------------------------|----------------------------|------------------------------------|-------------------------------------------------------------------|--------------|-------------------|--------------------------------|--------------------------|-------------|-------------|
| Type                                    |                            | (GWd/t(HM))                        | ОСОН                                                              | AUPuC        |                   |                                | (OCOM/                   | AUPuc       | /ERU)       |
| Obrigheim<br>(KWO)<br>14x14-16          | MOX-Standars               | 6 - 9<br>17 - 20<br>29 - 36<br>38  | 2<br>2<br>17                                                      | 1<br>16<br>1 |                   | 1<br>2<br>3<br>4               | 2 2 3 1                  | i<br>1<br>2 |             |
|                                         | ERU-Standard               | 13<br>22<br>32 - 36<br>41 - 42     |                                                                   |              | 2<br>1<br>10<br>2 | 1<br>2<br>3<br>4               |                          |             | 1<br>1<br>1 |
|                                         | MOX Segmented<br>Fuel Rods | 9 - 10<br>20 - 23<br>32 - 34<br>39 | 2<br>3<br>6<br>1                                                  | 2<br>2<br>1  |                   | 1<br>2<br>3<br>4               | 2<br>1<br>2              | 2<br>2<br>1 |             |
| Neckarwest-<br>heim (GKN),<br>15x15-20  | MOX-Standard               | 33 - 41<br>35 - 41                 | 16                                                                |              |                   | 3                              | 4                        |             |             |
| Grafenrhein-<br>feld (KKGf)<br>16x16-20 | MOX-Standard               | 31 - 38                            | 17                                                                |              |                   | 3                              | ·                        | •           |             |
| Total                                   | <u>,,,,,</u> ,             | 6 - 42                             | 78                                                                | 24           | 15                | 1 - 4                          | 17                       | 10          | 4           |

<sup>\*</sup> Eddy Current, Length, Diameter, Oxide Layer

Table III: SIEMENS'/KWU's Pool-Measurements and Hot Cell Examinations on Individual MOX/OCOM/AUPuC and ERU Fuel Rods/(Status Oct. 89)

|                                  | •                 |
|----------------------------------|-------------------|
| Pufiss in natural uranium (wt %) | 3.2/3.5           |
| Pellet diameter (mm)             | 9.08              |
| MOX fuel density: AUPuC (g/cm3)  | 10.35             |
| OCOM (g/cm <sup>3</sup> )        | 10.32             |
| •                                |                   |
| Fuel length (mm)                 | 310               |
| Fuel rod length (mm)             | 382               |
| Zircaloy-4 cladding              | Stress relieved   |
| Cladding dimensions (mm)         | 10.75 x 9.29/9.27 |
| Diametrical gap (mm)             | 0.210/0.190       |
| Helium prepressure (bar)         | 22.5              |

Table IV: Ramp Experiments with MOX Fuel Rods (AUPuC and OCOM) at HFR Petten Design Data of the Ramped Test Rods

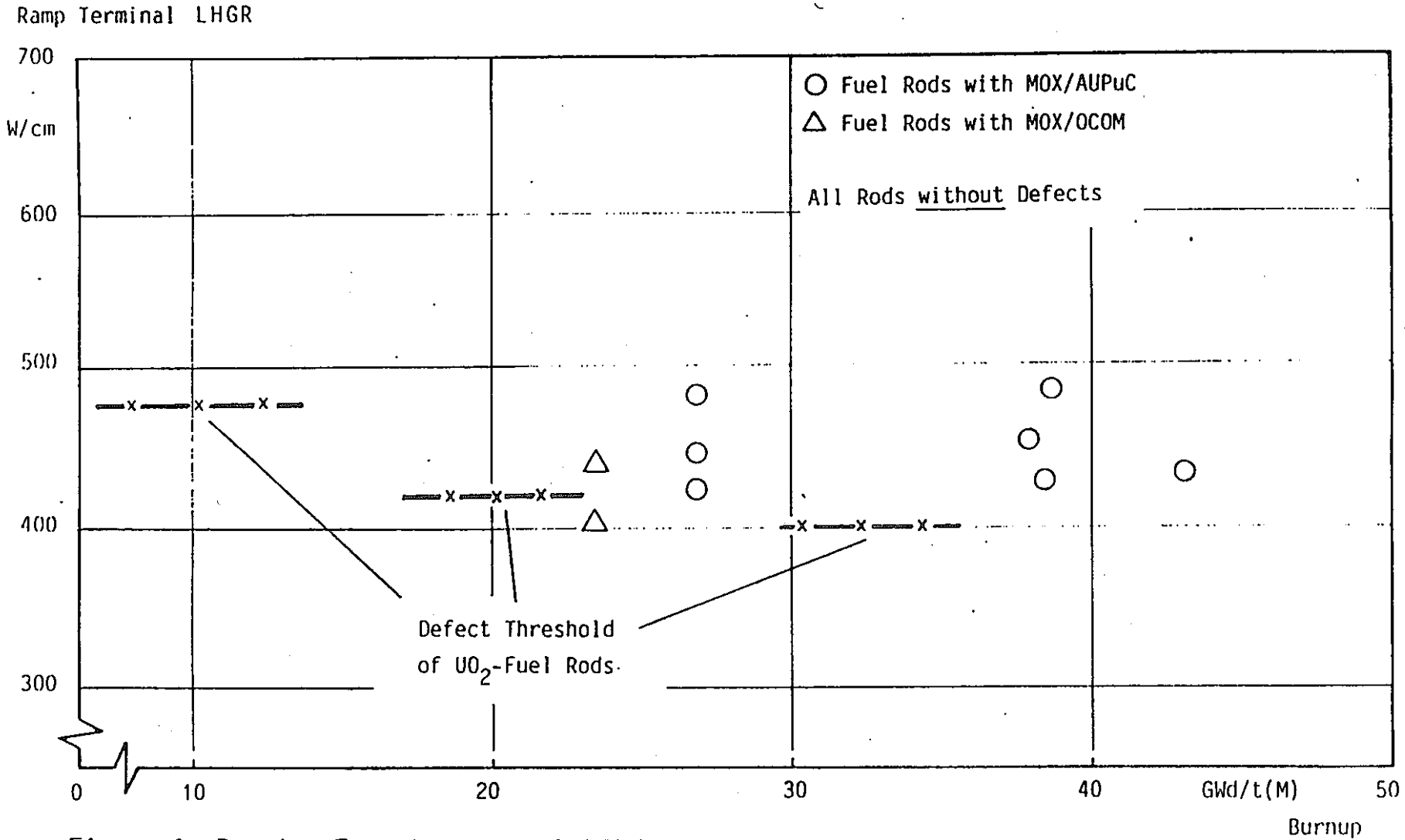


Figure 1. Ramping Experiments with MOX/AUPuC/OCOM Fuel Rods in the HFR Petten

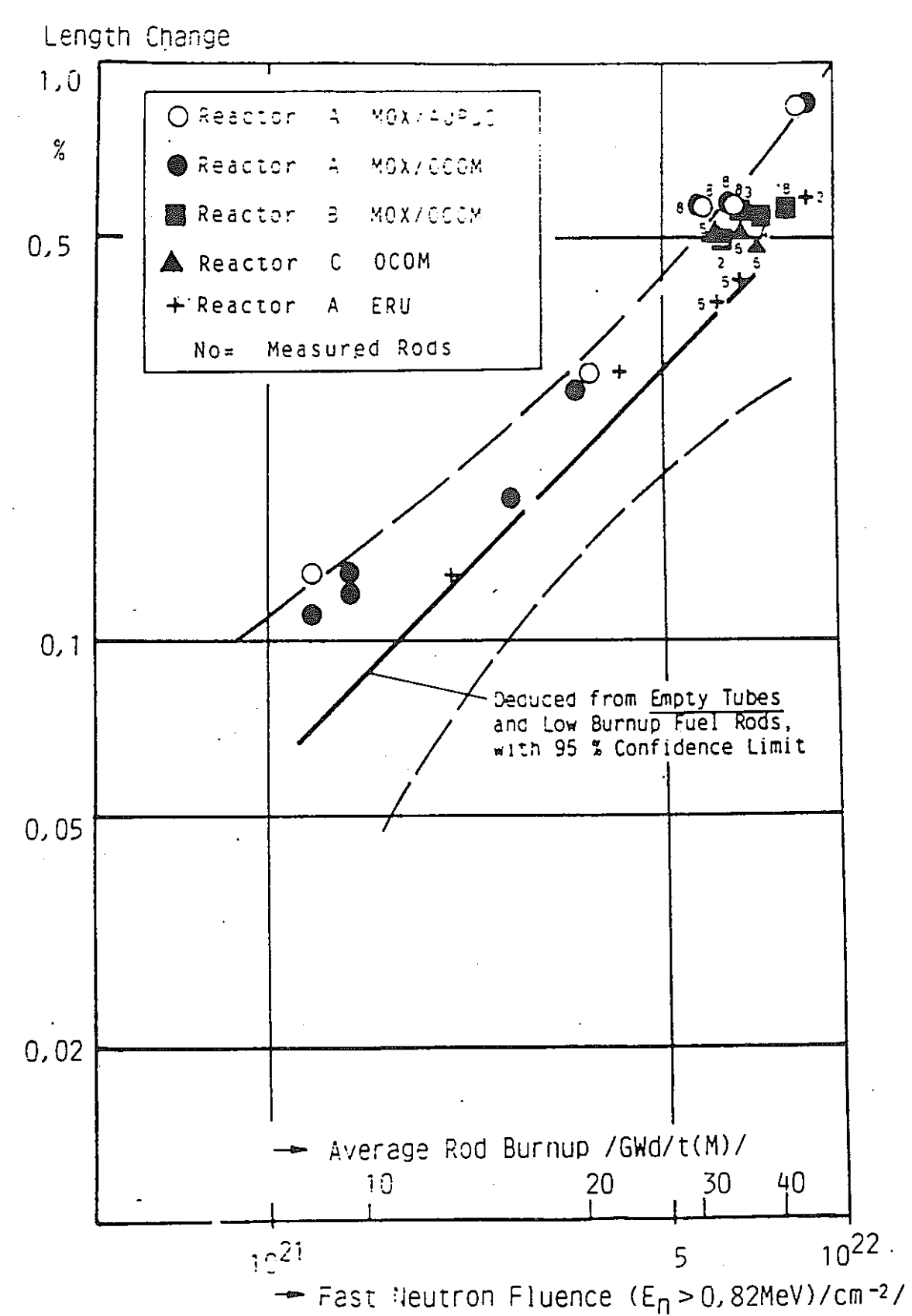


Figure 2.Length Change of MOX/AUPuC/OCOM Fuel Rods as a Function of Burnup or Fast Neutron Fluence

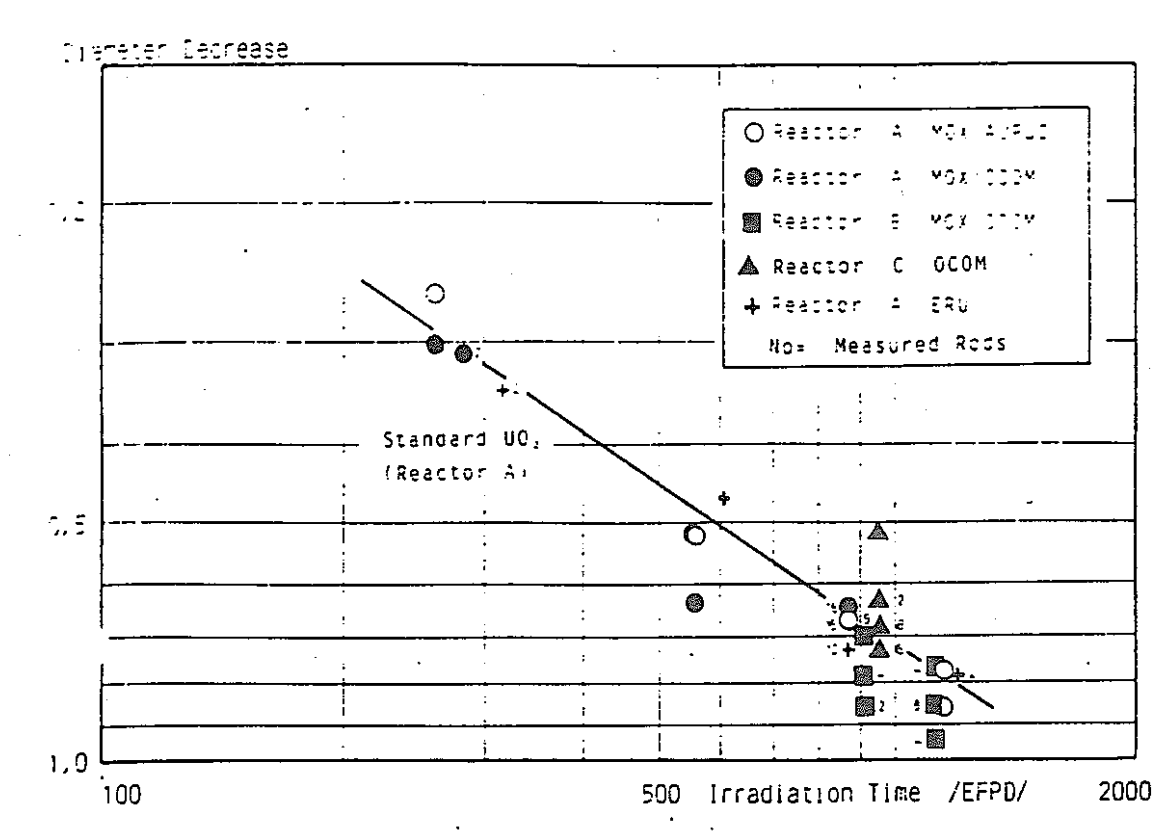


Figure 3 .Maximum Diameter Decrease of MOX/AUPuC/OCOM and ERU Fuel Rods as a Function of Irradiation Time :

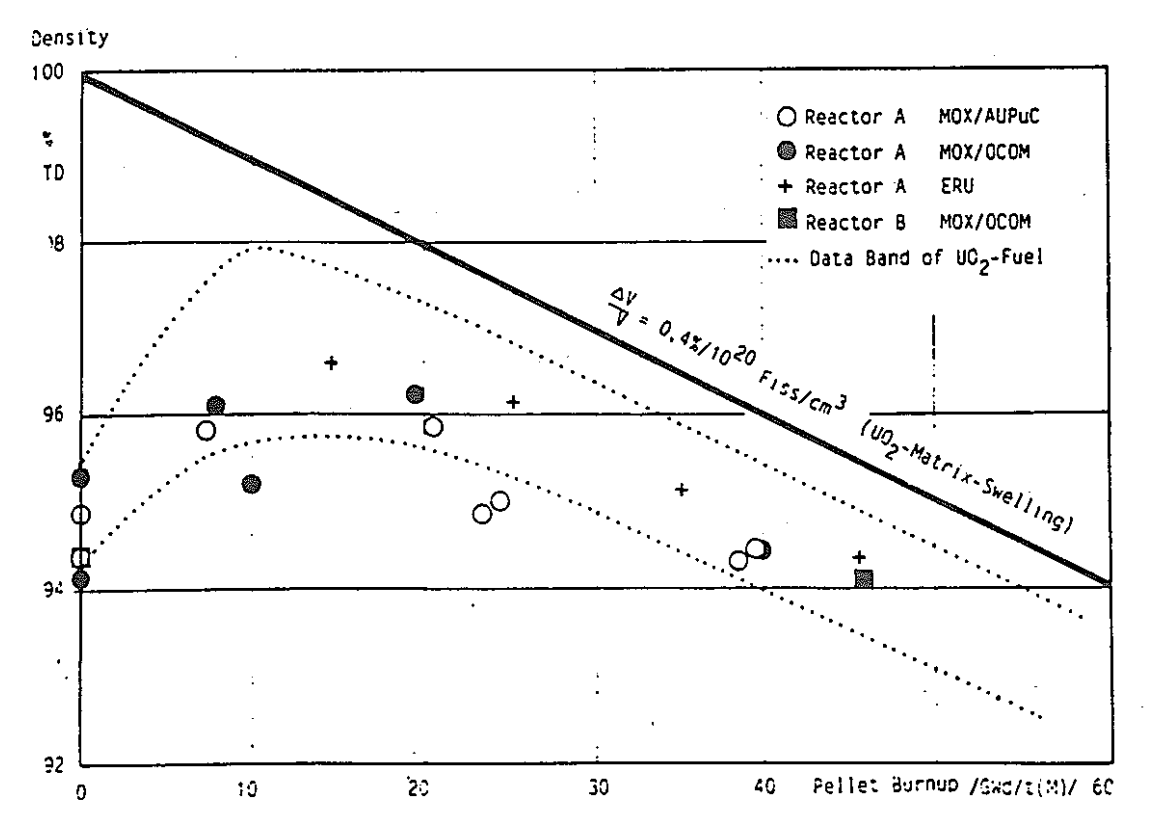


Figure 4.Densification /Swelling Behaviour of MOX/AUPuC/OCOM and ERU Fuel as a Function of Burnup

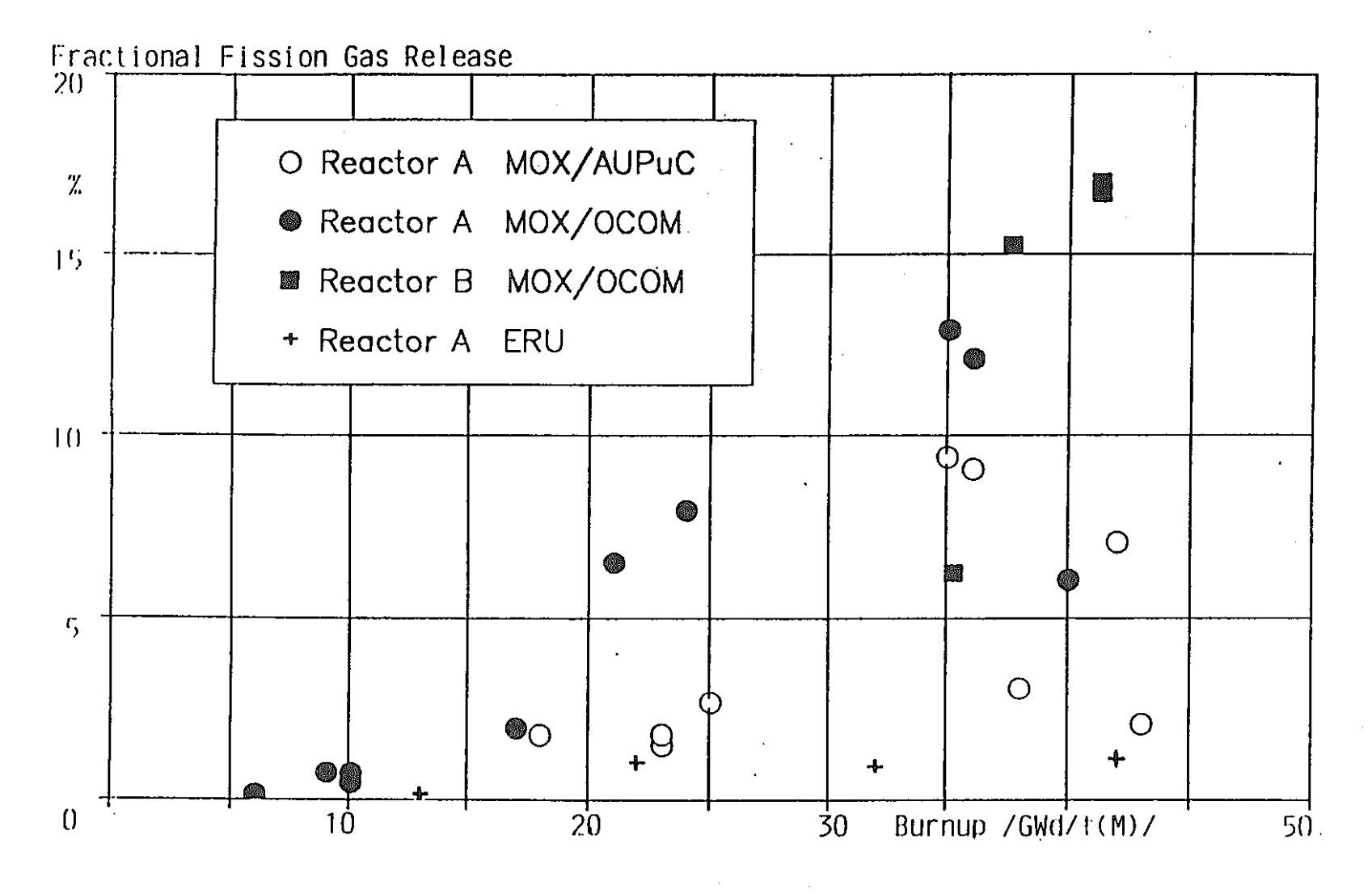


Figure 5. Fractional Fission Gas Release of MOX/AUPuC/OCOM and ERU Fuel Rods as a Function of Fuel Rod Burnup

# INVESTIGATION OF HIGH-BURNUP LWR URANIUM, MOX AND RECYCLED-URANIUM FUEL ON THE BASIS OF JEF-1 DATA VALIDATED AT KFK

#### H.W. Wiese

Kernforschungszentrum Karlsruhe Institut für Neutronenphysik und Reaktortechnik P.O. Box 3640, D-7500 Karlsruhe 1, F.R.G.

#### ABSTRACT

Based on the Joint Evaluated File JEF-1, with the KfK burnup code system KARBUS and subsequent KORIGEN calculations the characteristics of high-burnup PWR uranium, mixed-oxide (MOX) and recycled uranium (RU) fuels are analysed. Actinide masses, decay heat, radioactivities and radiation are discussed for exposures from 40 - 60 GWd/tHM both in case of reprocessing and in case of a direct storage of used fuel. A comparison with recent results from LANL for uranium fuel burnt to 50 GWd/tHM shows good agreement for important actinides and fission products.

#### INTRODUCTION

Validation of the European Nuclear Data File JEF-1 for LWR burnup applications by comparisons of calculated nuclide concentrations with experimental values from post-irradiation analyses had been performed successfully at KfK for PWR uranium fuel with burnups up to 30 GWd/tHM¹. In this paper, advanced PWR uranium-, MOX- and recycled-uranium (RU) fuel characteristics are analysed for burnups up to 60 GWd/tHM. With respect to fuel reprocessing, final storage of waste, and a direct storage of spent fuel elements, the high-burnup behaviour of actinide nuclides and the emission of neutron, y- and a-radiation from spent fuel and waste is investigated. Our calculational results for radioactivities are compared to theoretical values found in recent literature.

### METHODS FOR DATA PROCESSING AND INVENTORY CALCULATIONS

The JEF-data are processed to a 69-group-constant set with NJOY2. For the KARBUS3 cell and burnup calculation, special attention is paid to the self-shielding of the most important actinide and fission product nuclides with the KfK-version of the code RESAB4 by properly determining the resonance neutron flux used for weighting. Fuel decay calculations are performed with KORIGEN5, which is also used for stand-alone burnup and decay calculations with consistent cross sections from the preceding KARBUS runs.

# INVESTIGATED FUELS AND CONDITIONS OF IRRADIATION

In order to maintain criticality at least up to a burnup of about 50 GWd/tHM, uranium fuel with 4.0 w/o U235, MOX-fuel with 3.7 w/o fissile plutonium in natural uranium, and RU-fuel with 4.5 % U235 is chosen. The MOX plutonium and the RU uranium vector are

Pu238/Pu239/Pu240/Pu241/Pu242 = 1.8/59./23./12.2/4. (w/o) U232/U234/U235/U236/U238 = 3.35-6/.15/4.5/2.2/93.15 (w/o)

The fuel atomic number density is  $2.155 \cdot 10^{22}$  atoms of heavy material per ccm. Since the investigation aims at the long-term fuel and waste behaviour, simplified irradiation conditions, namely a constant-power operation with 36.7 MW/tHM, is modelled; additionally, the boron concentration is kept constant to the average value of 500 ppm. The reactor lattice is of BIBLIS-type, i.e. pin radius of 0.4659 cm, canning thickness .0725 cm, and a moderator - to - fuel ratio of 2.06.

# COMPARISON OF SELECTED CHARACTERISTICS OF IRRADIATED FUELS 7 YEARS AFTER DISCHARGE

In <u>Table II</u> for U-, MOX- and RU-fuel the amounts of U, Pu, Am, Cm and Np, the total actinide and total fission product radioactivities and decay heat releases, and the neutron and y-emission 7 years after discharge for burnups of 40, 50 and 60 GWd/tHM are listed. For comparison, also values for lower-burnup uranium fuel after 33 GWd/tHM are given.

Decay Heat and Main Contributors

For the actinide total heat releases a characteristic ratio of

U:MOX:RU = 1:5.4:1.8 at 50 GWd/tHM

is found. From <u>Table I</u>, where the contributions of the main decay heat nuclides Cm244, Pu238 and Am241 7 years after discharge are given, it is seen that the large decay heat in MOX-fuel mainly originates from Cm244 (64%) and to a lesser part from Pu238 (22%), whereas in RU-fuel Pu238 with 71% is the main contributor. In U-fuel, Cm244 and Pu238 both yield ca. 40% of the actinide decay heat 7 years after discharge.

Table I

Decay Heat (absolute in W/tHM and relative to total actinide in %)
of main Decay Heat Contributors after 50 GWd/tHM Burnup

| Nuclide      | U-Fuel  |      | MOX   | MOX-Fuel |      | Fuel |
|--------------|---------|------|-------|----------|------|------|
|              | W/tHM % |      | W/tHM | W/tHM %  |      | %    |
| Cm244        | 197.    | 40.5 | 1691. | 63.7     | 151. | 17.6 |
| Pu238        | 191.    | 39.3 | 572.  | 21.5     | 607. | 70.7 |
| Am241        | 60.6    | 12.5 | 260.  | 9.8      | 62.3 | 7.3  |
| Other Actin. | 37.4    | 7.7  | 133.  | 5.0      | 37.7 | 4.4  |

Table II

Characteristics (per tHM) of High-Burnup PWR Fuels 7 Years after Discharge (no Reprocessing)

| Fuel →<br>Burnup<br>GWd/tHM | <b>→</b> | 40.   | Uraniu<br>4.0 % U<br>50. |             |        | X 3.7 % P<br>nat. Ura<br>50. |       | Red   | eycled U1<br>4.5 % U2<br>50. |       | Uranium*<br>3.2 %<br>33. |
|-----------------------------|----------|-------|--------------------------|-------------|--------|------------------------------|-------|-------|------------------------------|-------|--------------------------|
| Masses                      | U        | 947.7 | 936.0                    | 924.5       | 919.5  | 911.6                        | 903.5 | 945.6 | 933.3                        | 921.3 | 955.8                    |
|                             | Np       | 0.57  | 0.73                     | 0.85        | 0.23   | 0.29                         | 0.33  | 2.00  | 2.36                         | 2.63  | 0.44                     |
| kg                          | Pu       | 9.78  | 10.86                    | 11.74       | 35.64  | 32.95                        | 30.57 | 10.43 | 11.90                        | 13.16 | 9.19                     |
|                             | Am       | 0.57  | 0.74                     | 0.92        | 3.40   | 3.49                         | 3.50  | 0.54  | 0.72                         | 0.90  | 0.46                     |
|                             | Cm       | 0.03  | 0.08                     | 0.16        | 0.46   | 0.69                         | 0.97  | 0.02  | 0.06                         | 0.13  | 0.02                     |
|                             | FP       | 41.4  | 51.7                     | 61.9        | 40.7   | 50.8                         | 61.0  | 41.4  | 51.7                         | 61.9  | 34.0                     |
| Activity                    | Act.     | 4.3   | 5.1                      | 5.8         | 20.9   | 20.3                         | 19.5  | 4.5   | 5.6                          | 6.6   | 3.5                      |
| Bq <sup>-</sup>             | FP       | 16.3  | 19.7                     | 22.9        | 14.1   | 17.3                         | 20.3  | 16.4  | 19.9                         | 23.2  | 13.8                     |
| x 1015                      | Total    | 20.6  | 24.8                     | 28.7        | 35.0   | 37.6                         | 39.8  | 20.9  | 25.5                         | 29.8  | 17.3                     |
|                             | α        | 0.30  | 0.53                     | 0.87        | 2.25   | 2.87                         | 3.55  | 0.62  | 0.96                         | 1.39  | 0.22                     |
| Heat                        | Act.     | 0.28  | 0.49                     | 0.80        | 2.09   | 2.67                         | 3.12  | 0.56  | 0.87                         | 1.26  | 0.20                     |
| kW                          | FP       | 1.36  | 1.70                     | 2.03        | 1.18   | 1.49                         | 1.79  | 1.36  | 1.70                         | 2.03  | 1.16                     |
|                             | Total    | 1.64  | 2.19                     | 2.83        | 3.27   | 4.16                         | 4.91  | 1.92  | 2.57                         | 3.29  | 1.36                     |
| Neutrons                    | Act.     | 3.1   | 8.1                      | 17.0        | 46.0   | 68.7                         | 95.1  | 2.4   | 6.3                          | 13.4  | 2.2                      |
| /sec x 108                  | only     |       | ·                        | <del></del> |        |                              |       | ļ     |                              |       |                          |
| Gammas                      | Act.     | 0.79  | ′ 1.21                   | 1.78        | . 5.28 | 6.18                         | 7.15  | 1.27  | 1.88                         | 2.60  | 0.61                     |
| /sec x 1014                 | FP       | 86.9  | 111.                     | 134.        | 81.1   | 104.                         | 126.  | 86.0  | 110.                         | 133.  | 70.8                     |

Act. = Actinides, FP = Fission Products, Total = Act. + FP

<sup>\*</sup> lower-burnup PWR reload fuel for comparison with high-burnup fuels with increased initial enrichment

The large amount of Cm in MOX-fuel is generated from plutonium present already from the begin of irradiation (initially 52 kg/tHM). In U- and RU-fuel, the build-up of Cm is delayed, since there because of zero initial plutonium this has to be generated from uranium before partly being converted to Cm.

Pu238 is generated in MOX-fuel via Pu241, Cm242, from Pu239 and from U238, Np237. In RU-fuel, the generation of Pu238 is due to U236 and to U238 via Np237. The Pu238 ratio 7 years after discharge is found as

U:MOX:RU = 1:3:3.2 at 50 GWd/tHM

The factor 3.2 from U- to RU-fuel is a consequence of the U236 already initially present in RU-fuel.

Burnup Dependance of Spent-Fuel Characteristics

With respect to burnup in the range of 40 - 60 GWd/tHM the characteristics compiled in <u>Table II</u> show the following behaviour:

- (a) The amounts of fresh-fuel constituents (U in U- and RU-fuel, Pu in MOX-fuel) decrease with increasing burnup. The total amount of plutonium in U- and RU-fuel slightly increases with burnup; at 50 GWd/t burnup there are 10.9 and 11.9 kg Pu/tHM, respectively.
- (b) The minor actinides Np, Am and Cm are generated during irradiation; they do not reach their equilibrium concentrations within the considered burnup range up to 60 GWd/tHM. In particular, Cm, which 7 years after discharge predominantly consists of Cm244, doubles every 10 GWd/t in U-and RU-fuel. In MOX-fuel the relative increase of Cm in the high-burnup range is smaller. But, remember, there is about 10 times more Cm in MOX-fuel than in U-fuel due to the short-way production from plutonium see also  $\underline{\text{Table I}}$ . Since the emission of neutrons is predominantly caused by spontaneous fissions of Cm244, the relative changes in the neutron source in  $\underline{\text{Table II}}$  are similar to those of Cm.
- (c) The characteristics in  $\underline{\text{Table }\Pi}$  related to fission products of course linearly increase with burnup.
- (d) The plutonium compositions dependent on burnup are listed in <u>Table III</u>.

Table III

Plutonium Compositions (w/o) 7 Years after Discharge

| Burnup                                             | U-Fuel                                      |                                             |                                              | U-Fuel MOX-Fuel                              |                                                |                                              | RU-Fuel                                    |                                             |                                              |
|----------------------------------------------------|---------------------------------------------|---------------------------------------------|----------------------------------------------|----------------------------------------------|------------------------------------------------|----------------------------------------------|--------------------------------------------|---------------------------------------------|----------------------------------------------|
| GWd/t→                                             | 40                                          | 50                                          | 60                                           | 40                                           | 50                                             | 60                                           | 40                                         | 50                                          | 60                                           |
| Pu236<br>Pu238<br>Pu239<br>Pu240<br>Pu241<br>Pu242 | 9.5-6<br>2.1<br>57.9<br>23.7<br>10.6<br>5.7 | 1.3-5<br>3.1<br>52.2<br>25.4<br>11.0<br>8.3 | 1.7-5<br>4.1<br>47.8<br>26.4<br>11.0<br>10.8 | 1.1-6<br>2.6<br>41.2<br>32.1<br>13.7<br>10.4 | 1.7-6<br>3.0<br>• 37.9<br>32.4<br>13.9<br>12.8 | 2.5-6<br>3.5<br>35.5<br>32.1<br>13.7<br>15.2 | 3.6-5<br>7.0<br>57.7<br>21.0<br>9.8<br>4.5 | 4.4-5<br>9.0<br>51.8<br>22.4<br>10.3<br>6.5 | 5.1-5<br>10.9<br>47.2<br>23.2<br>10.3<br>8.4 |

Since Pu239 as a main fissile nuclide at larger burnups essentially contributes to energy production, its relative-to-total-plutonium ratio becomes smaller with increasing burnup whereas the contributions of all other plutonium isotopes increase. Pu241 reaches its relative equilibrium at about 50 GWd/t burnup in U-and RU-fuel. In MOX-fuel it decreases after 50 GWd/t.

Of special interest is Pu238. Its increase with burnup in the higher burnup region is strongest in U-fuel, almost doubling from 40 to 60 GWd/t and reaching 3.1 % at 50 GWd/t. But in RU-fuel it amounts to 7 % already at 40 GWd/t and is still increasing! This large fraction of Pu238 is prohibitive for RU-fuel reprocessing and a reuse of the plutonium product for fuel refabrication because of its strong heat production and neutron radiation. However, if Pu238 is a wanted product to be used for e.g. pacemakers and outer-space batteries, the long-term irradiation of RU-fuel is the best way to get it.

Pu236, generated by (n, 2n)-reactions at Np237 and, via U232, leading to Th208

(2.6 MeV gamma-radiation), is produced favourably in RU-fuel.

# Decay Heat Time Dependence

The long-term time dependence of irradiated fuel and of waste after reprocessing, important for final repository investigations for direct storage of used fuel elements or vitrified high active waste e.g. to determine the heat loading of the repository, can be seen from <u>Table V</u> and <u>Fig. 1</u>.

Because of the assumed identical power density of 36.7 MW/t the decay heat

shortly after discharge (1 day) is nearly the same for all fuels considered.

The most evident difference in the succeeding course of time is that the MOX-fuel/waste decay heat is distinctly larger than the decay heat from U- and RU fuel/waste up to 500 000 years from discharge (factor 2 and 4 at 100 and 1000 years, resp.). From Table IV may be seen, that the fission product heat releases are largely the same for U- and MOX waste. The actinide decay heat contributions, however, are distinctly larger in MOX-fuel. Depending on their half-lives, the dominating nuclides are Cm242 (short term), Cm244 and Am241 (up to several 100 years), and Am243 and the Pu isotopes in the long-term range.

Table IV

Contributions (kW/tHM) of Actinides and Fission Products to the Heat Release after 50 GWd/t Burnup and Reprocessing 7 Years after Discharge

| Time after           |        | Actini   | Fissio       | on Products |          |
|----------------------|--------|----------|--------------|-------------|----------|
| Discharge<br>(years) | U-Fuel | MOX-Fuel | Dom. Nucl.   | U-Fuel      | MOX-Fuel |
| 1                    | 1.14   | 6.57     | Cm242, 244   | 12.4        | 13.6     |
| -10                  | 0.24   | 1.79     | Cm244        | 1.35        | 1.16     |
| 100                  | 0.063  | . 0.30   | Am241, Cm244 | 0.14        | 0.11     |
| 103                  | 0.015  | 0.067    | Am241        | 2.6-5       | 3.2-5    |
| 104                  | 1.2-3  | 6.8-3    | Am243, Pu    | 2.5-5       | 3.1-5    |

Table V Decay Heat (kW/tSM) from Actinides and Fission Products in U-, MOX-and RU-Fuel and Waste after 50 GWd/tHM Burn-Up and Reprocessing 7 y after Discharge

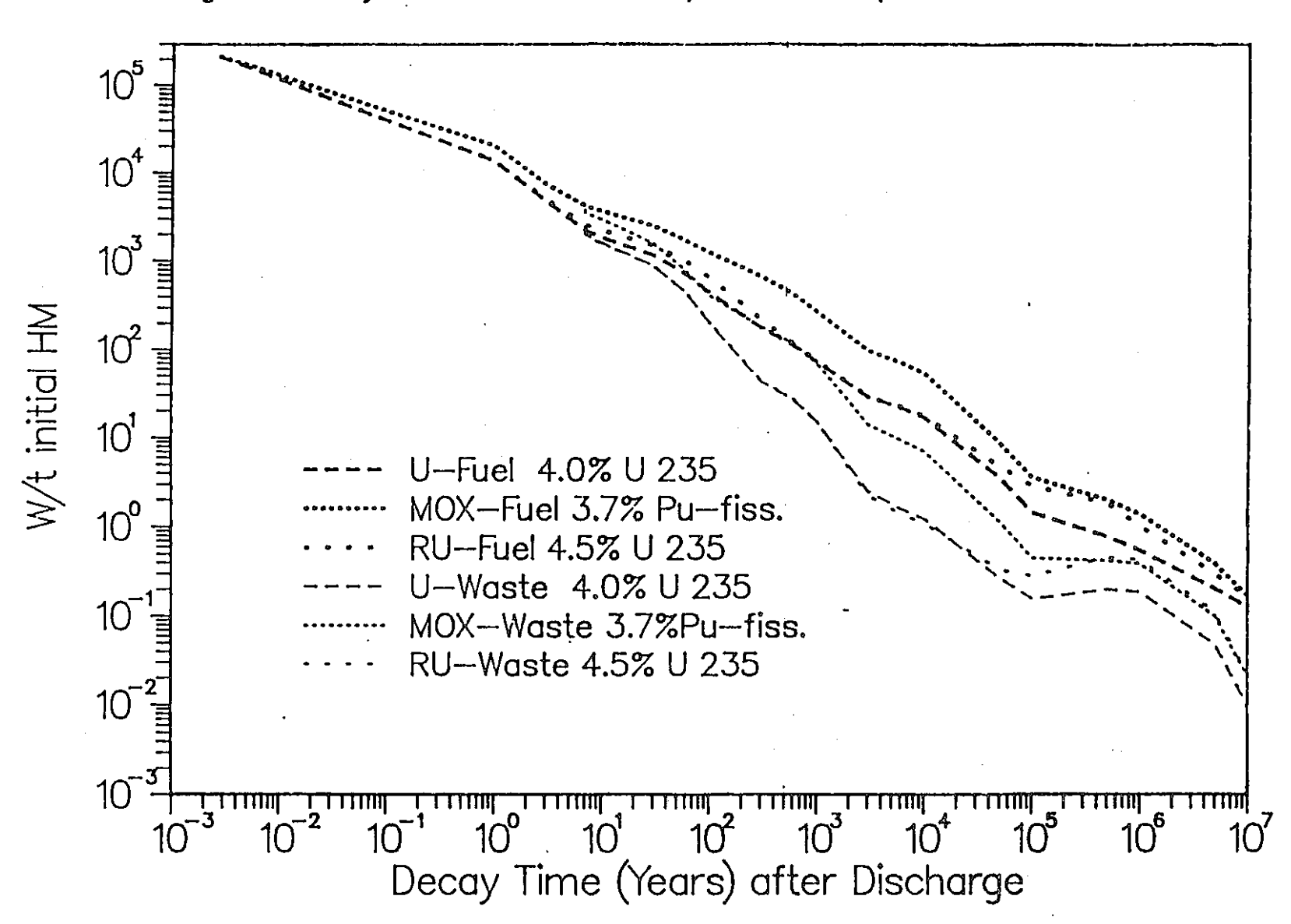
| Decay<br>Time | U-Fuel  |         | МО      | X-Fuel  | RU-Fuel |         |  |
|---------------|---------|---------|---------|---------|---------|---------|--|
| (y)           | 4.0 w/o | U235    | 3.7 w/o | Pu-fiss | 4.5 w/o | U235    |  |
| .0027(c)      | 213.    |         |         | 218.    | 2       | 216.    |  |
| 1             |         | 13.5    |         | 20.1    | 1       | 3.5     |  |
| 3             |         | 4.82    |         | 7.48    | 5       | 5.08    |  |
| 7             |         | 2.19    |         | 4.16    | 2       | 2.57    |  |
| 7             | 2.19(a) | 1.98(b) | 4.16(a) | 3.51(b) | 2.57(a) | 1.93(b) |  |
| 8             | 2.05    | 1.81    | 3.98    | 3.27    | 2.42    | 1.77    |  |
| 10            | 1.84    | 1.59    | 3.69    | 2.95    | 2.21    | 1.56    |  |
| 30            | 1.16    | .876    | 2.49    | 1.57    | 1.50    | .870    |  |
| 60            | .714    | .441    | 1.70    | .770    | .991    | .443    |  |
| 100           | .441    | .201    | 1.23    | .407    | .645    | .204    |  |
| 300           | .179    | 4.27-2  | .672    | .183    | .223    | 4.39-2  |  |
| 600           | .111    | 2.63-2  | .424    | .117    | .117    | 2.67-2  |  |
| 1000          | 7.17-2  | 1.49-2  | .269    | 6.75-2  | 7.31-2  | 1.49-2  |  |
| 3000          | 2.79-2  | 2.43-3  | 9.55-2  | 1.37-2  | 2.84-2  | 2.19-3  |  |
| 6000          | 2.13-2  | 1,56-3  | 6.99-2  | 9.12-3  | 2.18-2  | 1.36-3  |  |
| 104           | 1.64-2  | 1.19-3  | 5.16-2  | 6.79-3  | 1.71-2  | 1.06-3  |  |
| 5.104         | 3.42-3  | 2.62-4  | 8.49-3  | 1.10-3  | 4.60-3  | 3.24-4  |  |
| 105           | 1.40-3  | 1.53-4  | 3.46-3  | 4.38-4  | 2.78-3  | 2.78-4  |  |
| 5-105         | 7.51-4  | 1.95-4  | 1.91-3  | 4.06-4  | 1.75-3  | 4.46-4  |  |
| 106           | 5.31-4  | 1.82-4  | 1.34-3  | 3.75-4  | 9.82-4  | 4.17-4  |  |
| 5.106         | 1.96-4  | 4.71-5  | 3.73-4  | 9.73-5  | 2.87-4  | 1.08-4  |  |
| 107           | 1.23-4  | 9.77-6  | 1.63-4  | 2.08-5  | 1.60-4  | 2.18-5  |  |

<sup>(</sup>a)

Irradiated fuel without reprocessing Waste after reprocessing 7 years after fuel discharge with 0.3 % U and (b) 1.0 % Pu losses

<sup>(</sup>c) ·1 day

Fig. 1: Decay must after 50GWd/tHM Burnup



For decay times larger 500 000 years in case of reprocessing the decay heat from the RU-waste exceeds the MOX- and U-waste decay heat. This is due to the large build-up of Np237 in RU-fuel during irradiation. The Np237 ratio after 50 GWd/t burnup is found as

U:MOX:RU=2.7:1.:8.7 at discharge.

Within 10 000 years after discharge via the decay of Am 241 to Np237 this ratio has attained

$$U:MOX:RU = \begin{cases} 0.5 : 1.: 1.1 & \text{with reprocessing} \\ 0.34: 1.: 0.58 & \text{without reprocessing} \end{cases}$$

where in case without reprocessing in MOX-fuel the initial drawback is over-compensated by the decay of Pu241 to Am241. The interesting phenomenon of a late increase of the RU-waste decay heat reaching a relative maximum at about  $6.4 \cdot 10^5$  years of decay results from U233 in the decay chain of Np237.

#### COMPARISON WITH RECENT LITERATURE VALUES

In 1988, Wilson et al. from Los Alamos National Laboratory (LANL) published calculational results on radionuclide inventories of high-exposure LWR fuels<sup>6</sup>. In <u>Table VI</u>, for the case of 4 % enriched uranium fuel in a PWR, their results are compared to ours for 50 GWd/tHM burnup.

Table VI

Selected Calculated Nuclide Radioactivities (Ci/tHM) at Discharge for 4 % Enriched PWR Uranium Fuel from LANL and KfK

| Nuclide                                            | LANL                                                  | KfK                                               | % (a)                                           | Nuclide                                  | LANL                                           | KfK                                            | %                            |
|----------------------------------------------------|-------------------------------------------------------|---------------------------------------------------|-------------------------------------------------|------------------------------------------|------------------------------------------------|------------------------------------------------|------------------------------|
| Pu238<br>Pu239<br>Pu240<br>Pu241<br>Am241<br>Cm242 | 4862.<br>349.<br>550.<br>1.91 + 5<br>225.<br>8.07 + 4 | 5734.<br>348.<br>622.<br>1.73+5<br>183.<br>8.14+4 | 17.9<br>- 0.3<br>13.1<br>- 9.4<br>- 18.7<br>0.9 | Sr90<br>Ru106<br>Cs134<br>Cs137<br>Ce144 | 1.03+5<br>7.52+5<br>2.80+5<br>1.54+5<br>1.31+6 | 1.03+5<br>7.61+5<br>2.80+5<br>1.56+5<br>1.31+6 | 0.<br>1.2<br>0.<br>1.3<br>0. |
| Cm244                                              | 9030.                                                 | 7462.                                             | - 17.4                                          |                                          |                                                |                                                |                              |

#### (a) (KfK-LANL)/LANL \* 100.

For Pu239, Cm242 and the leading fission products the agreement is excellent. For the other plutonium isotopes and for Am241 and Cm244 deviations up to about 20% are stated. Obviously, the crucial nuclide is Pu240 which, in the LANL calculation because of a less shielded capture reaction, is transmuted stronger to Pu241 and hence to heavier actinides. The KfK results are supported by independent calculations with OREST7.

#### CONCLUSIONS

Based on the Joint Evaluated Data File JEF-1, with the KfK burnup code system KARBUS/KORIGEN the characteristics of high-exposure PWR U-, MOX- and RU-fuel are analysed. Special attention is paid to heat generation and neutron/gamma emission. A comparison with recent results from Los Alamos shows good agreement for fission products and for important actinides; discrepancies very probably arise from different data and/or a different treatment of neutron capture in Pu240.

#### ACKNOWLEDGEMENT

The author is gratefully indebted to C.H.M. Broeders for his valuable support in KARBUS calculations.

#### REFERENCES

- 1. A. MATEEVA, "Qualification of the JEF-1 Nuclear Data Library for Pressurized-Water Reactor Burnup Analysis," KfK 4461 (1988) and A. MATEEVA, "Qualification of the JEF-1 Nuclear Data Library for PWRs.," Proc. Jahrestagung Kerntechnik, Düsseldorf 1989, p. 67
- 2. I. BROEDERS, B. KRIEG, "Die KfK-Version des Gruppenkonstanten-Erstellungsprogramms NJOY," Jahrestagung Kerntechnik '89, p. 63
- 3. C.H.M. BROEDERS, "Validation of Calculational Procedures for the Design of Light Water Tight Lattice Reactors (LWTLR) with Epithermal Spectrum," "State of the Art" Seminar on Nuclear Data, Cross Section Libraries, and their Application in Nuclear Technology, Bonn, October 1985
- 4. B. RIIK, R. RÜHLE, "RESAB II, ein Programm zur Berechnung von Gruppenkonstanten im Resonanzbereich nach der Stoßwahrscheinlichkeitsmethode," IKE-Ber. Nr. 3.3 6.1209 (1972)
- U. FISCHER, H.W. WIESE, "Verbesserte konsistente Berechnung des nuklearen Inventars abgebrannter DWR-Brennstoffe auf der Basis von Zell-Abbrand-Verfahren mit KORIGEN," KfK 3014 (1983), ORNL-tr-5049
- 6. W.B. WILSON, T.R. ENGLAND, R.J. LA BAUVE, J.A. MITCHELL, "Calculated Radionuclide Inventories of High-Exposure LWR-Fuels," Nuclear Safety, Vol. 29, No. 2 (1988)
- 7. U. HESSE, "OREST The HAMMER-ORIGEN Burnup Program System: Method and Results," Nuclear Technology Vol. 82, No. 2 (1988), p. 173

セッション1.3

# 33rd NEACRP MEETING PARIS OCTOBER 15-19, 1990

# COMPARATIVE STUDY OF THE NEUTRONIC PERFORMANCES OF A LARGE LMFBR USING OXIDE FUEL OR METALLIC FUEL

by

J.C. GARNIER, A. ZAETTA CEA

## COMPARATIVE STUDY OF THE NEUTRONIC PERFORMANCES OF A LARGE LMFBR USING OXIDE FUEL OR METALLIC FUEL

J.C. GARNIER - A. ZAETTA
CEA/DRN/DER/SPRC/LEDC

#### **ABSTRACT**

A primary study has been carried out on the respective merits of oxide and metallic fuels used in a Fast Breeder Reactor on a neutronic point of view. Differences concerning burn-up reactivity loss, discharge burn-up, damage rate, Doppler and sodium void reactivities are evaluated. The sensitivity of the metal fueled core performances to design parameter variations is also examined. The conclusion, at this intermediate stage of progress, is in favour of a specific optimised design for metallic fuel use, particularly with respect to the positive sodium void reactivity reduction.

#### INTRODUCTION

LMFBR development remains closely dependant on significant economics and safety improvements. Pursuing that goal, the CEA core design studies have been enlarged to nitride fuel (UN,PuN) and metallic fuel [(U,Pu)10%Zr], both considered for the long term as possible alternatives to oxide fuel (UO2,PuO2).

A core design optimisation, for each candidate, is underway that will enable a realistic comparison with oxide performances and a more definitive evaluation of their respective merits as advanced fuel.

In a preliminary phase, a neutronic comparison between oxide and metal fueled cores has been made using a homogeneous core design, optimised for oxide fuel: the First Consistent Design of E.F.R. e.g. the European Fast Reactor [1]. Then, variations of these performances with smear density and clad thickness have been examined. Results discussed in this paper are related to this work.

#### CORE DESIGN DESCRIPTION

Main characteristics of the core are outlined below and the core layout is given in figure 1.

| Total thermal power (MW)       | 3600 |
|--------------------------------|------|
| Number of fuel subassemblies   | 346  |
| Number of fuel zones           | 2    |
| Subassembly pitch (mm)         | 190  |
| Number of pins per subassembly | 271  |
| Pin outer diameter (mm)        | 8.65 |
| Fissile height (m)             | 1.40 |
| Number of refuelling batches   | 3    |

The metal core is assumed to be identical to the oxide one, except with regard to smear density and gas plenum. The gas plenum in the metal fuel pin is higher and entirely located in the upper part of the pin and the smear density used for metallic fuel is lower than the value retained for oxide fuel: 0.68 and 0.83 respectively. This difference concerning smear density is justified by the high swelling propensity of metallic fuel.

#### **METHODOLOGY**

The basic cross section data used for the neutronic calculations were CAR-NAVAL IV. Twenty-five group cross section sets were generated for general use. Core calculations were carried out in RZ geometry using the CCRR code system and a diffusion theory methodology.

The shutdown systems were not taken into account, so the fuel zone contained 33 additional subassemblies, compared with the reference EFR core. To be consistent with this approximation, enrichments of the fresh fuel have been chosen to give an excess reactivity of 3000 pcm at end-of-cycle (the ratio between the two enrichments being equal to 0.8).

The cycle length was adjusted to achieve a peak damage rate of 180 dpa-NRT which is the target value for EFR.

Both Doppler and sodium void reactivities were obtained by direct calculation, the Doppler reactivity being performed between 180 °C and nominal operating temperatures and the sodium void reactivity being performed for a complete voiding of the fuel + axial breeder zones.

#### CORE PERFORMANCE CHARACTERISTICS

Main results can be found in table I.

The fresh fuel mass inventory makes clear the higher heavy atom content of metallic fuel: compared with oxide, the theorical density rises by +44% but, because of the lower smear density, the practical increase of the heavy atom content is close to +20%. This additional mass is mainly supplied by depleted uranium leading to a better breeding gain.

The target of a zero reactivity loss is here exceeded: instead of the standard reactivity loss with burn-up of the oxide core, the metal fueled core offers a substantial reactivity gain. However, this behaviour is closely dependant on the large core size of EFR: an oxide/metal comparison applied to a smaller core would show a reduced but negative reactivity variation in favour of the metal fueled core and a more convincing benefit on control requirements.

Corresponding to an equal damage rate, the peak discharge burn-up is inexorably lower in the metal core than it is in the oxide one, mainly due to lower enrichments. This disadvantage of metallic fuel could be partly compensated by the use of a heterogeneous design. Doppler and sodium void reactivities are also greatly modified by the use of metallic fuel: decrease for the Doppler reactivity and increase for the sodium void reactivity in factors about 2. These differences are mainly related to neutron energy spectrum and also, for Doppler reactivity, to operating temperatures.

#### PERFORMANCE SENSITIVITY TO SMEAR DENSITY AND CLAD THICKNESS

The present knowledge on metallic fuel use in LMFBR being very far from the one achieved for oxide fuel, uncertainties affecting design parameters are obviously larger when metallic fuel is used.

Particularly, because of the swelling, the smear density capable of achieving high discharge burn-up could be lower than the value previously mentioned. So, it was interesting to evaluate the metal core performances considering a smear density equal to 0.63 and 0.58, the reference value being 0.68.

Most of the results (table II) are intermediate to those previously obtained for oxide and metal fueled cores (closer to the last one), except the cycle length that is reduced again with respect to the "reference" metal core. This difference can be explained by the higher instantaneous damage rate due to the higher mean flux level and also to the spectrum hardening (related to higher enrichments).

However, the main result is the burn-up reactivity variation that remains clearly in favour of the metal core in spite of the reduced smear density. Moreover, the damage rate over discharge burn-up ratio is still far from the one of oxide fuel.

The clad thickness is an other design parameter that is likely to evolve with knowledge improvement. A major advantage foreseen in using metallic fuel is the non-corrosion of the clad and consequently, the possible clad thickness reduction. Results reported in table III show the consequences on core performances of a 20% reduction of the clad thickness.

The steel volume fraction reduction induces direct favourable effects related to neutron parasitic absorption and scattering, but is also profitable to the fuel volume fraction acting like an increase of the smear density. As a consequence, enrichment and reactivity gain with burn-up differ appreciably from the "reference" values.

Moreover, both parameters, smear density and clad thickness do not provoke any significant changes of Doppler and sodium void reactivities (a few percent for the variations considered above).

#### SAFETY IMPLICATIONS

More detailed explanations can be found in reference [2], so the purpose of the following lines will be limited to a few comments on safety aspects involving the above results.

When going further in such an oxide/metal core comparison, the metal fueled core disadvantage concerning sodium density coefficient and Doppler coefficient can be seen in the same manner as it has been here for integral reactivity effects.

Taking into account the higher sodium density coefficient and the lower Doppler coefficient, the analysis of 3 types of transient (slow loss of flow, fast loss of flow and slow overpower) leads to the following conclusions:

- in the case of a slow loss of flow, higher sodium and clad temperatures are reached at the beginning of the transient in the metal fueled core because of the higher sodium density coefficient. Then, the equilibrium temperature is in favour of the metal core due to its reduced Doppler coefficient.
- in the cases of fast loss of flow and slow overpower, higher sodium and clad temperatures are reached during the transient due, for the first transient, to the higher sodium density coefficient and for the second, to this unfavourable effect joined with the lower Doppler coefficient.

These considerations make clear that the demand for low void cores is to be considered of prime interest when metallic fuel is used.

#### CONCLUSION

A comparative study is underway to identify and quantify the physic parameters that differentiate metal and oxide fuel types when they are used in a LMFBR. In a preliminary phase, a neutronic comparison has been carried out using a large and homogeneous core, optimised for oxide fuel use, e.g. the European Fast Reactor core. Compared with oxide fueled core performances, the differences mainly noticed are the following:

- a strong reduction of the burn-up reactivity loss, up to reach a reactivity gain instead of the characteristic reactivity loss (5.65 pcm/EFPD) of the oxide fueled core.

- a lower discharge burn-up (-30%) corresponding to an equal damage rate.
- a nearly twice larger positive sodium void reactivity associated with a reduced Doppler reactivity in a factor close to 2.

Moreover, these results are not qualitatively modified when using a smear density of the metallic fuel reduced from 0.68 up to 0.58 or a reduced clad thickness, design parameters still likely to evolve.

Among these differences, the disadvantage on sodium void reactivity, because of the resulting core dynamic behaviour, certainly constitutes a main draw-back for the use of metallic fuel. So, the further developments of our study will examine some geometrical and conceptual improvements to achieve a optimised design, particularly with respect to this safety aspect.

#### References

- [1] Core optimisation studies for the European Fast Reactor EFR
  - U. Wehmann, R. de Wouters, R. Suderland, H. Sztark International Conference on the Physics of Reactors, Marseille, April 90 Proceedings, Vol 1, p II.34
- [2] Reactivity effects and dynamic behaviour: comparative performances of large LMFBR's oxide and metallic fuel cores.
  - P. Bergeonneau NEACRP-A-991, 32nd NEACRP meeting, 9-13 Oct 89, Argonne (USA)

TABLE I

| Fuel                           |              | UO2 PuO2 | UPu 10Zr |
|--------------------------------|--------------|----------|----------|
| Initial Pu loading             | (tonne)      | 8.15     | 6.35     |
| Initial U+Pu loading           | (tonne)      | 48.3     | 56.9     |
| Cycle length                   | (EFPD)       | 503      | 428      |
| Reactivity rods up at BOEC     | (pcm)        | 5837     | 241      |
| Reactivity rods up at EOEC     | (pcm)        | 3000     | 3000     |
| B.U. reactivity loss           | (pcm/EFPD)   | 5.65     | <b></b>  |
| Peak linear rating at BOEC     | (W/cm)       | 427      | 419      |
| Peak linear rating at EOEC     | (W/cm)       | 438      | 490      |
| Average discharge B.U.         | (MWd/t)      | 99700    | 71900    |
| peak discharge B.U.            | (MWd/t)      | 161000   | 118000   |
| peak damage rate               | (dpa NRT,Fe) | 180      | 180      |
| Doppler reactivity at EOEC     | (pcm)        | 1283     | 547      |
| Sodium void reactivity at EOEC | (pcm)        | 2726     | 4616     |

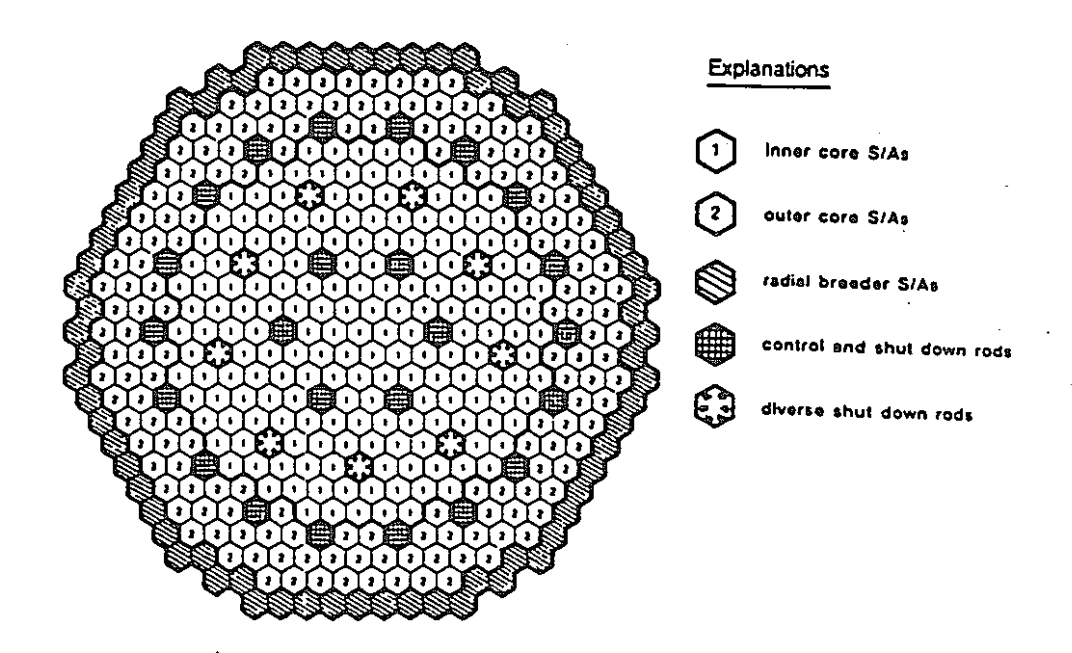
TABLE II

| Smear density              | (%)          | ref=68 | 63     | 58     |
|----------------------------|--------------|--------|--------|--------|
| Initial Pu loading         | (tonne)      | 6.35   | 6.18   | 6.02   |
| Initial U+Pu loading       | (tonne)      | 56.9   | 52.8   | 48.8   |
| Cycle length               | (EFPD)       | 428    | 407    | 386    |
| Reactivity rods up at BOEC | (pcm)        | 241    | 911    | 1664   |
| Reactivity rods up at EOEC | (pcm)        | 3000   | 3000   | 3000   |
| Average discharge B.U.     | (MWd/t)      | 71900  | 73700  | 75700  |
| peak discharge B.U.        | (MWd/t)      | 118000 | 121000 | 126000 |
| peak damage rate           | (dpa NRT,Fe) | 180    | 180    | 180    |

TABLE III

| Clad thickness         | (mm)         | ref=0.534 | 0.437  |
|------------------------|--------------|-----------|--------|
| Initial Pu loading     | (tonne)      | 6.35      | 6.36   |
| Initial U+Pu loading   | (tonne)      | 56.9      | 60.4   |
| Cycle length           | (EFPD)       | 428       | 433    |
| Average discharge B.U. | (MWd/t)      | 71900     | 68600  |
| peak discharge B.U.    | (MWd/t)      | 118000    | 113000 |
| peak damage rate       | (dpa NRT,Fe) | 180       | 180    |

FIGURE I



NEACRP-A-1057 Topic 1.3

# 33rd NEACRP MEETING PARIS OCTOBER 15-19, 1990

# COMPARATIVE STUDY OF THE NEUTRONIC PERFORMANCES OF A LARGE LMFBR USING OXIDE FUEL OR METALLIC FUEL

bу

J.C. GARNIER, A. ZAETTA CEA

#### COMPARATIVE STUDY OF THE NEUTRONIC PERFORMANCES OF A LARGE LMFBR USING OXIDE FUEL OR METALLIC FUEL

J.C. GARNIER - A. ZAETTA
CEA/DRN/DER/SPRC/LEDC

#### **ABSTRACT**

A primary study has been carried out on the respective merits of oxide and metallic fuels used in a Fast Breeder Reactor on a neutronic point of view. Differences concerning burn-up reactivity loss, discharge burn-up, damage rate, Doppler and sodium void reactivities are evaluated. The sensitivity of the metal fueled core performances to design parameter variations is also examined. The conclusion, at this intermediate stage of progress, is in favour of a specific optimised design for metallic fuel use, particularly with respect to the positive sodium void reactivity reduction.

#### INTRODUCTION

LMFBR development remains closely dependant on significant economics and safety improvements. Pursuing that goal, the CEA core design studies have been enlarged to nitride fuel (UN,PuN) and metallic fuel [(U,Pu)10%Zr], both considered for the long term as possible alternatives to oxide fuel (UO2,PuO2).

A core design optimisation, for each candidate, is underway that will enable a realistic comparison with oxide performances and a more definitive evaluation of their respective merits as advanced fuel.

In a preliminary phase, a neutronic comparison between oxide and metal fueled cores has been made using a homogeneous core design, optimised for oxide fuel: the First Consistent Design of E.F.R. e.g. the European Fast Reactor [1]. Then, variations of these performances with smear density and clad thickness have been examined. Results discussed in this paper are related to this work.

#### CORE DESIGN DESCRIPTION

Main characteristics of the core are outlined below and the core layout is given in figure 1.

| Total thermal power (MW)       | 3600 |
|--------------------------------|------|
| Number of fuel subassemblies   | 346  |
| Number of fuel zones           | 2    |
| Subassembly pitch (mm)         | 190  |
| Number of pins per subassembly | 271  |
| Pin outer diameter (mm)        | 8.65 |
| Fissile height (m)             | 1.40 |
| Number of refuelling batches   | 3    |

The metal core is assumed to be identical to the oxide one, except with regard to smear density and gas plenum. The gas plenum in the metal fuel pin is higher and entirely located in the upper part of the pin and the smear density used for metallic fuel is lower than the value retained for oxide fuel: 0.68 and 0.83 respectively. This difference concerning smear density is justified by the high swelling propensity of metallic fuel.

#### **METHODOLOGY**

The basic cross section data used for the neutronic calculations were CAR-NAVAL IV. Twenty-five group cross section sets were generated for general use. Core calculations were carried out in RZ geometry using the CCRR code system and a diffusion theory methodology.

The shutdown systems were not taken into account, so the fuel zone contained 33 additional subassemblies, compared with the reference EFR core. To be consistent with this approximation, enrichments of the fresh fuel have been chosen to give an excess reactivity of 3000 pcm at end-of-cycle (the ratio between the two enrichments being equal to 0.8).

The cycle length was adjusted to achieve a peak damage rate of 180 dpa-NRT which is the target value for EFR.

Both Doppler and sodium void reactivities were obtained by direct calculation, the Doppler reactivity being performed between 180 °C and nominal operating temperatures and the sodium void reactivity being performed for a complete voiding of the fuel + axial breeder zones.

#### CORE PERFORMANCE CHARACTERISTICS

Main results can be found in table I.

The fresh fuel mass inventory makes clear the higher heavy atom content of metallic fuel: compared with oxide, the theorical density rises by +44% but, because of the lower smear density, the practical increase of the heavy atom content is close to +20%. This additional mass is mainly supplied by depleted uranium leading to a better breeding gain.

The target of a zero reactivity loss is here exceeded: instead of the standard reactivity loss with burn-up of the oxide core, the metal fueled core offers a substantial reactivity gain. However, this behaviour is closely dependant on the large core size of EFR: an oxide/metal comparison applied to a smaller core would show a reduced but negative reactivity variation in favour of the metal fueled core and a more convincing benefit on control requirements.

Corresponding to an equal damage rate, the peak discharge burn-up is inexorably lower in the metal core than it is in the oxide one, mainly due to lower enrichments. This disadvantage of metallic fuel could be partly compensated by the use of a heterogeneous design. Doppler and sodium void reactivities are also greatly modified by the use of metallic fuel: decrease for the Doppler reactivity and increase for the sodium void reactivity in factors about 2. These differences are mainly related to neutron energy spectrum and also, for Doppler reactivity, to operating temperatures.

#### PERFORMANCE SENSITIVITY TO SMEAR DENSITY AND CLAD THICKNESS

The present knowledge on metallic fuel use in LMFBR being very far from the one achieved for oxide fuel, uncertainties affecting design parameters are obviously larger when metallic fuel is used.

Particularly, because of the swelling, the smear density capable of achieving high discharge burn-up could be lower than the value previously mentioned. So, it was interesting to evaluate the metal core performances considering a smear density equal to 0.63 and 0.58, the reference value being 0.68.

Most of the results (table II) are intermediate to those previously obtained for oxide and metal fueled cores (closer to the last one), except the cycle length that is reduced again with respect to the "reference" metal core. This difference can be explained by the higher instantaneous damage rate due to the higher mean flux level and also to the spectrum hardening (related to higher enrichments).

However, the main result is the burn-up reactivity variation that remains clearly in favour of the metal core in spite of the reduced smear density. Moreover, the damage rate over discharge burn-up ratio is still far from the one of oxide fuel.

The clad thickness is an other design parameter that is likely to evolve with knowledge improvement. A major advantage foreseen in using metallic fuel is the non-corrosion of the clad and consequently, the possible clad thickness reduction. Results reported in table III show the consequences on core performances of a 20% reduction of the clad thickness.

The steel volume fraction reduction induces direct favourable effects related to neutron parasitic absorption and scattering, but is also profitable to the fuel volume fraction acting like an increase of the smear density. As a consequence, enrichment and reactivity gain with burn-up differ appreciably from the "reference" values.

Moreover, both parameters, smear density and clad thickness do not provoke any significant changes of Doppler and sodium void reactivities (a few percent for the variations considered above).

#### SAFETY IMPLICATIONS

More detailed explanations can be found in reference [2], so the purpose of the following lines will be limited to a few comments on safety aspects involving the above results.

When going further in such an oxide/metal core comparison, the metal fueled core disadvantage concerning sodium density coefficient and Doppler coefficient can be seen in the same manner as it has been here for integral reactivity effects.

Taking into account the higher sodium density coefficient and the lower Doppler coefficient, the analysis of 3 types of transient (slow loss of flow, fast loss of flow and slow overpower) leads to the following conclusions:

- in the case of a slow loss of flow, higher sodium and clad temperatures are reached at the beginning of the transient in the metal fueled core because of the higher sodium density coefficient. Then, the equilibrium temperature is in favour of the metal core due to its reduced Doppler coefficient.
- in the cases of fast loss of flow and slow overpower, higher sodium and clad temperatures are reached during the transient due, for the first transient, to the higher sodium density coefficient and for the second, to this unfavourable effect joined with the lower Doppler coefficient.

These considerations make clear that the demand for low void cores is to be considered of prime interest when metallic fuel is used.

#### CONCLUSION

A comparative study is underway to identify and quantify the physic parameters that differentiate metal and oxide fuel types when they are used in a LMFBR. In a preliminary phase, a neutronic comparison has been carried out using a large and homogeneous core, optimised for oxide fuel use, e.g. the European Fast Reactor core. Compared with oxide fueled core performances, the differences mainly noticed are the following:

- a strong reduction of the burn-up reactivity loss, up to reach a reactivity gain instead of the characteristic reactivity loss (5.65 pcm/EFPD) of the oxide fueled core.

- a lower discharge burn-up (-30%) corresponding to an equal damage rate.
- a nearly twice larger positive sodium void reactivity associated with a reduced Doppler reactivity in a factor close to 2.

Moreover, these results are not qualitatively modified when using a smear density of the metallic fuel reduced from 0.68 up to 0.58 or a reduced clad thickness, design parameters still likely to evolve.

Among these differences, the disadvantage on sodium void reactivity, because of the resulting core dynamic behaviour, certainly constitutes a main draw-back for the use of metallic fuel. So, the further developments of our study will examine some geometrical and conceptual improvements to achieve a optimised design, particularly with respect to this safety aspect.

#### References

- [1] Core optimisation studies for the European Fast Reactor EFR
  - U. Wehmann, R. de Wouters, R. Suderland, H. Sztark International Conference on the Physics of Reactors, Marseille, April 90 Proceedings, Vol 1, p II.34
- [2] Reactivity effects and dynamic behaviour: comparative performances of large LMFBR's oxide and metallic fuel cores.
  - P. Bergeonneau NEACRP-A-991, 32nd NEACRP meeting, 9-13 Oct 89, Argonne (USA)

TABLE I

| Fuel                           |              | UO2 PuO2 | UPu 10Zr |
|--------------------------------|--------------|----------|----------|
| Initial Pu loading             | (tonne)      | 8.15     | 6.35     |
| Initial U+Pu loading           | (tonne)      | 48.3     | 56.9     |
| Cycle length                   | (EFPD)       | 503      | 428      |
| Reactivity rods up at BOEC     | (pcm)        | 5837     | 241      |
| Reactivity rods up at EOEC     | (pcm)        | 3000     | 3000     |
| B.U. reactivity loss           | (pcm/EFPD)   | 5.65     | -6.45    |
| Peak linear rating at BOEC     | (W/cm)       | 427      | 419      |
| Peak linear rating at EOEC     | (W/cm)       | 438      | 490      |
| Average discharge B.U.         | (MWd/t)      | 99700    | 71900    |
| peak discharge B.U.            | (MWd/t)      | 161000   | 118000   |
| peak damage rate               | (dpa NRT,Fe) | 180      | 180      |
| Doppler reactivity at EOEC     | (pcm)        | 1283     | 547      |
| Sodium void reactivity at EOEC | (pcm)        | 2726     | 4616     |

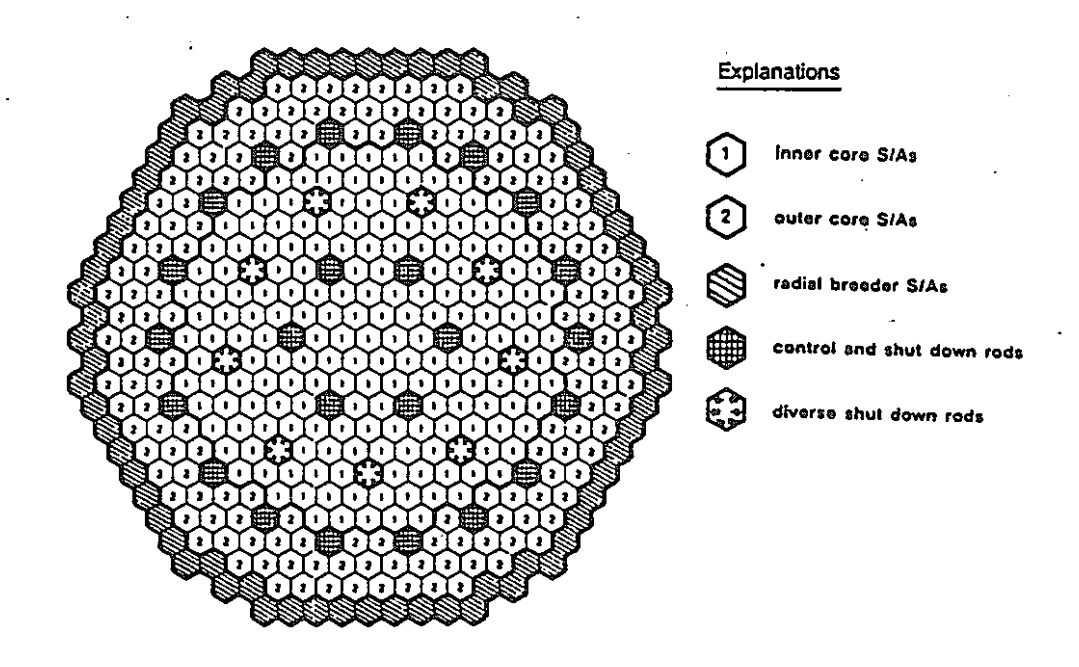
TABLE II

| Smear density              | (%)          | ref=68 | 63     | 58     |
|----------------------------|--------------|--------|--------|--------|
| Initial Pu loading         | (tonne)      | 6.35   | 6.18   | 6.02   |
| Initial U+Pu loading       | (tonne)      | 56.9   | 52.8   | 48.8   |
| Cycle length               | (EFPD)       | 428    | 407    | 386    |
| Reactivity rods up at BOEC | (pcm)        | 241    | 911    | 1664   |
| Reactivity rods up at EOEC | (pcm)        | 3000   | 3000   | 3000   |
| Average discharge B.U.     | (MWd/t)      | 71900  | 73700  | 75700  |
| peak discharge B.U.        | (MWd/t)      | 118000 | 121000 | 126000 |
| peak damage rate           | (dpa NRT,Fe) | 180    | 180    | 180    |

TABLE III

| Clad thickness         | (mm)         | ref=0.534 | 0.437  |
|------------------------|--------------|-----------|--------|
| Initial Pu loading     | (tonne)      | 6.35      | 6.36   |
| Initial U+Pu loading   | (tonne)      | 56.9      | 60.4   |
| Cycle length           | (EFPD)       | 428       | 433    |
| Average discharge B.U. | (MWd/t)      | 71900     | 68600  |
| peak discharge B.U.    | (MWd/t)      | 118000    | 113000 |
| peak damage rate       | (dpa NRT,Fe) | 180       | 180    |

### FIGURE I



NEACRP-A-1058 Topic 1.3

# 33rd NEACRP MEETING PARIS OCTOBER 15-19, 1990

## SODIUM-VOIDING REACTIVITY EFFECT REDUCTION IN FAST BREEDER REACTORS

by

J. TOMMASI, A. ZAETTA CEA

### SODIUM VOIDING REACTIVITY EFFECT REDUCTION IN FAST BREEDER REACTORS

Jean TOMMASI, Alain ZAETTA
CEA/DRN/DER/SPRC/LEDC

August 29, 1990

#### **ABSTRACT**

This paper deals with the studies already or to be conducted at CEA on sodium voiding reactivity effect (SVRE) reduction in fast reactors. It considers first the variations of SVRE with single parameters affecting core composition, geometry, and design options. This parametric study will give hints on the best ways to reduce SVRE. Then, the parameters considered being dependent and not exhaustive, one has to take into account neutronic and design basis considerations to achieve realistic (functional) core designs; that gives a new set of constraints on the different kinds of design modification examined. Two examples of such optimizations are given.

#### 1. INTRODUCTION

Two strong incentives lead the design of new fast reactors:

- 1) these reactors must be economically competitive with thermal reactors;
- 2) they must ensure as high a safety level as possible,

These two objectives are antagonistic to some extent, and tradeoffs must be found between them. In this paper, we study a mean to improve fast reactors safety only, regardless of quantified consequences on economical competitiveness. A way to increase safety in fast reactors is to reduce the sodium voiding reactivity effect (abbreviated SVRE here), an ideal would be to achieve negative values for SVRE.

A program of parametric studies is under way at CEA to precise SVRE behavior in relation with core composition, geometry and design options. This series of studies will focus on two core types: PHENIX and SUPERPHENIX, representing two interesting power levels and sizes. Calculations are made by resolving the diffusion equation in RZ geometry, with 25 energy groups. SVREs are obtained either by difference between two direct calculations (especially when core geometry changes) or with perturbation theory formalism (to split SVREs into physically significant components).

#### 2. SVREs PRESENTATION

The influence of sodium on core neutronic balance is double: it slows down neutrons (moderating effect) and is a relatively weak absorber (compared to heavy atoms). When the in-core sodium concentration falls down the neutronic balance is altered:

- absorption decreases due to sodium voiding, and neutron leakage goes up due to the increase of diffusion coefficients:
- slowing down of neutrons decreases;
- resonance self-shielding increases (lesser dilution of heavy atoms into moderator), and heavy atoms cross-sections go down.

We can split SVRE into four components (splitting issued from perturbation theory formalism):

1) Leakage component

Always negative, due to the increase of the diffusion coefficient. As this component depends on the gradients of direct and adjoint flux its importance will be greater near interfaces (core-blanket for example) and generally in external core regions.

2) Slowing down (or spectral) component

This component depends on the variation of scattering cross-sections and the difference between initial and final importances of scattered neutrons. If sodium concentration goes down, scattering cross-sections decrease, and the sign of this component depends on the shape of the importance spectrum: a lesser scattering from a high importance energy to a lower importance one gives a positive contribution to SVRE, and conversely. For energies greater than 0.8 MeV, importance grows with energy, due to the increase of U8 fission cross-sections; from 20 keV to 0.8 MeV, importance grows with energy in the case of Pu9 fuel, the steepness of the curve increasing when enrichment decreases; for energies lesser than 20 keV, importance

decreases as energy grows. To calculate accurately this component, a few-group approximation is questionable, thus the 25-group formalism.

#### 3) Absorption component

It depends on the variation of absorption cross-sections and on the values of direct and adjoint flux. Absorption cross-sections go down as sodium is voided and as self-shielding increases for heavy atoms, and this component is positive. The highest values of direct and adjoint flux are generally obtained deep within the core (at core center for most homogeneous cores).

#### 4) Production component

It depends on the variation of production cross-sections and on the values of direct and adjoint flux. As self-shielding increases, the production cross-sections go down, and this component is negative, with a small amplitude.

The last three components are usually added to form the so-called central component, while the first is split into axial and radial leakage components. SVRE is then the balance between the central component, generally positive, and the negative leakage components; thus for small SVRE values the uncertainties become relatively large, and blur the sign of SVRE for near-zero values.

The principal ways to achieve a substantial reduction of SVREs are, according to the previous considerations:

- to modify neutron importance spectra to act on the spectral component (for example by modifying enrichments or by adding some moderator to driver subassemblies)
- 2) to increase leakage (mainly gradients of flux and adjoint flux) in flooded core configurations. This can be done by designing small cores, cores with a large area-to-volume ratio (for example pancake cores), by reducing reflector efficiency, by playing upon enrichment ratios (radially and axially), by decoupling core zones by fertile and/or non-active zones (heterogeneous and modular designs)...

The most promising way to decrease heavily SVRE seems to be the second. In either way, it is easy to realize that SVRE diminution is in contradiction with a good neutron economy and deteriorates core neutronic performances. A good example of performances/SVRE-reduction tradeoffs that can be made is given in ref. 1.

The main terms of the series of parametric studies initiated by CEA are the following:

| core composition | <ul> <li>volume fractions of sodium, fuel, steel</li> <li>mean enrichment, enrichment ratios</li> <li>fuel type (oxide, metal, nitride), steel type, Pu vector</li> <li>in-core moderator</li> </ul> |
|------------------|------------------------------------------------------------------------------------------------------------------------------------------------------------------------------------------------------|
| core geometry    | - height to diameter ratio - volume                                                                                                                                                                  |
| core design      | - concept: homogeneous, axially and/or radially heterogeneous - environment: blanket and/or reflector modifications                                                                                  |

The following paragraphs will comment the results already obtained (mainly in the case of a SUPERPHENIX-type core), and the directions to be prospected.

#### 3. CORE COMPOSITION MODIFICATIONS

These modifications are made on global values (volume fractions, mean enrichment, enrichment ratios, burnup...) independently of design basis correlative modifications. Quoted values can thus lead to unrealistic core designs, and advantages on SVRE expected can be offset to a large extent by design basis constraints; but the only aim of this part of the study is to clear parametric variations of SVRE with core composition modifications.

Here are some effects of parameter variations on SVRE, in SUPERPHENIX-type cores:

| Increase of                                    | Effect on SVRE                                                                              |
|------------------------------------------------|---------------------------------------------------------------------------------------------|
| Sodium volume fraction                         | Quasi-linear increase (50 pcm/%)                                                            |
| Steel volume fraction                          | Small decrease: <70 pcm from 10 to 40%                                                      |
| Fuel volume fraction                           | Increase, saturation and decrease over the 25-40% range; maximum amplitude of about 200 pcm |
| Mean enrichment                                | Decrease of about 30 pcm/%                                                                  |
| Enrichment ratio (at constant mean enrichment) | Increase: 550 pcm from 0.65 to 0.9                                                          |
| Виглир                                         | Increase of about 0.8 pcm/efpd                                                              |

Notes:

- Enrichment ratio is the ratio between internal and external zone enrichments; it will be recalled as  $E_1/E_2$  in the following.

$$-1 \text{ pcm} = 10^5 \frac{\Delta k}{k}$$

Some comments can be made on these figures:

#### 1) Volume fractions.

Design basis rules make these values correlated one with another; single variations have no practical sense and realistic modifications will have to integrate the three kinds of variations simultaneously.

#### 2) Sodium volume fraction alone.

In voiding sodium, SVRE central and leakage components have the following behaviors with respect to sodium volume fraction in corresponding flooded cores:

- Central component: its magnitude increases monotonically when sodium volume fraction goes up, as absorption and scattering cross-sections do (the production component is of lesser amplitude and can generally be neglected).
- Leakage component: it depends on the diffusion coefficient variation  $\delta D$ .  $D \approx \frac{1}{3(\Sigma_0 + \Sigma_{Na})}$ , where  $\Sigma_{Na}$  means sodium macroscopic cross-section, and  $\Sigma_0$  all-but-

sodium macroscopic cross-section. Then  $\delta D$  is proportional to  $\frac{\Sigma_{Na}}{\Sigma_0 + \Sigma_{Na}}$ ; that is,  $\delta D$ 

value is zero when sodium volume fraction is zero (obvious), increases as sodium volume fraction goes up, and comes to saturation with large values of sodium volume fraction (these large values may well be unrealistic ones).

SVRE results of the competition between these two effects. Depending on flooded core leakage level, this can give rise to two different behaviors:

- Low leakage cores: leakage component magnitude is not sufficient to counter central component increase with sodium volume fraction; SVRE monotonically increases from zero with sodium volume fraction.

- High leakage cores: for 'small' sodium volume fraction values, leakage component predominates: SVRE decreases while sodium volume fraction goes up. Then the leakage component goes to saturation, and central component effects become prevalent: SVRE becomes stationary, then goes up. Such sodium volume fraction values may well be unrealistic (too large) ones, and we may either see the decreasing part of the curve only, or its whole shape.

In this parametric study context, fuel and steel volume fractions are fixed.

3) Fuel volume fraction, mean enrichment and enrichment ratio.

Different core sizes and shapes can lead to different behaviors. For example, calculations made for a PHENIX-like core show a decrease in SVRE for enrichment ratios growing from 0.64 to 0.86; that is exactly the opposite trend compared to a SUPERPHENIX-type core within the same range of  $E_1/E_2$ . We can give the following sketch of explanation (which needs yet support calculations to test its value):

- a) For low enrichments an increase in enrichment gives an increase to the central component, because of spectrum hardening which activates the threshold fission cross-sections of U8; for high enrichments, an increase in enrichment makes the central component decrease because the slope of the importance spectrum decreases in the 20keV to 0.8 MeV range.
- b) An increase in enrichment lowers the absolute value of the leakage component, because of the diminution of the diffusion coefficient; this leakage component reduction goes to saturation for very high enrichments, when flux shapes are little altered by an increase in enrichment.

The expected shape for the SVRE vs enrichment curve is then a steep increase followed by a gentler decrease (as was obtained for the SVRE vs fuel volume fraction curve), the position of the maximum depending on the size and shape of the core: for a flooded core with important leakage, the position of the maximum should be shifted towards high enrichment values. This means for example that for sufficiently small cores SVRE could grow with mean enrichment: it would be interesting to determine the relevant sizes and/or shapes relative to these maxima.

For enrichment ratios, we can guess asymptotic behaviors: if  $E_1/E_2$  reaches near-zero values, we get the equivalent of an annular core with a large and growing enrichment  $E_2$ . SVRE decreases as  $E_2$  goes up, so SVRE grows with  $E_1/E_2$ . To the contrary, if  $E_1/E_2$  reaches large values, we get the equivalent of a smaller active core with a large and growing enrichment  $E_1$ . SVRE decreases as  $E_1$  grows up, that is as  $E_1/E_2$  grows up. The position of the maximum depends here again on the size and shape of the core, and particularly of the width of the external zone, which allows a more or less important flux curvature within it (in small width external zones a higher enrichment is required to increase gradients and leakage, and not only to flatten flux distribution). Small external zone widths lead to a displacement of the maximum towards high  $E_2$  values, that is low  $E_1/E_2$  values; this explanation scheme is coherent with calculations: for a PHENIX-like core we should be on the descendent slope of the SVRE vs  $E_1/E_2$  curve, while we should be on the ascendent slope for a SUPERPHENIX-like core for the same range of  $E_1/E_2$  values with which calculations were made. It could also be interesting to check SVRE values vs mean enrichment in relation to  $E_1/E_2$ . Note that we can have different enrichment zones not only radially but also axially.

4) Burnup.

Flux hardening due to voiding reduces absorption by fission products at intermediate energies; we see that high burnup and SVRE reduction are opposite objectives, and that multibatch management, reducing mean burnup values over a long part of core life can present advantages for SVRE reduction.

#### 4. CORE GEOMETRY MODIFICATIONS

These modifications allow the easiest significant reductions of SVRE (regardless to correlated neutronic penalties), mainly because of the massive increase of neutron leakage level they consent. They are only size and shape modifications.

The following results are drawn from calculations on a SUPERPHENIX-type core:

| Increase of                                             | Effect on SVRE                                                                    |
|---------------------------------------------------------|-----------------------------------------------------------------------------------|
| H/D (at constant volume)                                | Increase then saturation in the 0.1 to 0.8 range; amplitude: from 100 to 2200 pcm |
| Volume (at constant H/D)                                | Quick increase, then saturation (the higher the H/D, the earlier the saturation)  |
| Core radius                                             | Increase, saturation and decrease (amplitude 320 pcm, range 120 to 300 cm)        |
| Core height                                             | Increase from 500 to 2600 pcm in the 50 to 200 cm range                           |
| Internal core height only .                             | Increase from 0 to 2500 pcm in the 20 to 200 cm range                             |
| External core height only                               | Increase from 1500 to 1750 pcm in the 20 to 200 cm range                          |
| Internal and external core heights (at constant volume) | Increase from 500 to 1700 pcm in the 20-200 to 100-100 cm range                   |

Note: H/D = height-to-diameter ratio

#### Comments on these figures:

0) Expression of area-to-volume ratio for a cylinder.

$$\frac{S}{V} = \left[\frac{2\pi}{V}\right]^{\frac{1}{3}} \left[2\left[\frac{H}{D}\right]^{\frac{1}{3}} + \left[\frac{H}{D}\right]^{\frac{-2}{3}}\right]$$

1) Height-to-diameter ratio.

As expected, for area-to-volume ratio at constant volume is minimal for H/D=1, has a steep slope for H/D<1, and a gentler slope for H/D>1.

2) Volume.

As expected, for area-to-volume ratio at constant H/D presents a steep slope for small volume values, which goes gentler as volume grows. When H/D grows from 0 to 1, lesser volume values are needed to reach the same values of S/V, which explains the quicker saturation with growing (<1) H/D values.

3) Core radius.

This behavior results of a two-effect compensation: a positive effect with saturation due to volume increase, and a negative one due to H/D decrease when core radius values grow up.

4) Core height.

This behavior too is a two-effect combination: a positive effect with saturation due to volume increase, an a positive (then negative when H/D>1) effect due to H/D increase.

5) Internal and/or external core heights.

Due to the large core dimensions, the major part of SVRE is concentrated in the internal core zone, thus the behavior observed: large variations of SVRE with internal core height variations, minor ones with external core height variation. It could be interesting to examine what would happen in a smaller core, to compare in that situation the respective weights of internal and external core height individual variations on SVRE. The last table entry shows the interest (with respect to SVRE only) of a H-shaped core, which keeps reference core volume constant.

#### 5. DIFFERENT CORE DESIGNS

#### A) Heterogeneous cores.

#### A1) Axially heterogeneous cores.

We check here the effect of a fertile slab insertion at core half-height on a SUPERPHENIX-type core. Slab width varies in the 0 to 50 cm range. In the case of fuel zone voiding only, SVRE decreases from its reference value (1710 pcm) to 0 pcm for 50 cm width. Two points temperates this good behavior: if we void the fertile slab too, SVRE increases to about 2000 pcm then decreases to 1000 pcm for 50 cm width; and if we check the behavior of the SVRE vs slab width curve at 1000 EFPD the gain obtained at 50 cm slab width becames less than one dollar.

#### A2) Radially heterogeneous cores.

Optimization of radially heterogeneous core designs with respect to SVRE is an uneasy task, because of the wide range of possible design options, particularly the positions, widths, sizes and number of in-core fertile zones. However, the general trend is the following: for the same in-core fertile to fissile ratio (heterogeneity factor, HF in the following), large-size fertile islands, well decoupling fissile zones, should be preferred to multiple small-size fertile islands. Thus, compact and thick heterogeneous designs (a central slab, one thick fertile ring) lead to the greatest SVRE reductions. More details will be given in section 6.B.

#### B) Modular cores.

Decoupling even more core zones leads to modular core design: small fissile islands are embedded in a thick fertile and/or non-active matrix. The high leakage level from the fissile islands allows very low values of SVRE to be achieved, for volumes comparable to those of big homogeneous cores. The main drawbacks of this solution are the necessity to achieve very high fuel enrichments to keep a good reactivity level (this can give problems for reprocessing) and problems of power control due to the different fissile zones high decoupling. In return, flux characteristics of this core type might help for actinide burning. For more details, see ref. 2.

#### C) Different core environments.

Studies are under way to quantify the modifications of SVRE brought by modifying core environment. Such modifications are for example: suppression of axial blankets, use of low density steel structures for neutronic protections, exchange of positions between axial blanket and fission gas plenum... The main goal of these changes is here again to increase neutron leakage. These solutions degrades neutronic performances and may lead to protection problems; they give relatively small SVRE reductions compared to those achieved with core geometry modifications, but do not modify core bulk. As an indication, we can give the following values:

- Reference core: EFR-type core with reduced height (100 cm); SVRE=1163 pcm.
- Reference core with 5-cm-wide axial blankets: SVRE=1109 pcm.
- -Reference core with 5-cm-wide axial blankets and 'lightened' plenum steel (half Fe, Cr, Ni nuclides): SVRE=965 pcm.
- Reference core without axial blankets and with lightened plenum steel: SVRE=792 pcm.

#### D) Use of in-core moderator.

Moderators can be used to shift neutron spectrum towards low energies to increase negative contributions to SVRE slowing down component. This can be done by mixing moderator pins with fuel pins in fuel subassemblies. The result should be a diminution of SVRE due to the combination of the decrease of the central component (slowing down, absorption and production) with an adverse diminution of leakage. Studies are in progress.

#### E) Use of other coolants.

A radical change of approach to minimize voiding reactivity effects is to change coolant, and use other liquid metals or alloys instead of sodium. Most solutions use lead or lead alloys (with lithium or bismuth). Studies are in progress to precise this point.

#### 6. TAKING INTO ACCOUNT NEUTRONIC AND DESIGN BASIS CONSTRAINTS

To determine individual trends is not sufficient: the parametric variations examined above are dependent one from another, and are furthermore constrained by design basis rules and neutronic performances considerations if they are to result in realistic core designs. Such calculations were performed with the MECONG code, currently under development at CEA, which is able to take into account simple design basis constraints and to adjust some parameters such as enrichment ratio, mean enrichment and cycle duration, to achieve predetermined neutronic performances (burnup, damage on steel, reactivity levels at beginning and end of cycle...). We give here two examples of such investigations:

#### A) Some interesting core designs.

The reference is a SUPERPHENIX-like core (core radii 141 and 188 cm, core height 100 cm). Three different cores are considered:

- 1) A pancake core of same fissile volume and H/D=0.1.
- 2) A variable height core (internal core height 50 cm, external 160 cm) with the same fissile volume.
- 3) A radially heterogeneous core with a central fertile slab of 100 cm radius, which replaces fuel subassemblies.

The thermal output is fixed at 3000 MW; enrichments are adjusted to obtain at end of life with a single-batch management scheme a zero reactivity associated with a 100000 MWd/t (oxide) burnup. The figures in the following table speak for themselves.

|                              | reference | pancake<br>core | variable<br>height<br>core | radially<br>heterogeneous<br>core |
|------------------------------|-----------|-----------------|----------------------------|-----------------------------------|
| Mean enrichment (%)          | 16.7      | 23.2            | 20.2                       | 20.4                              |
| Initial reactivity (pcm)     | 5473      | 9655            | 7774                       | 9238                              |
| Reactivity swing (pcm/efpd)  | 5.8       | 8.5             | 8.95                       | 13.8                              |
| Residence time (efpd)        | 940       | 1134            | 870                        | 678                               |
| Mean burnup (MWd/t)          | 67000     | 78000           | 63000                      | 67000                             |
| Qmax (half-life, W/cm3)      | 400       | 319             | 419                        | 537                               |
| SVRE (beginning of life) pcm | 1520      | 484             | 960                        | 443                               |
| SVRE (end of life) pcm       | 2363      | 1451            | 1728                       | 1068                              |
| SVRE (half-life) pcm         | 1942      | 968             | 1344                       | 756                               |

Note: To convert quickly SVRE into \$ values take a 1\$=400 pcm basis (1\$ worth ranges between 430 and 350 pcm when enrichment varies from 10 to 35%).

#### B) Radially heterogeneous cores SVRE optimization.

The aim of this study is to optimize SVRE reduction in relation with neutronic performances and design basis constraints. To standardize calculations and to make easy comparisons between them, a group of fixed constraints has been set. These are peak burnup (150000 MWd/t), BOC reactivity (5500 pcm), EOC reactivity (2700 pcm); an upper value for peak linear rating is 480 W/cm. Parameters are of two kinds:

- Core size and shape: volume and height-to-diameter ratio. Three core volumes are taken into account: EFR volume ( $16~m^3$ , 3600~MW thermal output), PHENIX volume ( $1.5~m^3$ , 600~MW), PRISM volume ( $0.5~m^3$ , 400~MW). Reference H/D is 0.35. Other calculations are made at H/D=0.15 and H/D=0.5.
- Radial heterogeneity: different heterogeneity factors (from 0 to 30 %) and fertile patterns (central slab, fertile rings, and combinations) are taken into account.

When shifting from an homogeneous to an heterogeneous core design, at constant core bulk, there is a decrease in fuel volume; that needs an higher enrichment to achieve fixed reactivity levels. This higher enrichment leads in turn to a greater reactivity swing, which shortens cycle length, and requires a higher-frequenced multibatch fuel management. In relation to fissile volume diminution, the power distribution is flattened with respect to homogeneous cores: higher  $E_1/E_2$  values are sufficient to balance the outputs of the two fissile zones; for high HFs, a unique enrichment is achievable.

As regards design basis constraints, a fissile subassembly number diminution leads to a correlative increase of pin number per subassembly to try to maintain the same peak linear rating (as pin number per S/A can only vary in a discrete way, this adjustment can only be a loose one). Such variations need in turn an adjustment in sodium, steel and fuel volume fractions; furthermore, a larger pin number per S/A increases core pressure drop.

This brief review shows that SVRE reduction, all constraints taken into account, is the result of the complex interaction of multiple single variations which can individually offset or reinforce each other.

The first part of the study was devoted to the choice of radial heterogeneity patterns which affect less core neutronic performances. As was said in section 5A.2, the thicker fertile patterns are the better to decrease SVRE, at fixed HF. For both EFR and PHENIX core volumes, the retained pattern was the central slab, with 20% HF for EFR volume core, 30% for PHENIX volume core (due to lesser dimensions, the same thickness is reached for higher HFs). The PRISM-volume homogeneous core, having yet a sufficiently negative SVRE needs no modification. The second part of the study examines SVRE reductions brought by a H/D shift from 0.35 to 0.15. To achieve a less-than-1\$ SVRE in the case of a maximum effect voiding, the sizes needed are:

- for a homogeneous core: a volume between those of PRISM and PHENIX, and a thermal output of about 500 MW;
- for a heterogeneous core: a volume between those of PHENIX and EFR (about 6 m<sup>3</sup>), and a thermal output of about 1500 MW.

This shows the interest of radially heterogeneous core designs. The following table gathers most important parameter variations with design options and geometry modifications:

| Volume/thermal output        | EFR   | EFR   | PX     | PX     | EFR    | EFR   |
|------------------------------|-------|-------|--------|--------|--------|-------|
| H/D                          | 0.35  | 0.35  | 0.35   | 0.35   | 0.15   | 0.15  |
| Heterogeneity factor (%)     | 0     | 20    | 0      | 30     | 0      | 20    |
| Fuel volume fraction (%)     | 32.21 | 30.66 | 35.85  | 31.22  | 37.12  | 33.31 |
| Sodium volume fraction (%)   | 37.90 | 37.75 | 33.39  | 38.87  | 32.68  | 35.96 |
| Steel volume fraction (%)    | 25.30 | 25.30 | 25.55  | 25.53  | 24.77  | 24.57 |
| Pin number per S/A           | 271   | 331   | 217    | 271    | 271    | 331   |
| Pressure drop (bar)          | 5.20  | 8.70  | 2.89   | 2.93   | 2.54   | 2.99  |
| Mean enrichment (%)          | 16.40 | 18.30 | 24.30  | 36.60  | 17.19  | 19.19 |
| Enrichment ratio             | 0.80  | 1.00  | 0.65   | 1.00   | 0.85   | 1.00  |
| Mean burnup (MWd/t)          | 93744 | 90271 | 104266 | 113573 | 101402 | 93739 |
| BOC pin linear rating (W/cm) | 403   | 427   | 364    | 367    | 329    | 352   |
| Reactivity swing (pcm/efpd)  | 6.04  | 13.03 | 14.90  | 23.09  | 6.00   | 11.35 |
| Cycle length (day)           | 476   | 212   | 168    | 117    | 458    | 244   |
| Multibatch frequence         | 3     | 5     | 6      | 6      | 4      | 5     |
| Fuel in-core lifetime (day)  | 1428  | 1060  | 1008   | 702    | 1832   | 1220  |
| BOC SVRE (pcm)               | 2297  | 1137  | -19    | -1462  | 1170   | 1003  |
| EOC SVRE (pcm)               | 2756  | 1377  | 135    | -1369  | 1563   | 1050  |

#### 7. CONCLUSION

This review is open-ended, for a great part of the studies quoted within are still in progress. Two points can yet already be underlined:

- 1) As there are close interrelations between the parameters that can lead to SVRE modifications, SVRE results of complex interactions between individual variations; furthermore, to get to realistic core designs and SVRE values needs to take into account neutronic performances and design basis constraints.
- 2) The major part of core modifications made in order to decrease substantially SVREs lead to high leakage flooded core designs, in order to increase the leakage component magnitude in voided cores. An easy way to do so is to act on core size (volume) and shape (H/D, heterogeneity), with subsequent penalties on neutron economy.

Complementary studies are therefore needed in order to optimize core design and to achieve good tradeoffs between safety and economics.

#### 8. REFERENCES

- [1] R.N. Hill, H. Khalil: An evaluation of LMR design options for reduction of sodium void worth, proc. PHYSOR 90, International conference on the physics of reactors: operation, design and computation, oral session II, pp. 19-33, April 90
- [2] C. de Pascale: Modular island cores, NEACRP, August 90

#### NEACRP-A-1059 Topic 1.3

# 33rd NEACRP MEETING PARIS OCTOBER 15-19, 1990

MODULAR ISLAND CORES

by

C. DE PASCALE, A. ZAETTA CEA

October 1990

### MODULAR ISLAND CORES

Claire de Pascale - Alain Zaetta

CEA/DRN/DER/SPRC/LEDC September, 1990.

#### Abstract:

Since the most essential characteristics of fast reactors must be safety as well as economics, a modular island core concept is proposed to nullify sodium voiding reactivity effect, while keeping neutronic performances of big conventional cores.

The General Electric design is presented as an illustration of a modular island core.

Then are presented the CEA studies which turn on module optimizations, coupling study and modular core reconstitutions.

Very low sodium voiding reactivity are reached, but to the detriment of the core reactivity level, the loss of reactivity during operating fuel cycle and the power control.

Two interesting coupling materials are composed of three rows of fertile/absorber/fertile assemblies or three rows of stainless steel/absorber/stainless steel assemblies, depending on whether breeding gain or recycling costs are preferred.

The possibility of actinide recycling in modular cores is discussed.

#### 1. Introduction

The current studies on fast breeder reactors tend to improve reactor safety and particularly to reduce the sodium voiding reactivity effect: in large conventional breeders of about 1500 MWe the maximum sodium void reactivity is about \$5 to \$8, and a corresponding reactivity insertion in unprotected accident situations may lead to an energy release.

An approach to enhance the safety of cores is to modify core designs such that the removal of sodium from the core would only add a near-zero value of reactivity or even a negative one.

However, another necessity is to make fast reactors economically competitive in comparison with PWR:

- \* reduced cycle costs with high discharge burnup values,
- \* reduced structure costs with limited vessel sizes, though associated with large thermal powers.

First of all, sodium void reactivity effect is presented in part 2.

### 2 . Sodium void reactivity effect

The two major components of the sodium void worth are:

- \* the leakage component, which contributes a negative reactivity, and
- \* the spectral component (spectrum hardening due to voiding), which gives positive reactivity.

Many variations of the conventional homogeneous core design that will limit the sodium void worth have been identified. These can be classified as follows:

- \* pancake core with large axial neutron leakage,
- \* heterogeneous core with large local neutron leakage from high-importance fuel regions to low-importance internal blanket zones, (see ref. 1)
- \* and also, modular island cores as extremely decoupled designs (the larger the degree of decoupling, the greater the leakage).

### 3. The modular concept

Modular core configurations consist of small cores which are arranged in one reactor vessel.

The individual modules are separated from each other by several rows of radial blanket assemblies (or other assemblies of any "insulating" material).

The target parameters are:

- \* the maximum burnup fraction,
- \* the global thermal power, and
- \* the vessel diameter.

The values of these parameters must be comparable with those of a conventional homogeneous core, for economic reasons.

### 4. The General Electric study

The General Electric fast reactor study is presented as an illustration of a modular core (ref 2).

In the design study, (Pu,U)O2 fuel is assumed for the core. This modular core has seven modules separated by three rows of radial blankets. The design data are given in table and figure 1.

The sodium void worth for the total core height is \$0.25, whereas a conventional homogeneous core of similar size and thermal power would have a sodium void worth about \$5.

figure I
the General Electric modular island design

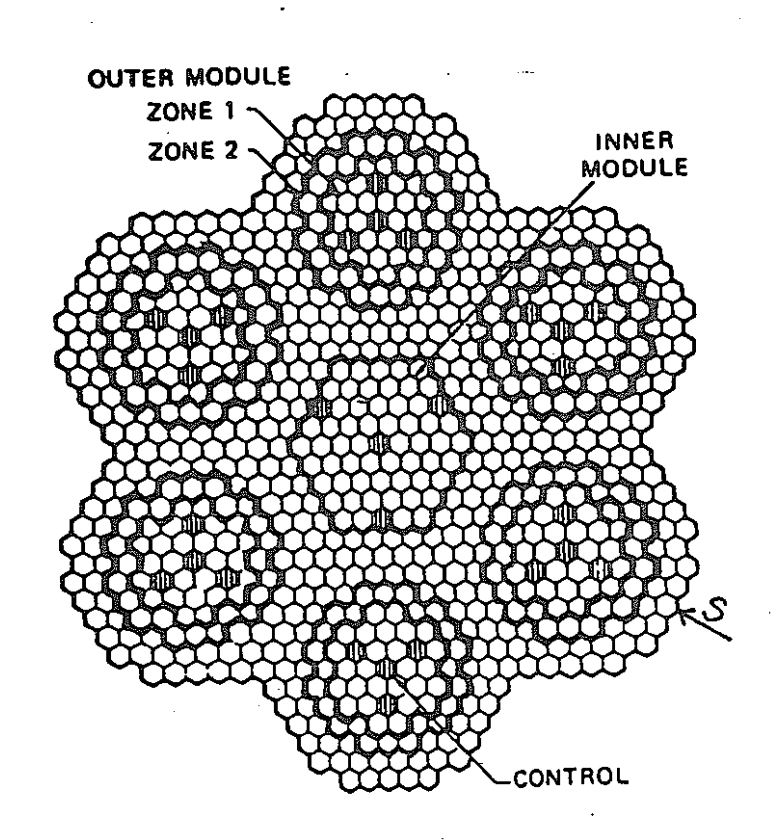


table 1

The General Electric modular core data

| reactor electric power        | MW      | 1200  |
|-------------------------------|---------|-------|
| reactor thermal power         | MW      | 3077  |
| number of modules             |         | 7     |
| refueling intervals           | days    | 365   |
| capacity factor               |         | 0.7   |
| number of fuel assemblies     |         |       |
| 1 inner module                |         |       |
| fuel zone 1                   |         | 57    |
| fuel zone 2                   |         | 0     |
| control                       |         | 4     |
| 6 outer modules               |         |       |
| fuel zone 1                   |         | 27    |
| fuel zone 2                   |         | 24    |
| control                       |         | 4     |
| maximum fuel zone radius      | cm      | 200   |
| fuel zone height              | cm      | 106.7 |
| assembly channel pitch        | cm      | 13.89 |
| fuel assembly volume fraction | -       |       |
| fuel                          | %       | 45.75 |
| structure                     | %       | 17.68 |
| sodium                        | %       | 36.57 |
| enrichments                   | 70.4    |       |
| zone 1                        | %       | 18.3  |
| zone 2                        | %       | 23.7  |
| peak of linear power          | W/cm    | 597   |
| sodium void worth             | dollars | 0.25  |
| (for the total core height)   |         |       |
| dollar value                  | pcm     | 385   |
|                               |         |       |

The current CEA studies are:

- \* module
- \* coupling
- \* modular core, optimizations.

Here after are presented the first CEA studies.

# 5. The module optimization

As module power and module size are conditionned by the number of modules in the vessel, and by the way they are arranged in the vessel, the studied modules are 90 to 150 MWe reactors.

Two studied cores of 90 to 150 MWe are described in figures and tables 2 and 3.

It can be noticed that each small reactor needs a separate control system, because of the weak neutronic coupling between the modules.

The reduction in sodium void reactivity is very promising: near-zero values or even negative ones are reached. But this has some important consequences: higher fissile enrichments are needed to obtain a high discharge burnup, thus the loss of reactivity during operating cycle is increased and the initial reactivity to be controlled, also. Refueling intervals will have to be reduced.

The linear power peak is near the objective and there is no problem with the damage dose.

To conclude with those studies, the sodium void reactivity is very interesting but to the detriment of the loss of reactivity during the operating fuel cycle.

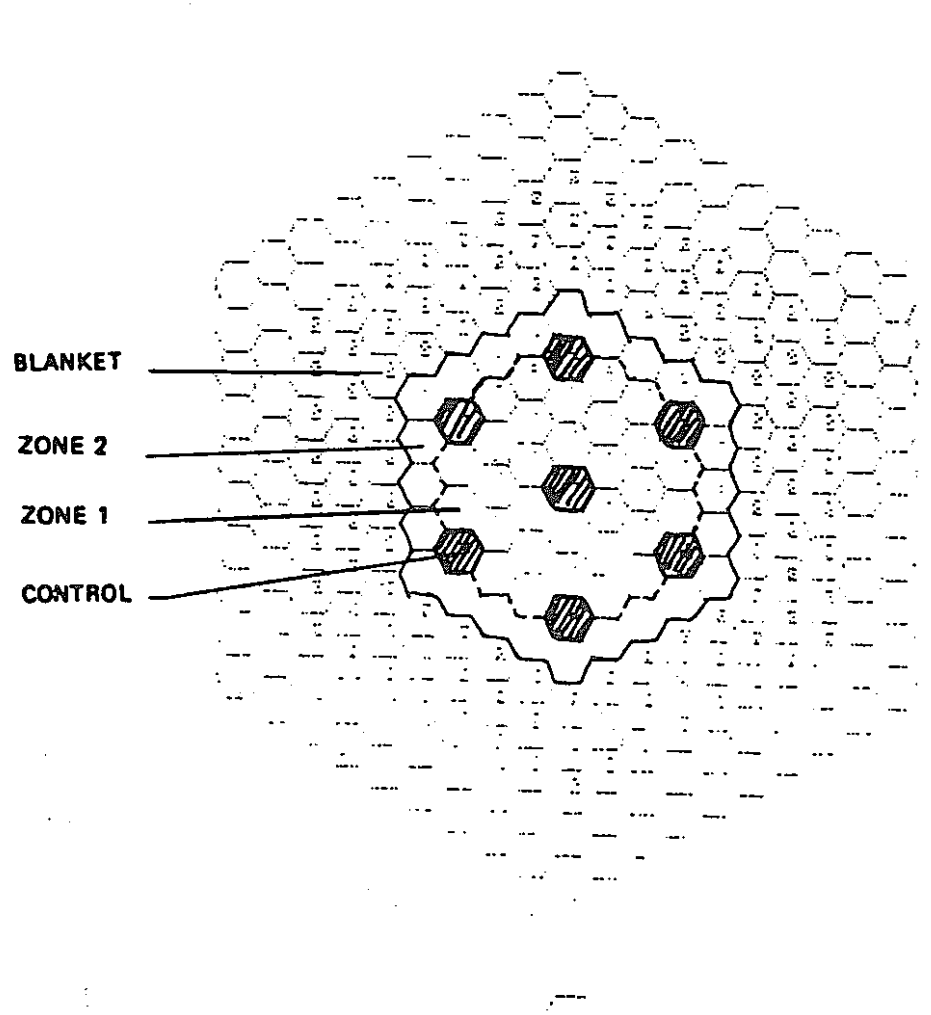


figure 2 the 150 MWe module

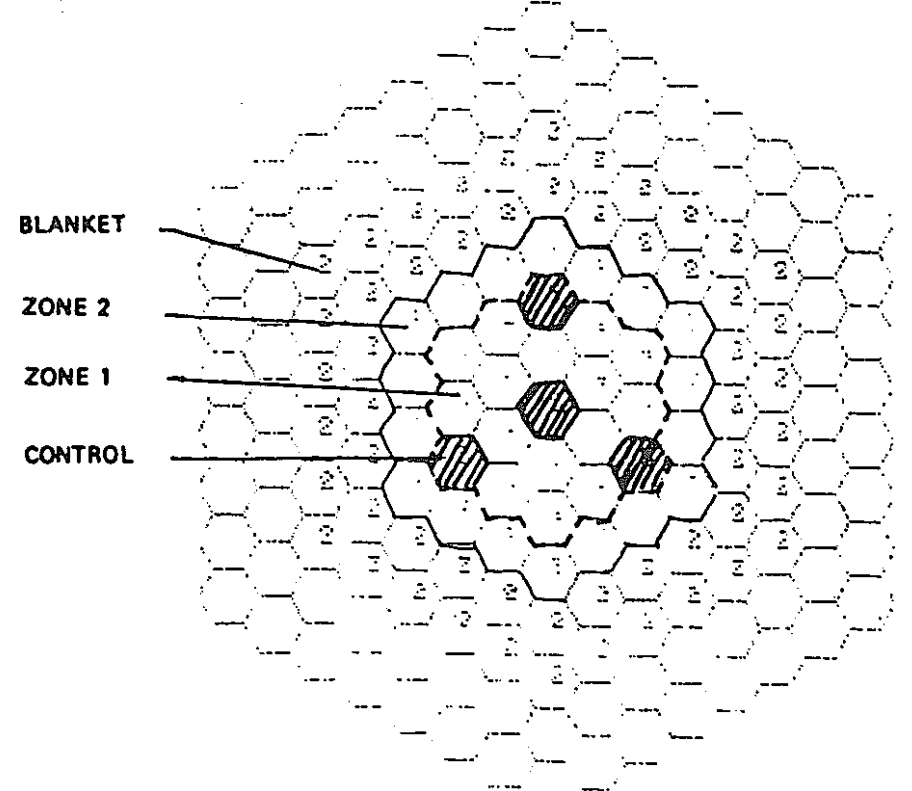


figure 3
the 90 MWe module

table 2

| data                          |      | the 150 MWe reactor | the 90 MWe reactor |
|-------------------------------|------|---------------------|--------------------|
| reactor thermal power         | MW   | 385                 | 231                |
| refueling intervals           | days | 730                 | 730                |
| capacity factor               | -    | 0.7                 | 0.7                |
| number of fuel assemblies     |      |                     |                    |
| fuel zone 1                   |      | 30                  | 15                 |
| fuel zone 2                   | _    | . 24                | 18                 |
| control                       | •    | 7                   | 4                  |
| maximum fuel zone radius      | cm   | 58                  | 45                 |
| fuel zone height              | cm   | 100                 | 100                |
| assembly channel pitch        | cm   | 12.8                | 12.8               |
| fuel assembly volume fraction |      |                     |                    |
| fuel                          |      | 38.7                | 38.7               |
| structure                     |      | 25.3                | 25.3               |
| sodium                        |      | 36                  | 36                 |
| enrichments                   |      |                     |                    |
| zone 1                        | %    | 22.5                | 30.8               |
| zone 2                        | %    | 37.4                | 35.1               |

table 3

| nuclear performance predictions                         |         | the 150 MWe reactor | the 90 MWe reactor |
|---------------------------------------------------------|---------|---------------------|--------------------|
| peak of linear power                                    | W/cm    | 454                 | 493                |
| peak of DPA                                             | nrt     | 146                 | 131                |
| discharge burnup                                        | MWd/t   |                     |                    |
| peak                                                    |         | 119600              | 116390             |
| average                                                 |         | 67800               | 67440              |
| loss of reactivity per day                              |         |                     |                    |
| at nominal power                                        | . pcm   | 19.7                | 20.5               |
| dollar value                                            | pcm     | 360                 | 350                |
| sodium voiding effect                                   | dollars |                     |                    |
| total -> beginning of cycle -> end of cycle             |         | -2.6<br>-2.5        | -6<br>-3.5         |
| fissile zone only -> beginning of cycle -> end of cycle | ÷.,:    | 0.5<br>1.           | -1<br>-0.8         |

# 6. Coupling optimization

The reduction in sodium voiding reactivity depends on the thickness of the internal blanket zones. The blankets tend to enhance the leakage component, and thus the neutronic decoupling among the modules.

Blankets may here be composed with "insulating assemblies" such as:

- \* fertile (53% fertile + 28% sodium + 19% stainless steel)
- \* stainless steel (50% stainless steel + 50% sodium)
- \* absorber (46% natural B4C + 20% stainless steel + 34% sodium)
- \* sodium (90% sodium + 10% stainless steel)

and all combinations of those materials: for example, one row of stainless steel / one row of absorber / one row of stainless steel assemblies.

However, the size of the vessel must be limited for economic reasons.

It is seen in figure 4 that three rows of internal fertile assemblies decouple sufficiently enough the core zones so that the sodium voiding reactivity does not decrease a lot with increasing blanket thickness. Thus, three rows of any insulating assembly is an optimum for those studies.

In table 4 are given tendances (values not to be considered as absolute ones) on core reactivities, with different kinds of insulating materials. That coupling optimization has been made with the General Electric modular reactor and at the beginning of the operating fuel cycle.

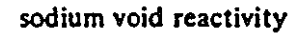
The best results are obtained with three rows of stainless steel / absorber / stainless steel assemblies. Such solution is also attractive because of the low recycling costs of those non-fissile materials.

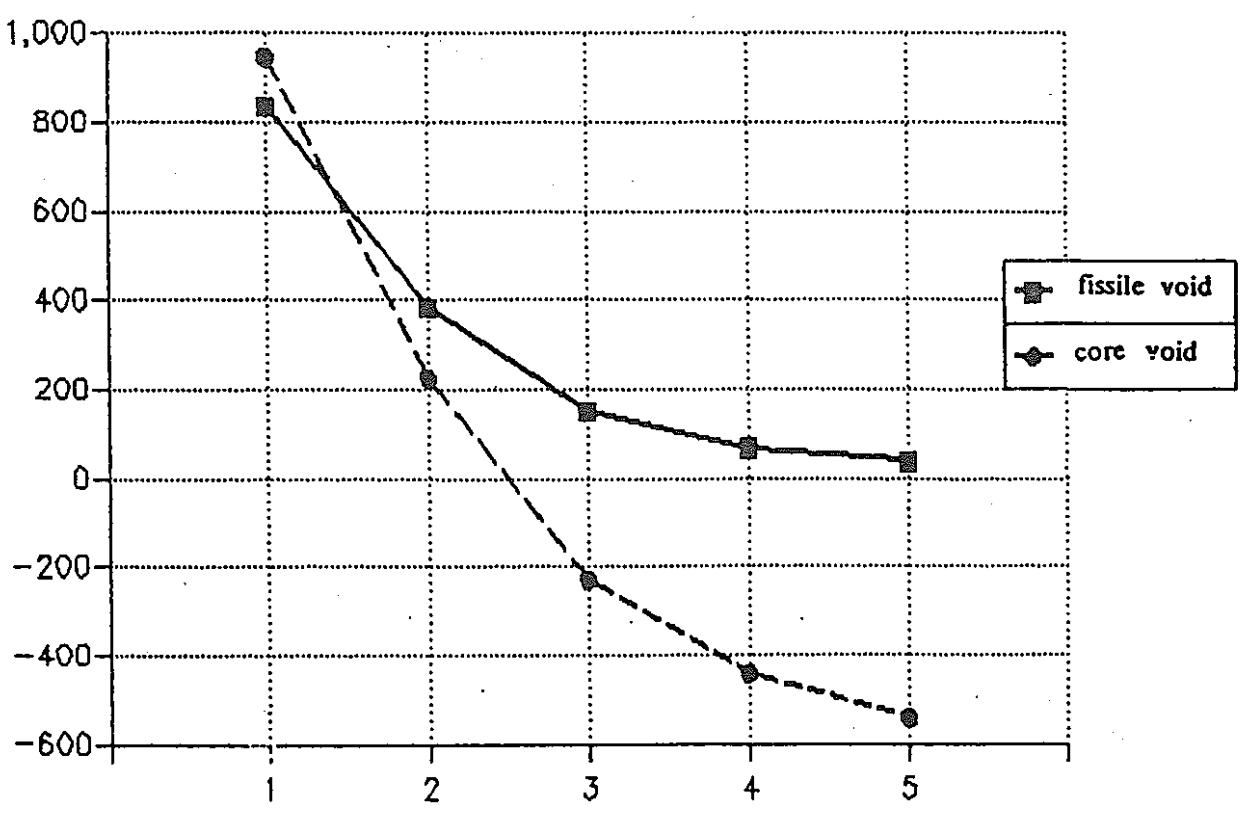
However, breeding gain during operating fuel cycle has been preferred in that study, and so three rows of fertile / absorber / fertile assemblies have been chosen for the optimized modular core.

table 4 coupling optimization

|                                         | core reactivity pcm | voiding effect for<br>the fissile zone (pcm) | voiding effect for<br>the total core (pcm) |
|-----------------------------------------|---------------------|----------------------------------------------|--------------------------------------------|
| 3 rows of fertile (G.E)                 | 4300                | 150                                          | -230                                       |
| fertile/stainless steel/fertile         | 4570                | 210                                          | 50                                         |
| fertile/absorber/fertile                | 3340                | -40                                          | -740                                       |
| stainless steel/absorber/stainless stee | 1 3580              | -90                                          | -1460                                      |
| 3 rows of sodium                        | 9170                | 750                                          | -6250                                      |
| 1 row of absorber                       | 480                 | -340                                         | -990                                       |

figure 4





rows of internal blanket assemblies

## 7. Modular island cores

An example of a modular island core created with seven modules of 150 MWe (see figure and table 2), surrounded by three rows of fertile / absorber / fertile assemblies, is given in figure and table 5.

That reactor has an electric power of 1050 MWe.

However the core size is quite good.

Sodium voiding reactivities for the fuel zones and for the whole core seem very promizing. But, to conclude with the safety of that modular core when voiding sodium, a balance with the new Doppler coefficient value has to be made.

A supplementary study illustrating the difficulty of power control in modular island cores has been made with the General Electric design: two radial sections of linear power rating (in S direction - see figure 1 - and in the maximum flux plane) has been drawn for two different rod insertions (see figure 6 and the diagram below).

When criticality is obtained with rod insertions of 44.7 cm for the seven modules, the linear power in the inner module exceeds 1600 W/cm, whereas it is below 300 W/cm in the outer modules.

However, very slight rod movements restore the linear power equilibrium at 500 W/cm for the seven modules.

It is why very deep attention must be brought to the high power sensitivity in case of slight assymetries in the control rod insertions, which could be a negative characteristic of modular cores.

That kind of core, by its modular aspect, could also lead to a better approach of actinide recycling, with:

- \* high neutron spectra and significant flux levels in the modules and especially the inner one.
- \* the use of the non-fissile zones surrounding the modules.

figure 5
the 1050 MWe reactor

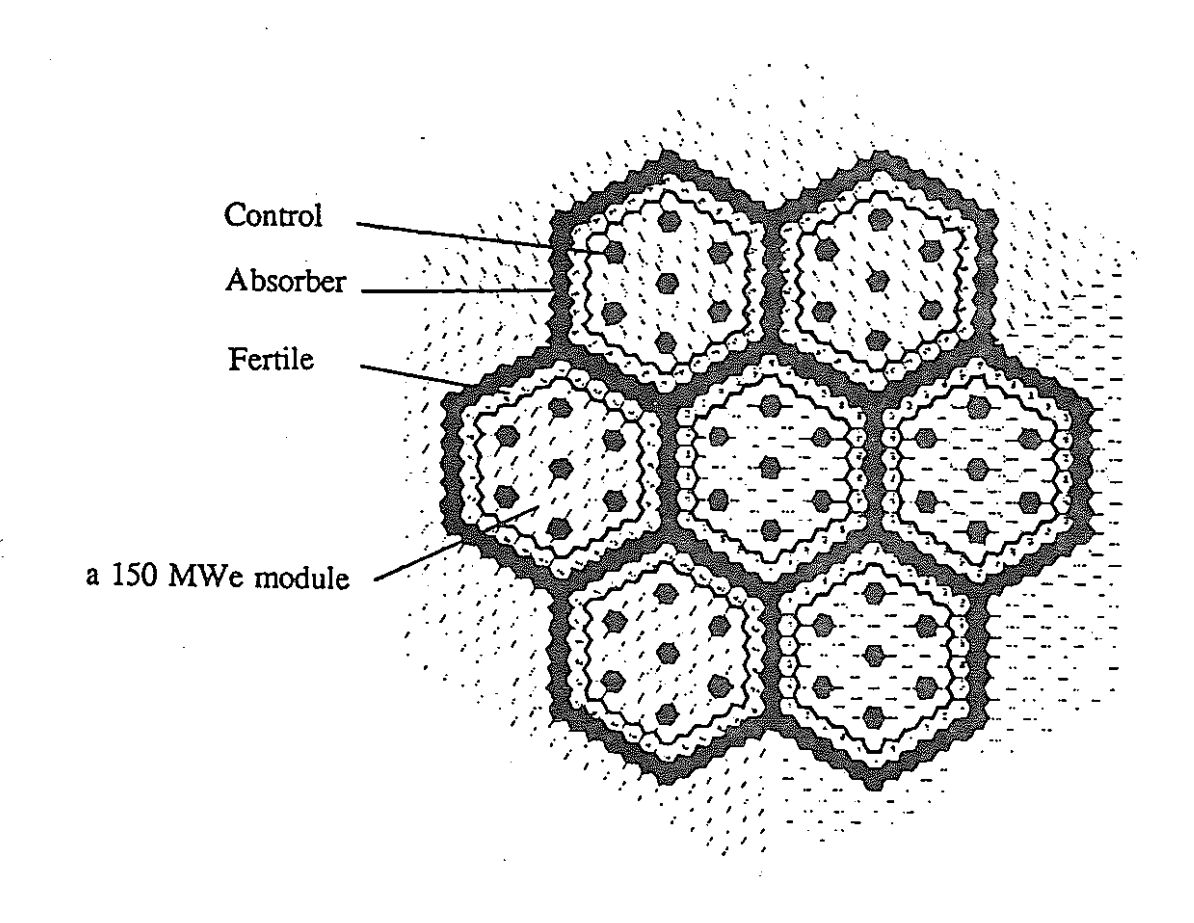
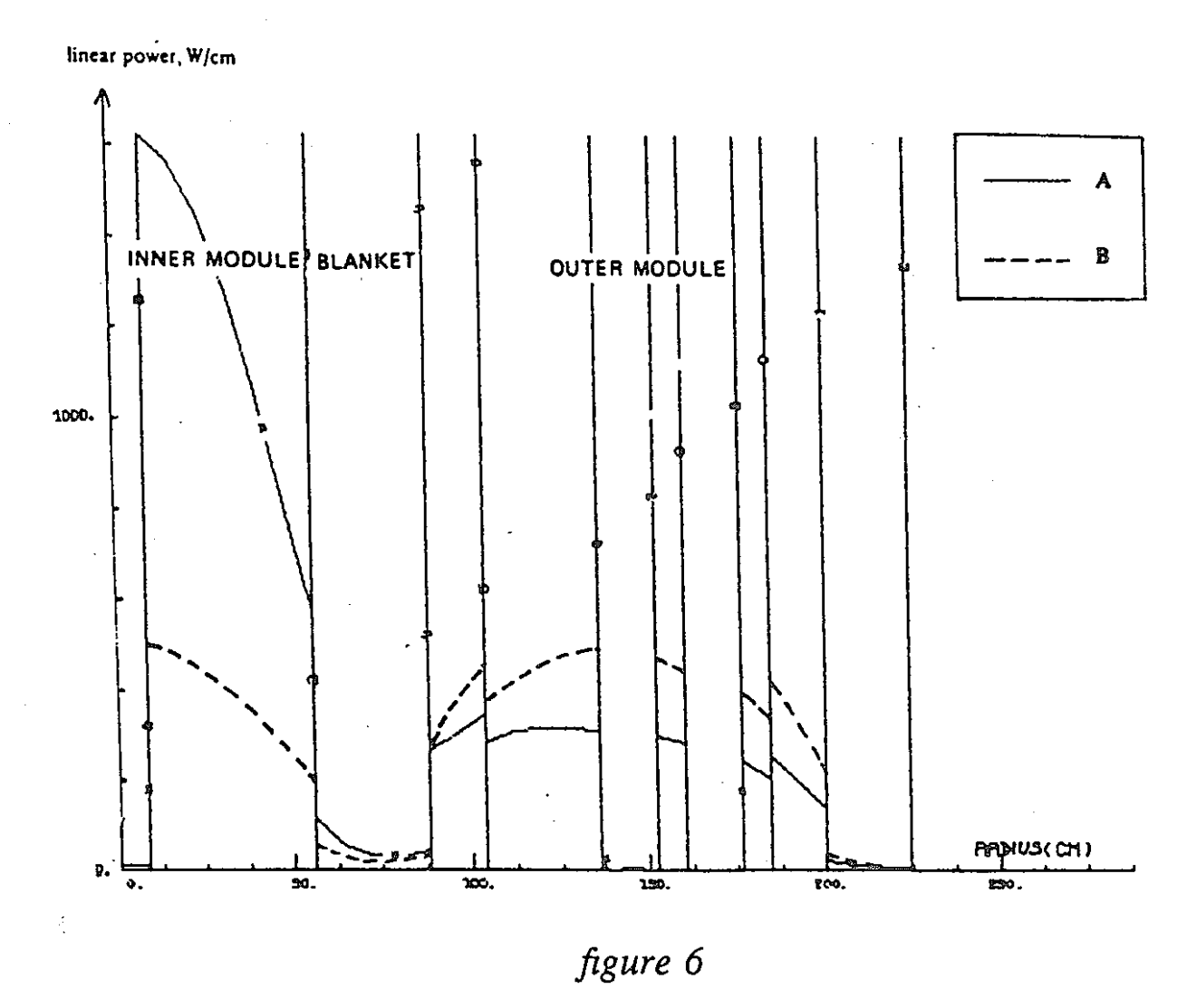


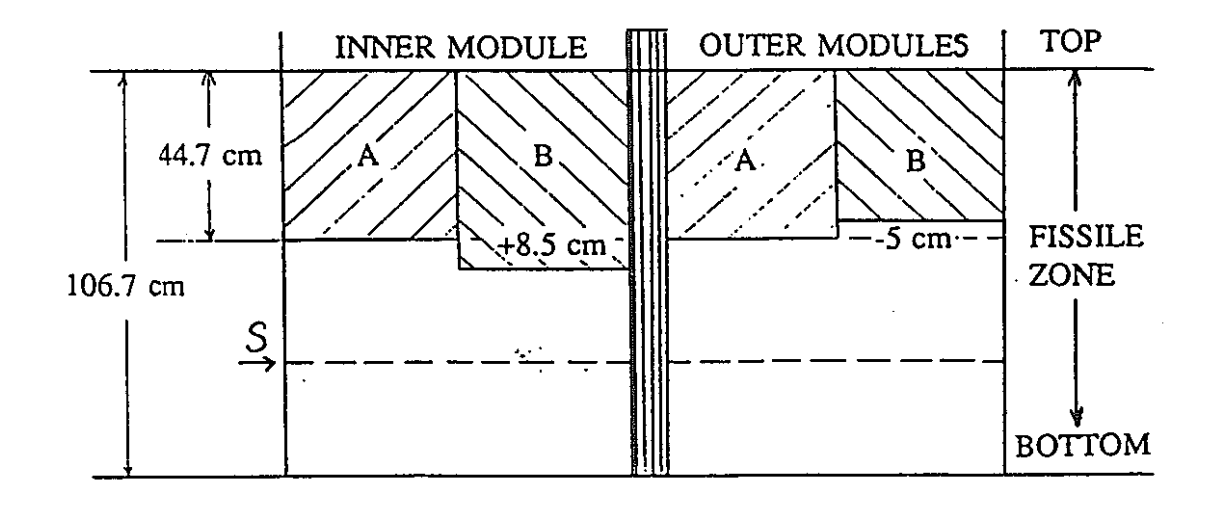
table 5
the 1050 MWe reactor

| reactor thermal power          | -    | 2695  |
|--------------------------------|------|-------|
| number of modules              |      | 7     |
| (150 MWe each)                 |      |       |
| refueling intervals            | days | 730   |
| capacity factor                |      | 0.7   |
| maximum fuel zone radius       | cm   | 185   |
| fuel zone height               | cm   | 100   |
| assembly channel pitch         | cm   | 12.8  |
| enrichments                    | -    |       |
| (not recalculated values)      |      |       |
| zone 1                         | %    | 22.5  |
| zone 2                         | %    | 37.4  |
| core reactivity                |      |       |
| at the beginning of cycle      |      |       |
| ->control rod in high position | pcm  | 11110 |
| ->control rod in low position  | pcm  | -3420 |
| sodium voiding effect          |      |       |
| at the beginning of cycle      |      |       |
| ->total                        | pcm  | -40   |
| ->fissile zone only            | pcm  | 540   |



Control of the power distribution for two different rod insertions:

- A criticality obtained with rod insertions of 44.7 cm for the seven modules.
- B criticality obtained with rod insertions of 53.2 cm for the inner module, and of 39.7 cm for the six outer modules.



### 7. Conclusion

The modular core concept can give a good compromise between safety and economics.

Near-zero values of sodium voiding reactivity effect can be reached, while thermal power, discharche burnup and vessel size keep competitive values.

Such low values of sodium voiding reactivity are achieved, thanks to high neutron leakage from the modules, and therefore to the detriment of the reactivity level.

The power control during the operating fuel cycle could also be problematic.

Coupling optimization has given two interesting solutions: three rows of stainless steel / absorber / stainless steel assemblies or fertile / absorber / fertile assemblies depending on whether recycling costs or breeding gains are preferred.

Some complementary studies are needed in order to estimate burnup fractions, damage doses and breeding gains after operating cycle.

The problem of actinide recycling in modular cores is set out.

# References

- Sodium voiding reactivity effect. Reduction in fast breeder reactors. J Tommasi. NEACRP. 1990.
- Nuclear performance of liquid-metal fast breeder reactors to preclude energetic hypothetical core disruptive accident. H.S.Bailey and Y.S.Lu of General Electric Company. Nuclear Technology article (volume 44, page 76). February 1979.

Study on Enhanced Safety Core Characteristics of Nitride Fuel FBR
Y.Ohkubo and T.Wakabayashi

Power Reactor and Nuclear Fuel Development Corporation

Japan

#### Abstract

In order to enhance FBR safety, core characteristics of nitride fuel have been investigated. A safety map relative to sodium void reactivity has been made for ULOF to make clear the core characteristics expected to prevent CDA. Parametric survey calculations for various core specifications have been performed and a 1000MWe nitride fuel core with core height 40cm has been chosen as enhanced safety core. It has been found that the nitride fuel core can make the sodium void reactivity small while keeping high core performances.

#### I. Introduction

In a view of FBR safety, it is recognized that following improvements of core characteristics are needed;

- (1) Reduction of the sodium void reactivity at the coolant boiling or babble passing through the core.(1)(2)(3)
- (2) Reduction of the burn up reactivity swing in order to suppress the reactivity insertion at anticipated withdrawal of control rods.

Nitride fuels have high heavy metal density and high thermal conductivity, and it seems to be able to design cores with nitride fuels having low burn up reactivity and low sodium void reactivity because of their high breeding ratios and high linear heat rates leading to the small core size.

The nitride fuel is considered to be one of attractive FBR fuels in future owing to its good core characteristics and thermal performances.

In this study, a development of nitride fuel core is focused on enhancement of its safety aspects. The transient calculations have been performed parametrically to clarify the expected core characteristics of sodium void reactivity and doppler coefficient. The parametric calculations have also been performed to survey core specifications satisfying the expected values described above.

From these calculations, a core concept of nitride fuel FBR has been selected from a point of view of core safety, and the core characteristics have been investigated and compared with a mixed oxide fuel core.

## II. A safety map for ULOF

Although several sequences leading to CDA (Core Disruptive Accidents) are considered, it is recognized that ATWS (Anticipated Transient Without Scram) is a most important event.

In this study, we pay attention to ATWS, especially to ULOF (Unprotected Loss Of Flow) in order to investigate core characteristics that are effective to prevent CDA.

A safety map regard to sodium void reactivity and doppler coefficient has been made by parametric calculations of transients. It shows a region of which the reactivity inserted in transient is less than that of a given value. We set the following condition of making the safety map;

"The net insertion reactivity in transient is less than 1\$"

In order to prevent CDA, it must be avoided that fuels and claddings get damages, and no fuel melting conditions can not be attained without a suitable negative sodium void reactivity so far as a large amount of coolant flow not supplied in ULOF. The safety condition described above is a minimum essential of not to reach the prompt critical before the melting of core materials occurs.

By setting the condition that the net insertion reactivity is less than 1\$ in transient, it can be expected that the negative reactivity feedback effects by structural characteristics around the core such as control rod drive line thermal expansions, fuel subassembly radial thermal expansions, and core support plate thermal expansions etc. suppress the power excursions in timely.(4)(5)(6)

We choose a 1000MWe nitride fuel core with core height 60cm as a reference core. The specifications of the reference core are shown in

Table 1. The transient calculations have been performed for various sodium void reactivities and doppler coefficients with respect to the reference nitride fuel core.

Figure 1 shows the safety map for ULOF. The shaded region of this figure corresponds to the region of which the net insertion reactivity in transient is less than 1\$.

The sodium void reactivity and the doppler coefficient of the reference core are 1.08%∆k/k and -7.4×10-3Tdk/dT respectively. In order to improve safety characteristics of the reference core, it has been proved that the sodium void reactivity must have been reduced to 60% of that of the reference core.

### III. Parameter survey of core characteristics

The core characteristics calculations for various specifications such as H/D's, fuel materials, core configurations, and reactor powers have been performed to investigate the possibilities of reduction of sodium void reactivity and burn up reactivity.

The calculation cases are shown in Table 2. The evaluated core characteristics are sodium void reactivity, doppler coefficient, burn up reactivity, and breeding ratio. The results are also shown in Table 2.

The results are summarized as follows;

#### (1) Core height (H/D)

The calculations have been performed for the nitride fuel cores with core height 40cm, 60cm (reference core), and 100cm. The decreasing of core height is very effective to reduce the sodium void reactivity. It is found that the sodium void reactivity can be reduced to 0.51%Δk/k by adoption of core height 40cm, and it corresponds to 50% of the value of the reference core.

## (2) Fuel materials

The sodium void reactivity of the nitride fuel core with core height 100cm is found to be less than that of oxide fuel core with same core height. The one of reason is owing to that the nitride fuel core is small than the oxide core in the radial dimension. In addition to this reason, the following reason is considered. The sodium void reactivities shown in Table 2 are evaluated at BOC. The inner core power of the nitride

fuel at BOC is lower than that of oxide fuel because of its high internal conversion ratio, and it might be thought the reason that the sodium void reactivity of the nitride fuel core is less than that of the oxide fuel core.

The effects on core characteristics of addition of TRU have also been investigated. TRU has been added in the outer core with 10w/o. The additions of TRU lead to low burn up reactivity, but they result in increasing sodium void reactivity because of their hard neutron spectra.

## (3) Core configuration

The comparisons of core characteristics have been made between the homogeneous core and the axially heterogeneous core with nitride fuel. The axially heterogeneous core has the advantage of reducing the sodium void reactivity due to existence of the inner blanket.

## (4) Reactor power

The core characteristics of 1000MWe and 300MWe nitride fuel cores have been calculated. The sodium void reactivity can be substantially reduced with small cores. The 300MWe nitride fuel core with core height 30cm can make the sodium void reactivity less than zero.

## IV. Consideration of external reactivity

We have selected the 1000MWe nitride fuel core with core height 40cm as a enhanced safety core. The sodium void reactivity of this core is 0.51% \( \Delta k/k \), and it does not result in prompt critical so far as no fuel and cladding melting. However, the fuel integrity of this core is not actually guaranteed unless some external negative reactivity insertions during transient..

Considerations have been made to estimate the amount of external negative reactivity insertion necessary to keep the fuel pin integrity. Once the coolant boiling occurs it is so difficult to avoid the fuel and cladding melting, that the prevention of coolant boiling is adequate to the condition of keeping fuel integrity.

In order to avoid fuel pins get damages, it strongly depends on thermal and structural characteristics of the plant system in addition to the core characteristics. In this study, the amount of external reactivity necessary to avoid coolant boiling has been estimated relative to core flows by static analyses of temperature distributions after transients. By comparing the differences between the initial temperature distributions and that of attainable power levels with core flows in stable states, it can be obtained reactivities compensating the values that will be inserted up to reaching stable power levels.

The external reactivity insertions to prevent coolant boiling for the enhanced safety core with nitride fuels evaluated by analyses described above are shown in Figure 2. Figure 2 shows the correlations between the core flows by natural convections or pony motors and the necessary reactivities inserted externally to prevent the coolant boiling for the hottest pin, the nominal hottest pin and the nominal pin. The hottest pin means the pin of maximum temperature with uncertainties. The nominal hottest pin and the nominal pin correspond to the pin of maximum temperature and the pin of average temperature without uncertainties respectively.

It has been found that the coolant boiling of the nominal hottest pin can be prevented with the external reactivity of 70¢ within 10sec by control rod drive line expansions and fuel assemblies radial expansions and so on, as far as the 5% of core flow can be secured.

#### V. Conclusion

Nitride fuel cores have been investigated in view of safety enhancement. The safety map relative to the sodium void reactivity and the doppler coefficient has been made for ULOF in the condition that the net insertion reactivity during transients is less than 1\$. From the survey of various core specifications, the 1000MWe nitride fuel core with core height 40cm has been chosen as enhanced safety core.

It has been found that the enhanced safety nitride fuel core can make the net reactivity insertion during transient less than 1\$ while keeping the burn up reactivity same as that of oxide fuel core with core height 100cm. The breeding ratio of the nitride fuel core can be increased in 0.3 than that of the oxide fuel core.

It has been proved to be able to design the enhanced safety core by using the nitride fuel without decreasing core performances.

#### References

- (1) M. Martini, M. Salvatores CEN / CADARACHE NEACRP-A-988 "Analysis of the Possibility to Reduce Sodium Void Reactivity Worth in Large Fast Breeder Reactors", September, 1989
- (2) R.N. Hill, H.S. Khalil, ANL, NEACRP-A-1005
  "An Evaluation of LMR Design Options for Reduction of Sodium Void Worth", September, 1989
- (3) Alekseev P.N, et. al. NEACRP-A-1014

  "Feasibility of Nonpositive Void Reactivity Effect in the Fast Sodium Reactors of Enhanced Self-Protection", September, 1989
- (4) NUREG-1368 PRISM Draft Safety Evaluation Report
- (5) A. Gouriou et. al., "The dynamic behavior of the Super-phenix reactor under unprotected transient", July., 1982, Lyon Conf.
- (6) P. Bergeonneau et. al., "Comparative studies of feed-back effects in Rapsodie, Phenix and Super-phenix", 1986, Guernsey Conf.

Table 1 Specifications of nitride fuel reference core

| Parameter                          |         | Spec.       |
|------------------------------------|---------|-------------|
| Electric power                     | (MWe)   | 1000        |
| Thermal power                      | (MWt)   | 2600        |
| Core configuration                 |         | Homogeneous |
| Reactor inlet/outlet temperature   | (°C)    | 375 / 530   |
| Core height                        | (mm)    | 600         |
| Axial blanket length (upper/lower) | (mm)    | 300/300     |
| Fuel pin diameter                  | (mm)    | 8.5         |
| Cladding thickness                 | (mm)    | 0.4         |
| Fuel pellet diameter               | (mm)    | 7.28        |
| Smear density                      | (%TD)   | 85          |
| Spacer wire diameter               | (mm)    | 1.5         |
| Number of fuel pins per subassemb  | oly (-) | 271         |

Table 2 Core performance of various core specifications

| Electric power (MWe)                  |           | 1000              |          |             |               |                 |                    | 300       |
|---------------------------------------|-----------|-------------------|----------|-------------|---------------|-----------------|--------------------|-----------|
| Core configuration                    |           | Homo              |          |             |               |                 | Axially<br>Hetero. | Homo      |
| Fuel type                             |           | Nitride           |          | Oxide       | Oxide<br>+TRU | Nitride<br>+TRU | Nitride            | Nitride   |
| Core height (cm)                      | 40        | 60<br>(Reference) | 100      | 100         | 100           | 40              | 60                 | 30        |
| Inner core diameter(cm)               | 293       | 239               | 185      | 254         | . 254         | 293             | IB = 239           | 185       |
| Outer core diameter(cm)               | · 417     | 340               | 263      | 362         | 362           | 417             | Core=340           | 263       |
| Pu enrichment (in/out) (wt%)          | 17.5/22.2 | 12.94/17.52       | 9.1/14.6 | 16.35/19.60 | 16.1/20.1     | 17.1/19.1       | 18.5               | 20.9/30.8 |
| Na void reactivity<br>(%Ak/k)' (BOC)' | 0.51      | 1.08              | 1.72     | 2.30        | 2.85          | 1.34            | 0.84               | -0.01     |
| Doppler coefficient<br>(×10-3Tdk/dT)  | -4.8      | -7.4              | -10.2    | -8.6        | -7.0          | -4.5            | -6.6               | -3.1      |
| Burn up reactivity<br>(%Δk/k)         | 3.4       | 1.5               | -1.3     | 3.3         | 2.6           | 1.6             | 1.2                | 3.9       |
| Breeding ratio                        | 1.4       | 1.5               | 1.7      | 1.1         | 1.2           | 1.6             | 1.5                | 1.3       |



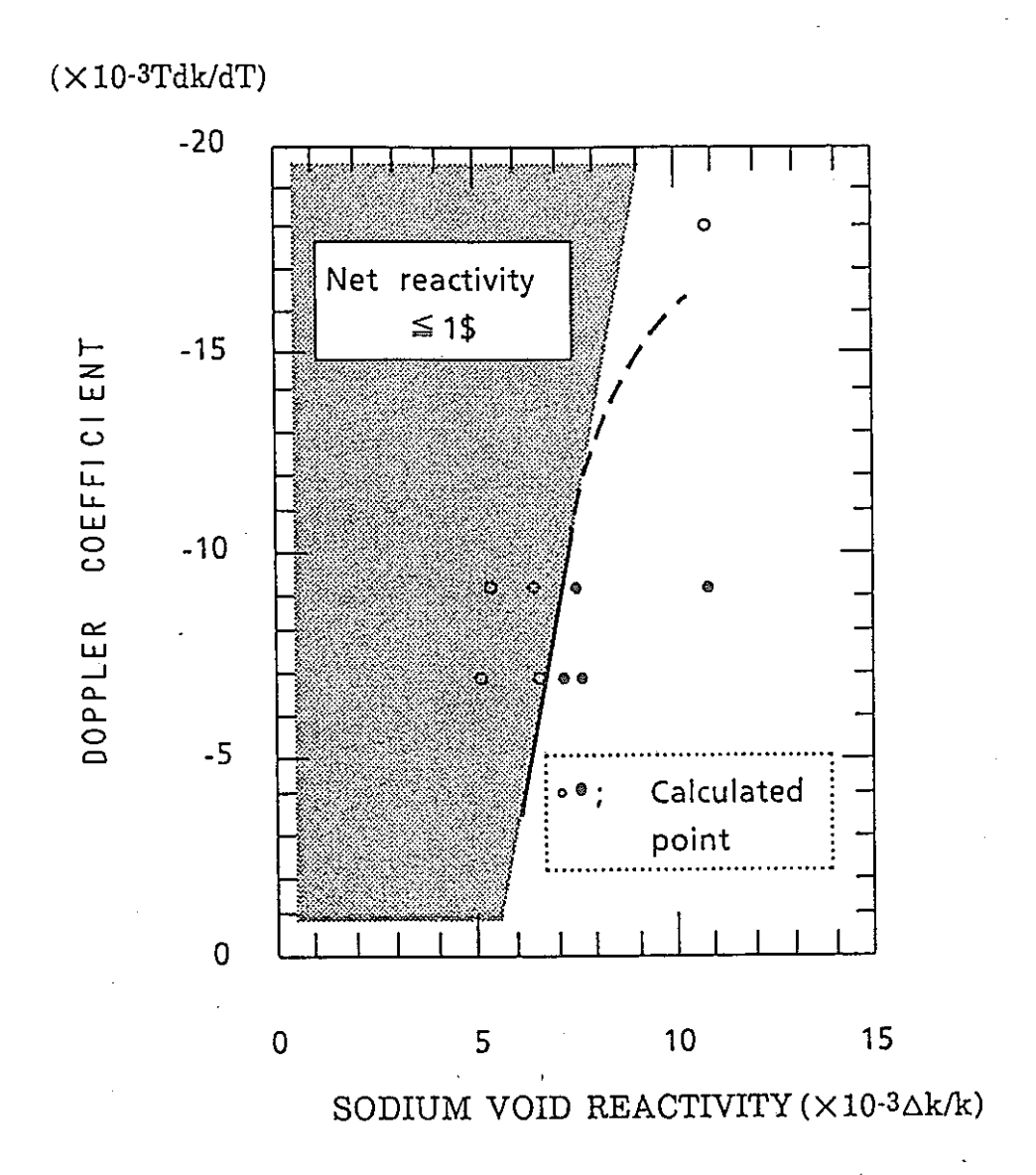


Figure 1 Safety map for ULOF

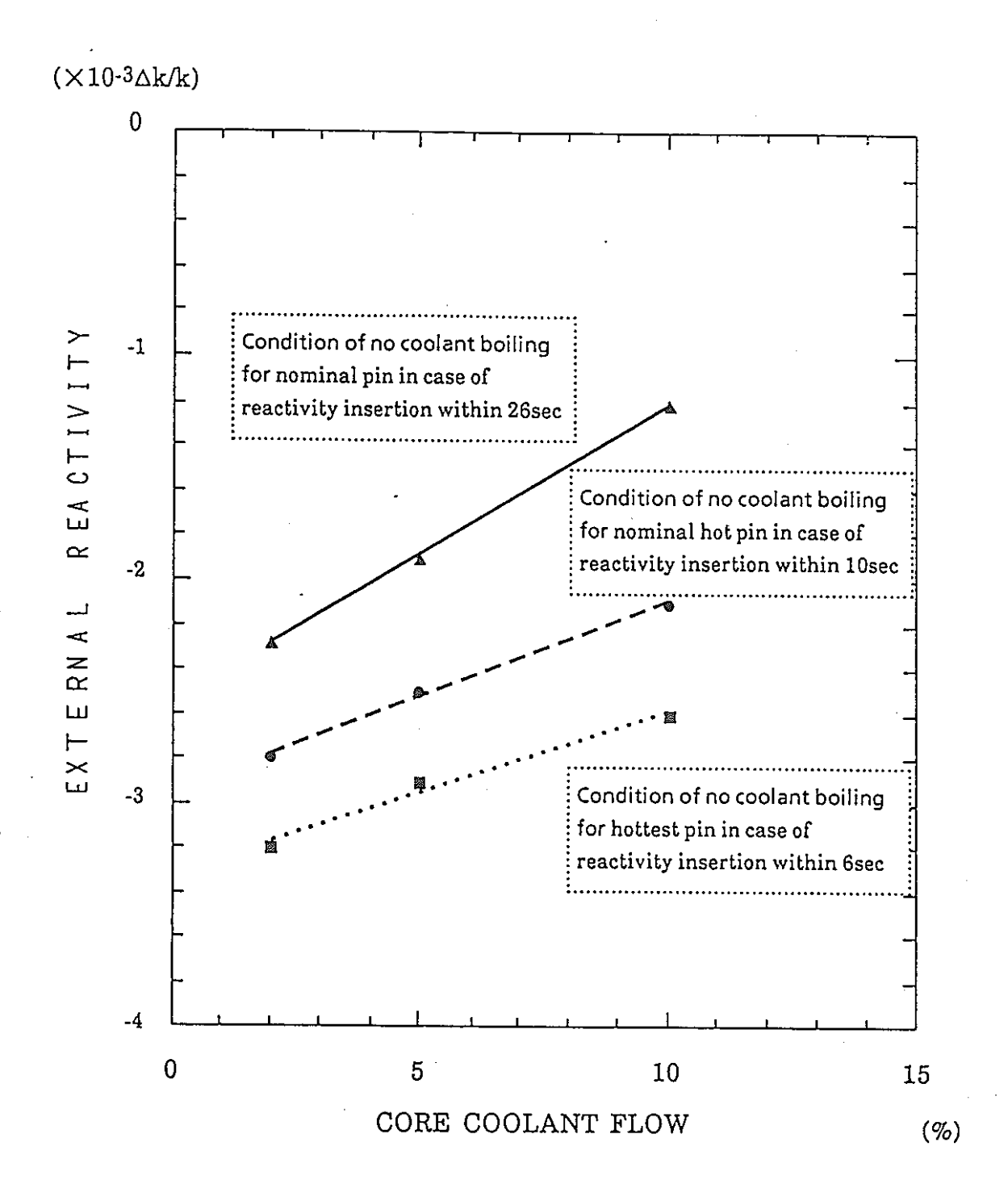


Figure 2 External reactivity necessary to prevent coolant boiling with respect to the coolant flow of natural convection or a pony motor. (ULOF)

NEACRP-A-1086 /-3

# A MEASUREMENT-BASED METHOD FOR PREDICTING MARGINS AND UNCERTAINATIES FOR UNPROTECTED ACCIDENTS IN THE INTEGRAL FAST REACTOR

R. B. Vilim

Argonne National Laboratory 9700 S. Cass Avenue Argonne, IL 670439



# GOAL

- o To Develop a Means for Verifying that the Reactivity
  Feedbacks that Ensure Passively Safe Characteristics in
  a Metal Fueled LMR are in Place in the As-Built Plant
- o Why?
  - Credit will be Taken in Safety Analysis for Inherently Safe Characteristics
- o Constraints
  - Measurement-Based
  - Unobtrusive
  - Periodic
  - Treatment of Uncertainties

## THE METHOD

- o Classify Unprotected Accidents According to Boundary
  Conditions Presented at the Core
  - Primary Flowrate
  - Inlet Temperature
  - External Reactivity
- o Perturb these Boundary Conditions Using Pseudo Random Binary Signals
- o Deduce a Model for Core Behaviour from Measurements
- o Predict Unprotected Accident Response by Driving Model with Appropriate Core Boundary Conditions

# **ALGORITHM STEPS**

# 1. Model Order Determination

Linear Stochastic System Framework

$$\delta \underline{x}(k+1) = \overline{\phi}(k) \delta \underline{x}(k) + \Theta(k) \delta \underline{u}(k) + \Omega(k)\underline{\xi}_{\underline{u}}(k) + \underline{\xi}_{\underline{x}}(k)$$

$$\delta \underline{y}(k) = C(k) \delta \underline{x}(k) + D(k) \delta \underline{u}(k) + E(k) \underline{\xi}_{\underline{u}}(k) + \underline{n}(k)$$

Akaike's Criterion

$$\min_{\underline{\alpha}} \min_{\mathbf{M}} \mathsf{AIC}(\underline{\alpha}, m)$$

$$AIC(\alpha,m) = -2 \ln f(x|\alpha,m) + 2 \dim (\alpha)$$

## 2. Model Parameter Estimation

- Non-Linear Stochastic System Framework

$$\underline{x}(k+1) = f_{\underline{d}}[\underline{x}(k), \underline{u}(k), \underline{\xi}_{u}(k)] + \underline{\xi}_{x}(k)$$

$$\underline{y}(k) = \underline{g}[\underline{x}(k), \underline{u}(k), \underline{\xi}_{n}(k)] + \underline{\eta}(k)$$

- Maximize Likelihood Function

$$\ln f[\delta \underline{y}_{m}(1), \dots, \delta \underline{y}_{m}(n)] =$$

$$-\frac{1}{2} \sum_{k=1}^{n} [\delta \underline{r}_{m}(k)^{T} \Sigma (k|k-1)^{-1} \delta \underline{r}_{m}(k) +$$

r 
$$\ln 2\pi + \ln |\det \Sigma(k|k-1)|$$

# ALGORITHM STEPS (CONTINUED)

- 3. Model Validity Test
  - Test for Whiteness of Measurement Residuals

$$R(1) = \frac{1}{N-1} \sum_{k=1}^{N-1} \tilde{\underline{r}} (k) \tilde{\underline{r}} (k+1)^{T}$$

$$\frac{|R(1)^*_{ij}^{-\mu}_{R(1)}^{-\mu}|}{\sigma_{R(1)}^{\sigma_{R(1)}}} < 3$$

4. Uncertainty Prediction

$$\underline{x}(k+1) = f[\underline{x}(k), \underline{u}(k), \underline{\xi}_{u}(k)] + \underline{\xi}_{x}(k)$$

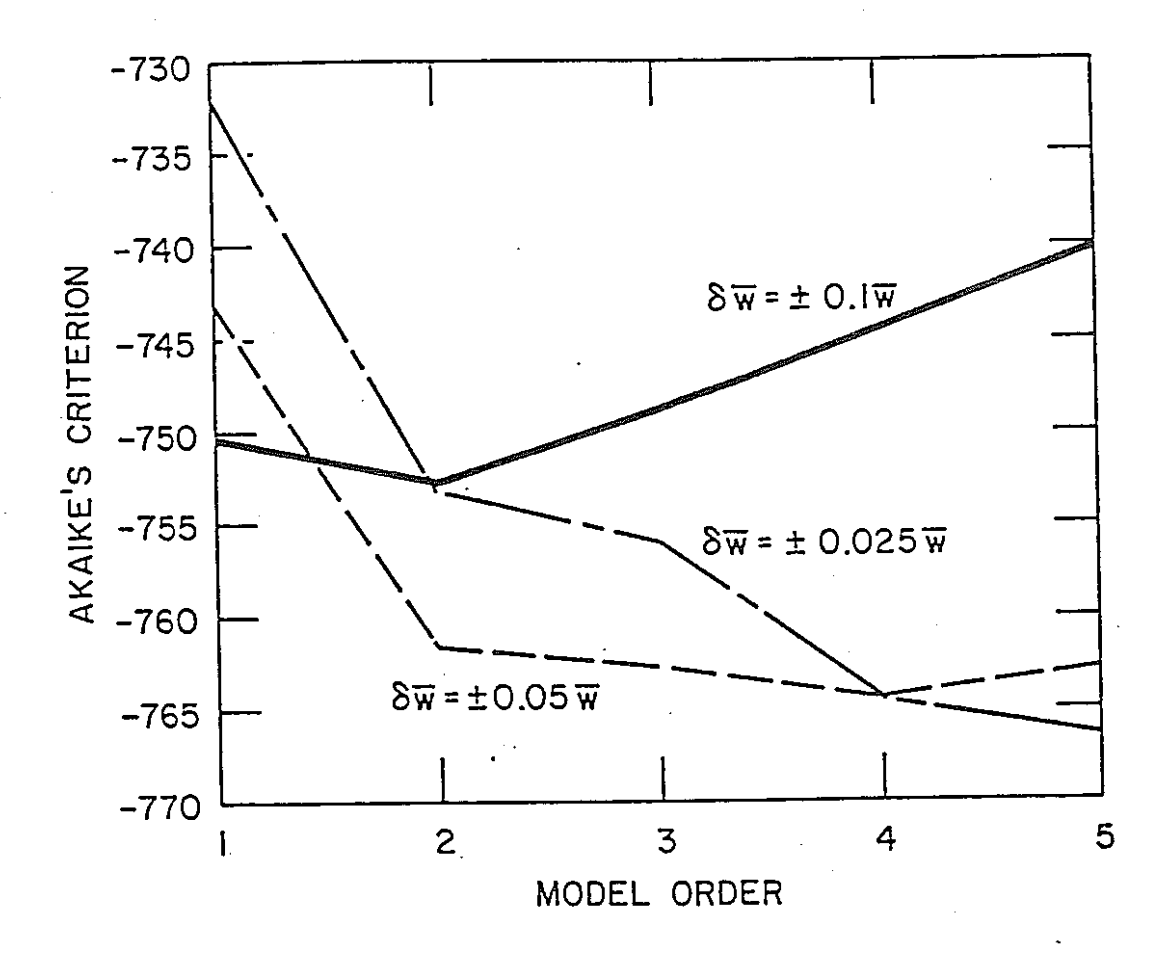
$$\underline{z}(k) = \underline{g}[\underline{x}(k), \underline{u}(k), \underline{\xi}_{u}(k)]$$

$$\underline{z}(k) \sim N[\underline{\nu}(k), \Sigma(k|k-1)]$$

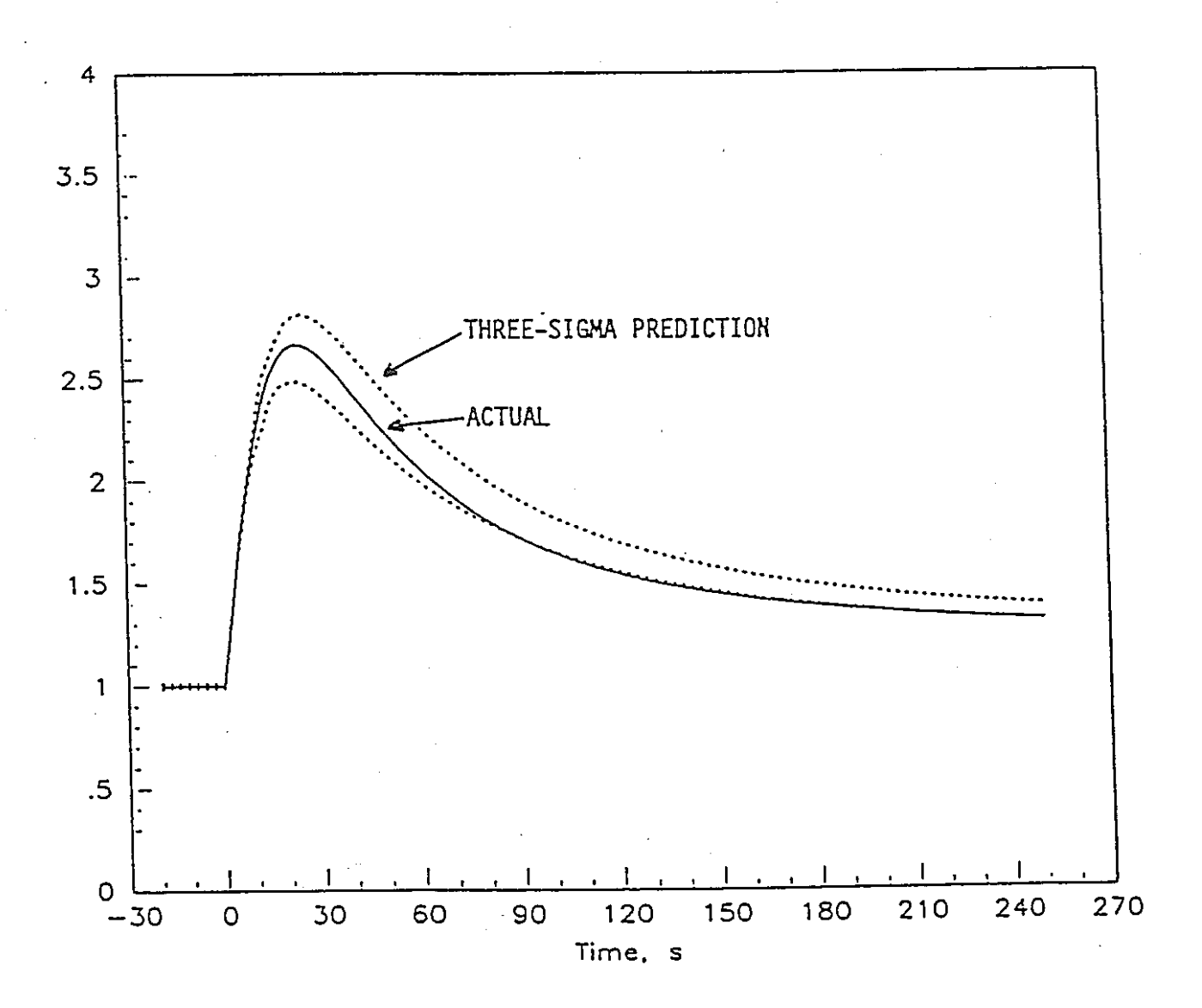
# **TEST PROBLEM**

- o Description
  - EBR-II Core
  - Primary Flowrate Forcing Function
- Use Simple Model to Generate Measured Data
  - Point Kinetics
  - One Group Neutron Precursor
  - Lumped Parameter Control Rod
- o Predict Core Response for Unprotected Loss of Flow

# RESULTS OF MODEL ORDER DETERMINATION



# RESULTS OF UNCERTAINTY PREDICTION



# **FUTURE WORK**

- o Method Works Well for Simulations Performed to Date
- o More Detailed Simulations are Underway Using the SASSYS Code
- o Method Will be Tested in EBR-II

NEACRP-A-1086 1.3

Paper to be presented at the ANS 1990 Fast Reactor Safety Meeting, Snowbird, Utah, August 12-16, 1990.

A MEASUREMENT-BASED METHOD FOR PREDICTING MARGINS AND UNCERTAINTIES FOR UNPROTECTED ACCIDENTS IN THE INTEGRAL FAST REACTOR CONCEPT\*

bу

R. B. Vilim

Argonne National Laboratory 9700 S. Cass Avenue Argonne, IL 60439

The submitted manuscript has been authored by a contractor of the U. S. Government under contract No. W-31-109-ENG-38. Accordingly, the U. S. Government retains a nonexclusive, royalty-free license to publish or recroduce the published form of this contribution, or allow others to do so, for U. S. Government purposes.

<sup>\*</sup>Work supported by the U.S. Department of Energy, Nuclear Energy Programs under contract W-31-109-ENG-38.

A MEASUREMENT-BASED METHOD FOR PREDICTING
MARGINS AND UNCERTAINTIES FOR UNPROTECTED ACCIDENTS
IN THE INTEGRAL FAST REACTOR CONCEPT

#### R. B. Vilim

Argonne National Laboratory Argonne, Illinois 60439, U.S.A.

#### ABSTRACT

A measurement-based method for predicting the response of an LMR core to unprotected accidents has been developed. The method processes plant measurements taken at normal operation to generate a stochastic model for the core dynamics. This model can be used to predict three sigma confidence intervals for the core temperature and power response. Preliminary numerical simulations performed for EBR-II appear promising.

#### INTRODUCTION

If the economic and safety benefits of an inherent shutdown capability in the Integral Fast Reactor (IFR) concept are to be realized, then the concept of passive safety, and the associated risk reduction, must be incorporated in the plant probabilistic risk assessment. In order to claim passive safety, however, it must be shown that sufficient inherent feedback mechanisms for safe shutdown are present in the plant as built. The only way to demonstrate this is to routinely perform dynamic tests on the plant. An analogous situation exists in light water plants. Tests are periodically performed to verify that the Engineered Safety Systems meet design requirements. These tests are mandated by the Technical Specifications upon which the reactor has been licensed.

The goal is to show that the required shutdown capability is in place. To do so, periodic and unobtrusive testing of plant dynamics will be performed. The plant measurements from these tests will be processed to yield a dynamic model that comprises a measured basis upon which the response to unprotected accidents will be predicted. If the response is within safety limits, then it will be concluded that the mechanisms for safe shutdown are in place.

Other approaches exist for predicting the response of the core<sup>1,2</sup> but they do not make use of current measurements and as a result suffer two shortcomings. First, estimates for uncertainty magnitudes made without consideration for current operating data will always be larger than those obtained by direct measurement. Since the core rating must be decreased as

the uncertainty increases, an economic penalty is imposed. In principle, the minimum uncertainty levels for the method proposed in this paper depend only on measurement noise levels. Second, a direct confirmation of model validity requires that the identified model be compared against current measurements and that the goodness of the fit be consistent with the statistical properties of the identified model. This comparison can be done only if current measurements are available.

While the preferred form of the identified model is one developed from measured data without regard to model structure, some structure beyond that of a transfer function is required to handle nonlinearities. A linear model simply cannot represent core behavior during a rapid loss of flow.

In addition to the requirement for a measurement-based approach and the need for some nonlinear model structure, there are other factors that influence the type of scheme used to generate the model. First, experience at EBR-II<sup>3,4</sup> indicates that neither process noise in the core nor rod drop tests provide sufficient excitation energy to identify dynamic behavior. Test signals in the form of perturbations to reactor flowrate, rod position and inlet temperature will have to be introduced. Second, to be practical from an operations standpoint, this excitation must take place at normal power. Third, measurement noise and its effect on the uncertainty of the model prediction must be explicitly dealt with. Finally, a statistical test is required to verify that the identified model of the core dynamics is consistent with the measurements.

This paper describes a methodology developed to meet these goals. The methodology is a synthesis of existing methods and an extension of others.

#### MODEL EQUATIONS

The system to be identified is in general composed of three elements: sensors, actuators and process hardware. The behavior of each element is governed by the conservation laws, and these laws are normally represented in lumped parameter form. The system equations then take the form

$$\frac{d}{dt}x(t) - f_c[x(t), u(t)] \tag{1}$$

and

$$Y(t) - g[X(t), u(t)]$$

where

 $\underline{x}(t) = n \times 1$  state vector,

 $\underline{u}(t) = \mathbf{m} \times 1$  input vector,

 $\underline{\mathbf{y}}(t) - \mathbf{r} \times \mathbf{1}$  output vector.

The stochastic or random components of the plant behavior are assumed superimposed on the deterministic model of Eq. (1). This equation is transformed to discrete-time form and augmented with the random vectors  $\underline{\xi}_u(k)$ ,  $\underline{\xi}_x(k)$  and  $\underline{n}(k)$  to give

$$\chi(k+1) = f_d[\chi(k), \mu(k), \xi_u(k)] + \xi_{\chi}(k)$$
 (2)

and

$$\underline{y}(k) = \underline{g}[\underline{x}(k),\underline{u}(k),\underline{\xi}_{\underline{u}}(k)] + \underline{n}(k).$$

where k denotes the sample time.

#### METHODOLOGY

The methodology is sufficiently general that it can be used to determine a probabilistic model for any system whose underlying basis is a set of ordinary differential equations.

A prudent first step is to determine the minimum model order necessary to describe the plant. The model order that best describes the measured data is determined using Akaike's minimum information criterion (AIC). The criterion is used as follows. For order one we identify at the full power operating point, a discrete-time linear canonical stochastic model. The maximum of the likelihood function is a by-product and we use this to calculate AIC. This procedure is repeated for orders 2,3,... until the minimum AIC is found. The model associated with the minimum AIC is, according to Akaike, the one that best describes the data at the operating point.

The model order, and time constants which are output in the above step, and a knowledge of the underlying physics are used to hypothesize a model structure whose parameter values are to be estimated. The only constraint on the form of the structure is that it can be written in the form of Eq. (2). In addition to  $\underline{u}(k)$  representing a forcing function, it can also be used to represent a model parameter. For example, if the ith element of  $\underline{u}(k)$  is to represent the deterministic parameter  $\alpha_d$ , then  $\underline{u}(k)_i - \alpha_d$  and  $\operatorname{Var}[\underline{\xi}_u(k)_i] = 0$  in Eq. (2). Alternatively, if the ith element of  $\underline{u}(k)$  is to represent the stochastic parameter  $\alpha_s$ , then  $\underline{u}(k)_i - \mathrm{E}[\alpha_s]$  and  $\operatorname{Var}[\underline{\xi}_u(k)_i] = \operatorname{Var}[\alpha_s]$ . The symbols E and Var denote expected value and variance, respectively.

The parameter values sought are those that maximize the logarithm of the likelihood function of Eq. (2).

$$\max_{\alpha} \ln f[\underline{y}_{n}(1), \dots, \underline{y}_{n}(n) | \underline{\alpha}]$$
(3)

where the dependence on the parameters  $\underline{\alpha}$  has been written explicitly.

If the plant output measurements are  $\underline{v}_n(1)$ , ...,  $\underline{v}_n(n)$ , then

$$\ln f[\underline{y}_{m}(1), \dots, \underline{y}_{m}(n)] \tag{4}$$

$$= -\frac{1}{2} \sum_{k=1}^{n} \left[ r_{m}(k)^{T} \sum_{k=1}^{n} (k|k-1)^{-1} r_{m}(k) + r \ln 2n + \ln |\det \sum_{k=1}^{n} (k|k-1)| \right]$$

where

$$\mathcal{I}_{m}(k) - \mathcal{Y}_{m}(k) - g\left[\hat{x}(k|k-1), \underline{u}(k), 0\right]$$

and where  $\Sigma(k|k-1)$  is the covariance matrix of the measurement residual and  $\mathcal{L}(k|k-1)$  is the Kalman filter state estimate.

As a necessary condition for the model to be declared valid, we require that the statistical properties of the identified model be consistent with the measured data. A reasonable test is to check to see that the measurement residuals are white as they should be. This can be done by computing the covariance of measurement residuals displaced in time and looking to see that

$$E[\chi(k) \chi(k+1)^{T}] = 0, 1 \neq 0.$$
 (5)

The test for measurement residual whiteness used in this paper is that of Peterson. He proposes the matrix

$$R(1) = \frac{1}{N-1} \sum_{k=1}^{N-1} \tilde{I}(k) \tilde{I}(k+1)^{T}$$
(6)

where

$$\tilde{I}(k) - \sum (k|k-1)^{-1/2} I(k)$$
 (7)

as a measurement of the covariance between residuals. The statistical properties of R(1) were, however, not given by him so they were derived independently as part of this work.

The validity test is as follows. The values of the elements of R(1) are computed from plant measurements  $\underline{y}_{m}(1)$ , ...,  $\underline{y}_{m}(N)$  using Eq. (6) to give

$$R(1)_{ij}$$
\* = value of  $R(1)_{ij}$  computed using plant measurements  $\underline{y}_a(1), \ldots, \underline{y}_a(N)$ .

Now if Eq. (2) is a valid representation of the plant and if the errors introduced by the linearization are small, then  $R(1)_{ij}$  must be consistent with the statistical properties of  $R(1)_{ij}$ . To be specific, if the identified model given by Eq. (2) is a valid representation of the measurements  $\underline{y}_n(1)$ , ...,  $\underline{y}_n(N)$ , then for f defined to be the fraction of R(1)\* elements for which

$$\frac{|R(1)_{ij}^* - \mu_{R(1)_{ij}}|}{\sigma_{R(1)_{ij}}} < 3$$
 (8)

we must have f > 0.995 where  $\mu$  denotes the mean and  $\sigma$  the standard deviation.

The identified model can be used to predict the uncertainty in the plant response for a given input forcing function. The state variables  $\underline{x}(k)$  and the outputs  $\underline{y}(k)$  in Eq. (2) correspond to temperatures and powers that are of interest from a safety standpoint. Further, these quantities are random variables whose statistics can be calculated. However, in Eq. (2),  $\underline{y}(k)$  is a sensor signal which includes the effect of sensor noise. We are more interested in predicting the process variable itself, not the noise corrupted version output by the sensor. The more appropriate form of Eq. (2) for prediction is

$$x(k+1) = f_d[x(k), u(k), \xi_u(k)] + \xi_x(k)$$
(9)

and

$$z(k) - g[x(k), u(k), \xi_u(k)]$$

where the output measurement noise term, n(k), has been dropped.

#### APPLICATION

The methodology was evaluated by processing simulated measurements generated for the EBR-II reactor. This approach provides a starting point for the eventual demonstration of the methodology at the EBR-II plant using real data.

The results presented here considered only the effect of primary flowrate on reactor behavior. The effect of external reactivity and inlet temperature are to be studied in future work.

The simulation model used in this example while relatively simple -- it consists of the point kinetics equation with one precursor and the prompt jump approximation and a lumped parameter equation for the control rod -- predicts the core power behavior observed in EBR-II flow coastdown tests quite well. The solution for quasi-static changes in flow depends on a parameter  $\alpha_{\rm qs}$ , a function of all reactivity feedbacks. The solution for more rapid changes depends on the additional parameters  $\alpha_{\rm dl}$ , the one-group

neutron precursor half-life,  $\alpha_{d2}$ , a function of all reactivity feedbacks except the control rods, and  $\alpha_{d3}$ , the control rod temperature time constant.

Measurement data were generated by adding white noise to reactor power and primary flow obtained from a noise-free simulation.

#### Quasi-Static Identification

A slowly varying transient in which some parameters do not affect the quasi-static plant response presents an opportunity to identify a subset of parameters. In turn, the task of identifying the remaining parameters through a fast transient is made easier. Specifically, if flow is varied in a quasi-static manner, then the parameters  $\alpha_{d1}$ ,  $\alpha_{d2}$ , and  $\alpha_{d3}$  do not affect the power. This leaves the expected value of  $\alpha_{qs}$ , the variance of  $\alpha_{qs}$ , the variance of the measured power,  $\eta_{\bar{p}}(k)$ , to be identified. The state equation errors  $\xi_{\bar{p}}(k)$  and  $\xi_{T_{ca}}(k)$  are set to zero for the present.

A quasi-static transient was initiated by ramping flowrate from 100 to 85 percent and back again over a period of one hour. Simulated measurements were generated by adding white noise to the flowrate forcing function and to the calculated reactor power.

The parameter values identified from the quasi-static transient simulated measurements are shown in Table I. As seen in the table, the "initial" values used to start the parameter search algorithm are a factor of two different from the "actual" values used to generate the simulated measurements.

#### Model Order Identification

A determination of model order was made by perturbing the plant at full power and processing the measurements using Akaike's criterion. The input signal consisted of a pseudo-random binary sequence superimposed on the full power primary flowrate. The AIC criterion is plotted as a function of model order in Fig. 2. The results indicate that flow perturbations of at least five percent but no more than ten percent are needed to correctly determine the model order. Further, the system is very nearly first order which is consistent with the fact that the control rod feedback coefficient is small.

Based on the above findings, flowrate perturbations of five percent and a system order of one were determined as appropriate for performing dynamic identification. One concludes that the effect of the control rod on plant dynamic behaviour is minor.

#### Dynamic Identification

Identification was performed for the first order system obtained by setting the control rod driveline time constant to zero. In doing so we find the parameters  $\alpha_{d2}$  and  $\alpha_{d3}$  assume fixed values in the problem.

We are left with a reduced set of parameters to be estimated and these are listed in Table II.

This first order system was identified using simulated measurement data generated from the second order model. The input signal consisted of the signal in the quasi-static case with a plus and minus five percent pseudo-random binary signal superimposed on this.

The parameter values identified are shown in Table II.

Test for Model Validity

The validity test given by Eq. (8) was applied to the identified model. The model passed the test.

#### Prediction Uncertainty

The validated model was used to predict the response of the core to an unprotected loss of flow accident. A hyperbolic flow decay with a halving time of five seconds was used and is typical of a flow coastdown in EBR-II following a loss of electric power to the primary pumps.

The results of the uncertainty prediction are shown in Fig. 2. The solid line is the power-to-flow ratio given by the model used to generate simulated measurements throughout this work. The two dotted lines show the three-sigma confidence level of the identified model. As it should, the identified model prediction envelopes the response of the model that was used to generate the simulated measurements.

#### SUMMARY AND FUTURE WORK

A method was developed to obtain a probabilistic model for the dynamic behavior of a reactor core from measurements made at normal operation. The method tests initially for the dynamic order of the plant. Time constants are then determined once the order is known. From a knowledge of time constants and the underlying physics, one develops a stochastic model structure to describe the plant. The parameter values in this structure are then selected to maximize the likelihood that the model produced the measured data. A validity test is then used to check for statistical consistency between model and measurements. The model once validated can be used to predict three-sigma core response uncertainty levels for different forcing functions.

It is envisioned that this capability will be used to predict the response of an as-built IFR core to unprotected accidents. This capability will be required if credit for a passive shutdown capability is to be taken in the plant probabilistic risk assessment. Measurements will be gathered in an unobtrusive manner and on a periodic basis. The resulting model will be driven by core boundary conditions -- primary flowrate, reactor inlet temperature and external reactivity -- corresponding to five classes of

unprotected accidents: loss of flow, loss of heat sink, rod withdrawal, primary pump overspeed and chilled core inlet temperature. The three-sigma confidence levels generated by the model will then be compared against cladding eutectic, sodium boiling and fuel melting safety limits. If the predicted response is within safety limits, then it will be concluded that the mechanisms for safe shutdown are in place.

The method was evaluated by processing simulated measurements from the EBR-II reactor. Although the simulation model is relatively simple, it predicts the core behavior observed in EBR-II tests quite well. The method appears very promising. The model order test proved effective for determining the minimum signal-to-noise ratio required, for determining the actual system order and for determining an appropriate model order. In particular, pseudo-random binary signals of ten percent peak-to-peak superimposed on full power flowrate proved sufficient for identifying core dynamics.

Future work will be directed toward eventual demonstration in EBR-II. The next step will be to generate new simulated measurements using the more detailed models in the SASSYS code. A more detailed investigation of the effect of the input signal's energy spectrum and time duration on the uncertainty in the identified model will be made. In addition to including primary flowrate as a forcing function as was done in this report, inlet temperature and external reactivity will also be examined.

#### REFERENCES

- 1. R. S. MAY, J. M. SORENSON and R. E. ENGEL, "Probabilistic Methods for Evaluating Operational Transient Margins and Uncertainties," <u>Nuclear Science and Engineering</u>, 103, 81-93 (1989).
- C. J. MUELLER and D. C. WADE, "Probabilities of Successful Inherent Shutdown of Unprotected Transients in Innovative Liquid Metal Reactors," <u>Proc. Int. Topical Meeting Safety of Next Generation Power</u> <u>Reactors</u>, Seattle, Washington, May 1-5, 1988, p. 704, American Nuclear Society (1988).
- D. D. EBERT, "An Inherent Noise Analysis Investigation on the Experimental Breeder Reactor II," <u>Nuclear Science and Engineering</u>, <u>55</u>, 470 (1974).
- 4. A. J. FOLTMAN, "Limitations of EBR-II Rod-Drop Tests and Proposed Improvements Using Frequency-Response Testing," <u>Proceedings Second Power Plant Dynamics</u>. Control. Testing Symposium, Knoxville, Tennessee (1975).
- 5. H. AKAIKE, "A New Look at The Statistical Model Identification," <u>IEEE Transactions on Automatic Control</u>, Vol. AC-19, No. 6 (1974).
- D. W. PETERSON, "Residual Processes for Model Validation and Bad-Data Detection," unpublished data, Massachusetts Institute of Tech. (1976).

TABLE I. Parameters Identified from Quasi-Static Transient

| Identification | Parameter                          | Parameter Values       |                             |                        |  |  |  |  |
|----------------|------------------------------------|------------------------|-----------------------------|------------------------|--|--|--|--|
| Methods        |                                    |                        | Initial                     |                        |  |  |  |  |
|                |                                    | Actual                 | Guess                       | Identified             |  |  |  |  |
| A Priori       | $Var[\xi_{\overline{u}}(k)]^{1/2}$ | 5.000×10 <sup>-3</sup> | <b>-</b>                    | 5.000×10 <sup>-3</sup> |  |  |  |  |
| Least squares  | $E[\alpha_{qs}(k)]$                | 8.000                  | 8.000×2.0                   | 7.517                  |  |  |  |  |
| Maximum        | $Var[lpha_{qs}]^{1/2}$             | 0                      | 8.000×0.5                   | 3.989                  |  |  |  |  |
| Likelihood     | $Var[n_p(k)]^{1/2}$                | 5.000×10 <sup>-3</sup> | 5.000×10 <sup>-3</sup> ×2.0 | 4.926×10 <sup>-3</sup> |  |  |  |  |

TABLE II. Parameters Identified from Dynamic Transient

| Identification | Parameter                                           | Parameter Values       |                           |                        |  |  |  |  |
|----------------|-----------------------------------------------------|------------------------|---------------------------|------------------------|--|--|--|--|
| Methods        |                                                     |                        | Initial                   |                        |  |  |  |  |
|                |                                                     | Actual                 | Guess                     | Identified             |  |  |  |  |
| Least squares  | $E[\alpha_{d1}(k)]$                                 | 3.000×10 <sup>-3</sup> | 3.000×10 <sup>-3</sup> ×2 | 2.903×10 <sup>-3</sup> |  |  |  |  |
| Maximum        | $Var[\alpha_{d1}(k)]^{1/2}$                         | <b>O</b>               | 3.000×10 <sup>-3</sup>    | 1.175×10 <sup>-7</sup> |  |  |  |  |
| Likelihood     | $Var[\xi_{\overline{p}}(k)]^{1/2}$                  | 0                      | 0.010                     | 0.000                  |  |  |  |  |
|                | $Var[\xi_{p}(k)]^{1/2}$ $Var[\alpha_{qs}(k)]^{1/2}$ | 0                      | 8.000×0.5                 | 1.136                  |  |  |  |  |

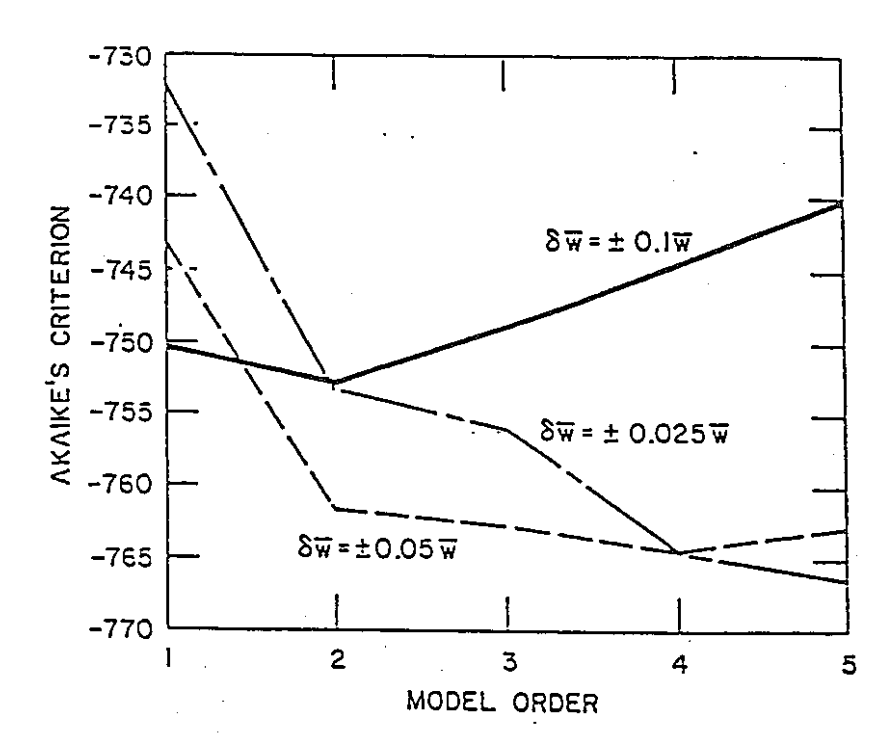


Fig. 1. Akaike's Criterion as a Function of Primary Flowrate Perturbation Magnitude.

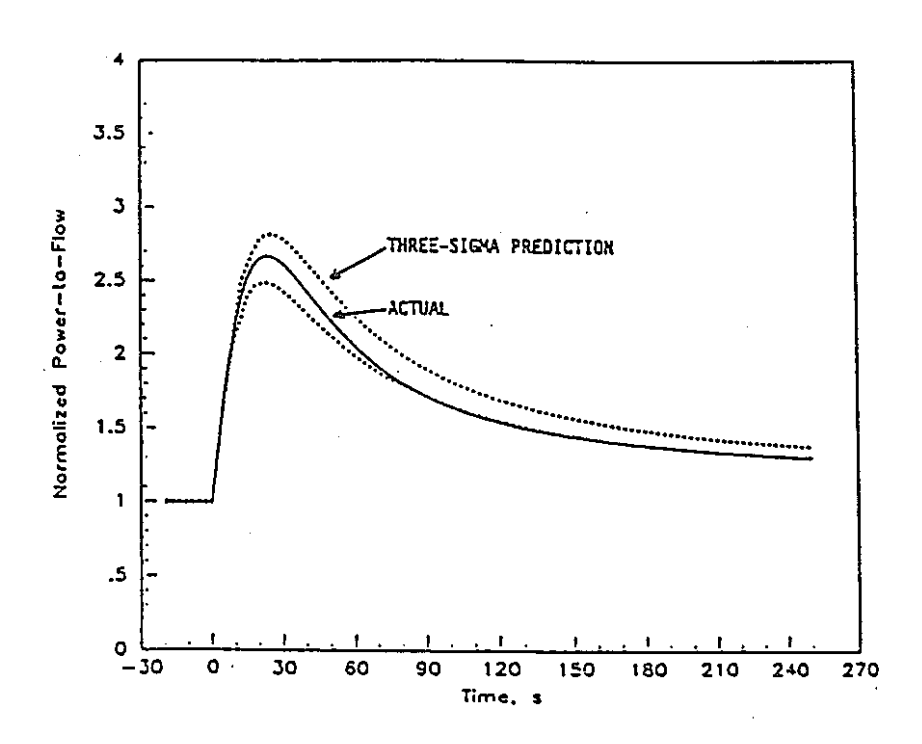


Fig. 2. Three-Sigma Power-to-Flow Uncertainty Prediction for Flow Coastdown.

NEACRP-A-1441 Session B13

SENSITIVITIES TO NUCLEAR CONSTANTS AND RELATED CALCULATIONAL ERRORS IN SAFETY CHARACTERISTICS OF FAST REACTORS WITH DIFFERENT COOLANTS

G.G.KULIKOV, V.B.GLEBOV - Moscow Engineering Physics Institute

A.G.MOROZOV - I.V.Kurchatov Institute of Atomic Energy, Moscow, USSR

The purpose of the investigations performed was to determine safety parameters sensitivity coefficients to nuclear constants, to evaluate calculational errors due to uncertainty in nuclear data, to analyze the components of the errors. Sensitivity S of reactor characteristic F to nuclear constant & was determined in a standard way as

 $S = \frac{\partial F}{\partial \lambda} \cdot \frac{\partial}{F} \tag{1}$ 

The advanced reactors considered include fast sodium reactor BN-1600 [1], steam-water cooled power reactor SWPR [2] and lead-cooled natural convection reactor RB-EZ [3]. MOX fuel was used for BN-1600 and SWPR, while UN - for RB-EZ; stainless steel was structural material for all reactors considered. In burnup calculations the chain used included <sup>235</sup>U, <sup>238</sup>U, <sup>239</sup>Pu, <sup>240</sup>Pu, <sup>241</sup>Pu, <sup>242</sup>Pu. Fission products were simulated by single effective nuclide.

The parameters in study included: effective multiplication factors in nominal ( $K_{ef}^{nom}$ ) and voided ( $K_{ef}^{void}$ ) states of the reactor; void effect of reactivity (VER) determined as:

$$VER = 1/K_{ef}^{nom} - 1/K_{ef}^{void};$$
 (2)

dopler effect determined as

$$DER = 1/K (600°K)-1/K(1500/1100°K),$$
 (3)

where 1100°K was for SWPR;  $K_{ef}$  at burnup of 3% h.a.  $(K_{ef}(\mathcal{T}))$ ; corresponding reactivity change due to burnup determined as

$$RC = 1/K_{ef}(0) - 1/K_{ef}(7)$$
 (4)

The method used takes into account time dependence of fluxnuclide reactor field and is based on generalized perturbation theory [4]. As is shown in [4], sensitivity S may be split to components:

$$S = F + Fl + P + N, \qquad (5)$$

where F is responsible for functional, Fl - for flux, P - for power, N - for nuclide. These components simulate the contributions to sensitivity from functional changes, neutron flux changes, power to flux ratio changes and nuclide concentration changes correspondingly. The method described is implemented in SENS code for multigroup diffusion calculations in homogeneous media. Space structure of the reactor is taken into account by specially elaborated collapsing procedure involving nuclear data and nuclide concentrations reduction [5]. It was shown that reduction using value weight function  $(\Phi^+)$  radically improves sensitivities calculation accuracy. The reduction model sensitivities differ from those obtained in full-scale calculations not more than by 5% (for reactors considered).

The constant supply used was ABBN-78 [6], and it included corresponding covariation mattrices of constant errors.

Main results are presented in Tables 1 and 2.

As is seen from the results of calculations, the main error in functionals is due to uncertainties in generation and absorption constants of heavy nuclides. In the voided states the contribution of "high-energy" processes increases ( $\mathcal{E}_{f}, \mathcal{E}_{in}, \mathcal{X}$ ), while that of resonance capture decreases. With burnup the sensitivities to fission and capture constants decrease by 20-30% and 50-60% correspondingly. This is due to appearance of nuclide component N(5), opposite in sign to the main functional component F. Fl and P components are least important. An essential contribution of in-

elastic scattering on Pb should be noted.

Results of Table 2 are based on sensitivities of reactivity characteristics  $S_{\mathrm{px}}$ :

$$S_{px} = (K_{ef}S' - K'_{ef}S)/(K'_{ef} - K_{ef}), \qquad (7)$$

where  $K_{ef}$ , S are for unperturbated state and  $K_{ef}^{'}$ , S' are for perturbated state. It is evident that the value and sign of  $S_{pX}$  are determined by those of the corresponding reactivity effect  $K_{ef}^{'} - K_{ef}$  that may vary essentially under slight changes in calculational model of the reactor. It especially concernes VER. However, the contributions of processes to error (like the value of error itself) are conservative if measured in  $K_{ef}$  units.

Main contributions to VER error come from inelastic scattering on coolant. The exception is SWPR, where the hydrogen cross sections are known quite accurately. Then, essential contributions are from  $\frac{238}{6}$ U and  $\frac{239}{6}$ Pu that are most sensitive to spectrum "fastening".

DER error is mainly due to fission and capture of  $^{239}$ Pu and  $^{238}$ U. The major contribution to RC comes from  $\lambda_{\rm f}^{239}$ Pu,  $\lambda_{\rm c}^{238}$ U and  $\lambda_{\rm c}^{238}$ O of fission products that also determine reactor criticality. With this the sensitivity of RC to  $\lambda_{\rm f}^{239}$ Pu is determined by N-component (5) greatly, to  $\lambda_{\rm c}^{238}$ U - by N-component exclusively.

Table 3 presents results for effective delayed neutron fraction ( $\beta_{\rm ef}$ ) and neutron lifetime (1) calculations. As may be seen,  $\beta_{\rm ef}$  increases dramatically with increase in <sup>235</sup>U and <sup>241</sup>Pu contents.

Increase in neutron lifetime may be obtained with gaining of a more resonance-area-oriented type of neutron spectrum.

The main conclusions are:

<sup>1.</sup> Sensitivity calculations should be performed taking into account fuel burnup, as nuclide component contribution to sensitivity may reach 20-30% for  $K_{\rm ef}(\mathcal{T})$  and totally determines the sensitivity of RC;

- $^{2.K}_{\rm ef}$  error is essentially the same for all reactors in all states considered, it has a value of 2.0-2.4%  $\rm K_{\rm ef}.$  The exception is the error in  $\rm K_{\rm ef}^{\rm nom}$  for lead cooled RB-EZ that reaches 2.9%  $\rm K_{\rm ef}$  due to uncertainty in  $\rm \partial_{i}$  Pb. For  $\rm K_{\rm ef}$  error decrease  $\rm \partial_{f}^{239} \rm Pu$ ,  $\rm \partial_{f}^{235} \rm U$  and  $\rm \chi$  should be refined. In voided states the contribution of  $\rm \partial_{in}^{238} \rm U$  to  $\rm K_{\rm ef}$  error increases, with burnup so does the contribution of fission products.
- 3. DER and RC errors in reactors with  $\lesssim$  3% h.a. average burnup are 0.03-0.07%  $\rm K_{ef}$  and 0.18-0.28%  $\rm K_{ef}$  correspondingly. BN-1600 has smaller values of VER error  $\sim$  0.4%  $\rm K_{ef}$ ; for SWPR and RB-EZ VER errors are essential 1.15%  $\rm K_{ef}$  and 1.95%  $\rm K_{ef}$  correspondingly. In SWPR this is due to uncertainties in  $\rm \lambda_c^{238}U$  (31% contribution), in RB-EZ due to  $\rm \lambda_{in}$  PB (60% contribution).
- in RB-EZ due to  $\partial_{iN} PS$  (60% contribution).

  4. As a whole,  $\partial_{r}^{239}$ Pu,  $\partial_{r}^{235}$ U,  $\partial_{c}^{238}$ U,  $\partial_{c}^{238}$ U,  $\partial_{c}^{238}$ U,  $\partial_{iN}^{238}$ U,  $\partial_{iN}^{238}$ Na,  $\partial_{iN}^{238}$ Pb and  $\mathcal X$  should be refined within the used constant supply. Specific directions of refinement for a given functional can be driven from Tables 1,2.

#### REFERENCES

- Troyanov M.F., Rinejskii A.A. Status of Fast Reactor Activities in the USSR. - In: Status of National Programmes of Fast Breeder Reactors, 21 Annual Meeting in Seattle, USA, 9-12 May 1988, IAEA, Vienna, 1988, p. 102.
- Alekseev P.N., Grishanin E.I., Zverkov Yu.A. et al.
   Steam-Water Power Reactor Concept. Atomnaya Energya, v. 67, 1989, p. 239-243.
- Alekseev P.N. et al. High Safety Liquid Metal Advanced Reactor Concept. Atomnaya Energya, 1989, v. 66, issue 3, p. 155-158.
- 4. Takeda T., Umano T., Nucl. Sci. Eng., 1985, v. 91, p. 1-10.
- 5. Khromov V.V. et al. Method of Spatial Reactor Structure Reduction for Calculations of Reactor Functionals Sensitivities to Nuclear Data. Moscow, MIFI, 1990.
- 6. Abagyan L.P. et al. Group Constants for Reactor and Shield Calculations. Moscow: Energoatomizdat, 1981, 232p.

TABLE I Contributions of processes to  $K_{ef}$  error: up - the value of error due to uncertainty in constant (%  $K_{ef}$ ); down - sensitivity coefficient of  $K_{ef}$  to constant  $3(-10^{-3})$ 

| Reactor                |            | BN-1600                   |                     |                     | SWPR                    |                     | RB-EZ               |                      |                     |
|------------------------|------------|---------------------------|---------------------|---------------------|-------------------------|---------------------|---------------------|----------------------|---------------------|
| functional onstant     | Kef        | K <mark>void</mark><br>ef | K <sub>ef</sub> (て) | K <sup>nom</sup> ef | K <sup>void</sup><br>ef | K <sub>ef</sub> (で) | K <sup>nom</sup> Ev | oid<br>ef            | K <sub>ef</sub> (で) |
| 8, <sup>239</sup> Pu   | 27<br>418  | 27<br>424                 | 24<br>345           | 19<br>348           | 24<br>419               | 12<br>265           |                     | 28<br>486            | 17<br>372           |
| ک <sub>ر 235</sub> ں   | 21<br>652  | 22<br>656                 | 18<br>522           | 16<br>622           | 20<br>676               | 12<br>. 472         |                     | 20<br>694            | 9<br>510            |
| X                      | 18<br>1000 | 18<br>1000                | 24<br>1000          | 14<br>1000          | 14<br>1000              | 17<br>1000          |                     | 13<br>1000           | 18<br>1000          |
| პ <sup>238</sup> υ .   | 10<br>-206 | 10<br><b>–</b> 185        | 4<br><b>–1</b> 10   | 13<br>-231          | 10<br><b>–</b> 195      | 4<br>-115           |                     | 9<br>- <b>1</b> 51 - | 3<br>-92            |
| 238 <sub>U</sub><br>in | 7<br>-47   | 9<br><b>-</b> 54          | 7<br>-44            | 14<br>-63           | 21<br>83                | 17<br>62            | 4<br>-49 -          | 19<br>-84            | 3<br>-37            |
| in 208 <sub>Pb</sub>   |            | -                         | -                   | -                   | 644<br>645              | pro<br>em           | 27<br>-53           | <b>,</b>             | 30<br><b>-</b> 46   |
| dc fission products    | 2<br>18    | 1<br>-15                  | 3<br>-31            | 6<br>-34            | 1<br>-13                | 21<br><b>-</b> 56   | 3<br>-33 -          | 2<br>-20             | 9<br><b>~</b> 45    |
| total error, % Kef     | 2.2        | 2.2                       | 2.0                 | 2.3                 | 2.3                     | 2.1                 | 2.9                 | 2.4                  | 2.4                 |

TABLE 2 Contributions of processes to reactivity effects errors,%

| Reactor                                                             | BN-1600 |        |       | SWPR |      |       | R <b>B</b> –EZ |      |       |  |
|---------------------------------------------------------------------|---------|--------|-------|------|------|-------|----------------|------|-------|--|
| functional constant                                                 | VER     | DER    | RC    | VER  | DER  | RC    | VER            | DER  | RC    |  |
| Sin coolant                                                         | 31      | 1      | 0     |      |      | :     | 60             | 20   | 4     |  |
| ි <sub>c</sub> <sup>238</sup> U<br>∂ <sub>f</sub> <sup>239</sup> Pu | 12      | 3      | 39    | 33   | 23   | 33    | 2              |      | 40    |  |
| ბ f <sup>239</sup> Pu                                               | - 10    | 27     | 1.5   | 12   | 19   | 10    | 3              | 9    | 26    |  |
| ∂ <sub>f</sub> <sup>235</sup> U                                     | 9       | 18     | 10    | 15   | 13   | 7     | 4              | 5    | 13    |  |
| 3 in 238 <sub>U</sub>                                               | 5       | 11     | 0     | 4    | 23   |       | 14             | 7    | 3     |  |
| 6 products                                                          | 3       | 11     | 17    | 13   | 14   | 27    | 1              | 10   | 6     |  |
| Sel coolent                                                         | 5       | 8      |       |      |      |       | 7              | 44   | · . 2 |  |
| unctional error                                                     | 0.37    | . 0.04 | 0.18* | 1.15 | 0.07 | 0.26* | 1.95           | 0.03 | 0.28  |  |

per 1% h.a. of burnup

Sensitivities (·10<sup>-3</sup>) of  $\beta_{\rm ef}$  and 1 to reactor contents. Values of  $\beta_{\rm ef}$  and 1 (sec.-10<sup>-7</sup>)

| Reactor             | BN-16                 | 00           | SWPR                          |                 | RBEZ                          |            |  |
|---------------------|-----------------------|--------------|-------------------------------|-----------------|-------------------------------|------------|--|
| functional nuclide  | $\mathcal{S}_{	t ef}$ | 1            | $oldsymbol{eta}_{	exttt{ef}}$ | 1               | $oldsymbol{eta}_{	exttt{ef}}$ | 1.         |  |
| 235 <sub>U</sub>    | 30                    | -40          | 21                            | -24             | 18                            | -11        |  |
| 238 <sub>U</sub>    | 122                   | <b>-</b> 347 | 119                           | -300            | 152                           | -341       |  |
| 239 <sub>Pu</sub>   | -182                  | -884         | -183                          | -863            | -159                          | -884       |  |
| 240 <sub>Pu</sub>   | -62                   | -169         | -87                           | -222            | -40                           | -119       |  |
| 241 <sub>Pu</sub>   | 74                    | -172         | 54                            | <b>-1</b> 25    | 40                            | -61        |  |
| 242 <sub>Pu</sub>   | -4                    | -21          | <b>-</b> 5                    | -23             | -1                            | <b>-</b> 9 |  |
| O/N                 | -9                    | 275          | -16                           | 141             | 6                             | 142        |  |
| oolant              | -10                   | 145          | 24                            | 316             | <b>-</b> 79 .                 | 253        |  |
| ission products     | -10                   | -49          | -13                           | <b>-</b> 73 · . | -10                           | -58        |  |
| tructural materials | -54                   | 183          | -35                           | 74              | -14                           | 72         |  |
| alue                | 0.00341               | 4.29         | 0.00363                       | 5.22            | 0.00301                       | 5.26       |  |

セッション2.1

NEACRP-A-1089

#### PIN POWER AND DEPLETION OF EBR-II

W. S. Yang and R. D. McKnight

Argonne National Laboratory 9700 S. Cass Avenue Argonne, IL 67.0439



## Pin Power and Depletion of EBR-II W. S. Yang and R. D. McKnight

Motivated by the analysis needs resulting from the Integral Fast Reactor (IFR) fuel cycle demonstration and other advanced Fast Breeder Reactor (FBR) designs, a method for recovering detailed (pin-wise) information from coarse reactor representations has been developed for hexagonal-z geometry and implemented in a computer code RCT. This code, in conjunction with the REBUS-3 reactor burnup code, has been used to calculate in detail the depletion in EBR-II over a long series of runs. These calculations are being used to validate the REBUS/RCT fuel management methodology as adequate for the EBR-II/HFEF-S fuel cycle for both operational and material control and accountancy purposes. The development of these reconstruction methods was essential to the practical application of the REBUS methodology to the EBR-II fuel cycle.

#### Reconstruction of Pin Burnup Characteristics

Reconstruction methods have reached a high level of development for Light Water Reactors, and are becoming standard analysis tools because they extend the usefulness of computationally efficient nodal schemes and eliminate the need to perform fine-mesh computations. However, the existing reconstruction methods are not directly applicable to full-core FBR's because they have been designed for Cartesian geometry and macroscopic depletion calculations. Therefore, RCT has been developed to reconstruct the intra-nodal distributions of power density, burnup, nuclide densities, group fluxes, and fast and total fluences from nodal-diffusion/depletion calculations performed in hexagonal-z geometry using the REBUS-3/DIF3D Argonne code system.

The spatial reconstruction techniques in RCT are based on higher order polynomial expansions of the nuclide densities as well as the group fluxes. The intra-nodal pointwise group flux is approximated for each node assuming the flux within a node is separable in the hex-plane and axial directions. With this separability assumption, the axial flux distribution of a node is interpolated for each group by a cubic polynomial constrained to preserve the node-average flux, the top and bottom surface-average fluxes, and z-directional flux moment.

The hex-plane distribution is interpolated for each group by a non-separable sixth order polynomial required to preserve the 13 nodal quantities (one node-average flux, six surface-average fluxes, and six surface-average currents) and six local corner fluxes. A unique sixth order polynomial for the hex-plane distribution is obtained with additional constraints requiring the polynomial to be invariant under the symmetry operations of the hexagon and to reproduce lower order polynomial shapes exactly. The corner fluxes used in the hex-plane flux interpolation is approximated by assuming a biquadratic polynomial shape (less the  $x^2$   $y^2$  term) in each of the three adjacent nodes. A simple expression for a corner flux is obtained by preserving node-average and surface-average fluxes, requiring flux and current continuity at mid-points, and imposing a source free condition at a corner point.

The intra-nodal nuclide densities are calculated in one of two ways. In the first way, which is applicable to conventional assemblies with nominally uniform beginning of life (BOL) densities and smooth density variation after depletion, the surface and corner densities are first calculated by solving the nuclide transmutation equations using the surface-average and corner fluxes. Using these surface-average and corner densities as well as the node-average density from the nodal solution and making the assumption of hex-planar and axial separability, the hex-plane densities are interpolated at the center of each fuel pin by a fourth order polynomial. Similar to the case of flux interpolation, the interpolation polynomial is required to preserve the above 13 base values and to be invariant under the symmetry operation of the hexagon. The axial density distribution is interpolated by a quadratic polynomial using the node-average density and the top and bottom surface-average densities. The second method of computing local nuclide densities is applied to specified "special" pins in assemblies with different types of fuel pins (e.g., experimental assemblies in EBR-II); in this case, the densities are not smooth functions of position within the assembly and cannot be determined by interpolation. The special pin nuclide densities are, therefore, calculated by point depletion, i.e., solving the depletion equations with the interpolated fluxes. For each axial pin segment contained in a given node, the top, axial-average, and bottom densities are

calculated along the center line of the segment. Using these three values, the axial density distribution is interpolated by a quadratic polynomial.

The intra-nodal distribution of the power density is calculated using the interpolated flux and nuclide density distributions. On the other hand, the intra-nodal burnup and fluence distributions are calculated in a similar manner as the nuclide densities. For conventional assemblies, the hex-plane distributions of burnup and fluences are interpolated by fourth order polynomials, and the respective axial distributions are interpolated by quadratic polynomials, using the node-average, surface-average, and corner values. For the special pins, the burnup and fluences are explicitly calculated using the interpolated fluxes at the center of each fuel pin.

Several important capabilities have been implemented in RCT to permit its application to a wide range of core designs and fuel management strategies. As mentioned above, the burnup characteristics are explicitly calculated for user-defined "special pins" by point depletion using the interpolated fluxes at the center of each fuel pin. The radioactive decay during the out-of-core storage is also considered in the nuclide density calculation. Since non-uniform intra-nodal distributions are considered in reconstruction calculations, the rotational shuffling of assemblies is allowed and is specified by integer multiples of 60 degrees. To permit assembly reconstitution from different types of fuel pins, pin-by-pin shuffling is allowed for the special pins. The axial displacement of fuel (e.g., arising from the movement of the fueled portion of the control rods in EBR-II) is also treated, consistent with the data provided in the REBUS-3 input dataset. Multi-cycle reconstruction calculations are performed as a sequence of single cycle RCT calculations.

#### Depletion Calculations of EBR-II

One of the first steps undertaken to demonstrate the technical feasibility of the IFR concept was to irradiate three lead subassemblies of U-Pu-Zr fuel in EBR-II. In February of 1985 three 61-element subassemblies (X419, X420 and X421) began operation in EBR-II with D9-clad U-10Zr, U-8Pu-10Zr, and U-19Pu-10Zr fuel. Interim examination and reconstitution and subsequent chemical analysis of

elements from these three subassemblies provide measured burnup data for the testing of the REBUS/RCT methodology.

In order to analyze the burnup history for these subassemblies with REBUS, detailed modeling of the reactor loading and the reactor power level history began with Run 130A (Aug. 3, 1984). This process was then extended through a series of all subsequent EBR-II runs (up to the present), where input to the REBUS burnup calculations utilized the known heavy metal loadings for freshly-loaded subassemblies and the REBUS-calculated number densities for the remainder of the assemblies. Therefore, after a series of EBR-II runs had been analyzed, the effect of the initial conditions (i.e., coarse initial reactor loading data) should have diminished.

Because each of the lead test subassemblies were mixed fuel types, analysis with RCT was required for each EBR-II run in which these subassemblies were irradiated in order to determine local values (i.e., values for a specific pin at a specific axial position) of the burnup and nuclide densities. These values were then compared with burnup measurements (based on <sup>139</sup>La and <sup>148</sup>Nd indicators) and Pu and U isotopic ratio measurements.

Agreement between the REBUS/RCT calculations and results of chemical analysis of the burnup in X419, X420, and X421 are generally good (i.e., within the combined experimental uncertainties of -6%). C/E values range from 0.94 to 1.09, with a mean  $\pm$   $1\sigma$  of 1.026  $\pm$  0.041. Similarly, the comparison of the measured and calculated U and Pu isotopic fractions tend to agree within the experimental uncertainties.

Current effort is focused on better understanding the sensitivities of both the measured and calculated values, understanding the components of uncertainty in each, and refining both the analysis and measurement methods. We are collaborating with the reactor experimenters and analytical chemistry personnel to better understand the interpretation of the experiments (e.g., the extent and interpretation of irradiation fuel growth, fission product migration, sensitivity of fission yield data, etc.). Because the REBUS/RCT methodology is expected to

become a production tool in the closure of the IFR fuel cycle at EBR-II/HFEF-S, we are also working to improve the methods and models. Studies have been made of improved cross section preparation, and an effort has been made to incorporate Nodal Equivalence Theory in the framework of the nodal option of REBUS/DIF3D to reduce the nodal solution error. Database systems and software are being developed to interface with the Mass-Tracking System and to "automate" input preparation and execution of the REBUS/RCT codes. This database system will not only contain reactor loading information (e.g., identification of all subassemblies and elements with masses and locations), but also the axial profiles of nuclide densities, burnup, and fluence (which must be calculated with RCT). These data files will be required for both pre- and post-analysis of EBR-II operations, for input to the Mass-Tracking System, and for records verification.

In summary, the goal has been to validate the REBUS fuel management methodology as adequate to determine isotopic mass and neutronic data inputs to HFEF-S for both operational and material control and accountancy purposes. This required first developing and benchmarking the reconstruction capabilities of RCT and then validating REBUS/RCT as a system which can compute the burnup and isotopic distribution in binary and ternary fuel assemblies. Much progress toward this goal has been realized.

## **OVERVIEW**

- I. Reconstruction of Pin Burnup Characteristics
  - Objectives
  - Background
  - Methodology
  - Validation
  - Conclusions
- II. Depletion Calculations of EBR-II
  - Objectives
  - Procedure and Methodology
  - Results
  - Conclusions
  - Future Work

# RECONSTRUCTION OF PIN BURNUP CHARACTERISTICS

## **Objectives**

- Reconstruct Pin Values of Power, Burnup, and Nuclide Densities
  - -- from Fuel Cycle Analysis Performed with Hex-Z Nodal Option of REBUS-3/DIF3D
- Applicable to IFR Fuel Cycle Demonstration,
   EBR-II Experiments, and Analysis of Advanced
   LMR Designs
- Take into Account Operational Features Specific to EBR-II

## Background •

- Draw from LWR Experience
  - Flux Reconstruction by Collocation of Nodal Quantities
  - -- Need to Interpolate Corner Point Values
- Specific Features of LMR Applications
  - -- Simplifications:
    - No Intra-node Heterogeneity
    - Burnup Independent Microscopic X.S.
    - Block Depletion for Average Values
  - -- Challenges:
    - Hexagonal Geometry
    - Strong Flux Curvature
    - Transport Effects
- Specific Features of EBR-II Applications
  - -- Multiple Fuel Types
  - -- Moving Fuel
  - -- Reconstitution of Fuel

## Methodology

- Hex-planar and Axial Separability within Node
- Planar Distribution
  - -- Non-separable Polynomial of X and Y
    - Sixth Order for Flux
    - Fourth Order for Nuclide Density
  - -- Preservation of
    - Node-average Value
    - Surface-average Values
    - Corner-point Values
    - (Surface-average Currents for Flux)
  - -- Invariant under Symmetry Operations
- Axial Distribution
  - Cubic for Flux
     Quadratic for Nuclide Density
  - -- Preservation of
    - Node-average Value
    - Top and Bottom Surface-average Values
    - (Z-directional Flux Moment for Flux)
- Point Depletion for Special Pins

## Validation

- Reference: Fine Mesh, Finite Difference,
   Diffusion Theory, and Point Depletion
- Static Benchmarks
  - -- 2D 450 and 900 MWt LMRs
  - -- 3D 450 MWt LMR and EBR-II
  - -- Maximum Errors (Pointwise Power Density)
    - Drivers: 2 3%
    - Blankets: 3 6%
  - Error Sources: Planar Flux < Corner Flux</li>Separability < Nodal Information</li>
- Depletion Benchmark
  - -- 3-Cycle 450 MWt LMR (3D, 474.5 Day Cycle)
  - -- Maximum Errors in Power Density at BOC-3
    - Driver: 1.5%
    - Blankets: 4%
  - -- Maximum Errors in Pu-239 Density at EOC-3
    - Driver: 0.25%
    - Blankets: 1.0 3.5%

## Conclusions :

- Numerical Benchmarks Demonstrate Good
   Accuracy
- Comparison with EBR-II Measurements Show That Method is Accurate (within Experimental Uncertainties)
- To Improve Accuracy
  - -- Reduce Separability Error (Finer Axial Mesh)
  - More Accurate Nodal Solution (Nodal Equivalence Theory)

## CALCULATION OF FUEL BURNUP IN EBR-II

- Goal: to validate REBUS as a code to compute EBR-II burnup in binary- and ternaryfueled Mark-III and Mark-IV cores
- So as to give us a way to accurately estimate the fissile mass flows into HFEF-S
  - -- for MCA purposes
  - -- for operational purposes

## CALCULATION OF FUEL BURNUP IN EBR-II

## Procedure:

- -- Go to EBR-II Records
- -- Start at Loading for Run 130A
- -- Do detailed REBUS Modeling of core loadings core power level histories
- -- Compute Pin Depletion of Experimental S/A's with RCT
- -- Compare resulting pin discharge compositions with

La and Nd measurements
Pu and U isotopic ratio measurements

## CALCULATION OF FUEL BURNUP IN EBR-II

- Methodology (REBUS/RCT)
  - Three-Dimensional Hex-Z Model
  - Nodal Diffusion Theory (k-eff ~ 0.96)
  - ENDF/B-V.2 data (9 broad energy groups)
  - Each S/A (rows 1-16) and all fuel management operations are modeled for each sub-run of EBR-II
  - Pin Modeling of some Experimental S/A's for pin-depletion analysis with RCT
- Current Status
  - REBUS Analysis completed up to Run 154A (current run)
  - RCT Analysis performed only for select S/A's

## COMPARISON OF REBUS/RCT CALCULATED BURNUP (atom %) WITH 139La AND 148Nd BURNUP MEASURMENTS

| S/A                             |                      |                         |                         |                       |                         | REBUS                      |                         | E Relative              |                         |
|---------------------------------|----------------------|-------------------------|-------------------------|-----------------------|-------------------------|----------------------------|-------------------------|-------------------------|-------------------------|
| Pin No.                         | <u>L/Lo</u>          | 139 <u>La</u>           | 148 Nd                  | % Diff.               | <u>Avg.</u>             | RCT                        | 139 <u>La</u>           | 1 4 8 Nd                | <u>Avg.</u>             |
| X419<br>31<br>(U-19Pu-Zr)       | 0.08<br>0.57<br>0.94 | 1.571<br>1.828<br>1.426 | 1.624<br>1.834<br>1.486 | 3.37<br>0.33<br>4.21  | 1.598<br>1.831<br>1.456 | 1.6692<br>1.9324<br>1.4537 | 1.063<br>1.057<br>1.020 | 1.028<br>1.053<br>0.978 | 1.045<br>1.055<br>0.999 |
| 40<br>(U-8Pu-Zr)                | 0.12<br>0.57<br>0.90 | 1.628<br>1.791<br>1.550 | 1.665<br>1.831<br>1.544 | 2.27<br>2.23<br>-0.39 | 1.647<br>1.811<br>1.547 | 1.7160<br>1.9146<br>1.5160 | 1.054<br>1.069<br>0.978 | 1.031<br>1.046<br>0.982 | 1.042<br>1.057<br>0.980 |
| 13<br>(U-Zr)                    | 0.10<br>0.45<br>0.92 | 1.645<br>1.848<br>1.454 | 1.615<br>1.872<br>1.467 | -1.82<br>1.30<br>0.89 | 1.630<br>1.860<br>1.461 | 1.6748<br>1.9190<br>1.4687 | 1.018<br>1.038<br>1.010 | 1.037<br>1.025<br>1.001 | 1.028<br>1.032<br>1.005 |
| <u>X420</u><br>20<br>(U-8Pu-Zr) | 0.53                 | 5.339                   | 5.679                   | 6.37                  | 5.509                   | 5.1621                     | 0.967                   | 0.909                   | 0.937                   |
| X421                            |                      |                         |                         |                       |                         |                            |                         |                         |                         |
| 41                              | 0.45                 | 9.169                   | 9.220                   | 0.57                  | 9.195                   | 10.0495                    | 1.096                   | 1.090                   | 1.093                   |
| (U-8Pu-Zr)<br>39<br>(U-Zr)      | 0.45                 | 9.196                   | 9.278                   | 0.89                  | 9.237                   | 9.9929                     | 1.087                   | 1.077                   | 1.082                   |
| X419B<br>48                     | 0.44                 | 12.53                   | 12.17                   | -2.87                 | 12.350                  | 12.3526                    | 0.986                   | 1.015                   | 1.000                   |
| (U-19Pu-Zr)<br>25<br>(U-Zr)     | 0.44                 | 11.65                   | 12.14                   | 4.21                  | 11.895                  | 12.0882                    | 1.038                   | 0.996                   | 1.016                   |

## IFR FUEL NEUTRON INDUCED ISOTOPIC CHANGE U-10ZR

|          |                        | ·            |              |              |                |
|----------|------------------------|--------------|--------------|--------------|----------------|
|          |                        | 234[]        | 2351         | 235U         | 2381           |
| AS CAST  |                        | . 488        | 68.7         | .380         | 30.33          |
| X419 @ 2 | 2 <sup>a</sup> /o BU:  |              |              |              |                |
| TOP:     |                        |              |              |              |                |
|          | Measured<br>Calculated | .494<br>.496 | 68.0<br>68.4 | .603<br>.590 | 30.88<br>30.53 |
| CENTER:  |                        |              |              |              | •              |
|          | Measured<br>Calculated | .490<br>.496 | 67.8<br>68.2 | .658<br>.650 | 30.95<br>30.64 |
| BOTTOM:  |                        |              | •            |              |                |
| . }      | Measured<br>Calculated | .495<br>.496 | 67.9<br>68.3 | .655<br>.640 | 30.95<br>30.59 |
|          | 5 <sup>a</sup> /o BU:  | . 130        | 00.3         | .040         | 30.33          |
| TOP:     | <del>5 70 80</del> .   |              |              |              |                |
| 1        | Measured               | .605         | 66.9         | 1.23         | 31.30          |
|          | Calculated             | .501         | 66.8         | 1.30         | 31.36          |
| CENTER:  | Measured               | .606         | 66.5         | 1.37         | 31.58          |
|          | Calculated             | .501         | 66.7         | 1.29         | 31.53          |
| BOTTOM:  |                        |              |              |              |                |
|          | Measured<br>Calculated | .606<br>.501 | 66.6<br>66.9 | 1.34<br>1.29 | 31.45<br>31.35 |
| X421 0   | 10 <sup>a</sup> /o 8U: |              |              | •            |                |
| TOP:     |                        |              |              |              |                |
| 1        | Measured<br>Calculated | .588<br>.614 | 65.2<br>65.5 | 1.96<br>1.87 | 32.32<br>32.03 |
|          | carcaraced             | .014         | 03.3         | 1.07         | 32.03          |
| CENTER:  | Calculated             | .616         | 64.4         | 2.22         | 32.79          |
| воттом:  |                        |              |              |              |                |
|          | Calculated             | .616         | 64.7         | 2.17         | 32.52          |
|          |                        |              |              | · .          |                |

IFR FUEL NEUTRON INDUCED ISOTOPIC CHANGE U-8PU-ZR

|                |                                    | 2341         | <u>235U</u>  | 2 3 6 U      | 238U         | 23 s P U       | 240U         | 241PU      | 242PU |
|----------------|------------------------------------|--------------|--------------|--------------|--------------|----------------|--------------|------------|-------|
| AS CAS         | ST                                 | .460         | 64.3         | .295         | 34.8         | 93.8           | 5.72         | .39        |       |
| X419 @         | <sup>3</sup> 2 <sup>a</sup> ∕o BU: |              |              |              |              |                |              | •          |       |
| TOP:           | Measured<br>Calculated             | .466         | 63.6<br>64.0 | .573<br>.560 | 35.3<br>35.0 | 93.51<br>93.56 | 6.05<br>5.97 | .38<br>.40 | .08   |
| CENTER         | R:<br>Measured<br>Calculated       | .466<br>.469 | 63.4<br>63.8 | .622<br>.608 | 35.5<br>35.1 | 93.47<br>93.52 | 6.08<br>6.00 | .38<br>.40 | .08   |
| EOTTON         | Measured<br>Calculated             | .466<br>.469 | 63.4<br>63.9 | .617<br>.603 | 35.4<br>35.1 | 93.48<br>93.51 | 6.06<br>6.02 | .38<br>.40 | .08   |
| <u> X420 (</u> | <u>9 5ª/o BU</u> :                 | -            |              |              |              |                |              |            |       |
| TOP:           | Measured<br>Calculated             | .473<br>.459 | 62.4<br>61.1 | 1.10<br>1.15 | 35.9<br>37.3 | 92.9<br>93.1   | 6.62<br>6.48 | .39<br>.41 | .004  |
| CENTE          |                                    | 477          | co 1         | 1 00         | 26.0         | 00.0           | 6 70         | 40         | •     |
|                | Measured<br>Calculated             | .477<br>.459 | 62.1<br>61.0 | 1.23<br>1.15 | 36.2<br>37.4 | 92.8<br>93.0   | 6.72<br>6.57 |            | .01   |
| воттог         |                                    |              | •            |              |              |                |              |            | •     |
|                | Measured<br>Calculated             | .478<br>.459 | 62.3<br>61.1 | 1.22<br>1.15 | 36.0<br>37.3 | 92.6<br>93.0   | 6.76<br>6.62 | .41<br>.42 | .01   |
| X421           | <u>@ 10<sup>a</sup>/o BU</u> :     |              |              |              |              |                |              |            |       |
| TOP:           | Measured<br>Calculated             |              |              | 1.80<br>1.70 |              | 92.1<br>92.3   |              |            | .09   |
| CENTE          |                                    |              | · · · · ·    | 1470         | 50.0         | 22.0           | 7.20         | •          | •03   |
| GLII ( L.      | Measured<br>Calculated             | .487<br>.478 |              | 2.07<br>2.02 |              | 91.9<br>92.0   |              | .41<br>.46 | •09   |
| OTTOS          |                                    | 106          |              | 2 01         | 27.2         | 01.0           | 7 64         | A1         |       |
|                | Measured<br>Calculated             |              |              | 1.97         |              | 91.8<br>92.0   |              |            | .09   |
|                |                                    |              |              |              |              |                |              |            | •     |

IFR FUEL NEUTRON INDUCED ISOTOPIC CHANGE U-19PU-ZR

|        | •                            | 2341         | 2 3 5 <u>U</u> | 2 3 6 ប្រ    | 238[]        | 239PU          | 240U         | 241Pu      | 2 4 2 PU |
|--------|------------------------------|--------------|----------------|--------------|--------------|----------------|--------------|------------|----------|
| AS CAS | ST .                         | .410         | 57.0           | .263         | 42.3         | 93.84          | 5.68         | -39        |          |
| X419 @ | 2 <sup>a</sup> /o BU:        |              |                |              |              |                |              |            |          |
| TOP:   | Measured<br>Calculated       | .414<br>.415 | 56.3<br>56.7   | .503<br>.492 | 42.8<br>42.4 | 93.49<br>93.55 |              | .38<br>.40 | .07      |
| CENTE  | R:<br>Measured<br>Calculated | .415<br>.415 | 56.1<br>56.5   |              | 42.9<br>42.5 | 93.45<br>93.51 |              | .38<br>.40 | .07      |
| BOTTO  | Measured<br>Calculated       | .418<br>.415 | 56.3<br>56.5   | .540<br>.536 | 42.8<br>42.5 | 93.44<br>93.48 |              | .38<br>.40 | .07      |
| X420 ( | <u> </u>                     |              |                |              |              |                |              |            |          |
| TOP:   | Measured<br>Calculated       | .430<br>.417 | 54.9<br>55.1   | .978<br>1.05 |              | 92.80<br>92.95 |              | .39<br>.42 | .08      |
| CENTE  | R:<br>Measured<br>Calculated | .435<br>.417 | 54.6<br>55.0   |              | 43.9<br>43.5 | 92.65<br>92.83 |              | .40<br>.43 | .08      |
| BOTTC  | M:<br>Measured<br>Calculated | .417         | 55.1           | 1.05         | 43.4         | 92.78          | 6.72         | .43        | .08      |
| X421   | @ 10 <sup>a</sup> /o BU:     |              |                |              |              |                | ٠            |            |          |
| TOP:   | Measured<br>Calculated       |              |                | 1.69<br>1.55 |              | 91.90<br>92.13 |              |            | .08      |
| CENTE  | R:<br>Measured<br>Calculated | .570<br>.419 | 52.5<br>52.9   | 1.89<br>1.73 | 44.9<br>44.9 | 91.60<br>91.89 | 7.82<br>7.55 | .45<br>.47 | .08      |
| 80176  | M:<br>Measured<br>Calculated |              |                |              |              | 91.60<br>91.77 |              |            | .08      |
|        |                              |              |                |              |              |                |              |            |          |

### SUMMARY OF BURNUP COMPARISONS

- Agreement is generally good

   (i.e., within 1-sigma uncertainties of ~6%).
- Some discrepancies are attributed to poor measurement values.
- Chemistry techniques are most difficult for ternary fuel, especially w/ high Pu fraction.
- There is a slight misprediction (~1-2%) of axial tilt which should improve with newer methods.
- Uncertainty in calculated predictions may improve with application of isotope correlations (combined with mass spectrometer measurements) to better define fluence.
- Burnup data is limited and new data (e.g., X-444) will be very helpful.
- Burnup comparisons for radial blanket S/A's are needed and will be more difficult to obtain.

#### FUTURE WORK WITH REBUS/RCT

### Short Term

- Implement additional checking of fuel management by REBUS input processor
- Modify STACK file to include ISOTXS subset

## Long Term

- Improve plots currently produced in SUMMARY
- Produce REBUS input from Master File of S/A masses
- Interface with Mass-Tracking System
- Perhaps produce utilities to calculate and plot Isotope Correlations from RCTDEN files
- Improve Methodology as Available (e.g., Equivalence Theory, X-Sections, etc.)
- Better Understand the Interpretation of the Experiments (e.g., irradiation fuel growth, FP migration, fission yield sensitivity, etc.)

NEACRP-A-1072
Topic ♣9

## Prediction Accuracies of Safety Related Core Design Parameters for FBR

Keisho Shirakata and Toshio Sanda\*

Power Reactor and Nuclear Fuel Development Corporation (PNC) 4002, Narita-cho, O-arai machi, Ibaraki-ken, 311-13, JAPAN

#### Abstract

Prediction accuracies of safety related core design parameters for a large Liquid Metal Fast Breeder Reactor (LMFBR) core were evaluated by using the current calculation method for core design. Target accuracies for them were also evaluated by estimating impacts of calculation uncertainties on the core design. The technical level of the current calculation method for core design was assessed and discussed.

#### 1. Introduction

Neutronics analysis methods for fast reactor core have been developed in Japan to support the national project on LMFBR. From the standpoint of core design for large LMFBR, it is required to reduce the uncertainties for core design parameters.

The analysis of JUPITER experiments (US/Japan joint physics large core critical experiment program) has been almost concluded in Japan, and an adequacy and accuracy of the current core analysis method has been assessed when it was applied to critical assembly experiments on large FBR core. Utilizing these C/E (Calculation/Experiment) results by the core analysis method, prediction accuracies by the current calculation method for core design were evaluated. Safety related core design parameters, i.e., control rod reactivity, sodium void reactivity and Doppler reactivity were evaluated for a large FBR core design.

The purpose of this work is to assess the technical level of the current calculation method for core design, and to investigate trends and problems of it.

<sup>\*</sup>Present address: Hitachi Ltd.

#### 2. Calculation method for core design

The 70-group cross section set JFS-3-J2<sup>1)</sup>, processed from the JENDL-2 library, was used. Effective cross sections for individual regions were produced by cell calculations, considering double heterogeneous configuration of sub-assembly, heterogeneous arrangement of different material adjacent to each other, reaction rate preservation, background cross section based on collision probability method, and so on. The base calculation used diffusion theory in three dimensional geometry, and employed Benoist's diffusion coefficients. Mesh and Transport corrections to base calculations were considered.

#### 3. Present prediction accuracies

where

A present prediction accuracy  $\Delta_{Present}$  can be treated to consist of systematic error and random error, and is obtained from the following equation:

 $\Delta_{\text{Present}} = 100 \text{ (C/E - 1.0)} + \text{S} \pm (\Delta_{\text{S}} + \sqrt{\Delta_{1}^{2} + \Delta_{2}^{2} + \Delta_{3}^{2}}),$ 

C/E: JUPITER experiments and calculations 2),3)

S: Systematic error other than C/E

 $\Delta_S$ : Random error in S

 $\Delta_1$ : Random error in C/E

 $\Delta_2$ : Random error in extrapolation from critical assembly to

designed core

 $\Delta_3$ : Uncertainty of the designed core.

That is,  $\Delta_{Present}$  is obtained, based on the JUPITER C/E results.

 $\Delta_{Present}$  of control rod, sodium void and Doppler reactivities for a 1,000 MWe size homogeneous FBR core were evaluated according to the equation. Values of  $\Delta_{Present}$  in 2 $\sigma$  level, in percent units, were shown in Table 1, 2 and 3 respectively, together with their components. Items in the bracket of  $\Delta_{i}$  were considered for the evaluation of  $\Delta_{i}$ . A systematic error means there is a systemtic problem on the calculation method, and a random error means the breadth of uncertainty on the calculation method.

#### 4. Target accurancies

An impact of a calculation uncertainty on core design was evaluated and summarized in the form of event trees, and the sensitivity coefficients were obtained between various design parameters.<sup>4)</sup> Based on these data,

target accuracies  $\Delta_{\text{Target}}$  of control rod, sodium void and Doppler reactivities were evaluated considering the allowable design limits and compromising between design margins and excessive cost. Results were shown in Table 4.

#### 5. Results

It was made clear from Table 4 that  $\Delta_{Present}$  did not satisfy  $\Delta_{Target}$  for all the cases, and that there were some spatial dependences in  $\Delta_{Present}$ . It was also shown that there were large systematic errors for the sodium void reactivities. In order to make  $\Delta_{Present}$  satisfy  $\Delta_{Target}$ , it is necessary to reduce both the amount of systematic error and random error. In near future,  $\Delta_{Present}$  and  $\Delta_{Target}$  will also be evaluated for different type of core designs.

#### References

- 1) Takano, H., et al.: JAERI-M 82-135 (1982).
- 2) Shirakata, K., et al.: Proc. Int. Reactor Physics Conference, Jackson Hole, II-297 (1988).
- 3) Sanda, T., et al.: JPNC TN9600 90-013 apan, Vol.31, No.16, 16, (In Japanese), (1989). PNC TN9600 90-013
- 4) Shirakata, K., et al.: Proc. Topical Mtg. on Reactor Physics and Shielding, Chicago, 347 (1984).

Table 1. Present Prediction Accuracy of Control Rod Reactivity Worth for Large LMFBR Core (2σ level, Percent units)

| Systematic error                                                                               |     |            |                |            | termost |
|------------------------------------------------------------------------------------------------|-----|------------|----------------|------------|---------|
|                                                                                                |     | <u>Cen</u> | <u>ter Rod</u> | <u>Rin</u> | g Rods  |
| C/E                                                                                            | =   | 0.94       |                | 1.0        | 0       |
| $eta_{	ext{eff}}$ error                                                                        | = ` | 2.5        | ± 2.5          | 2.5        | ± 2.5   |
| <sup>10</sup> B loading error                                                                  | =   | 0.5        | ± 0.5          | 0.5        | ±0.5    |
| Random error                                                                                   |     |            |                |            |         |
| $\Delta_1$ (Measurement, Calculation,                                                          | =   |            | ± 5.8          |            | ± 5.8   |
| $\beta_{\rm eff}$ random error, C/E fluctuation) $\Delta_2$ (Geometry of control rod assembly, |     |            | ± 2.8          |            | ± 2.8   |
| Cross section, Geometry of absorbe                                                             |     | •          | ± 2.0          |            | ± 2.0   |
| Amount of <sup>10</sup> B loaded, Core compo                                                   |     |            |                |            |         |
| $\Delta_3$ (Operation condition,                                                               | ==  |            | ± 2.2          |            | ± 2.2   |
| Driver fuel composition)                                                                       |     |            |                |            |         |
| Total error $\Delta_{Present}$                                                                 |     | - 3        | ± 9.8          | 3          | ± 12.6  |

Table 2 Present Prediction Accuracy of Sodium Void Reactivity Worth for Large LMFBR Core (2σ level, Percent units)

|                       | Systematic error                                                                                                          |                 | <u>Non-leakage</u>        | Leakage                   | -013 |
|-----------------------|---------------------------------------------------------------------------------------------------------------------------|-----------------|---------------------------|---------------------------|------|
| -                     | C/E<br>β <sub>eff</sub> error                                                                                             | <b>=</b><br>= ` | 1.20<br>2.5 ± 2.5         | 1.20<br>2.5 ± 2.5         |      |
|                       | Random error                                                                                                              |                 | •                         |                           |      |
| <b>–</b> 318 <b>–</b> | $\Delta_1$ (Measurement, Calculation, $\beta_{eff}$ random error, C/E fluctuation)                                        | =               | ± 11.9                    | ± 17.2                    |      |
|                       | $\Delta_2$ (Core dimension, Core composition, Driver fuel composition, Operation core temperature, Control rod effectives |                 | ± 19.2                    | ± 28.8                    |      |
|                       | $\Delta_3$ (Driver fuel composition)                                                                                      |                 | ± 1.5                     | ± 0                       |      |
|                       |                                                                                                                           | ,               | Central small region void | Central large region void |      |
|                       | As the result, total error $\Delta_{Preser}$                                                                              | nt =            | 23 ± 25                   | 29 ±34                    |      |

Table 3 Present Prediction Accuracy of <sup>238</sup>U Doppler Reactivity Worth for Large LMFBR Core (2σ level, Percent units)

| Systematic error                                                                                                                                                  |             |      | core                       |
|-------------------------------------------------------------------------------------------------------------------------------------------------------------------|-------------|------|----------------------------|
| C/E<br>β <sub>eff</sub> error<br>Mox fuel composition                                                                                                             | =<br>=<br>= | 0.87 | <u>°K→1100°K)</u><br>± 2.5 |
| Random error                                                                                                                                                      |             | •    |                            |
| $\Delta_1$ (Measurement, Calculation, $\beta_{eff}$ random error, C/E fluctuation. Effective cross section of sample)                                             | =           |      | ± 9.9                      |
| $\Delta_2$ (Core dimension, Core composition, Operational core temperature, Heterogeneity effect, Extrapolation to full core, Blanket effect, Control rod effect) | <b>::</b>   |      | ± 10.1                     |
| $\Delta_3$ (Operational core temperature)                                                                                                                         | 1<br>1      |      | ± 8                        |
| Total error $\Delta_{Present}$                                                                                                                                    |             | -5.5 | ± 18.7                     |

|     |                                           | Present<br>Predictio | n accuracy | Target | accuracy |
|-----|-------------------------------------------|----------------------|------------|--------|----------|
|     | Control rod reactivity worth              | ,                    |            |        |          |
|     | Center rod                                | -3                   | ±9.8       |        | ± 10     |
| 220 | Outermost ring rods                       |                      | ± 12.6     |        | ± 10     |
|     | Sodium void reactivity worth              |                      |            |        |          |
|     | Central small region void                 | 23                   | ± 25       |        | ± 15     |
|     | Central large region void                 | 29                   | ±34        |        | ± 15     |
|     | <sup>238</sup> U Doppler reactivity worth | -5.5                 | ± 18.7     |        | ± 15     |

### Analysis of JOYO Burnup Characteristics

### Akihiro Hara\* and Kastuya Kinjo

Power Reactor and Nuclear Fuel Development Corporation (PNC) 4002, Narita-cho O-arai-machi, Ibaraki-ken, 311-13, JAPAN

#### Abstract

All the post irradiation experiment (PIE) data on the experimental fast reactor JOYO MK-I core were collected, and complied into a data base. Burnup calculations were done by using the JFS-3-J2 cross section set and the three dimensional diffusion code MOSES with modified coarse-mesh method. Comparisons of calculations (C) with experiments (E) are as follows:

① Burnup coefficient (reactivity loss for 50MW·day)

$$C/E = 1.02 + (7 \sim -13)\%$$

② Relative change of isotope ratio to burnup (a/o)

| Pu-239/Pu | C/E = 1.05 | ±2% |
|-----------|------------|-----|
| Pu-240/Pu | C/E = 1.06 | 土4% |
| Pu-242/Pu | C/E = 1.14 | 士5% |
| U-235/U   | C/E = 1.11 | ±1% |
| U-236/U   | C/E = 1.08 | ±2% |
| U-238/U   | C/E = 1.11 | ±1% |

3 Pu build-up in radial blanket

| 5th layer | $C/E = 1.01 \sim 1.06$ | ±7%  |
|-----------|------------------------|------|
| 6th layer | $C/E = 1.02 \sim 1.14$ | ±7%  |
| 7th layer | C/E = 1.07             | ±7%  |
| 8th layer | C/E = 1.02             | ±7%. |

#### 1. Introduction

Burnup characteristics of JOYO were analyzed and the results were reported in the past.1),2),3) In case of those previous reports, the number of

<sup>\*</sup> Present address: Toshiba Corporation

analyzed PIE data was limited, and the maximum burnup of them was 35GWd/t.

This time, all the PIE data on the JOYO MK-I core were collected and analyzed. As the result, the number of PIE data was twice as many as the previous report, and the maximum burnup extended to 55GWd/t.

Number of assemblies on which PIE was performed were 28 and 11 for core fuel and blanket fuel assemblies. Numbers of points or pellets on which PIE was performed were 147, 28 and 43 for core fuel, axial blanket fuel and radial blanket fuel, respectively. Fig.1 and 2 show the distributions of PIE data for core and blanket fuel pellets as a function of burnup.

#### 2. PIE data

The PIE was done through the processes of chemical separation by ion-exchange resin and mass-spectrometry. As the result of PIE, following data were obtained for each specimen:

Ratio of Pu to total heavy metal (a/o): 
$$\frac{N (Pu)}{N (Pu) + N(U)}$$
Isotopic ratio of Pu (a/o): 
$$\frac{N (Pu238)}{N (Pu)} , \frac{N (Pu239)}{N (Pu)} , \frac{N (Pu240)}{N (Pu)}$$

$$\frac{N (Pu241)}{N (Pu)} , \frac{N (Pu242)}{N (Pu)}$$
Isotopic ratio of U (a/o): 
$$\frac{N (U234)}{N (U)} , \frac{N (U235)}{N (U)} , \frac{N (U236)}{N (U)}$$

$$\frac{N (U238)}{N (U)}$$
Burnup (a/o): 
$$\frac{N (FP)}{N (Pu) + N(U) + N(FP)}$$

Specific burnup, i.e., GWd/t was also obtained from isotopic compositions of Nd.

Fig.3 and 4 show changes of isotopic ratio of <sup>239</sup>Pu for the core and axial blanket fuels as a function of burnup. In these Figures, identifications for fuel fabrication lots are noted. This is because the initial isotopic ratios are a little different between the fabrication lots.

#### 3. Calculation method

A core configuration of the JOYO MK-I core is shown in Fig.5. Hexagonal-Z geometry diffusion calculations were performed for the analysis of burnup characteristics of the core. The JFS-3-J2 cross section set and the modified coarse-mesh diffusion code MOSES were employed for the calculations.

#### 4. Results

C/E result for the burnup coefficient was  $1.02+(7\sim-13)\%$ . It means, the nominal value of calculation agrees with the experiment, but the uncertainty is relatively large.

Fig.6 shows the results of calculation and experiment for the change of isotopic ratio of <sup>239</sup>Pu as a function of burnup. There is some difference in the gradient between them.

Results for relative change of isotope ratio to burnup(a/o) are

| Pu-239/Pu | C/E = 1.05 | $\pm 2\%$ |
|-----------|------------|-----------|
| Pu-240/Pu | C/E = 1.06 | ±4%       |
| Pu-242/Pu | C/E = 1.14 | ±5%       |
| U-235/U   | C/E = 1.11 | ±1%       |
| U-236/U   | C/E = 1.08 | ±2%       |
| U-238/U   | C/E = 1.11 | +1%       |

Calculations overpredict experiments in all the cases.

C/E results for Pu build-up in radial blanket are

| 5th layer | $C/E = 1.01 \sim 1.06$ | ±7%      |
|-----------|------------------------|----------|
| 6th layer | $C/E = 1.02 \sim 1.14$ | $\pm7\%$ |
| 7th layer | C/E = 1.07             | $\pm7\%$ |
| 8th layer | C/E = 1.02             | ±7%.     |

The uncertainty is relatively large.

In order to detail the calculation, possible corrections for pin and wrapper tube heterogeneity, diffusion calculation, temperature effect, etc. will be considered in near future.

#### References

- 1) Kawashima, M., et al.: NEACRP-A-680, (1984).
- 2) Watari, Y., et al.: NEACRP-A-686, (1984).
- 3) Ikegami, T., et al.: NEACRP-A-746, (1985).

Table 1 The ratio of isotopic composition change rate to burnup (PU8230\*)

|                      | Calculation                     | Experiment                      | C/E       |
|----------------------|---------------------------------|---------------------------------|-----------|
| <sup>239</sup> Pu/Pu | $-3.751\pm0.036 \times 10^{-1}$ | $-3.541\pm0.035 \times 10^{-1}$ | 1.059 ±2% |
| <sup>240</sup> Pu/Pu | $3.714\pm0.022 \times 10^{-1}$  | 3.522±0.028 ×10 <sup>-1</sup>   | 1.055 ±2% |
| <sup>242</sup> Pu/Pu | 1.506±0.003 ×10 <sup>-2</sup>   | 1.345±0.023 ×10 <sup>-2</sup>   | 1.120 ±2% |

<sup>\*</sup> Feul fabrication lot No.

Table 2 The ratio of isotopic composition change rate to burnup (PU8231)

|                      | Calculation                     | Experiment                      | C/E       |
|----------------------|---------------------------------|---------------------------------|-----------|
| <sup>239</sup> Pu/Pu | $-3.832\pm0.027 \times 10^{-1}$ | $-3.656\pm0.022 \times 10^{-1}$ | 1.048 ±1% |
| <sup>240</sup> Pu/Pu | 3.724±0.057 ×10 <sup>-1</sup>   | $3.534\pm0.076 \times 10^{-1}$  | 1.054 ±5% |
| <sup>242</sup> Pu/Pu | $1.503\pm0.004 \times 10^{-2}$  | $1.300\pm0.099 \times 10^{-2}$  | 1.156 ±8% |

Table 3 The ratio of isotopic composition change rate to burnup (EU0004)

|                    | Calculation                      | Experiment                      | C/E       |
|--------------------|----------------------------------|---------------------------------|-----------|
| <sup>235</sup> U/U | $-5.398\pm0.044 \times 10^{-1}$  | $-4.835\pm0.030 \times 10^{-1}$ | 1.116 ±1% |
| <sup>236</sup> U/U | 1.451±0.014 ×10 <sup>-1</sup>    | 1.355±0.005 ×10 <sup>-1</sup>   | 1.071 ±1% |
| <sup>238</sup> U/U | $3.879 \pm 0.003 \times 10^{-1}$ | 3.475±0.033 ×10 <sup>-1</sup>   | 1.116 ±1% |

Table 4 The ratio of isotopic composition change rate to burnup (EU0013)

|                    | Calculation.                    | Experiment                      | C/E       |
|--------------------|---------------------------------|---------------------------------|-----------|
| <sup>235</sup> U/U | $-5.376\pm0.024 \times 10^{-1}$ | $-4.907\pm0.041 \times 10^{-1}$ | 1.096 ±1% |
| <sup>236</sup> U/U | 1.467±0.015 ×10 <sup>-1</sup>   | 1.351±0.020 ×10 <sup>-1</sup>   | 1.086 ±3% |
| <sup>238</sup> U/U | $3.909\pm0.010 \times 10^{-1}$  | 3.548±0.037 ×10 <sup>-1</sup>   | 1.102 ±1% |

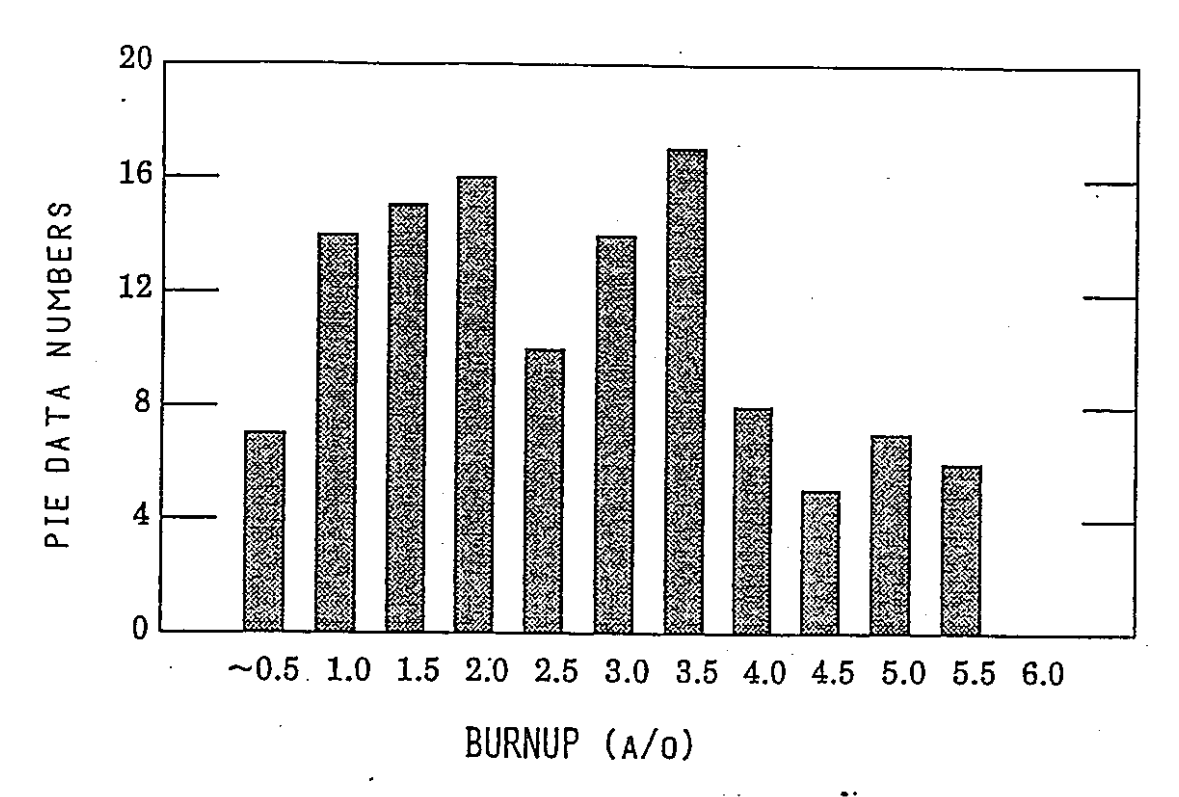


Fig.1 Distribution of PIE data for core fuel pellets as a function of burnup

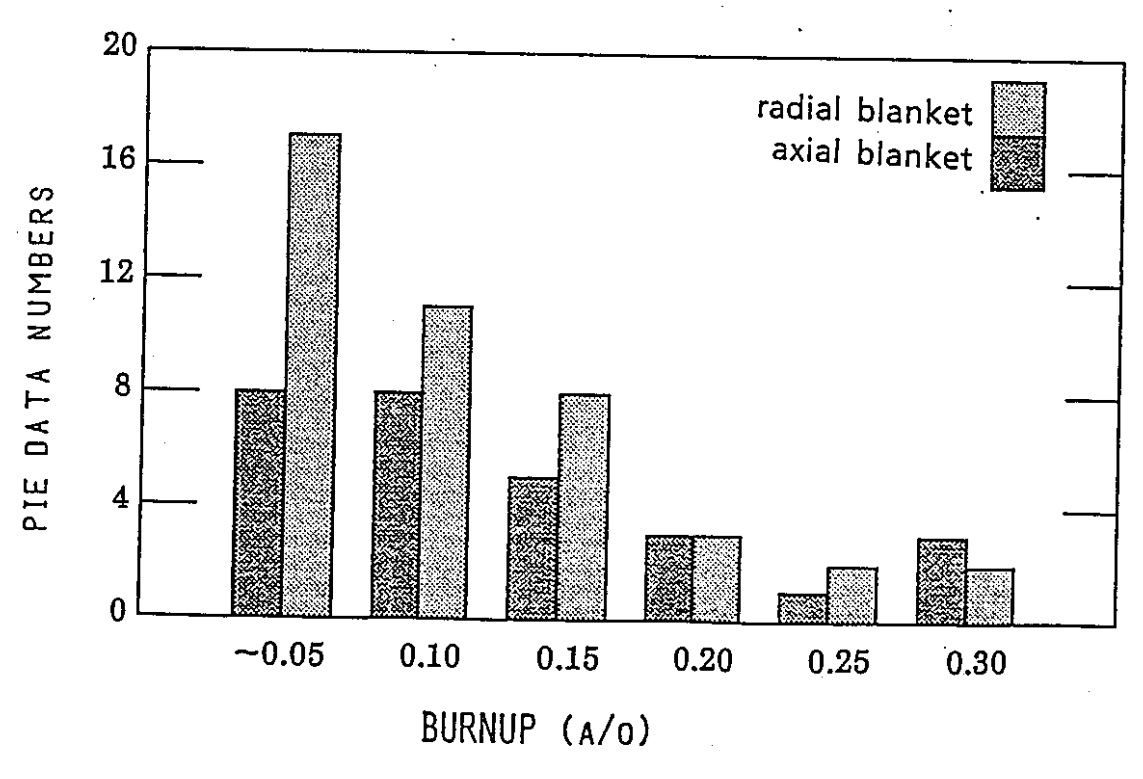
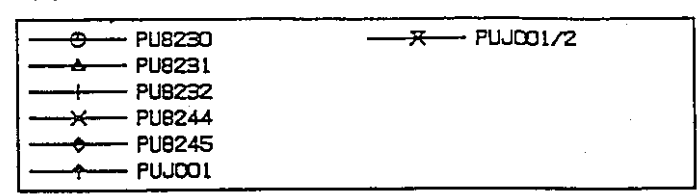


Fig.2 Distribution of PIE data for blanket fuel pellets as a function of burnup

Fuel fabrication lot



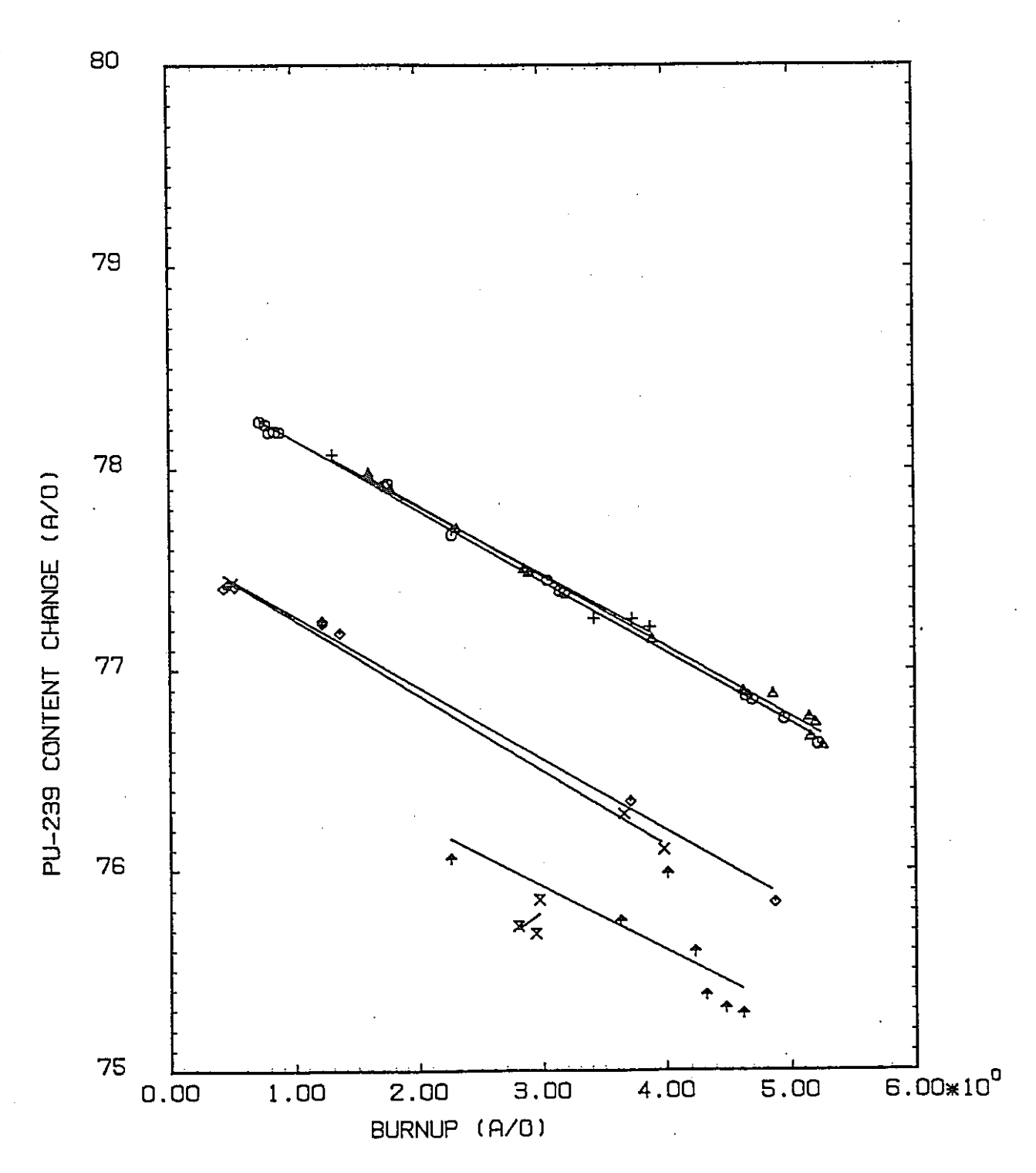


Fig.3 Change of isotopic ratio of <sup>239</sup>Pu for the core fuel as a function of burnup

Fuel fabrication lot

| ——— PU8230  |  |
|-------------|--|
| ——— PU8231  |  |
|             |  |
| ———— PUJ001 |  |

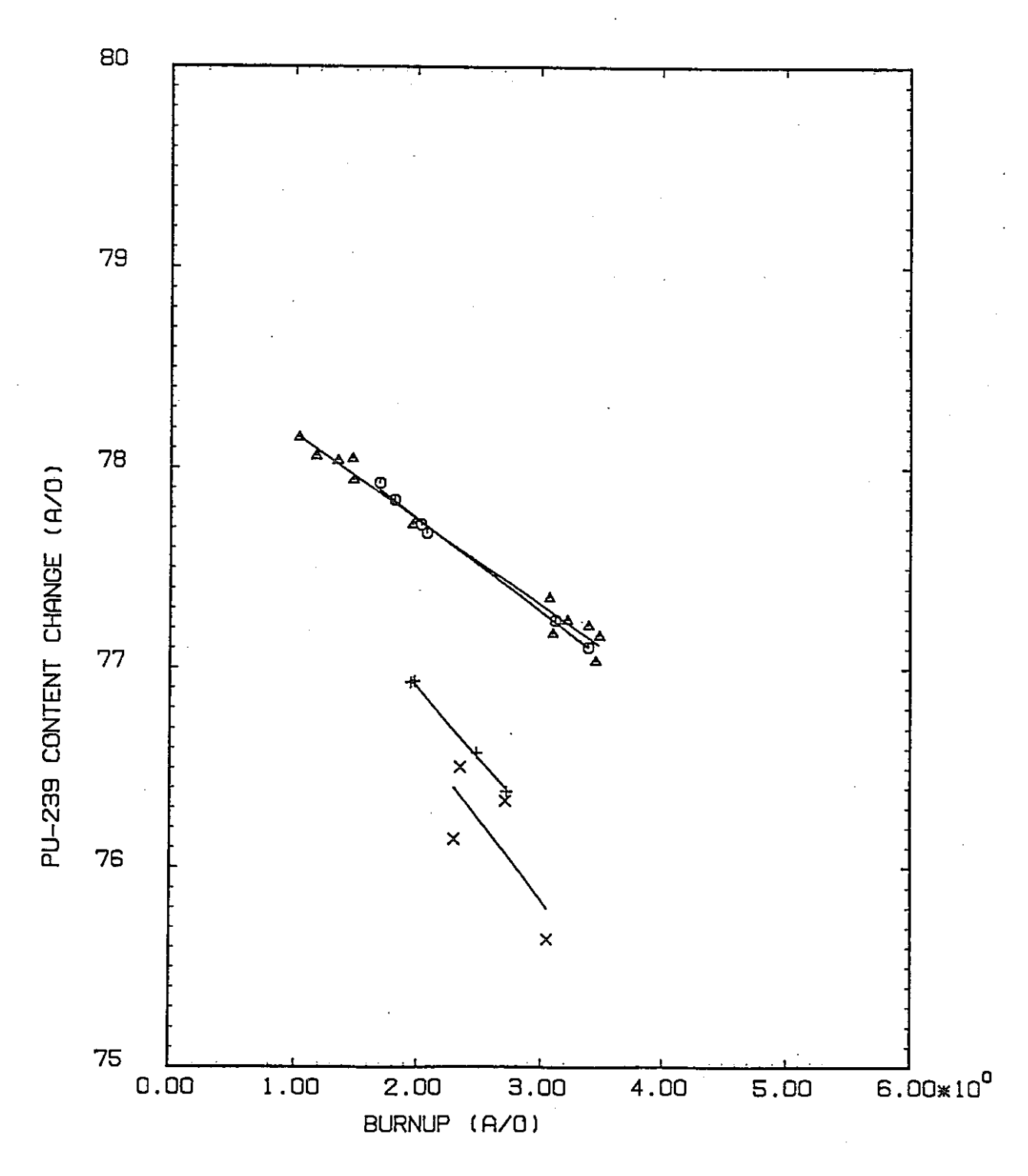


Fig.4 Change of isotopic ratio of <sup>239</sup>Pu for the axial blanket fuel as a function of burnup

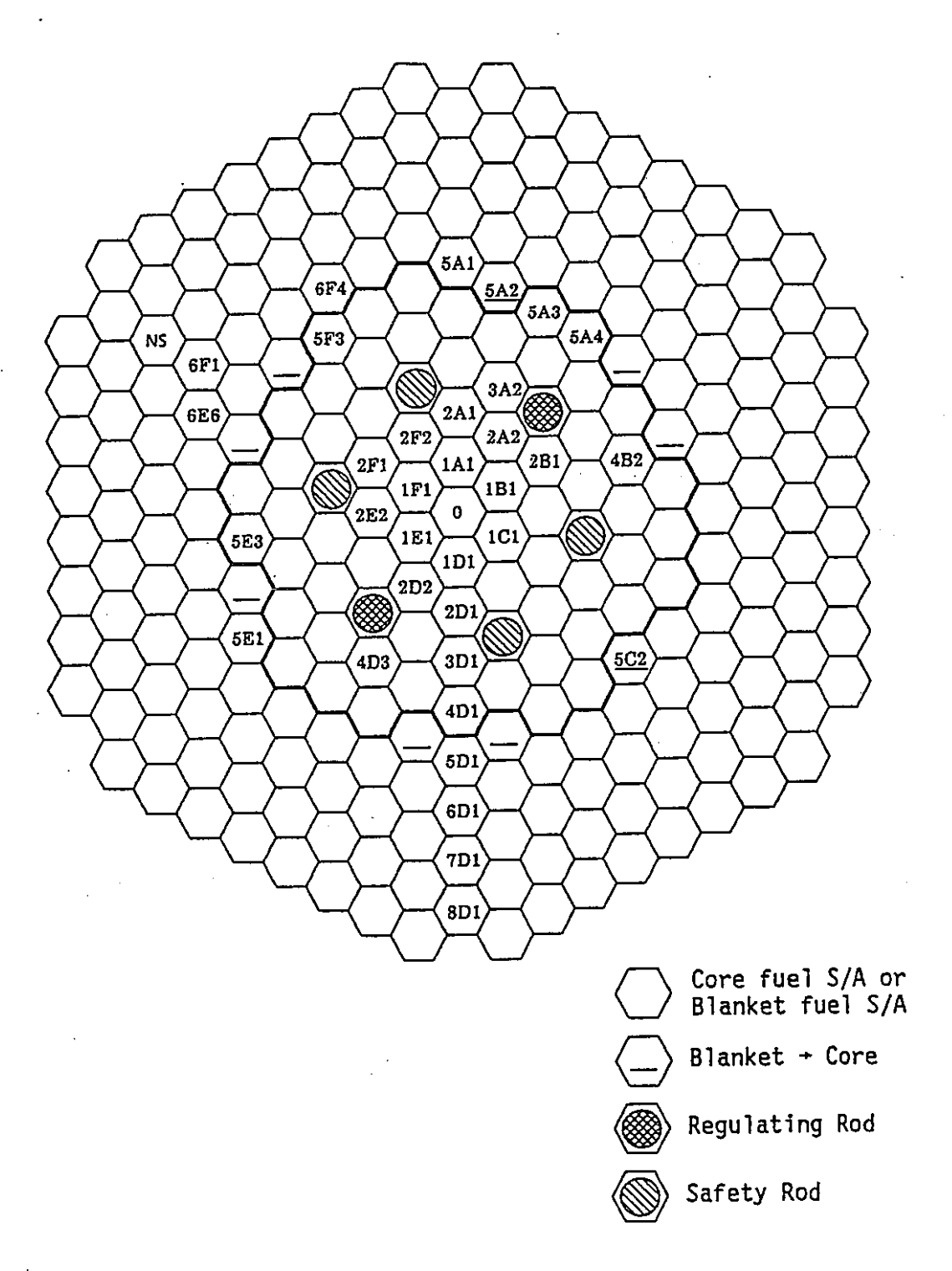
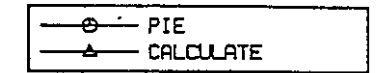


Fig.5 Core configuration of the JOYO MK-I core



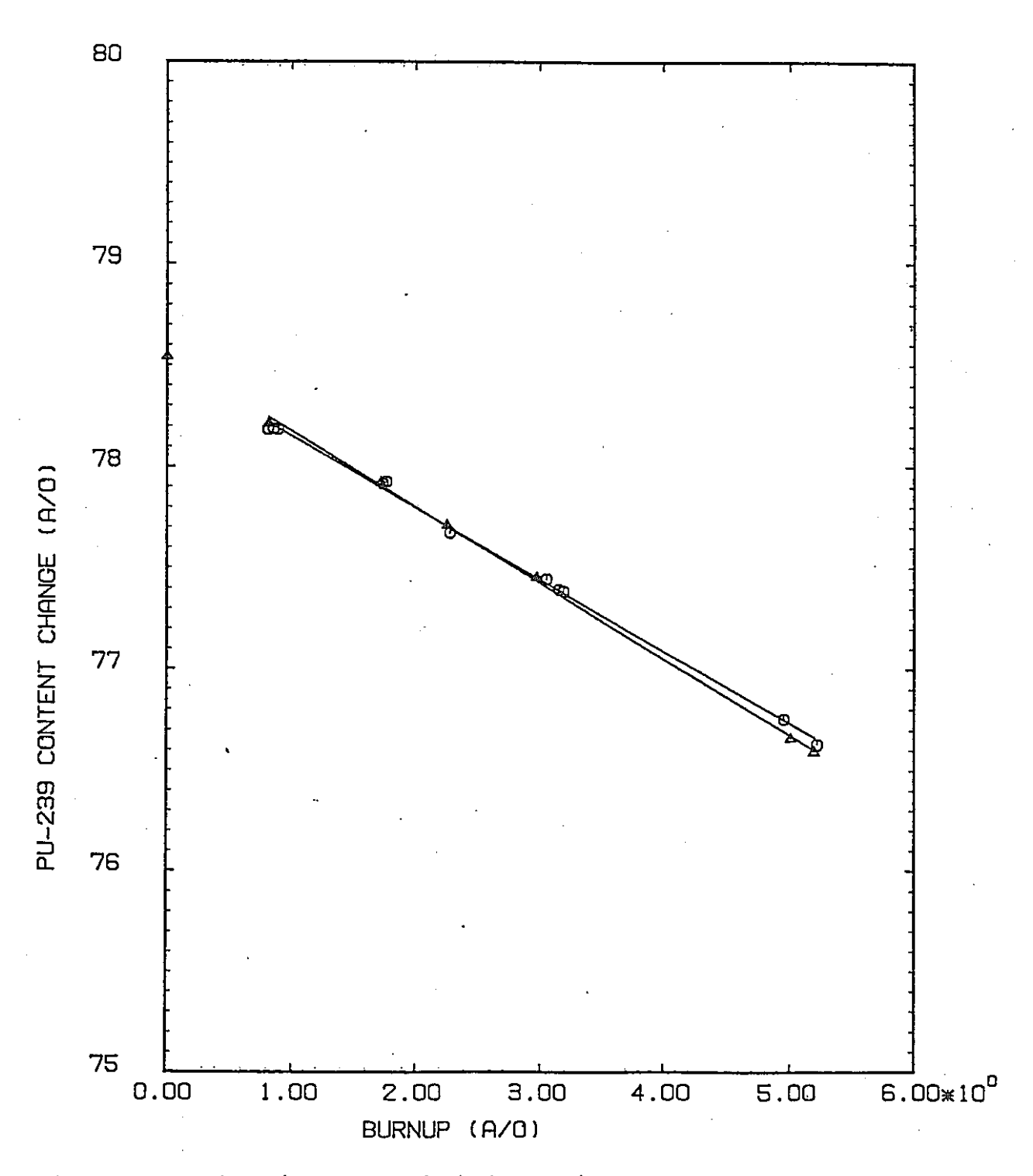


Fig.6 Comparison between calculation and experiment for the change of isotopic ratio of <sup>239</sup>Pu as a function of burnup

セッション2.3

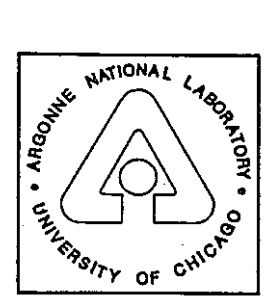
NEACRP-A-1090

2.3

#### HAZARD QUANTIFICATION FOR LWR SPENT FUEL

R. N. Hill

Argonne National Laboratory 9700 S. Cass Avenue Argonne, IL 670439



#### Hazard Quantification for LWR Spent Fuel

#### R. N. HIII

# Argonne National Laboratory Argonne, Illinois 60439

The actinide management features of the Integral Fast Reactor (IFR) fuel cycle have several potential payoffs which are under investigation. First, by stripping transuranics from the IFR waste stream and recycling them for fission in the reactor, the engineering and licensing aspects of sending IFR reprocessing wastes to a geologic repository can be expected to be eased. Second, the energy content of the minor actinides can be used for resource extension because they are fissionable in the fast neutron spectrum, and when combined with flexibility in the breeding ratio of IFR designs, they can be used to provide either a steady-state or a growing IFR energy economy without an external source of fissile material. Finally, breeding ratio < 1 designs combined with repeated recycle for fission can potentially provide for a means to "burn" transuranics supplied from a source external to the IFR cycle, such as LWR spent fuel or decommissioned sibling IFRs. In this paper, the importance of transuranics in LWR waste will be addressed by quantifying their hazard contribution.

LWR spent fuel waste consists of both fission product and actinide elements. Fission products comprise hundreds of various isotopes with differing decay characteristics. Actinide isofopes include the remaining uranium which has not fissioned (the vast majority of the initial load) as well as transuranics produced by neutron capture. The purpose of this analysis is to assess the hazard associated with the various isotopes in LWR spent fuel. A comprehensive risk analysis would require a detailed modeling of the radionuclide release and transport; whereas, hazard analysis addresses only the consequences of exposure. Hazard has been quantified using various measures and databases. In this paper, the cancer dose (CD) measure developed by Cohen, the annual limit of intake (ALI) International Commission on Radiological Protection (ICRP) limits, and the water dilution (WD) limits from 10 CFR 20<sup>3</sup> will be compared. ICRP data from 1959, 1980, and 1988 will be utilized as well as data from the Biological Effects of Ionizing Radiation (BEIR) I and BEIR III reports.

The cancer dose measure described by Cohen in Ref. 1 utilizes the dose exposure data from the ICRP publications and the cancer risk data from the BEIR reports. Committed dose equivalent data are presented in ICRP Publication No. 30¹ for each isotope in each tissue; this factor represents the dose from intake of radioactive materials during the current year assuming a 50 year life after intake. These data are given for both oral and inhalation exposure where the biological retention time will vary. The BEIR reports are a comprehensive evaluation of the cancer effects of radiation. The BEIR results can be interpreted to yield fatal cancer risk per dose factors as shown in Ref. 1. These factors vary by organ and radiation type; alpha radiation in vital organs is the most likely to cause a fatal cancer. The Cohen methodology sums over all organs to achieve the cancer hazard.

The most recent ICRP oral intake data (Ref. 5) was utilized in conjunction with the BEIR-III (Ref. 7) data to generate fatal cancer risk per unit activity factors for the actinides and fission products. The product of isotopic activities and the cancer risk factors embodies the CD hazard measurement. Detailed isotopic activities were calculated, using the ORIGEN code, for 1 MT of fuel in a typical LWR (3.2% enrichment, 33000 MWd/MT burnup) with post-irradiation decay for times up to 10 million years. To put the cancer hazard in perspective, the CD hazard is normalized to the CD hazard associated with the natural uranium required to produce the 1 MT of fuel (5 MT of natural uranium in equilibrium with its daughters).

The dominant isotopic hazards are shown in Fig. 1. The fission products dominate the hazard curve at discharge; however, their hazard quickly decreases as the short-lived fission products decay dropping

below the level of the initial ore (below 1.0) after about 500 years. The hazard associated with the transuranics extends over a much longer time scale; it does not fall below the level of the original ore for nearly a million years. For the first 5000 years, Am-241 with its 432 year half-life dominates the hazard. Pu-239 and Pu-240 dominate in the 10,000 year time scale, and Np-237 with its 2 million year half-life is hazardous for millions of years.

The ICRP dose commitment data were initially evaluated in 19594; the entire data set was reevaluated in 1980<sup>2</sup> and select isotopes were again modified in 1988.<sup>5</sup> The effect of these data changes on the CD hazard curves is quite significant. In Figure 2, CD hazard curves based on 1959 ICRP data -BEIR I, 1980 ICRP data - BEIR III, and 1988 ICRP data - BEIR III are compared. The normalization factor (hazard associated with 5 MT of natural uranium) is computed using each database; thus, the 1959 curves are normalized to the initial ore hazard calculated using the 1959 data. The old (1959) data shows very different trends from the contemporary data. These differences are caused primarily by the treatment of bone dose; the old data leads to high estimates of the cancer risk for Sr-90 and Ra-226, whereas, the new data greatly enhances the bone cancer hazard for the transuranics. Thus, the 1959 data shows much lower relative transuranics hazards because of the presence of radium in the initial ore and the dominance of transuranics in the spent fuel actinide hazard. In the 1980 ICRP evaluation, the biological retention factor of neptunium is 100 times larger than the retention factor for plutonium; thus, the neptunium hazard (and the long-term actinide hazard) is much higher for this evaluation. In the 1988 ICRP evaluation, the neptunium and plutonium retention values are equal giving an order of magnitude increase in the plutonium hazard and decrease in the neptunium hazard (this causes the crossing of the 1980 and 1988 data curves between 10,000 and 1 million years, see Fig.1 for isotopic curves).

Since food or water contamination is generally agreed to be the most likely mechanism for LWR spent fuel radioisotope release, oral exposure data have been utilized in the preceding analysis. Cancer dose hazards can be calculated in a similar manner for inhalation exposure; the oral and inhalation CD hazards based on the most recent ICRP data are compared in Fig. 3. The fission product contribution to the hazard is much lower for inhalation exposure. This is primarily caused by the fact that actinides are retained much longer in the lungs than in the gastrointestinal tract; whereas, most fission products are nearly totally absorbed through either path. Since the initial ore is also composed of actinides, the relative actinide hazard is similar for inhalation or oral exposure as shown in Fig. 3.

The CD hazard measure is compared to the ALI and WD measures in Figures 4 and 5 for oral exposure; once again the normalization factor is calculated separately for each measure. The ALI hazard measure is based on limits published in the ICRP reports. These limits utilize the dose commitment factors developed by the ICRP and a constant tissue weighting. Basically, the hazard/dose is calculated using the tissue weighting formula described in Ref. 2; whereas, the CD hazard utilizes a more detailed tissue weighting model based on the BEIR data. The ALI hazard curves appear to agree well with the CD hazard curves as shown in Fig. 4. The WD hazard measure expresses the volume of water necessary to dilute a given activity to acceptable drinking standards. This curve generated from 10 CFR 20 values does not agree well with the CD hazard curves as shown in Fig. 5; in particular, the actinide hazard is significantly lower using the WD hazard measure. However, the WD hazard curves are similar to the 1959 ICRP - BEIR I curve shown in Fig. 2. This suggests that the 10 CFR 20 standards are likely to have been based on the old data and will underestimate the relative transuranic hazard.

In conclusion, fatal cancer dose for complete exposure was used as a hazard measure for LWR spent fuel. The evolution of the cancer dose hazards from 1959 data to the present was shown, and the cancer dose hazard was compared to annual limit of intake and water dilution measures. All cases indicate that the transuranics dominate the long term hazard with Am-241, Pu-239, Pu-240, and Np-237 being the most important contributors. Thus, actinide recycle would significantly reduce the long term radiological hazard associated with the LWR spent fuel. Therefore, actinide recycle should allow the technical requirements placed on a repository to be met more easily, and seems highly desirable from the point of view of public acceptance. At the same time, however, actinide recycle is not a requirement for high-level waste management, and actinide recycle does not replace the need for a geologic repository.

#### REFERENCES -

- 1. B. L. COHEN, Health Physics, 42, 133 (1982).
- 2. INTERNATIONAL COMMISSION ON RADIOLOGICAL PROTECTION, Annals of the ICRP, 30, Parts 1-3 (1979).
- 3. CODE OF FEDERAL REGULATIONS, 10 CFR 20, (rev. 1990).
- 4. INTERNATIONAL COMMISSION ON RADIOLOGICAL PROTECTION, Annals of the ICRP, 2, (1959).
- 5. INTERNATIONAL COMMISSION ON RADIOLOGICAL PROTECTION, *Annals of the ICRP*, 30, Part 4 (1988).
- NATIONAL ACADEMY OF SCIENCE, "The Effects on Populations of Exposure to Low Levels of lonizing Radiation," BEIR I (1972).
- 7. NATIONAL ACADEMY OF SCIENCE, "The Effects on Populations of Exposure to Low Levels of Ionizing Radition," BEIR III (1980).
- 8. M. J. BELL, "ORIGEN The ORNL Isotope Generation and Depletion Code," ORNL-4628 (1973).

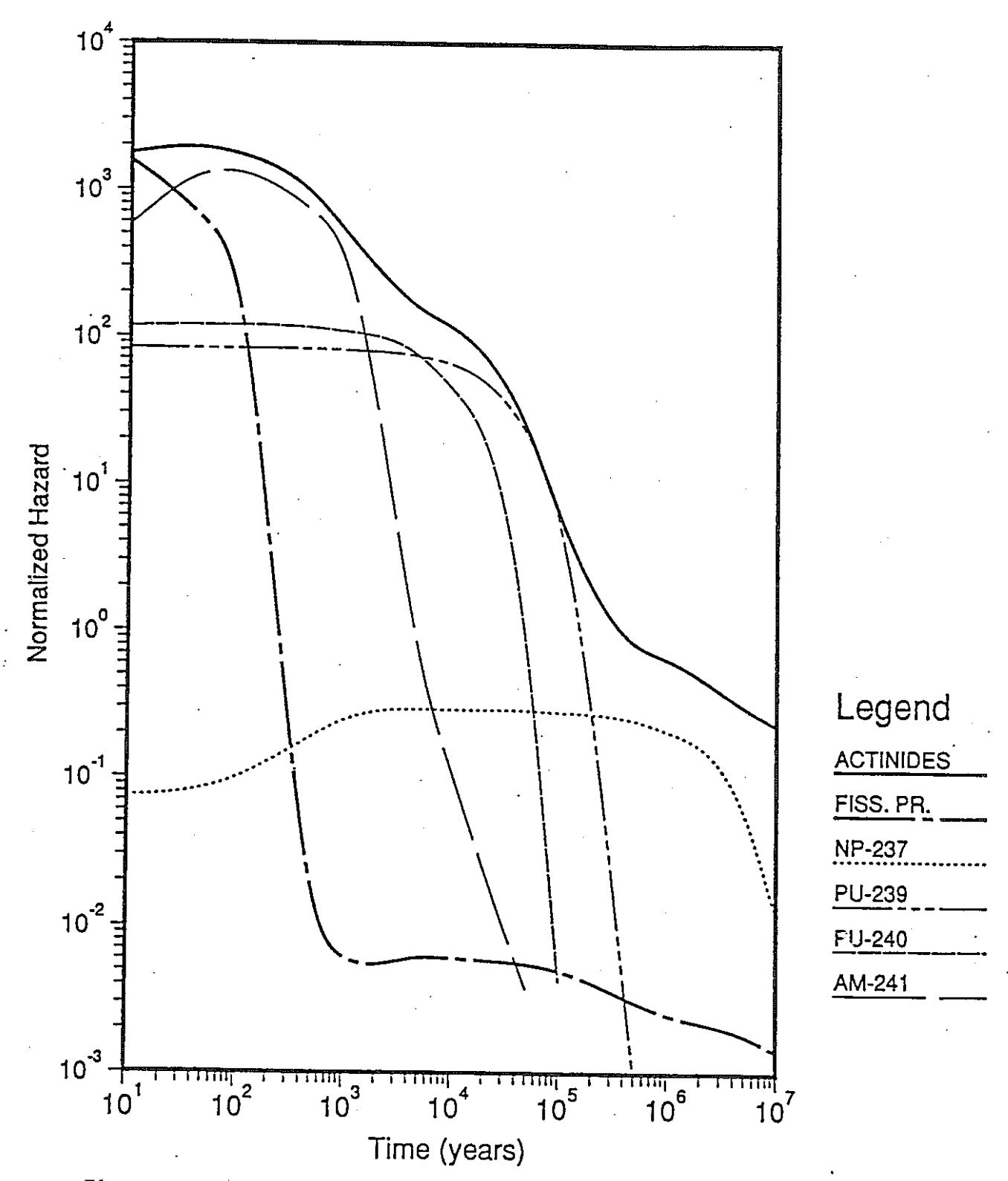


Figure 1: Isotopic Breakdown of Cancer Dose Hazard for oral intake.
Isotopic values are normalized to hazard of initial uranium ore (5 MT of natural uranium for 1 MT of fuel).

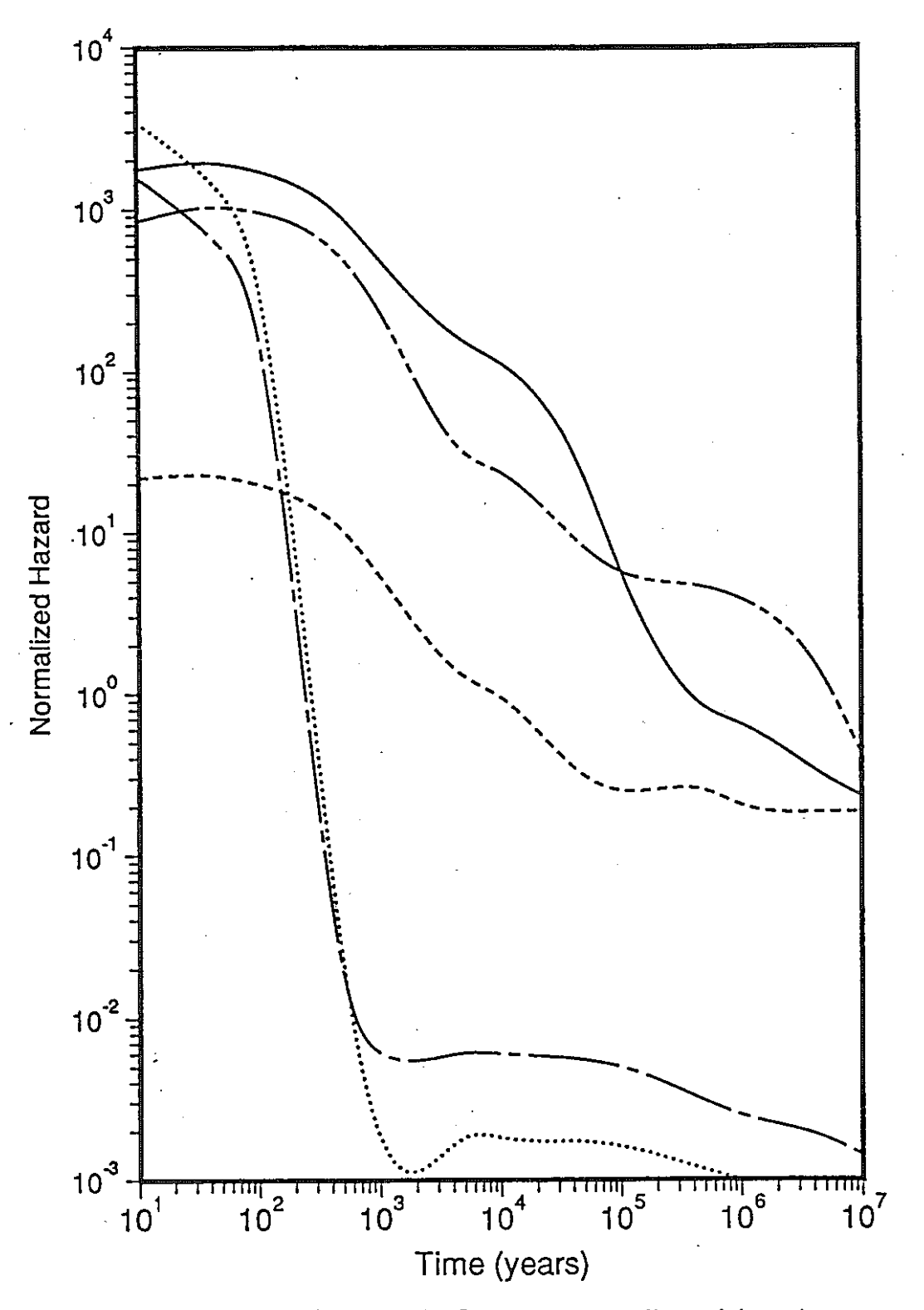


Figure 2: Comparison of Oral Cancer Dose Hazard based on 1959, 1980, and 1988 ICRP data.

Legend

ACTINIDES-88

ACTINIDES-80

ACTINIDES-59

FISS. PR.-80,88

FISS. PR.-59

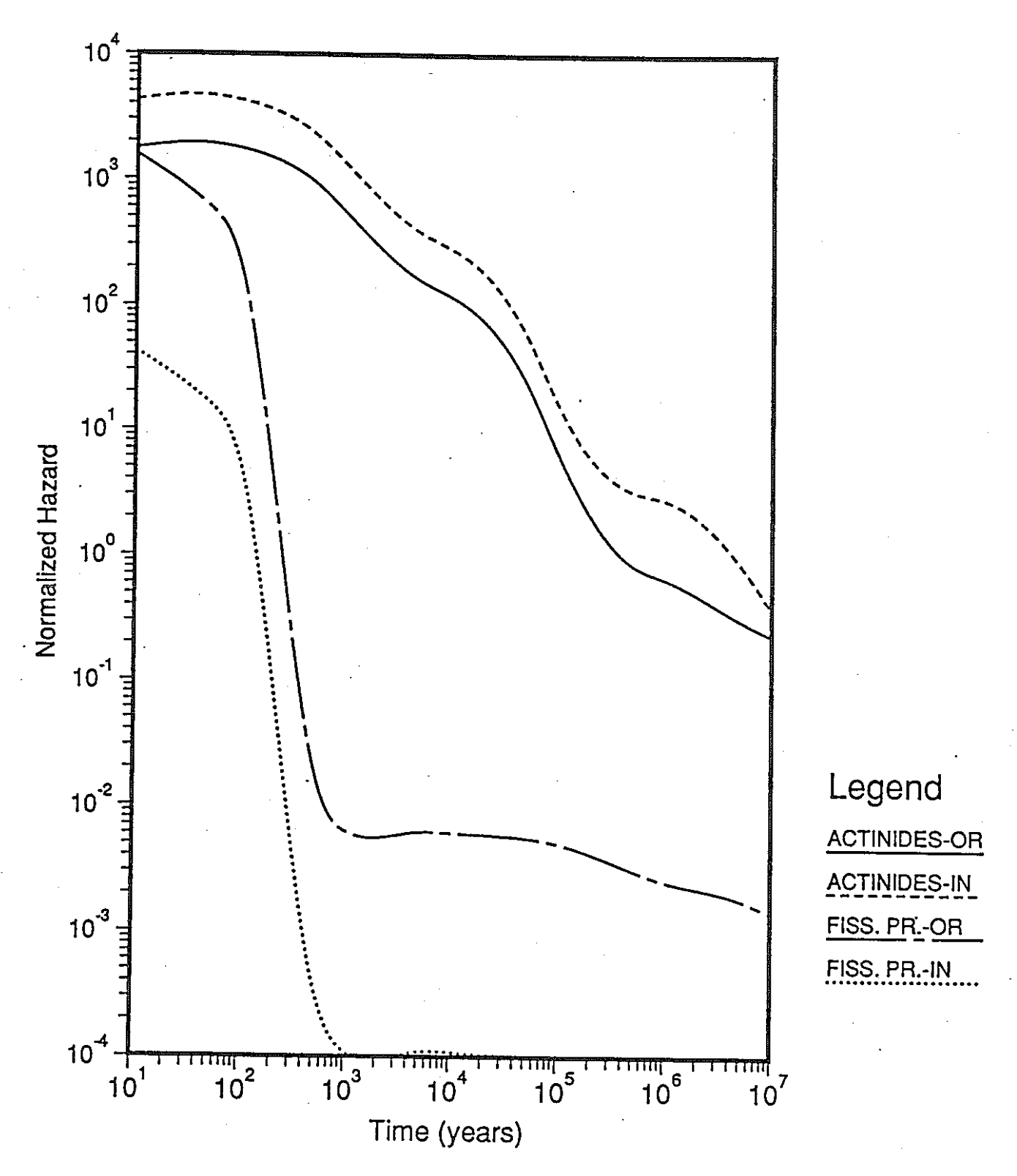


Figure 3: Comparison of Oral (OR) and Inhalation (IN) Cancer Dose Hazards.

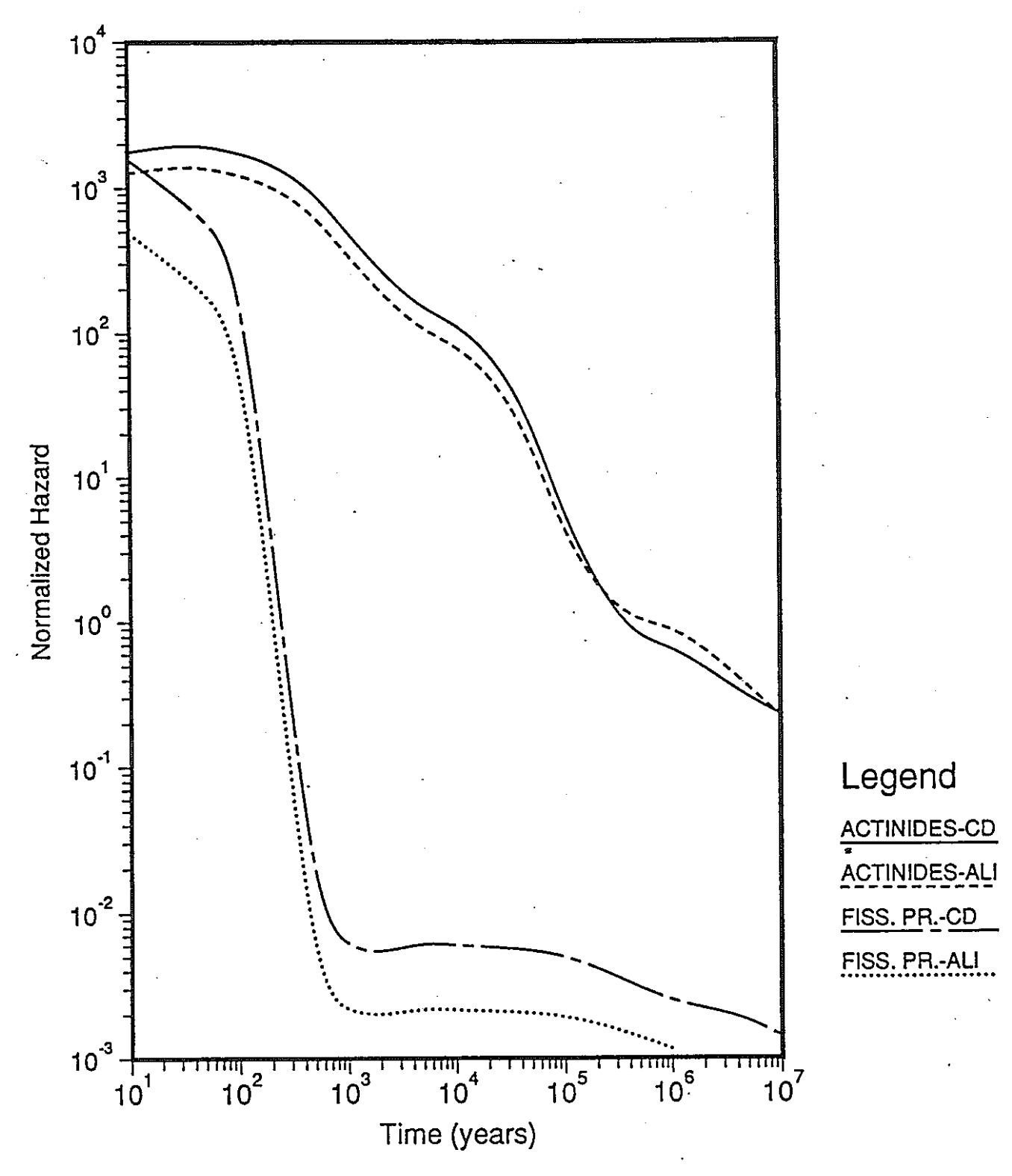


Figure 4: Comparison of Cancer Dose (CD) and Annual Limit of Intake (ALI) Hazard Measures for oral intake.

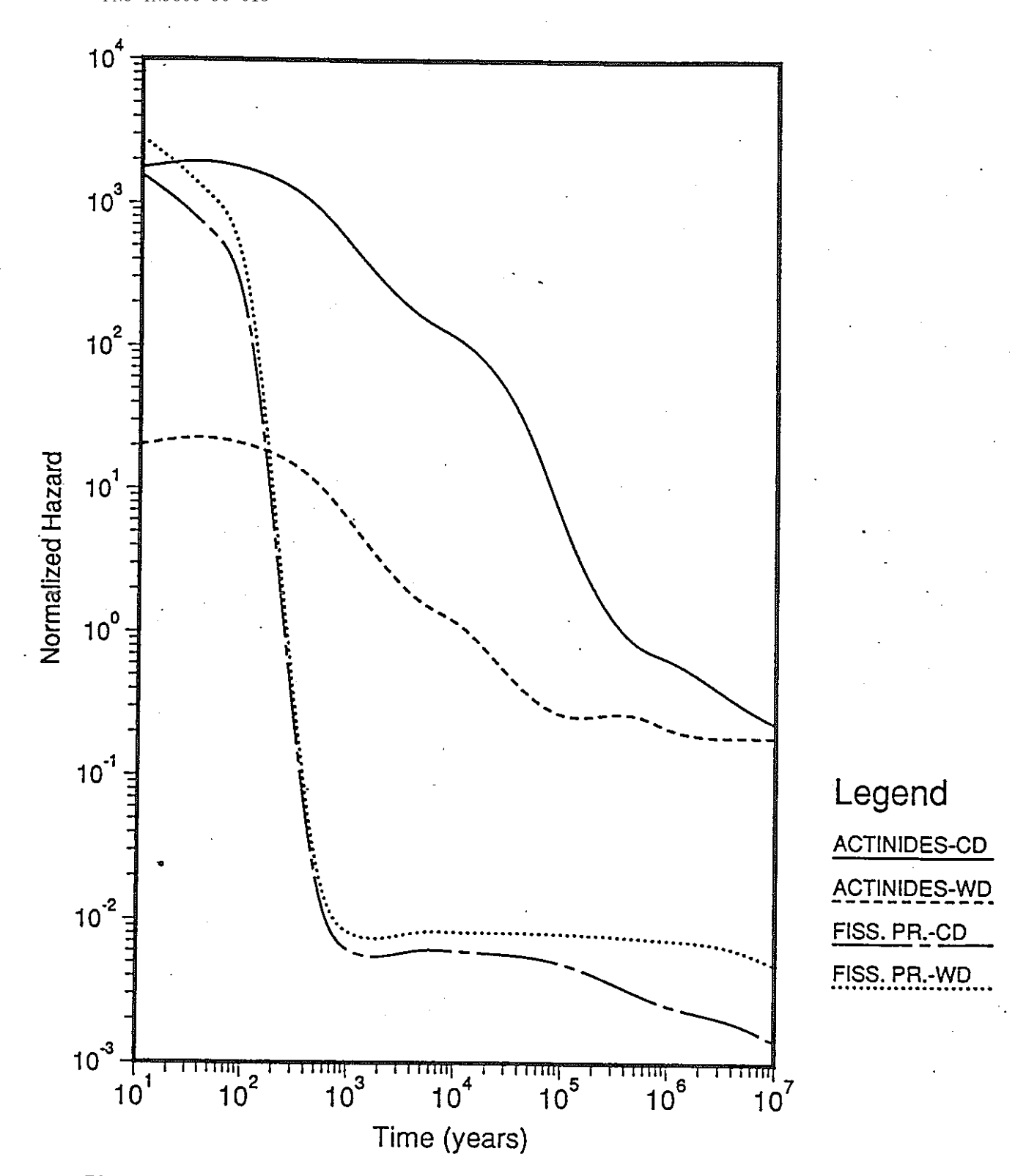


Figure 5: Comparison of Cancer Dose (CD) and Water Dilution (WD) Hazard Measures for oral intake.

NEACRP-A-1062 Topic 2.3

# 33rd NEACRP MEETING PARIS OCTOBER 15-19, 1990

# RADIOTOXICITY OF WASTES IMPACT OF PLUTONIUM RECYCLING

by

M. DARROUZET, G. FLAMENBAUM, J.P. GROUILLER CEA

#### ABSTRACT

Regarding long term radiological impact, the most important element beyond a few hundred years, is plutonium.

This paper aims to answer two questions.

Does the recycling of plutonium in a PWR permit the reduction of the radiotoxic wastes ?

Does the recycling of plutonium have a significant impact on the radiotoxicity of wastes for a large nuclear power capacity?

The conclusion is : plutonium recycling is rather favorable to the reduction of the radiotoxicity of the wastes but globally the impact is limited.

#### INTRODUCTION.

Some of the nuclides produced by irradiation of uranium oxide fuels in reactors, (or nuclides linked by radioactive decays) are radiotoxic during a very long time. They are a potential risk as far as their storage is concerned.

A possible solution to this problem is to destroy these nuclides by recycling them in reactors.

It is very important that the recycling does not increase the risks.

Regarding long term radiological impact, the most important element beyond a few hundred years, is plutonium (chap II).

Several studies have already been performed concerning this problem.

This paper aims to answer two questions.

Does the recycling of plutonium in a PWR permit the reduction of the radiotoxic wastes ? (chap. III).

Does the recycling of plutonium have a significant impact on the radiotoxicity of wastes for a large nuclear power capacity constituted with PWR as in France? (chap. IV).

#### 1 - THE CALCULATIONAL MODEL.

In order to perform this study, the charaterizations of irradiated fuels were calculated with the CEA subassembly CEA code APOLLO and for the post-irradiation decay with the MECCYCO code.

The reactors are 1000 MWe PWR's. The  $\rm U0_2$  fuel is made with enriched (3,7 %) uranium, oxide (from natural Uranium). The average burn up is 45 GWd/t.

To evaluate the radiotoxicity, the values of annual public limits of ingestion have been used. These values are taken from ICPR 30 guidelines modified by ICPR 48 guidelines.

For the MOX fuel, the Plutonium comes from the reprocessing of 45 GWd/t irradiated  $U0_2$  fuel (support : natural Uranium). The initial Plutonium content is about 7,6 %.

2.

2 - THE CONTRIBUTION OF PLUTONIUM TO THE RADIOTOXICITY OF IRRADIATED UOX - FUELS.

In the following table, we give the total radiotoxicity of the irradiated  $U0_2$  fuel  $\mid$  R  $(U0_2)\mid$  and the contribution due to the Plutonium component  $\mid$  R  $(Pu)\mid$ . The radiotoxicities are expressed in arbitrary units.

| Decay<br>(years)     | 101       | 102       | 10 <sup>3</sup>       | 104                  | 105                  | 106                  |
|----------------------|-----------|-----------|-----------------------|----------------------|----------------------|----------------------|
| R (UU <sub>2</sub> ) |           |           | 1.19 10 <sup>10</sup> |                      | 1.58 108             | 4.19 10 <sup>7</sup> |
| R (Pu)               | 4.94 1010 | 4.05 1010 | 1.05 1010             | 2.56 10 <sup>9</sup> | 1.39 10 <sup>8</sup> | 2.58 107             |
| Pu<br>contribution   | 72 %      | 87 %      | 88 %                  | 93 %                 | 88 %                 | 61 %                 |

We can see that the Plutonium contribution is always predominant.

After 10<sup>6</sup> years, following the disappearance of the plutonium, the "natural" radiotoxicity of 238 U and its descendents becomes the principal source.

# 3 - COMPARISON BETWEEN UO2 AND MOX FUEL RADIOTOXICITY AFTER A LONG DECAY.

In table 1 (UOX) and table 2 (MOX) the comparison of the radiotoxicity for a fresh fuel (column 1) and a (45  $\,\mathrm{GWd/t}$ ) irradiated fuel (column 2) is given.

If one examines only the radiotoxicity of irradiated fuels (columns 2) one can say that irradiated MOX fuel is more toxic than irradiated UOX fuel. Therefore recycling of plutonium should not be performed.

In fact, concerning the wastes, this conclusion is not valid.

In effect, the fresh MOX fuel contains Plutonium which, if not recycled, would be part of the wastes. However, the irradiation of this plutonium (in a MOX subassembly) reduces the radiotoxity (column 3, table 2).

This effect is due to the disappearance of  $239p_{\rm u}$  and  $240~p_{\rm u}$  during the irradiation. (35 % to 40 % of plutonium is consumed in reactor).

In conclusion we can see that the recycling of plutonium permits the reduction of the radiotoxicity of the wastes.

#### 4 - IMPACT OF RECYCLING OF PLUTONIUM IN A PWR POWER CAPACITY.

In order to evaluate this impact we have examined two schemes; the situation in France is placed between these two cases.

First, all energy is generated with UOX fuel. The spent fuels are considered as radioactive wastes.

This scheme represents the open cycle.

Second, the irradiated UOX fuels are reprocessed and the Plutonium is used to make MOX fuel. The irradiated MOX fuels are not reprocessed but put into storage. This case is a closed cycle with one recycling.

In the first case, one has in the wastes the radiotoxicity (R1) of the irradiated UOX fuel.

In the second case, one finds in the wastes the radiotoxicity (R2) of the no-recycled elements of the preceding UOX fuel (minor Actinides and lost Plutonium) and of the irradiated MOX fuel fabricated  ${\rm f1_{PNC\ TN9600\ 90-013}}$  Plutonium.

Figure 1 gives the comparison of the radiotoxicities (R2/R1) obtained in the PNC TN9600 90-013  $\,$  s for equivalent delivered energy quantities.

We state here that, even if the gains obtained are not decisive, Plutonium recycling reduces the radiotoxicity of the wastes.

#### CONCLUSION

In this paper, we have examined only long lived <-emitters.
The fission products are not treated, because they have
equivalent effects in the two scenarios. Furthermore, they are
only important in the short term (< 200 years).</pre>

In summary, Plutonium, recycling is rather favorable to the reduction of the radiotoxicity of the wastes.

Globally, the impact of Plutonium recycling is limited.

.../.

Tableau l

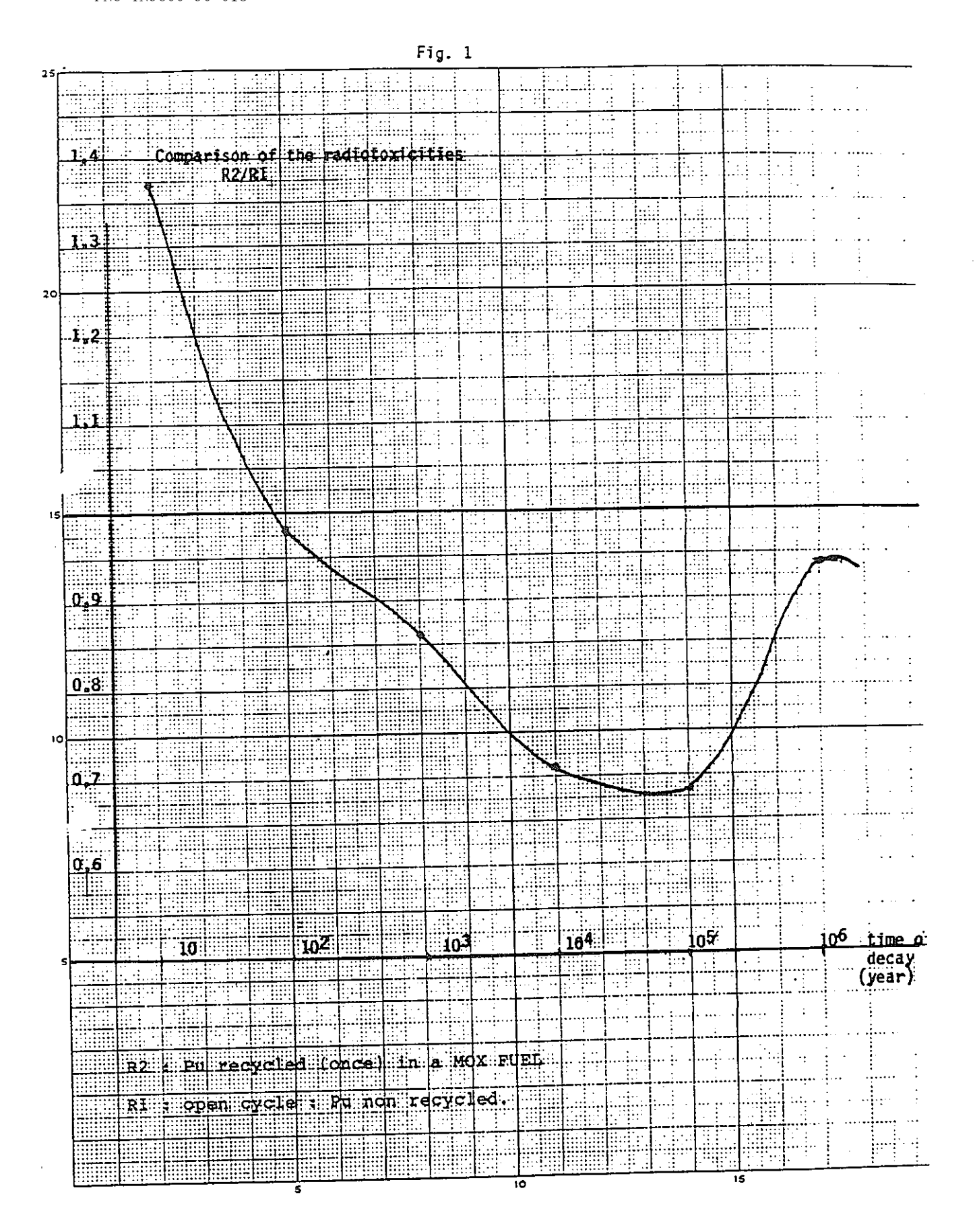
# RADIOTOXICITY (a.u.) UOX FUEL

| Time of decay<br>(years) | (1)<br>Fresh<br>fuel | (2) Irradiated fuel (45 Gwd/t) |
|--------------------------|----------------------|--------------------------------|
| 102                      | < 10 <sup>6</sup>    | 4.64 10 <sup>10</sup>          |
| 103                      | < 10 <sup>6</sup>    | 1.19 1010                      |
| 104                      | ≼ 106                | 2.77 10 <sup>9</sup>           |
| 105                      | < 10 <sup>6</sup>    | 1.58 108                       |
| 106                      | 2.5 106              | 4.19 107                       |

### Tableau 2

# RADIOTOXICITY (a.u) MOX FUEL

| Time of de decay<br>(years) | (1)<br>Fresh<br>fuel | (2)<br>Irradiated<br>fuel (45 GWd/t) | (3)<br>Difference<br>(2) - (1) |
|-----------------------------|----------------------|--------------------------------------|--------------------------------|
| 102                         | 2.70 1011            | 3.10 1011                            | 4.0.1010                       |
| 103                         | 7.00 1010            | 6.95 1010                            | -5.0 108                       |
| 104                         | 1.71 1010            | 1.39 1010                            | -3.2 10 <sup>9</sup>           |
| 105                         | 9.28 108             | 6.95 108                             | -2.3 108                       |
| 106                         | 1.72 108             | 1.96 108                             | 2.4 107                        |



# Reduction of the Long-Term Toxicity of Neptunium by Nuclear Spallation

H.U. Wenger, P. Wydler, F. AtchisonPaul Scherrer InstituteCH-5232 Villigen PSI

#### **ABSTRACT**

The paper reports results of a study of the effectiveness of high-energy particle induced reactions (spallation and fission) for reducing the long-term toxicity of Np-237, the nuclide which dominates the long-term toxicity of the high level radioactive waste from spent fuel.

For a (hypothetical) quasi-infinite Np-237 target and an incident proton energy of 1 GeV, the calculations give a favourable ratio of 3.9 between the high-energy fission and spallation reactions, indicating a good "burning" capability. The energy multiplication factor for the target due to the high-energy processes alone is 1.6; it could be improved by using the many free neutrons below 15 MeV (about 30 per incident proton) to generate additional fission power in a multiplying target assembly.

The toxicity of the transmutation products is dominated by spallation products and is 40 to more than 500 times smaller than the toxicity of the original Np-237 and its decay products. The residual long-term toxicity (beyond  $10^7$  years) is about the same as that of natural  $U_3O_8$ .

The theoretically achievable reduction of the toxicity depends on the high-energy fission model. An experimental verification is desirable in order to remove the associated uncertainties.

#### 1. INTRODUCTION

Transmutation by high-energy particle induced reactions has potential as a method for reducing the long-term toxicity of actinides. A practical spallation-based transmutation facility would involve a powerful high-energy proton accelerator and a multiplying target assembly to ensure a good overall energy balance. If the effective multiplication factor of the target assembly is close to 1, the transmutation properties are similar as those of a fast reactor with a hard neutron spectrum. This implies that the viability of accelerator-based transmutation systems depends on whether high-energy particle induced reactions in the target assembly can be enhanced while maintaining an adequate energy balance, and on whether these themselves are viable transmutation processes. This paper provides information relating to the second of these questions: it reports results of a study of the effectiveness of pure spallation processes for reducing the long-term toxicity of Np-237, the nuclide which dominates the long-term toxicity of the high level radioactive waste from spent fuel.

In a practical target assembly, the overall transmutation would come from a broad-band spectrum of (mainly) neutrons and protons; the exact nature of the irradiating spectrum will depend on the geometry and composition of the target. At this stage, the aim is to demonstrate not only that such a system is effective but also identify particular aspects of the overall process which work in favour of or against toxicity reduction. Calculations with speculative 'real' models could hide such information.

Two cases have been considered: both calculate the toxicity following irradiation of samples of pure Np-237 by high-energy protons. In the first case, the interaction products for a thin target are examined: this will examine the effectiveness of the basic high-energy reaction and also produce results that may be compared with those from thin-foil irradiation experiments. The second case considers all the products of the nucleon-meson cascade propagated by the incident high-energy protons in a quasi-infinite target: such a system is physically unreal (at the minimum it consists of many critical masses) but will show the maximum contribution from the nucleon-meson cascade.

#### 2. CALCULATIONAL METHODS

The interactions have been calculated using the PSI version of the HETC [1] code package. A full description of the physics may be found in references [2]-[5] so only a very brief summary will be given here.

The fundamental part of HETC is the calculation of the interaction of nucleons and mesons with nuclei. This is done with a two-stage model. The first stage is an intra-nuclear cascade of individual particle-nucleon interactions governed by the usual high-energy physics kinematics and conservation laws and 'free' particle-nucleon cross-sections; that the nucleons are bound in a nucleus enters the interaction via their Fermi momentum and the need to satisfy the exclusion principle. The outcome of this first stage is a set of escape particles and a residual nucleus in an excited energy state. The second stage of the calculation uses the statistical model to follow the de-excitation of this nucleus to the ground state. The PSI version of HETC has been modified to include a treatment of fission [6].

The lower limit of the valid energy-range for the model is indistinct but lies somewhat below 50 MeV for nucleons and comes from the increasing contribution of interactions which involve the nucleus collectively. Normally 15 MeV is selected as being slightly under the typical upper energy limit for neutron cross-section data sets; it provides a convenient link to fast-neutron transport codes.

Calculations, using this model, of an integral measurement performed at Los Alamos for proton irradiation of thick uranium and thorium targets [7] gave adequate agreement with experiment.

The thin target calculation considers only a single interaction of the incident proton; the thick target calculation adds the contribution of the high-energy interaction products through successive generations till the cut-off energy of 15 MeV is reached. The final residual nuclei are collected and transferred to a separate code module for chain-yield analysis and hence time-dependent toxicity estimates.

### 3. MASS YIELDS IN A THIN TARGET

The mass yield distributions resulting from the bombardment of thin Np-237 targets with 1 GeV and 590 MeV protons are shown in Fig. 1. (The contribution of light particles – n, p, deuterium, tritium, He-3, He-4 – has been omitted, since these particles are not relevant in the context of this study.) The two principal components, fission products (A < about 170) and spallation products (A > 170) both show a broader distribution at the higher proton energy. The prominent dip, from a mass of about 210 upwards, is a consequence of the assumptions built into the fission model concerning the transition from sub-actinide to actinide/transuranic fission. It is probably incorrect. As will be

seen below, in terms of toxicity, such details are not too important.

The total fission cross-sections which come out of the calculation ( $\sigma_{\rm fiss} = 1.2$  b,  $\sigma_{\rm tot,inel} = 1.9$  b for 1 GeV protons,  $\sigma_{\rm fiss} = 1.4$  b,  $\sigma_{\rm tot,inel} = 1.9$  b for 590 MeV protons) are within 20% of measured values [8,9]. On the other hand, comparison of the mass yield distributions with those reported by Nishida et al. from JAERI [10] reveals considerable differences. In particular, the high-energy fission model in NMTC/JAERI suggests fewer fissions than the respective HETC model.

The relatively large fission probability is an important advantage of spallation-based transmutation systems. However, Fig. 1 also illustrates a disadvantage of these systems, namely the simultaneous production of other undesirable long-lived nuclides such as U-236.

## 4. MASS YIELDS IN A QUASI-INFINITE TARGET

In order to investigate the effect of the nucleon-meson cascade on the mass yield distribution, a large cylinder of Np-237 is irradiated by an incident proton beam of 1 GeV. The length (60cm) and the radius (40cm) of the cylinder are chosen such that most particles slow down to the cutoff energy of 15 MeV within the target and the number of escaped particles is very small.

The mass yield distribution calculated by HET is shown in Fig. 2. Two obvious effects of the inclusion of the lower energy collisions from the inter-nuclear cascade reactions can be seen:

- The fission processes are even more favoured in relation to the spallation products.
- The double hump in the fission product distribution indicates the influence of the lower energy fissions.

Some important quantitative results (per incident 1 GeV proton) are:

| No. of spallation products   | 1.1      |  |
|------------------------------|----------|--|
| No. of high-energy fissions  | 4.2      |  |
| No. of transmuted nuclei     | 5.3      |  |
| No. of neutrons below 15 MeV | 30.9     |  |
| Total energy deposited       | 1.60 GeV |  |

The high ratio of fission to spallation reactions of 3.9 (1.6 for the thin target) indicates a good actinide burning capability. With a 300 MW proton beam and a load factor of 0.8, about 100 kg of Np-237 per year (i.e. the yearly production from about 7 LWRs) could be transmuted. However, with the calculated energy multiplication factor of 1.6, a thermal efficiency of 33% and an estimated maximum efficiency of 50% for converting the electric power into beam power, this (hypothetical) transmutation system would have a self-sufficiency of only about 25%, i.e. 450 MW or 6% of the power produced by the LWRs would have to be supplied externally. It is clear that a better overall energy balance is desirable, and this could be achieved by using the 31 free neutrons below 15 MeV to generate additional fission power in a (possibly isolated) multiplying assembly.

#### 5. TOXICITY OF THE TRANSMUTATION PRODUCTS

The evolution of the toxicity was evaluated for the mass yields in the quasi-infinite geometry. The decay time was assumed to begin after a short irradiation period, during which no radioactive decay and build-up was considered. All results are normalized to 1 kg of fully transmuted Np-237. Mass yield and activity over a period of 10<sup>7</sup> years were calculated for all decay products, and the activities were then multiplied by dose conversion factors for ingestion compiled from ICRP-30 [11]. The dose factors taken into account are summarized in Table 1.

Figs. 3 and 4 show the toxicity contributions resulting from the spallation products and the high-energy fission products, respectively. Analoguous decay calculations for the thin Np-237 target (mass yield distribution of Fig. 1a) gave essentially the same results, differing by not more than a factor of 2–3.

Within the first thousand years the toxicity of the spallation products is dominated by the decay products of Pu-236, with principal contributions from U-232, Th-228 and Ra-224. Pu-236 originates mainly from the  $\beta^-$ -decay of the spallation product Np-236, a nuclide with two different ground states with half-lives of 22.5 h and 1.1·10<sup>5</sup> y and  $\beta^-$ -decay probabilities of 50% and 9%, respectively. In the decay calculation the Np-236 was assumed to exist only in the short-lived state, since this gives an upper limit for the production of Pu-236.

Between 10<sup>3</sup> and 10<sup>7</sup> years the toxicity is mainly governed by Ra-226 and Pb-210 (from the precursor nuclides Np-234 and U-234), and by Ac-227 and Pa-231. About 65% of

the Pa-231 and Ac-227 originates from the spallation product U-231, the rest comes from direct production.

Beyond  $10^7$  years the toxicity stays almost constant. It is predominantly due to Ac-227 and Pa-231 produced by a second route from U-235 (22%) and Np-235 (76%). Its time behaviour is governed by the U-235 decay ( $T_{1/2} = 7 \cdot 10^8$  y).

The remaining toxicity of the spallation products beyond  $10^7$  years is about the same as that of 1 kg of pure  $U_3O_8$  with natural composition.

From the spallation products, only nuclides in the peak around A=236 give significant toxicity contributions. As mentioned before, the mass yields of the lighter spallation products may be incorrect. Adding these to the main peak would, however, increase the total toxicity of the spallation products by only 35%.

During different time periods the total fission product toxicity is dominated by single nuclides: between 10 and 10<sup>3</sup> years by Cs-137, then by Sn-126, and above 10<sup>6</sup> years by I-129. Between 500 and 10<sup>6</sup> years the contribution of the fission products to the overall toxicity is less than 1% and can therefore be neglected. Around 10<sup>7</sup> years, however, it rises to 15% and then again reduces to less than 1% after 8·10<sup>7</sup> years (beyond the scale of the figures).

Fig. 5 shows the toxicities of Np-237 and its main decay products under the assumption that the reference amount of 1 kg of Np-237 simply decays. Also plotted in the figure is the total spallation product toxicity from Fig. 3.

A comparison shows that between 10<sup>3</sup> and 10<sup>5</sup> years the spallation products are roughly 40 times less toxic than Np-237. After 10<sup>5</sup> years this ratio improves and reaches a maximum at 10<sup>7</sup> years when the toxicity of Np-237 and its decay products is more than 500 times larger. After 3·10<sup>7</sup> years, however, the toxicity of Np-237 decreases to the level of the spallation products and then disappears while the latter stays constant. For the first 300-400 years the spallation products are more toxic than the Np-237 itself, but for this period the transmutation products could be safely enclosed.

#### 6. CONCLUSIONS

The investigations described in this paper allow the following conclusions to be drawn:

- The basic potential of accelerator based transmutation systems for reducing the long-term toxicity of neptunium is confirmed. The high ratio of fission to spallation reactions is an important advantage of such systems. On the other hand, there is some simultaneous production of undesirable long-lived nuclides such as U-235 or U-236.
- The long-term toxicity is dominated by spallation products, and the toxicity of the high-energy fission products can be neglected. The remaining toxicity beyond 10<sup>7</sup> years is about the same as that of pure U<sub>3</sub>O<sub>8</sub> with natural composition.
- Compared with the direct decay of Np-237 and its decay products the toxicity of the spallation products is 40 to more than 500 times smaller for the time period between  $10^3$  and  $\sim 2 \cdot 10^7$  years.
- The theoretically achievable reduction of the toxicity depends on the high-energy fission model. An experimental verification is desirable in order to remove the uncertainties associated with this model.
- An accelerator based transmutation system which relies on high-energy reactions alone would not have a very favourable overall energy balance. There are, however, many free neutrons below 15 MeV which can be used to generate additional fission power in a multiplying target assembly.

#### 7. REFERENCES

- [1] RSIC Computer code collection number CCC-178
  - W.A.Coleman, T.W.Armstrong, ORNL-4606 (1970)
  - K.C.Chandler, T.W.Armstrong, ORNL-4744 (1972)
- [2] V.F.Weisskopf, Phys. Rev. <u>52</u>, 295 (1937)
- [3] R.Serber, Phys. Rev. <u>72</u>, 1114 (1947)
- [4] H.W.Bertini, Phys. Rev. <u>188</u>, 174 (1969)
- [5] L.W.Dresner, ORNL-TM-196 (1962)

- [6] F.Atchison, Paper II, Jul-Conf-34 (1980)
- [7] J.S.Gilmore, G.J.Russell, H.Robinson, R.E.Prael, Nucl. Sci. & Eng. <u>99</u>, 41 (1988)
- [8] V.A.Kon'shin, E.S.Matusevich, V.I.Regushevskii, Soviet Journal of Nuclear Physics 4, 69 (1967)
- [9] E.S.Matusevich, V.I.Regushevskii, Soviet Journal of Nuclear Physics 7, 708 (1968)
- [10] T.Nishida, Y.Nakahara, I.Kanno, H.Takada, Y.Kaneko, NEACRP-A-900 (1988)
- [11] ICRP Publication 30, Supplements to Part 1, 2 and 3, Annals of the ICRP, 3 No. 1-4 (1979), 5 No. 1-6 (1981), 7 No. 1-3 (1982), 8 No. 1-3 (1982)

Table 1: Dose conversion factors (mrem/Ci) for ingestion (from ICRP-30 [11])

| Nuclide              | Toxicity             | Nuclide | Toxicity            | Nuclide             | Toxicity            | Nuclide | Toxicity            |
|----------------------|----------------------|---------|---------------------|---------------------|---------------------|---------|---------------------|
| Mn-53                | 9.8 E4               | Fe-60   | 1.6 E8              | Co-60               | 1.0 E7              | Ni-59   | 2.0 E5              |
| Se-79                | 8.5 E6               | Zr-93   | 1.6 E6              | Nb-93m <sup>1</sup> | 5.3 E5              | Nb-94   | 5.2 E6              |
| Mo-93                | 1.3 E6               | Tc-99   | 1.3 E6              | Pd-107              | 1.4 E5              | Sn-126  | 2.7 E7 <sup>2</sup> |
| Sb-126m <sup>1</sup> | 7.5 E4               | I-129   | 2.7 E8              | Cs-135              | 7.0 E6              | Cs-137  | 5.0 E7              |
| Gd-148               | 2.1 E8               | Pt-193  | 1.1 E5              | Au-194              | 2.0 E6              | Hg-194  | 6.0 E6              |
| T1-202               | 1.5 E6               | Pb-202  | 3.9 E7              | Pb-209              | 2.0 E5              | Pb-210  | 5.0 E9              |
| Pb-211               | 4.4 E5               | Pb-212  | 6.2 E7              | Pb-214              | 5.8 E5              | Bi-210  | 4.8 E6              |
| Bi-213               | 6.8 E5               | Bi-214  | 2.4 E5              | Po-210              | 1.6 E9              | Ra-223  | 5.6 E8              |
| Ra-224               | 3.3 E8               | Ra-225  | 3.0 E8              | Ra-226              | 8.2 E9 <sup>2</sup> | Ac-225  | 9.6 E7              |
| Ac-227               | 1.5 E10 <sup>2</sup> | Th-227  | 3.6 E7              | Th-228              | 3.8 E8              | Th-229  | 3.9 E9 <sup>2</sup> |
| Th-230               | 5.6 E8               | Th-231  | 1.3 E6              | Pa-231              | 1.1 E10             | Pa-233  | 3.3 E6              |
| U-232                | 1.3 E9               | U-233   | 2.7 E8              | U-234               | 2.6 E8              | U-235   | 2.5 E8              |
| U-236                | 2.5 E8               | U-238   | 2.5 E8 <sup>2</sup> | Np-237              | 4.1 E10             | Pu-236  | 1.5 E8              |

<sup>&</sup>lt;sup>1</sup>nuclide with metastable state

<sup>&</sup>lt;sup>2</sup>including contribution of short-lived daughter nuclides

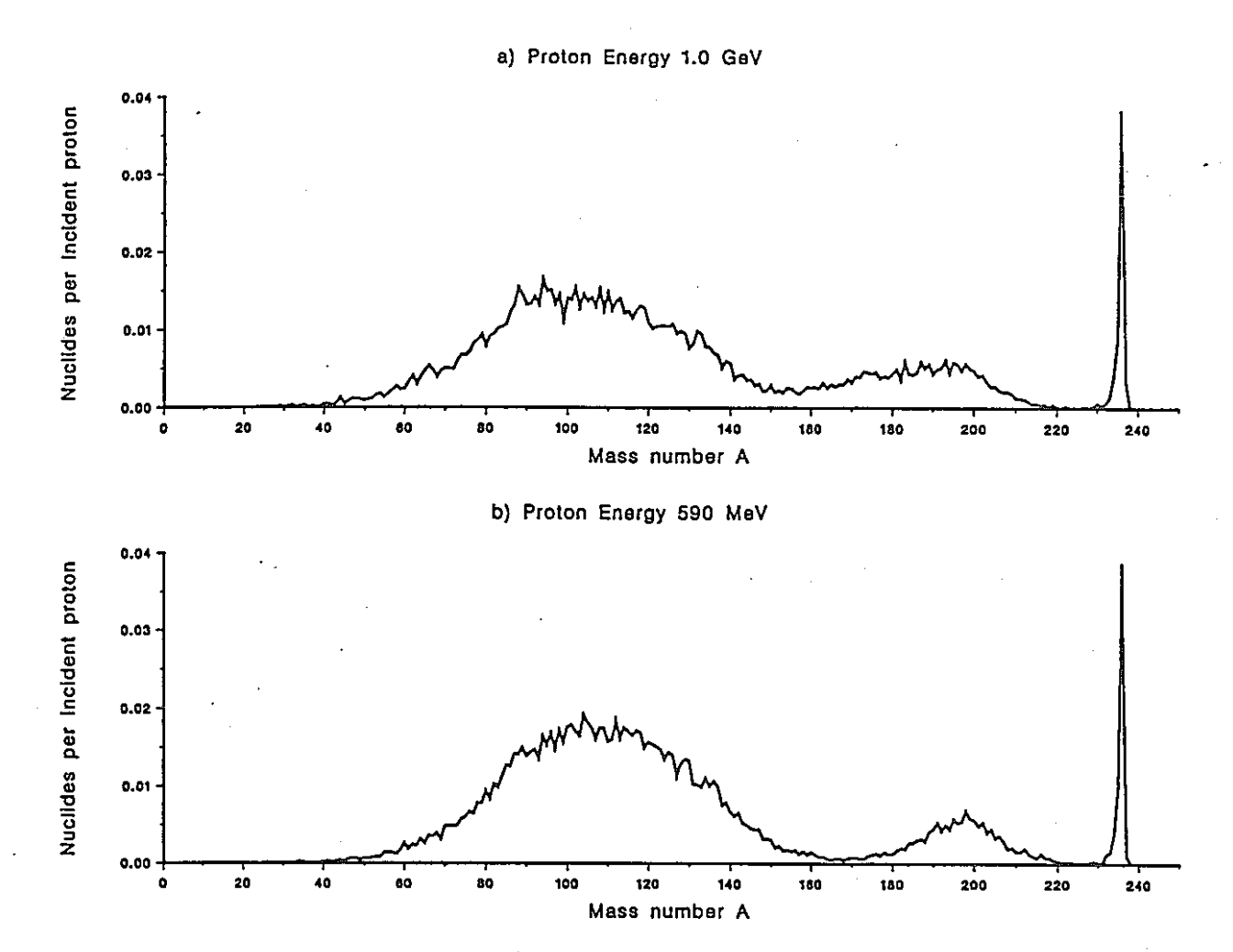


Figure 1: Mass yield distribution from bombardment of a thin Np-237 target with protons of different energies

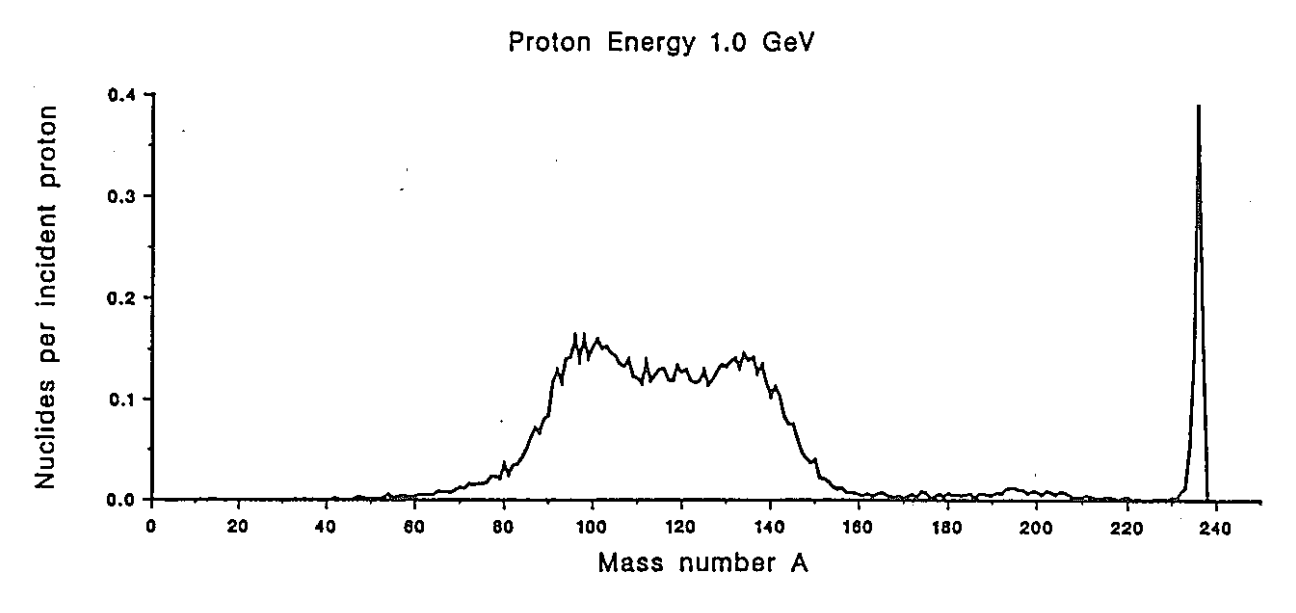


Figure 2: Mass yield distribution from bombardment of a quasi-infinite Np-237 target

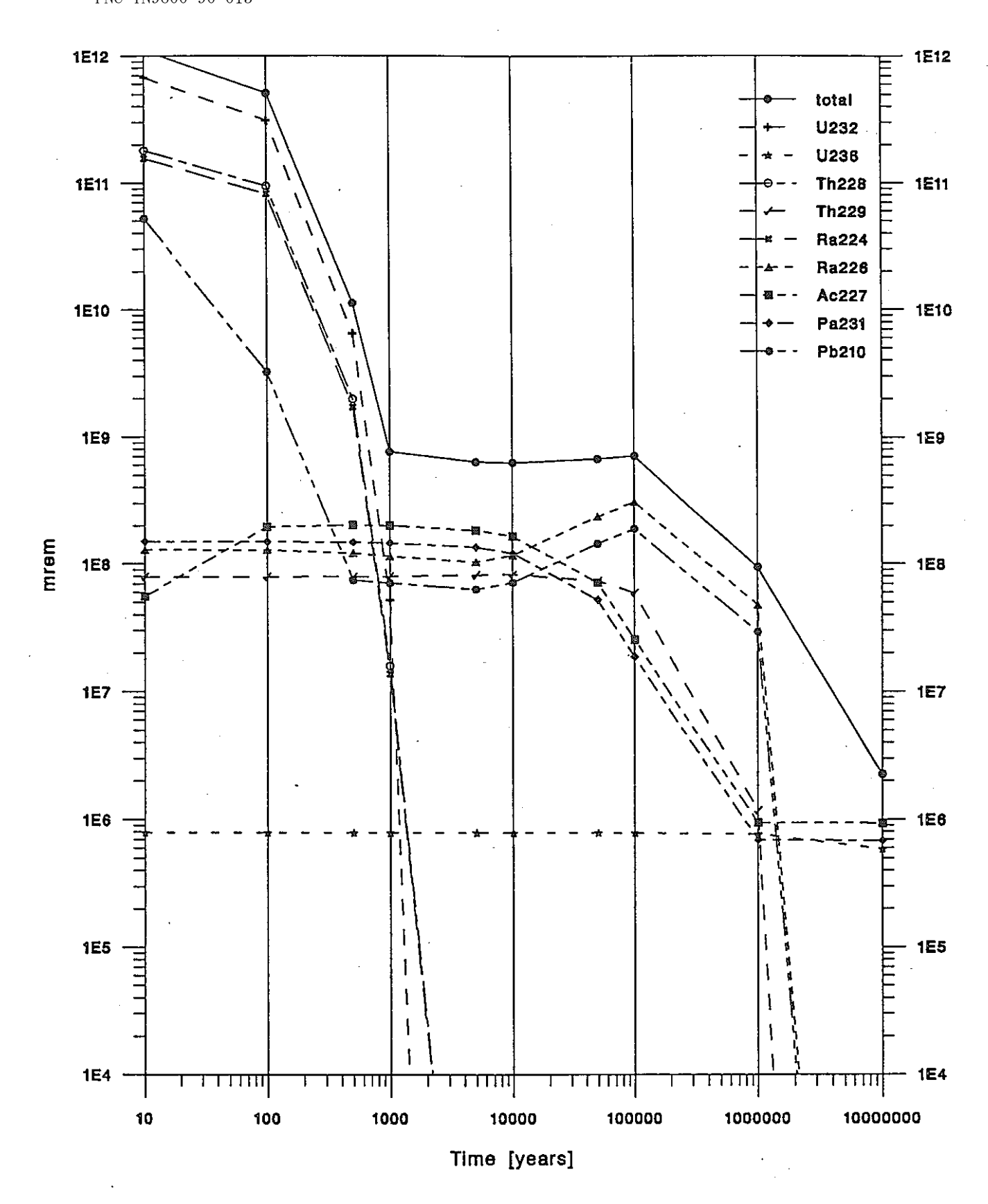


Figure 3: Long-term toxicity of Np-237 spallation products (1 GeV protons, quasi-infinite target)

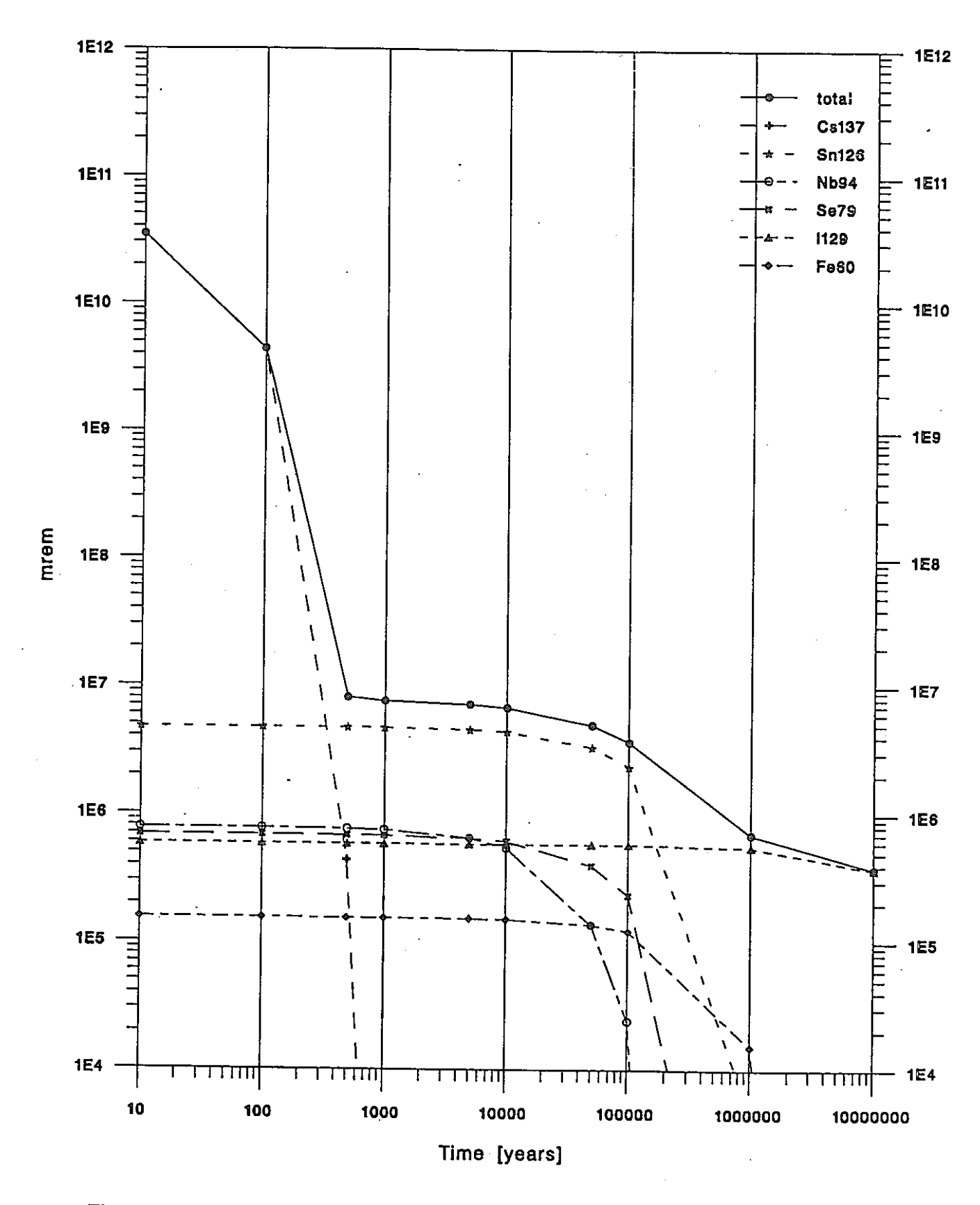


Figure 4: Long-term toxicity of Np-237 fission products (1 GeV protons, quasi-infinite target)

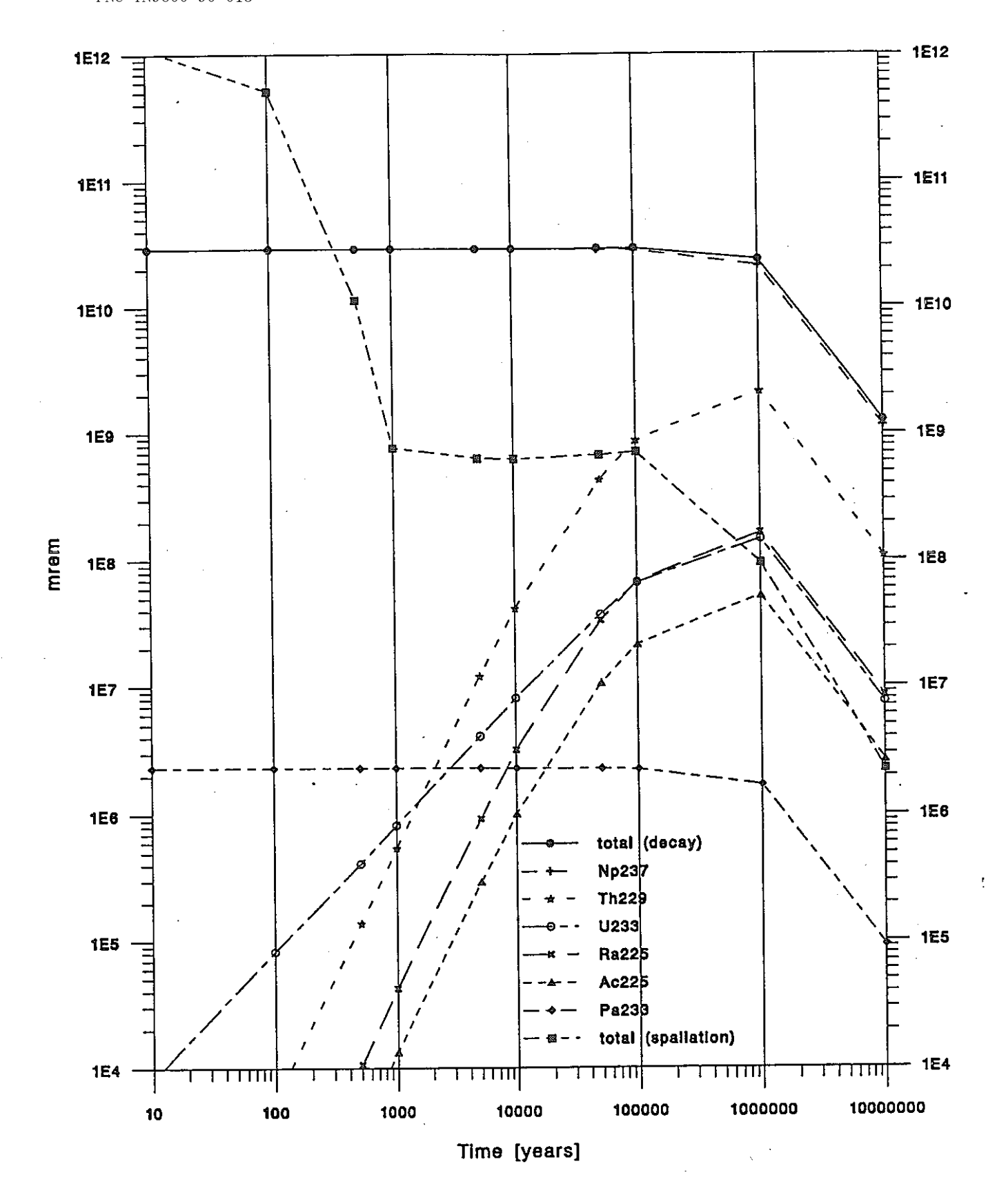


Figure 5: Long-term toxicity from direct Np-237 decay

NEACRP-A-1112

# ON ACTIVIDES TRANSMUTATION POSSIBILITY IN PAST REACTORS WITH VARIOUS COOLANTS

D.F. Tzurickov, A.N. Shmelyov, A.G. Morozov, V.B. Glebov, G.G. Koulickov, V.V. Kuznetzov

I.V.Kurchatov Institute of Atomic Energy, Moscow, USSR

#### INTRODUCTION

At the reprocessing of spent fuel of the reactors which operate in the uranium and uranium-plutonium fuel cycles one finds actinides (Np, Am, Cm) as well as uranium and plutonium traces in radioactive waste. Saying "The transmutation problem of radioactive waste" one means usually burning these actinides in nuclear reactors. Ther has been formed two approaches for solving the problem. The first one suggests that the actinides should be added as a small part to the reactor fuel so that equilibrium can be attained between their forming and burning. Some estimations have shown (see e.g. [11]) that the impact of such an addition on physical features of the reactors is relatively small. This approach suggests availability of numerous burner reactors.

The second approach is related with developping a special nuclear installation. We mean first of all a fast nuclear reactor [2], because the ratio of fission cross-section to radiation capture cross-section increases substantially in the energy range beyond 1 MeV.

In such a reactor a large part of power is to be provided by actinides burning, and the total capacity of burner reactors can be relatively low. In the given paper some physical characteristics of burner reactors are analyzed.

#### 1. NUMERIC MODEL AND SOURCE DATA

The purpose of the current paper is to study the principal neutron physical characteristics of a burner reactor. One should note that space configuration of the reactor is not considered here in details. In connection with this curcumstance the spatial reactor structure is modelled by a simplest homogeneous approximation. The energy dependance is described by multi-group approach.

As the nuclear data basis the ABBN-78 library [3] was used. It was realized in the FORTRAN program complex ARAMAKO-C1.

As the spent fuel the fuel from WWER-1000 reactor was used with initial enrichment 4.4% which was separated (after irradiation with burn-up density 40 MW·d/t) from fission products and kept aftermath during 3 years.

The following functionals are considered:

- (1) To estimate the effectiveness of actinides burning for Np, Am, Cm it is convenient to use the Actinides Annihilation Coefficient (AAC), i.e. the actinides fraction in the total number of fissions in the reactor.
- (2) The effective fraction of delayed neutrons,  $\beta_{eff}$ . Delayed neutrons-related data are taken from [4,5].
  - (3) The average life time of instant neutrons, l.
  - (4) The residual heat power related with radioactive decay,  $q_{_{
    m V}}$  (W/kg).

AAC is an analog to the efficiency of the burner reactor.  $\beta_{eff}$  and l characterize reactor safety and  $q_V$  estimates technological merits of fuel at reprocessing.

Besides the sodium coolant we considered melted lead and steam-water coolants.

#### 2. DISCUSSING RESULTS

The Table 1 represents the results of calculations for the reactor core with the volume composition and the laplacian value corresponding to those of the "low-enrichment core" in BN-350 reactor. The fuel included various actinides from radioactive waste. One can see that if the WWER-1000 spent fuel is used with addition of polluted plutonium to attain core criticality then the fission fraction resulting from Np, Am and Cm burning relatively small and comes up 1.6% - 1.7% depending on coolant. The main core fuel ingredient which is burned and formed again is plutonium. The physical characteristics did not change essentially as a result of adding Np, Am and Cm. But the characteristics do change substantially (see var.1 and 2, 3 and 4, 5 and 6 in The Table 1) if the fuel contains all Np, Am extracted from the WWER spent fuel as well as 1% of the accumulated Pu (Pu extraction at chemical reprocessing is supposed to be carried out with 99%-efficiency).

We should like to mark the following specific features of reactor cores with actinides fuel:

- 1. Small value of the delayed neutrons effective fraction (which has been reduced by 3 4 times depending on coolant). It might seriously complicate reactor control and come to a situation when reactivity effects considerably outweight that of delayed neutrons fraction. In thic case reducing the sodium density only by 10% (in average over the core) causes positive reactivity of value 5 for liquid metal coolants and that of value 14 for steam-water coolant.
- 2. Short life time of instant neutrons (which was reduced by 7 times for liquid metal coolants and by 13 times for steam-water coolant).
  - 3. High value of AAC (e.g. for Np, Am and Cm AAC was about

#### 71.6% - 75.4%).

4. — High values of specific heat power for actinide fuel due to radioactive decay:  $q_{_{\rm V}}\cong$  118.5 W/kg (for WWER-1000 spent fuel after 3 years keeping in a fuel storage  $q_{_{\rm V}}\cong$  3.4 W/kg). It may complicate fuel elements and assemblies production of such a fuel.

To increase the delayed neutrons effective fraction one can add "supporting" nuclides to the fuel which are characterized with two features: the increased fission cross-section for the energy values delayed neutrons appear with and the increased fraction of delayed neytron spectrum (235U, 233U, 240Pu, 241Pu, 242Pu).

To decrease the value of heat power conditioned by radioactive decay one should reduce fractions of the "most energy-producing" nuclides.

The isotopes of Cm constituting only 2% in the mixture give the biggest contribution in the general heat power (\$\approx\$ 76%). The conclusion suggests itself that it makes sense to extract curium from the mixture, and then it is possible to increase Np and Am percentage (taking into account subsequent \$^{239}Pu formation). in actinides-enriched fuel elements. As for Cm, it could be burned in separate fuel elements and in separate cores when being substantially mixed (to provide a reasonable heat power), with the corresponding neutron spectrum being formed. It is possible as well to include keeping the irradiated Cm (until decay of substantial amount of \$^{242}Cm) in the technology cycle. Still, in this case \$^{238}Pu is formed which is known as well by increased heat power though its heat power is lower than that of \$^{242}Cm by 210 times. So, the bulk of the actinides fraction added to fuel elements may be restricted by the heat power considerations.

Necessity to provide reactor criticality with the actinides fraction percentage being moderate prompts analyzing fuel assemblies with low absorbing inert diluter. The results of physical

characteristics calculation for BN-350 reactor are shown in the Table 2. All plutonium is supposed to have been extracted from the actinide fuel; calculation was performed for sodium coolant. Zirconium (Zr) and yttrium (Y) were used as inert diluters, and comparison is made with conventional non-inert diluter ( $^{238}\text{UO}_2$ ). One can see that adding "supporting" nuclide ( $^{235}\text{U}$ ) causes some growth of the delayed neutrons effective fraction. Besides, if the  $^{235}\text{U}$  contribution is 7.55%, then 45% of the  $\beta_{eff}$  growth is conditioned by the higher value of  $^{235}\text{U}$  percentage, and 50% is conditioned by the increased adjoint flux in the energy range inherent to delayed neutrons. Adding  $^{235}\text{U}$  to the fuel yields heat power decrease of the radioactive decay, with  $\beta_{eff}=0.335\%$ , that is comparable with the value of  $\beta_{eff}$  for U-Pu core of a fast reactor.

Using Y as diluter demands higher actinide nuclide fraction then using Zr. If  $^{238}\text{U}$  dioxide is used as the diluter then the fraction of actinides to be burned must be  $\cong$  46% to get the same value of  $\beta_{\text{eff}}$ .

Using inert diluters and decreased actinide fraction in fuel elements give the way to deep once-time burning the mixture which is important at intermediate stages of fuel reprocessing.

#### CONCLUSIONS

A nuclear reactor for transmutation of radioactive actinides, namely, for Am, Np and Cm was studied. It has been shown that actinides burning is performed in the most effective way when plytonium is extracted from the spent fuel and a rigid neutron spectrum is formed. Yet in this case a problem of safe reactor maintenance appears because the effective fraction of delayed neutrons becomes too small and the life time of instant neutrons

is too short. There are difficulties in fuel reprocessing because of high radioactive residual heat.

The following measures are offered to cope with these problems:

- 1. Adding nuclides to the fuel to increase the effective fraction of delayed neutrons. These nuclides are characterized by the increased fission cross-section just for the energy values delayed neutrons appear with, and by the increased generation of delayed neutrons per fission (233U,235U,240Pu,241Pu,242Pu).
- 2. Extracting Cm isotopes which have the highest specific heat power from the mixture and subsequent burning them in separate fuel elements in highly diluted status. Fast decaying 242Sm should be kept in storage until its virtual decay.
- 3. Using metallic fuel with low-absorbing inert diluter (e.g. Zr or Y). It would decrease specific heat power in the fuel and give way to deep once-time actinides burning.

The calculations have shown that using melted lead instead of sodium as coolant does not effect essentially on the analyzed characteristics of burner reactors.

#### References

- 1. S.Pilate, R.de Wonters, G.Evrard, H.W.Wiese, V.Wehmann. Mixed Oxide Fuels with Minor Actinides for the Fast Reactors. Proceedings of the International Conference on the Physics of Reactors: Operation, Design and Computation. April 23-27, 1990, Marceille, France, vol.1, p.73-82.
- 2. T.Mukaiyama, H.Takano, T.Takizuka. Higher Actinides Transmutation Using Higher Actinid Burner Reactors. - Ibid., p.97-107.
- 3. L.Abagyan, N.Bazaziyantz, M.Nikolayev, Tzibulya A.M. Group constants for reactors and shield calculations. (Russ.). Moscow, 1981.
- 4. R.S. Tanczyn, Q. Sharfuddin, W.A. Schier. Nucl. Sci. Eng., 94, 353 (1986).
  - 5. M.S.Brady, T.R.England. Nucl.Sci.Eng., 103, 129 (1989).

Table 1.

Parameters of Bn-350-type core with various coolants

| Coolant                    | wwkR<br>fuel        | enr*; | a <sub>9</sub> | ÅAC<br>% | β <sub>eff</sub><br>% | l<br>10 <sup>-7</sup> s | q <sub>γ</sub><br>k₩/kg | T**   | vari<br>ant |
|----------------------------|---------------------|-------|----------------|----------|-----------------------|-------------------------|-------------------------|-------|-------------|
|                            | Pu<br>present       | 17.7  | .267           | 1.7      | -345                  | 3.41                    | 22.7                    | 004   | 1           |
| sodium                     | Pu<br>extract<br>ed | 77.8  | .154           | 72.0     | .110                  | 0.49                    | 118.5                   | 052   | 2           |
|                            | Pu<br>present       | 17.3  | .253           | 1.7      | .334                  | 3.34                    | 22.7                    | +.004 | 3           |
| melted<br>lead             | Pu<br>extract       | 78.8  | .150           | 71.6     | .115                  | 0.52                    | 118.5                   | 057   | 4 .         |
| steam-<br>water<br>mixture | Pu<br>present       | 18.7  | .427           | 1.6      | -354                  | 4.94                    | 22.7                    | +.003 | 5           |
|                            | Pu<br>extract<br>ed | 92.5  | .222           | 75.4     | .089                  | 0.39                    | 118.5                   | 121   | 6           |

<sup>\*)</sup> enrichment means percentage of trans-uranium elements (Pu, Np, Fm, Cm) in fuel

<sup>\*\*)</sup>  $L = (dK_{eff}/K_{eff})/(d\rho/\rho)$  for coolant

Table 2
Low enrichment core physical characteristics of BN-350 reactor with various fuel

| 235 <sub>U</sub> | Trans-Pu<br>elements | Diluter     | β <sub>eff</sub> | Instant.<br>neutrons<br>life-time | Actinides<br>Annihilat<br>coeffic. |
|------------------|----------------------|-------------|------------------|-----------------------------------|------------------------------------|
| %                | %                    | %           | %                | sec.                              | %                                  |
|                  | Diluter              | is Zr , Fue | el 1s meta       | llic                              | •                                  |
| 0.00             | 54.5                 | 45.5        | 0.060            | 2.76E-8                           | 100                                |
| 6.00             | 30.0                 | 64.0        | 0.236            | 9.48E-8                           | 61.4                               |
| 7.20             | 24.0                 | 68.8        | 0.309            | 1.24E-7                           | 50.8                               |
| 7.60             | 22.2                 | 70.25       | 0.335            | 1.35E-7                           | 47.5                               |
| 7.90             | 19.9                 | 72.2        | 0.372            | 1.52E-7                           | 43.1                               |
| 9.25             | 9.25                 | 81.5        | 0.591            | 2.71E-7                           | 21.6                               |
|                  | Diluter              | is Y, Puel  | is metalli       | LC                                |                                    |
| 0.00             | 53.7                 | 46.3        | 0.060            | 2.79E-8                           | 100                                |
| 6.00             | 29.9                 | 64.1        | 0.232            | 9.23E-8                           | 62.2                               |
| 7.60             | 30.0                 | 62.4        | 0.329            | 1.30E-7                           | 48.4                               |
| 9.65             | 9.65                 | 80.7        | 0.581            | 2.48E-7                           | 22.8                               |
| ,                | Diluter              | is U–238, F | uel is dio       | xide                              |                                    |
| 11.50            | 57.6                 | 30.9        | 0.245            | 7.76E-8                           | 56.6                               |
| 13.80            | 46.1                 | 40.1        | 0.325            | 1.01E-7                           | 45.4                               |

MEACRP-A-1112 B Z-3 bij

## INVESTIGATIONS FOR DESIGN JUSTIFICATION OF ACTINIDES TRANSMUTATION REACTOR.

Bednyakov S.M., Dulin V.A., Korobeinikova I.V., Manturov G.N., Matveenko I.P., Tsibulya A.M.

Paper for 33-d NEACRP meeting, Paris, October, 1990

#### Abstract

Assessment of requirements for actinides nuclear data was carried out on the basis of achieved and required accuracies of physical parameters calculations for LMFBR core loaded by MOX fuel and evenly distributed TRU actinides from spent fuel of BB3P-1000. The influence of nuclear data uncertainties on a criticality calculation accuracy at different actinides content in the fuel was evaluated. Assessments of calculation accuracies was carried out by using sensitivity factors to different types of group constants and their uncertainty covariance matrixes.

Preliminary analysis of some reactivity experiments made on FCA (Japan) for actinide neutron cross-sections correction was carried out. Possible uncertainties due to uncorrect analysis of such experiments were evaluated.

An investigation programme on 6H-350 reactor,  $6\Phi C$  and 6P-1 facilities for near future is described.

1. Assessment of requirements of actinide neutron cross-sections corrections.

The problem of TRU actinides (plutonium, neptunium, americium, curium) contained in irradiated fuel of nuclear reactors can be solved by means of their transmutation to fission products that are accumulated at ordinary nuclear fuel

utilization. This problem in atomic power energetics can be solved by means of their recycling with mixed uranium-plutonium fuel in 5H-600 type reactors.

The number of BB3P-1000 reactors that are served by one 5H-800 may be equal near 20.

#### 1.1 Calculation model.

For the analysis the model of the BH-800 reactor was considered corresponding to the first loading using MOX fuel elements either with or without thermal reactor actinides. RZ-model consisted of three types of zones with different enrichments.

The calculations were carried out for 4 types of core composition: 25%, 50%, 75% and 100% of TRU actinides in fuel.

All physical calculations of different reactor states as well as perturbation theory calculations were carried out by TBK-2D code with APAMAKO-C1 constants preparation on the basis of  $\rm 5HAE-78\ library.$ 

#### 1.2. Accuracy assessment.

The neutron data component of calculational uncertainly of the reactor parameter F is defined as:

$$\mathcal{S}_{\mathsf{F}} = \sqrt{\mathsf{D}_{\mathsf{F}}} = \sqrt{\mathsf{H}_{\mathsf{F}} \mathsf{W} \, \mathsf{H}_{\mathsf{F}}^{\mathsf{T}}}$$

where  $H_F$  is matrix-vector of F sensitivity factors to group cross-sections  $\sigma_x$  of different types of reactions and nuclides, composing reactor core,

$$H_F = \left\| \frac{6x}{F} \frac{dF}{d6x} \right\|$$

and W is an uncertainty covariation matrix of the group cross-sections.

Sensitivity factors ( $H_{\text{F}}$ ) are calculated by TBK-2D code in line with reactor physics calculations.

The uncertainty matrixes of group constants W are still

being assessed for the BHAB-90 nuclear data library and assessment of such matrix for the investigated nuclides cross-sections is available now on the basis of BHAB-78 and ENDF/B-5 data sets.

Sensitivity factors of  $K_{e\!j\!j}$  to capture, fission and inelastic cross-sections (responsible for the main neutron data component in calculational uncertainty) for the different TRU actinides contents in a core are given in Table 1.

The applied estimated uncertainties of fissile nuclides group cross-sections are given in Table 2. The estimated required uncertainty levels resulting from the requirements to calculational accuracy of  $K_{eff}$  are also given in Table 2.

The contributions of different uncertainty sourses (uncertainty of  $\sigma_c$  ,  $\sigma_f$  ,  $\sigma_{in}$ ) to overall one uncertainty of calculational prediction of K  $\,$  5H-800 reactor with different TRU actinides contents are given on Fig.1. As it is seen the contributions of fission and inelastic scattering cross-sections uncertainties of Np-237 and Am-241 increases with TRU actinides content, both contributions being equal.

The dependence of overall K calculational uncertainty on the TRU actinides content in the reactor core is presented on Fig.2. This uncertainty increases from 2.5% for a core without TRU to 4.5% for the core with 100% TRU actinides content. The accuracy level achievable by testing and correction of 5HA5-78 library on the basis of critical assemblies and reactors macroexperiments is shown on the same figure.

2. Preliminary analysis of experimental data on actinides and assessment of possible uncertainties.

Published data on average fission cross-sections and central reactivity worths ratios of actinides interesting from the point of view of transmutation problem [1] were analysed in the way typical for similar BOC experiments [2,3]. Two aspects should be noted here. First, when analysing experimental reactivity worths of small samples by calculational codes, it is necessary to take into account not only a fine resonance and

spatial structure of an adjoint flux but also an angle depandance of neutron flux and adjoint flux. All these effects are calculated in HEEPC (without anisotropy) [3] and TULPE [4] codes used for such an assessment. The values of calculational reactivity worths ratios in heterogeneous media of  $\delta\Phi C$  critical assemblies with spectra similar those of large plutonium reactor are given as an example in Table 3. The hardest spectrum among considered ones in  $\delta\Phi C$ -49-3 critical assembly.

The calculations were carried out using 5HA5-78 library. It is seen that traditional way of analysis (with homogenisation of group constants on fine spatial structure of cell and neutron flux structure) in case of Pu-240 differ considerably from more accurate calculational ways for reactivity worths. The difference for Am-241 is less but it can exceed 10%.

Second, in our opinion, there exists a contradiction between experimental results. In Fig.3 a discrepancy value is given for measured and calculated reactivity worth ratios of Pu-240 and Pu-239 ( $\delta_{abs}$ ) in a number of critical assemblies (FCA and  $\Delta_{abs}$ ). Assessment of experiments (correction of calculation results for experimental conditions) was carried out by HEEPC code.

As seen from Fig.3 the FCA and E&C results are in essential contradiction except FCA-IX-I. It is interesting to find out a cause of such contradictions.

#### 3. Experiments on BH-350, BΦC and BP-1.

At present the first stage of manufacturing and attestation of samples for irraadiation in 5H-350 has been completed. The samples are hermetically sealed tubes  $\emptyset$  1.2\*0.1 mm and 100 long with tested materials inside. The samples in the hermetically sealed ampule (  $\emptyset$  1.6\*0.16 mm) were placed between pins in the fuel subassembly of 5H-350 core. The irradiation the samples of Np-237, Am-241, Pu-238, Pu-240 with masses the range of 0.2-0.5 g started in May, 1990. The analysis will be carried out after one year irradiation. It planned to continue these investigations for Am-243, Cm-244 other isotopes.

At  $5\Phi C$  and 5P-1 critical facilities preparations started for measurements of reactivity worths and fission rates distributions in critical assemblies with different neutron spectra.

#### Conclusion

- 1. The analysis of the neutron data uncertainty of  $K_{\mbox{eff}}$  calculation for BH-800 type reactor with different content of TRU actinides results in following:
- -the uncertainty increases with TRU actinides content and at 100% TRU fuel it is almost 2 times more than in the case of MOX fuel without TRU;
- -there exists a possibility to decrease considerably calculational uncertainty of  $K_{eff}(2-3 \text{ times})$  if neutron data are tested and corrected on the basis of integral experiments carried out on fast critical assemblies and power reactors (EH-350, EH-600) with a 20-30% TRU fuel;
- the main contribution to overall  $K_{eff}$  uncertainty for a core with a significant content of TRU actinides (more than 50%) is made by fission and inelastic cross-sections uncertainties of Np-237, Am-241, Am-243 and Pu-238. Their accuracy is rather low;
- the main contribution to Keffuncertainty at more than 75 % content of TRU actinides is made by inelastic scattering cross-sections uncertainty of Np-237 and Am-241. It is necessary to make in-core integral experiments on measurements of central reactivity worths for these isotopes and to carry out high presision accelerator experiments in order to decrease this uncertainty. It is impossible to decrease Keff calculational uncertainty below 2% without such experiments;
- the uncertainty contributions of Np-237, Am-241, Pu-238 fission cross-sections can be considerably decreased (2-3 times) if their fission cross-section ratios are measured.
- 2. Future development of fast reactor concept with TRU actinides in a fuel requires corrections of following nuclear data:

- -fission products yields for Np-237, Am-241, Am-243 and Pu-238;
  - -delayed neutron data for these nuclides;
- -data on Doppler self-shielding factors change, which are very uncertain now.
- 3. Preliminary analysis of reactivity worth experiments with some actinides indicated that:
- -neglection of resonance and spatial structure of adjoint flux when comparing calculational and experimental central reactivity worths can result in significant errors;
- —an essential discrepancy between results of Pu-240 reactivity worths experiments on FCA and  $\Phi$ C critical assemblies was noted. More accurate analysis is desirable to clarify the cause of the discrepancy.

#### References

- 1. Kajyama T., Obu M., Nakano M. et al. Actinide Integral Measurements on FCA for Evaluating and Improving Their Cross Section Data, NEACRP-A-684, 1985.
- 2. Дулин В.А. Оценка экспериментов по возмущению критичности реакторов при внесении малых образцов. Атомная энергия, 1989, т.66, с.79.
- 3. Бедняков С.М. Реализация метода оценки интегральных экспериментов в условиях стенда БФС. - Препринт ФЭИ - 2114, 1990.
- 4. Heinzelmann B. Das Stosswahrscheinlichkeitprogramm YARAB an der ES 1055, ZfK661, Rossendorf, 1988.
- 5. Бедняков С.М., Дулин В.А., Хайнцельман Б. Экспериментальное и расчетное изучение реактивности малых образцов в критсборках с разной гетерогенной структурой. В сб. "Вопросн атомной науки и техники", серия "Ядерные константы", 1989, вып.3, с.3.
- 6. Бедняков С.М., Безбородов А.А., Дулин В.А. и др. Проверка некоторых реакторных функционалов в экспериментах на быстрых критических сборках. Атомная энергия, 1990, т.69, с.3.

Table 1 One group coefficients of  $K_{\mbox{\it eff}}$  sensitivity to different cross-sections.

| Type of             | N 1 + 3        | TRU actinides contents |         |        |        |        |  |  |
|---------------------|----------------|------------------------|---------|--------|--------|--------|--|--|
| cross-<br>sectión   | Nuclide        | 0%                     | 25%     | 50%    | 75%    | 100%   |  |  |
| •                   | Pu -238        | 0                      | -0.005  | -0.004 | -0.003 | -0.002 |  |  |
|                     | Pu -239        | -0.046                 | -0.0I9  | -0.008 | -0.003 | 0      |  |  |
|                     | Pu-240         | -0.022                 | -0.0II  | -0.005 | -0.002 | 0      |  |  |
| $G_{\!f c}$         | Np -237        | 0                      | -0.06I  | -0.073 | -0.064 | -0.034 |  |  |
|                     | Am -24I        | 0                      | -0.045  | -0.056 | -0.05I | -0.030 |  |  |
| ·                   | Am -243        | 0                      | -0.0II  | -0.0I3 | -0.0II | -0.005 |  |  |
|                     | U -238         | -0.200                 | -0.082  | -0.033 | -0.0II | -0.00I |  |  |
|                     | Fe             | -0.016                 | -0.009  | -0.006 | -0.005 | -0.003 |  |  |
|                     | Ru -238        | 0                      | 0.040   | 0.04I  | 0.079  | 0.160  |  |  |
| -                   | Pu -239        | 0.482                  | 0.368   | 0.263  | 0.148  | 0.002  |  |  |
|                     | Pu -240        | 0.046                  | 0.04I   | 0.029  | 0.018  | 0      |  |  |
| $G_{\!{	extbf{f}}}$ | Pu -24I        | 0.107                  | 0.082   | 0.058  | 0.034  | 0      |  |  |
| J                   | Np -237        | 0                      | 0.070   | 0.147  | 0.200  | 0.300  |  |  |
|                     | Am -24I        | 0                      | 0.045   | 0.095  | 0.130  | 0.192  |  |  |
|                     | Am -243        | 0                      | 0.018   | 0.037  | 0.052  | 0.076  |  |  |
|                     | Np -237        | 0                      | -0.0I0  | -0.030 | -0.049 | -0.093 |  |  |
|                     | Am -24I        | 0                      | - 0.005 | -0.0I6 | -0.026 | -0.05I |  |  |
| $G_{i_n}$           | Am -243        | 0                      | -0.004  | -0.0IO | -0.0I7 | -0.03I |  |  |
| in                  | <b>V -</b> 238 | -0.043                 | -0.055  | -0.05I | -0.029 | -0.006 |  |  |
|                     | Na             | -0.0I3                 | -0.023  | -0.033 | -0.039 | -0.048 |  |  |
|                     | Fe.            | -0.023                 | -0.036  | -0.052 | -0.06I | -0.082 |  |  |

Table 2

Adopted one-group uncertainty values for fission cross-sections (required uncertainties are in brackets)

| Nuclide         | 8 Gc ,%         | 86 <sub>f</sub> ,% | 86 in, %  |
|-----------------|-----------------|--------------------|-----------|
| Np -237         | I5 (5)          | 7 (5)              | 30 (IO)   |
| U -238          | 5 (3)           | 3 (3)              | IO (IO) . |
| Pu –238         | 25 (IO)         | IO (5)             | 40        |
| Pu <b>–</b> 239 | 6 (4)           | 3 (3)              | 20 (I5)   |
| Pu -240         | IO (5)          | 5                  | 20 (15)   |
| Pu -24I         | I5 (5)          | 5 (3)              | 20        |
| Am -24I         | IO (5)          | IO (5)             | 30 (IO)   |
| Am-242m         | <b>3</b> 0 (IO) | I5 (5)             | 40        |
| Am-243          | 30 (IO)         | IO (5)             | 30        |
| Cm -242         | 50 (IO)         | I5 (5)             | 30        |
| Cm-243          | 50 (IO)         | I5 (5)             | 30        |
| Cm -244         | 30              | IO (5)             | 30        |

Table 3 Calculational values of  $\rho^{i}/\rho^{235}$  in EQC critical assemblies

|        | Code                    | Calculation                       | БФС-41                     | БФС-49-3                  | БФC-42                     | K5P-15                     |
|--------|-------------------------|-----------------------------------|----------------------------|---------------------------|----------------------------|----------------------------|
| Pu-240 | TULPE<br>TULPE<br>HEEPC | traditional * precise **) presise | ) 0.I53<br>0.097<br>0.I07  | 0.I22<br>-0.I43<br>-0.076 | 0.04I<br>-0.325<br>-0.286  | -0.310<br>-0.345<br>-0.356 |
| Am-241 | TULPE<br>TULPE<br>HEEPC | traditional<br>precise<br>precise | -0.233<br>-0.254<br>-0.244 |                           | -0.425<br>-0.486<br>-0.470 | -I.02<br>-I.00             |

<sup>\*)</sup> and \*\*) accordingly without and taking into account a resonance and spatial structure of adjoint flux.

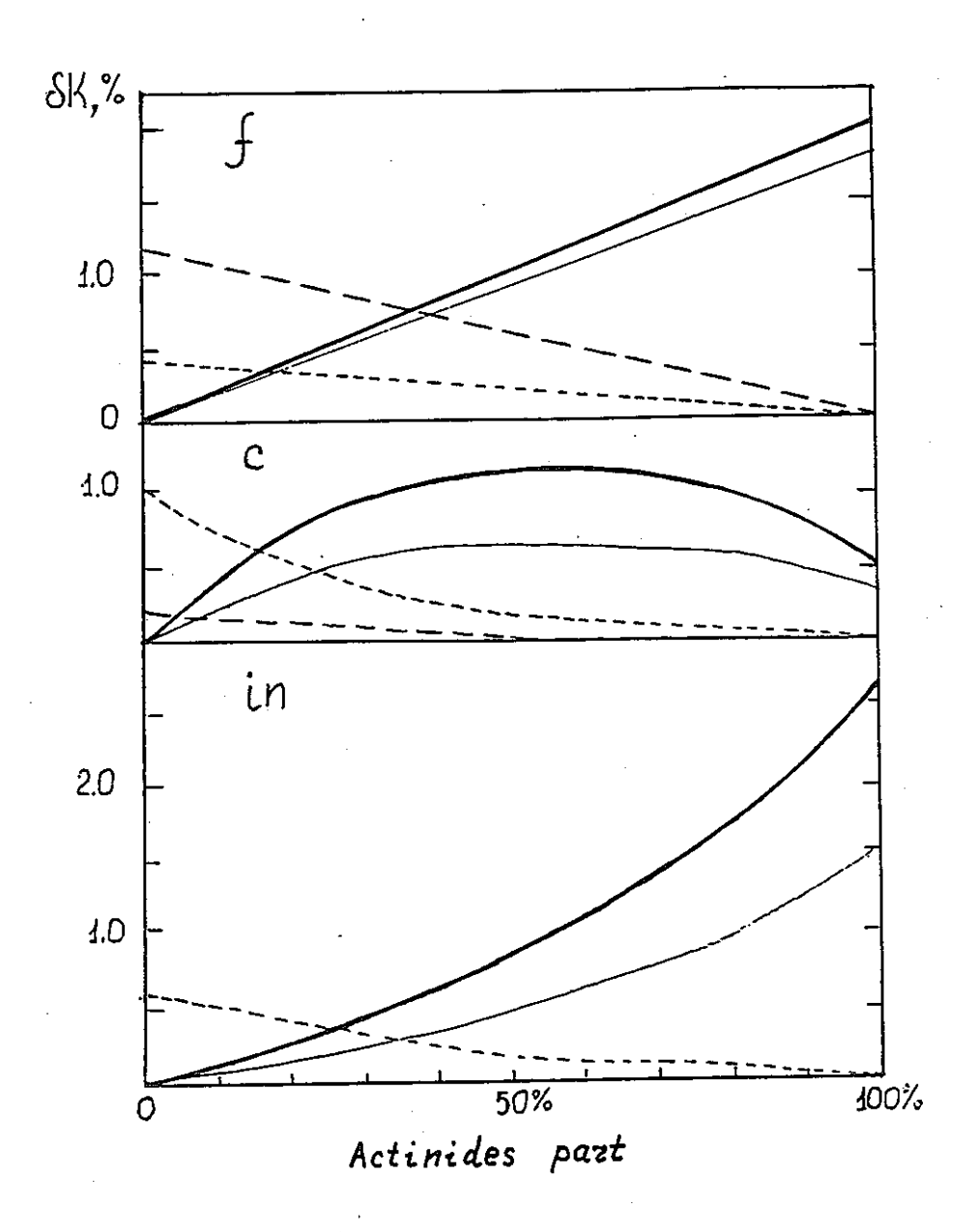
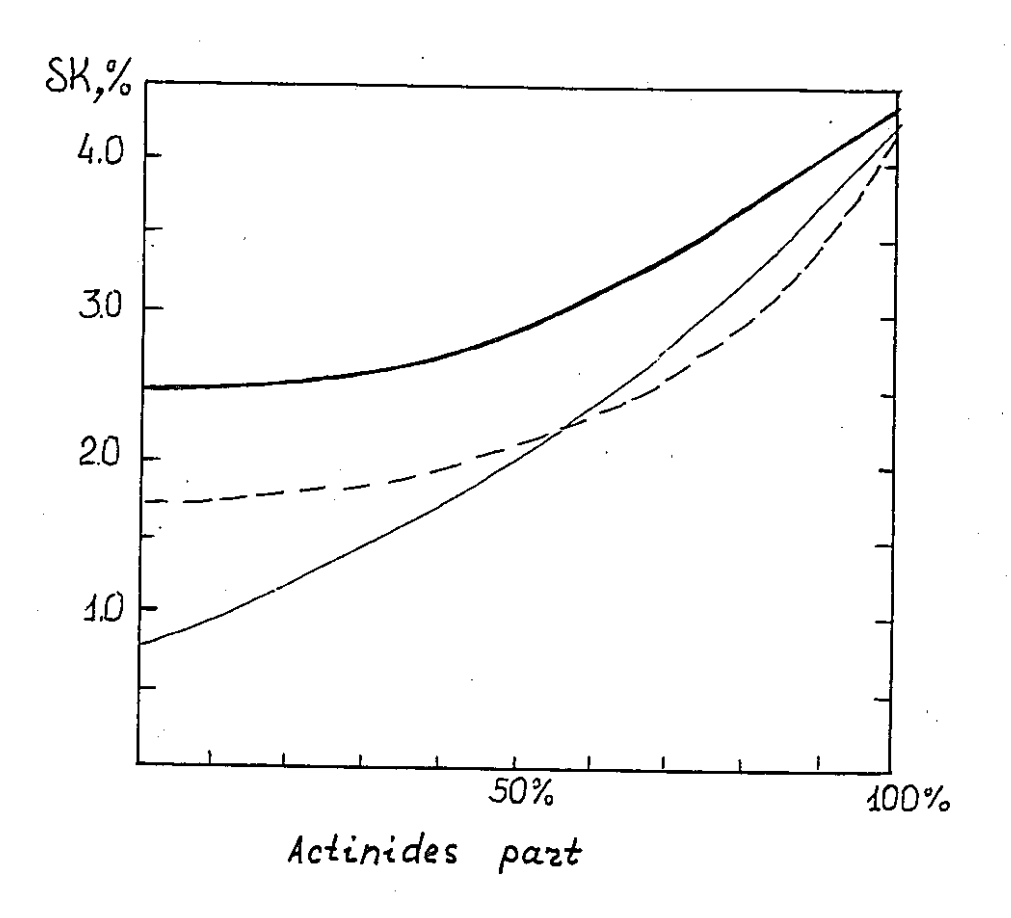


Fig.1. Uncertainty contribution of fission, capture and inelastic scattering cross-sections to overall uncertainty of calculational critical parameter:

---- U-238, ----Pu-239, ----Np-237, -----Am-241



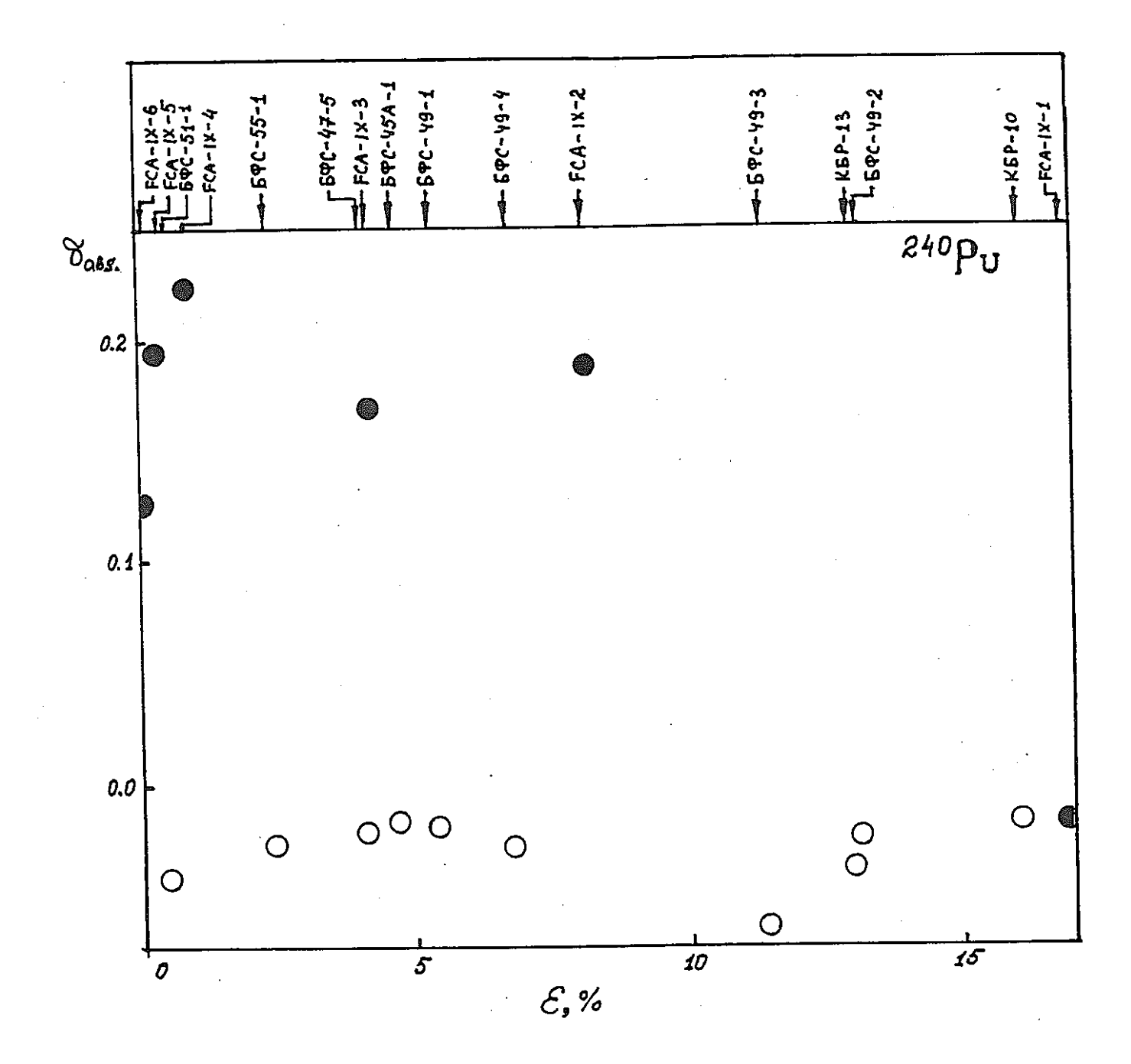


Fig. 3. Absolute discrepancy between experiment and calculation:

- FCA -IX experiments;

O-5ΦC experiments;

 $\mathcal{E}$  - neutron share in a core spectrum below 10 keV.

#### STUDY OF TRU TRANSMUTAION PLANT WITH A PROTON ACCELERATOR

- T. Nishida, I. Kanno, H. Takada, T. Takizuka, M. Mizumoto, M. Akabori,
  Y. Nakahara, Y. Okumura, H. Yasuda and Y. Kaneko
- Japan Atomic Energy Research Institute (Abstract)

Researches on the TRU transmutation with a proton accelerator, which were performed at JAERI in these years, have been promoted as one of main themes in the newly started national project OMEGA, which aims to establish new safer technologies to process long-lived radio-active wastes. Conceptual design studies of the transmutation plant have been made from the nucleonics and hydraulics analysis points of view. The proposed transmutation plant is a hybrid system of an intense proton accelerator, a tungsten target cooled with sodium and a subcritical core loaded with the TRU metal fuel. In this plant the transmutation rate of about 200 kg TRU a year (generated from about 8 units of 1 GWe PWR) are attainable and the marginal electricity more than one needed to drive the acclerator can be produced.

With the aim to make assessment of the plant design and to upgrade the computer codes for simulating nuclear spallation processes in the transmutation plant, the integral spallation experiment has been planned. The lead target has been set up along the 500 MeV beam line of a proton synchrotron booster at KEK. The first irradiation experiment is scheduled to start this Autumn.

The R & D schedules of the Engineering Test proton Accelerator(1.5 GeV, ~ 10 mA) have been made to ascertain the engineering feasibility of the transmutation plant. As the first step the Basic Technology proton Accelerator(10 MeV, 10mA) is to be constructed to develop the advanced technologies of higher beam intensity, high quality beam loading with low emittance, high efficient RF power, etc.

#### 1. Introduction

The management of minor actinides and fission products in the high level wastes is an important, hazardous problem due to their strong radio activities. In particular, transuranium nuclides(TRU) have a very long half lifetime of millions of years. Most of countries promoting the nuclear power generation have developed the vitrification and geological disposal techniques for managing these wastes. This subject, however, should be re-examined from the view piont of applying new, advanced technologies at present. By establishing new transmutation technologies the upgrade of safety assurance in the waste managnent will be achieved.

In Japan the OMEGA project(Option Making Extra Gains from Acitinides and fission products) started to research and develop the new technologies on nuclear waste partitioning and transmutation as the long term one. As a part of the project, Japan Atomic Energy Research Institute has set up the R & D plans mainly on

- 1) advanced partitioning technology,
- 2) TRU transmutation in burner and power reactors and
- 3) TRU transmutation with proton accelerators. 1).

The recent advance made in accelerator technology during the past decade has given the high possibility of providing the intense proton beam to the proposed transmutation system. Most of the products in the transmutation by using only the spallation reaction have halflives shorter than most of fission products. The nuclear spallation reaction between high energy protons (above 1 GeV) and heavy metal such as TRU generates many neutrons with the hard spectrum likely in a fast reactor. These facts makes the use of an proton accelerator attractive as a means of nuclear transmutation of TRU. At the present stage the accelerator-driven transmutation system mainly utilizing the fission reactions in duced by spallation neutrons has been studied as the type of transmutation plant because of high transmutation rate and good energy balance. The hybrid transmutation system of accelerator-target-core has the additional merits:

- (1) The system can be quickly shut down only by switching off the beam current of proton accelerator.
- (2) Since the hybrid target-core is always operated in a subcritical state, it can have a simpler structure without safety and control rods than the reactor.
- (3) The higher burnup rate is expected for the TRU fuel in this system with no constraints for the criticality. In this case the main limitation is the lifetime of fuel and structual material under the irradiation conditions.
- (4) The target-core designing is flexible because it is free from the safety requirements of non-positve Na void coefficients and the poisoning effect due to variation of isotope abundances in the fuel composition as the fuel is burning.

However there are technological items requiring further researches and developments:

- (a) an intense proton beam accelerator (1.5 GeV,  $\sim$ 10 mA),
- (b) TRU technologies,
- (c) high energy radiation shielding.

In the present paper the present status of the research at JAERI is described as following items,

- 1) development of the basic simulation code system,
- 2) conceptual study of the TRU transmutation plant,
- 3) spallation integral experiment,
- 4) development of a intense proton beam accelerator.

Tree structure illustration of R & D Items for the TRU Transmutation Plant and High Intensity Proton Beam Accelerator is shown in Fig. 1.

Moreover the spallation target system can be used for other applications such as the breeding of fissile nuclides and the creation of very intense neutron sources. The useful nuclides or short-life RI's used for special purposes can be produced from residual nuclides after transmutation and nuclide partitioning processes also.

2. Research of transmutation system driven with proton accelerator

#### 2-1. Development of simulation codes

The knowledge of residual nuclides accumulated in the target spallated by the proton beam irradiation is very improtant for the feasibility estimation of proton-induced TRU transmutation. Actually, however, it is almost impossible to obtain exactly the time evolution of yields of all the nuclides in the target due to enormous computing time. The SPCHAIN code has been developed to compute approximately the buildup and decay of spallation products (SP) by expanding the depletion code DCHAIN2 2) for fission products. By assuming that any complicated decay process of nuclides is disintegrated to linearized decay chains, the equation can be solved by the Bateman method. The new data of decay types, decay constants, branching ratios and decay schemes have been compiled in the SPCHAIN data library for about 1100 nuclides needed for the TRU spallation calculation. These data were mainly collected from Table of Isotope (7th version) and the data stored in the DCHAIN2 library. Figure 2 represents the nuclide distribution of both data sources in the (A,Z) plane. When the halflife time of a nuclide was not obtained by surveying the data, it was calculated by using the decay calculation program 3) or guessed from the trend of data of nuclides located in the neighborhood of the nuclide in the Nuclear Chart. The yields of SP in the spallation reaction were computed by using the code NUCLEUS.49 As a preliminary analysis the yields and radioactivities of residual nuclides in a 241 Am target irradiated by 1 GeV protons has been calculated. Figure 3 shows the activity rate distribution of buildup elements at the time stage of one year cooling after irradiation of ten hours.

The target-core design code system SP-ACE with a deterministic calculation method is being developed to simulate the transmutation process of TRU wastes in a subcritical system in reasonable computing time and precision. Figure 4 shows the main flow chart of this system. The neutron transport code RABBLE-THERMOS computes the region-wise neutron flux, using ultra fine group constants and the distribution of spallation neutron source, which can be obtained from Monte Carlo

calculations of high energy nuclear reactions and particle cascades in NMTC/JAER1. Using these fluxes the routine COLAPU gives the effective cross section and the average flux in each region for the burnup code COMRAD to calculate the yields of nuclides, heat generation and  $\gamma$ -ray intensity in the transmutation system.

#### 2-2. Basic design study of the TRU transmutation system

We have been promoting the conceptual studies on the TRU transmutation in the target-core system driven by an accelerated proton beam. <sup>5),6)</sup> The basic conditions settled for the system design are (1) high transmutation rate of TRU, the goal line of which is the transmutation of amount of TRU produced in about ten commercial 1 GWe PWR plants, and (2) good energy balance, in which it can generate enough electricity to operate the accelerator at least. The yields of TRU produced per year from 1 GWe PWR are summarized in Table 1. Total amount of TRU is about 26 kg/y, 56 % of which is <sup>237</sup>Np.

High energy nucleons generated in the spallation can transmute TRU nuclides through the cascade processes. Figure 5 shows the dependence of the number of spallated nuclides on the incident proton energy when the proton injects on the  $^{237}\,\mathrm{Np}$  metal target ( 20 cm  $\phi$  x 60 cm ). The number of nuclides transmutated at 1.5 GeV is about 5 per incident proton but it is too small to process TRU wastes in the commercial base unless the proton beam can have high current more than 300 mA. The heat generation is not sufficient to drive the intense accelerator. However it is noted that several tens neutrons with hard spectrum similar to the one in the fast reactor are emitted in the spallation. The computer simulation result shows that the number of spallation neutrons generated in the targets of actinides such as U, Np and Am, and heavy elements such as Pb and W increases monotonously when the proton energy increases up, as shown in Fig. 6. For the case of  $3^{237}\,\mathrm{Np}$  target bombarded by a 1.5 GeV proton the neutron number is  $\sim 40$ . As seen in Fig.76 the (n, f) cross section of 237 Np is larger by a factor of two or three than the (n,  $\gamma$  ) cross section of  $^{237}{\rm Np}$  in the energy range above 0.5 MeV.

Therefore it is considered to be advantageous to adopt high energy proton-induced spallation and the secondary neutron causing fission reactions as a means of the nuclear transmutation of TRU. Figure 8 shows the target-core of hybrid plant driven by high power proton beam with the energy of 1.5 GeV and the current of several tens mA. The core design parameters are summarized in Table 2. The tungsten target is 60 cm long in the direction of the incident beam, 1 m high and 10 cm wide and is installed in an TRU-fueled subcritical core ( $k_{eff}$ : 0.9~ 0.94). The core has dimensions of  $2\sim2.6$  m length, 1 m height and 1 m width, surrounded by the HT-9 steel container with thickness of 20 cm. A beam window is located at a depth of 0.7 m from the front face and has a rectangular cross section with dimensions of 1 m high and 0.1 m wide. The heat generated in the TRU fuel is removed by the forced circulation of liquid metal coolants Na/Pb-Bi. The heat removal performance is one of the major factors to determine the rate of TRU transmutation in the system. The core consists of metallic alloy fuel of TRU and provides considerably harder neutron spectrum than the other types of fuels. fuel consists of two types of alloys, Np-22Pu-20Zr and AmCm-35Pu-5Y and has the sufficiently high phase stability6). The fuel pin cell geometry is shown in Fig. 9, with a diameter of 4 mm cladded with HT-9 steel. The pin pitches has been adjusted to be 8 mm and 10 mm for Na and Pb-Bi cooled cores, respectively, to keep  $k_{eff}$  around 0.86  $\sim$  0.95. Here Pu is added initially to the fuel in order to suppress the reactivity swing within an acceptable burnup range. With addition of 20 wt% of Zr, the melting point of Np is supposed to increase from 640 °C up to about 900 C. The fuel assembly in the core is similar to that employed in a TRU burner reactor design. 7)

by an axially symmetric cylinder with the same volume as the original system for the efficient computation. A circular beam window located at the center line has a diameter of 0.36 m, and the maximum beam diameter is 0.2 m. The nuclear spallation processes above the cutoff energy of 15 MeV were calculated by NMTC/JAERI code 8). For the reaction below 15

MeV the Monte Carlo transport code MORSE-DD 9, was used with 52 neutron group constants edited from JENDL-2 and ENDF-84, where spallation neutrons were treated as the source. The results of the neutronics calculations, for four cases of the system cooled by Na and Pb-Bi, with and without the tungsten target, are summarized in Table 3. The number of TRU nuclei disintergated in fast fission reactions is much larger than that in the spallation reaction for each case. Profiles of the two-dimensional power distribution for these cases are shown in Fig.10(a) to (d), respectively. It is apparent that the power peaking which occurs just behind the beam window is lower in the system with the tungsten target than in the one without it due to the flatterning effect for cases of both coolants and the flatterned power distribution increases the number of transmuted nuclides. The maximum transmutation rate is 202 kg/year in the core with the target cooled by Na.

Thermal hydraulics calculations for the system were done to obtain the maximum achievable thermal power within the maximum temperature limits of fuel and cladding. Maximum temperatures in the TRU fuel and the HT-9 cladding tube are limited to 900  $^{\circ}$ C and 650  $^{\circ}$ C, respectively, where the temperature at the inlet of coolant is set to 300  $^{\circ}$ . The temperature distributions along the hottest fuel pins cooled by Na in the core with the tungsten target are shown in Fig. 11. - The maximum thermal power is limited by the maximum allowable fuel temperature of 900  $^{\circ}$ C. The operating conditions of the target-core system are summarized in Table 4.: In the case of Na cooling and the tungsten target the maximum thermal power is 691 MW with the maximum and average power densities of 889 W/cc and 307 W/cc. The thermal power is sufficietly large to supply the electric power to the accelerator while the beam current required for the power is 22.6 mA. Without tungsten target the thermal power is 405 MW with the maximum and average power densities of 776 W/cc and 159 MW/cc and its peaking factor is larger by a facter of 1.7 than the case with the tungsten target. The maximum powers of Pb-Bi cooled core with and without the target are considerably lower than those of the Na cooled one and the beam current required is

less than 8 mA. This is attributed mainly to the lower thermal conductivity of the coolant and the wider fuel pin pitch than in the case of Na cooling.

The variation of multiplication factor k<sub>eff</sub> with burnup days was calculated as shown in Fig. 12. The increase tendency of k<sub>eff</sub> at the initial stage turns the decrease around 1000 days and the subcritical operation of the system can be kept during the burning time. The changes of concentrations of some minor actinides with burn-up days in the reference system (Na cooling, with tungsten target) were also calculated, as shown in Fig.13, using the burnup code ORIGEN2. The amounts of <sup>237</sup>Np and <sup>241</sup>Am at 1500 burning days become one half of their initial inventries, while <sup>238</sup>Pu and <sup>242</sup>Cm, which are not contained in the initial loading, build up.

#### 2-3. Spallation intergal experiment

More accurate experimental data for the spallation reaction in the energy range of ~1 GeV to ~100 MeV are needed to examine the actual efficiency of TRU transmutation by spallation reaction 18). 11) and to upgrade the simulation code system for the TRU transmutation processes. The research plan of spallation integral experiment by using the high energy proton beam has started. The lead cylinder system for the experiment has been set up last March near the dump of beam line connected to the proton synchrotron booster at KEK. Figure 14 shows the lead cylider installed in a SS container with 100 cm length and 60 cm diameter. This has several small holes parallel to the central axis, which are pluged by specimen wires such as Ni, Au, Cu and Fe. Reaction products in these specimen by irradiation of 500 MeV protons are identified from their  $\gamma$  -ray emissions measured by a Ge(Li) detector. The energy of spallation neutron can be known from the activity of specimen foils with the threshold energy of neutron emission, imbedded in the holes in the cylinder. The safety analysis for spallation experiment has been made to know whether the activity in the irradiated specimen and the dose rate are lower than the values restricted by the

law when they are transported in the cask to be measured at JAERI. The irradiation experiment for the lead system will be started this Autumun according to the machine schedule. The switching magnet will be newly equipped in the near future on the booster beam line to control the intensity of irradiating beam by adjusting the number of pulses in current. In the next step, a tungsten or a depleted uranium target, which is inserted in the central region of the lead cylinder, will be used to simulate the TRU target spallation experiment.

### 2-4. Development of intense high energy proton accelerator

The basic concept of the Engineering Test Accelerator with a beam energy of 1.5 GeV and a current of 10 mA was proposed for the TRU transmutation as described at the last NEA/CRP meeting. The accelerator has a large scale compared with the conventional ones which are used for basic nuclear physics experiments. In particular, the proton beam is nearly 50 times more intense than that for exisiting machines. Only a linac can satisfy the requirements of such a high beam current with higher efficiency of beam extraction than other circular accelerators. As the first step of the development, the low energy portion of the accelerator structure will be carefully studied, since the beam quality determined at the low energy part is a key factor of dominating the beam efficiency in the high  $_2\beta_2$  accelating system. Therefore the smaller size proton linac, Basic Technology Accelerator, with current of 10 mA is going to be constructed to develop the element technology. Figure 15 shows:an illustration of the proposed arragement of BTA, which consists of (a)ion source, (b) Radio Frequency Quadrupole linac, (c) Drift Tube Linac and (d) high: energy beam transport & dump system, with the output beam energies of 100 keV, 2 MeV, 10 MeV for (a) to (c), respectively. The final beam energy of BTA is chosen to be 10~20 MeV.

Main items of the development of BTA are listed as

- . O lon source and its power supply,
  - @ Radio-frequency quadrupole (RFQ) linac,
  - ③ Drift tube linac (DTL),...

- @ RF power supply system,
- 6 Beam control technology.

The basic experiments of the negative ion source has started to increase the output beam current with high emittance using Neutral Beam Injection test equipment for the fusion experiment at JT-60. The preliminary calculations of beam transport in RFQ linac was made using the computer codes SUPERFISH and PARMTEQ. The trade-off study of ETA system will start this Autumn in coopration with LANL to optimize the concept of ETA arrangment. The input and output energy, the emittance and the acceptance for the various components such as ion source, RFQ and DTL have to be determined carefully and systematically. The high energy portion of the accelerator( high  $\beta$  structure, finally in CW operation) will be also studied in advance of the second stage development. As the operation mode of the accelerator in the first step, the low duty operation will be appropriate to adjust the various parameters so that the adequate parameters will be surveyed.

#### 3. Summary and Conclusion

The computer code solving the time evolution equation has been developed to calculate the yield of decay and buildup nuclides in the spallation reaction.

The conceptual design studies have been made for comparison of the accelerator driven TRU transmutation systems with and without the tungsten target. When the Na cooled TRU metal fuelled core with tungsten target is operated at the thermal power of 691 MW and the beam current of 23 mA, this system can transmute about 200 kg TRU per year. In the case of the Pb-Bi cooled system at the thermal power of 342 MW and the beam current of 7.5 mA, it can transmute 140 kg TRU annually. Improvement and optimization of target-core design will be carried out also in more detail through the plant design studies. The performance of transmutation plant of the type of molten TRU is examined as the next step.

The lead target has been set up along the 500 MeV beam line of a

proton synchrotron booster at KEK. The first irradiation experiment is scheduled to start this Autumn.

The R & D scheduele of a high intense Engineering Test Accelerator (1.5 GeV, ~ 10 mA) is being planned for examining the engineering feasibility of the transmutation system. As the first step basic researches of Basic Technology Accelerator(proton linac: 10~20 MeV, 10 mA) have started to obtain the advanced accelerator technologies.

#### REFERENCES

- 1) Y. Kaneko: "THE INTENSE PROTON ACCELERATOR PROGRAM," Proc. 2nd Int. Symp. on Advanced Nuclear Energy Research Evolution by Accelearator -, (1990)(Mito).
- 2) K. Tasaka : JAERI-M 8727 (1980).
- 3) T. Yoshida : JAERI-M 6313 (1975).
- 4) T. Nishida, Y. Nakahara, T. Tsutsui : JAERI-M 86-116 (1986).
- 5) T. Nishida, Y. Nakahara : Kerntechnik, <u>50</u>, 193 (1987).
- 6) T.Takizuka, J. Kanno, H. Takada, T. Ogawa, T. Nishida, Y. Kaneko:
  "A Study on Incineration Target System," Proc. ICENES (1989)(Karls ruhe)
- 7) H. Takano, T. Mukaiyama: "Nuclear Characteristic Analysis of TRU Burner Rreactors", JAERI-M 89-072 (1989)(in Japanese).
- 8) Y. Nakahara, T. Tsutsui: JAERI-M 82-198 (1982) (in Japanese).
- 9) M. Nakagawa, et al., "MORSE-DD A Monte Carlo Code Using Multi-Group Double Differential Form Cross Sections," JAERI-M 84-126 (1984)
- 10) S.S. Cierjacks, et al.: "High Energy Particle Spectra from Spallation Target," ICANS-V, (1981)
- 11) W. Amian, N.F. Peek, D.J. Shaddan, G. Sterzenbach: "Production Rates of Spallation and Fission Products in Depleted Uranium and Natural Lead Targets Bombarded by 600 MeV and 1100 MeV Protons", Proc. of ICANS-VII, (1983)

Table 1 TRU production per Year from 1 GWe PWR

| Nuclide           | Weight (kg) | Fraction (%) |
|-------------------|-------------|--------------|
| 237 <sub>Np</sub> | 14.5        | 56.2         |
| 241<br>Am         | 6.82        | 26.4         |
| 243<br>Am         | 3.1         | 12.0         |
| 243<br>Cm         | 0.0078      | 0.03         |
| <sup>244</sup> Cm | 1.32        | 5.1          |
| <sup>245</sup> Cm | 0.072       | 0.3          |
| Total             | 25.8 (kg)   | 100.0        |
|                   |             |              |

Fuel Burn Up : 33,000 MWD/T

Cooling Time before Reprocessing: 3 years
Cooling Time before Partitioning: 5 years
Collection Rate of U and Pu: 100%

Table 2 Plant design parameters

|                       | <u> </u>             |  |  |
|-----------------------|----------------------|--|--|
| Coolant               | Na/Pb-Bi             |  |  |
| Proton energy         | 1.5 GeV              |  |  |
| Target                |                      |  |  |
| Length                | 200 ~ 260 cm         |  |  |
| Height                | 100 cm               |  |  |
| Width                 | 100 cm               |  |  |
| Tungsten              |                      |  |  |
| Length                | 60 cm                |  |  |
| Height                | 100 cm               |  |  |
| <sup>2</sup> Width    | 10 cm                |  |  |
| Reflector             |                      |  |  |
| Composition           | Stainless steel      |  |  |
| Thickness             | 20 cm                |  |  |
| Fuel                  |                      |  |  |
| Composition           | Np-15Pu-30Zr         |  |  |
|                       | Am Cm - 35 Pu - 10 Y |  |  |
| Bond                  | Na                   |  |  |
| Clad                  | HT-9 steel           |  |  |
| Fuel slung diameter   | 4.00 mm              |  |  |
| Clad outside diameter | -5,22 mm             |  |  |
| Clad thickness        | 0.3 mm               |  |  |
| Pin length            | 1000 mm              |  |  |
|                       | •                    |  |  |

Table 3 Performance of the transmutation plant

| Torgel system                            | Reference | Version - 1 | Version - 2 | Version-3 |  |
|------------------------------------------|-----------|-------------|-------------|-----------|--|
| Coolant                                  | Na        | Pb-Bi       | , Na        | Pb-Bi     |  |
| Effective multiplication factor          | 0.92      | 0.86        | 0.94        | 0.95      |  |
| Pin pitch (mm)                           | 9.5       | 10.5        | 10.5        | 12.0      |  |
| Actinide looding (kg)                    | 2866      | 2013        | 2682        | 1584      |  |
| Beam current (mA)                        | 22.6      | 7.5         | 18.2        | 5.4       |  |
| Neutrons per proton                      | 38.1      | 52.8        | 35.3        | 55.1      |  |
| Fissions per proton (>15 MeV)            | 0.67      | 0.24        | 0.64        | 0.42      |  |
| ( < 15 MeV )                             | 150.6     | 171.3       | 108.0       | 147.4     |  |
| Average neutron energy (keV)             | 7.39      | 629         | 774         | 626       |  |
| Average neutron flux (x1015 n/cm2 ·sec)  | 4.6       | 6.6         | 2.0         | 1.9       |  |
| High energy component (>1.0 MeV)         | 20%       | 18%         | 20%         | 17%       |  |
| (>0.1 MeV)                               | 72%       | 78 %        | 71%         | 77 %      |  |
| Operation time (days)                    | 270       | 270         | 270         | 270       |  |
| Burnup rate (%)                          | 7.0       | 6.9         | 4.3         | 2.7       |  |
| weight (kg)                              | 202       | 139         | 114         | 42        |  |
| Unit of 3000 MWI LWR                     | 7.6       | 5.3         | 4.3         | 1.8       |  |
| Burnup reactivity swing (% $\Delta$ k/k) | 3.8       | 2.9         | 2.7         | 2.1       |  |

Table 4 Plant operation conditions

|                          |                     | Reference | Version-1 | Version-2 | Version-3 |
|--------------------------|---------------------|-----------|-----------|-----------|-----------|
| Pins                     |                     | TRU+'Y    | TRU+W     | TRU       | TRU       |
| Coolant                  |                     | Ха        | Pb-Bi     | Ха        | Pb-Bi     |
| Proton Beam Current [mA] |                     | 22.6      | 7.5       | 18.1      | 5.4       |
| Thermal Power (MY)       | •                   | 691       | 484       | 405       | 163       |
| Power Density [W/cc]     | max.                | 889       | 523       | 776       | 425       |
|                          | ave.                | 307       | 246       | 159       | 83        |
| Linear Power Rating (W/c | m) max.             | 695       | 499       | 713       | 530       |
|                          | ave.                | 240       | 235       | 146       | 103       |
| Coolant Temperature [°C] | outlet <sup>.</sup> | 389       | 451       | 352       | 377       |
| Clad Temperature [°C]    | max.                | 492       | 610       | 481       | 589       |
| Fuel Temperature [°C]    | max.                | 900       | 000       | 900       | 900       |
| Coolant Velocity [m/s]   | max.                | 8         | 2.35      | 8         | 2.35      |
| Pressure Drop (kPa)      |                     | 78        | 67        | 62        | 48        |

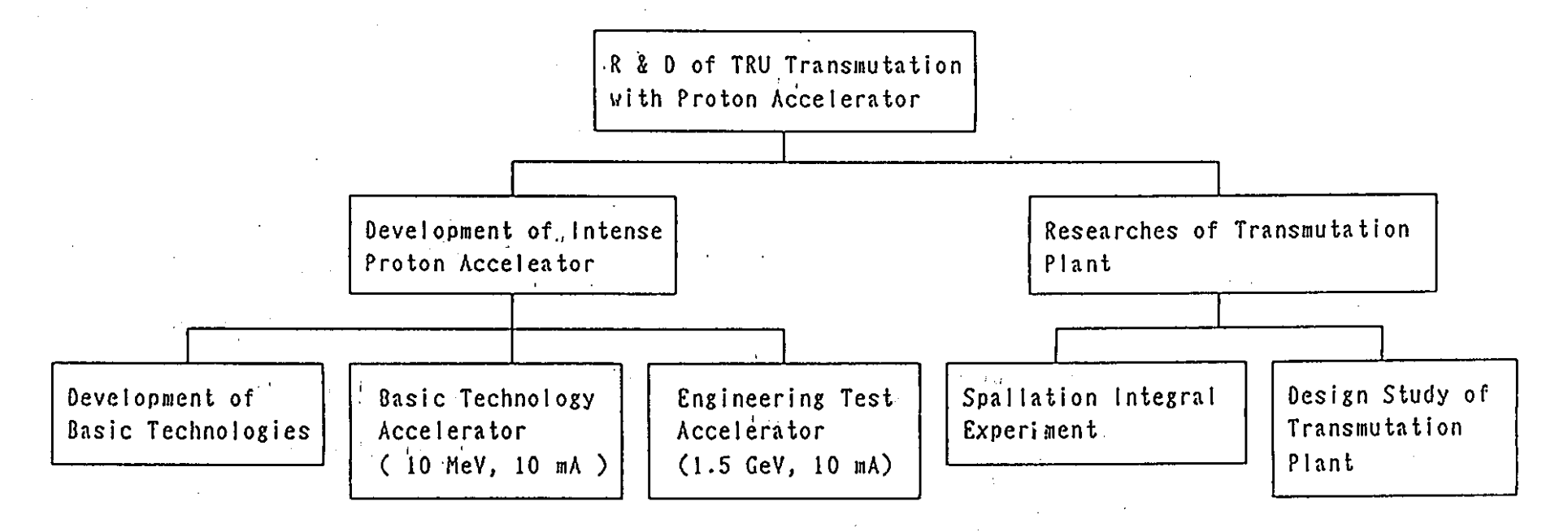


Fig. 1 Tree Structure of R & D Items for TRU Inceneration Plant Driven by High Intensity Proton Accelerator

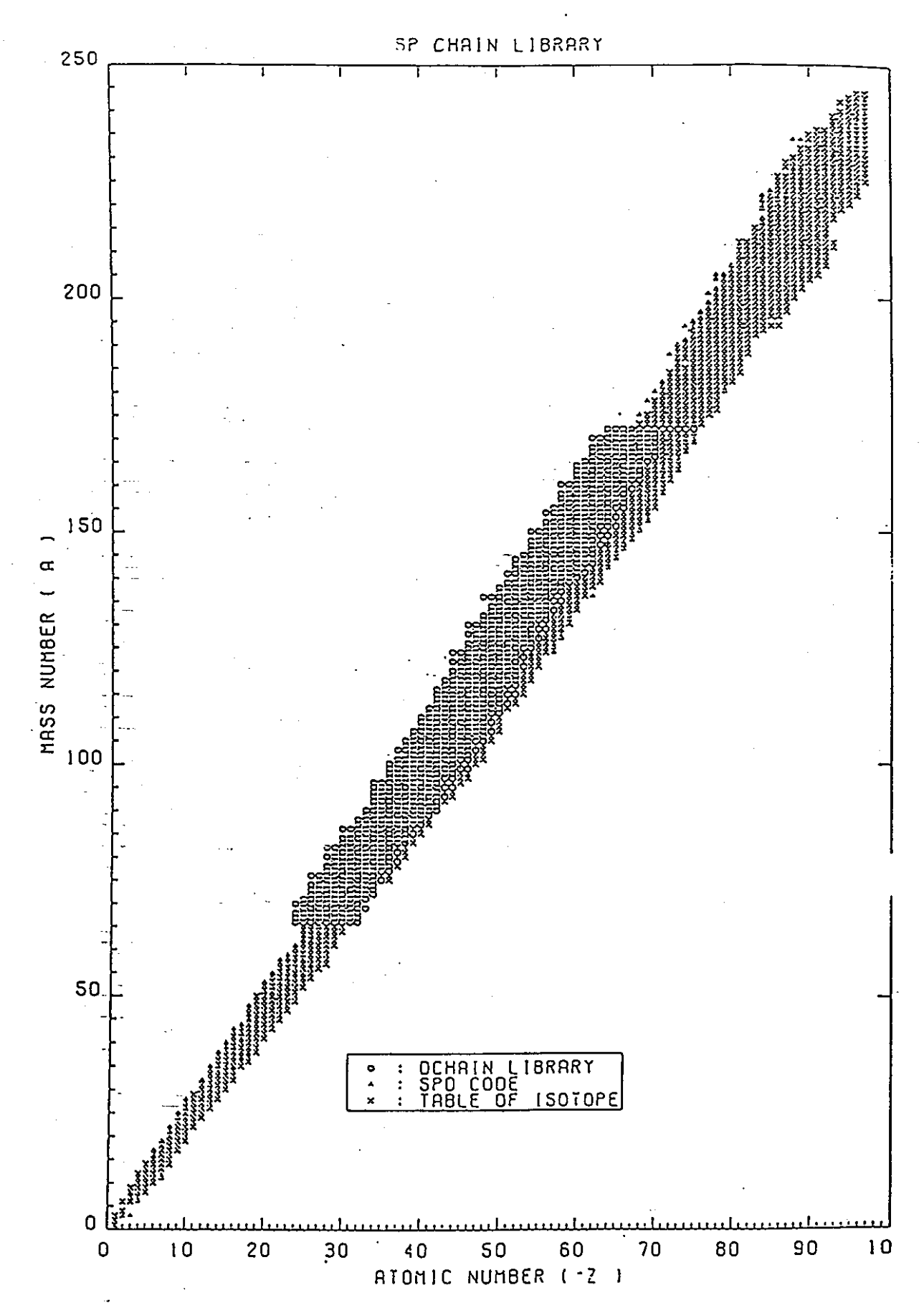


Fig. 2 Distribution of nuclides compiled in the SPCHAIN data file

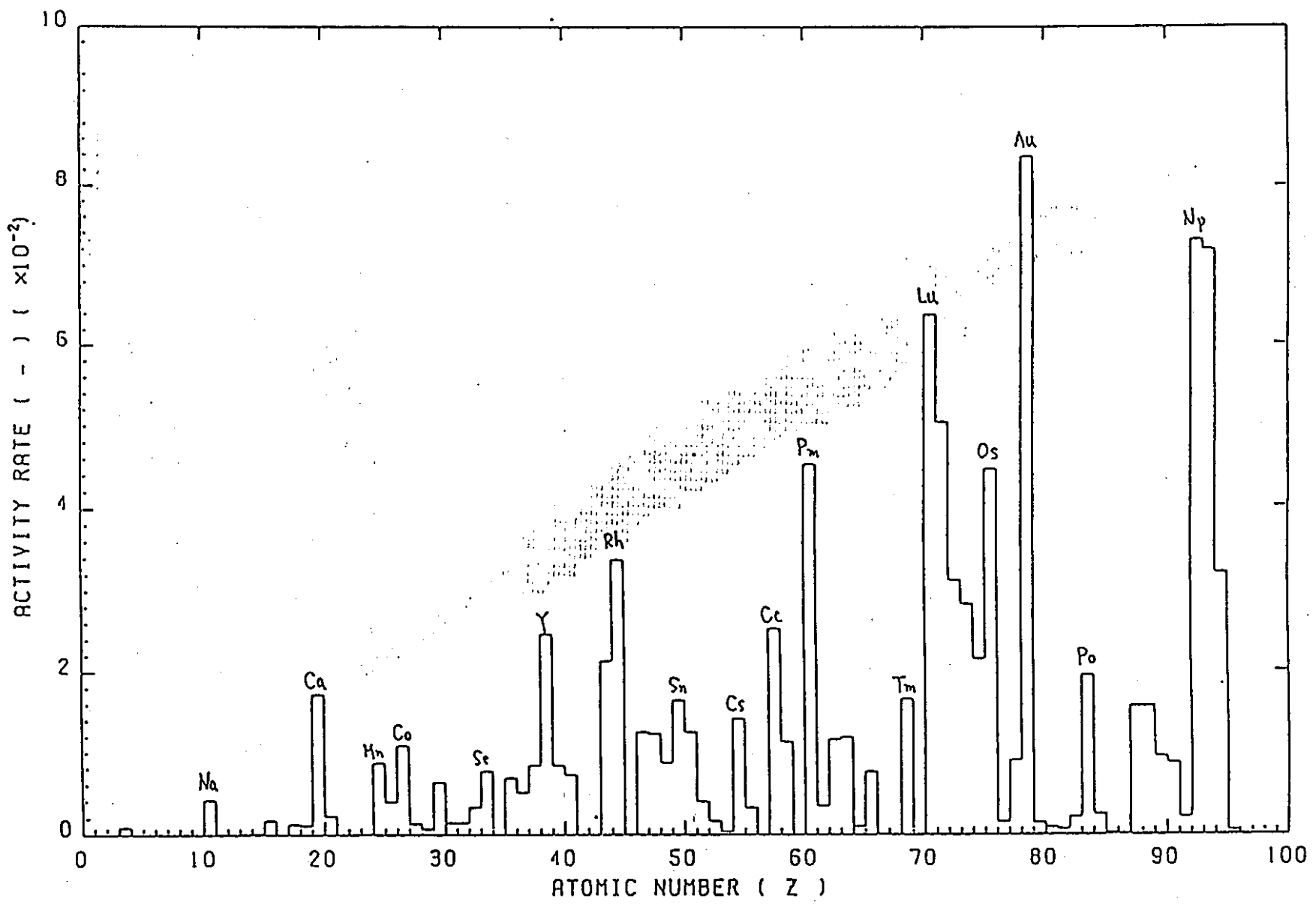


Fig. 3 Activity rate distribution of resibual elements in a <sup>241</sup>Am target at the time stage of one year cooling after irradiation of ten hours of 1 LeV protons

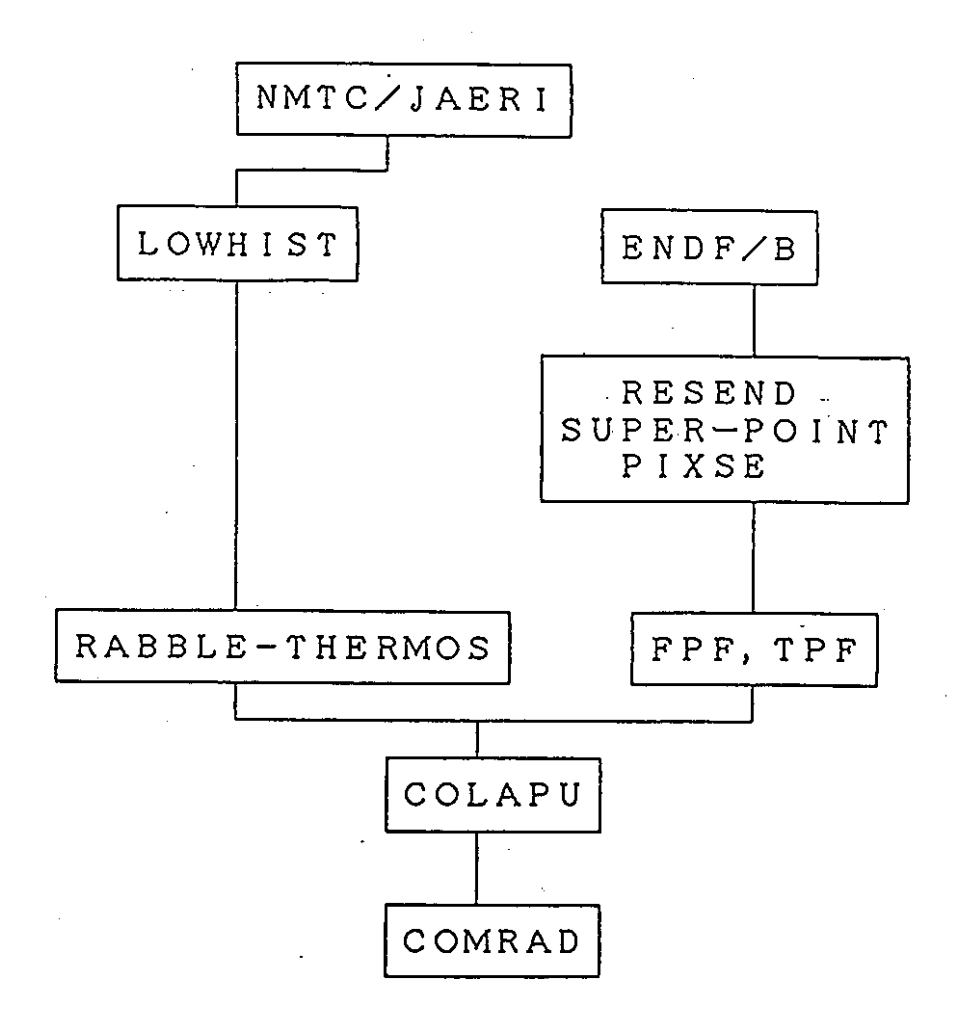


Fig. 4 SP-ACE code system for designing the transmutation core driven by a proton accelerator

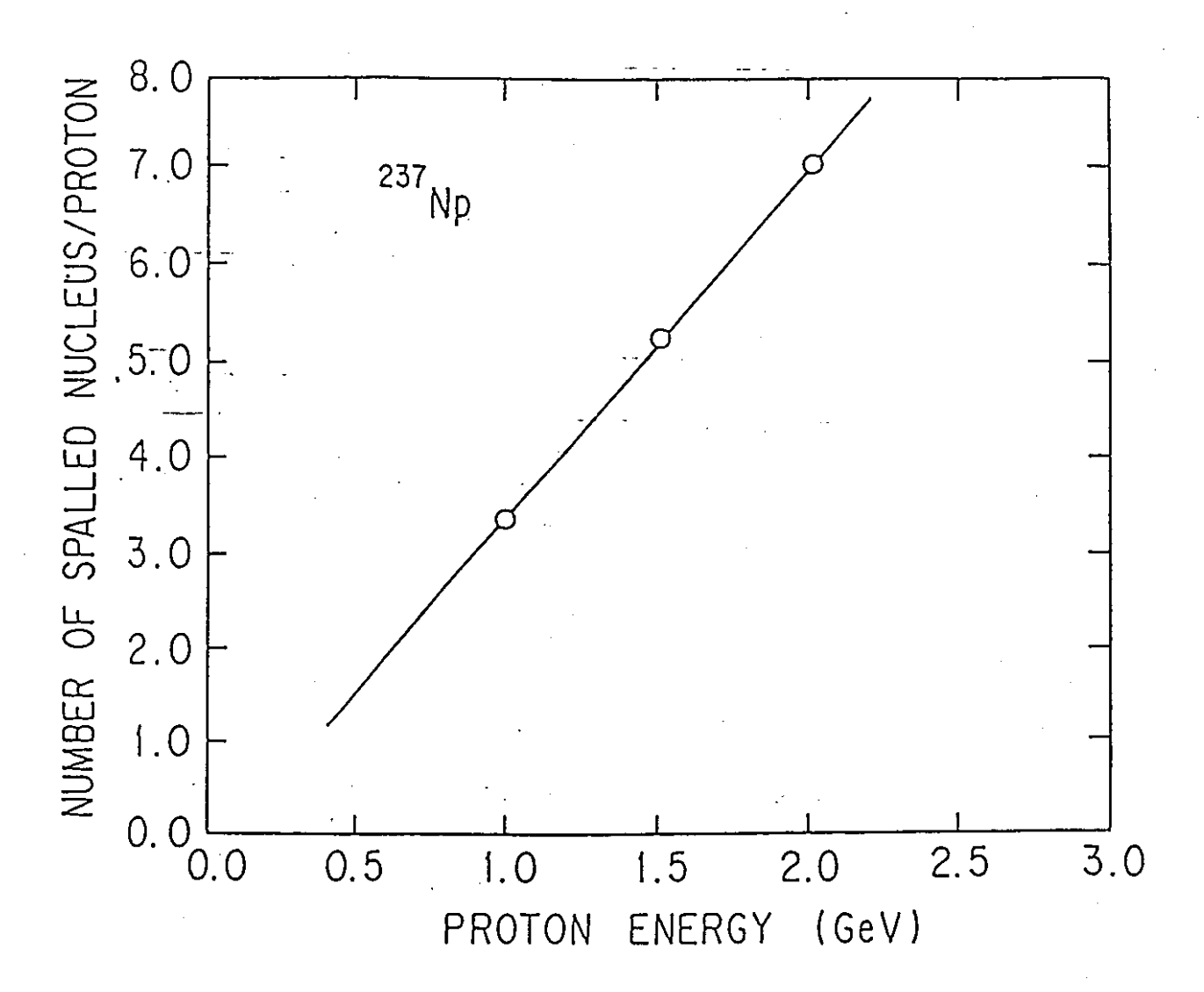


Fig. 5 Energy dependence on number of nuclei destructed due to spallation reaction

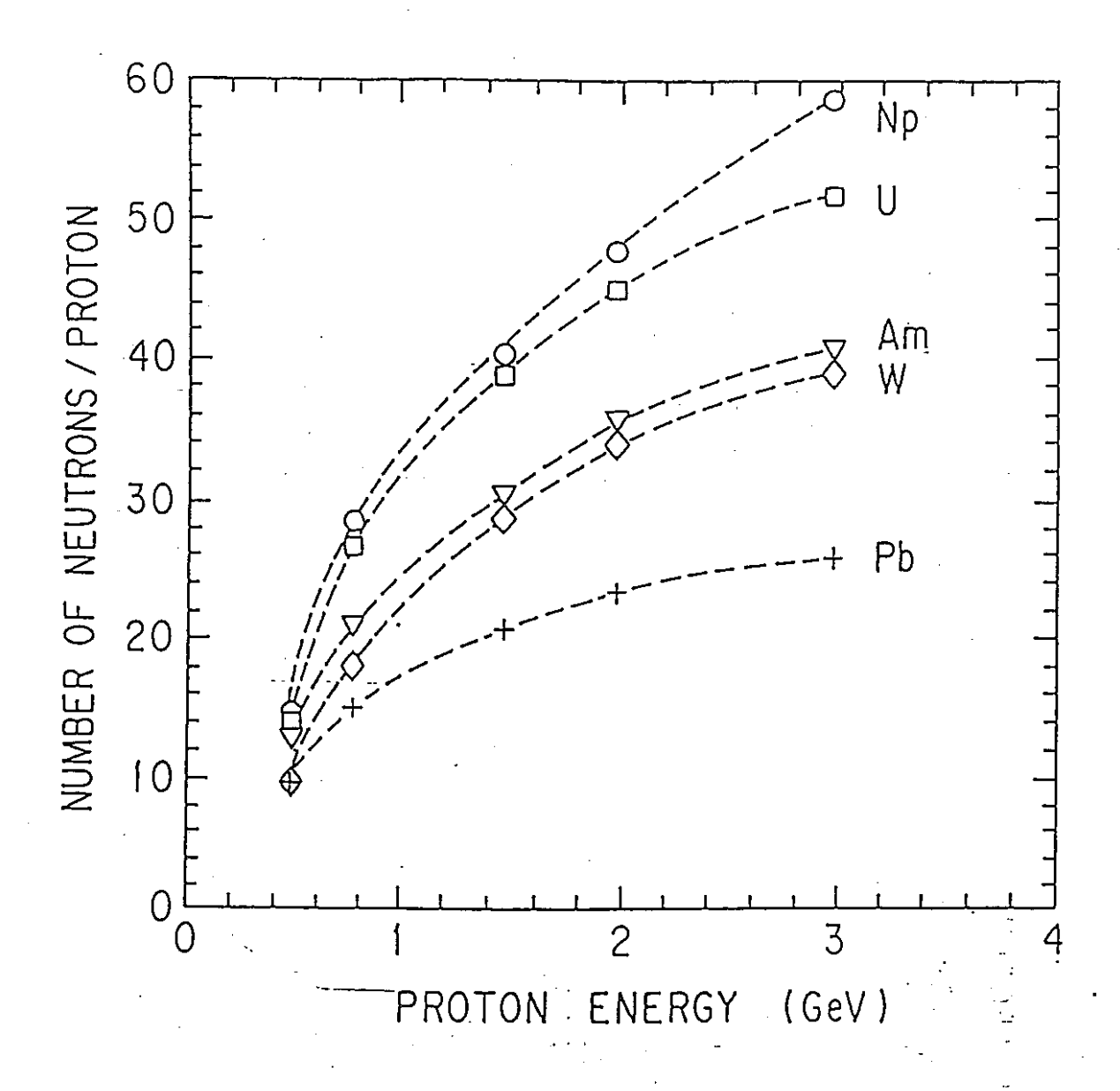
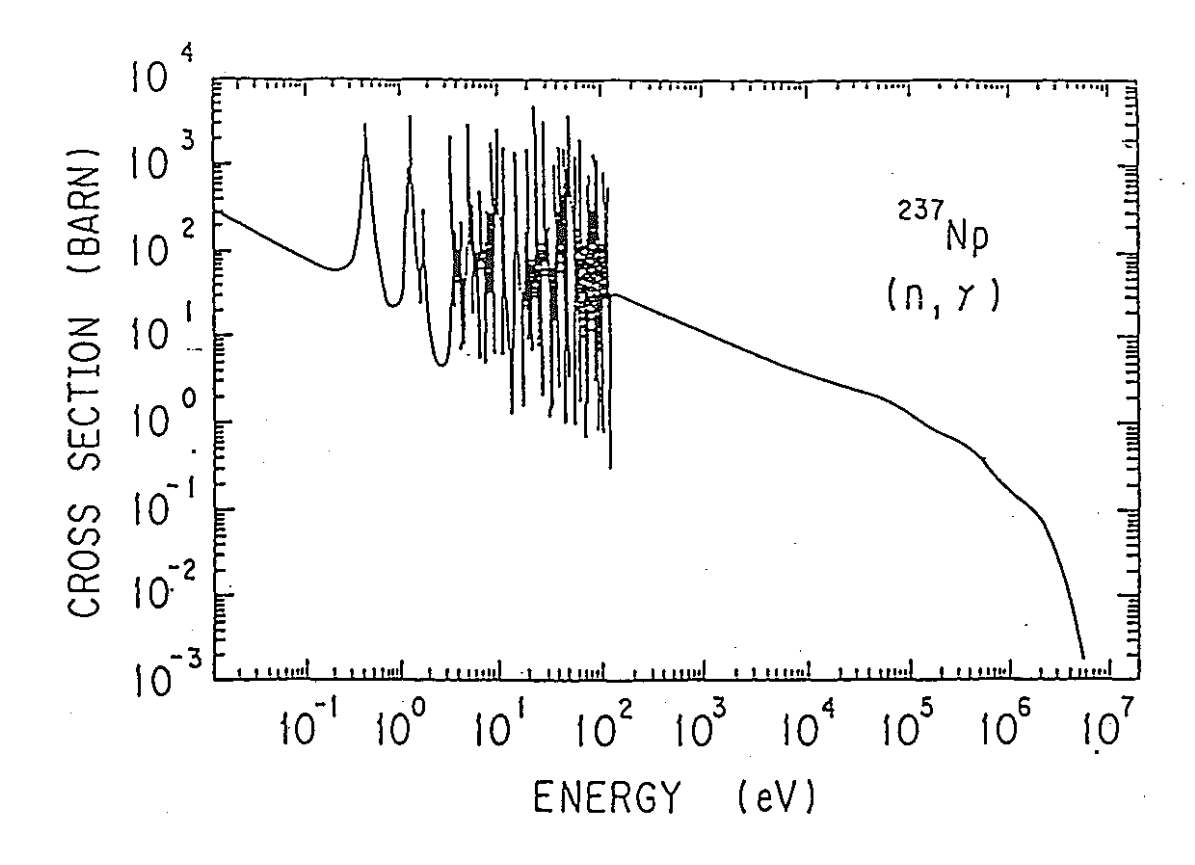


Fig. 6 Energy dependence on number of neutrons generated by spallation reaction



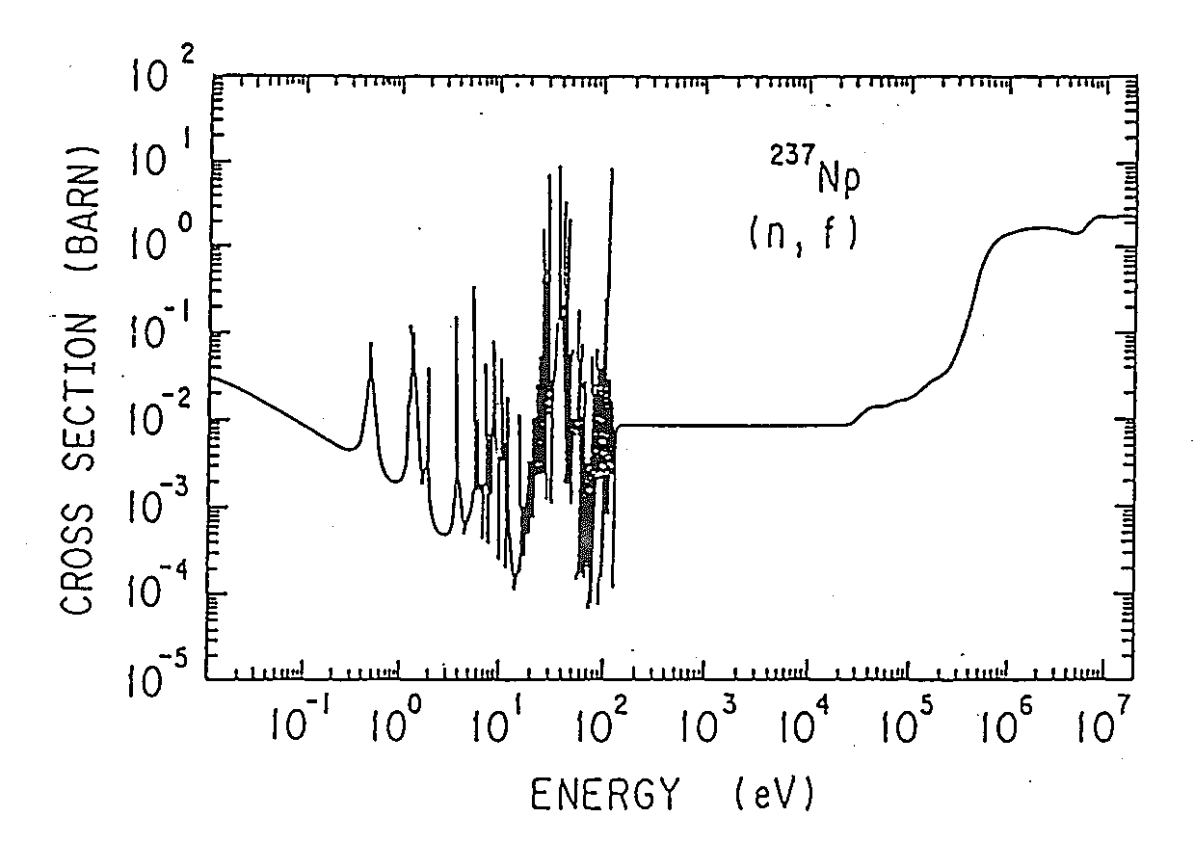


Fig. 7 Neutron cross section of 237Np

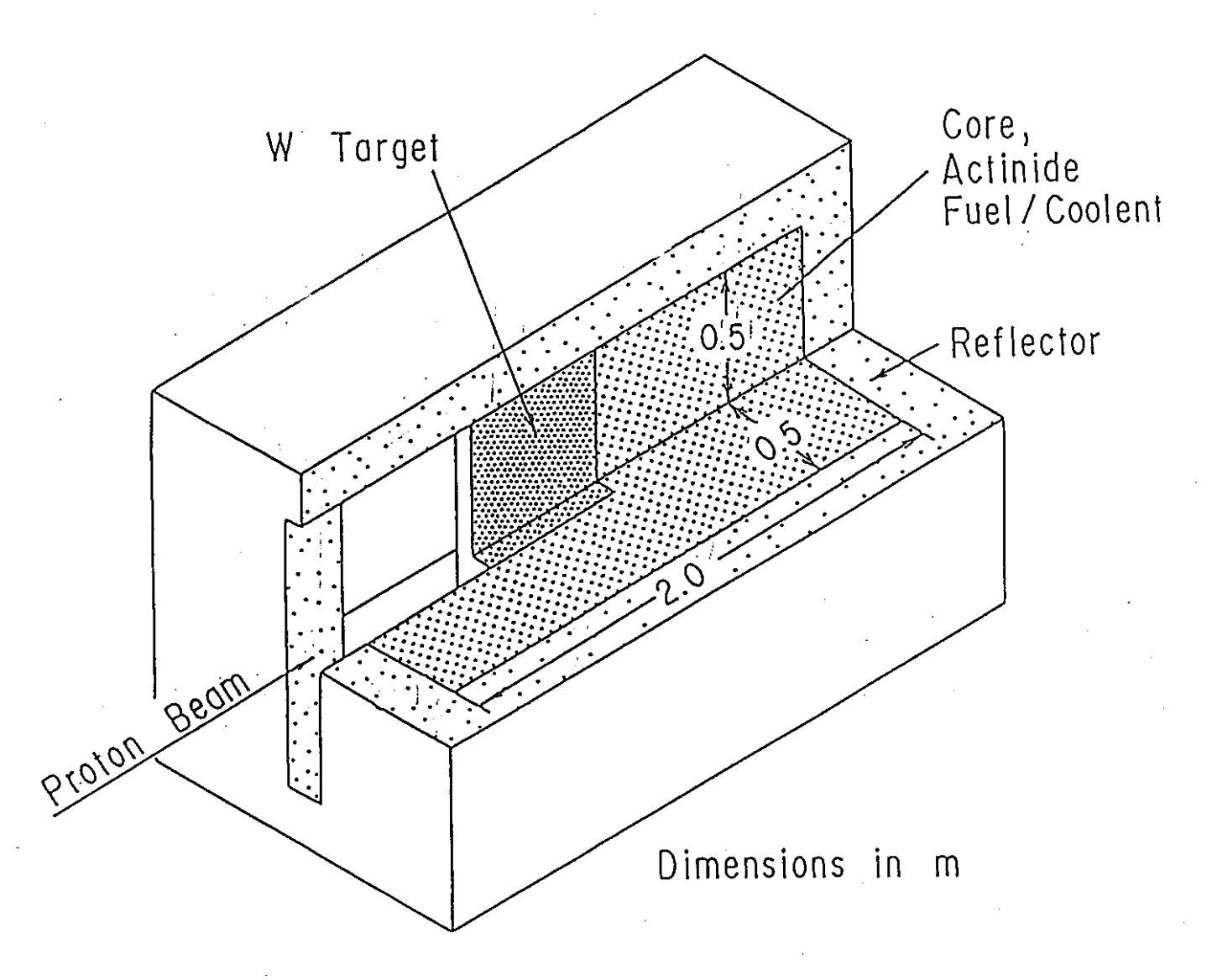


Fig. 8 Target-core configuration of hybrid plant(refernece system)

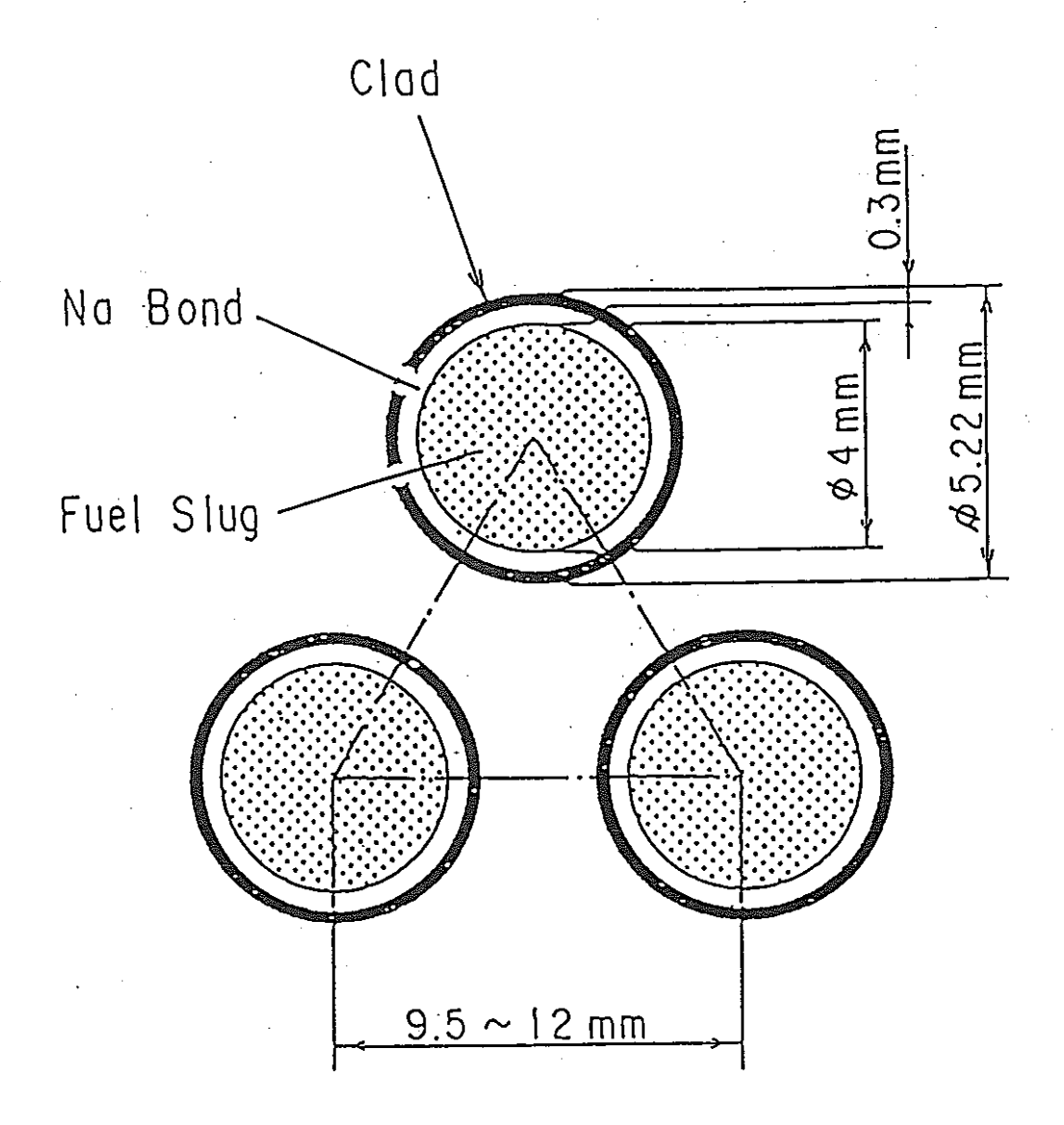


Fig. 9 Actinide fuel pin geometry

403 —

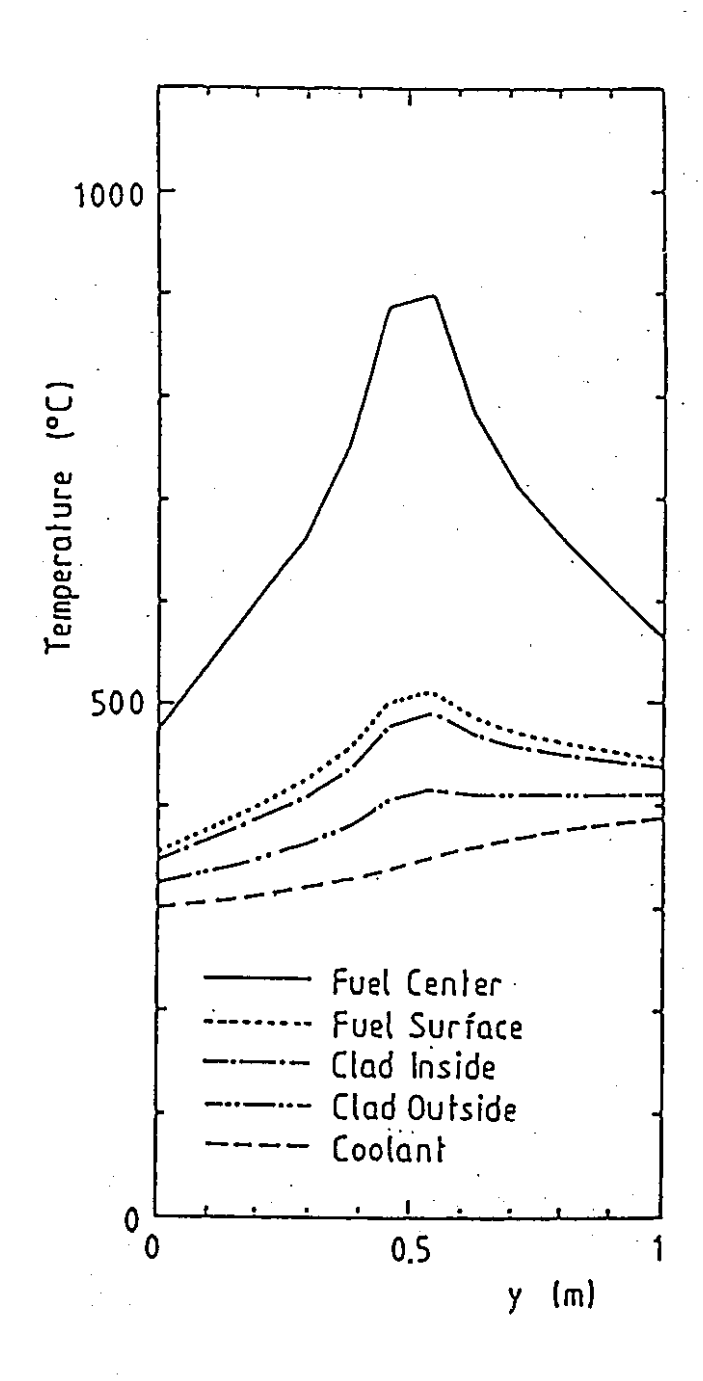
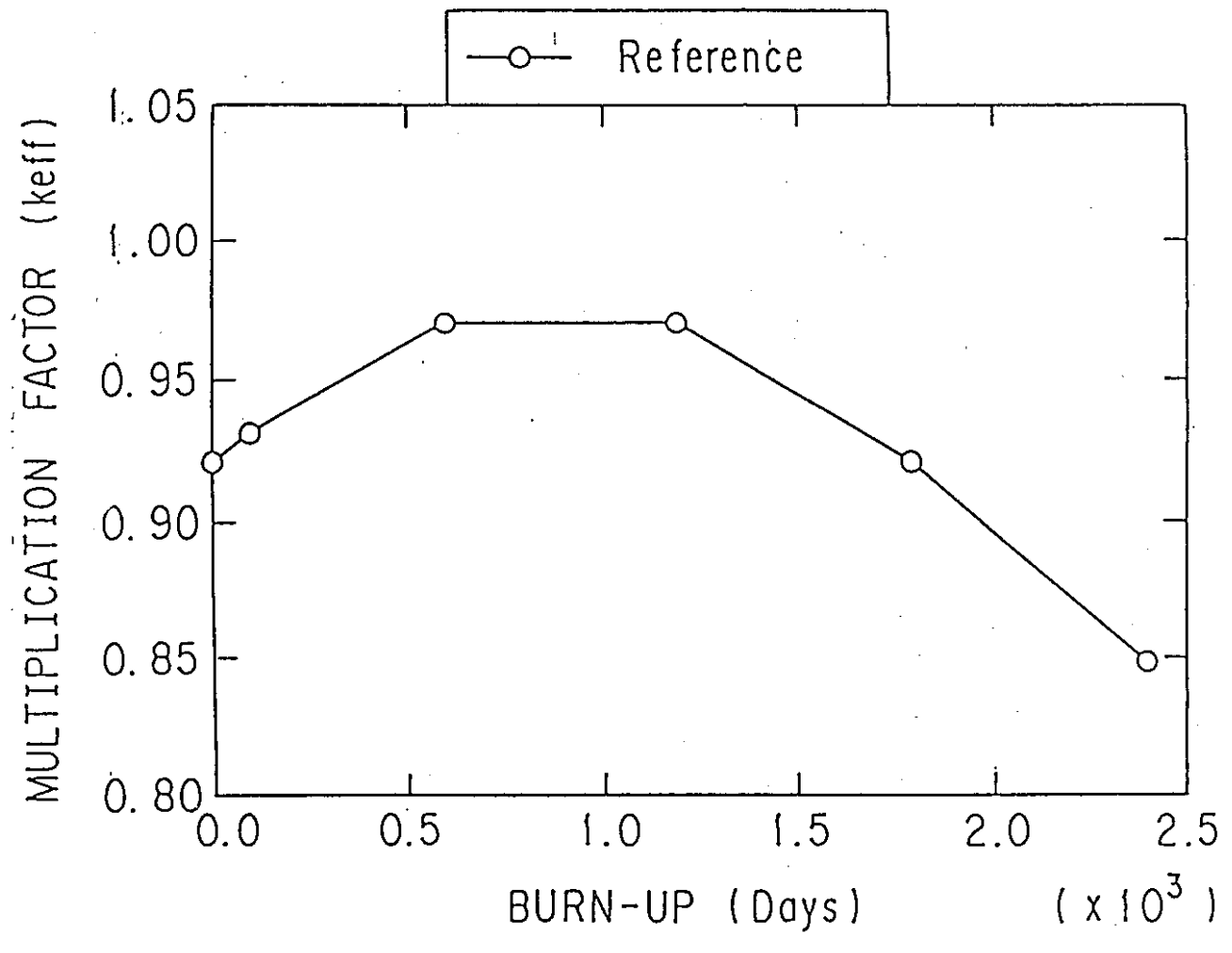
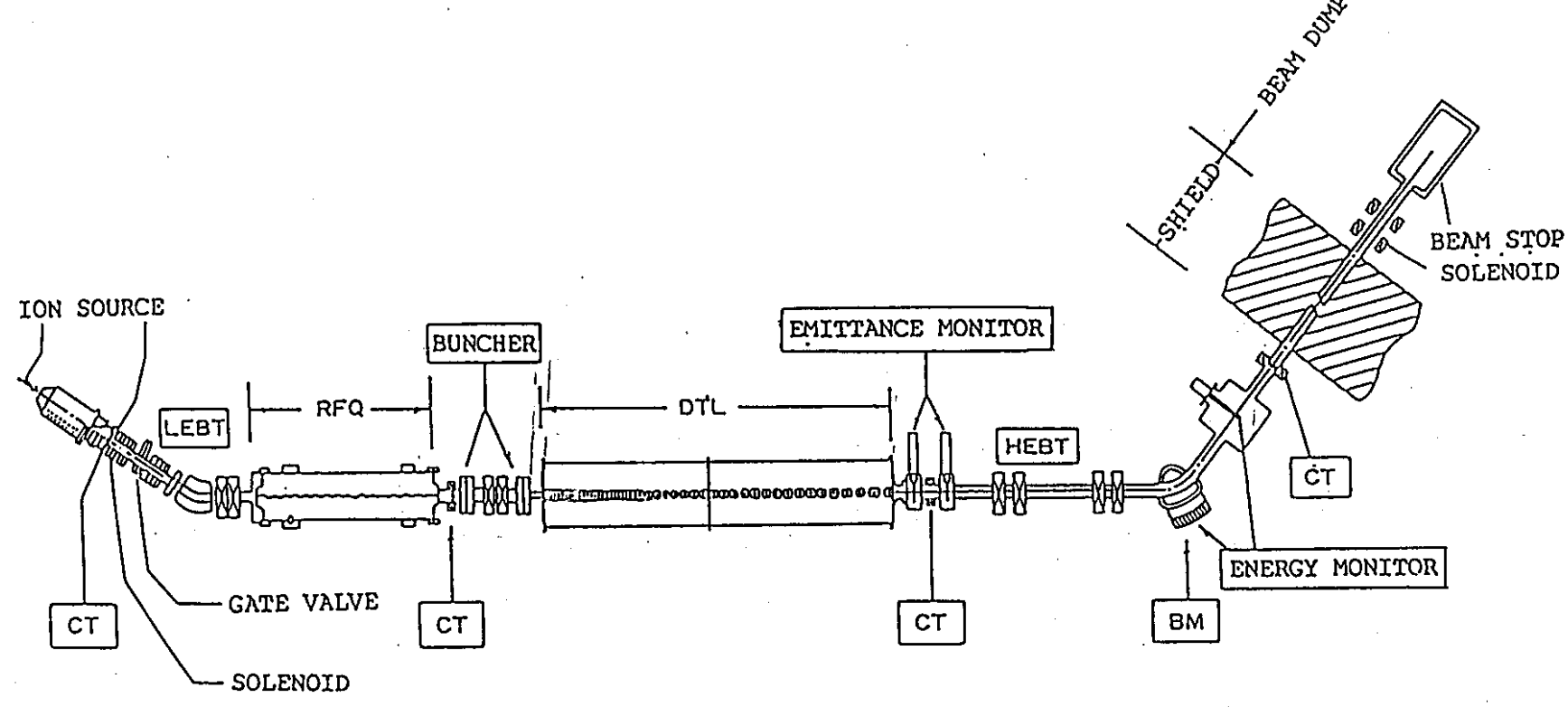


Fig. 11 Temperature distribution in the reference core



\* 1,000 burnup days correspond to  $\sim 10^5\,\text{MWD/ton}$  Fig. 12 Change of  $k_{\text{eff}}$  with burn-up



BM : BENDING MAGNET

CT : CURRENT TRANSFORMER

LEBT: LOW ENERGY BEAM TRANSPORT HEBT: HIGH ENERGY BEAM TRANSPORT

Fig. 15 Configuration of Basic Technology Accelerator (10 MeV, 10 mA)

## TRU Transmutation in an LMFBR

M. Ishikawa, M. Yamaoka and T. Wakabayashi
O-arai Engineering Center
Power Reactor and Nuclear Fuel Development Corporation
4002 Narita, O-arai-machi, Ibaraki-ken 311-13 JAPAN

# T. Kawakita Mitsubishi Atomic Power Industries, INC.

4-1 Shibakouen 2-chome, Minato-ku, Tokyo 105 JAPAN

### ABSTRACT

The characteristics of TRU transmutation in a 1000MWe-class LMFBR with mixed-oxide fuel were quantitatively studied to substantiate the feasibility.

We considered here two typical methods transmuting TRU in the LMFBR core. One is the method dispersing TRU homogeneously throughout the entire core (homogeneous TRU-loading method). It was found that the homogeneous method had no serious penalties of TRU loading to the reactor core performance, and the TRU transmutation rate reached approximately 11% per cycle with the loading of the weight ratio of 5% TRU in MOX fuel. The amount of the TRU transmutation in the LMFBR is almost six times as much as that of the TRU production from a 1000MWe-class LWR. As another desirable property, the TRU-loaded core was found to reduce the burnup reactivity loss by 40% compared with the reference core without TRU. It can be concluded that the TRU transmutation in an LMFBR has no problems from the viewpoint of the core performance, provided that the homogeneous method could be employed.

The other possible method is the use of small number of subassemblies (target S/As) which concentrate TRU in fuel (heterogeneous TRU-loading method). The weight ratio of 50% TRU fuel was assumed to be loaded in the target S/As. The calculating results showed that the swing of power peaking near the target S/As became quite severe and critical for the thermal design criteria, although the TRU transmutation rate and other reactor core performances of the heterogeneous method were roughly comparable to the homogeneous method. It seems from the present study that the heterogeneous method has quite a serious problem to be overcome and much effort would be needed to make the method feasible.

#### §1. Introduction

The proper management of High Level Wastes (HLW) which are inevitably produced with reactor operations is one of the most important problems to complete the nuclear fuel cycle (Ref. 1). Most of fission products in the HLW have relatively short half-lives and decay to stable form within a few hundred years, while the transuraniums (TRU) like Np237 and Am243, the  $\alpha$ -emitters, have extremely long half-lives of millions of years and contribute to the long-term radiotoxicity of the fuel cycle wastes. It is a strong social requirement not to leave these long-life HLW to future generations, and Power Reactor and Nuclear Fuel Development Corporation (PNC) has launched the project of the TRU transmutation study in LMFBRs from the view point of both reactor core characteristics and nuclear fuel cycle.

It is generally acknowledged that LMFBRs would be superior TRU transmutation devices, mainly due to their hard neutron spectrum (Ref. 2). In the course of the TRU study of PNC, we first surveyed the relation between the TRU transmutation rates and the various reactor core parameters which included amount of TRU loading, fuel type, reactor core size, reactor operation length per cycle, power density, isotopic composition of TRU. The objective of the parametric study was to understand the basic characteristics of TRU transmutation in LMFBRs (Ref. 3). As the second stage, we chose a large LMFBR with mixed-oxide(MOX) fuel as the TRU transmutation device and studied the characteristics of TRU transmutation in the large LMFBR quantitatively to substantiate the feasibility. The present report describes the summary of the second stage of the TRU transmutation study at PNC.

## §2. Survey of TRU Transmutation in a Large LMFBR

First, a 1000MWe-class LMFBR core with MOX fuel was defined as the reference whose main parameters are shown in Table 2.1 and Fig. 2.1. The nuclear characteristics of TRU-loaded core was calculated by two-dimensional diffusion theory with depletion chain. The cross sections used were seven effective group constants condensed from the Japanese standard 70-group constant set, JFS-3-J2 (Ref. 4), which is based on an evaluated nuclear data library, JENDL-2 (Ref. 5).

The loaded-TRU material was assumed to come from LWR spent fuel with fiveyear cooling time before reprocessing. The isotopic composition of the TRU was calculated by the ORIGEN2 code (Ref. 6). Table 2.2 shows the initial composition and the burnup dependency of the fission reaction rate of each isotope in 1 kg of the TRU. It is found that the total fiscion rate increases with burnup and reaches the maximum value of one and half times of initial value at 4-year burnup time. The increase of the total fission rate is caused by the fission of Pu238 which is generated from the capture reaction of Np237.

We consider here two typical methods transmuting TRU in the LMFBR core. One is the method dispersing TRU homogeneously throughout the entire core (homogeneous TRU-loading method), which is expected not to affect the core characteristics seriously. The other possible method is the use of small number of subassemblies (target S/As) which concentrate TRU in MOX fuel (heterogeneous TRU-loading method), which can have the advantage of the fuel cycle because of handling the small number of TRU-included fuels in fabrication factory. The followings are the results of parametric studies regarding these two TRU-loading methods.

## 2.1 Homogeneous TRU-loading Method

Reactor core characteristics evaluated here are amount of TRU transmuted, burnup reactivity loss and swing of power distribution with the TRU mass loaded in fuel as the parameter.

#### a. Amount of TRU Transmuted

Figure 2.2 shows the relationship between the amount of TRU transmuted and that of loaded-TRU in the FBR core. At least, one percent of TRU-loading to fuel would be needed to eliminate TRU, and the amount of TRU transmuted increases linearly with that of loaded-TRU. Since a 1000MWe-class LWR produces about 26 kg of TRU per year, an LMFBR with 5% TRU-loading can transmute the TRU mass from six LWRs in rough estimation.

## b. Burnup Reactivity Loss

The TRU-loading to core results in significant decrease of burnup reactivity loss mainly due to Pu238 build-up. As seen in Fig. 2.3, the burnup reactivity becomes positive when the amount of TRU-loading is over 10%, therefore, the maximum amount of TRU-loading in the FBR core would be limited to about 10% from the aspect of reactor operational safety. From other viewpoint, a proper amount of TRU-loading might be advantageous to the extension of reactor operation period.

## c. Swing of Power Distribution

Figure 2.4 shows the swing of power distribution between the beginning and the end of equilibrium cycle (BOEC and EOEC) with the parameter of TRU mass loaded in the outer core region. It could be possible to minimize the

power swing by optimizing the ratio of loaded-TRU amount between the inner and the outer core region.

## 2.2 Heterogeneous TRU-loading Method

Parameters surveyed here are the mass of TRU contained in the target S/As, loading position of the target S/As and plutonium enrichment of the target S/As. The survey cases and the TRU transmutation ratio calculated are summarized in Table 2.3.

#### a. TRU Transmutation Rate

As seen in cases A30 through A100, or B30 through B100 of Table 2.3, the TRU transmutation rate increases with the amount of TRU loading, but the tendency is not always linear and also depends on the position of the target S/As. About the dependence on loading position of the target S/As, the TRU transmutation rate in the case B50 where TRU is loaded at the periphery of the inner core is about four times as much as the case A50 of the core center loading with roughly identical TRU mass. This means that the target S/As perform high transmutation rate when they are loaded in a dispersive manner to avoid the depression of neutron flux.

In addition, quite a surprising fact was found from the case AB50, in which the target S/As with 50% TRU were loaded at just the same positions with cases A50 and B50. The amount of TRU transmuted in the case AB50 was 147 kg/cycle, which was by 80% larger than the summed value transmuted in the cases A50 and B50. This curious behavior of TRU transmutation was found to be caused by the increase of flux level in each TRU-loaded position due to the positive interference effect between two regions.

The case C50 shows the radial blanket region is another possibility to load TRU, since a large number of target S/As can be accepted there with no influence to core characteristics and transmute sufficient mass of TRU in spite of their low TRU transmutation rate.

Comparing cases A50, A50L and A50H, it is found that the TRU transmutation rate increases with plutonium enrichment of the target S/As. This can be interpreted as the consequence of neutron flux increase by plutonium enrichment. We should consider, however, the swing power of target S/As also increase, which is a large penalty for core thermal characteristics.

## b. Swing of Power Distribution

Figure 2.5 shows the power distribution of the cases A30, A50 and A100 where the target S/As are loaded in the core center region with 30%, 50% and 100% TRU in the target S/As, respectively. They are compared with no TRU-loading case REF. At BOEC, the power of TRU-loaded region is quite depressed in these TRU-loading cases.

At EOEC, all three cases shows larger power in the TRU-loaded region than that of BOEC. The degree of the power swing tends to increase with the mass of loaded-TRU in the target S/As, but the dependency on the mass of loaded-TRU is quite non-linear, especially in the case A100. This marked non-linearity can be interpreted as the complicated effect of the dominant isotope Np237 in TRU nuclides, which acts as both strong poison and fertile of active Pu238 as shown in Table 2.2.

#### §3. Nuclear and Thermal Characteristics of TRU-loaded Core

The influence of TRU-loading to the reactor core characteristics was quantitatively analyzed about a 1000MWe-class large LMFBR. Based on the previous survey, a typical TRU-loading core was assumed for each of the homogeneous and heterogeneous TRU-loading methods. The basic policies adopted here to set the loading patterns are: (a) as the main objective here is to understand physical mechanisms, a simple loading pattern is suitable rather than complicated one which might show better core performance, and (b) to compare the two loading methods, the total mass of loaded-TRU is set to be approximately identical between them, that is, 5% TRU in the whole core fuel in the case of the homogeneous method, and 37 target S/As which have 50% of TRU in fuel in the case of the heterogeneous TRU-loading method. Figure 3.1 shows the loading pattern of TRU-loaded S/As in the heterogeneous method. No TRU-loaded core was also analyzed as the reference case.

#### 3.1 Nuclear Characteristics

The basic nuclear characteristics was calculated by means of two-dimensional RZ diffusion-depletion theory. The three-dimensional distribution of power and burnup compositions were obtained with the combination of two-dimensional RZ and XY calculation. The plutonium enrichment of each core was determined to sustain criticality at EOEC, where the control rods are all withdrawn from the core. The characteristics evaluated here are power distribution, neutron spectrum, various reactivity coefficients, kinetics parameters and TRU transmutation rate.

Table 3.1 compares the calculated results about the nuclear characteristics of

the two TRU-loaded cores and the reference core.

#### a. Power Distribution

The swing of region-integrated power in the inner and outer core and blanket is almost identical among these three cores. The radial power distribution of the target S/A method, however, is quite different from that of the other cores as shown in Fig. 3.2. At BOEC, the power of TRU-loaded target S/As is very depressed compared with the reference core, while they get close at EOEC. This power swing would be a great obstacle for thermal characteristics.

### b. Neutron Spectrum

Fig. 3.3 shows the spectra of neutron and adjoint flux in the three cores. It is found that the neutron spectrum gets harder and the high-energy importance becomes larger with TRU-loading mass.

#### c. Control Rod Worth

The control rod worth of the TRU-loaded cores decreases from the reference core by 10~20%. This may be caused by the hardening of neutron spectrum.

### d. Burnup Reactivity Loss

Due to the production of Pu238 from Np237 in TRU, the burnup reactivity in the TRU-loading cores is 40% smaller than that of the reference core.

## e. Reactivity Coefficients

The Doppler coefficients of the TRU-loading cores are 20~30% smaller in absolute value, and the sodium density reactivity coefficients are 50% larger than the reference core because of the the spectrum hardening.

#### f. Kinetics Parameters

Similarly, the values of prompt neutron life time in the TRU-loaded cores become shorter by 20% than that of the reference core.

## g. TRU Transmutation Rate

Table 3.2 summarized the TRU inventory and transmutation rate of these three cores. Both TRU-loaded cores can transmute TRU by 11~12% (about 180kg/cycle), and there is no differences between the two TRU-loading methods. In detail, Np and Am were eliminated after depletion, but Cm increased on the contrary. This would be a problem from viewpoint of the fuel handling and transportation in fuel cycle.

#### 3.2 Thermal Characteristics

The coolant flow distribution was optimized for the no TRU-loaded reference core, and the influence of TRU-loading was evaluated about the thermal

characteristics. The results were shown in Table 3.3.

There is no thermal problems about the homogeneous TRU-loading core, since the power distribution hardly changes from the reference core. On the other hand, the position where maximum temperature of cladding occurs in the heterogeneous TRU-loading core moves from the reference core, and the hot spot temperature of the cladding reaches 775 degree-C which is higher than that of the reference core by 40 degrees.

Although there might be rooms for optimization of the flow distribution, the significant power swing is inevitable for the heterogeneous TRU-loading core. From the viewpoint of the thermal characteristics of the core, the homogeneous TRU-loading method is apparently superior to the heterogeneous TRU-loading method.

### §4. Decay Heat and Neutron Emission from TRU-loaded Fuel S/A

The problem of the fuel handling is another aspect to be considered related to the TRU transmutation in FBR plant. Table 4.1 shows the decay heat and neutron emission rate from a fresh fuel S/A with 100% TRU-loaded, in comparison with a conventional MOX fuel S/A. In the case of 5% TRU-loaded fuel S/A, these values will be one-twentieth since these quantities are expected proportional to TRU mass.

If the TRU composition contains all of Np, Am and Cm, both the decay heat and neutron emission rate of the 100% TRU-loaded fuel S/A will exceed that of a conventional spent fuel. Especially, the neutron emission rate will be severe even in the case of a 5% TRU-loading fuel S/A. From these facts, it seems that some modifications of shielding and heat removal in the fuel handling system of a FBR plant, fuel fabrication factory and/or transportation vessels are needed in order to make the TRU transmutation feasible.

Furthermore, it is also found in Table 4.1 the dominant element of these fuel properties is Cm. If it is possible to remove Cm from the TRU-loaded fuel, the decay heat value will decrease by one order, and the neutron emission rate by three orders. Since the dominant isotope, Cm244, has a relatively short half-life of 18 years, there might be another possibility of the fuel cycle, that is, partitioning of Cm from TRU in the reprocess and storing of Cm for a period separately. Some study will be needed to estimate the trade-off between the plant modification and the reprocessing.

#### §5. Conclusions

In the present study, the characteristics of TRU transmutation in a 1000MWeclass LMFBR with MOX fuel were quantitatively investigated to substantiate the feasibility.

There would be two typical methods transmuting TRU in the LMFBR core. One is the homogeneous TRU-loading method. It was found that the homogeneous method had no serious penalties of TRU loading to the reactor core performance, and the TRU transmutation rate reached approximately 11% per cycle with the loading of the weight ratio of 5% TRU in MOX fuel. The amount of the TRU transmutation in the LMFBR is almost six times as much as that of the TRU production from a 1000MWe-class LWR. As another desirable property, the TRU-loaded core was found to reduce the burnup reactivity loss by 40% compared with the reference core without TRU. It can be concluded that the TRU transmutation in an LMFBR has no problems from the viewpoint of the core performance, provided that the homogeneous method could be employed.

The other possible method is the heterogeneous TRU-loaded method. The weight ratio of 50% TRU fuel was assumed to be loaded in target S/As. The calculating results showed that the swing of power peaking near the target S/As became quite severe and critical for the thermal design criteria, although the TRU transmutation rate and other reactor core performances of the heterogeneous method were roughly comparable to the homogeneous method. It seems from the present study that the heterogeneous method has quite a serious problem to be overcome and much effort would be needed to make it feasible.

As another aspect, the decay heat and neutron activity of the TRU-loaded S/A were estimated. As a result, it is recognized that the fuel handling system in an LMFBR plant, a fuel fabrication factory and/or fuel transportation vessels should be modified to treat the TRU-loaded fuel with high decay heat and strong neutron activity.

Finally, we list up the remaining items of researches to accomplish the TRU transmutation in an LMFBR,

- Accumulation of data related to material property and irradiation characteristics of TRU-loaded fuel.
- Improvement of nuclear data for TRU isotopes,
- Establishment of reactor core design method including uncertainties of nuclear and thermal data of TRU,
- Optimization of TRU-loading method in FBR cores,
- and, Consideration of FBR plants to treat TRU, especially fuel handling system.

#### REFERENCES

1. L. KOCH, "Formation and Recycling of Minor Actinides in Nuclear Power Stations," Handbook on the Physics and Chemistry of the Actinides, Chapter 9, North-Holland Physics Publishing, (1986)

.

- 2. J. W. Watchter and A. G. Croff, "Actinide Partitioning Transmutation Program Final Report II. Transmutation Studies," Oak Ridge National Laboratory report, ORNL/TM-6983, (1980)
- 3. T. Wakabayashi, et al., "TRU Transmutation by LMFBR," Power Reactor and Nuclear Fuel Development Corporation, the 32nd NEACRP Meeting, A-982, (1989)
- 4. H. Takano, et al., "Revision of Fast Reactor Group Constant Set JFS-3-J2," Japan Atomic Energy Research Institute report, JAERI-M 89-141 (1989)
- 5. T. Nakagawa, "Summary of JENDL-2 General Purpose File," Japan Atomic Energy Research Institute report, JAERI-M 84-103 (1984)
- 6. A. G. Croff, "A User's Manual for the ORIGEN2 Computer Code," Oak Ridge National Laboratory report, ORNL/TM-7175, (1980)

Table 2.1 Main design parameters of the 1000MWe-class reference LMFBR:

| Design parameters                    | Data                             |
|--------------------------------------|----------------------------------|
| 1. Plant parameters                  |                                  |
| ·Reactor thermal power               | 2517 MWt                         |
| ·Coolant temperature                 | 530/375°C                        |
| (Reactor outlet / inlet)             |                                  |
| ·Coolant flow rate                   | $1.27 \times 10^4 \mathrm{kg/s}$ |
| ·Operation cycle length              | 456 days                         |
| ·Plant life time                     | 40 years                         |
| 2. Core parameters                   |                                  |
| ·Core concept                        | 2-region homogeneous core        |
| ·Core layout                         | see Fig.2.1                      |
| ·Number of core fuel S/As            | 175/180                          |
| (inner/outer)                        | • •                              |
| ·Number of radial blanket S/As       | 72                               |
| ·Number of control rods              | 18/6                             |
| (primary / backup)                   |                                  |
| ·Number of shielding                 | 78 / 277                         |
| (Stainless Steel / B <sub>4</sub> C) |                                  |
| ·Core diameter / core height         | 3.68/1.00 m                      |
| ·Thickness of axial blanket          | 0.20/0.20m                       |
| (upper/lower)                        |                                  |
| 3. Core fuel parameters              |                                  |
| ·Fuel composition                    | $PuO_2 \cdot UO_2$               |
| Pu isotope ratio(239/240/241/242)    | 58/24/14/4                       |
| ·Pu enrichment(inner/outer)          | 15.3 /19.3 wt%                   |
| ·Pattern of fuel exchange            | 3 dispersed batches              |
| 4. Blanket fuel parameters           |                                  |
| Fuel composition                     | UO <sub>2</sub>                  |
| ·U isotope ratio(235/238)            | 0.3/99.7                         |
| Pattern of fuel exchange             | 4 dispersed batches              |

### REFERENCES

1. L. KOCH, "Formation and Recycling of Minor Actinides in Nuclear Power Stations," Handbook on the Physics and Chemistry of the Actinides, Chapter 9, North-Holland Physics Publishing, (1986)

:

- 2. J. W. Watchter and A. G. Croff, "Actinide Partitioning Transmutation Program Final Report II. Transmutation Studies," Oak Ridge National Laboratory report, ORNL/TM-6983, (1980)
- 3. T. Wakabayashi, et al., "TRU Transmutation by LMFBR," Power Reactor and Nuclear Fuel Development Corporation, the 32nd NEACRP Meeting, A-982, (1989)
- 4. H. Takano, et al., "Revision of Fast Reactor Group Constant Set JFS-3-J2," Japan Atomic Energy Research Institute report, JAERI-M 89-141 (1989)
- 5. T. Nakagawa, "Summary of JENDL-2 General Purpose File," Japan Atomic Energy Research Institute report, JAERI-M 84-103 (1984)
- 6. A. G. Croff, "A User's Manual for the ORIGEN2 Computer Code," Oak Ridge National Laboratory report, ORNL/TM-7175, (1980)

Table 2.1 Main design parameters of the 1000MWe-class reference LMFBR:

| No                                   | •                         |
|--------------------------------------|---------------------------|
| Design parameters                    | Data                      |
| 1. Plant parameters                  |                           |
| ·Reactor thermal power               | 2517 MWt                  |
| ·Coolant temperature                 | 530/375°C                 |
| (Reactor outlet / inlet)             |                           |
| ·Coolant flow rate                   | $1.27 \times 104$ kg/s    |
| ·Operation cycle length              | 456 days                  |
| ·Plant life time                     | 40 years                  |
| 2. Core parameters                   |                           |
| ·Core concept                        | 2-region homogeneous core |
| ·Core layout                         | see Fig.2.1               |
| ·Number of core fuel S/As            | 175 / 180                 |
| (inner/outer)                        | ·                         |
| ·Number of radial blanket S/As       | 72                        |
| ·Number of control rods              | 18/6                      |
| (primary/backup)                     |                           |
| ·Number of shielding                 | 78/277                    |
| (Stainless Steel / B <sub>4</sub> C) |                           |
| ·Core diameter/core height           | 3.68/1.00 m               |
| ·Thickness of axial blanket          | $0.20/0.20 \mathrm{m}$    |
| (upper/lower)                        | ·                         |
| 3. Core fuel parameters              |                           |
| ·Fuel composition                    | PuO₂·UO₂                  |
| Pu isotope ratio(239/240/241/242)    | 58/24/14/4                |
| ·Pu enrichment(inner/outer)          | 15.3 /19.3 wt%            |
| ·Pattern of fuel exchange            | 3 dispersed batches       |
| 4. Blanket fuel parameters           |                           |
| ·Fuel composition                    | UO <sub>2</sub>           |
| ·U isotope ratio(235 / 238)          | 0.3/99.7                  |
| Pattern of fuel exchange             | 4 dispersed batches       |

Table 2.2 Isotopic composition of TRU fuel loaded and burnup dependency of fission reaction rate of each nuclide

| Nuclide   | TRU<br>composition<br>discharged      | 1-group cro |         | Fission reaction rate vs. irradiation time (flux: $4\times1$ (Units: $10^{15}$ fissions/sec/1kg of initial TRU amou |         |         | 015 <sub>nv</sub> )<br>int) |          |
|-----------|---------------------------------------|-------------|---------|---------------------------------------------------------------------------------------------------------------------|---------|---------|-----------------------------|----------|
|           | from LWR<br>(10 <sup>24</sup> atm/cc) | Capture     | Fission | Initial                                                                                                             | 1 years | 4 years | 7 years                     | 10 years |
| Np237     | 4.55×10-3                             | 1.44        | 0.39    | 1.92                                                                                                                | 1.53    | 0.77    | 0.39                        | 0.19     |
| Pu238     | 0.0                                   | 0.70        | 1.18    | <del>-</del>                                                                                                        | 1.04    | 2.35    | 2.06                        | 1.45     |
| Pu239     | 0.0                                   | 0.47        | 1.82    | <u>-</u>                                                                                                            | 0.06    | 0.56    | 0.84                        | 0.82     |
| Pu240     | 0.0                                   | 0.49        | 0.42    | •                                                                                                                   | 0.01    | 0.04    | 0.07                        | 0.10     |
| Pu241     | 0.0                                   | 0.44        | 2.44    | -                                                                                                                   | -       | 0.02    | 0.05                        | 0.08     |
| Pu242     | 0.0                                   | 0.42        | 0.30    |                                                                                                                     | 0.02    | 0.05    | 0.06                        | 0.05     |
| Am241     | 2.73×10-3                             | 1.33        | 0.34    | 1.02                                                                                                                | 0.80    | 0.38    | 0.18                        | 0.09     |
| Am242m    | 6.93×10-6                             | 0.37        | 3.91    | 0.03                                                                                                                | 0.27    | 0.32    | 0.19                        | 0.10     |
| Am243     | 1.40×10-3                             | 0.051       | 0.27    | 0.41                                                                                                                | 0.35    | 0.22    | 0.15                        | 0.10     |
| Cm242     | 7.95×10-8                             | 0.31        | 0.20    |                                                                                                                     | 0.04    | 0.02    | 0.01                        | 0.01     |
| Cm243     | 4.57×10-6                             | 0.23        | 2.60    | 0.01                                                                                                                | 0.02    | 0.03    | 0.02                        | 0.01     |
| Cm244     | 4.49×10-4                             | 0.80        | 0.48    | 0.20                                                                                                                | 0.27    | 0.29    | 0.25                        | 0.20     |
| Cm245     | 2.31×10-5                             | 0.30        | 2.60    | 0.07                                                                                                                | 0.16    | 0.34    | 0.38                        | 0.35     |
| TRU total | 9.17×10-3                             | :           |         | 3.66                                                                                                                | 4.56    | 5.39    | 4.65                        | 3.55     |

| Case name | Loading region of target S/As                                    | Number of<br>target S/As | TRU-loading<br>ratio in target<br>S/As (%) | amount of<br>TRU<br>transmuted<br>(kg/cycle) | TRU<br>transmutation<br>rate (%/cycle) |
|-----------|------------------------------------------------------------------|--------------------------|--------------------------------------------|----------------------------------------------|----------------------------------------|
| REF       | -                                                                | 0                        | 0                                          | -47                                          | · <b>-</b>                             |
| A30       | Center of the inner core                                         | 19                       | 30                                         | 5                                            | 0.9                                    |
| A50       | Center of the inner core                                         | . 19                     | 50                                         | 18                                           | 1.9                                    |
| A100      | Center of the inner core                                         | 19                       | 100                                        | 72                                           | 4.0                                    |
| B30       | Periphery of the inner core                                      | 18                       | 30                                         | 25                                           | 4.8                                    |
| B50       | Periphery of the inner core                                      | 18                       | 50                                         | 65                                           | .7.9                                   |
| B100      | Periphery of the inner core                                      | 18                       | 100                                        | 153                                          | 9.5                                    |
| C50       | Radial blanket                                                   | 72                       | 50                                         | 153                                          | 2.3                                    |
| A50L      | Center of the inner core<br>(Pu enrichiment decreased<br>by 30%) | 1.9                      | 50                                         | 9                                            | 0.9                                    |
| A50H      | Center of the inner core<br>(Pu enrichiment increased<br>by 30%) | 19                       | 50                                         | 32                                           | 3.5                                    |
| AB50      | Center and periphery of the inner core                           | 37<br>(19+18)            | 50                                         | 147                                          | 8.7                                    |

Table 3.1 Comparison of nuclear characteristics of TRU-loaded cores

|                                                                                                                               |                                                                     |                                                                     | <u></u>                                      |
|-------------------------------------------------------------------------------------------------------------------------------|---------------------------------------------------------------------|---------------------------------------------------------------------|----------------------------------------------|
|                                                                                                                               | Reference core<br>(no TRU-loaded)                                   | Homogeneous<br>TRU-loaded core                                      | Heterogeneous<br>TRU-loaded core             |
| Pu enrichment<br>(inner core/outer core)                                                                                      | 15.3/19.3 wt%                                                       | 16.2/19.6 wt%                                                       | 15.3/19.3 wt%                                |
| Region-integrated power ratio (BOEC/EOEC) Inner core Ouetr core Radial and axial blankets                                     | 46.8/50.9 %<br>47.6/41.8 %<br>5.6/7.4 %                             | 49.9/53.5 %<br>44.7/39.5 %<br>5.3/7.0 %                             | 48.8/53.6 %<br>45.4/38.9 %<br>5.8/7.5 %      |
| Max.linear heat rate<br>(BOEC/EOEC)<br>Inner core<br>Outer core<br>Radial blanket                                             | 380/419 w/cm<br>420/357 w/cm<br>427/397 w/cm                        | 376/431 w/cm<br>416/355 w/cm<br>411/369 w/cm                        | 391/419 w/cm<br>411/332 w/cm<br>502/425 w/cm |
| Control rod worth (BOEC、33cm insertion of primary rods)                                                                       | 1.67 %∆k/kk´<br>(1.00)*                                             | 1.46 %∆k/kk´<br>(0.87)*                                             | 1.36 %∆k/kk <sup>′</sup><br>(0.81)*          |
| Neutron spectrum<br>(core center)                                                                                             | see Fig.3.3                                                         | <del></del>                                                         | <del>(-</del>                                |
| Burnup reactivity loss                                                                                                        | 3.31 %∆k/kk <sup>′</sup>                                            | 1.88 %Ak/kk′                                                        | 1.97 %∆k/kk <sup>′</sup>                     |
| Doppler coefficient                                                                                                           | -1.05×10-2 Tdk/dT                                                   | -7.08×10-3 Tdk/dT                                                   | $-8.35 \times 10^{-3} \mathrm{Tdk/dT}$       |
| Density reactivity coefficient (Δρ/ρ/100%density change) Fuel Structure Coolant                                               | $2.87 \times 10^{-1}$ $-5.70 \times 10^{-2}$ $-1.73 \times 10^{-2}$ | $2.83 \times 10^{-1}$ $-6.20 \times 10^{-2}$ $-2.50 \times 10^{-2}$ | 2.92×10-1<br>-6.51×10-2<br>-2.67×10-2        |
| Geometric reactivity coefficient Radial ( $\Delta \rho / \rho / \Delta R / R$ ) Axial ( $\Delta \rho / \rho / \Delta H / H$ ) | 7.27×10-2<br>1.43×10-1                                              | 6.69×10-2<br>1.35×10-1                                              | 9.21×10-2<br>1.31×10-1                       |
| $eta_{	t eff}$                                                                                                                | 3.71×10-3                                                           | 3.47×10-3                                                           | 3.31×10-3                                    |
| Prompt neutron life time                                                                                                      | 0.406 μsec                                                          | 0.338 µsec                                                          | 0.326 μsec                                   |

<sup>\*)</sup> Values in parentheses denote relative control rod worth

Table 3.2 Summary of TRU inventory and transmutation rate

| Core             | Isotope   | Loaded<br>amount of | TRU inventory |          | Discharged amount of | Transmuted amount of | TRU<br>transmutation |
|------------------|-----------|---------------------|---------------|----------|----------------------|----------------------|----------------------|
| 00.0             | . 13010рс | TRU<br>(kg/cycle)   | BOEC(kg)      | EOEC(kg) | TRU<br>(kg/cycle)    | TRU<br>(kg/cycle)    | rate<br>(%)          |
| Reference core   | Np        | 0                   | 6             | 11       | 5                    | -5                   | _                    |
| (no TRU loaded)  | · Am      | 0                   | 46            | 82       | 36                   | -36                  | ·<br>•               |
|                  | Cm        | 0                   | 4             | 8        | 5                    | -5                   | -                    |
|                  | Total     | 0                   | 55            | 101      | 46                   | 46                   | -<br>-               |
| Homogeneous      | Np .      | 289                 | 719           | 590      | 160                  | 129                  | 18.0                 |
| TRU- loaded core | Am        | 268                 | 710           | 624      | 182                  | 86                   | 12.2                 |
|                  | Cm        | 31                  | 142           | 173      | 63                   | -31                  | -22.1                |
|                  | Total     | 589                 | 1571          | 1387     | 404                  | 184                  | 11.7                 |
| Heterogeneous    | Np        | 302                 | 769           | 647      | 180                  | 122                  | 15.8                 |
| TRU-loaded core  | Am        | 280                 | 752           | 669      | 197                  | 83                   | 11.0                 |
|                  | Cm        | 33                  | 140           | 168      | 61                   | -28                  | -20.4                |
|                  | Total     | 614                 | 1660          | 1485     | 438                  | 176                  | 10.6                 |

Table 3.3 Comparison of thermal characteristics of TRU-loaded cores

| Core               | flow region number<br>in which max.<br>hot spot cladding<br>temperature<br>occurred | Assembly<br>flow rate | Max.<br>assembly<br>power* | Max. hot spot<br>cladding<br>temperature* |
|--------------------|-------------------------------------------------------------------------------------|-----------------------|----------------------------|-------------------------------------------|
| Homogeneously      | •                                                                                   |                       |                            |                                           |
| TRU- loaded core   |                                                                                     |                       |                            |                                           |
| • Inner core(EOEC) | 1                                                                                   | 31.9 kg/s             | 9.89 MW                    | 723 °C                                    |
|                    | ·                                                                                   |                       | (9.65 MW)                  | (714°C)                                   |
| Outer core(BOEC)   | 6                                                                                   | 29.2 kg/s             | 8.84 MW                    | 727 °C                                    |
|                    |                                                                                     |                       | (8.87 MW)                  | (728°C)                                   |
| Heterogeneously    |                                                                                     |                       |                            |                                           |
| TRU- loaded core   |                                                                                     |                       |                            |                                           |
| • Inner core(EOEC) | 2                                                                                   | 31.5 kg/s             | 9.86 MW                    | 756 °C                                    |
|                    |                                                                                     |                       | (9.08 MW)                  | (724°C)                                   |
| Outer core(BOEC)   | 7                                                                                   | 27.1 kg/s             | 8.98 MW                    | 775 °C                                    |
| :                  |                                                                                     |                       | (8.06 MW)                  | (732°C)                                   |

<sup>\*)</sup> Values in parentheses denote the power for the assembly at the same position as in the reference core

Table 4.1 Decay heat and neutron emission rate of fresh TRU fuel

|                                            |                          | fresh fuel<br>ars before and a<br>eprocessing) | •           | al MOX fuel<br>I loaded)                        |
|--------------------------------------------|--------------------------|------------------------------------------------|-------------|-------------------------------------------------|
|                                            | Np+Am+Cm (e              |                                                | Fresh fuel  | Discharged fuel<br>(after cooled<br>for a year) |
| Decay heat<br>(per assembly)               | 21KW                     | 2.9KW                                          | 0.063KW     | 10KW                                            |
| Neutron<br>emission rate<br>(per assembly) | 6.9×10 <sup>10</sup> n/s | 8.7×107 n/s                                    | 6.8×106 n/s | 5.8×108 n/s                                     |

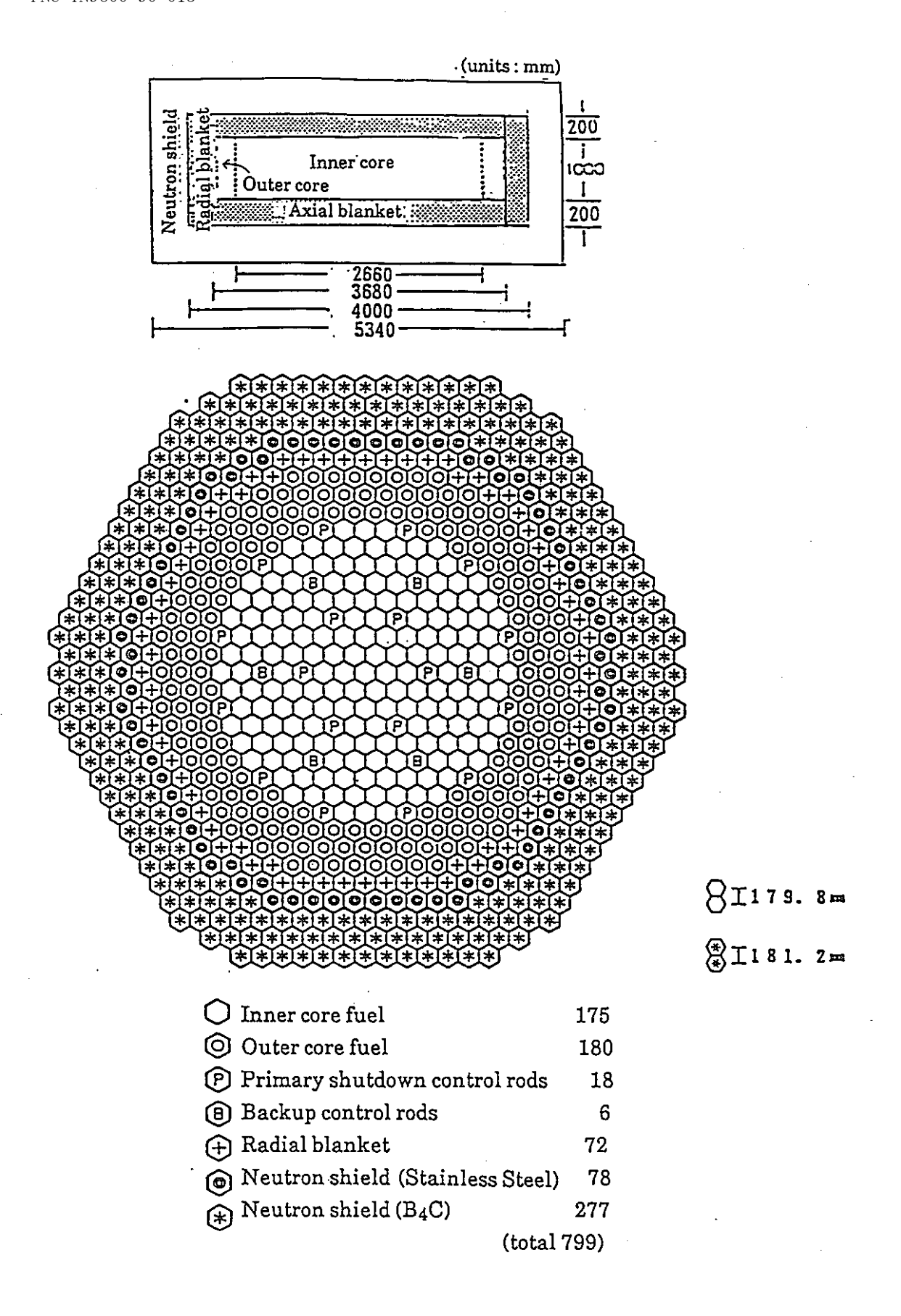


Fig. 2.1 Core layout of 1000MWe-class reference LMFBR

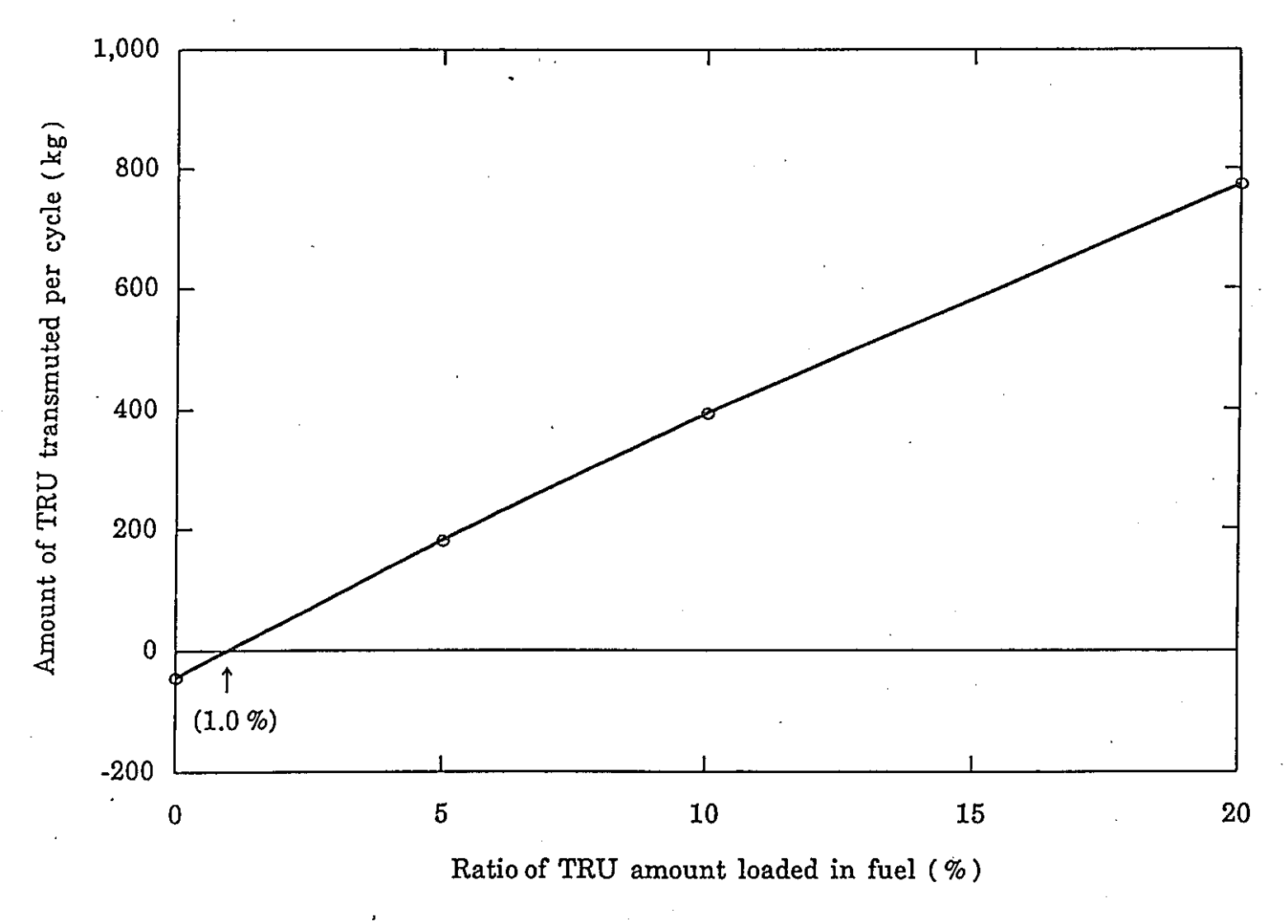


Fig. 2.2 Relationship between Amount of TRU Transmuted and Ratio of TRU Amount loaded in Fuel (Homogeneous TRU-loading Method)

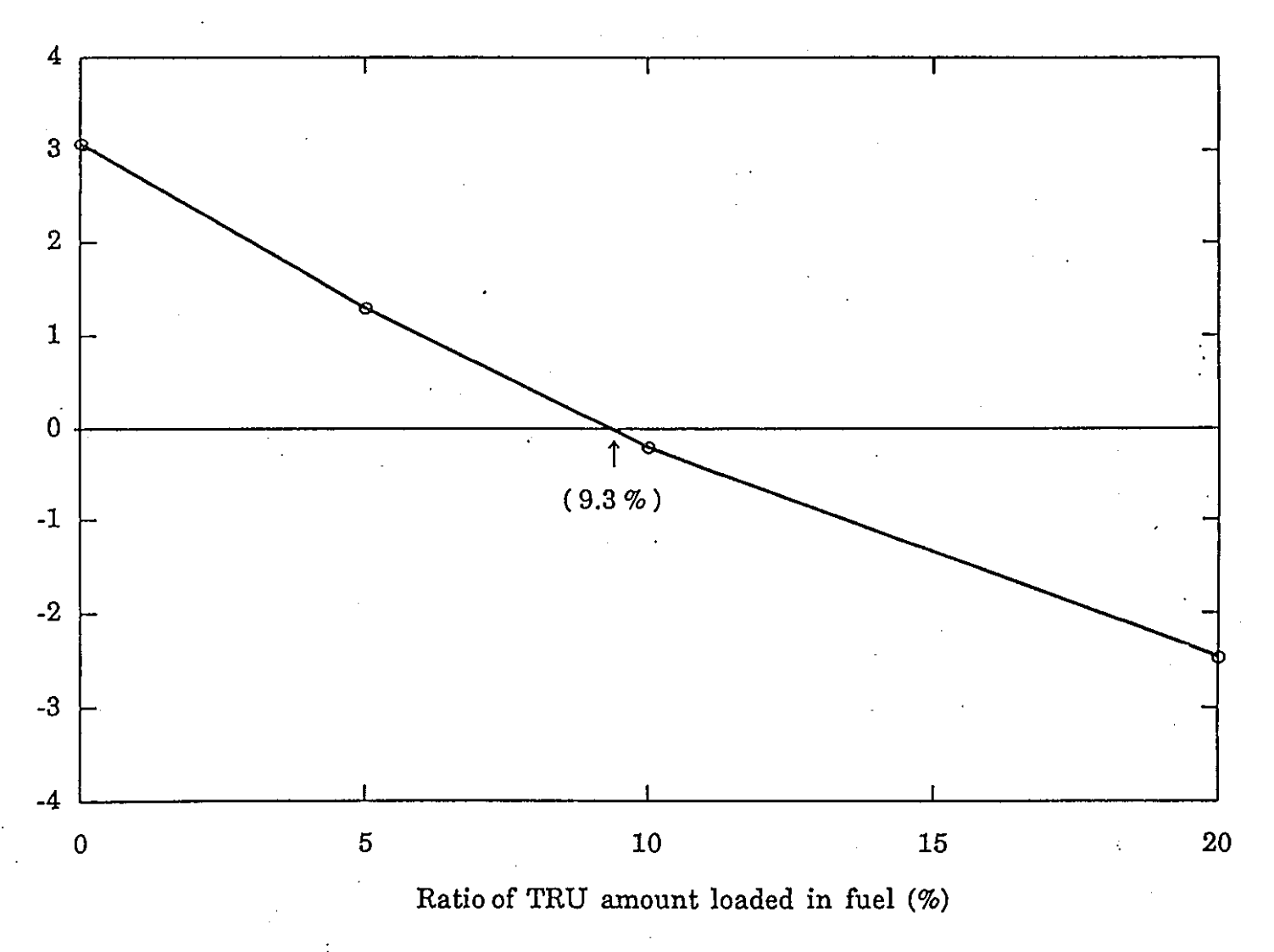
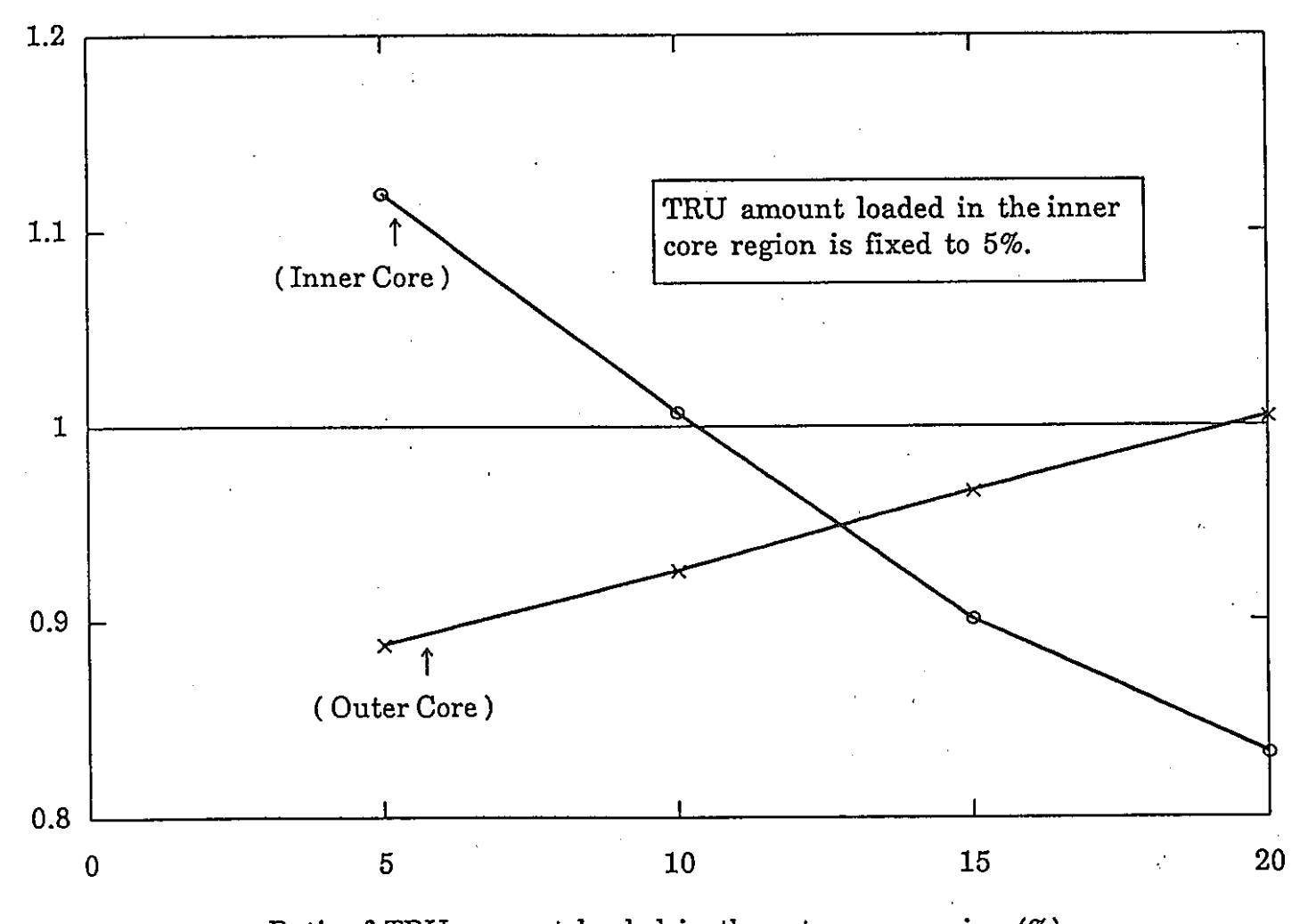


Fig. 2.3 Relationship between Burnup Reactivity Loss and Ratio of TRU Amount loaded in Fuel (Homogeneous TRU-loading Method)



Ratio of TRU amount loaded in the outer core region (%)

Fig. 2.4 Relationship between Power Peaking Swing and Ratio of TRU amount loaded in the Outer Core Region with Fixed TRU Amount in the Inner Region (Homogeneous TRU-loading Method)

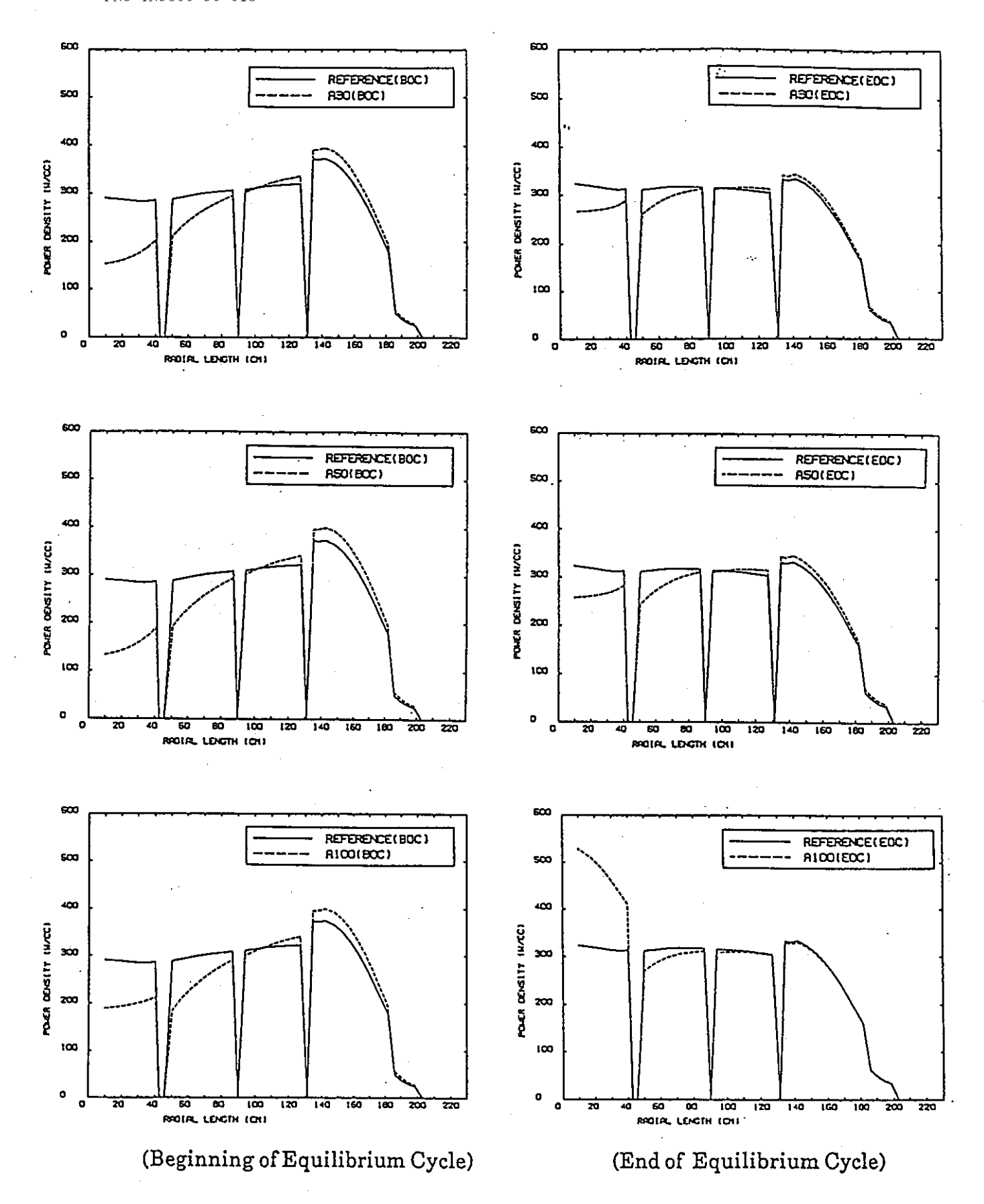
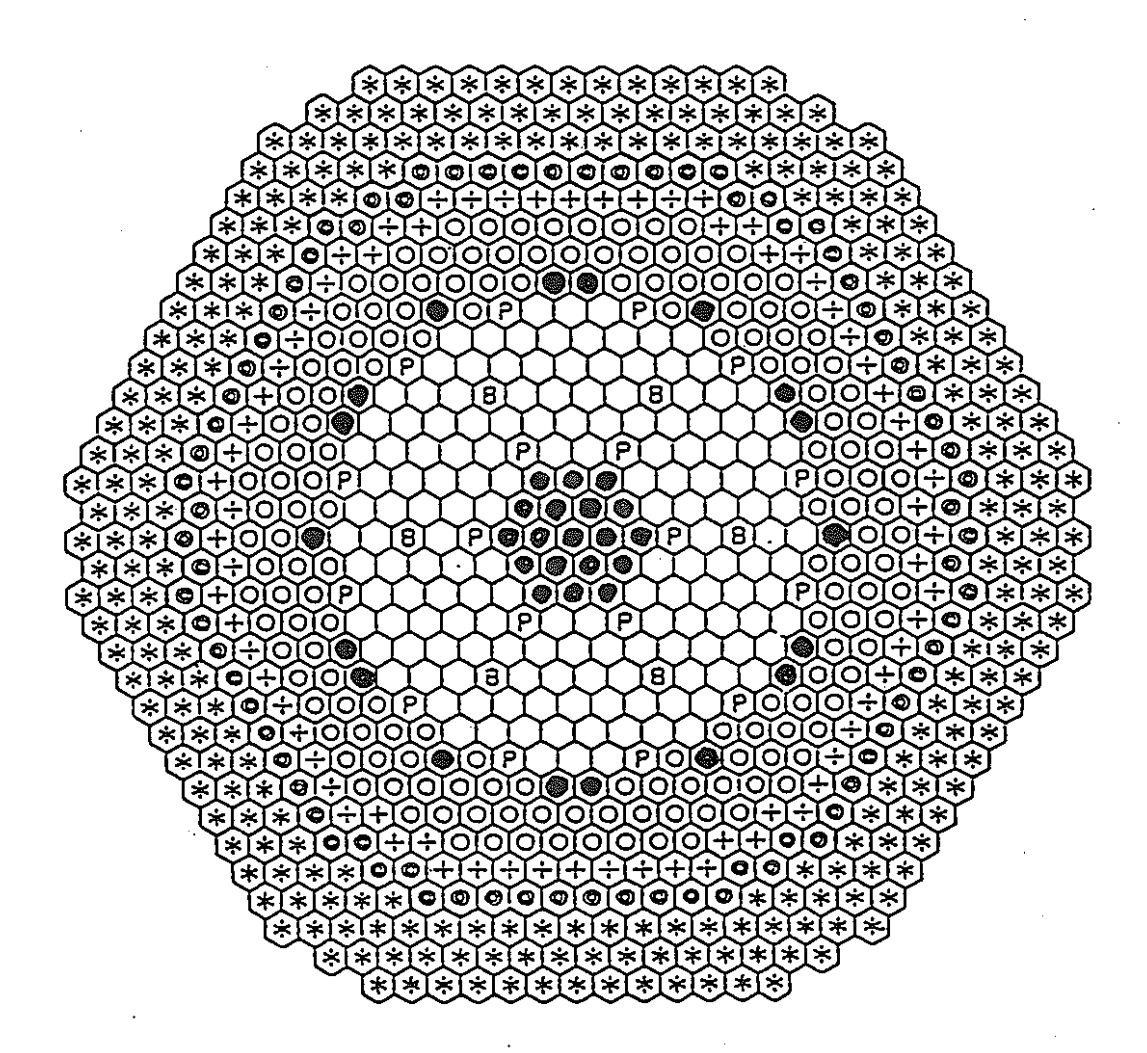


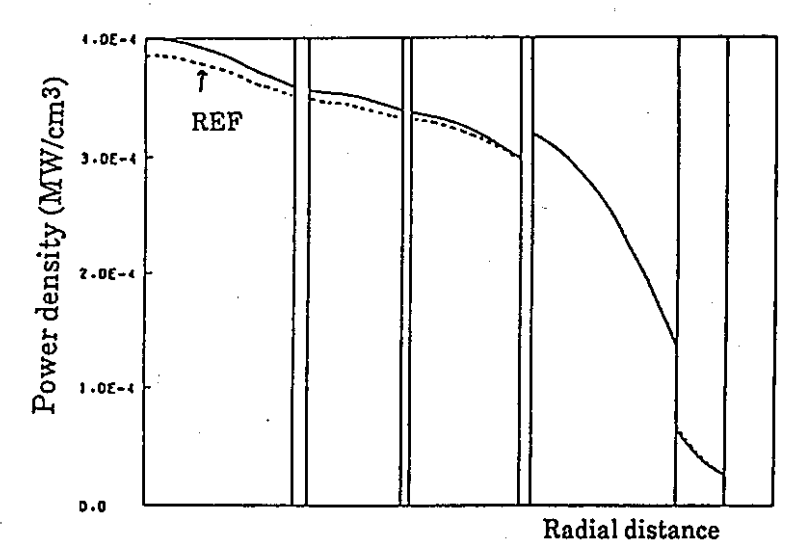
Fig.2.5 Power distribution of heterogeneous TRU-loaded cores



Target S/A including TRU

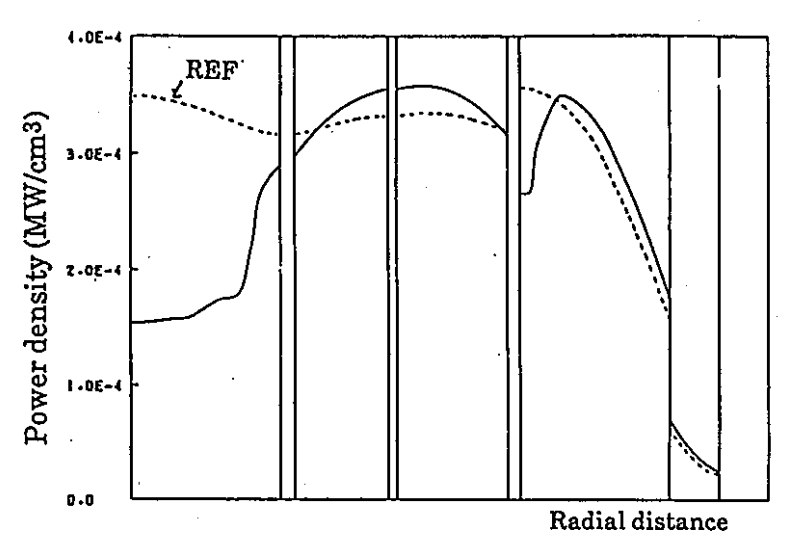
Fig.3.1 Loading pattern of target S/As (Heterogeneous TRU-loaded core)

Radial power distribution of homogeneous TRU-loaded core at BOEC (Primary control rods partially inserted)

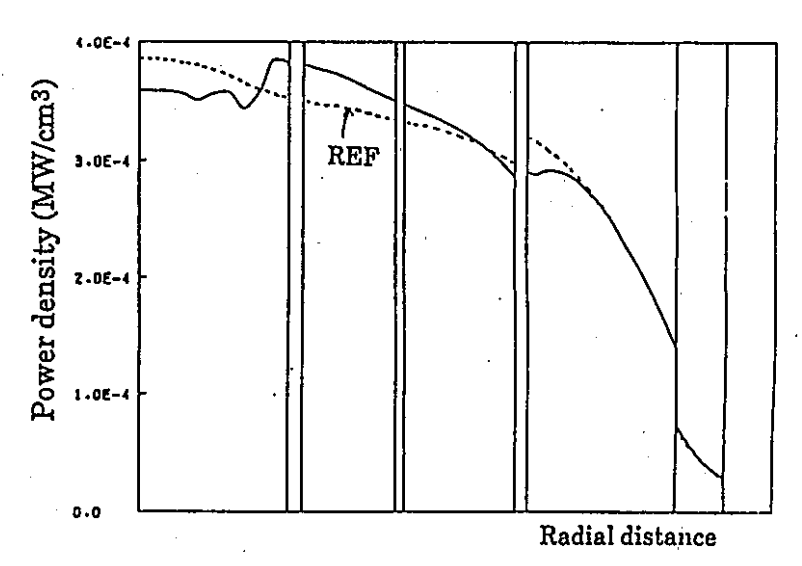


431 -

Radial power distribution of: homogeneous TRU-loaded core at EOEC (Primary control rods fully withdrawn)

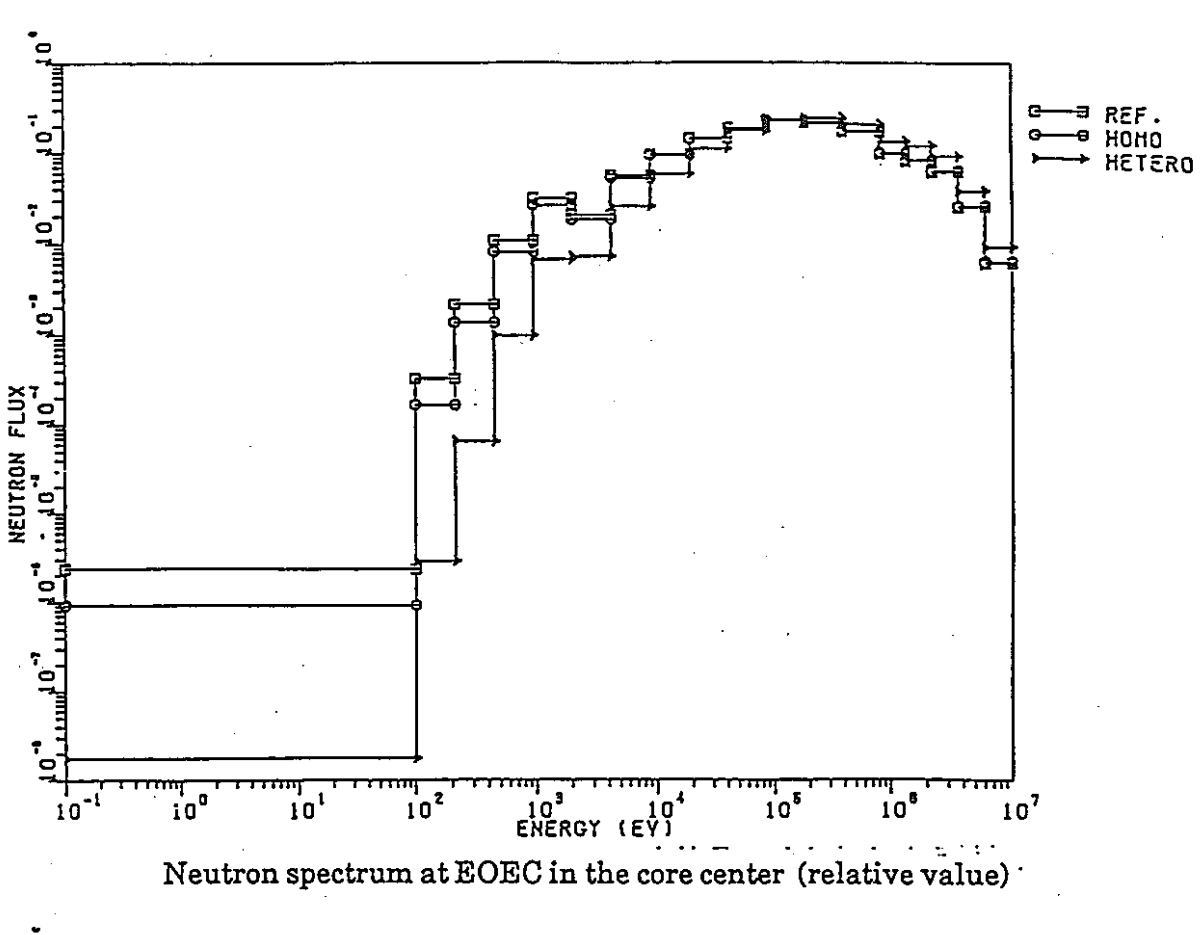


Radial power distribution of heterogeneous TRU-loaded core at BOEC (Primary control rods partially inserted)



Radial power distribution of: heterogeneous TRU-loaded core at EOEC (Primary control rods fully withdrawn)

Fig. 3.2 hadial power distribution of TRU-loaded cores



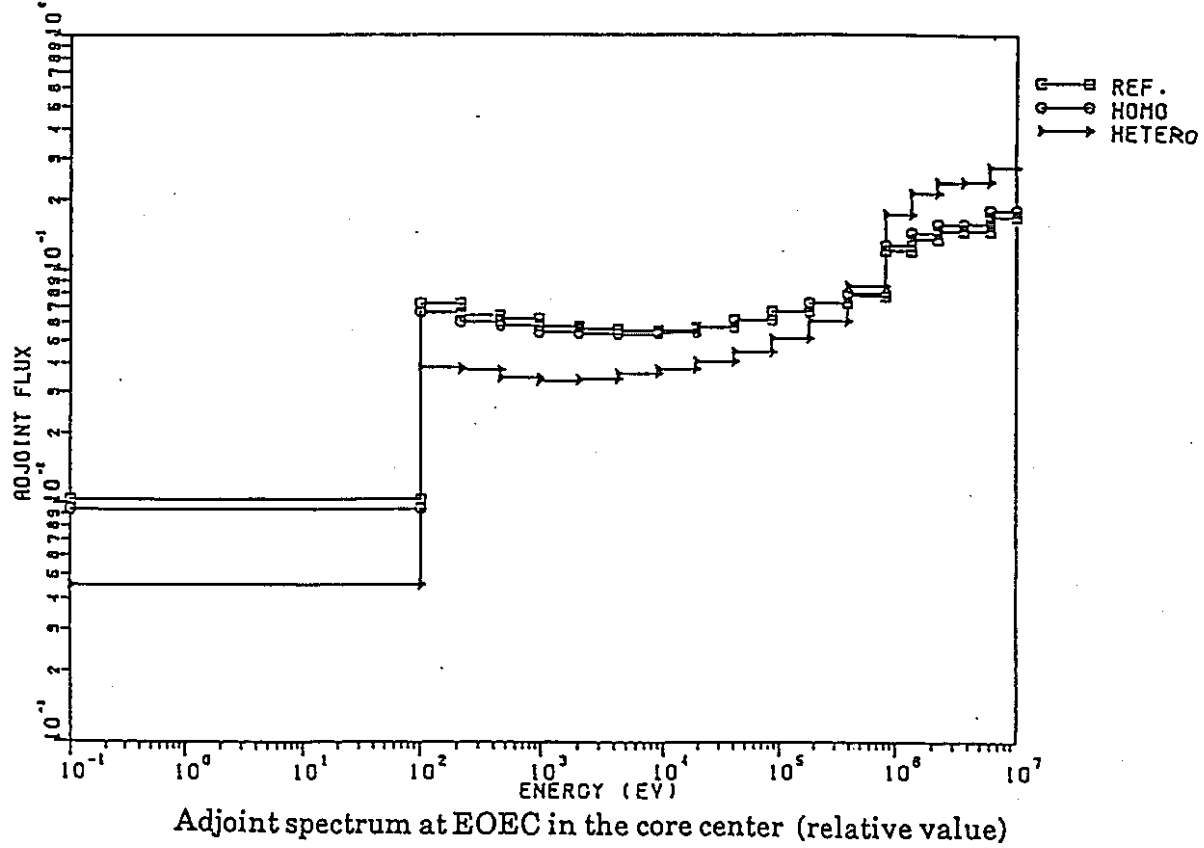


Fig. 3.3 Neutron and adjoint spectrum in the TRU-loaded cores